

AD-A164 847

TABULAR AND GRAPICAL SOLUTIONS OF REGULAR AND MACH
REFLECTIONS IN PSEUDO- (U) TORONTO UNIV DOWNSVIEW
(ONTARIO) INST FOR AEROSPACE STUDIES T C HU ET AL.

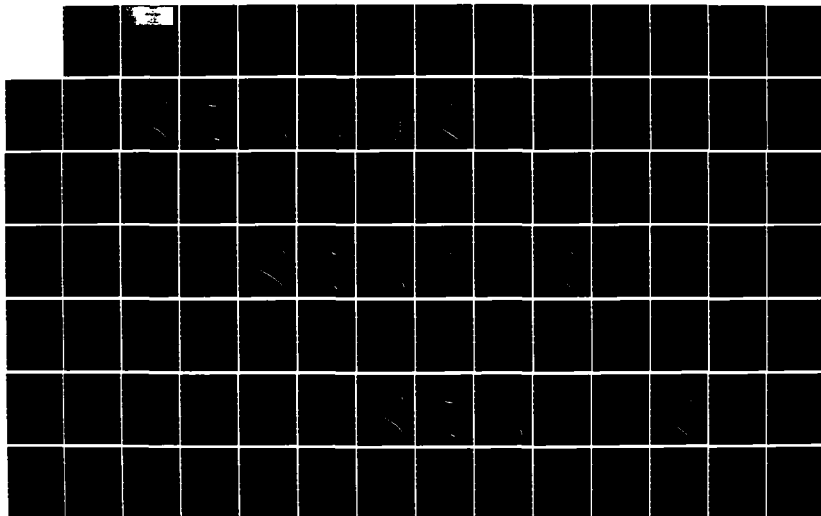
1/3

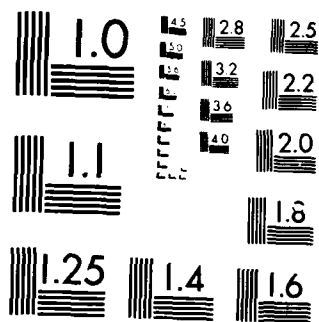
UNCLASSIFIED

JUN 85 UTIAS-283-PT-2 AFOSR-TR-85-1231

F/G 20/4

NL





MICROCOPY RESOLUTION TEST CHART
NATIONAL BUREAU OF STANDARDS 1963-A



INSTITUTE
FOR
AEROSPACE STUDIES

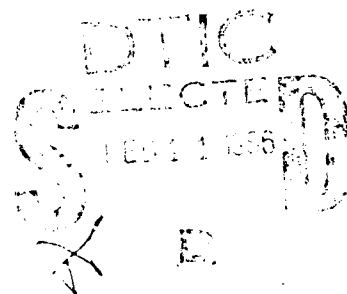
UNIVERSITY OF TORONTO

AFOSR-TR. 85-1231

TABULAR AND GRAPHICAL SOLUTIONS OF REGULAR AND MACH REFLECTIONS
IN PSEUDO-STATIONARY FROZEN AND VIBRATIONAL-EQUILIBRIUM FLOWS

PART 2

by



T. C. J. Hu and M. Shirouzu

Approved for public release;
distribution unlimited.

June 1985

UTIAS Report No. 283
CN ISSN 0082-5255

86 2 11 034

AD-A164 047

UNCLASSIFIED

SECURITY CLASSIFICATION OF THIS PAGE

AD-716-407

REPORT DOCUMENTATION PAGE

| 1a. REPORT SECURITY CLASSIFICATION Unclassified | | 1b. RESTRICTIVE MARKINGS | | | | | | | | | | | | | |
|---|-------------|---|---------------|---------------------|-------------|----------|---------------|--------|------|----|--|--|--|--|--|
| 2a. SECURITY CLASSIFICATION AUTHORITY | | 3. DISTRIBUTION/AVAILABILITY OF REPORT Approved for public release; distribution unlimited. | | | | | | | | | | | | | |
| 2b. DECLASSIFICATION/DOWNGRADING SCHEDULE | | | | | | | | | | | | | | | |
| 4. PERFORMING ORGANIZATION REPORT NUMBER(S) UTIAS Report No. 283 (in two parts) | | 5. MONITORING ORGANIZATION REPORT NUMBER(S) AFOSR-TR- 123 | | | | | | | | | | | | | |
| 6a. NAME OF PERFORMING ORGANIZATION University of Toronto, Inst. for Aerospace Studies | | 7a. NAME OF MONITORING ORGANIZATION AFOSR/NA | | | | | | | | | | | | | |
| 6b. OFFICE SYMBOL (If applicable) | | 7b. ADDRESS (City, State and ZIP Code) Building 410 Bolling AFB, DC 20332-6448 | | | | | | | | | | | | | |
| 6c. ADDRESS (City, State and ZIP Code) 4925 Dufferin Street, Downsview, Ontario, Canada M3H 5T6 | | | | | | | | | | | | | | | |
| 8a. NAME OF FUNDING/SPONSORING ORGANIZATION Air Force Office of Scientific Research/NA | | 9. PROCUREMENT INSTRUMENT IDENTIFICATION NUMBER AF-AFOSR 82-0096 | | | | | | | | | | | | | |
| 8b. OFFICE SYMBOL (If applicable) AFOSR/NA | | | | | | | | | | | | | | | |
| 8c. ADDRESS (City, State and ZIP Code) Bldg. 410, Bolling Air Force Base, DC 20332, U.S.A. | | 10. SOURCE OF FUNDING NOS. <table border="1"><tr><th>PROGRAM ELEMENT NO.</th><th>PROJECT NO.</th><th>TASK NO.</th><th>WORK UNIT NO.</th></tr><tr><td>61102F</td><td>2307</td><td>A1</td><td></td></tr></table> | | PROGRAM ELEMENT NO. | PROJECT NO. | TASK NO. | WORK UNIT NO. | 61102F | 2307 | A1 | | | | | |
| PROGRAM ELEMENT NO. | PROJECT NO. | TASK NO. | WORK UNIT NO. | | | | | | | | | | | | |
| 61102F | 2307 | A1 | | | | | | | | | | | | | |
| 11. TITLE (Include Security Classification) Tabular and Graphical Solutions of Regular and Mach Reflections in | | | | | | | | | | | | | | | |
| 12. PERSONAL AUTHOR(S) Pseudo-Stationary Frozen and Vibrational-Equilibrium Flows, Part 2 T. C. J. Hu and M. Shirouzu | | | | | | | | | | | | | | | |
| 13a. TYPE OF REPORT Interim | | 13b. TIME COVERED FROM TO | | | | | | | | | | | | | |
| 14. DATE OF REPORT (Yr., Mo., Day) 1985, June | | 15. PAGE COUNT 352 | | | | | | | | | | | | | |
| 16. SUPPLEMENTARY NOTATION | | | | | | | | | | | | | | | |
| 17. COSATI CODES <table border="1"><tr><th>FIELD</th><th>GROUP</th><th>SUB. GR.</th></tr><tr><td></td><td></td><td></td></tr><tr><td></td><td></td><td></td></tr><tr><td></td><td></td><td></td></tr></table> | | FIELD | GROUP | SUB. GR. | | | | | | | | | | 18. SUBJECT TERMS (Continue on reverse if necessary and identify by block number) Oblique-shock-wave reflections; regular reflection; Mach reflection; numerical and graphical solutions; frozen and equilibrium flows. | |
| FIELD | GROUP | SUB. GR. | | | | | | | | | | | | | |
| | | | | | | | | | | | | | | | |
| | | | | | | | | | | | | | | | |
| | | | | | | | | | | | | | | | |
| 19. ABSTRACT (Continue on reverse if necessary and identify by block number) Flow properties of pseudo-stationary oblique-shock-wave reflections are given as solutions of two-shock and three-shock theories. The calculations were performed for Ar, air, CO ₂ and SF ₆ using both frozen and vibrational equilibrium gas assumptions. The flow properties are tabulated for initial shock Mach numbers $1.2 < M_s < 10.0$ and wedge angles $1^\circ < \theta_w < 85^\circ$. The flow properties are plotted as a function of the incident shock Mach number for a series of wedge angles for both regular and Mach reflections. Another set of graphs is presented for Mach reflection with the flow properties plotted against the effective wedge angle θ_w' for a series of shock Mach numbers. The latter set is used when the effective wedge angle is chosen as the parameter for comparison. The second triple-point system, which exists only in double-Mach reflection, is solved numerically for the first time, and the solutions are presented both in tabular and graphical forms. The tables and graphs are designed to serve the analyst and experimenter working on oblique-shock-wave reflections. | | | | | | | | | | | | | | | |
| 20. DISTRIBUTION/AVAILABILITY OF ABSTRACT UNCLASSIFIED/UNLIMITED <input checked="" type="checkbox"/> SAME AS RPT. <input type="checkbox"/> RIC USERS <input type="checkbox"/> | | 21. ABSTRACT SECURITY CLASSIFICATION Unclassified | | | | | | | | | | | | | |
| 22a. NAME OF RESPONSIBLE INDIVIDUAL JAMES D WILSON | | 22b. TELEPHONE NUMBER (Include Area Code) (202) 767-4935 | | | | | | | | | | | | | |
| | | 22c. OFFICE SYMBOL AFOSR/NA | | | | | | | | | | | | | |

TABULAR AND GRAPHICAL SOLUTIONS OF REGULAR AND MACH REFLECTIONS
IN PSEUDO-STATIONARY FROZEN AND VIBRATIONAL-EQUILIBRIUM FLOWS

PART 2

by

T. C. J. Hu and M. Shirouzu

Submitted October 1984

AIR FORCE OFFICE OF SCIENTIFIC RESEARCH (AFOSR)
NOTICE OF SCIENTIFIC RESEARCH (AFOSR)
This document is the property of the Air Force Office of Scientific Research (AFOSR) and is loaned to you for your use only. It is not to be distributed outside your organization without the prior written consent of the AFOSR. The AFOSR is not responsible for the content or the use of this document. The AFOSR is not responsible for the content or the use of this document. The AFOSR is not responsible for the content or the use of this document.
Chief, Technical Information Division

June 1985

UTIAS Report No. 283
CN ISSN 0082-5255

Table of Contents

PART 1

| | |
|------------------------------------|-----|
| Acknowledgements | ii |
| Summary | iii |
| Notation | v |
| 1. INTRODUCTION | 1 |
| 2. METHOD OF CALCULATION | 1 |
| 3. REMARKS | 6 |
| 4. DISCUSSIONS | 7 |
| 5. WORKED EXAMPLES | 18 |
| 6. CONCLUSIONS | 19 |
| REFERENCES | 21 |

TABLE 1. γ_0 , T_k and n_k of Relevant Gases

FIG. 1. Regions and angles in RR and MR

FIG. 2. The Analogy between the Two Triple-Point Wave System
in a Double-Mach Reflection

LIST OF TABLES

LIST OF FIGURES

TABLES: T-1 to T-120

FIGURES: F-1 to F-120

PART 2

FIGURES: F-121 to F-320

APPENDIX A : Actual Sidewall Pressure Histories and Numerical Results; ✓

APPENDIX B : Computer-Program Listing for the Analytical Solution of
Regular and Mach Reflections.

1. 15-A164046

2. 15-A164047

Notation

Notations used in tables are shown in parentheses.

| | |
|-----------------|---|
| a | sound speed (A) |
| Ar | argon |
| CO ₂ | carbon dioxide |
| h | specific enthalpy |
| K | kink |
| M | Mach number (relative to P or T unless otherwise indicated) (MACH) |
| m | molecular weight |
| MR | Mach reflection |
| M _s | incident shock Mach number (MACHS) |
| n _k | number of modes in mode k |
| N ₂ | nitrogen |
| O ₂ | oxygen |
| P | reflection point |
| p | pressure (P) |
| R | universal gas constant |
| RR | regular reflection |
| SF ₆ | sulphur hexafluoride |
| T | temperature |
| T | triple point |
| T' | second triple point |
| T _k | characteristic temperature of mode k |
| u | flow velocity |
| γ | specific heat ratio |
| γ _p | specific heat ratio of perfect gas |
| γ _o | specific heat ratio of frozen gas |

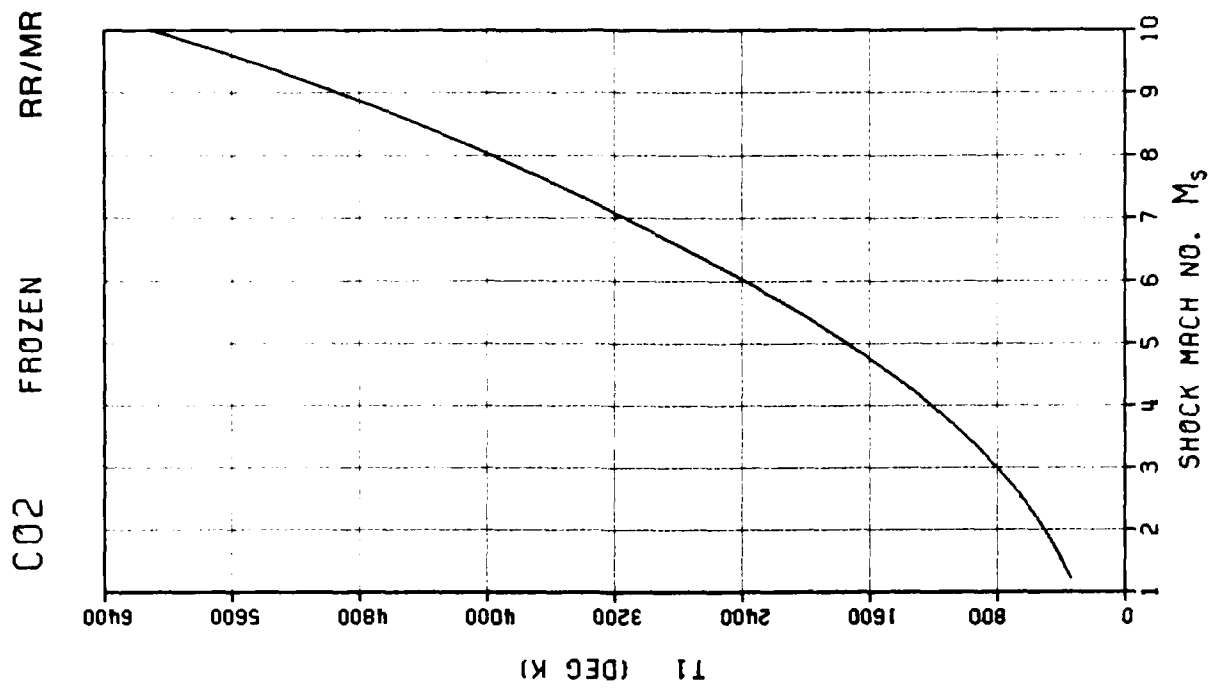
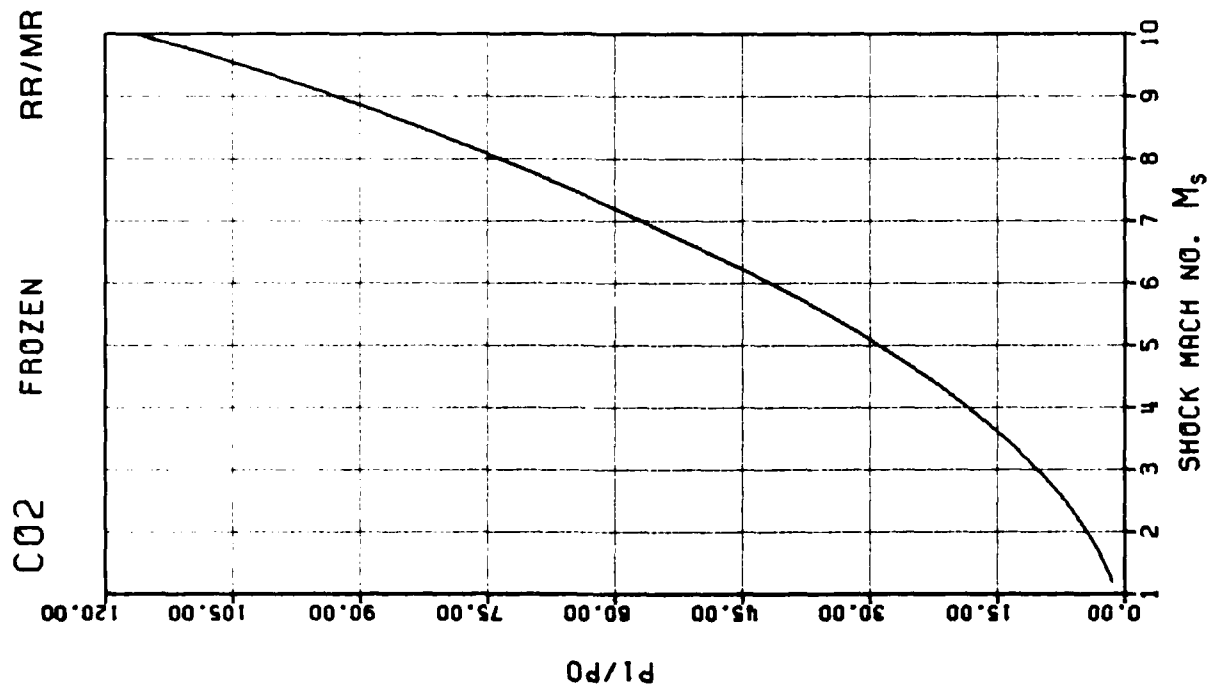
| | |
|--------------------------------------|---|
| Accession For | |
| NTIS | CRA&I <input checked="" type="checkbox"/> |
| DTIC | TAB <input type="checkbox"/> |
| Unannounced <input type="checkbox"/> | |
| Justification | |
| By | |
| Distribution / | |
| Availability Codes | |
| Dist | Avail and/or Special |
| A-1 | |

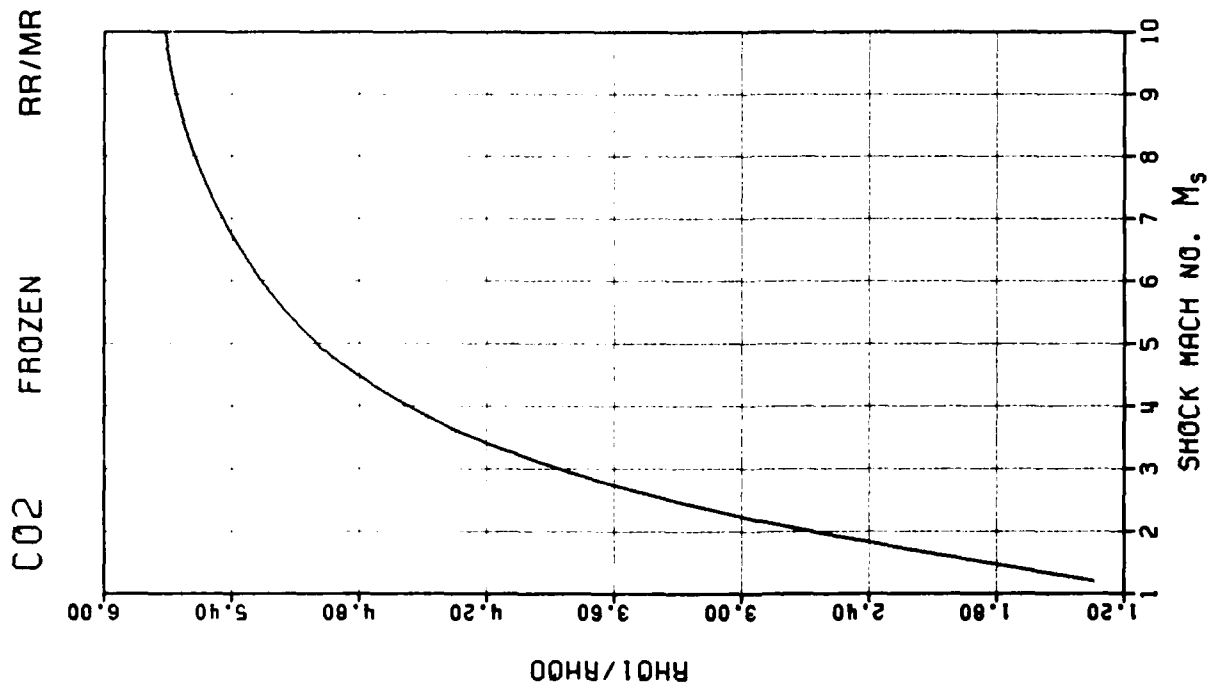


ξ angle between incident shock wave and reflected shock wave at triple point (DELTA)
 η angle between reflected shock wave and second Mach stem (ETA)
 θ deflection angle of flow from its original direction while passing through a shock wave (THETA)
 θ_w actual wedge angle (THETA WALL)
 θ'_w effective wedge angle (THETA WALL PRIME)
 ξ angle between the two reflected shock waves R and R' in region (1) (XI)
 ρ density (RHO)
 ϕ incident wave angle (PHI)
 χ triple-point-trajectory angle (CHI)
 χ' second-triple-point-trajectory angle (CHI PRIME)
 ω angle between reflected shock wave and wedge surface (in RR) or triple-point-trajectory (in MR) (OMEGA PRIME)

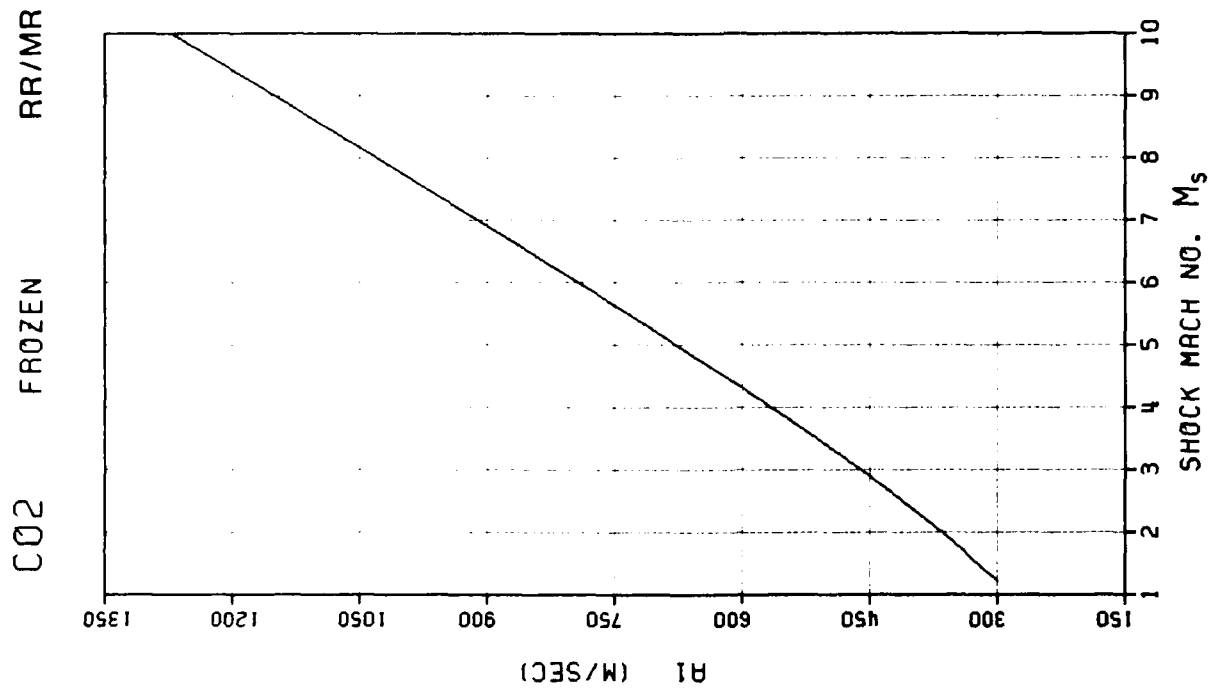
Subscripts

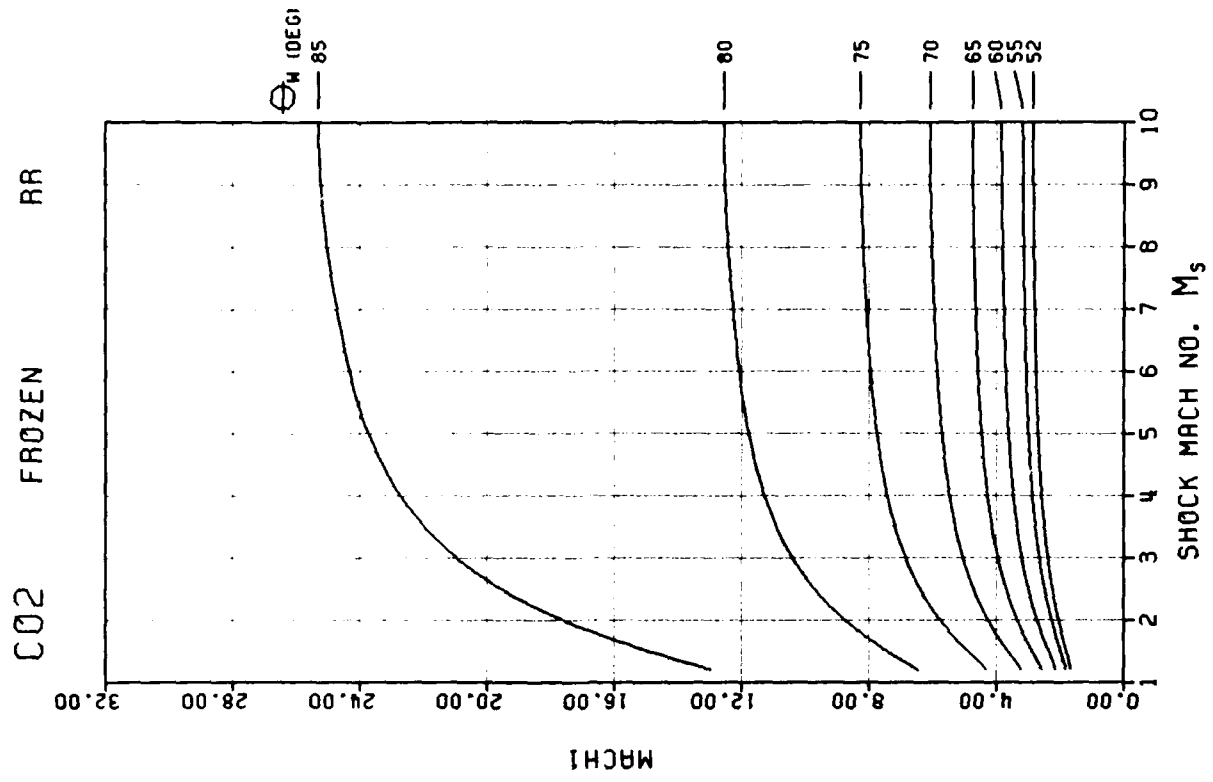
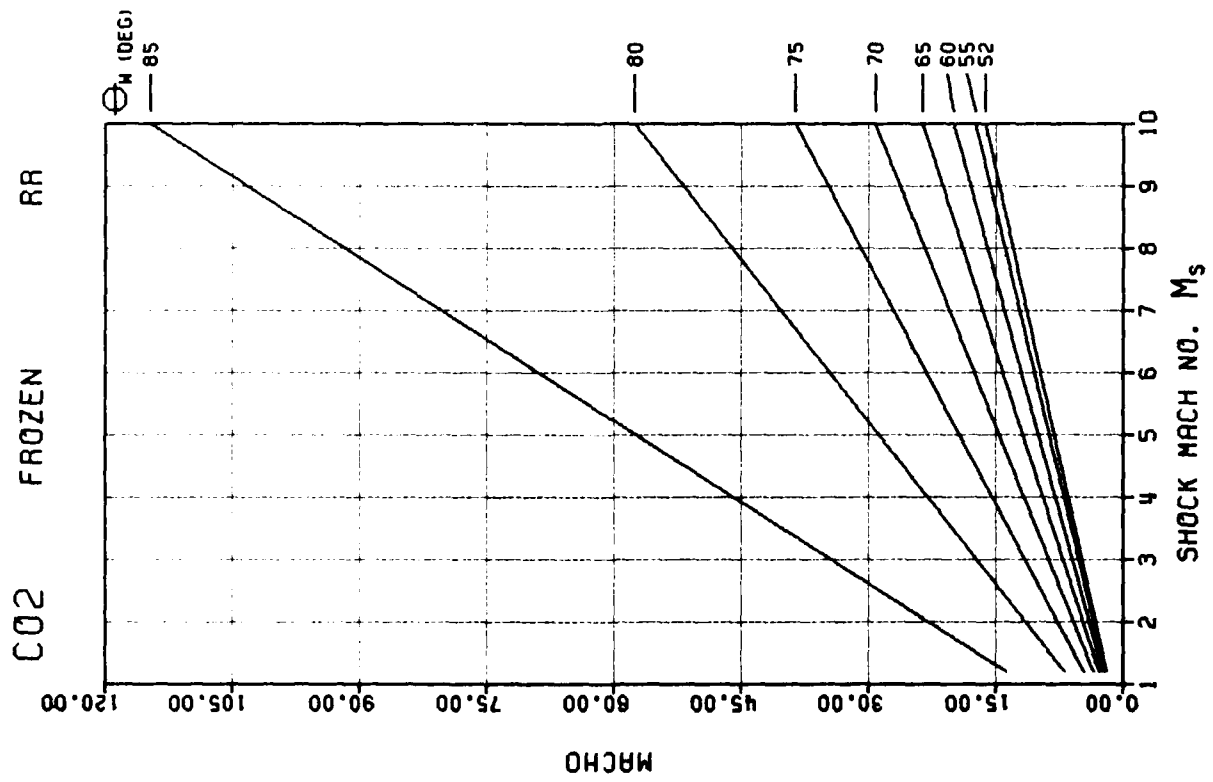
0, 1, 2, 3 regions 0, 1, 2, 3 (0, 1, 2, 3)

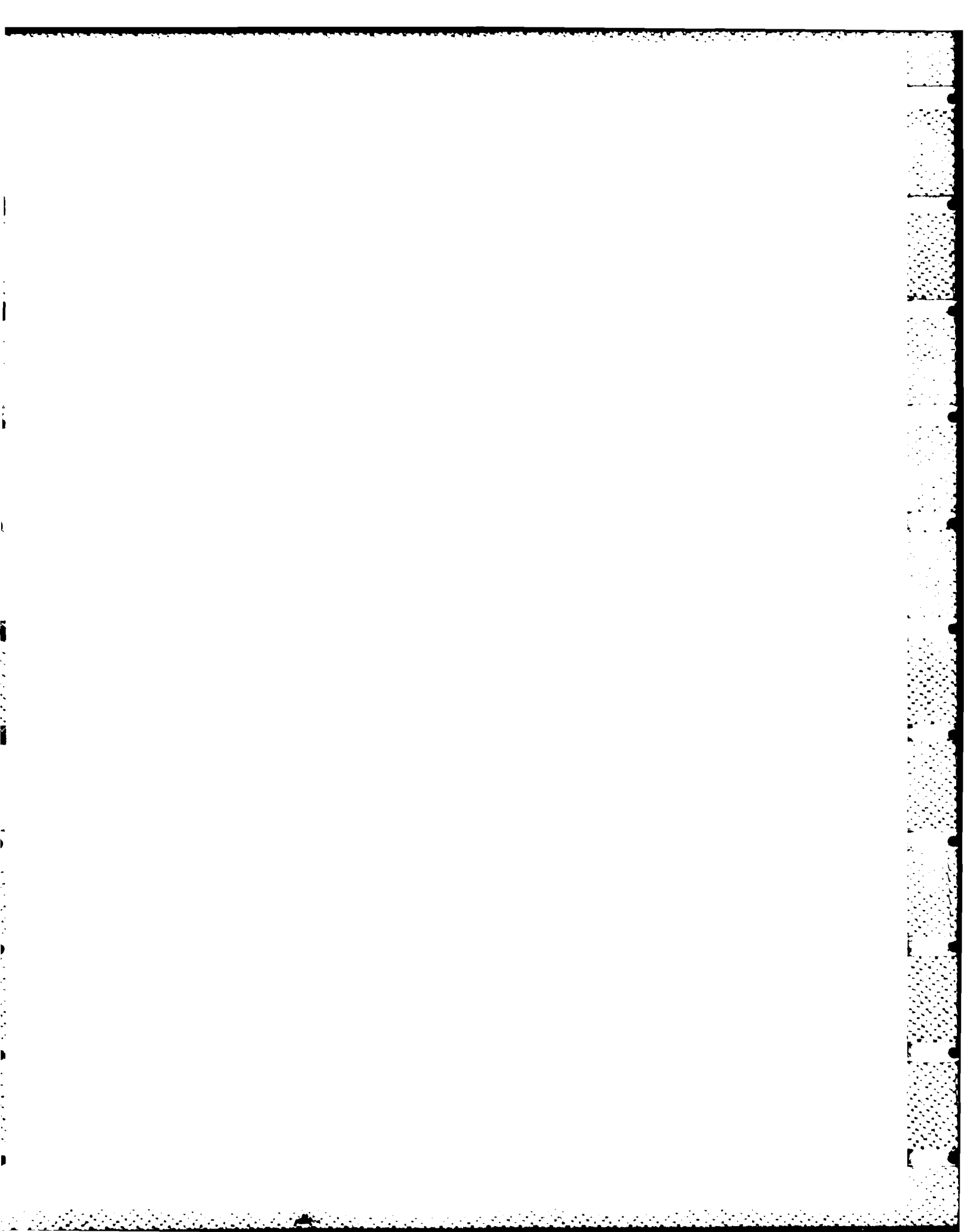


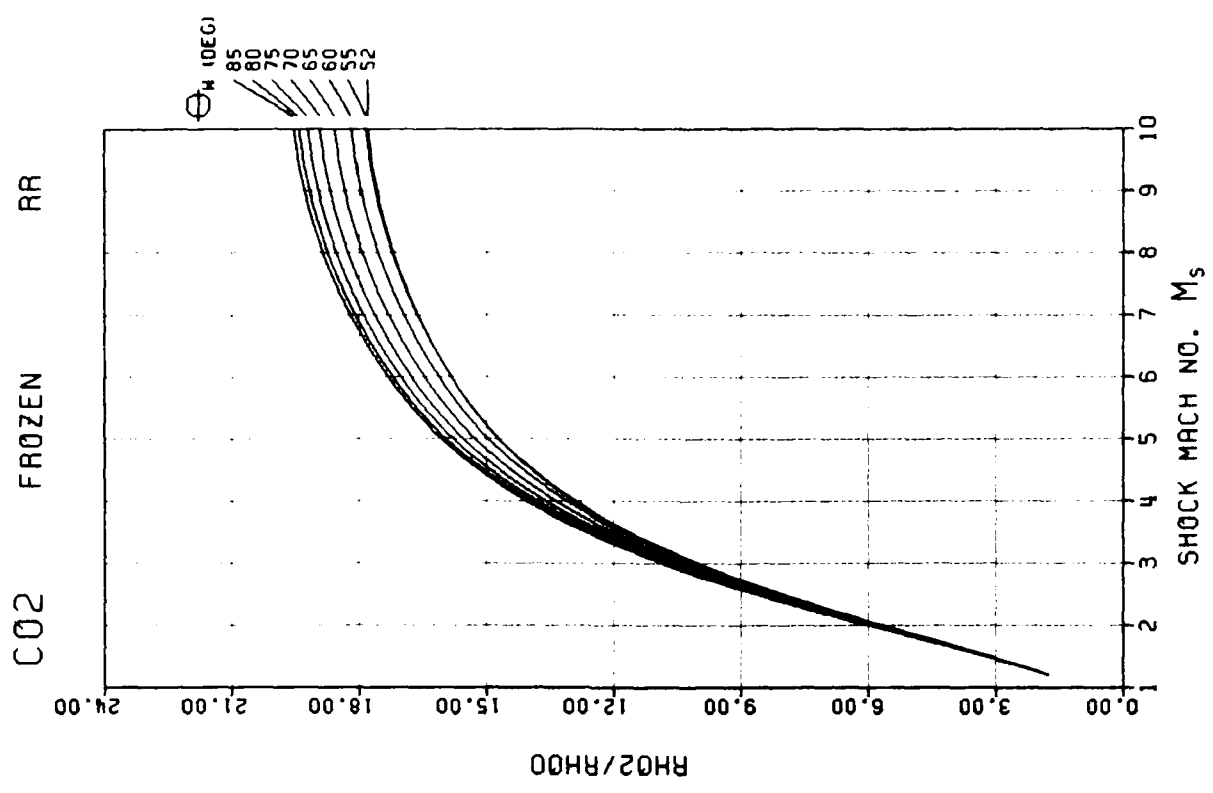
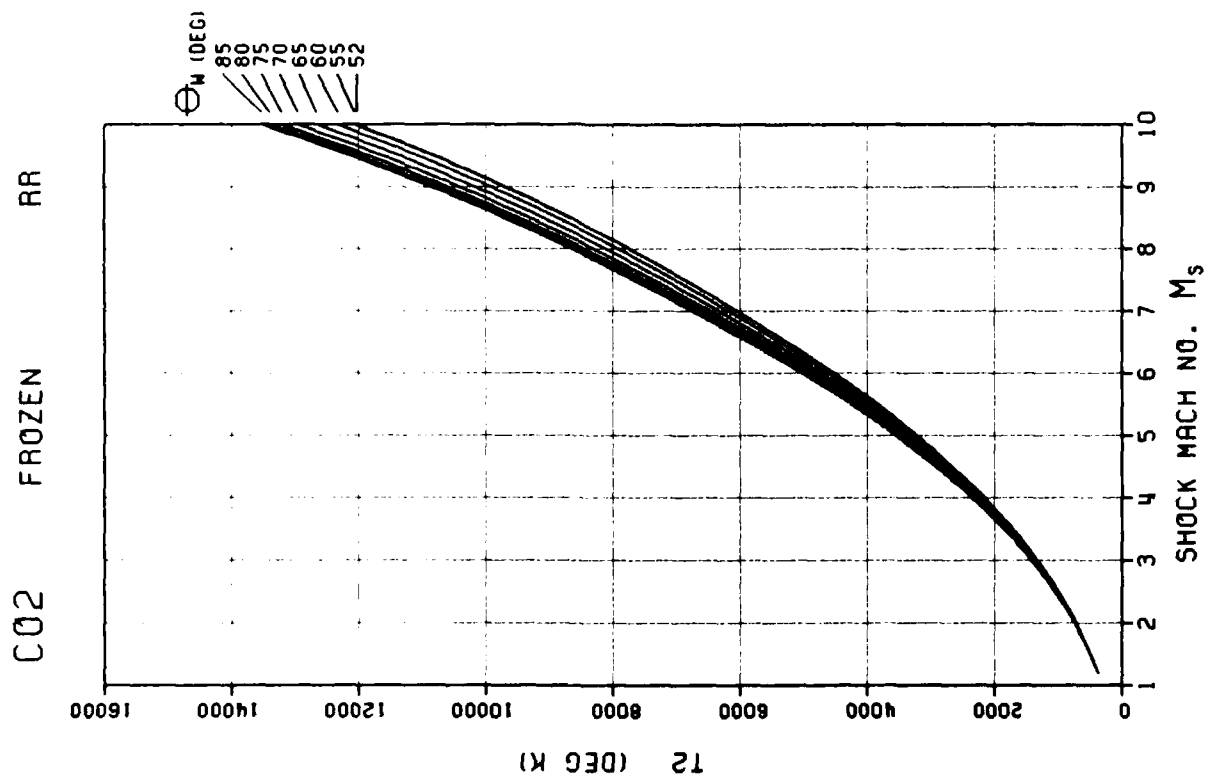


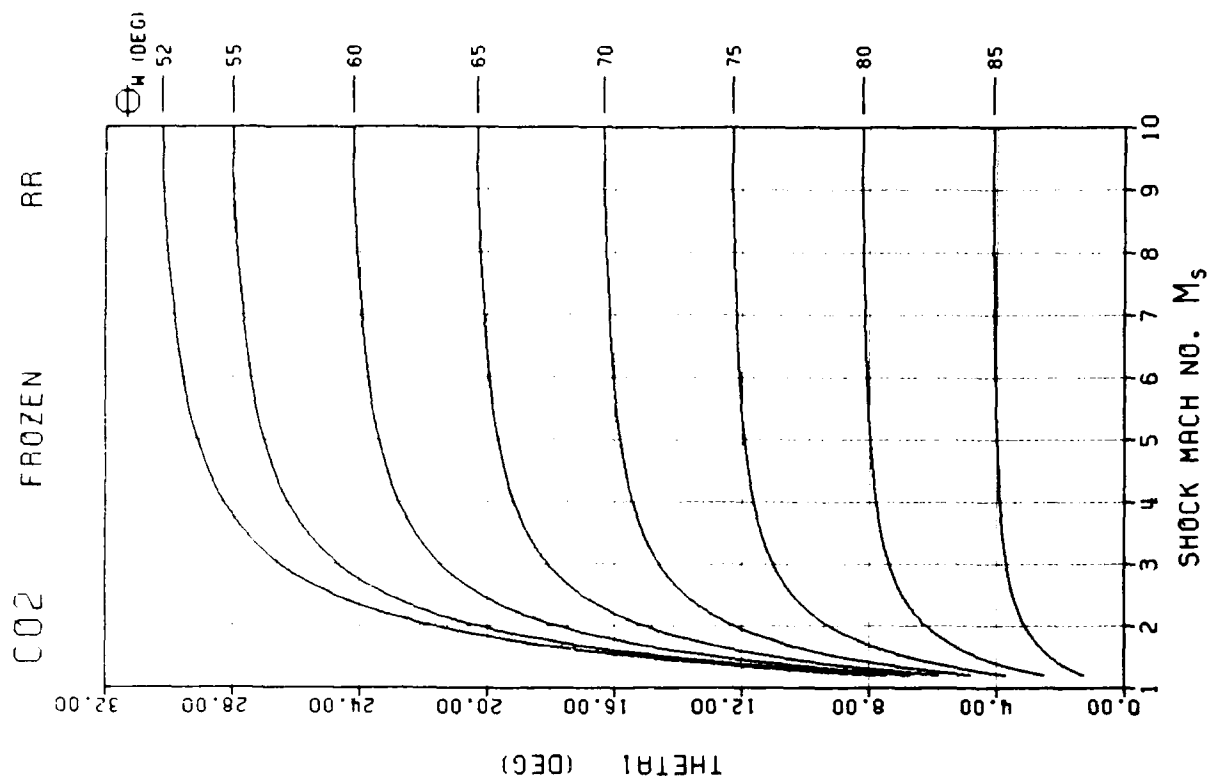
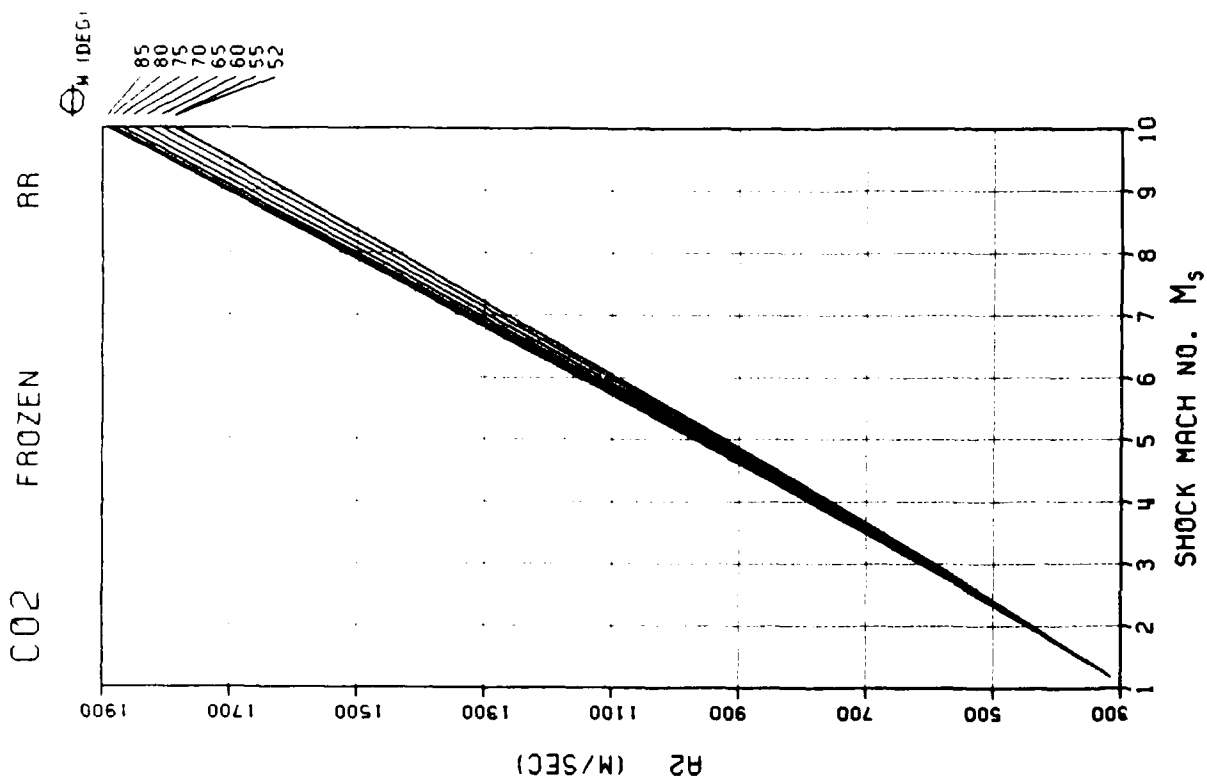
F - 122

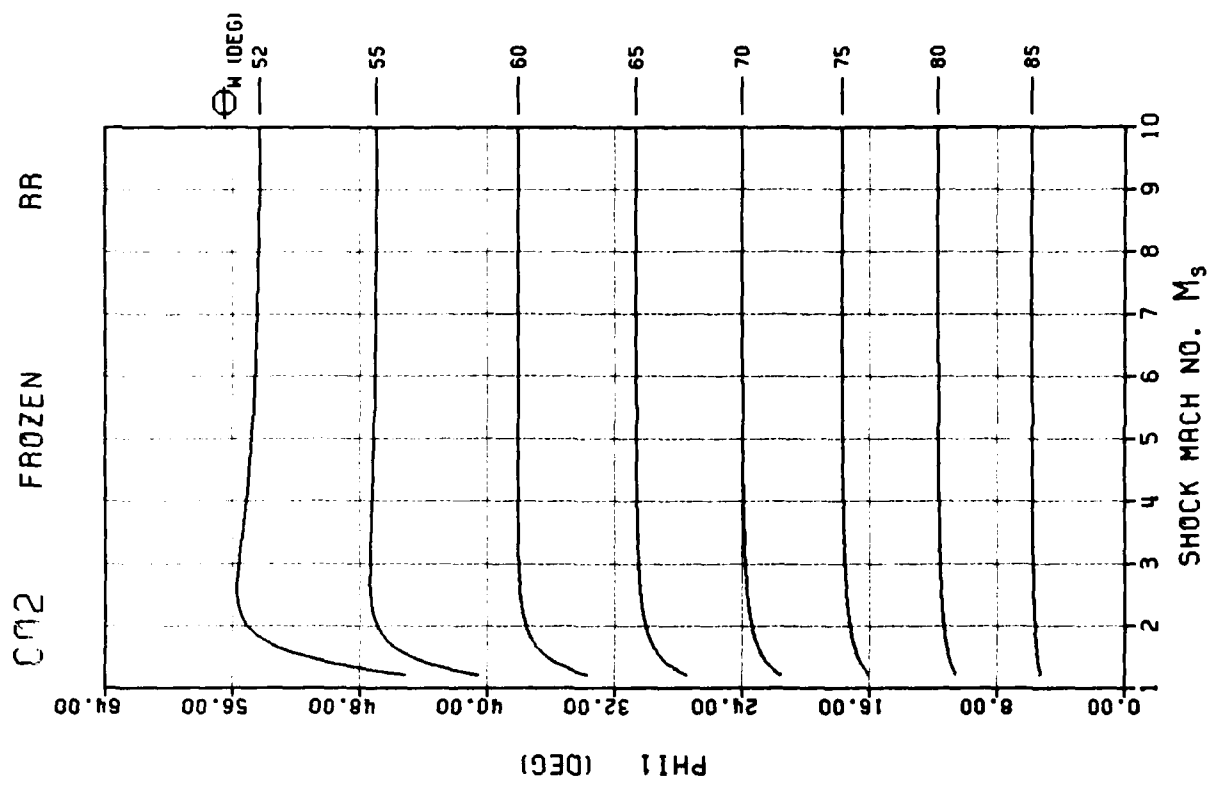
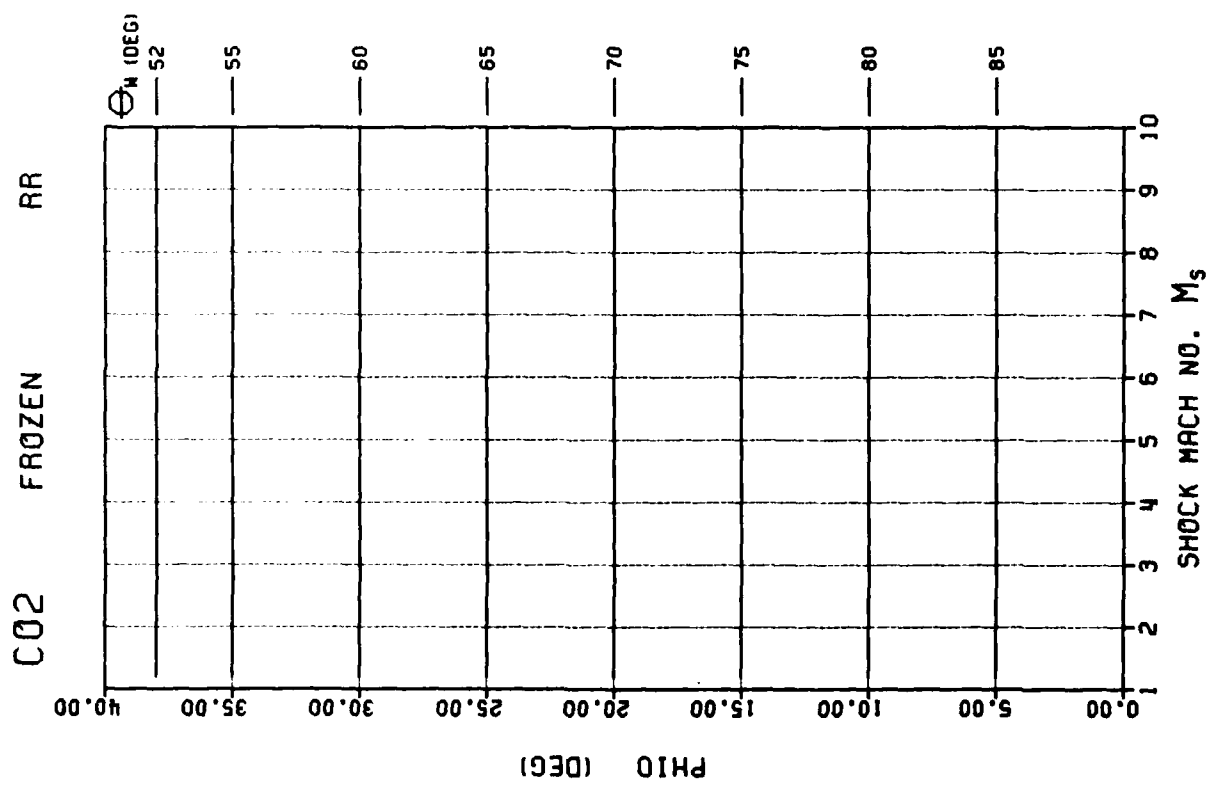


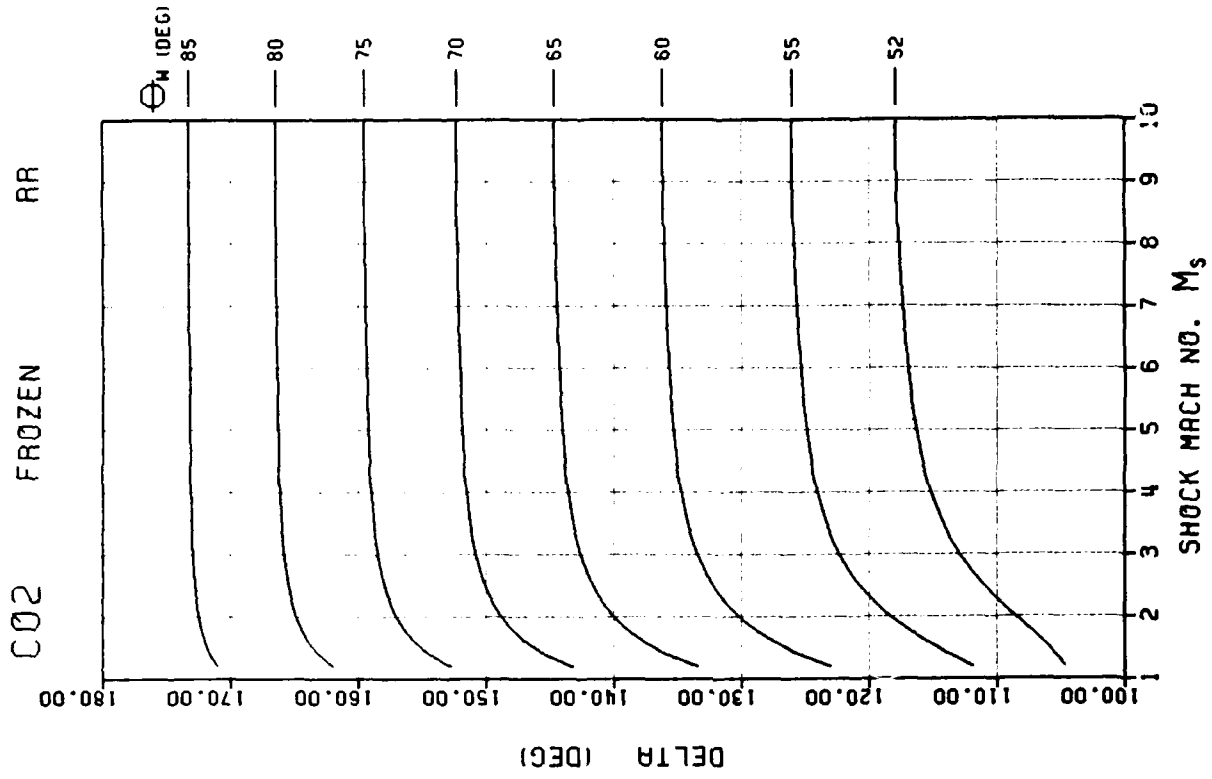
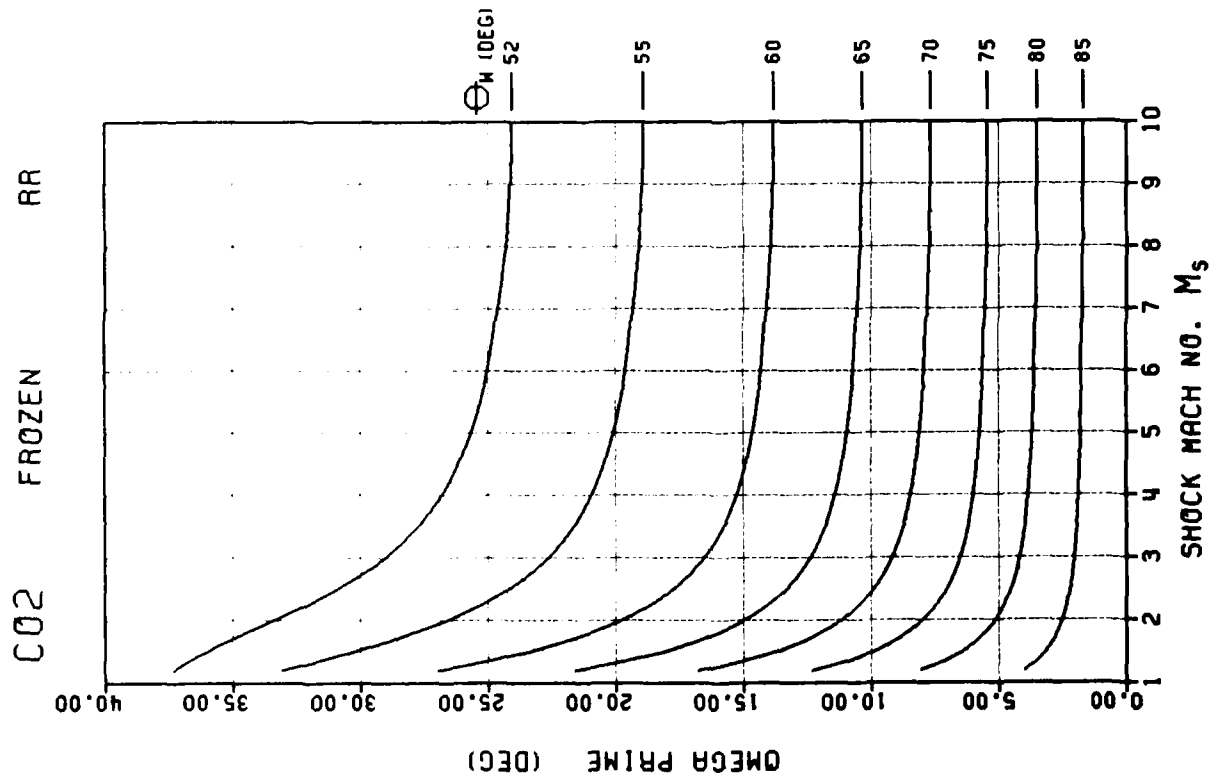


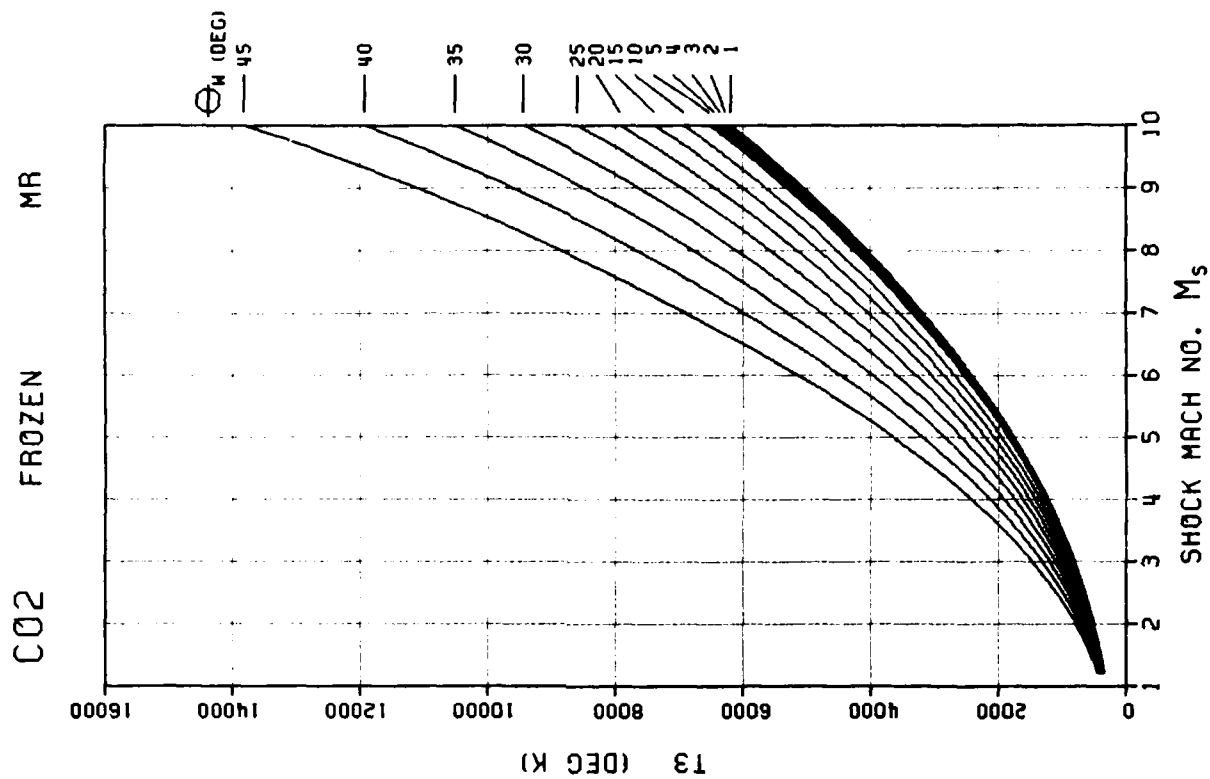
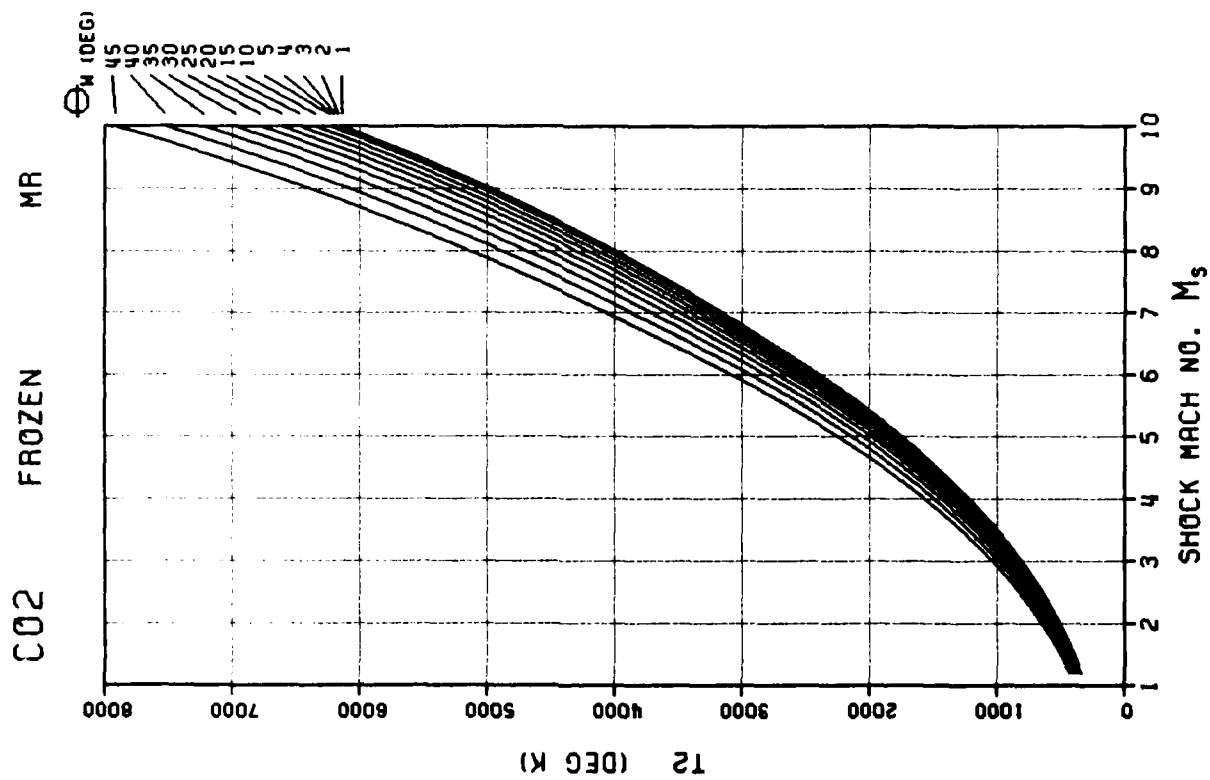


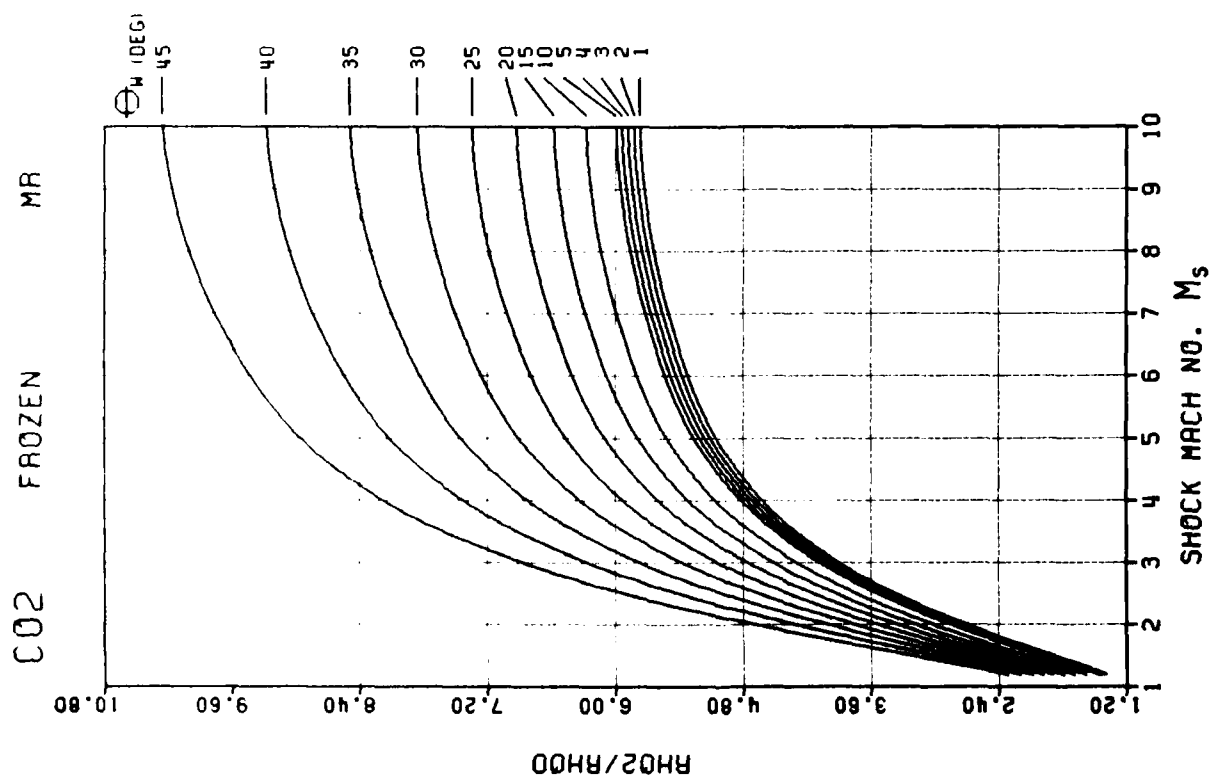
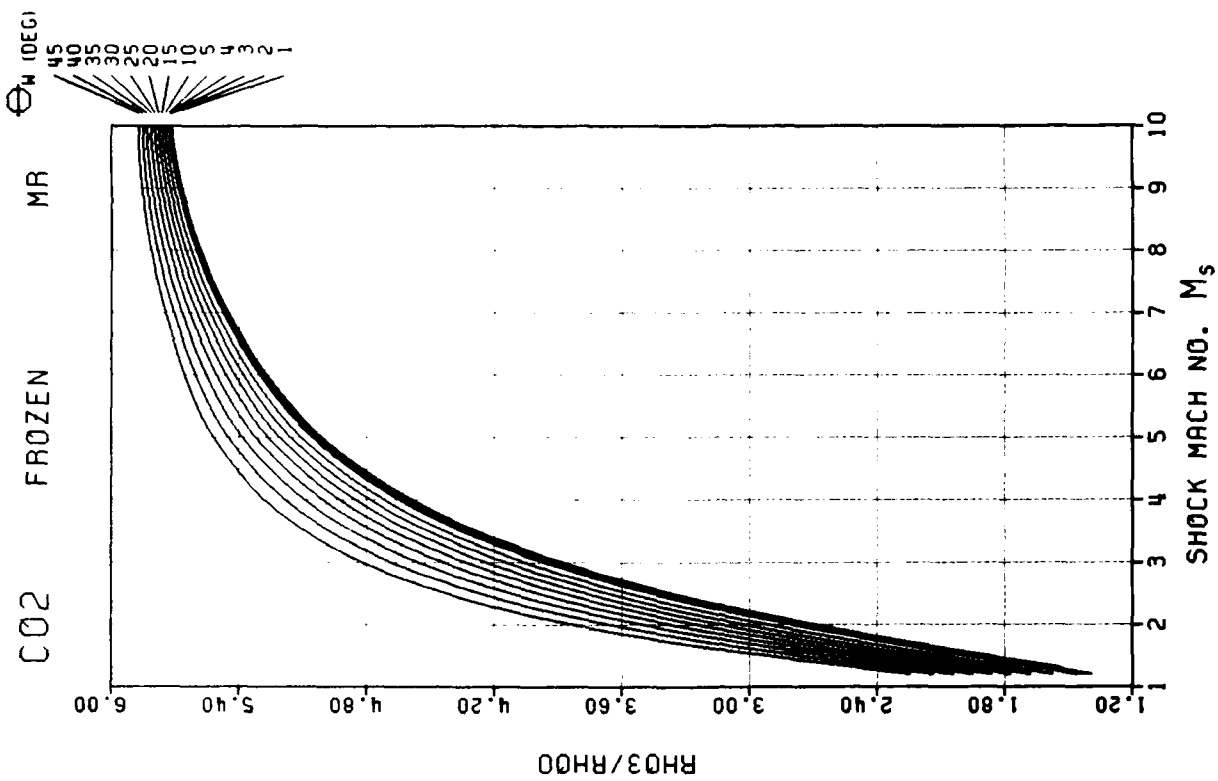


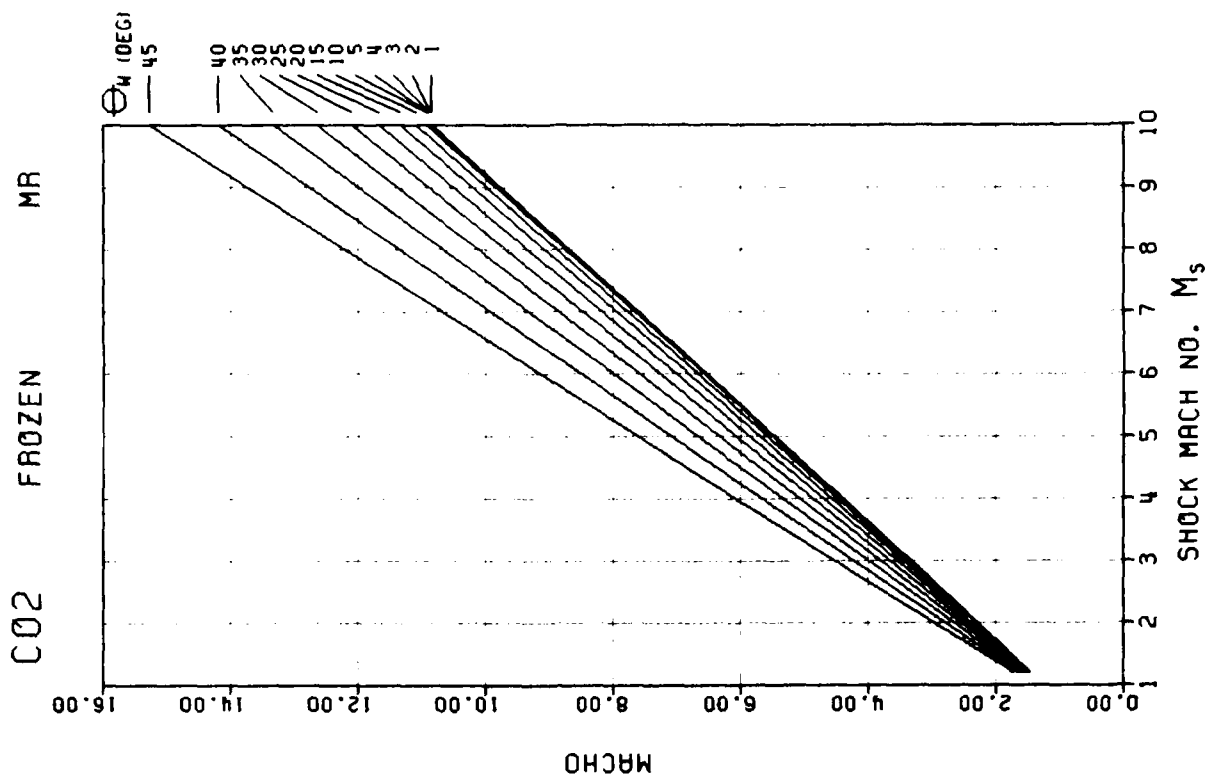
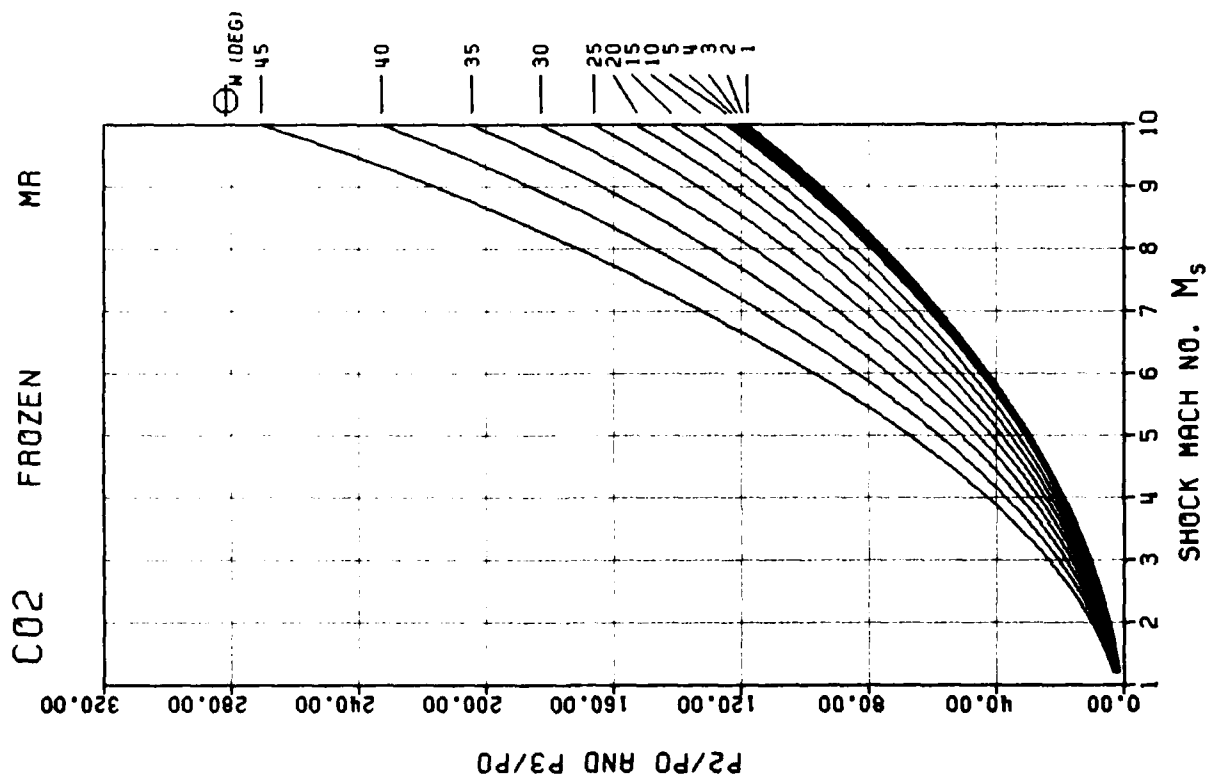


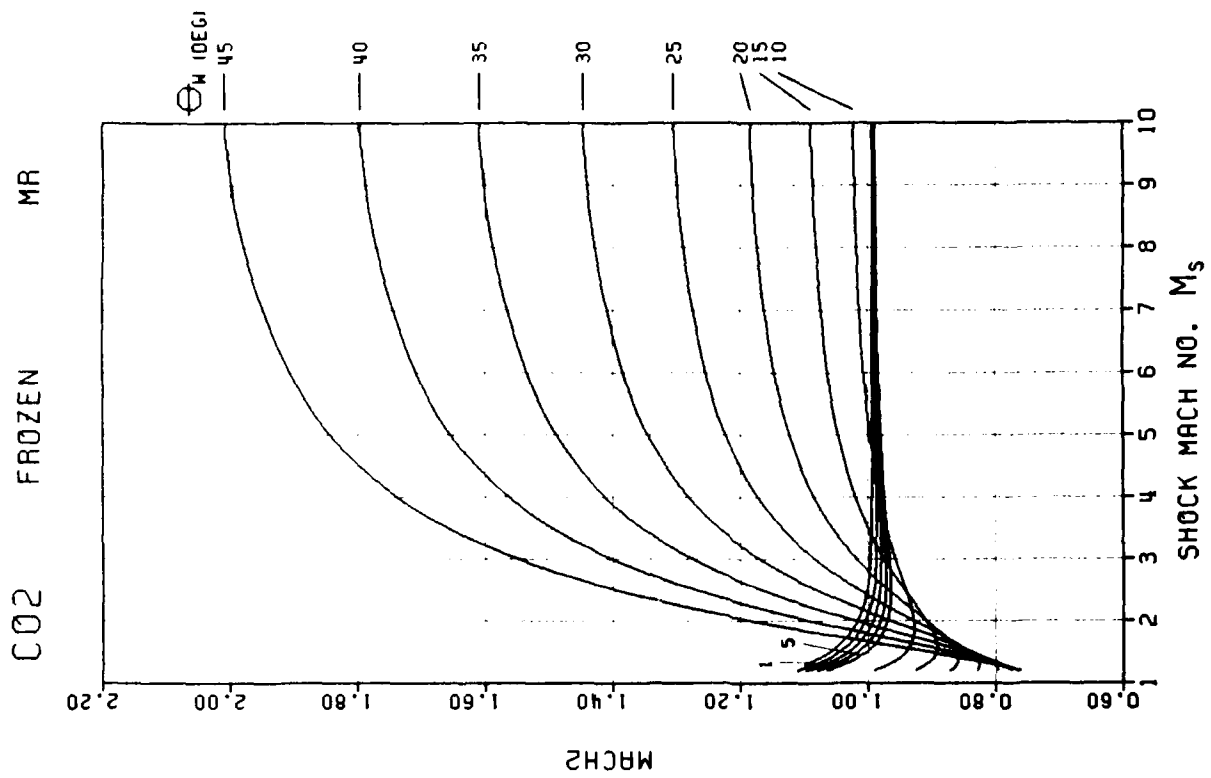
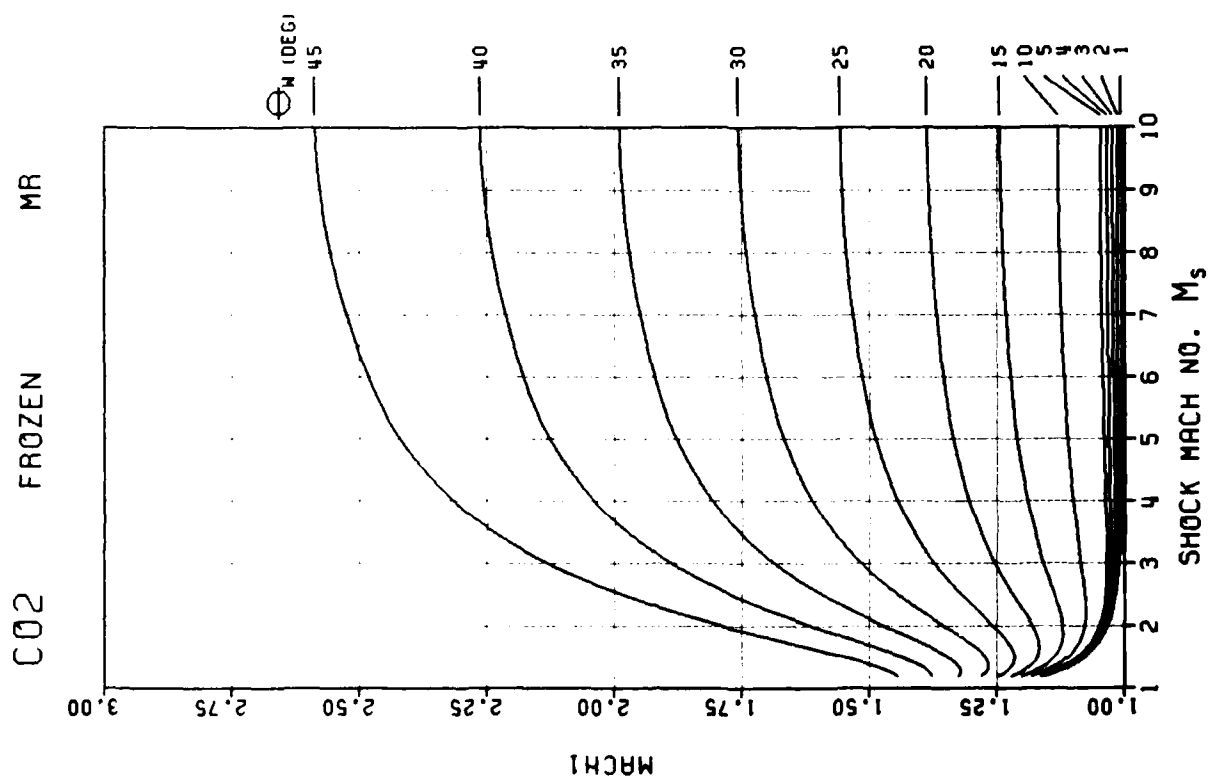


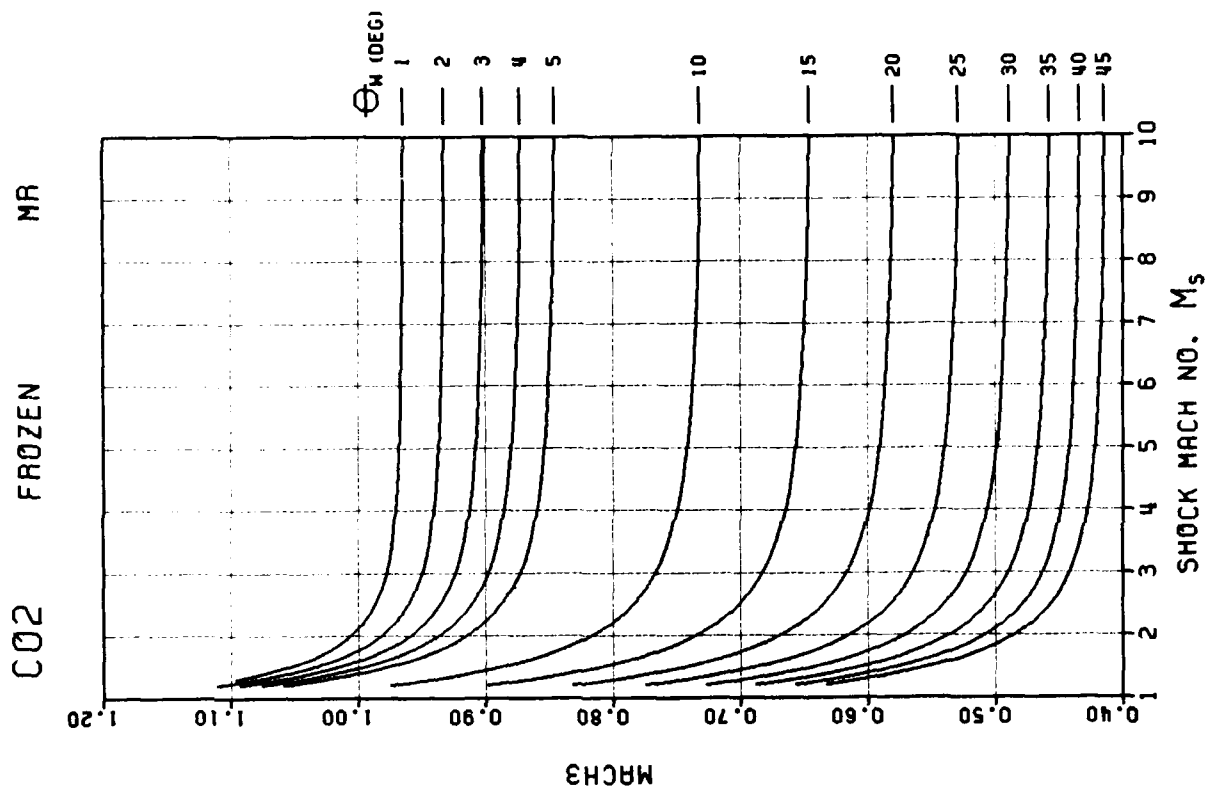
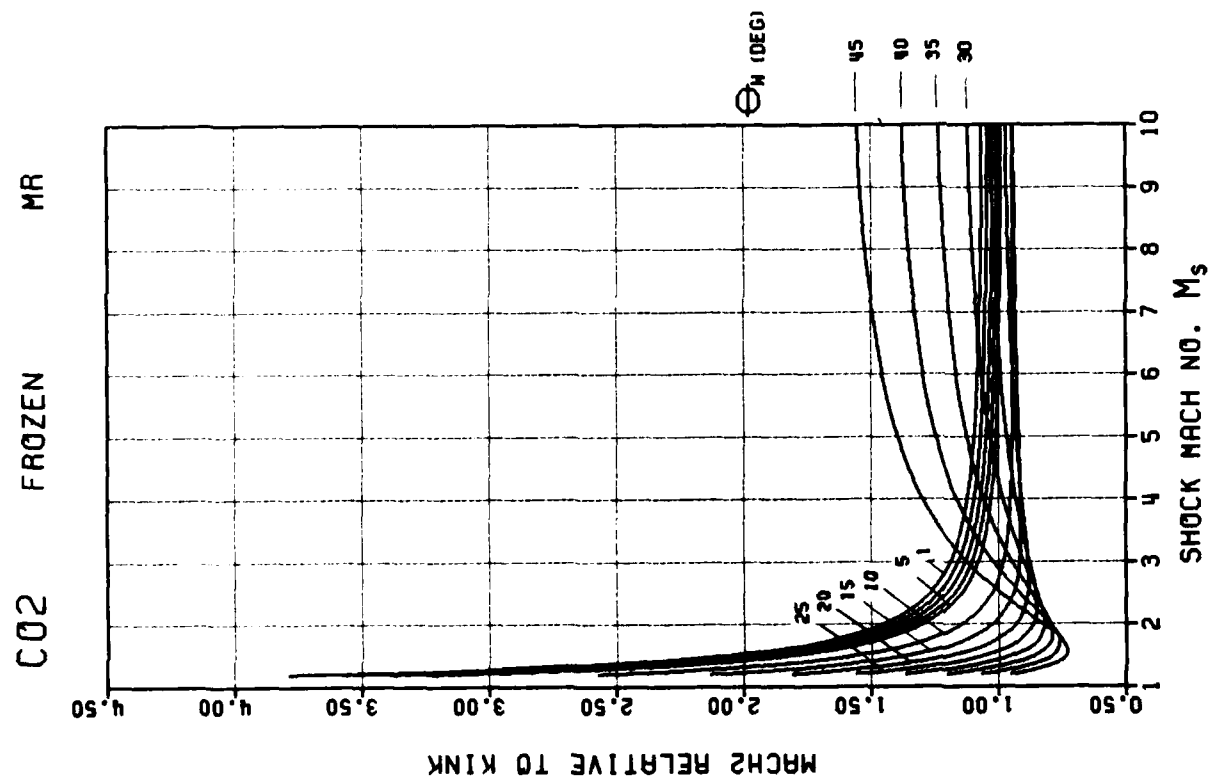


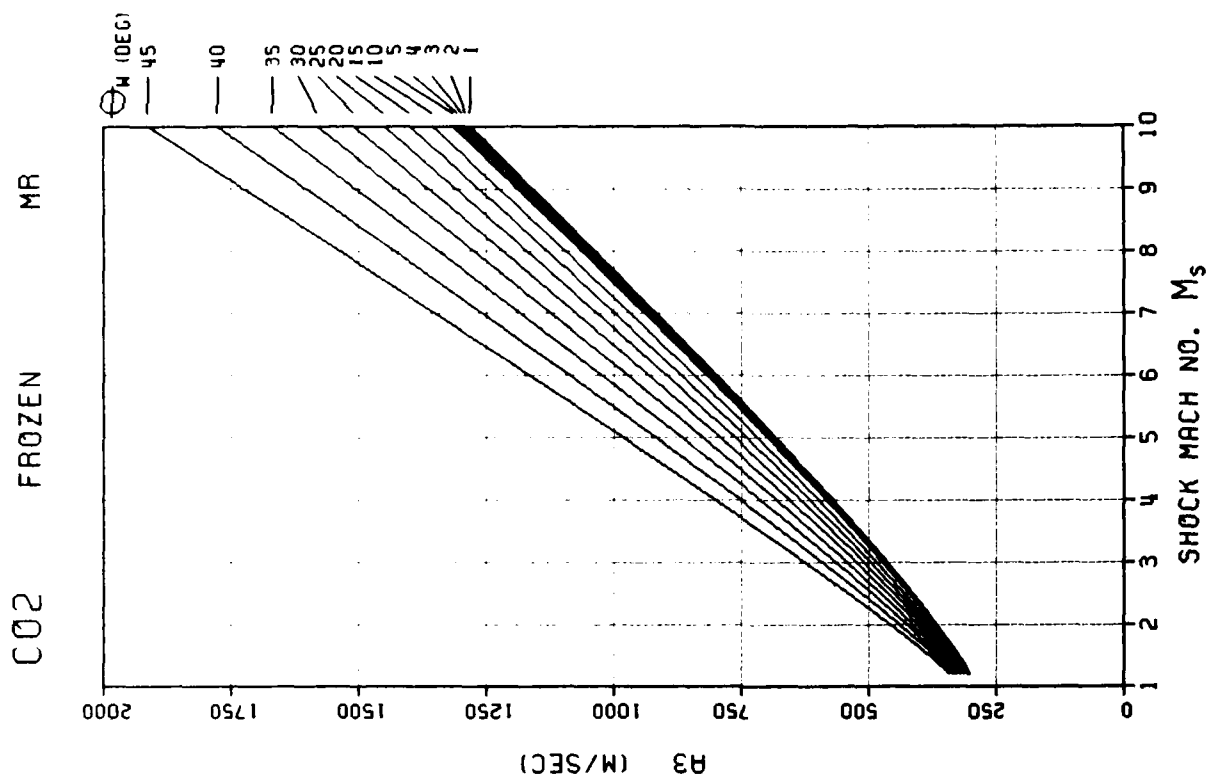
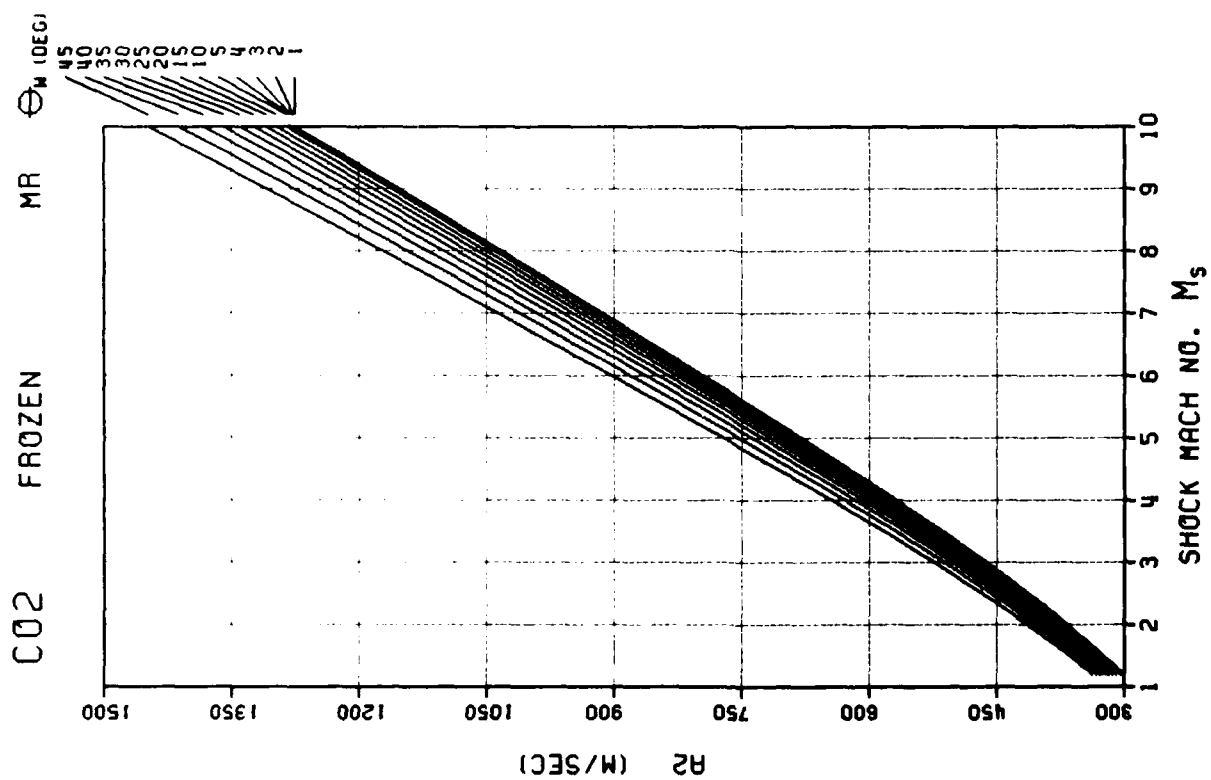


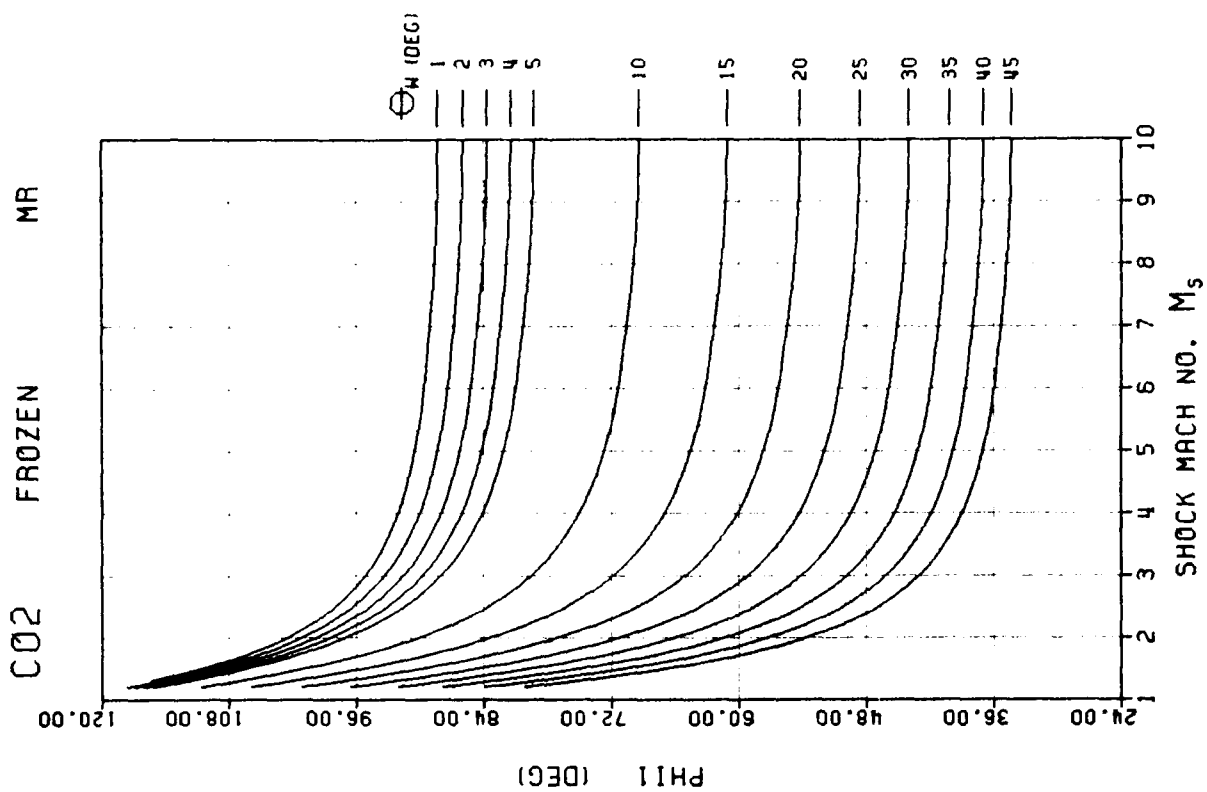
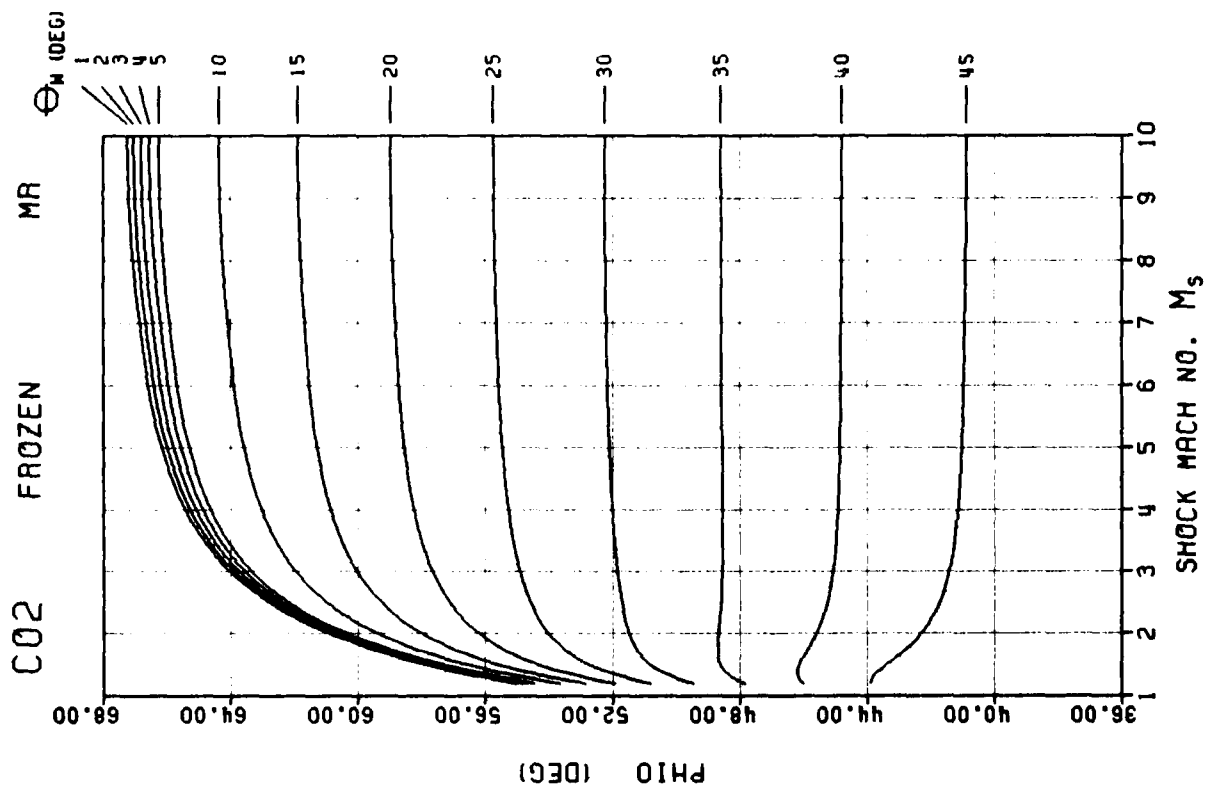


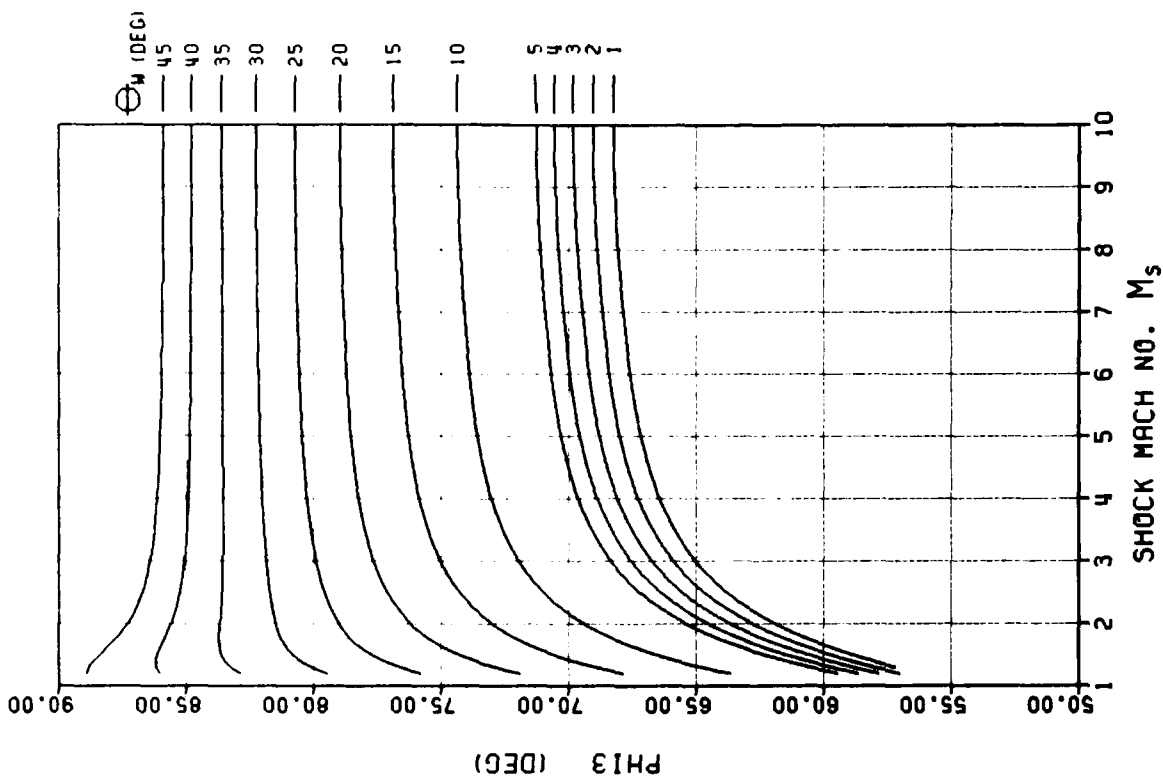
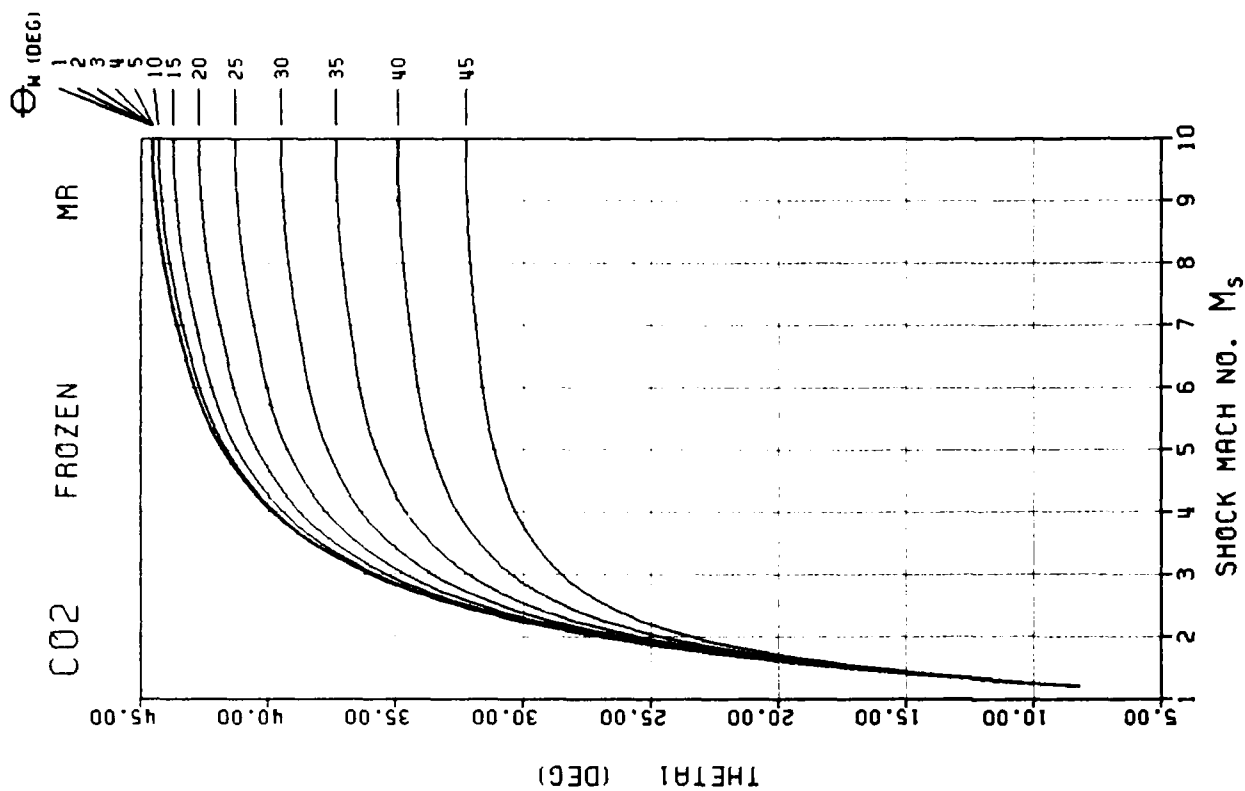


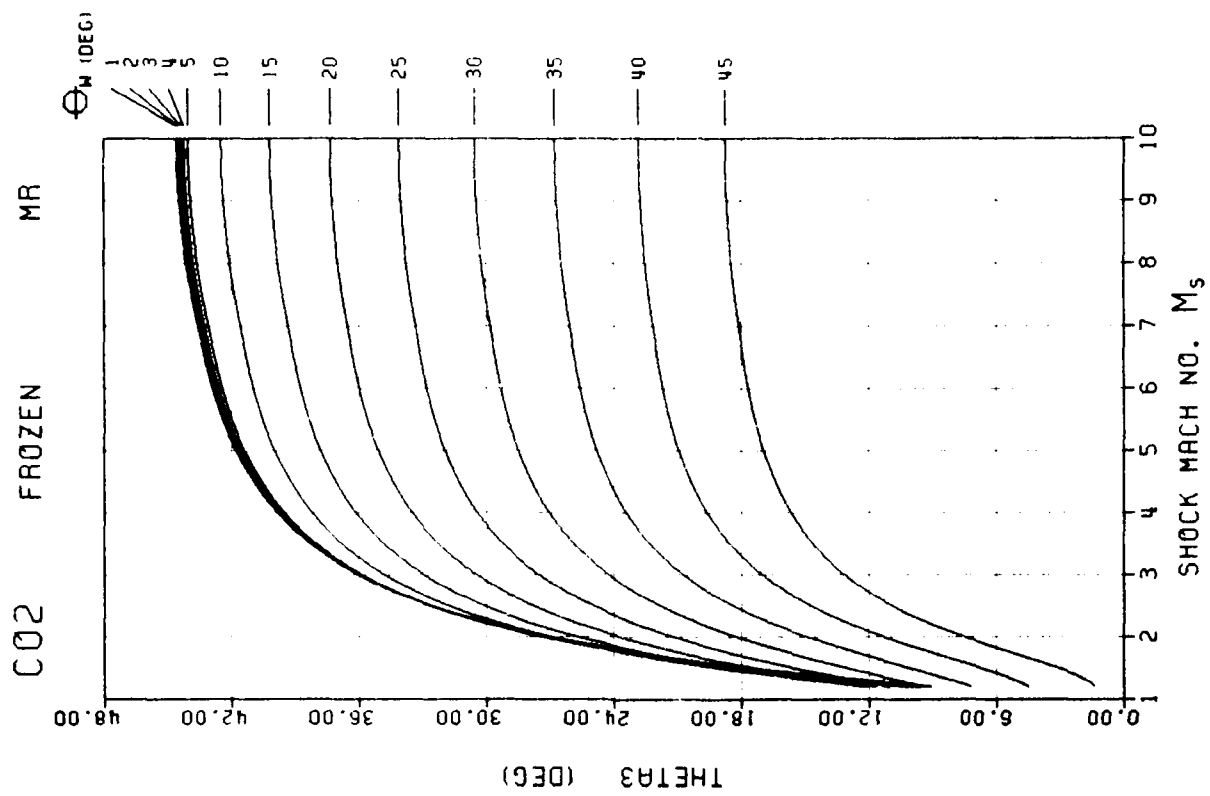
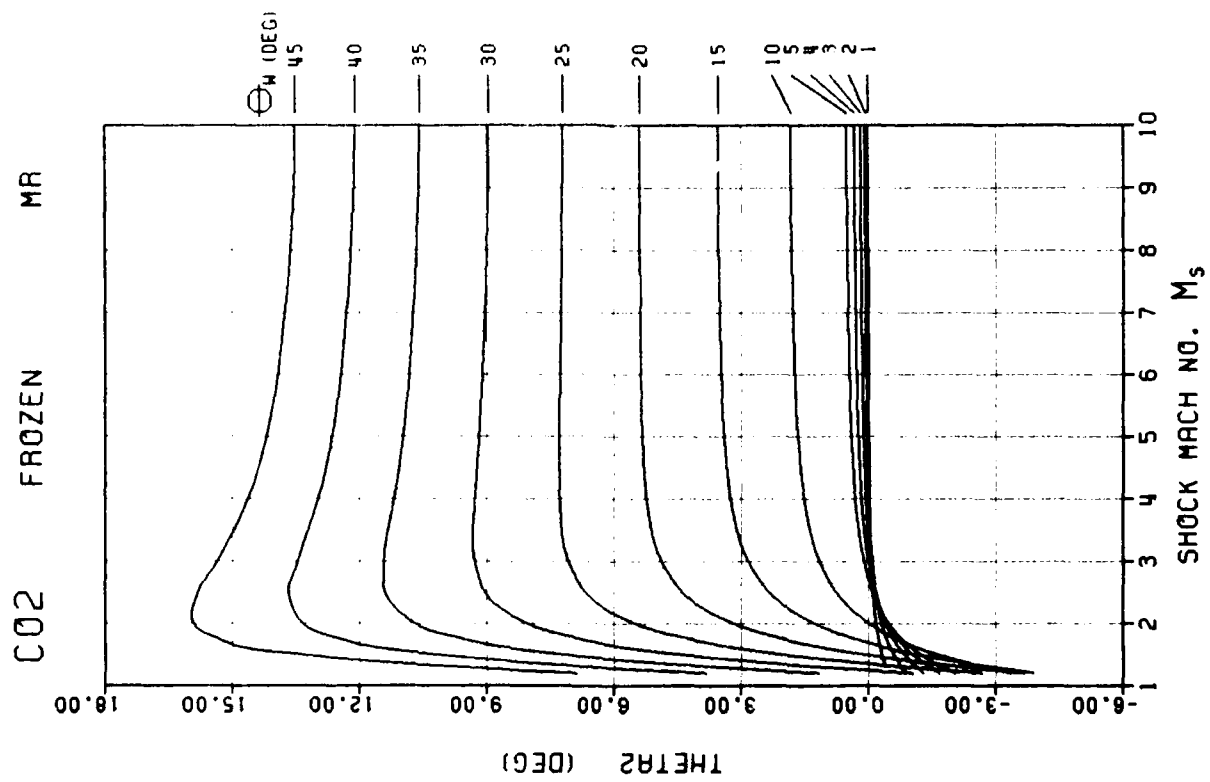


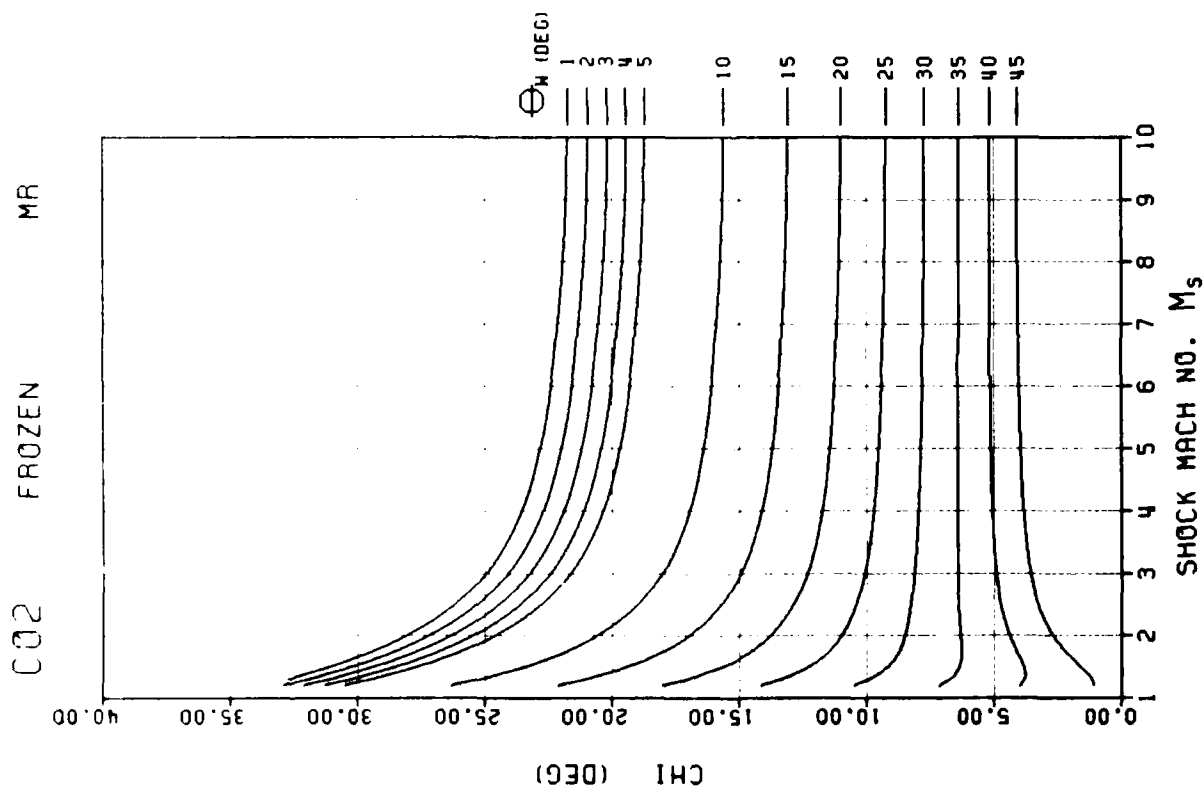




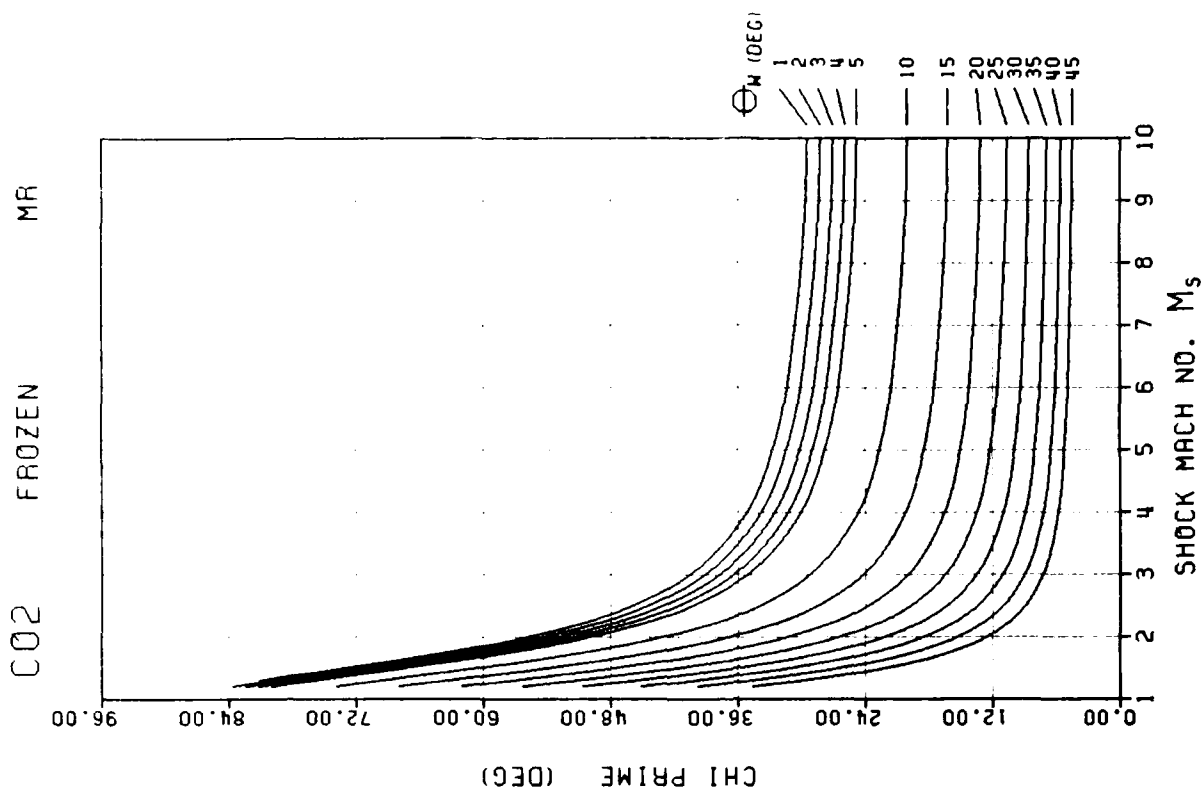


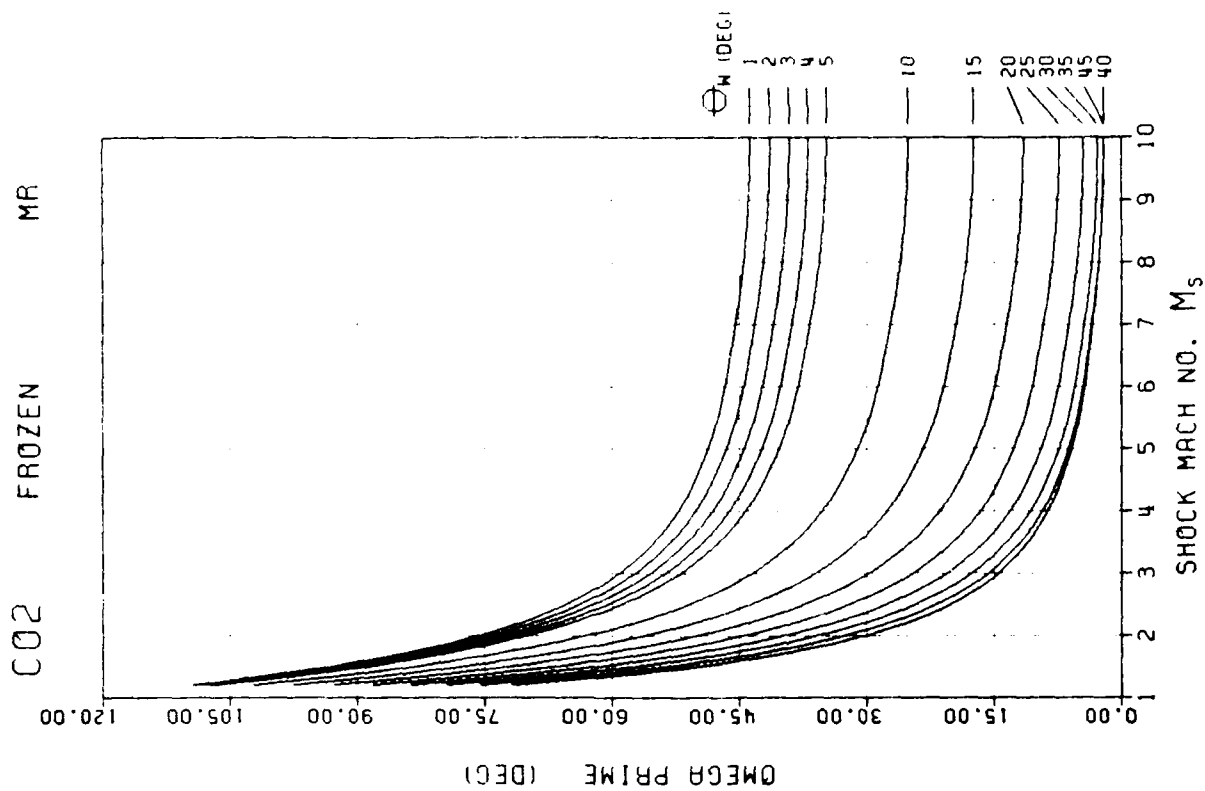
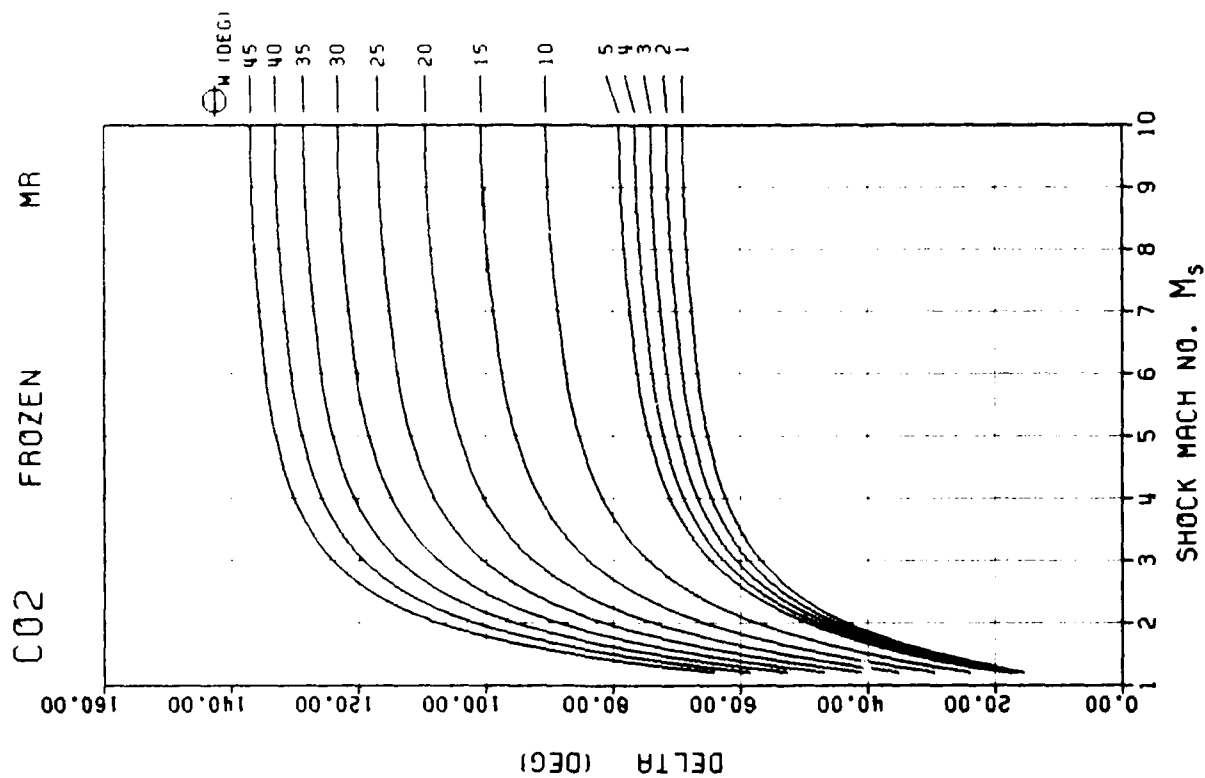


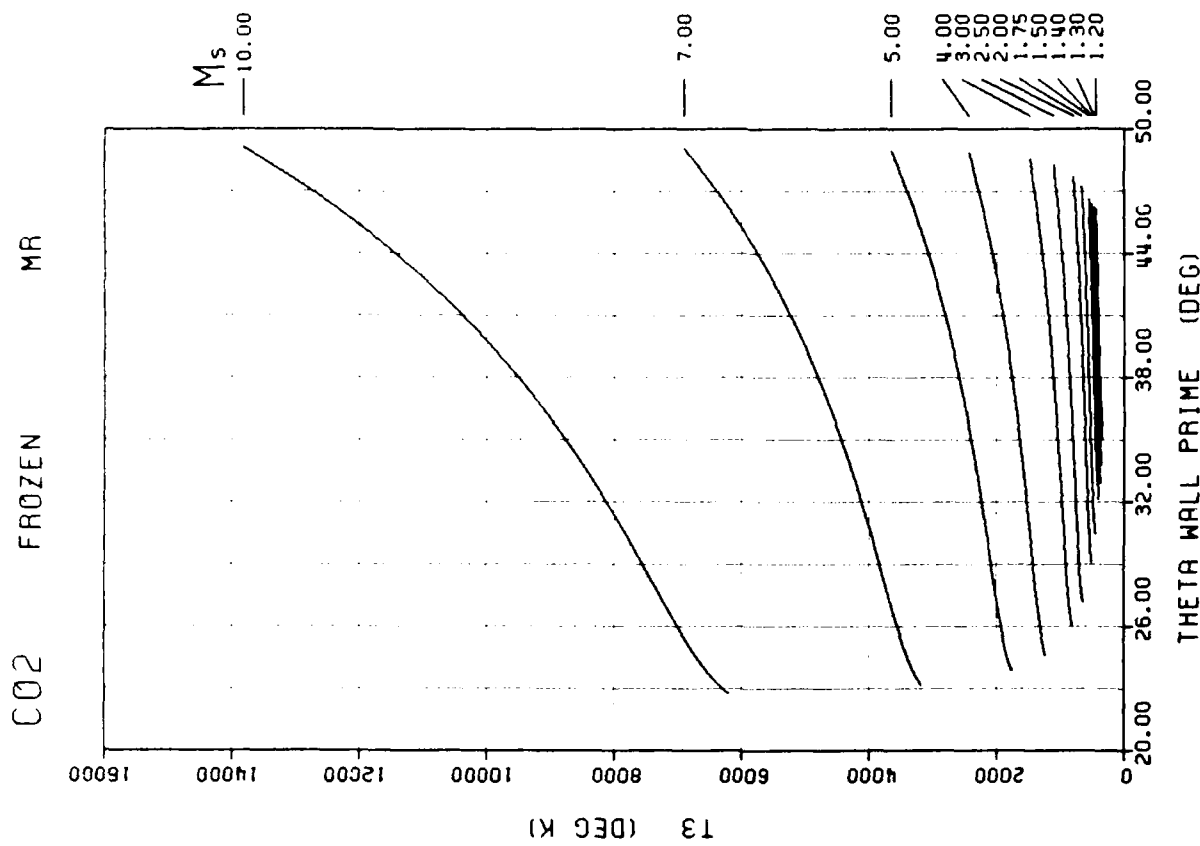
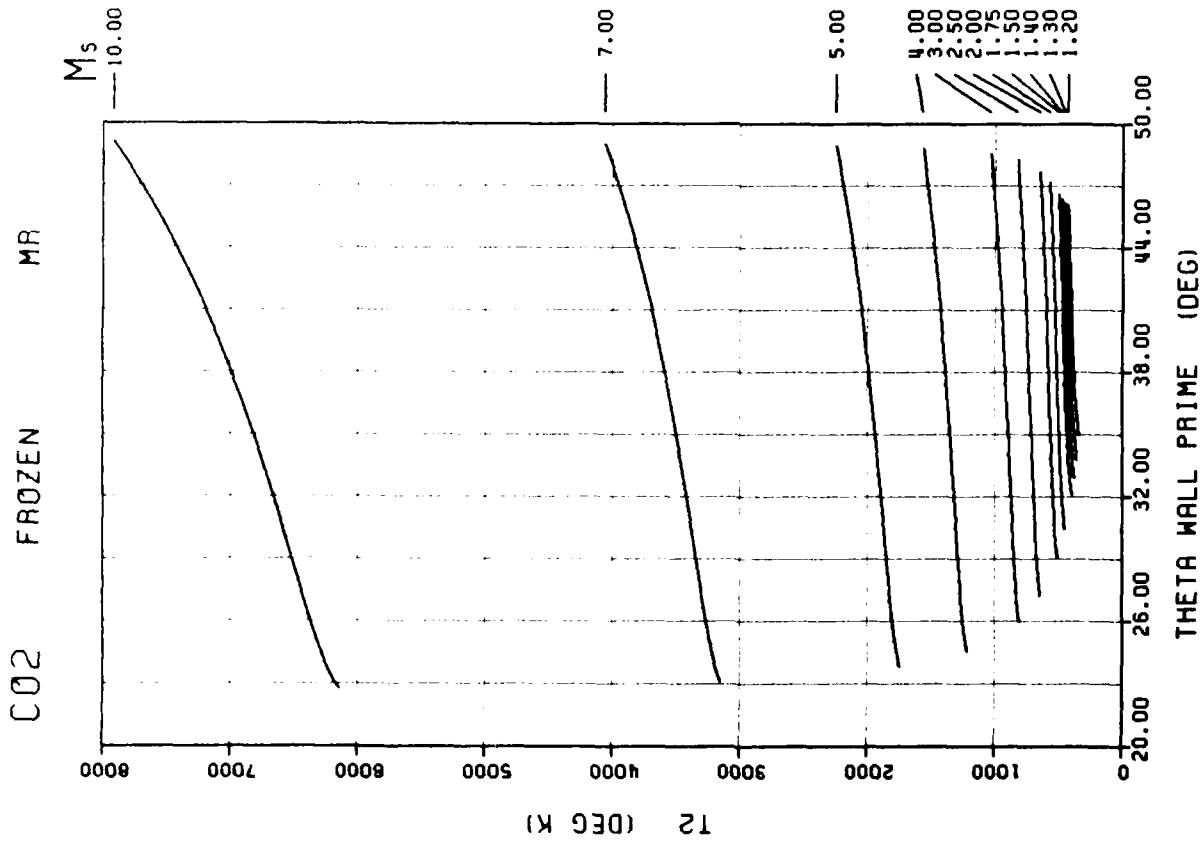


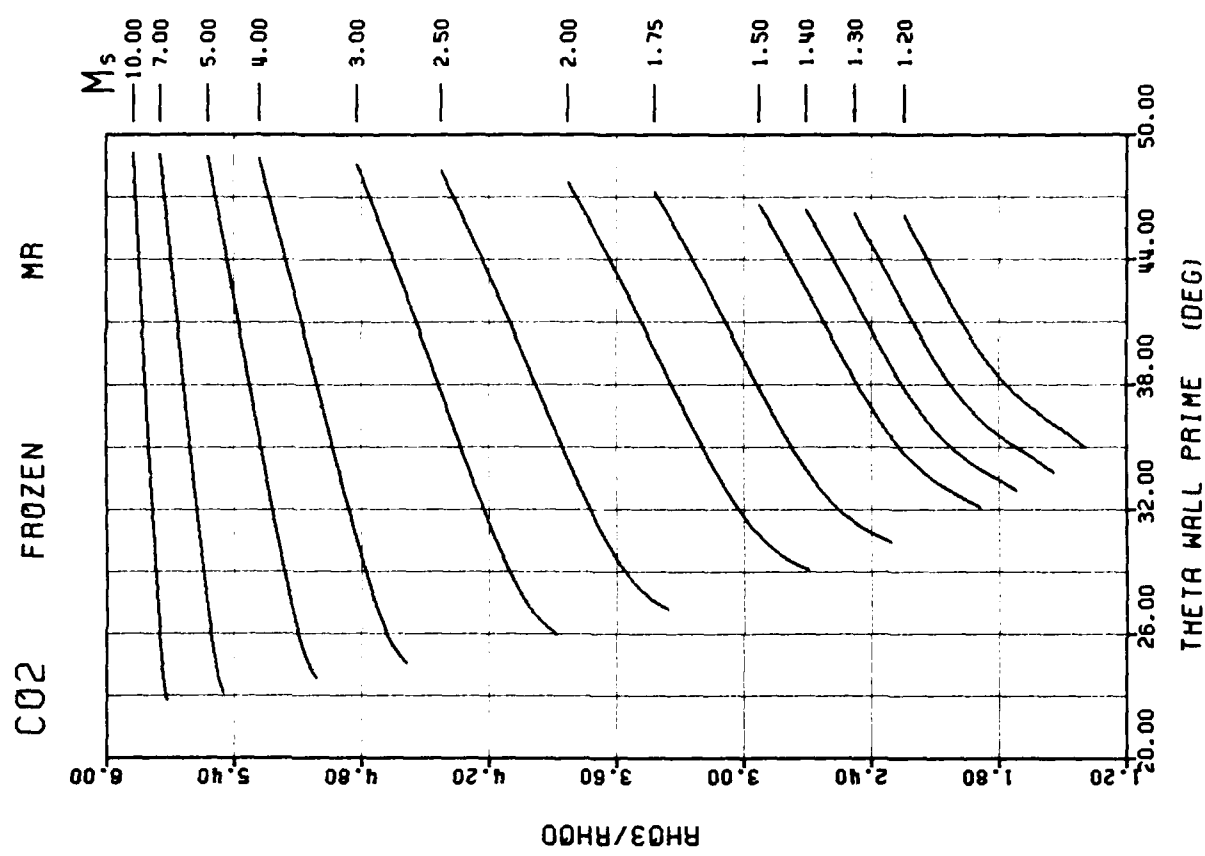
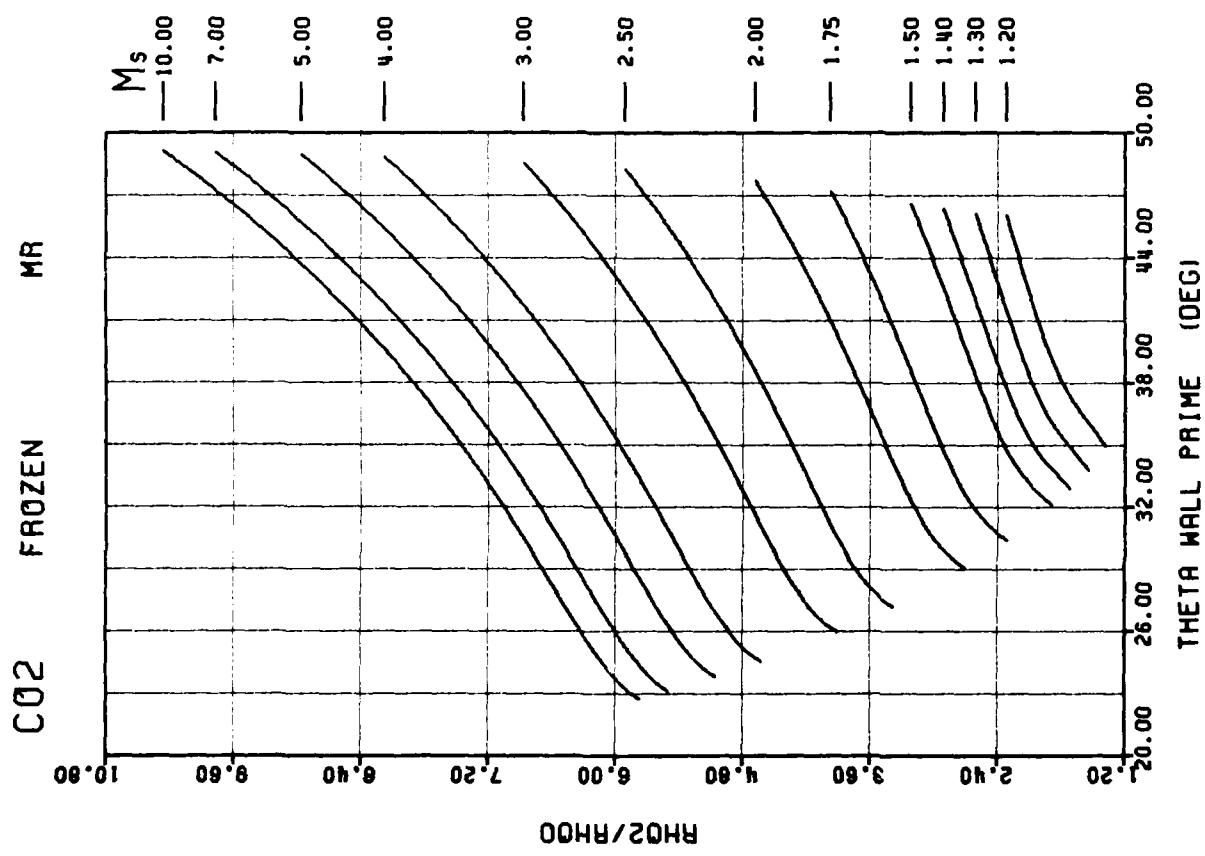


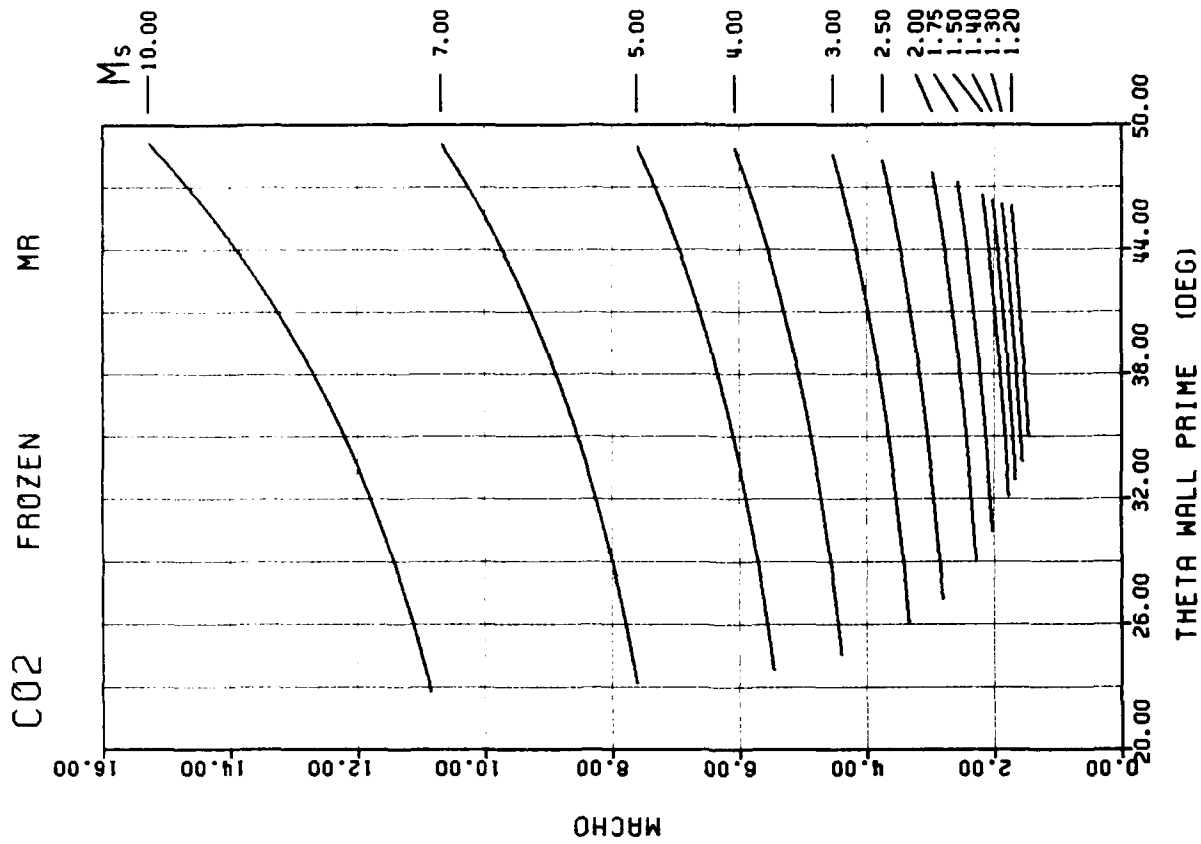
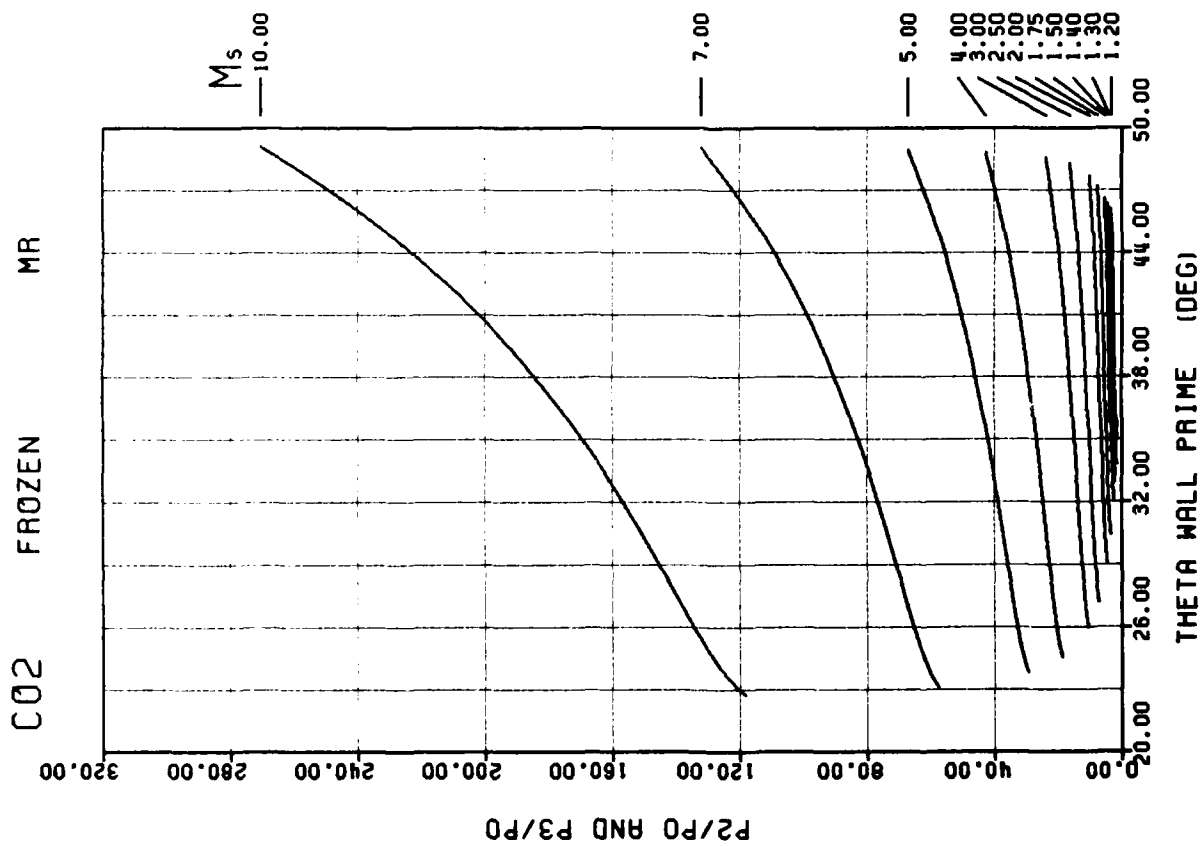
F - 138

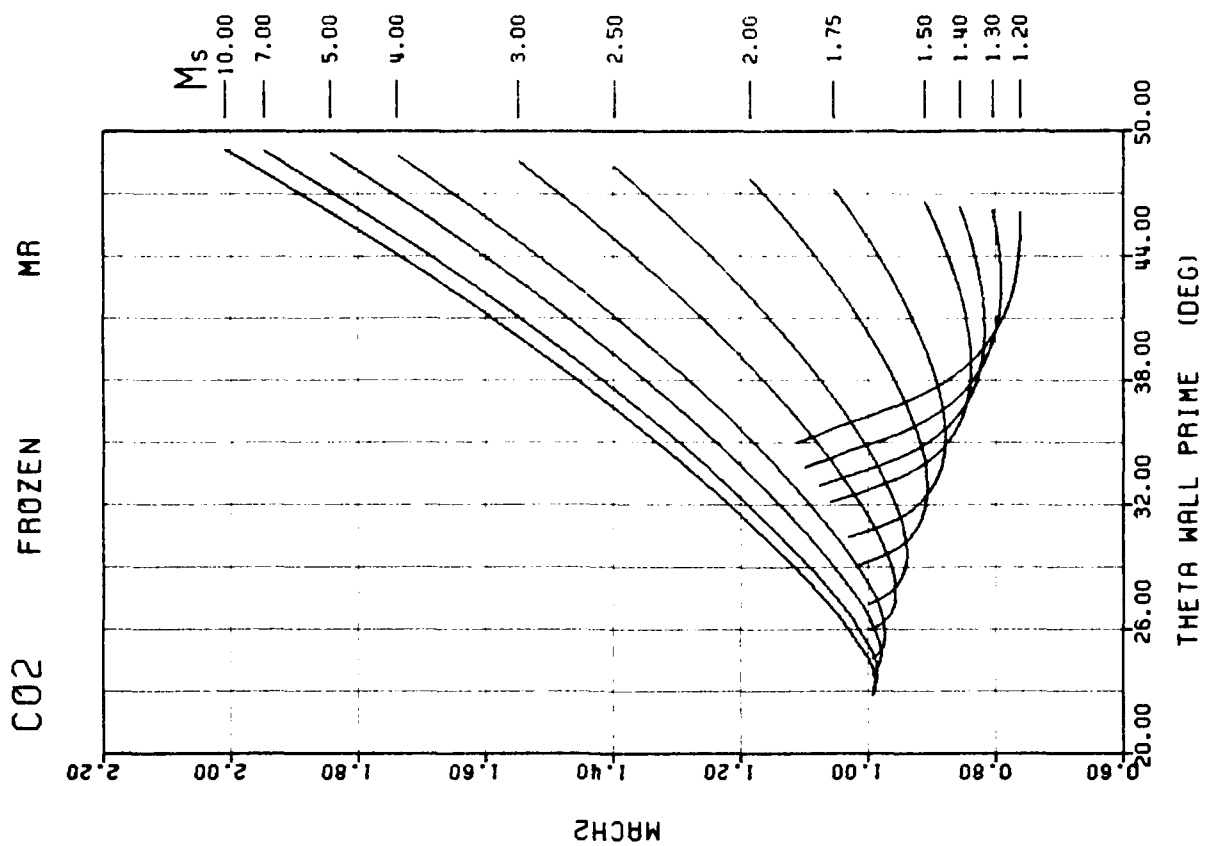
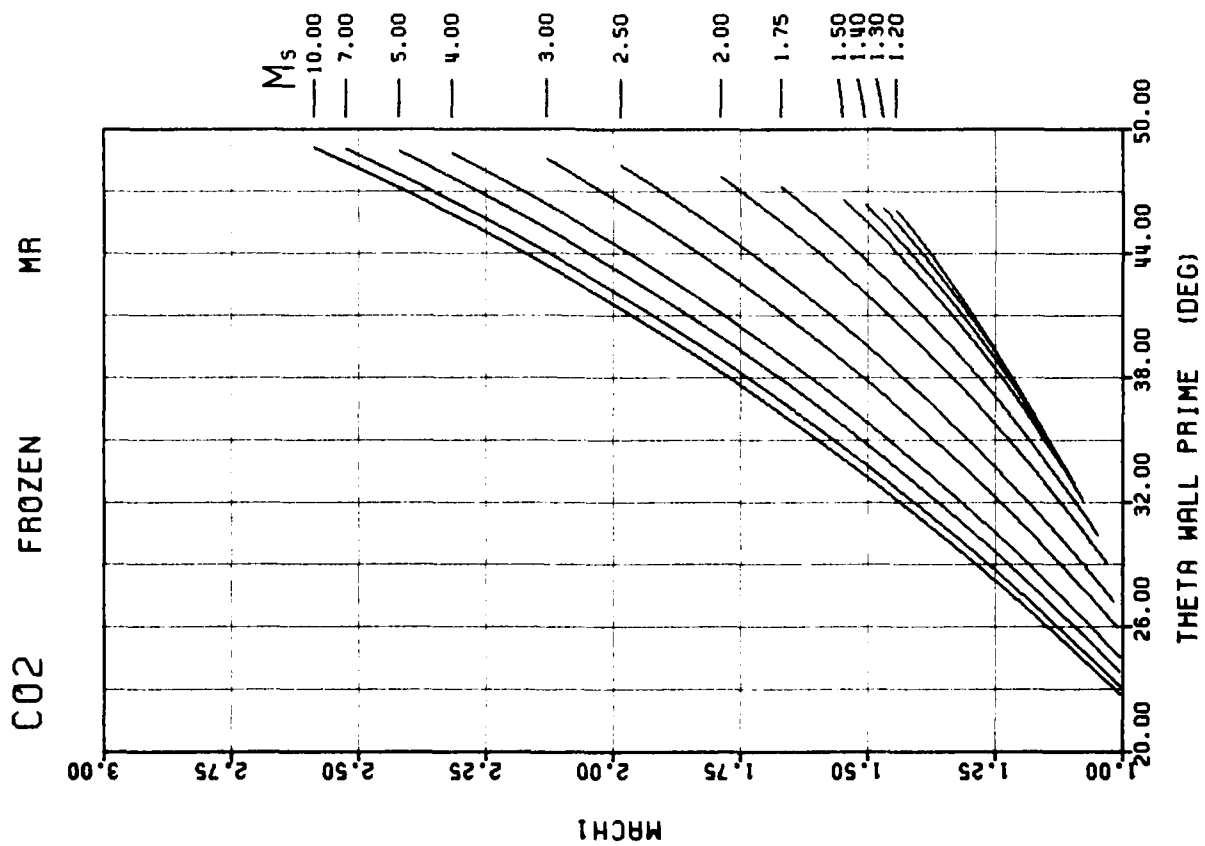


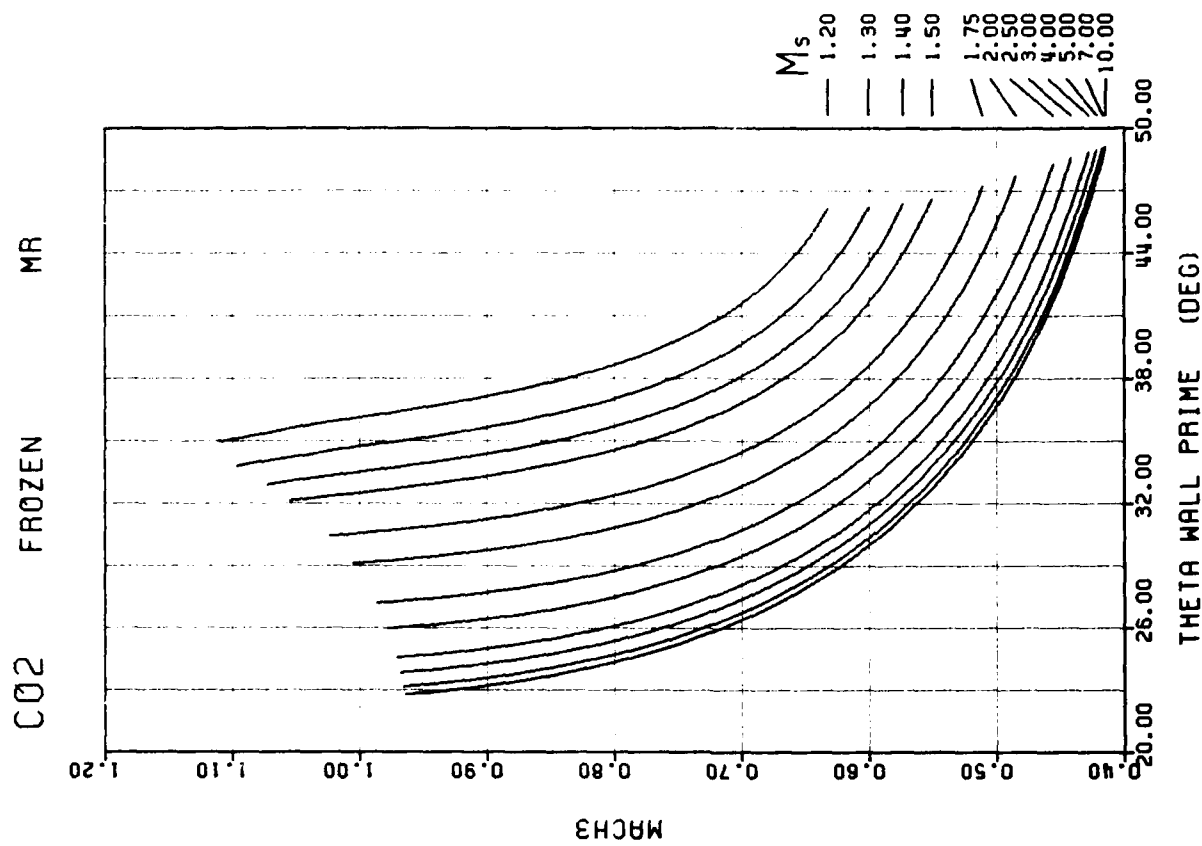
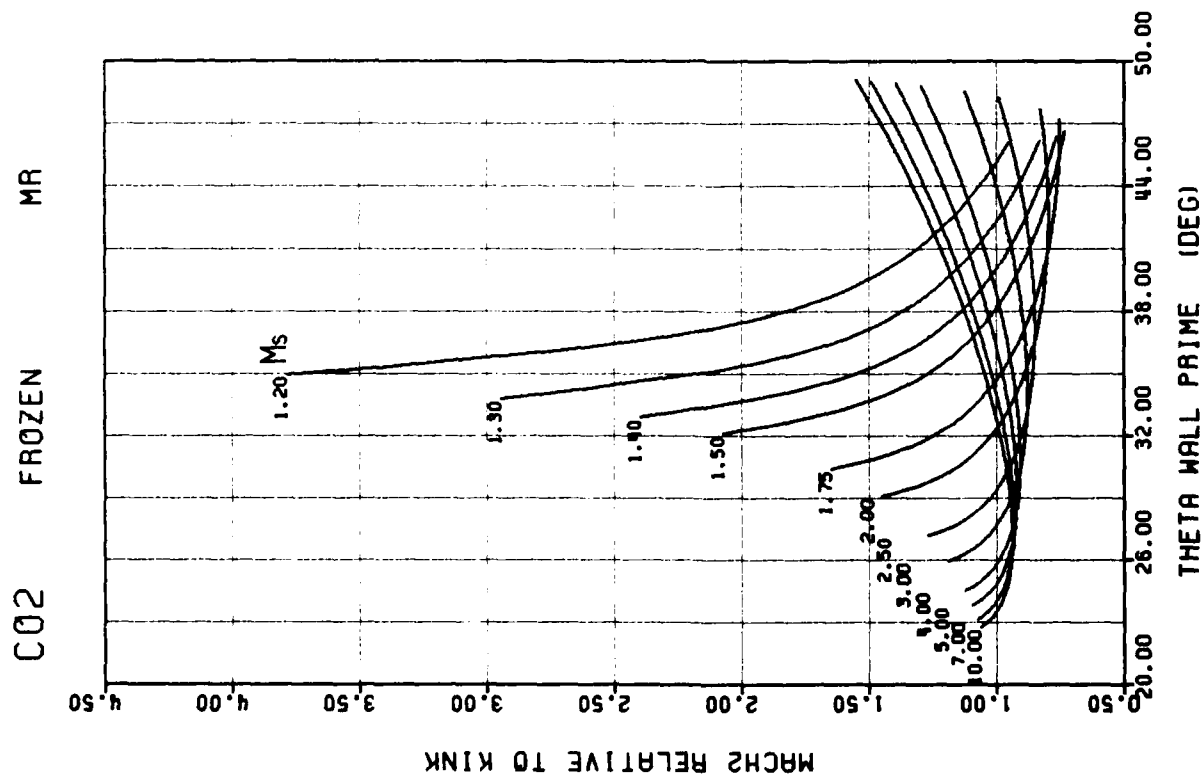


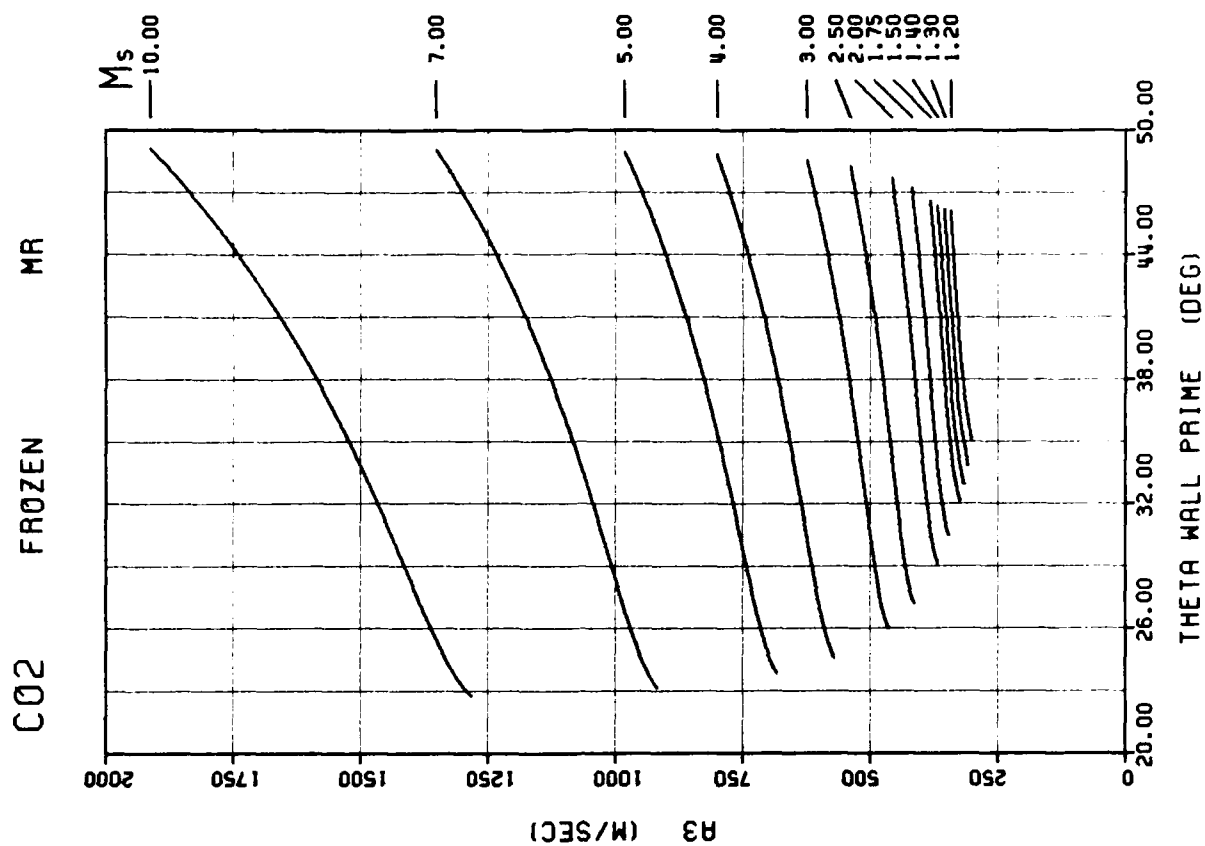
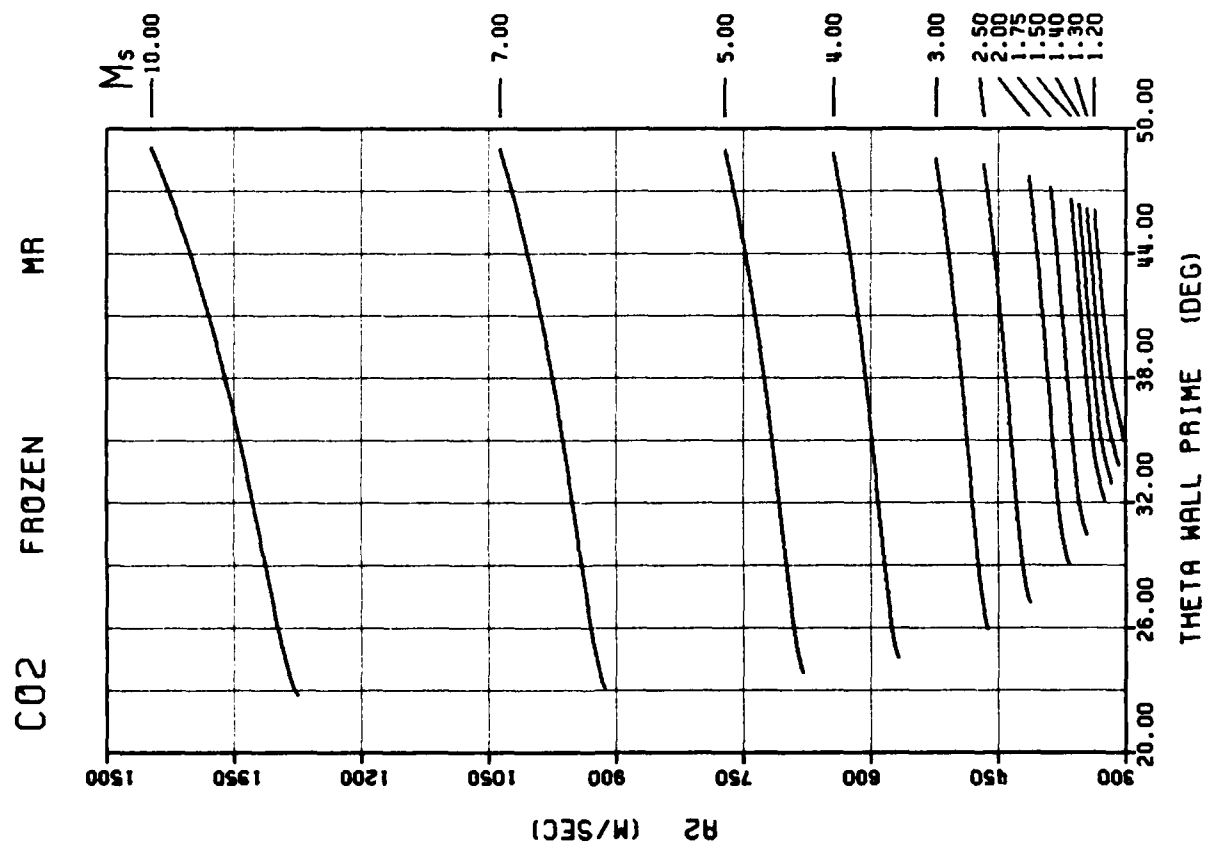


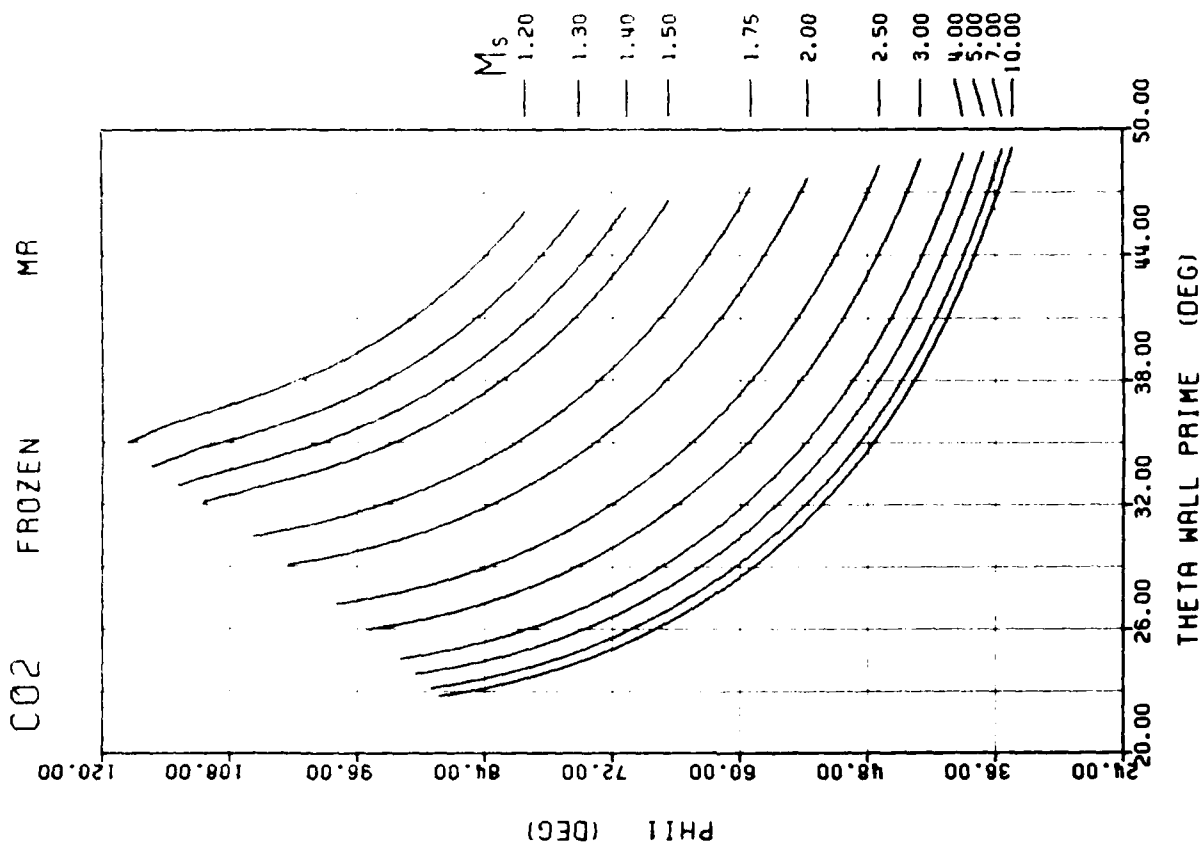
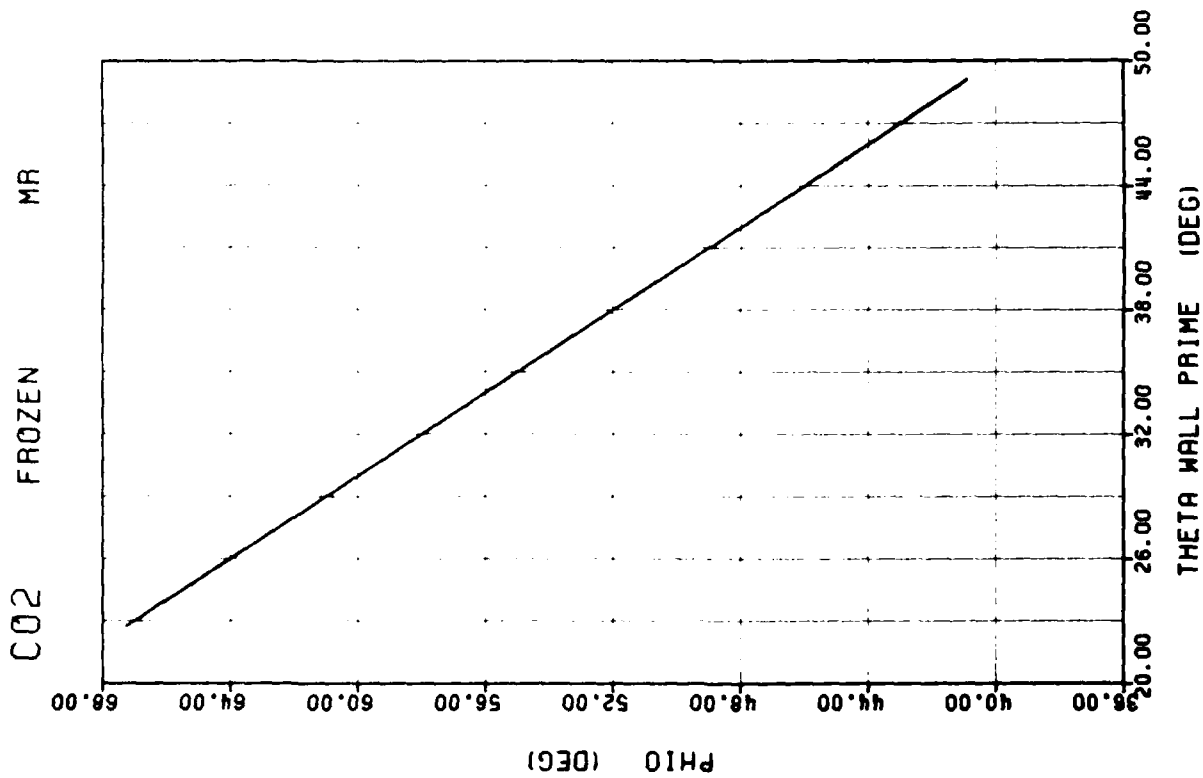


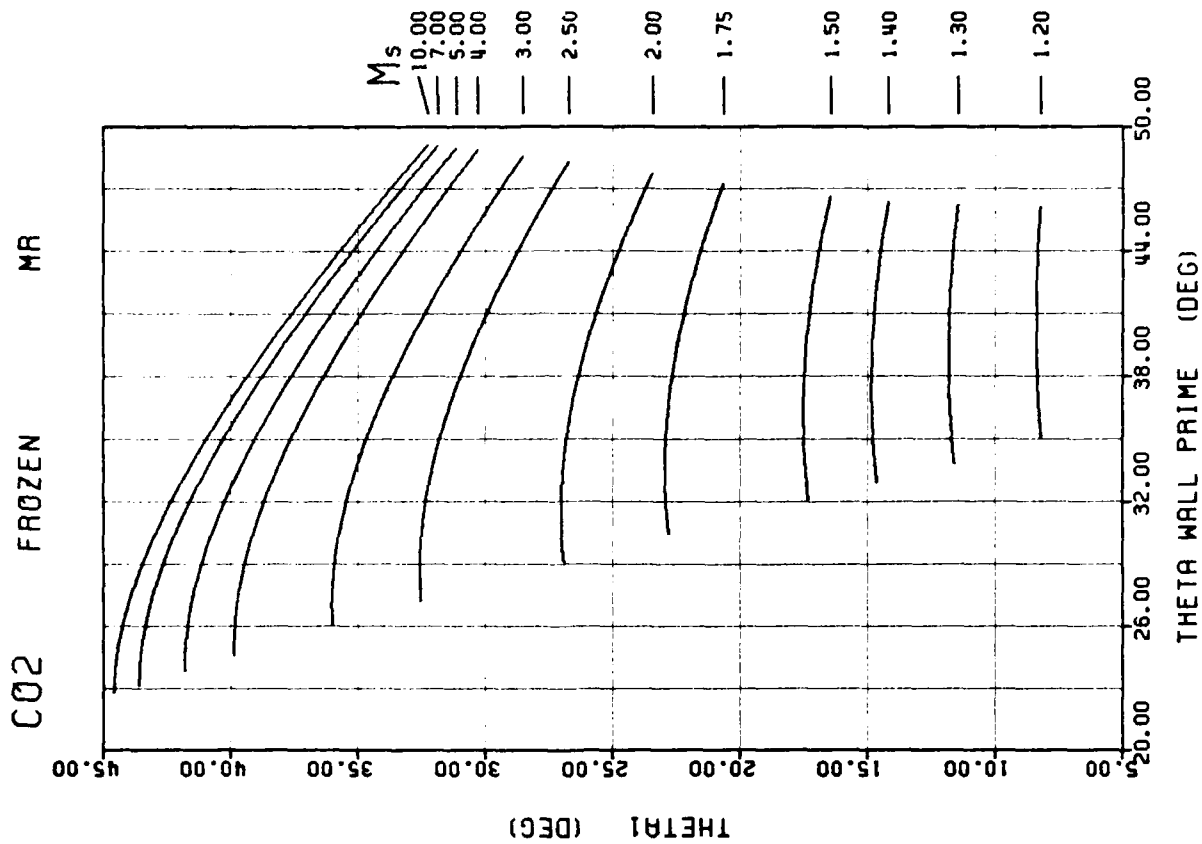
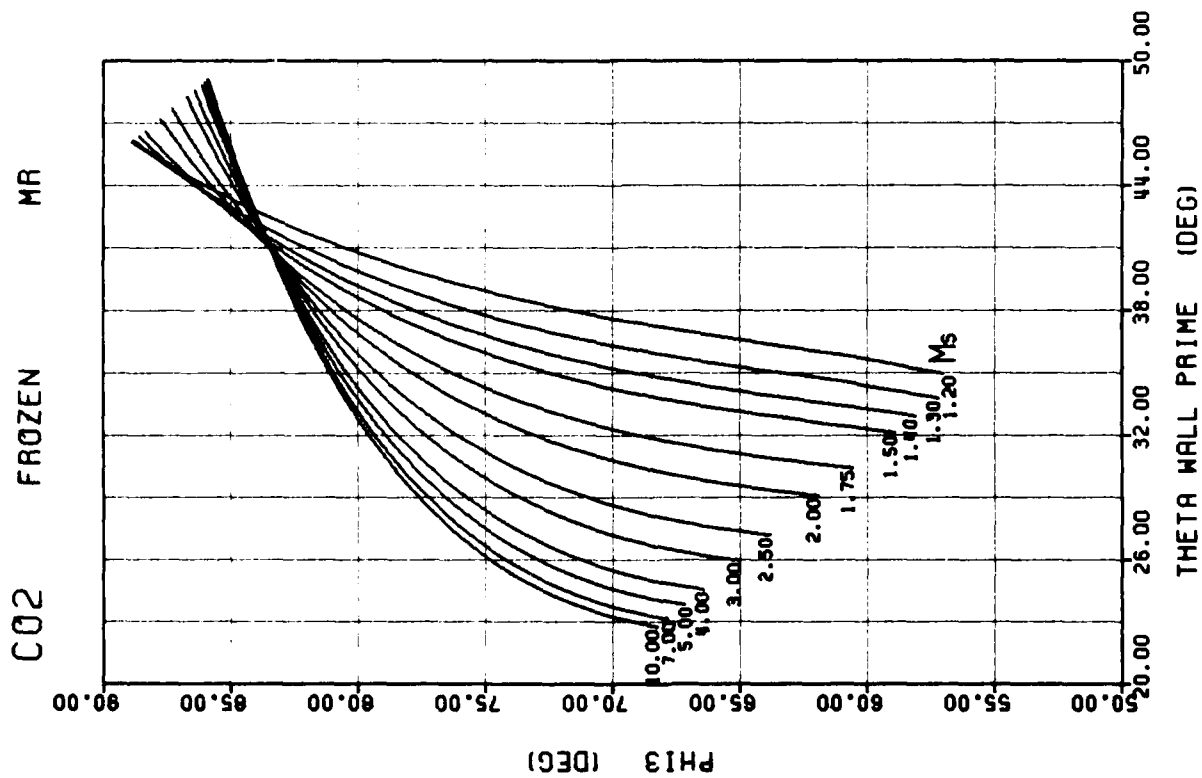


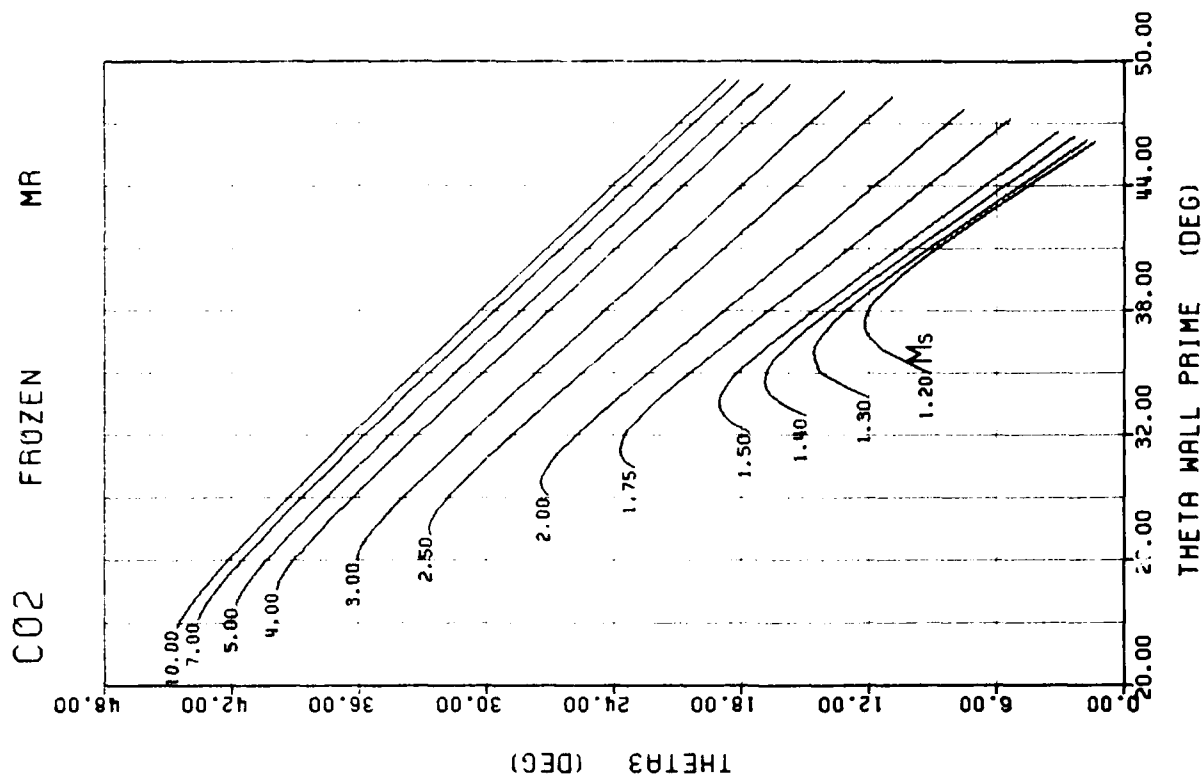
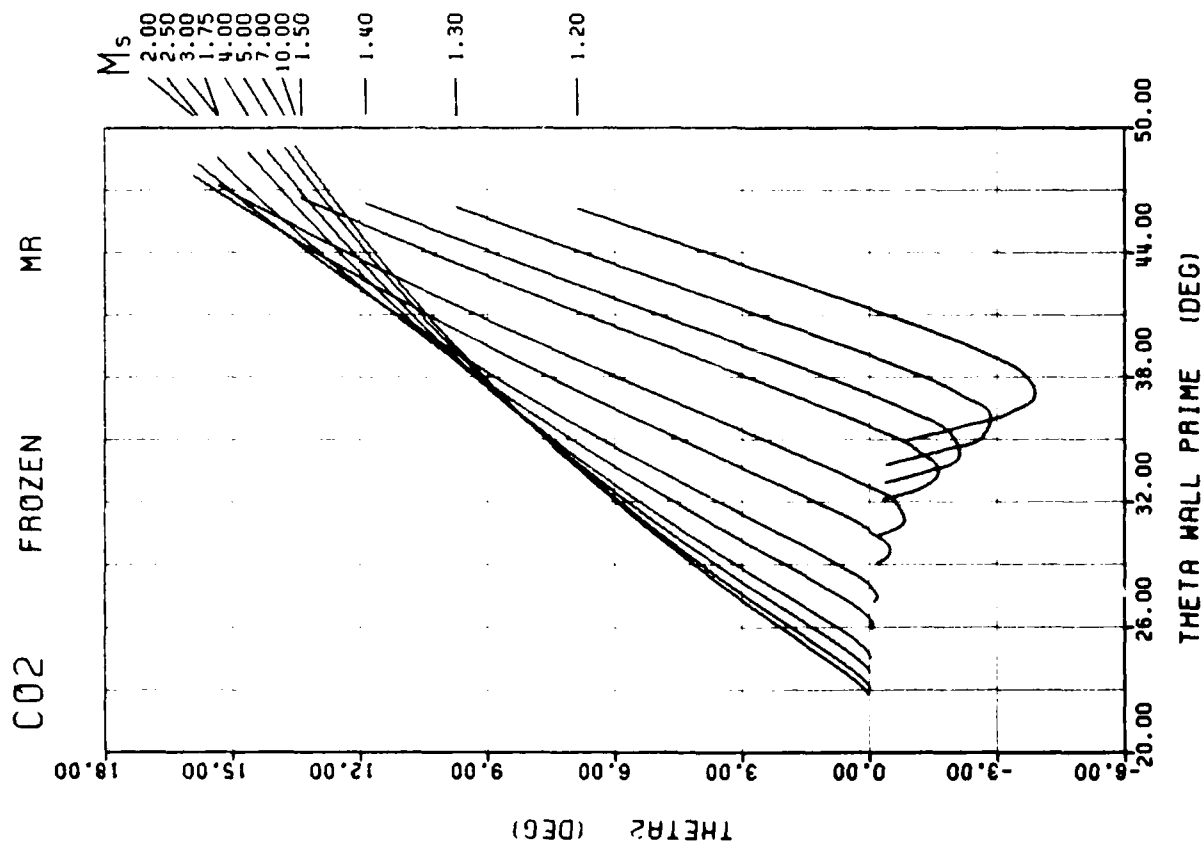


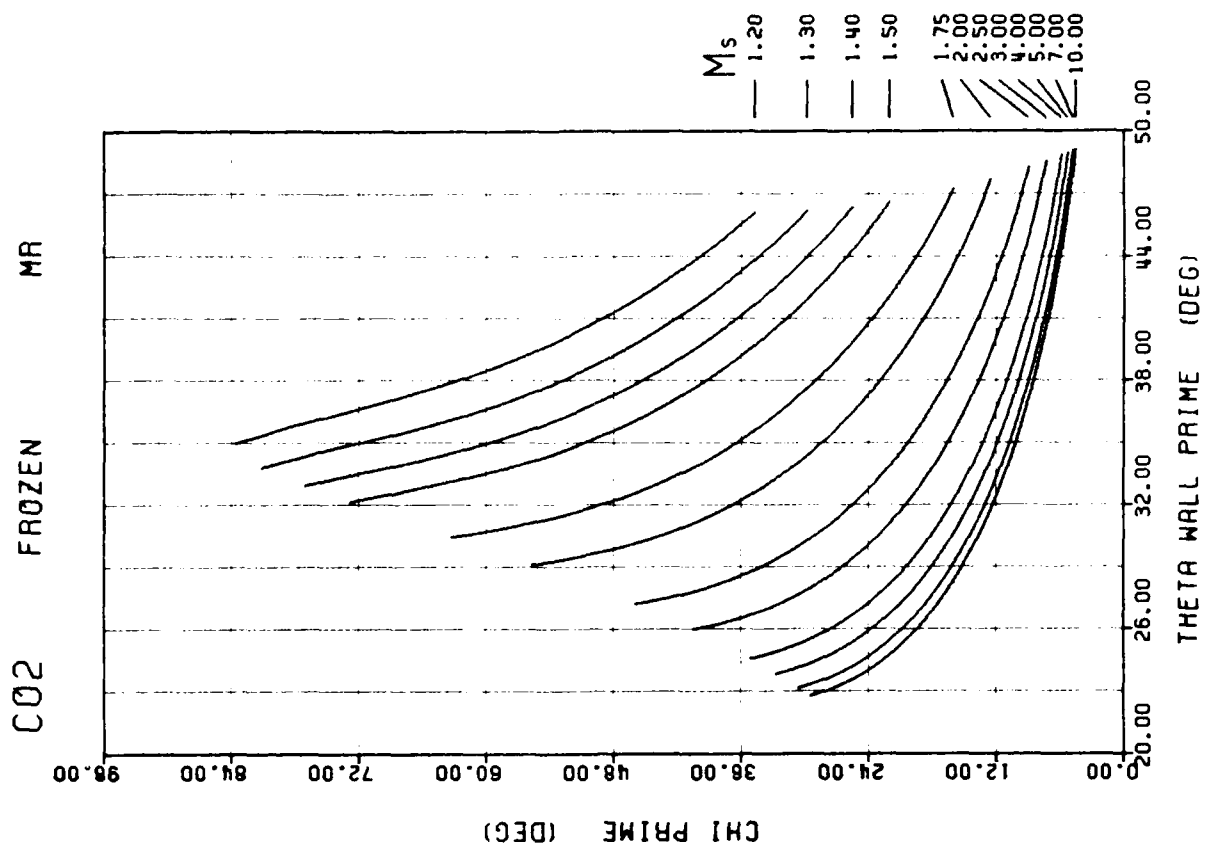
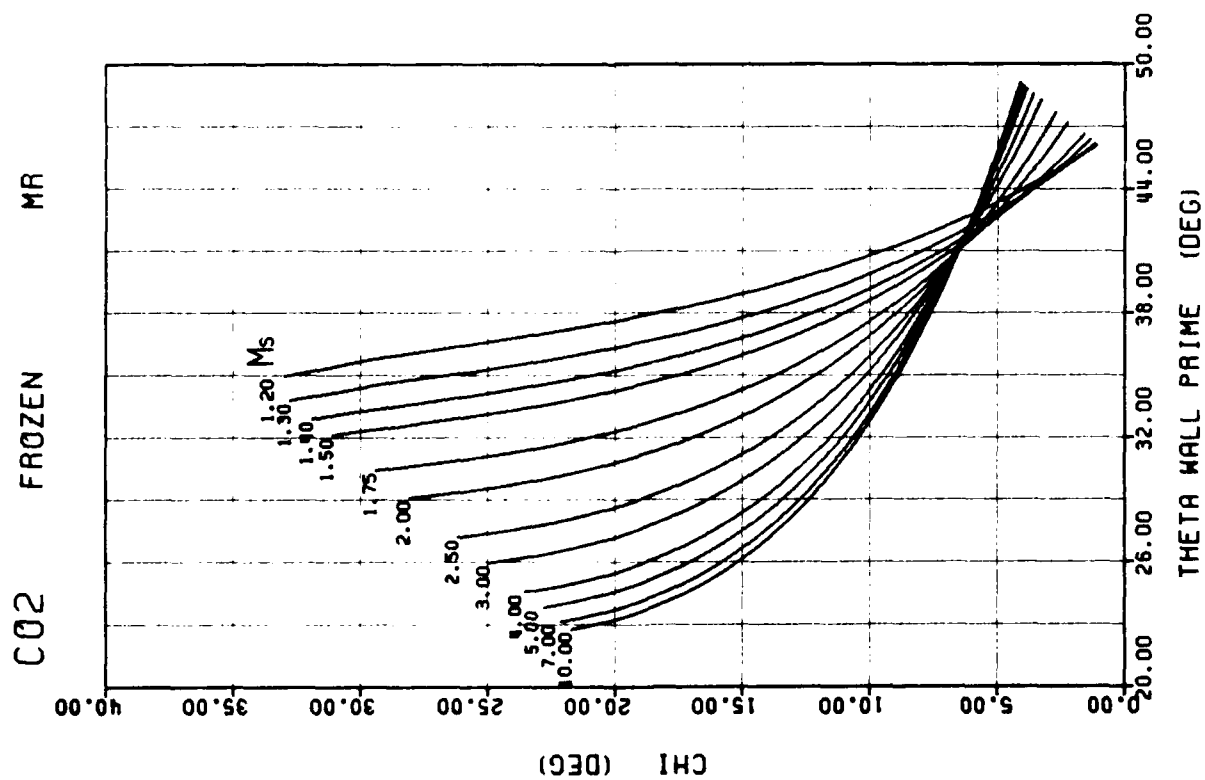


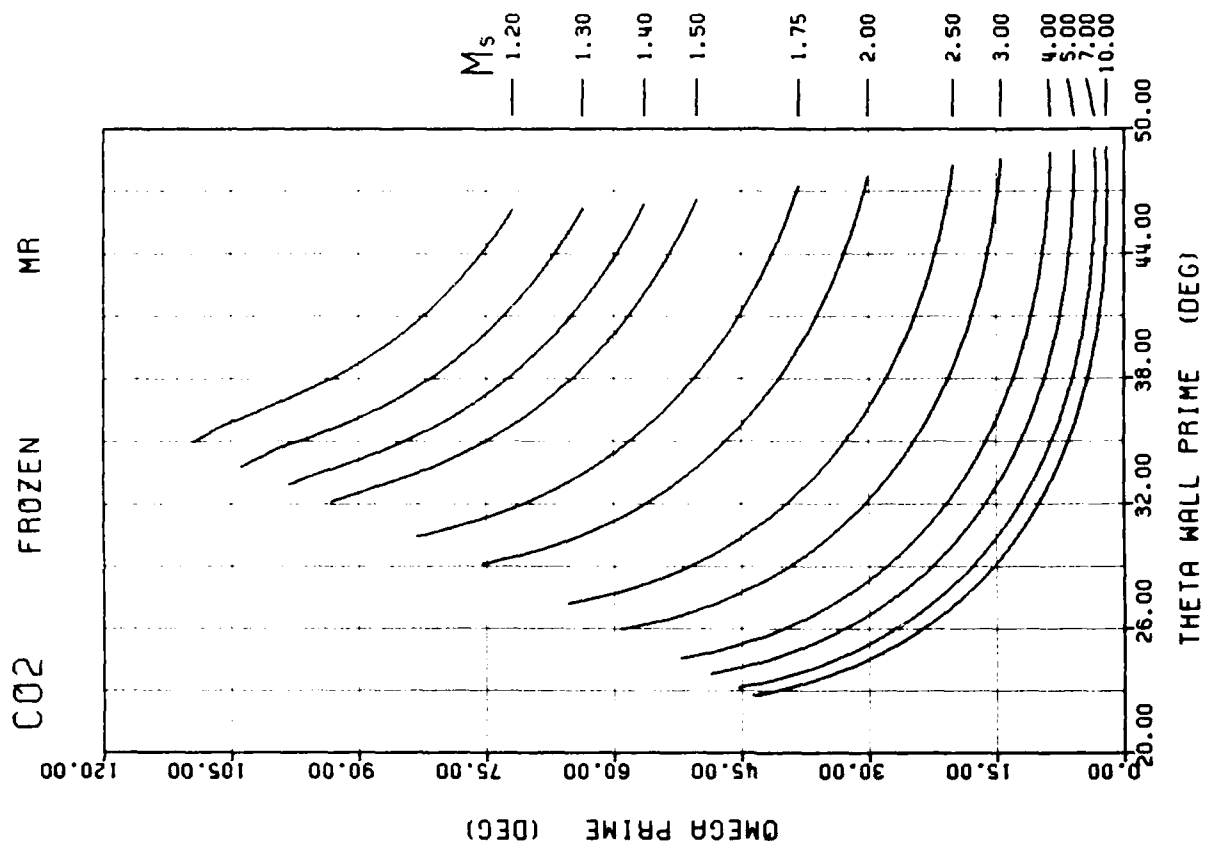
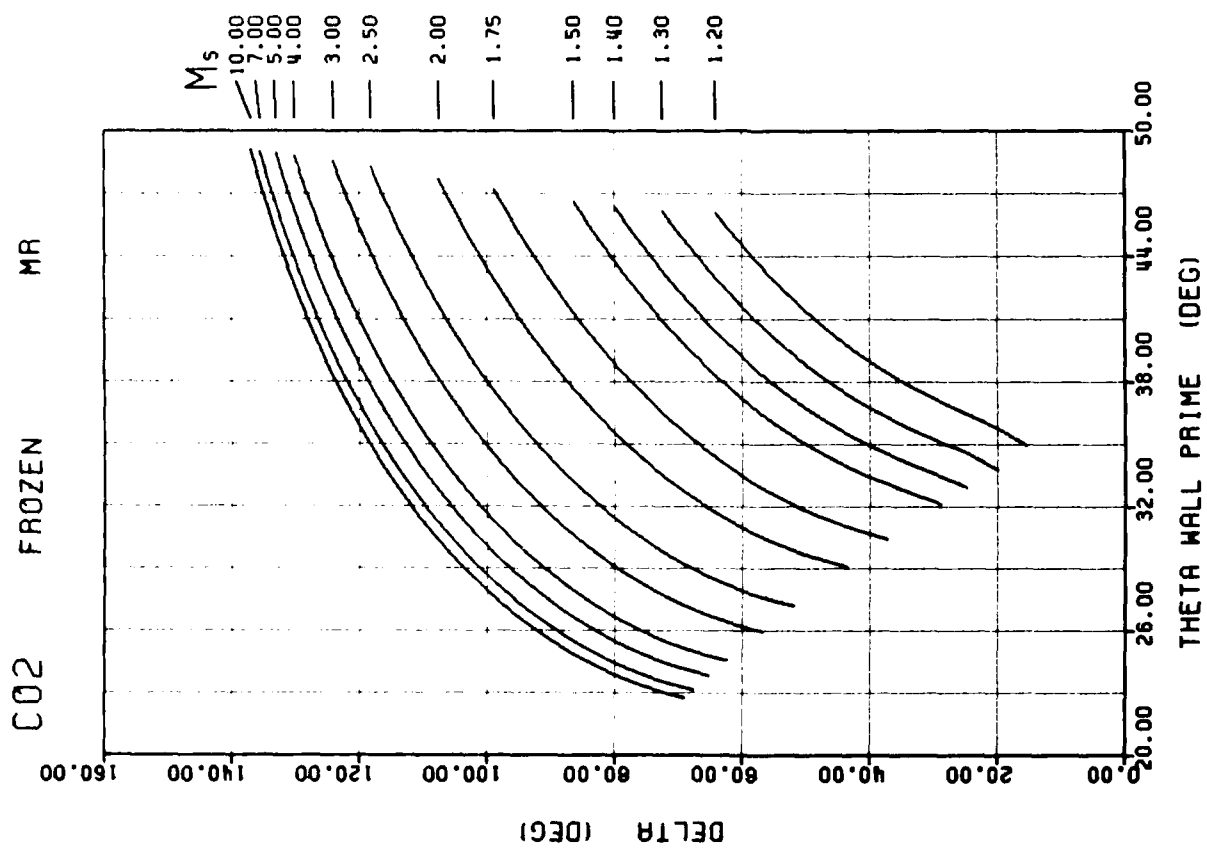


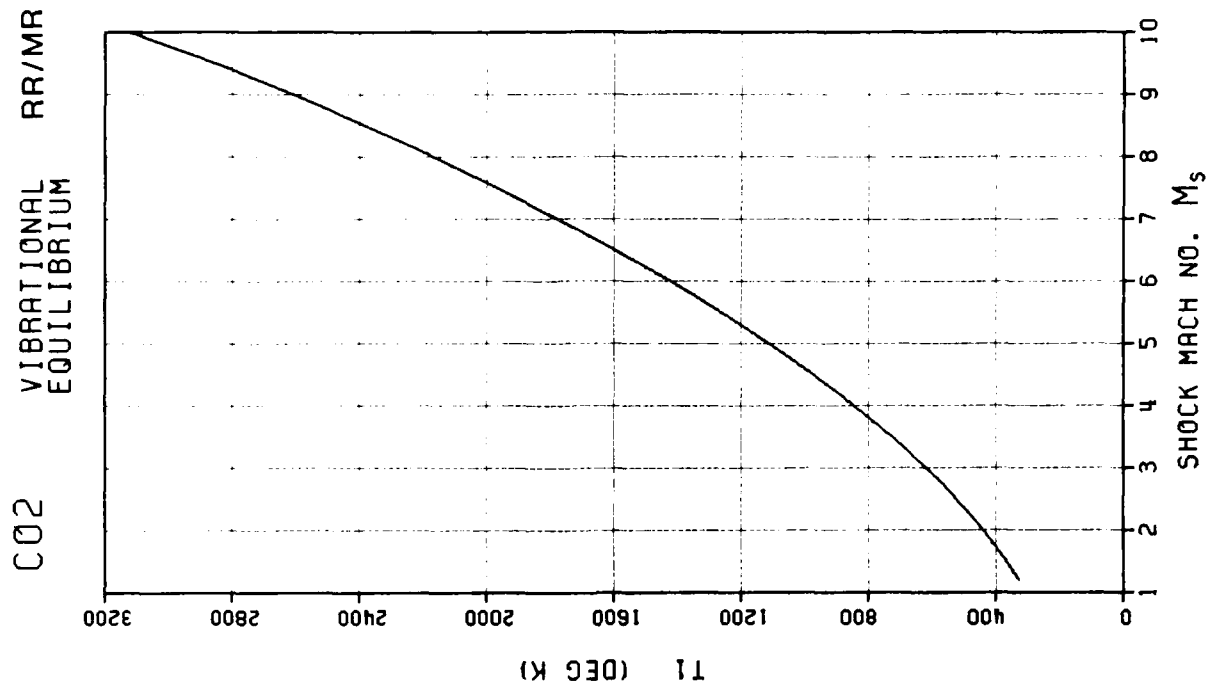
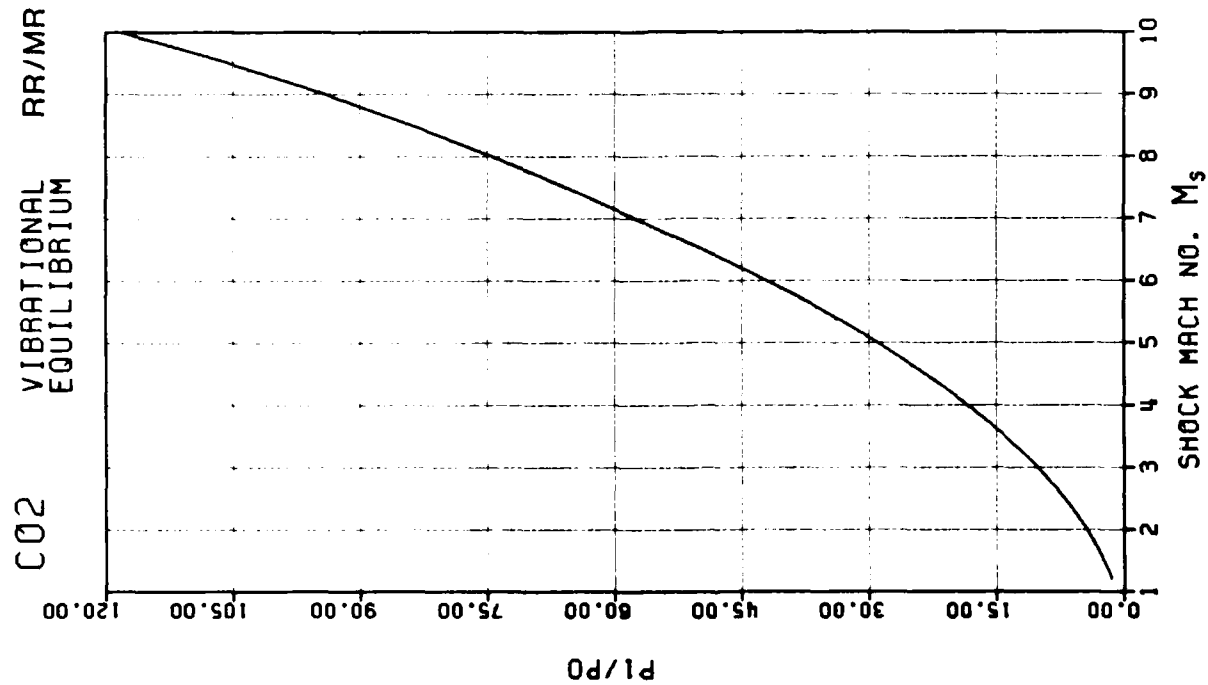


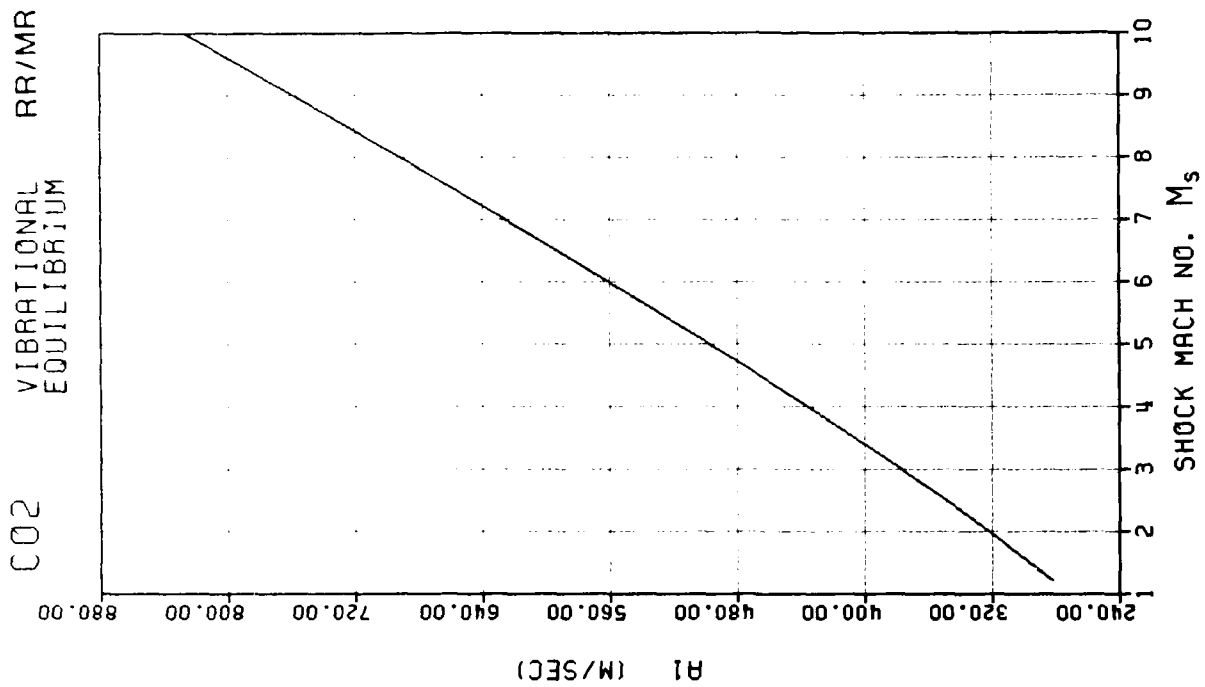
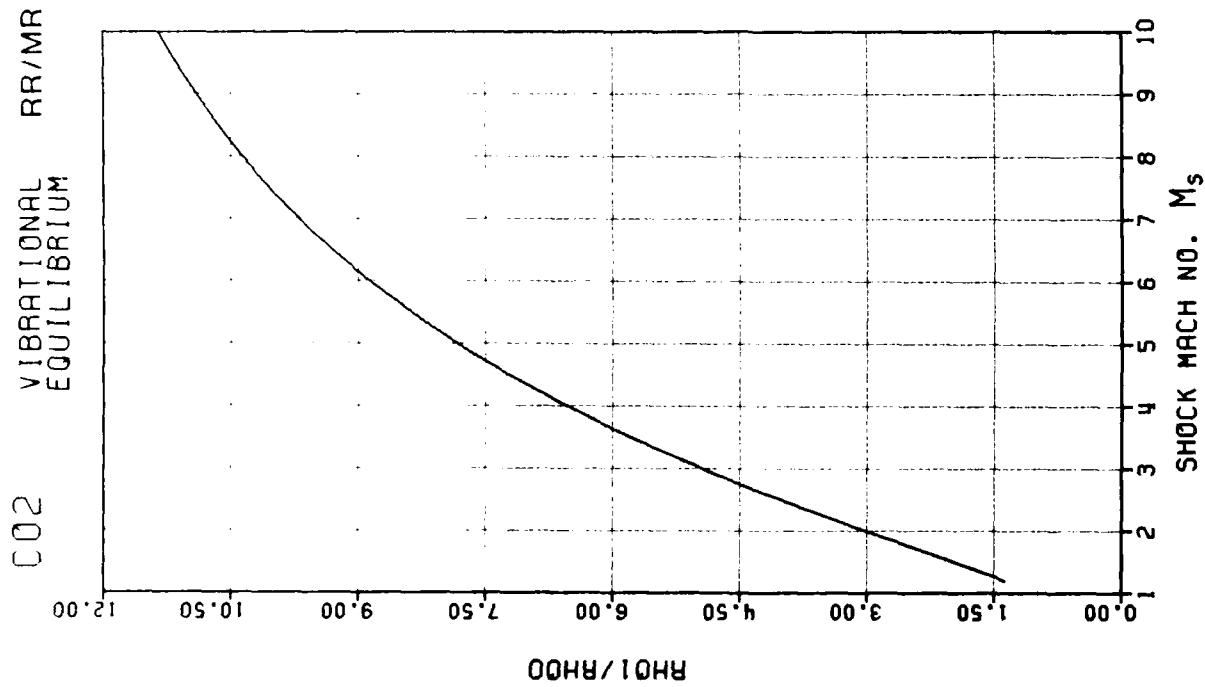




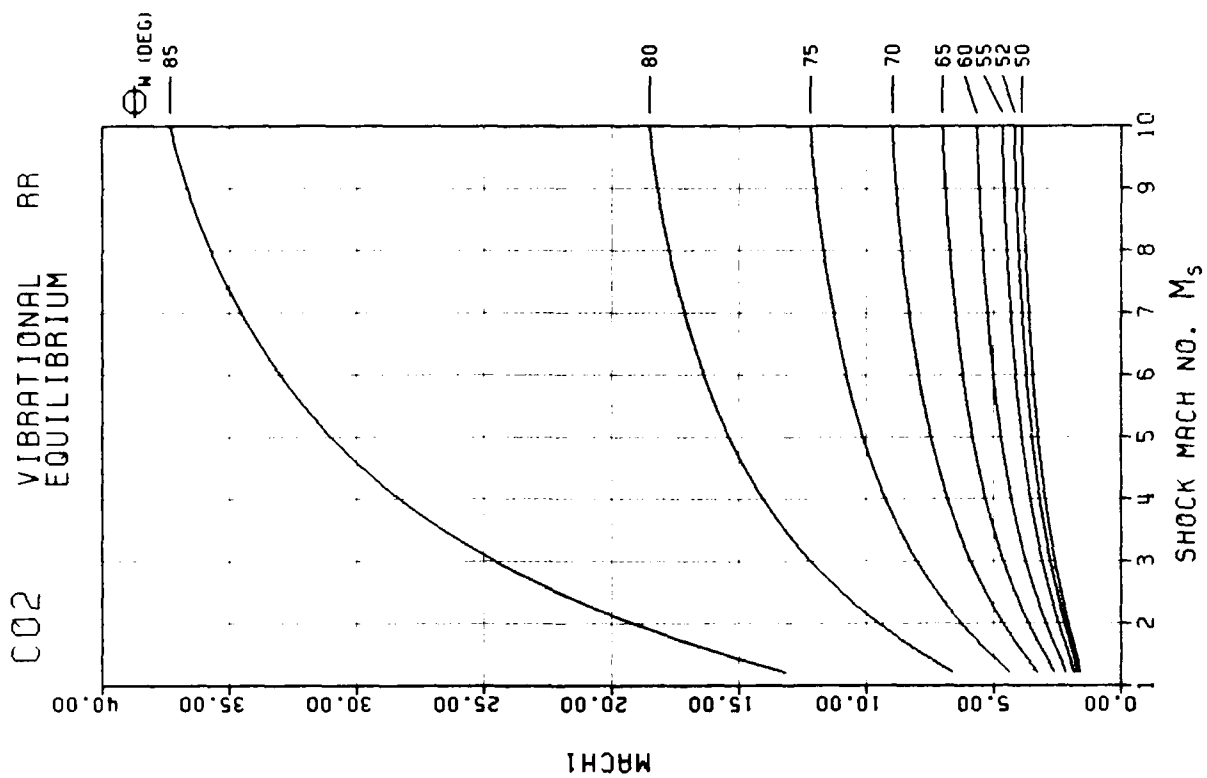
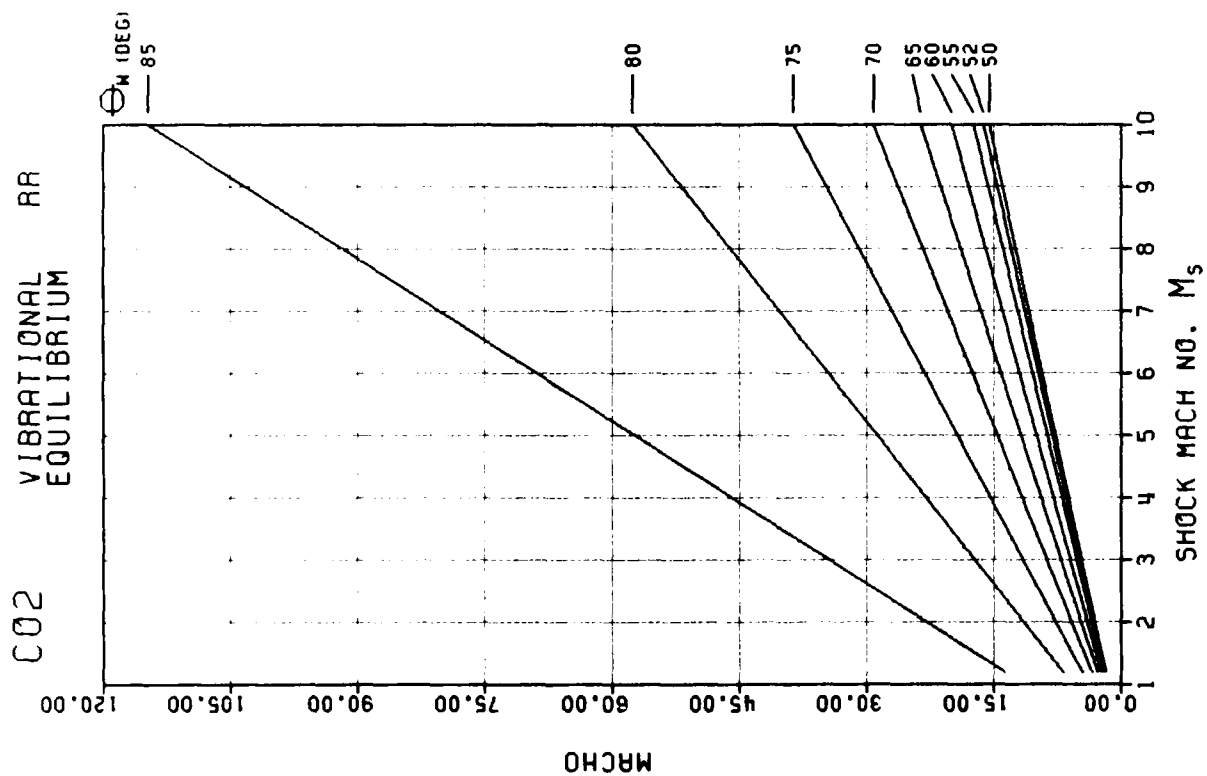


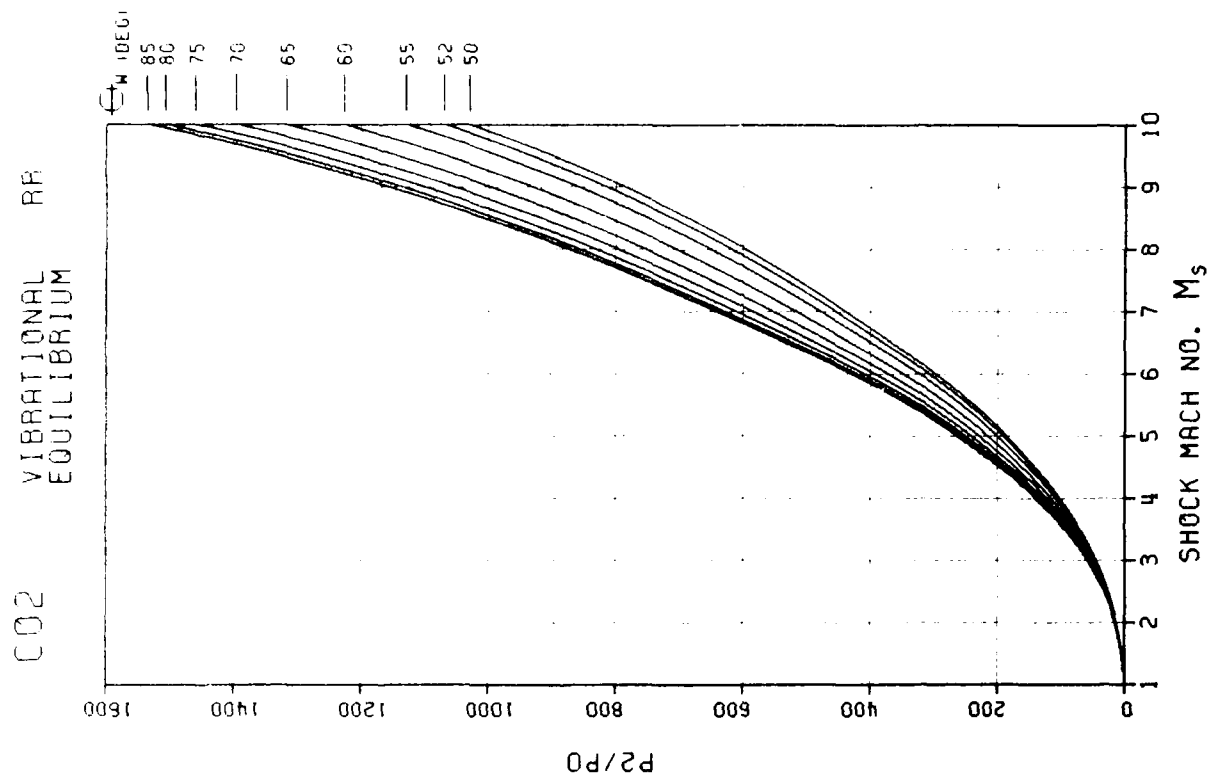
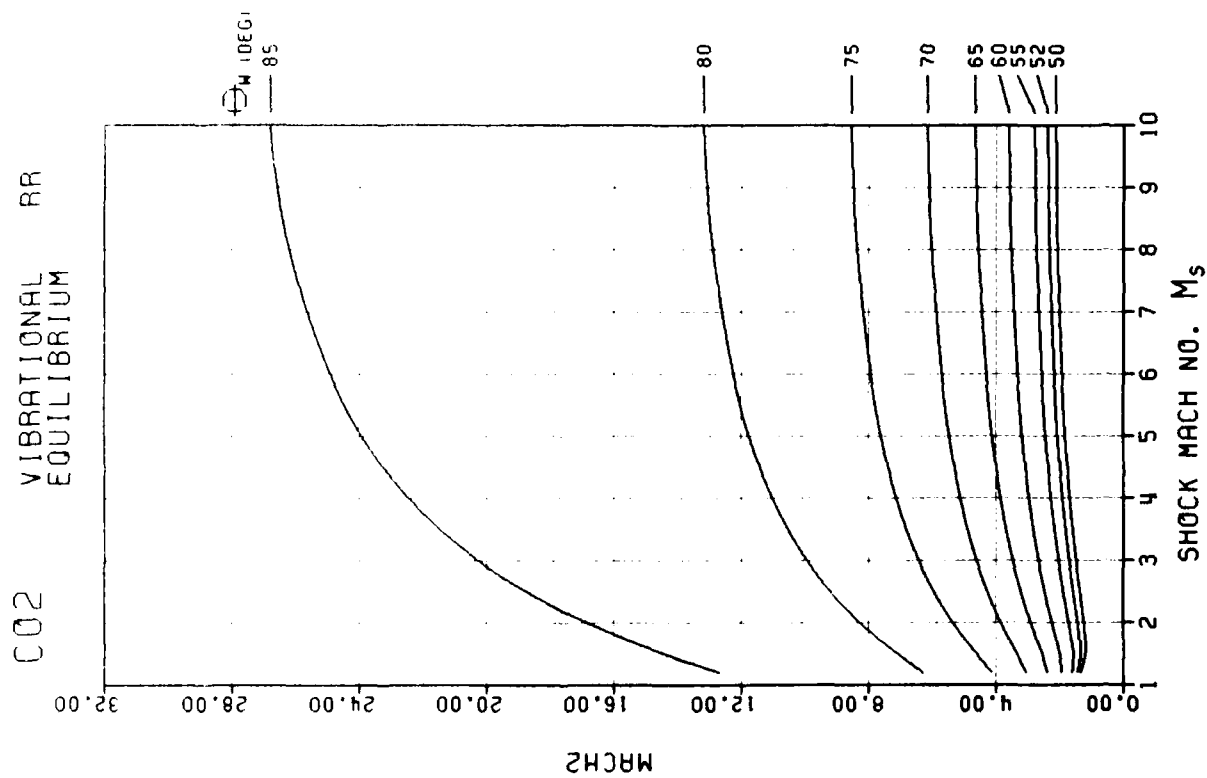


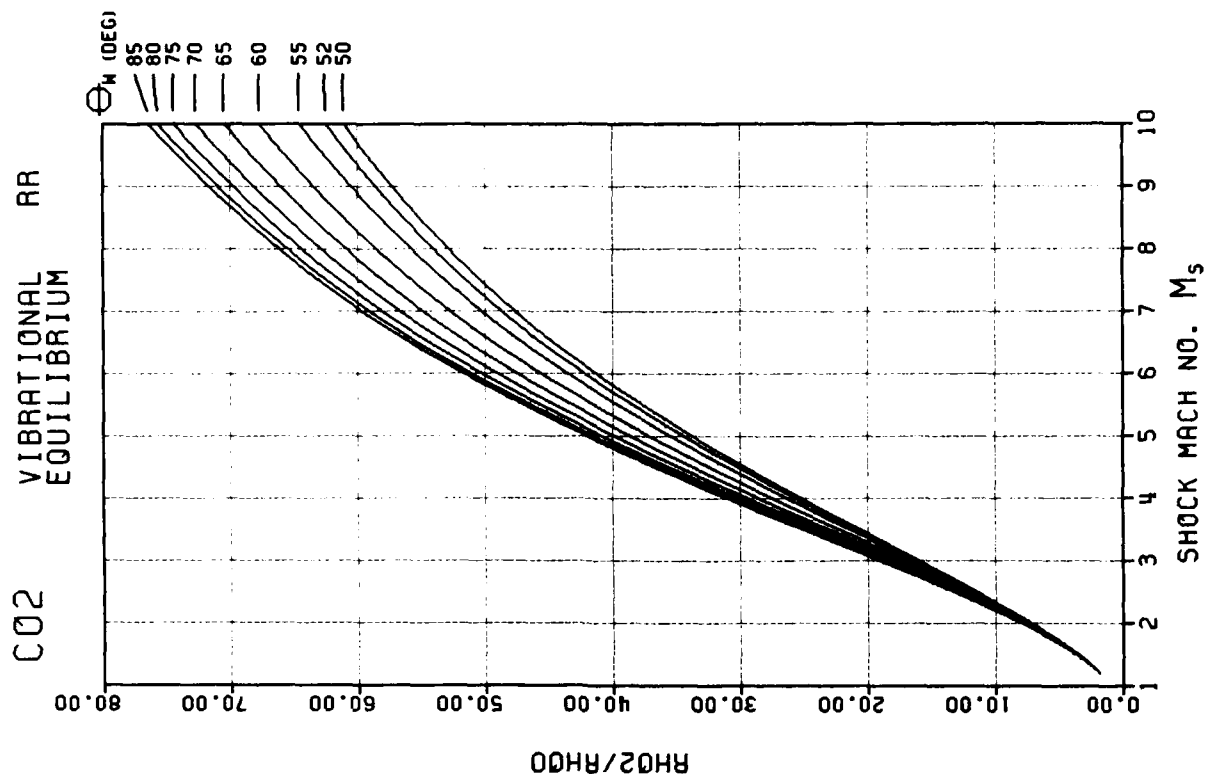
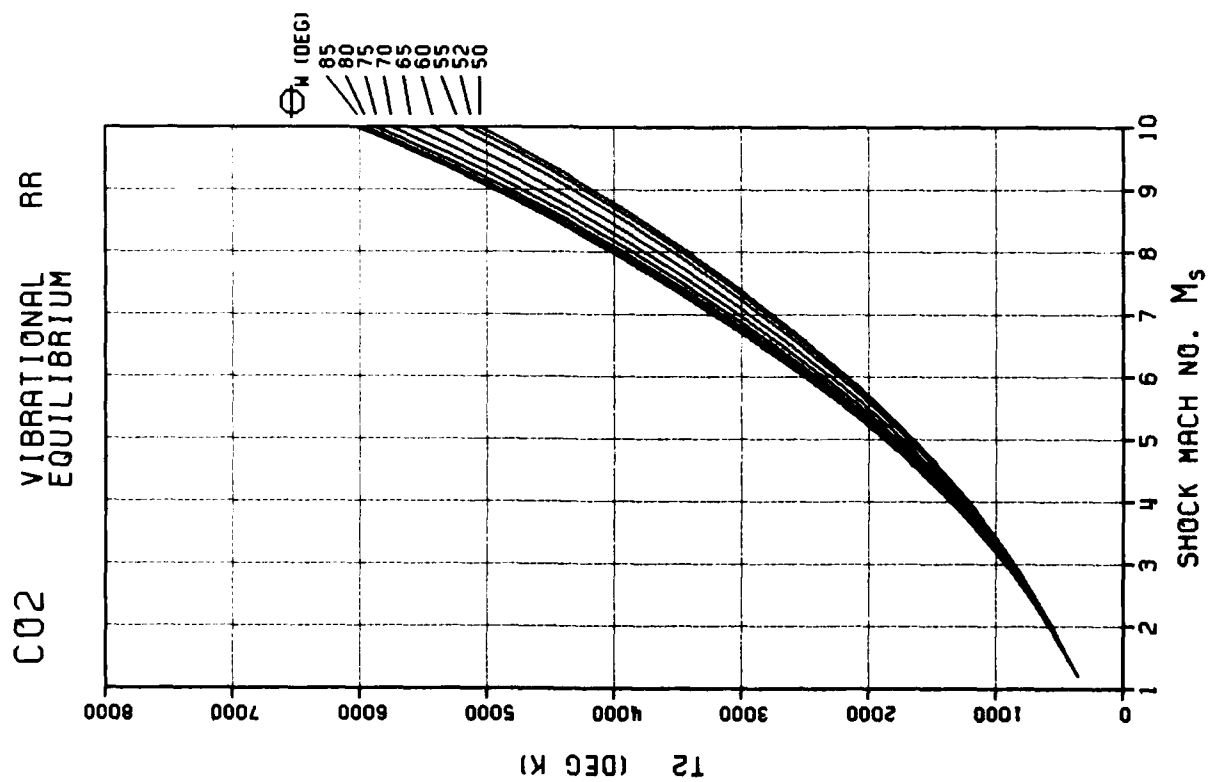


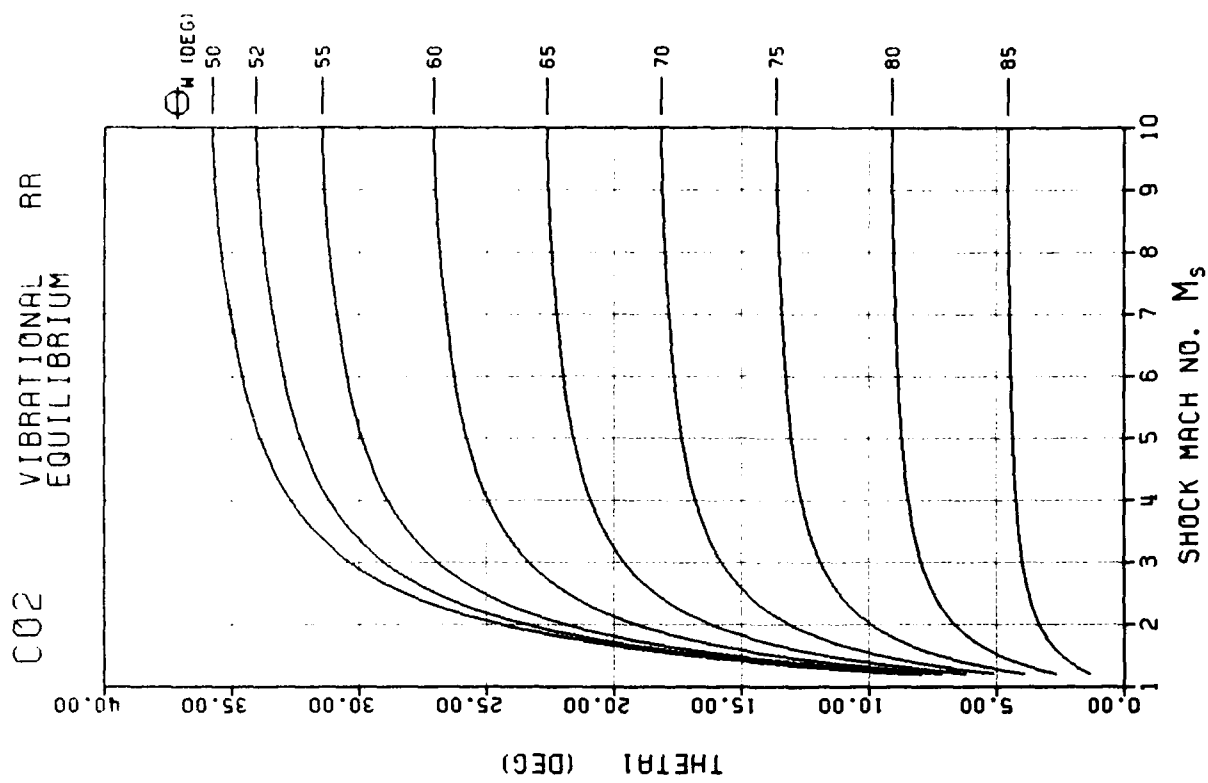
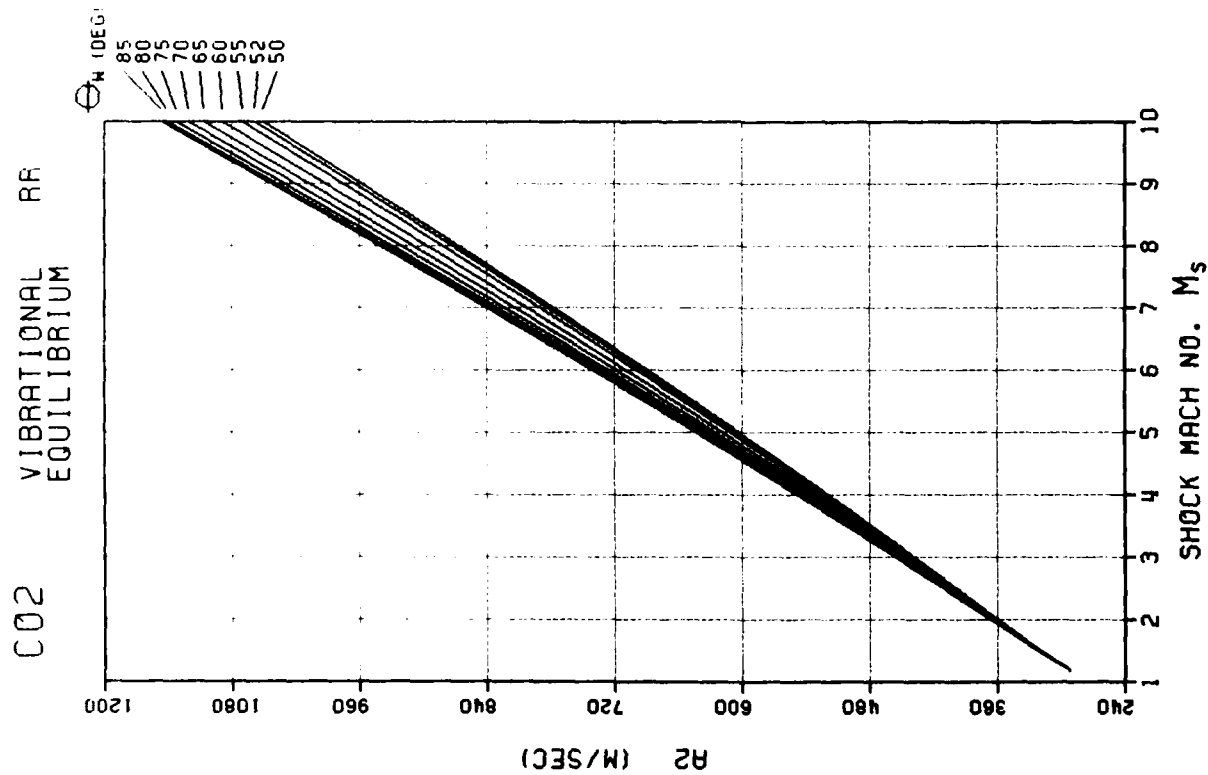


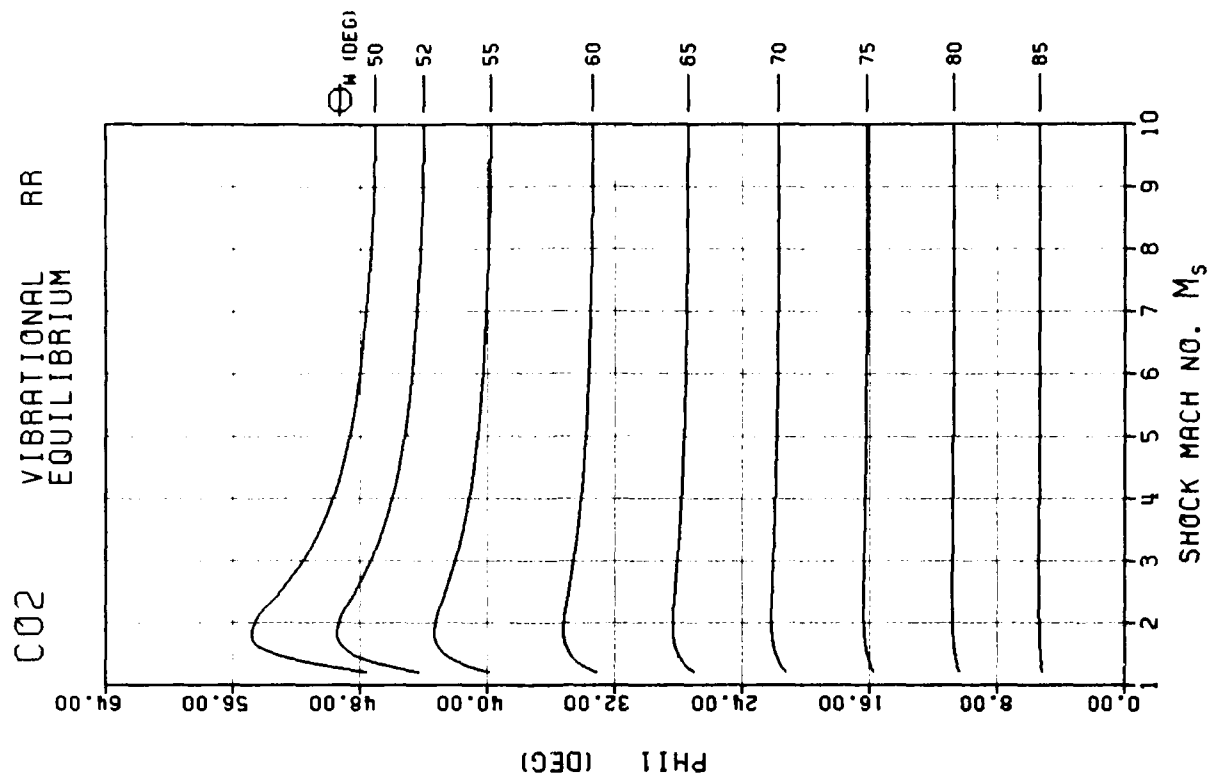
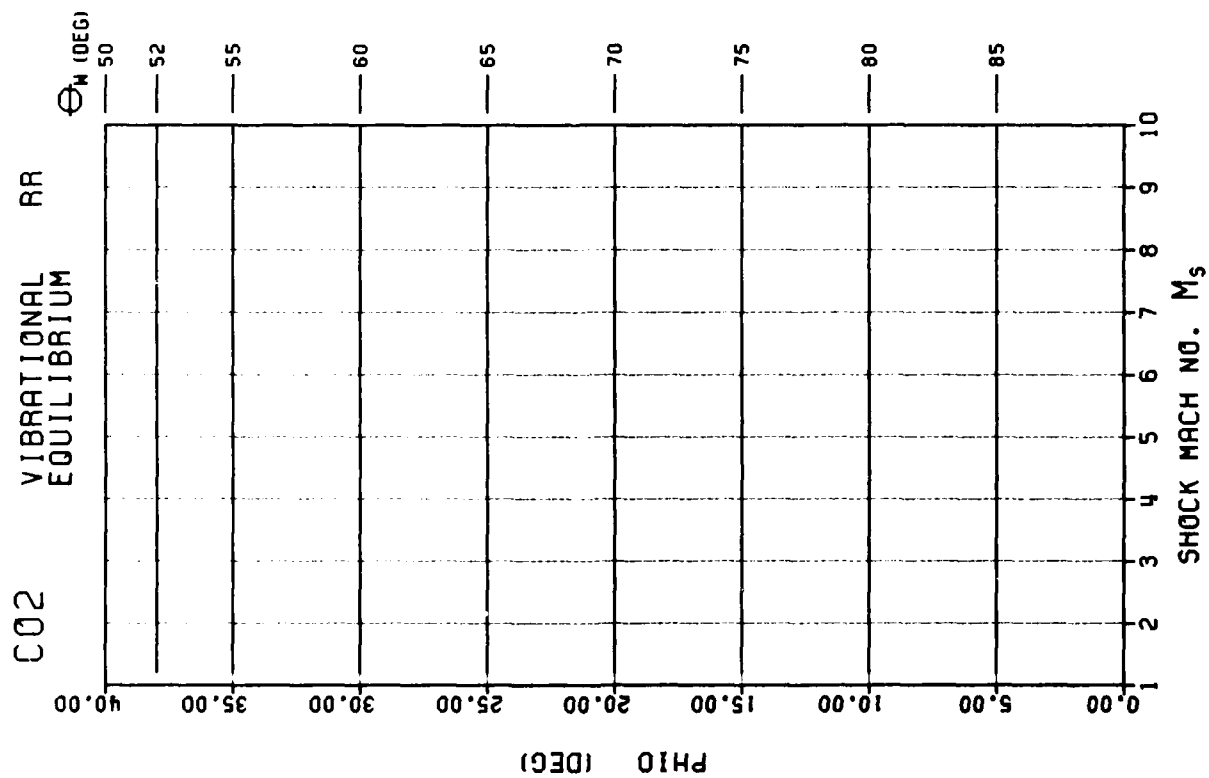
F - 152

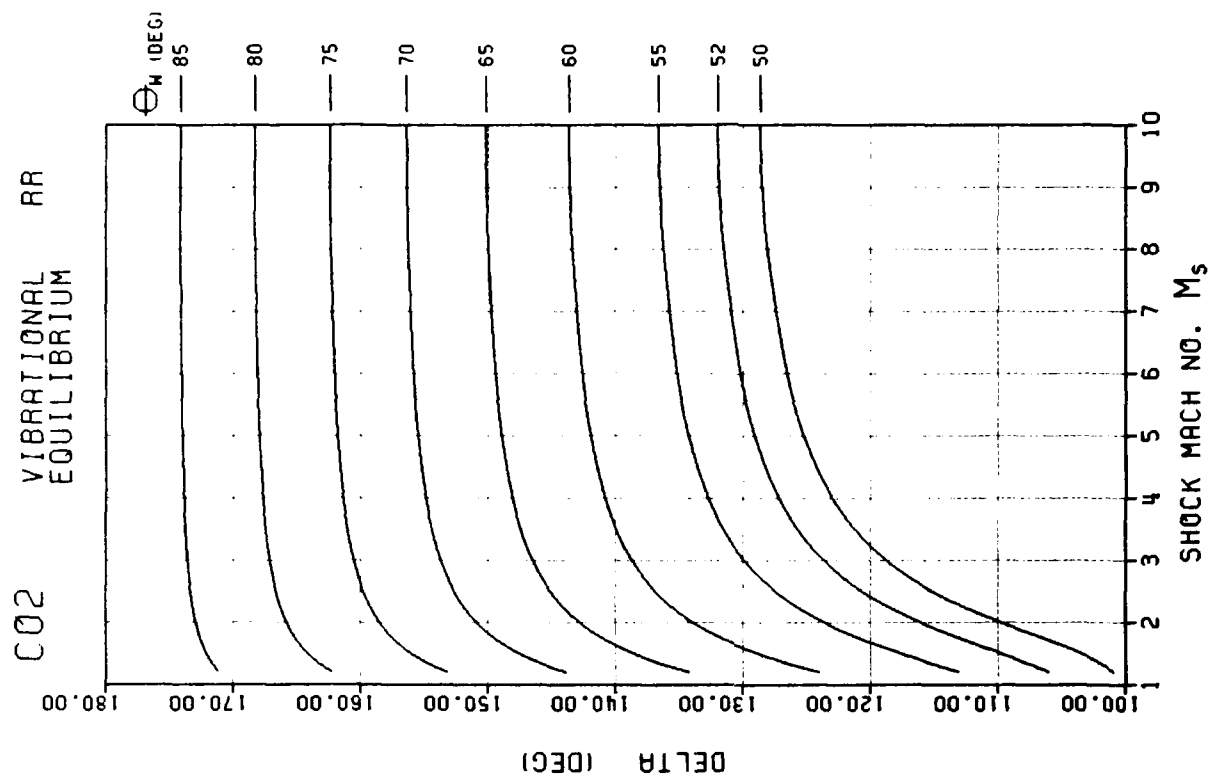
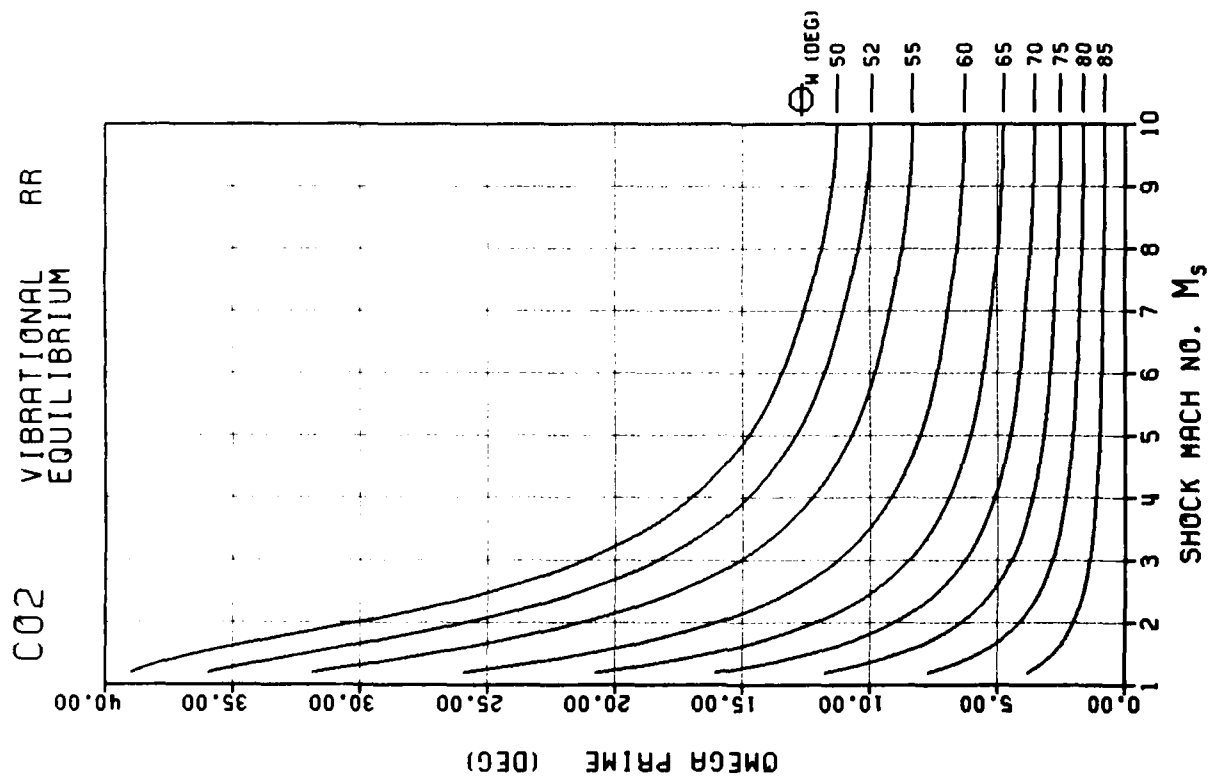


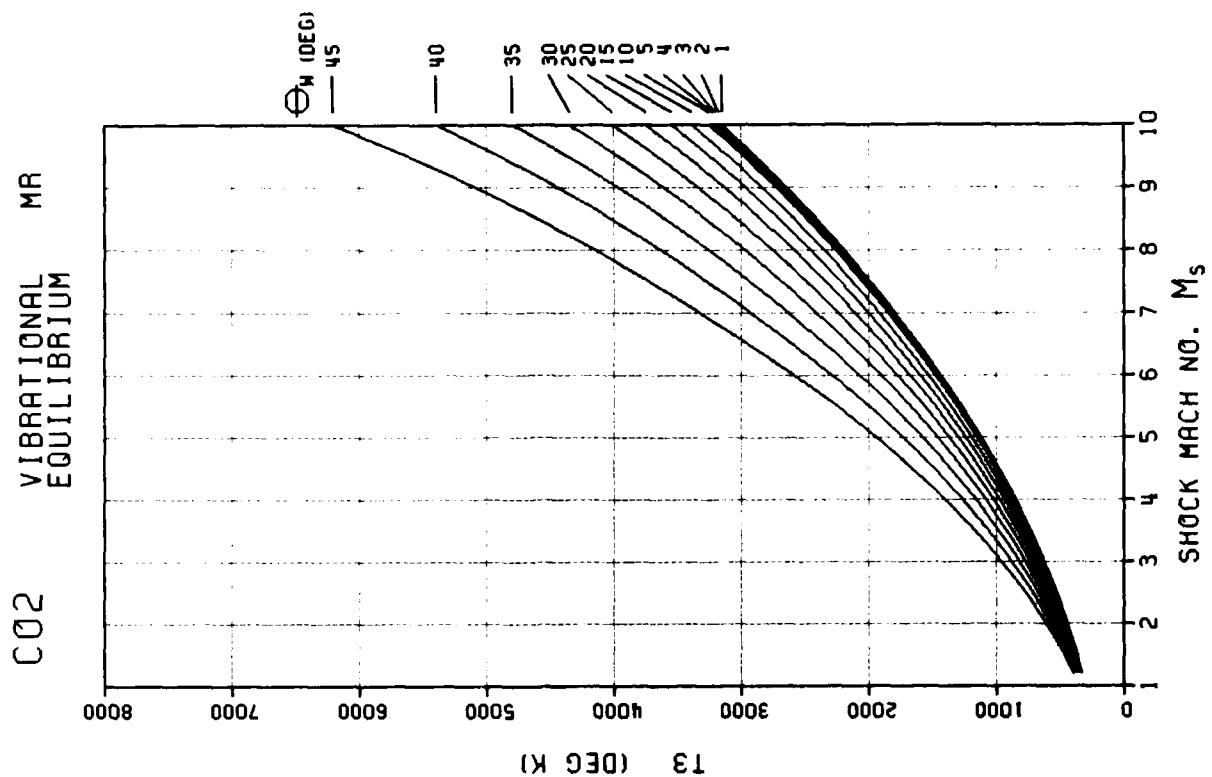
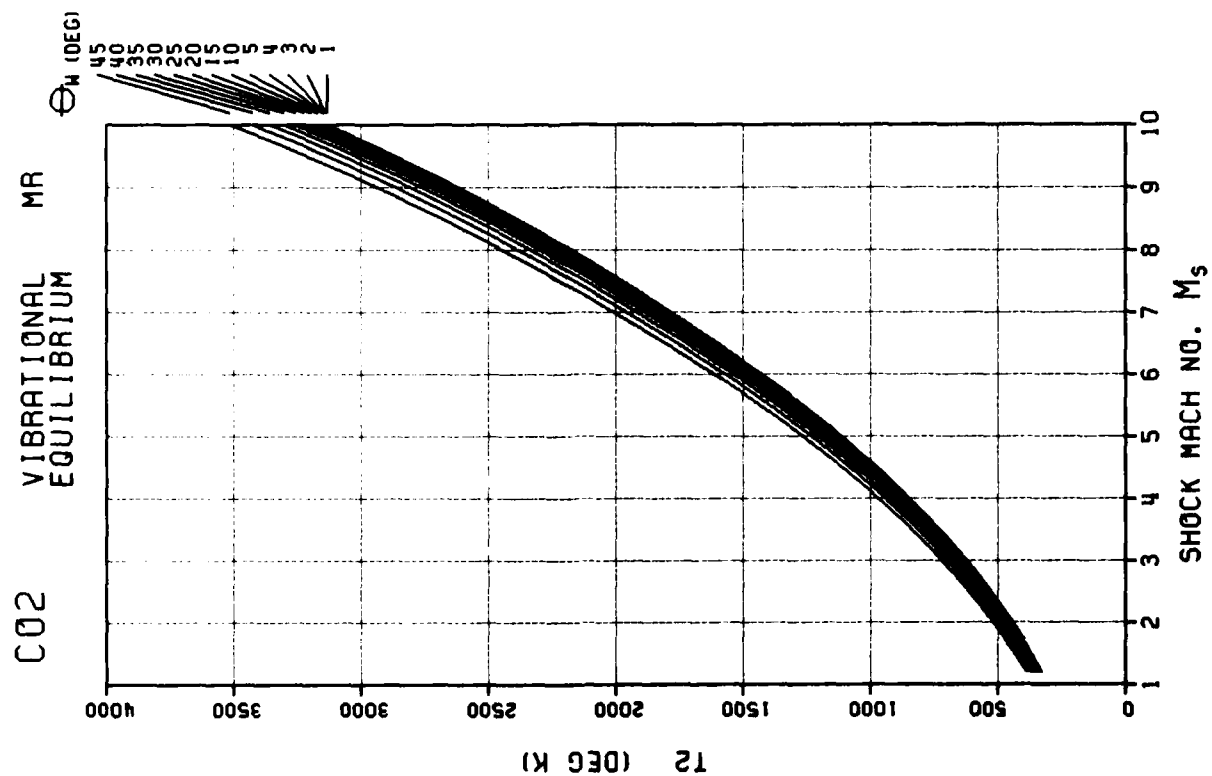


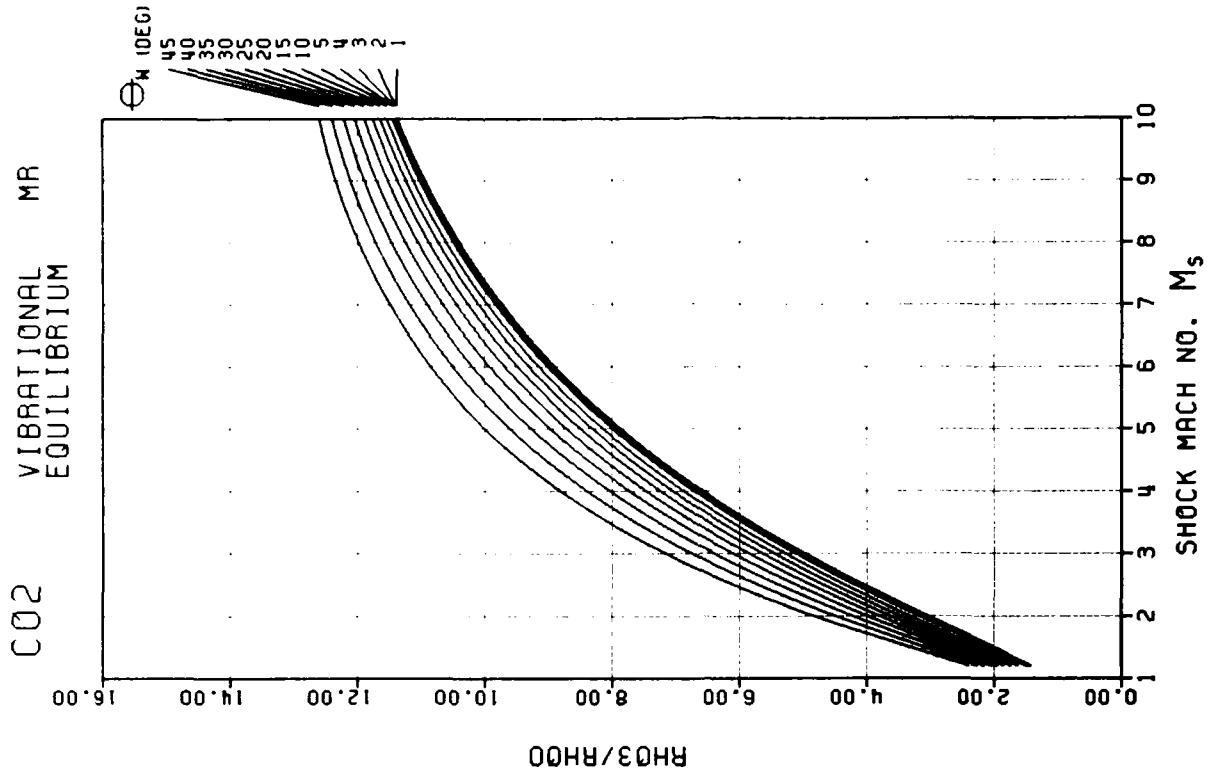
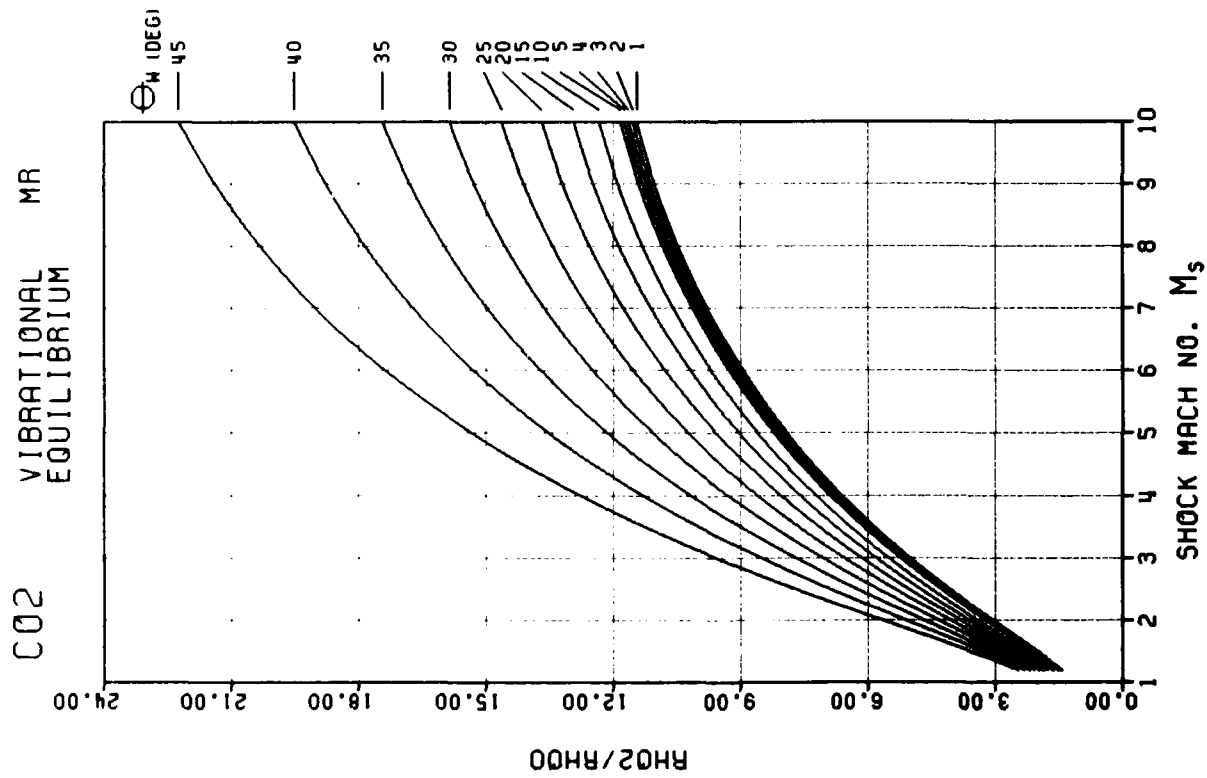


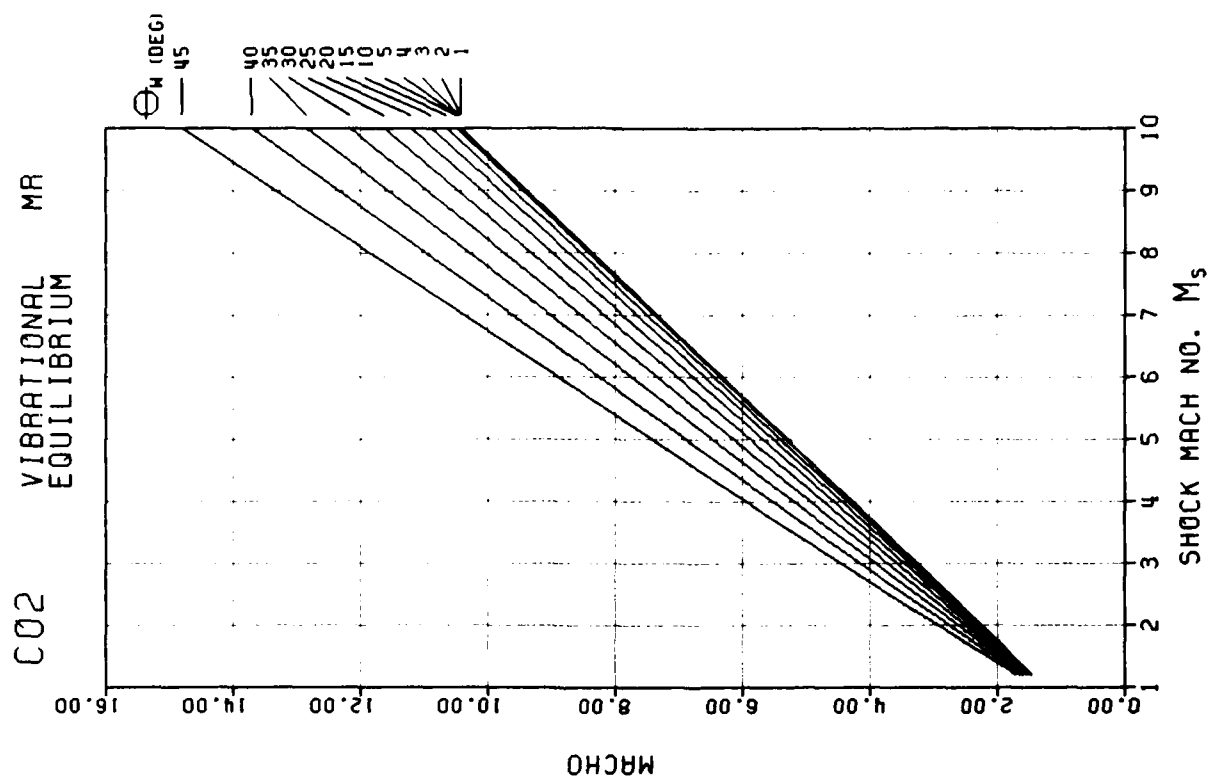
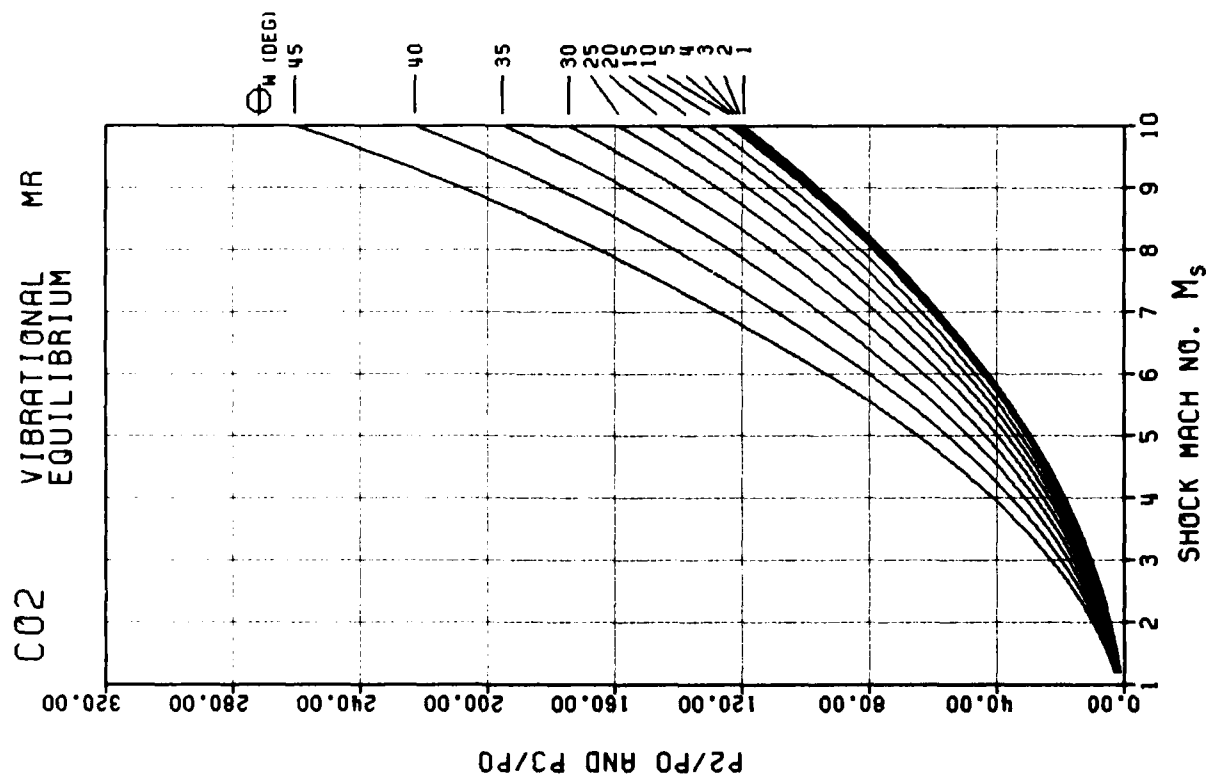


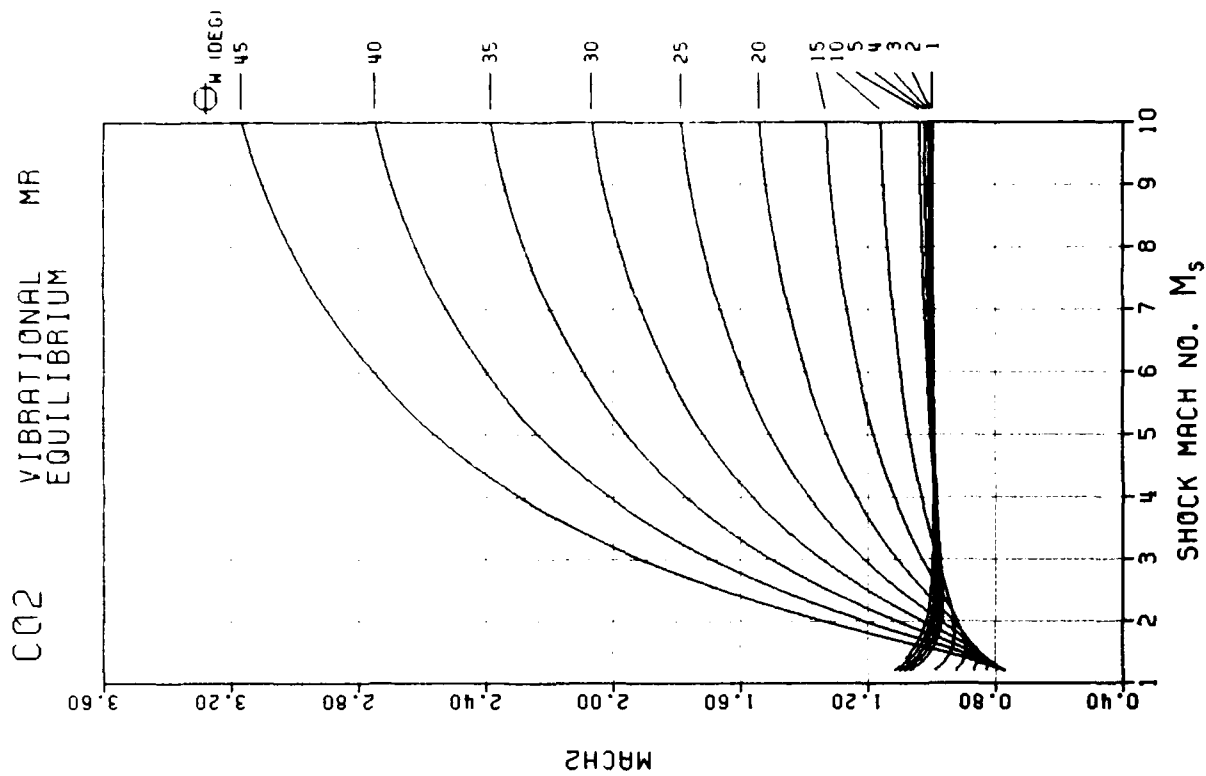
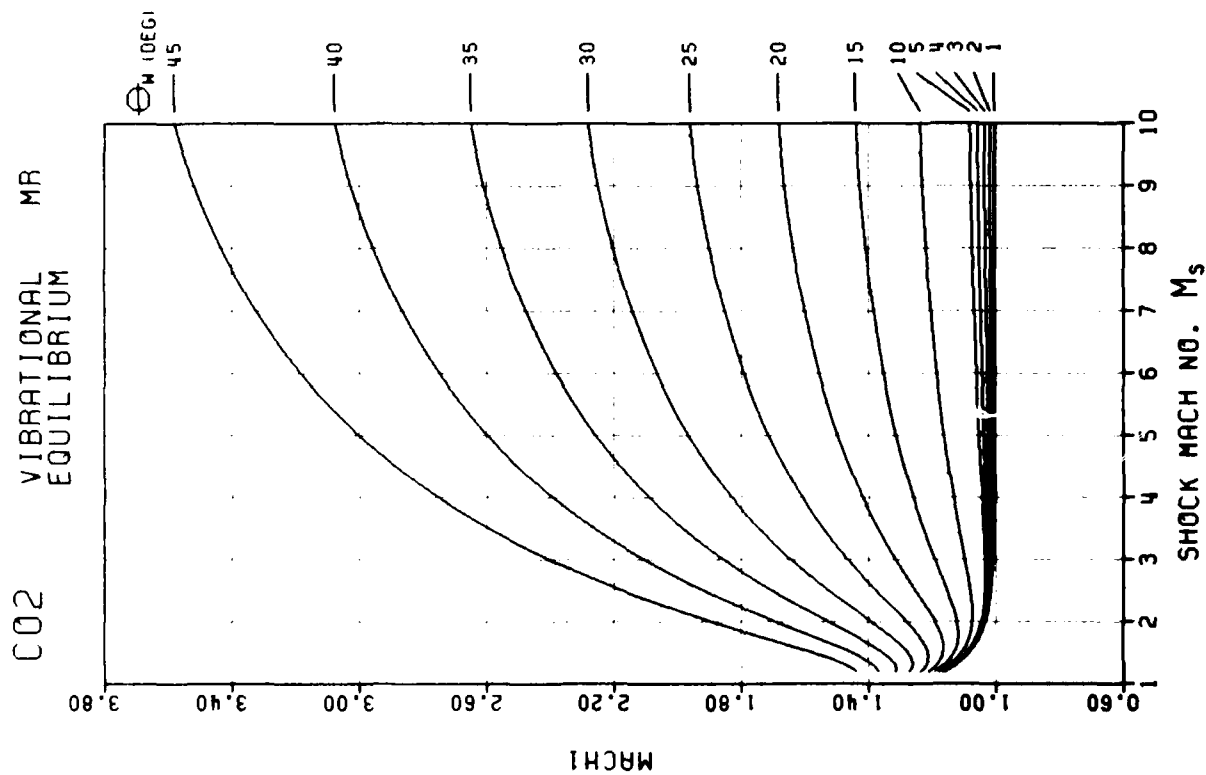


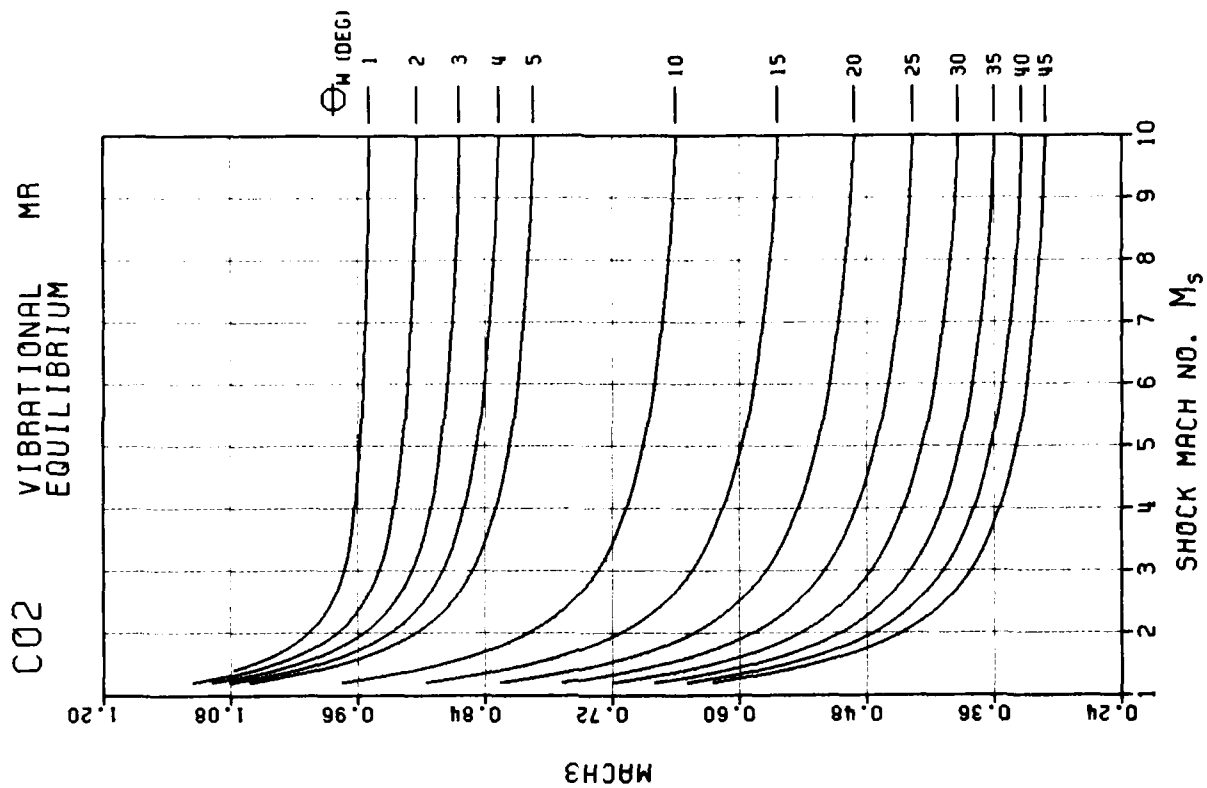
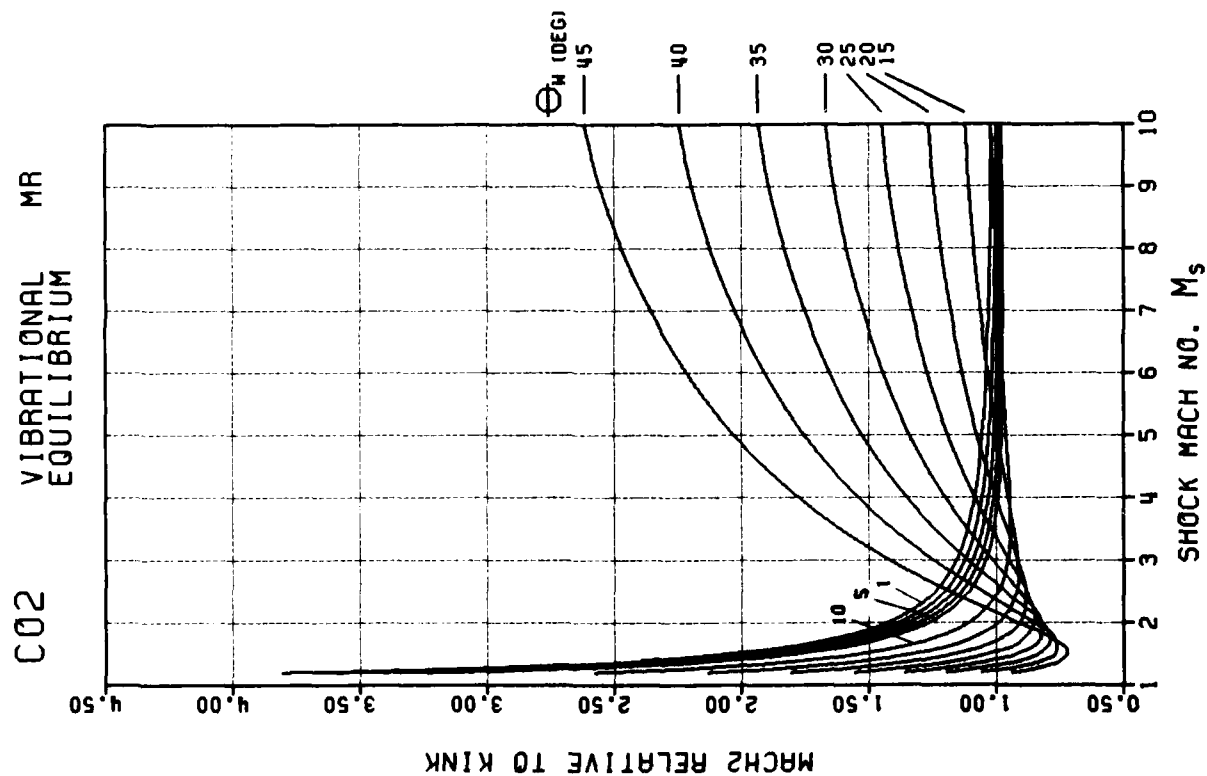


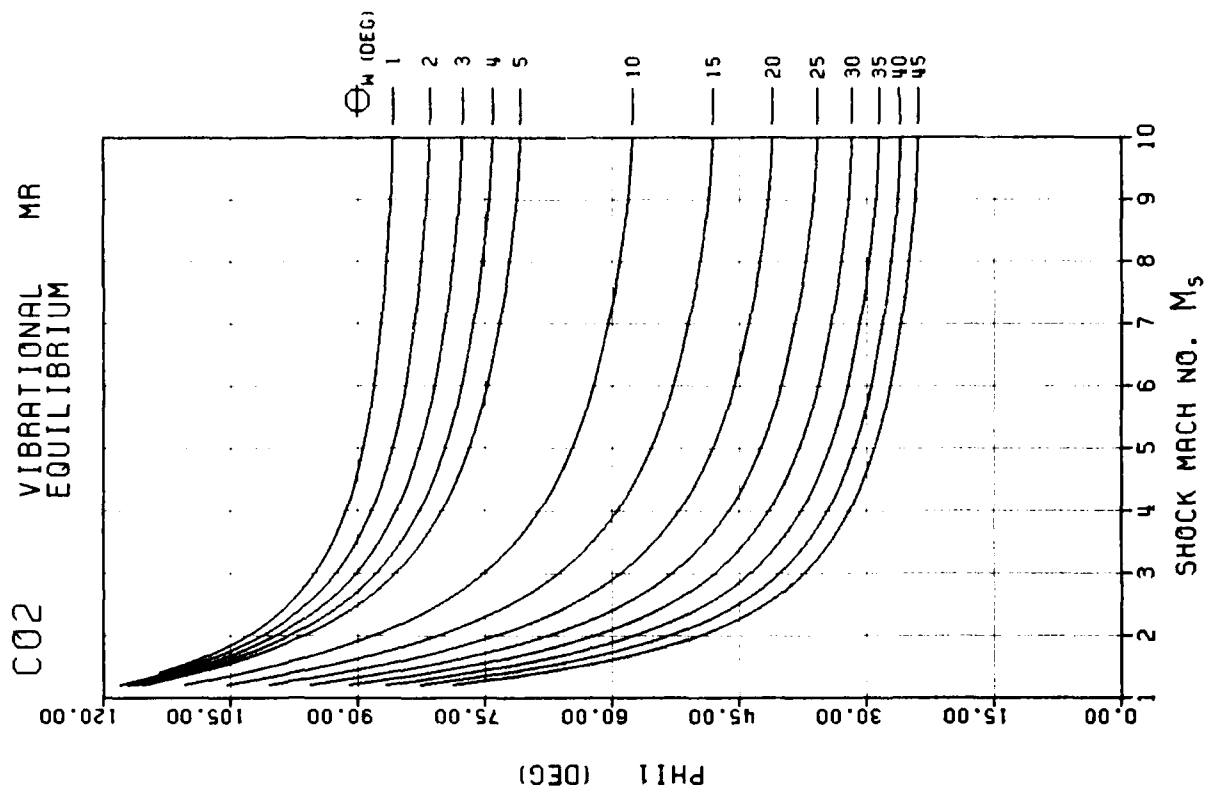
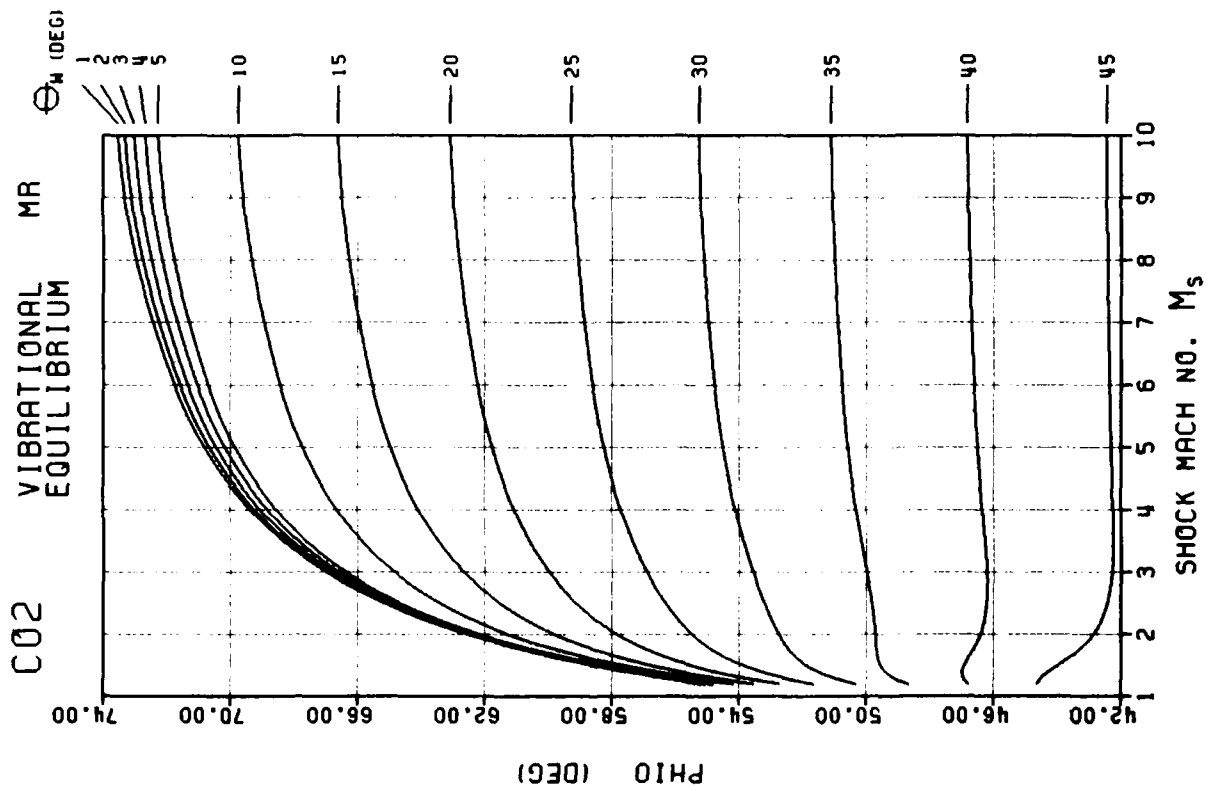


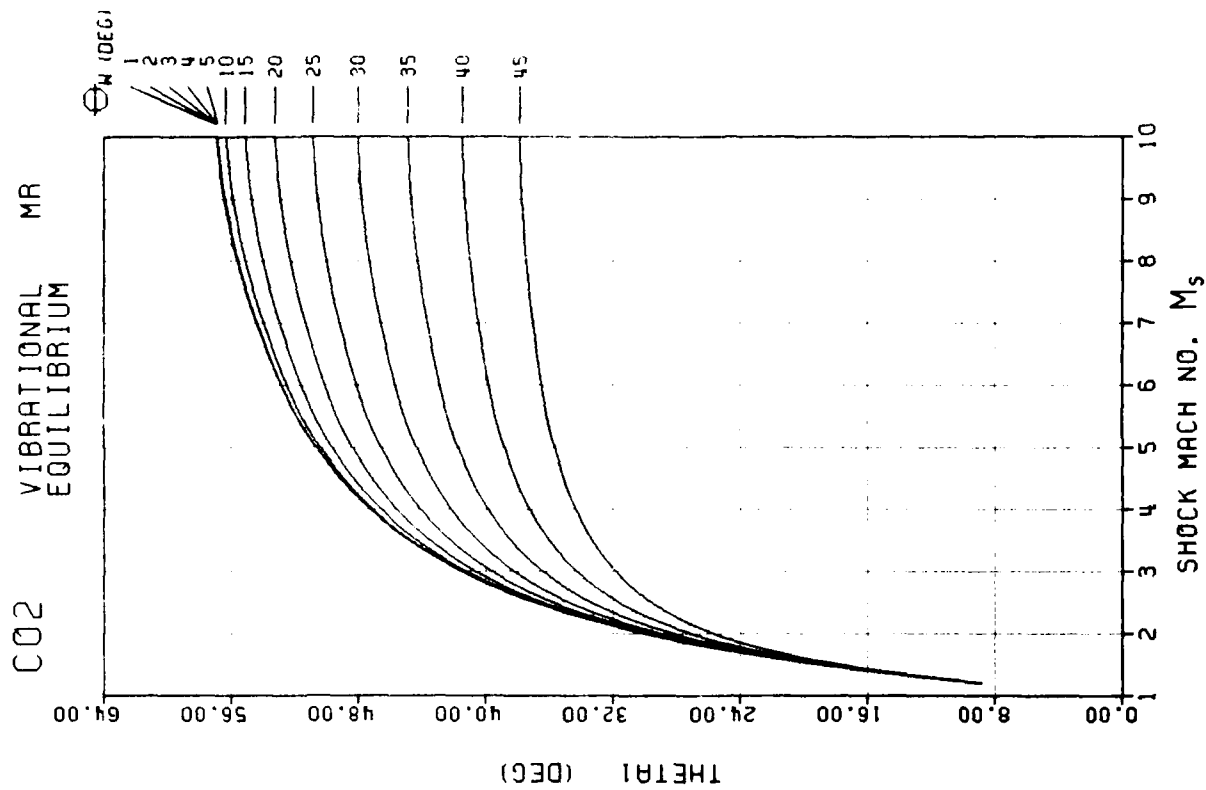
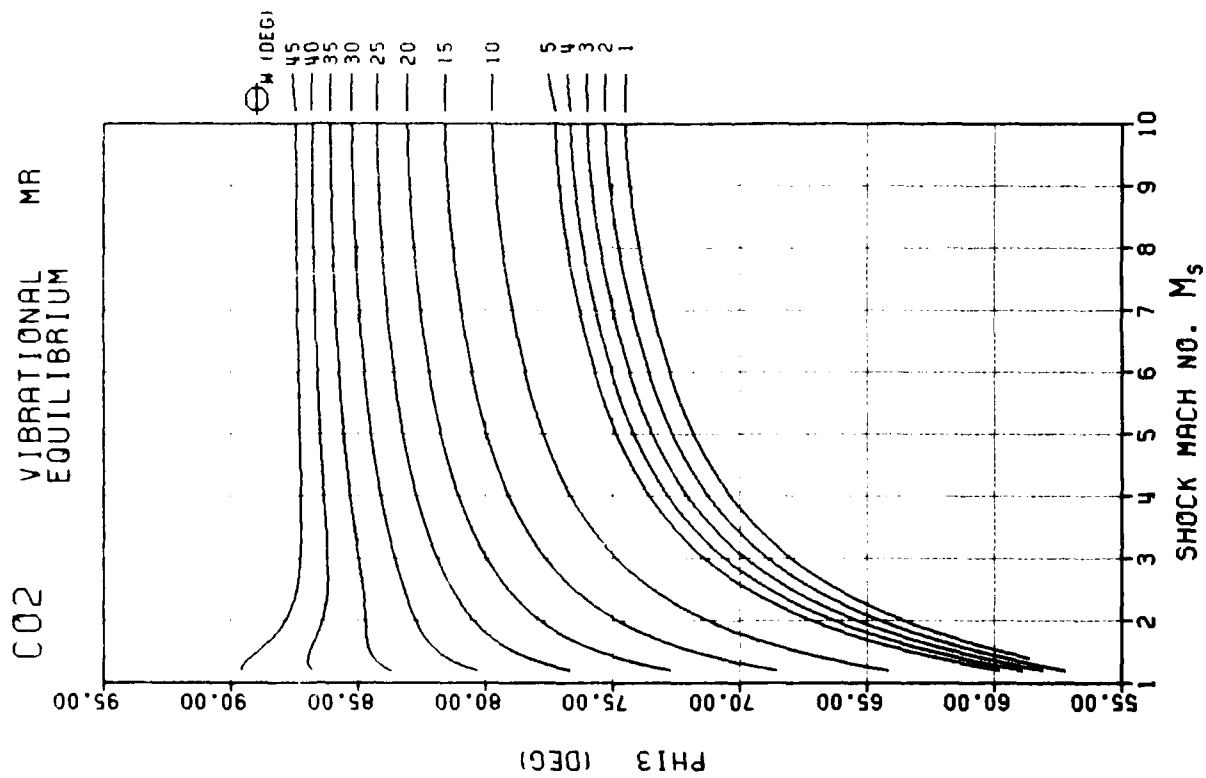


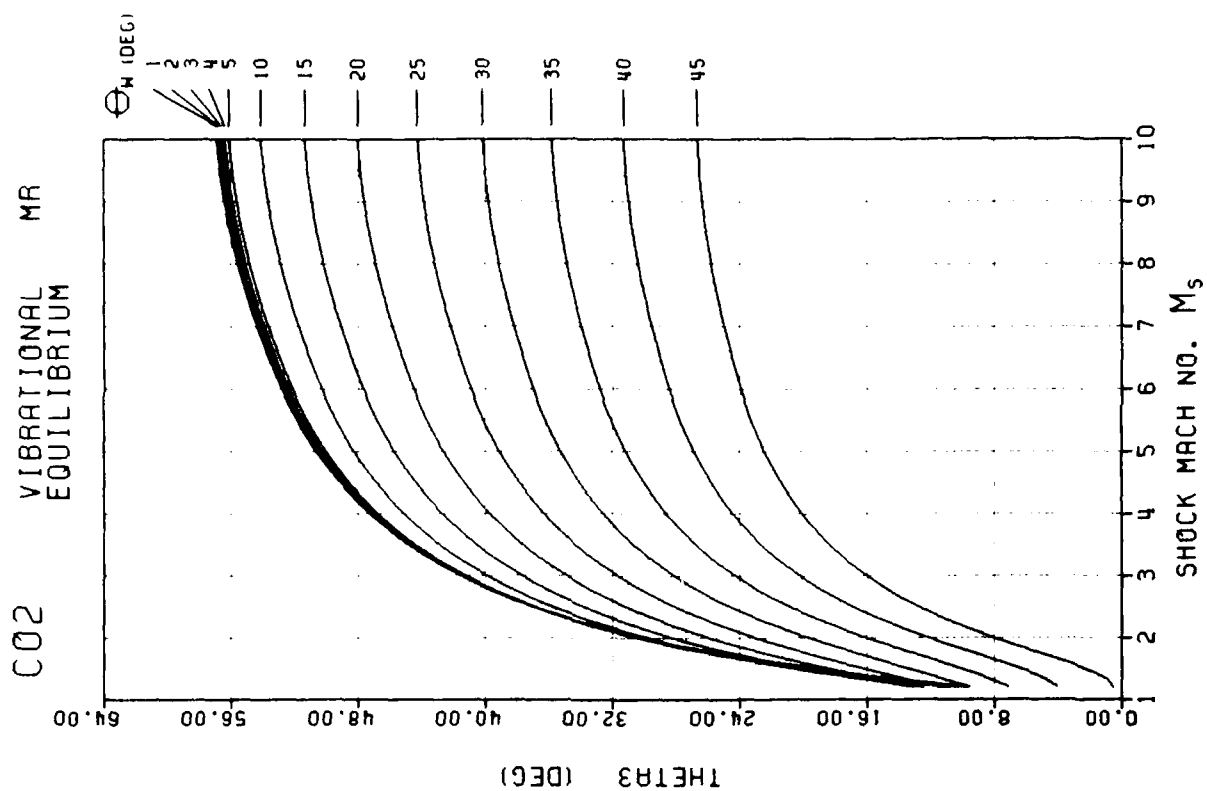
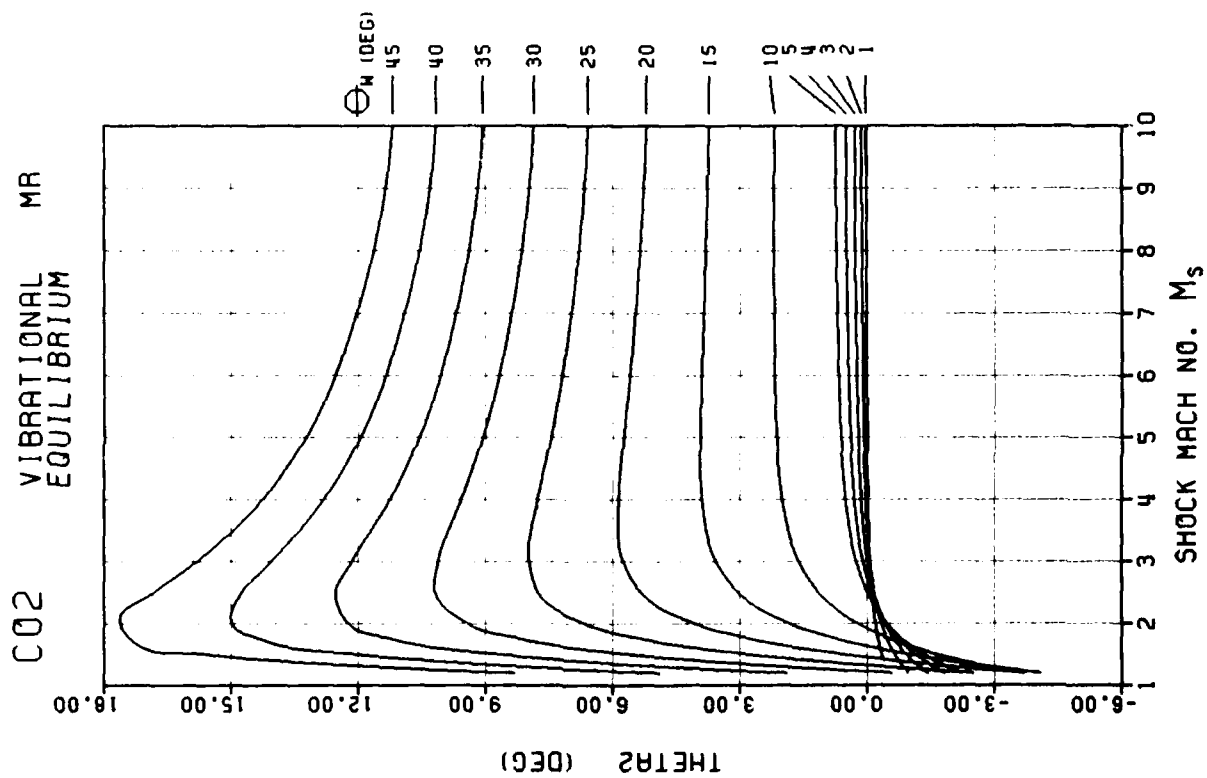


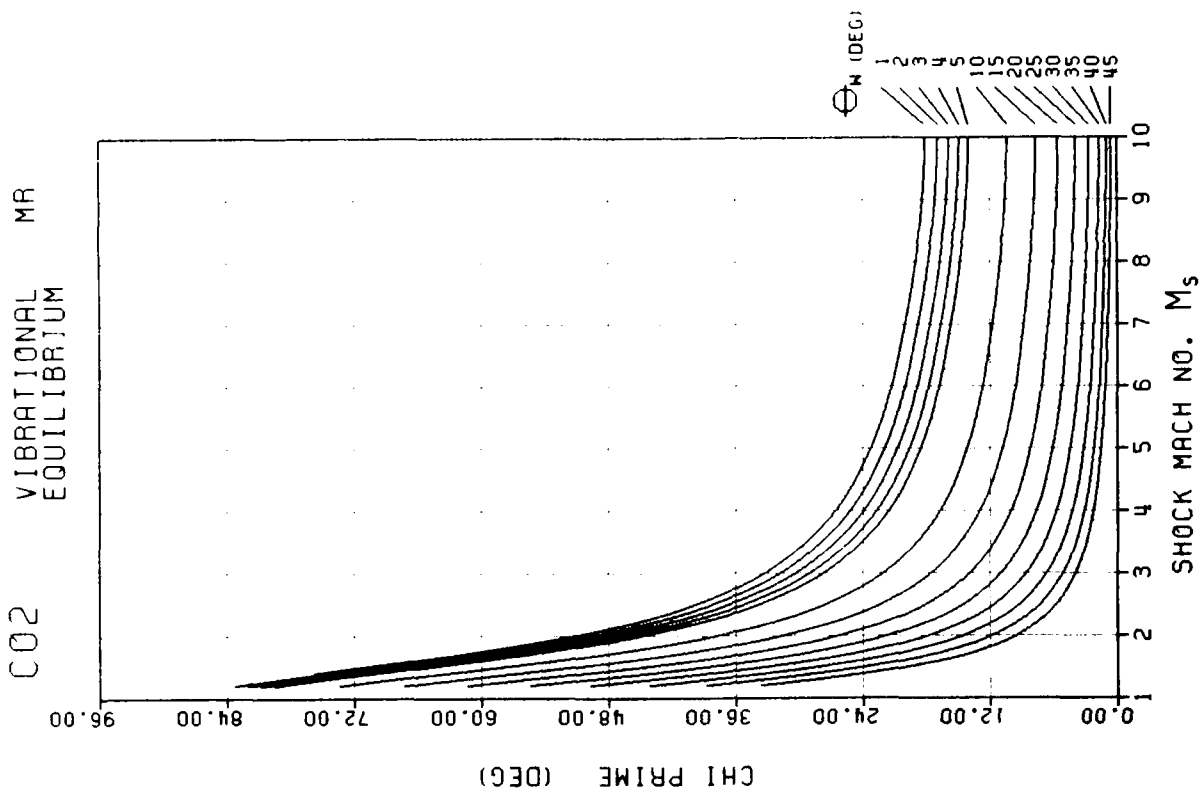
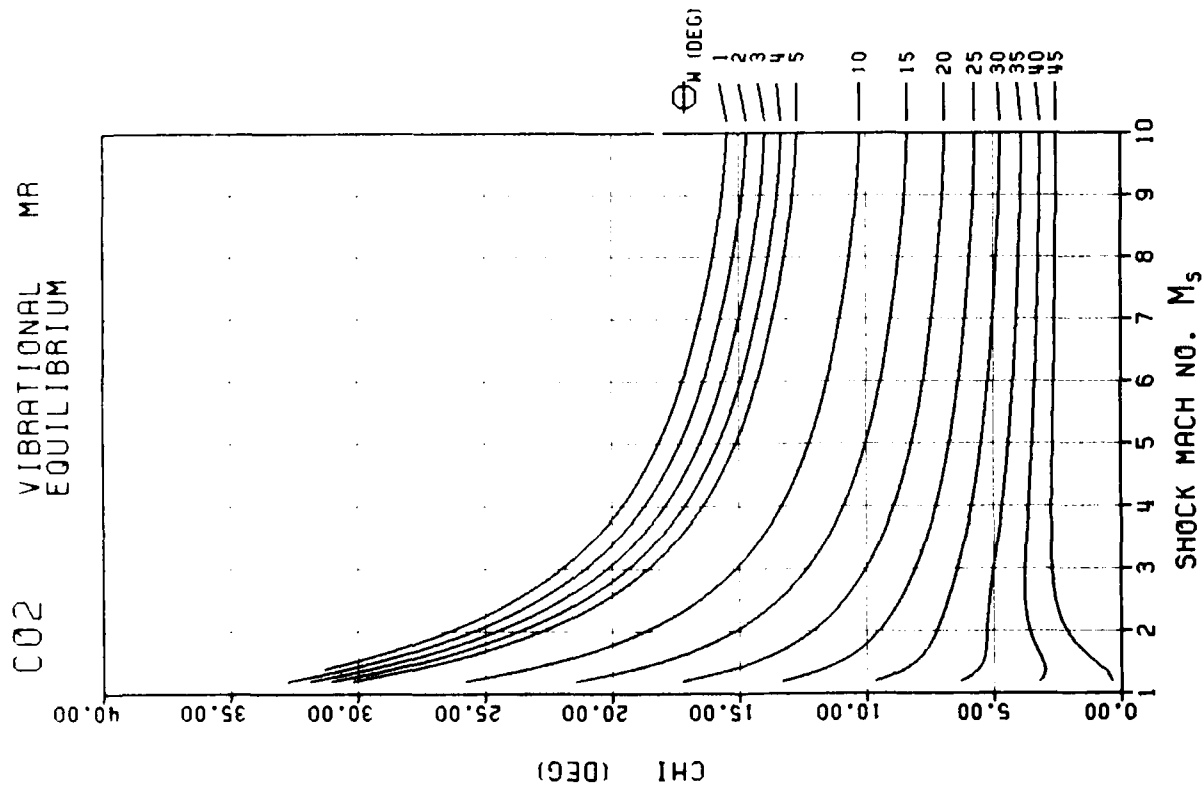


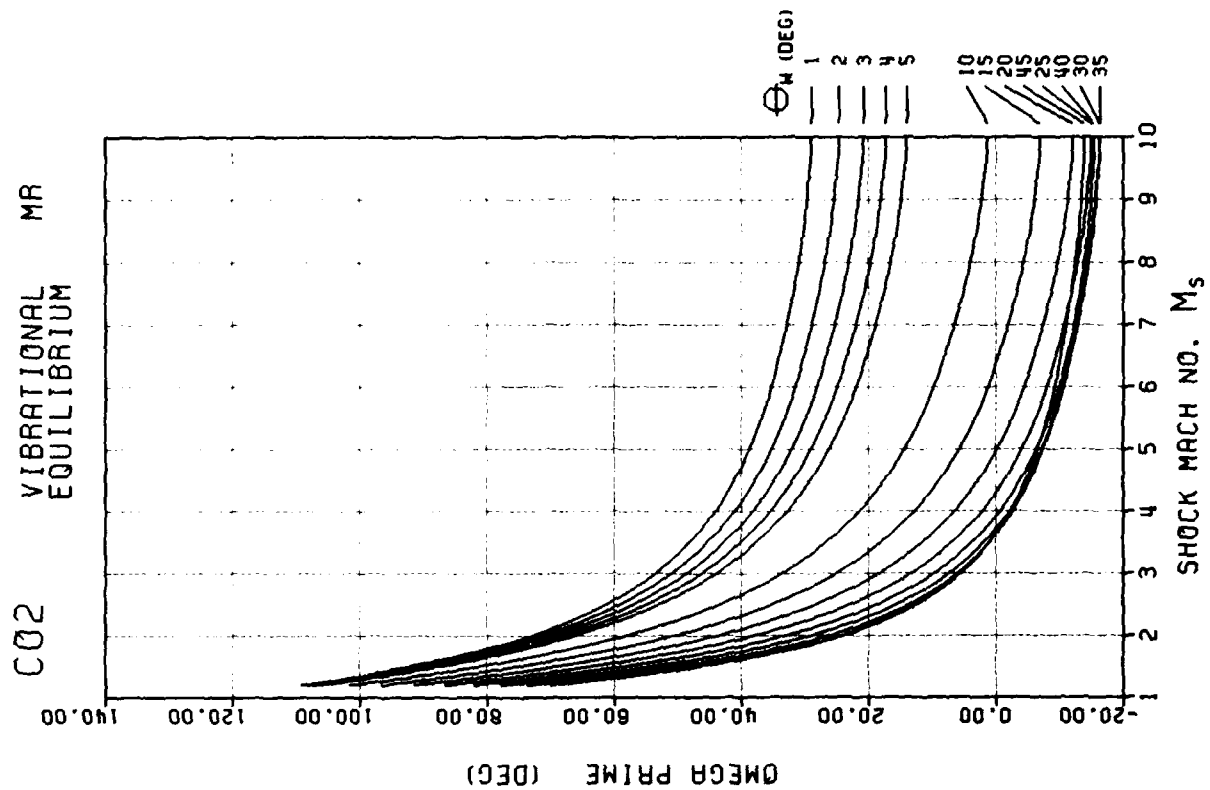
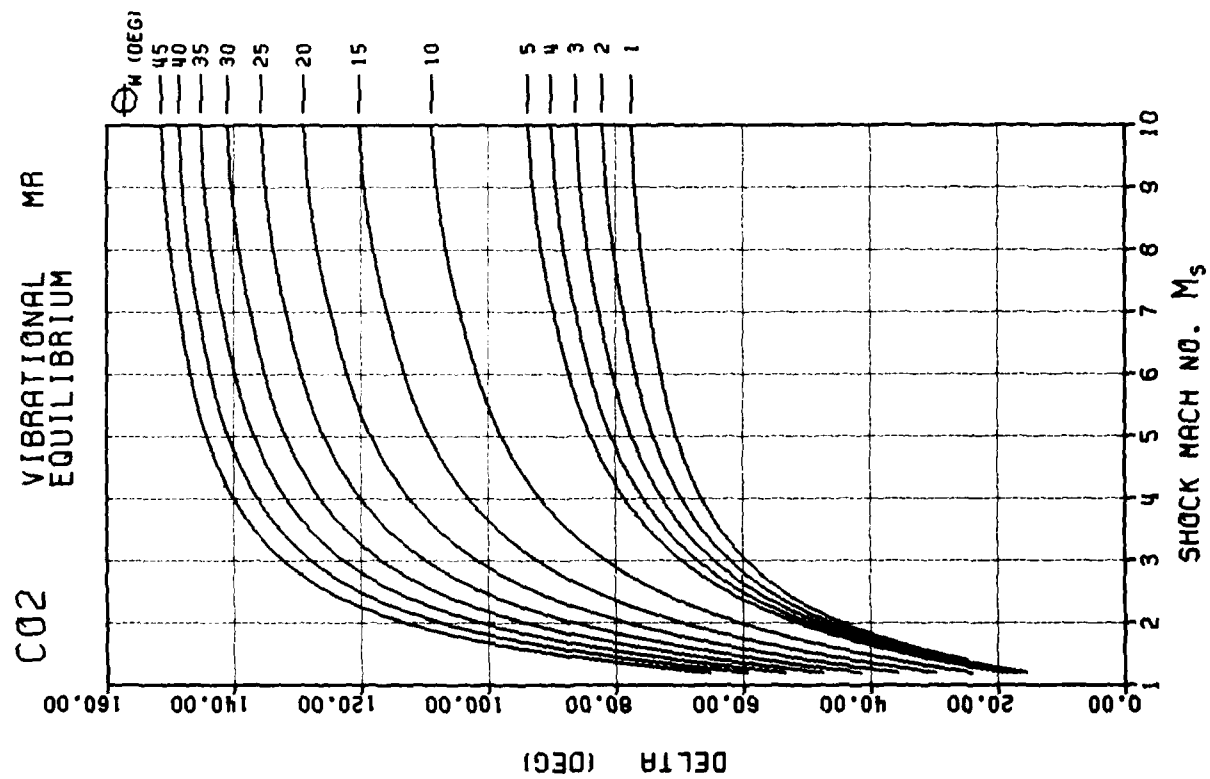




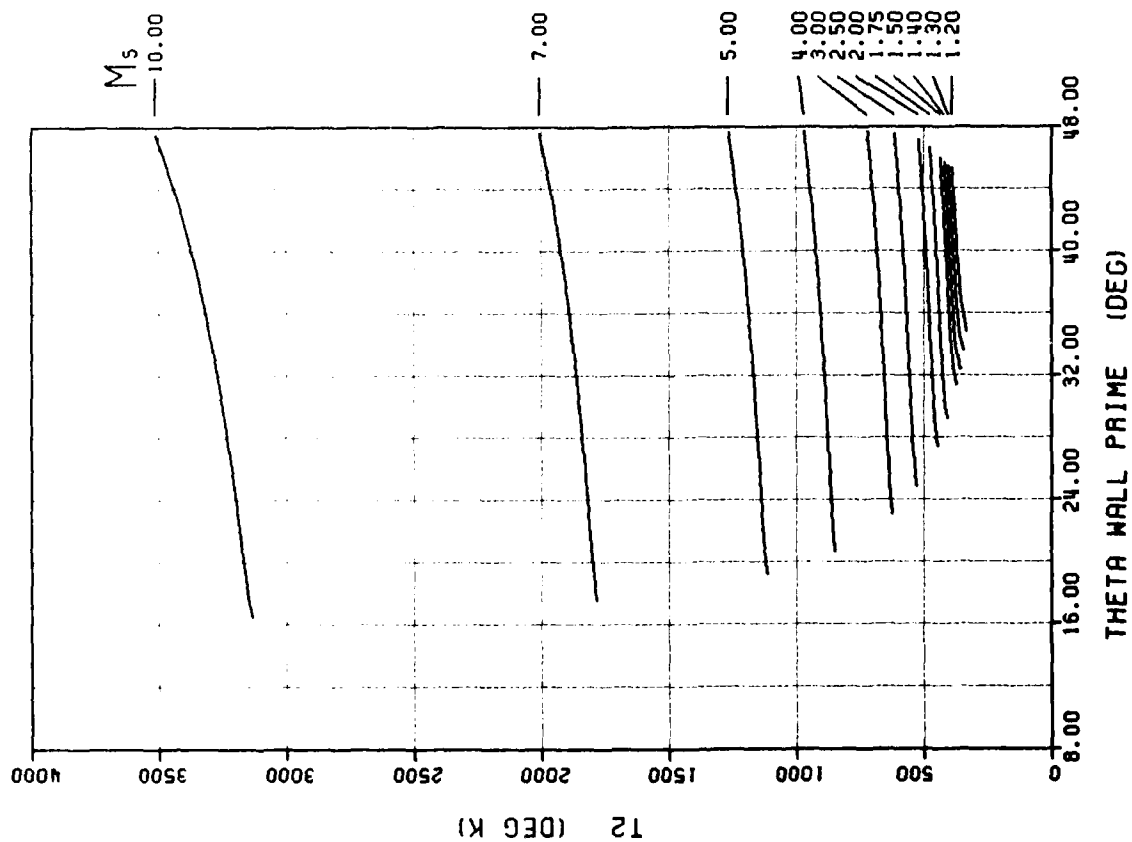




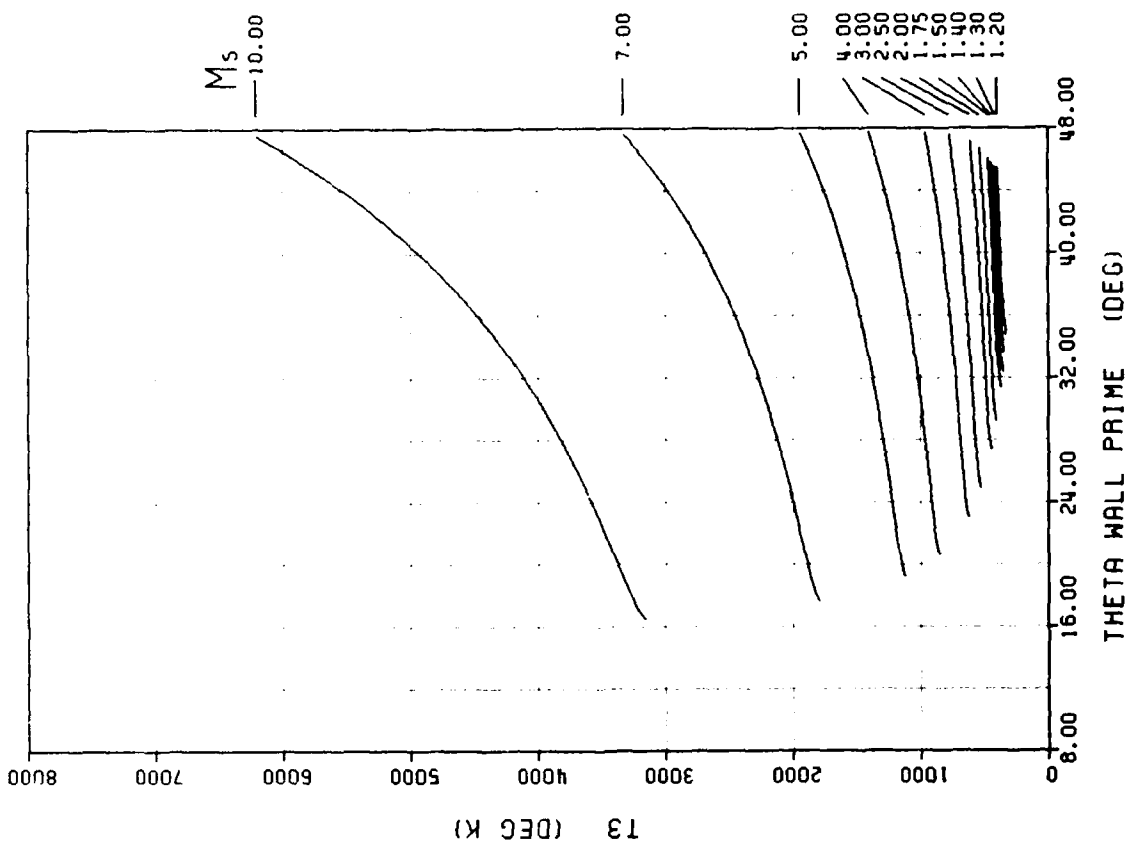


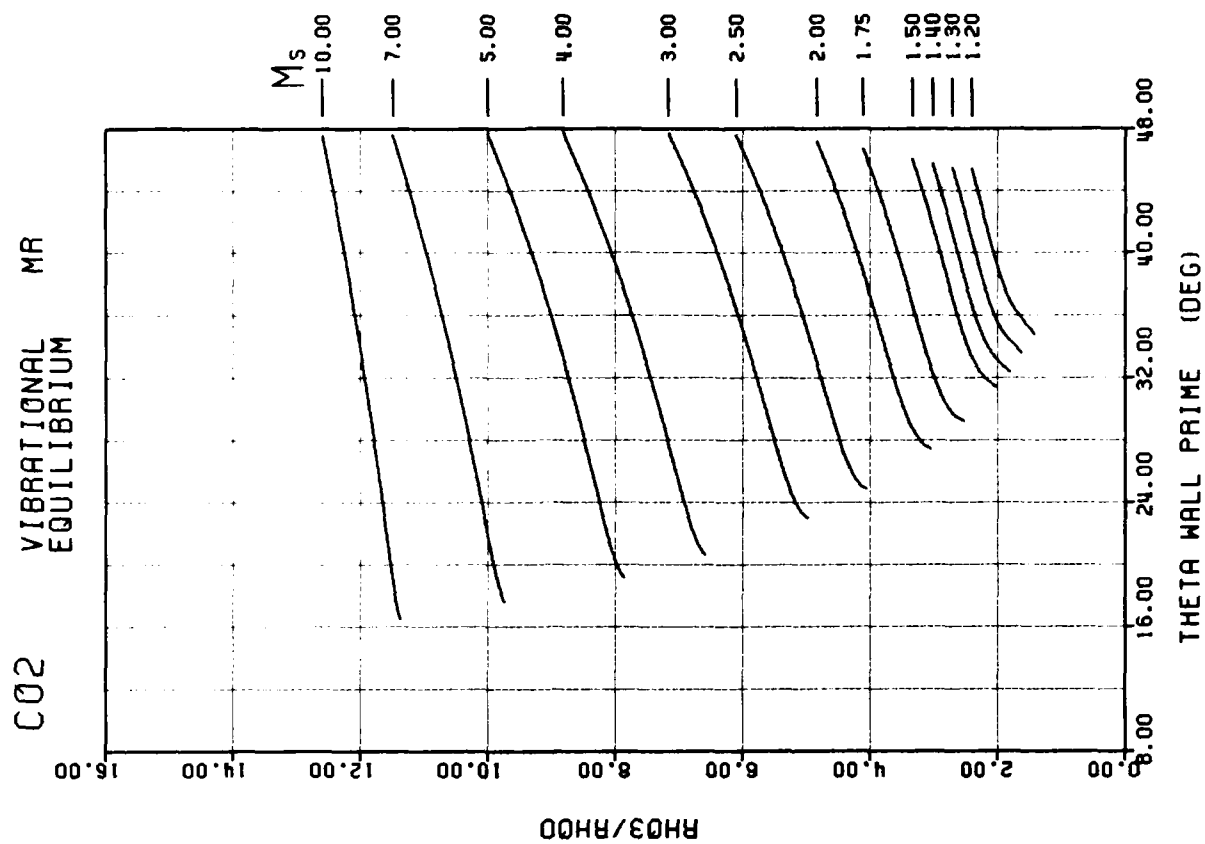
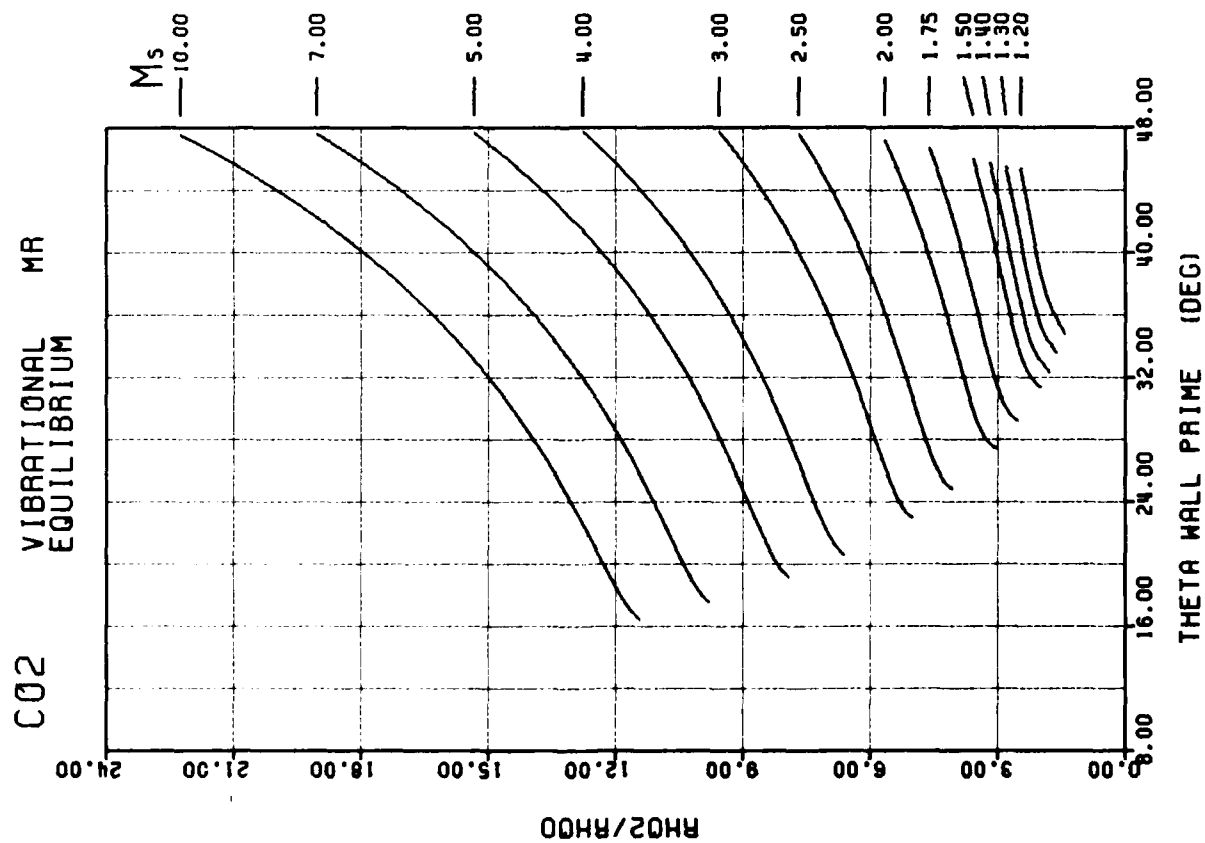


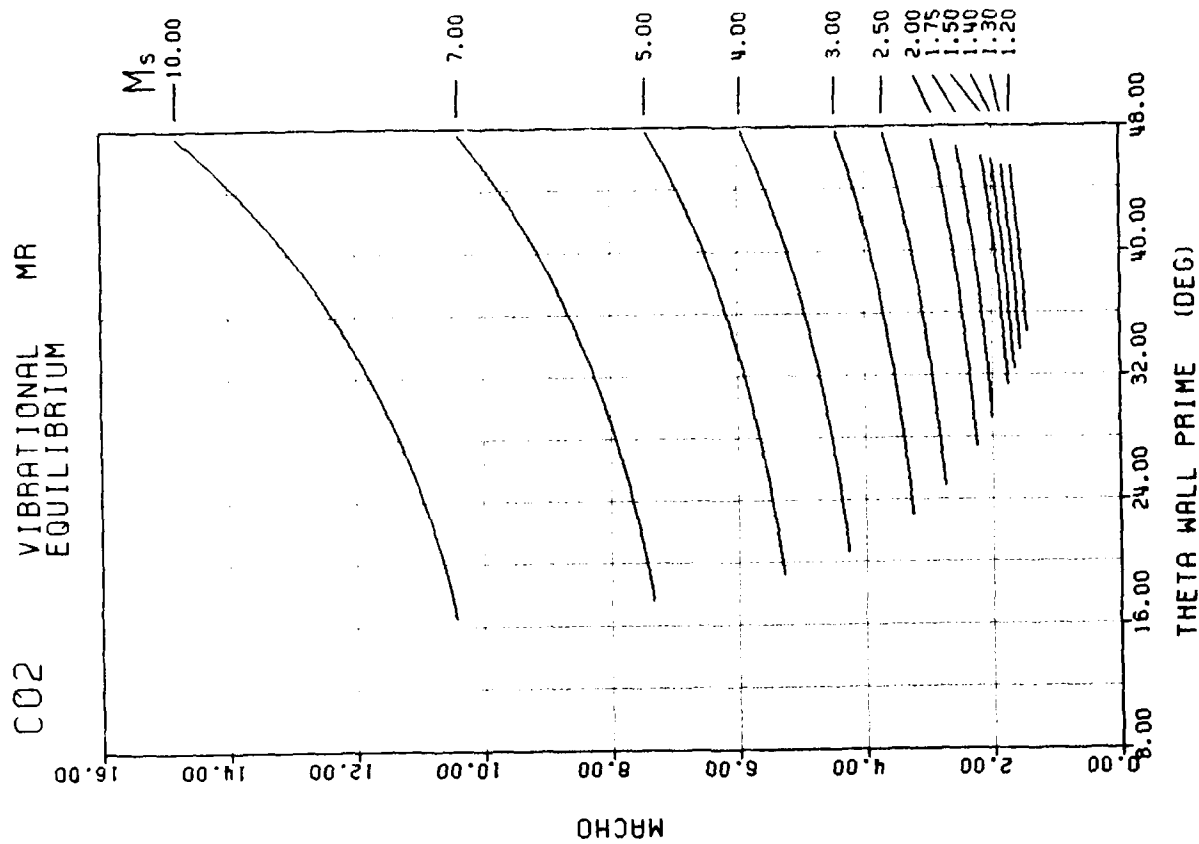
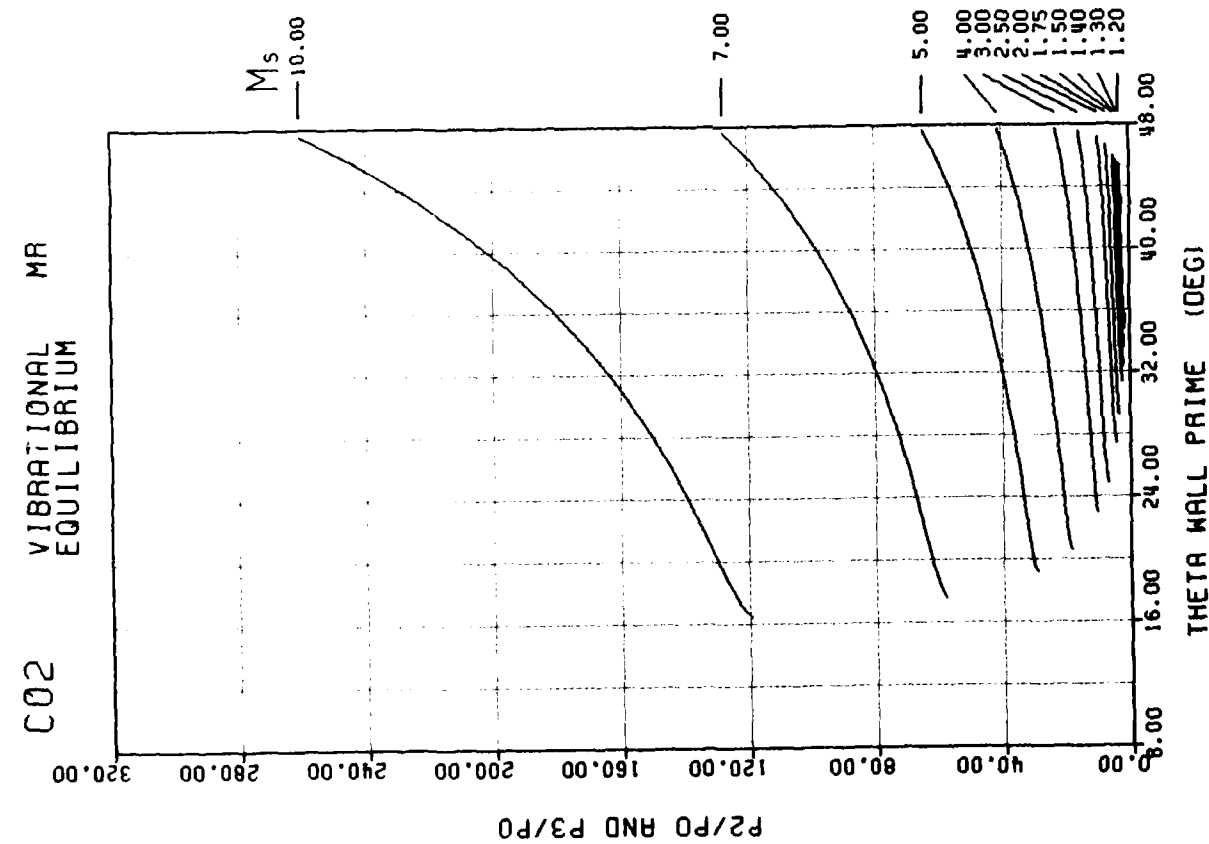
C02 VIBRATIONAL EQUILIBRIUM MR

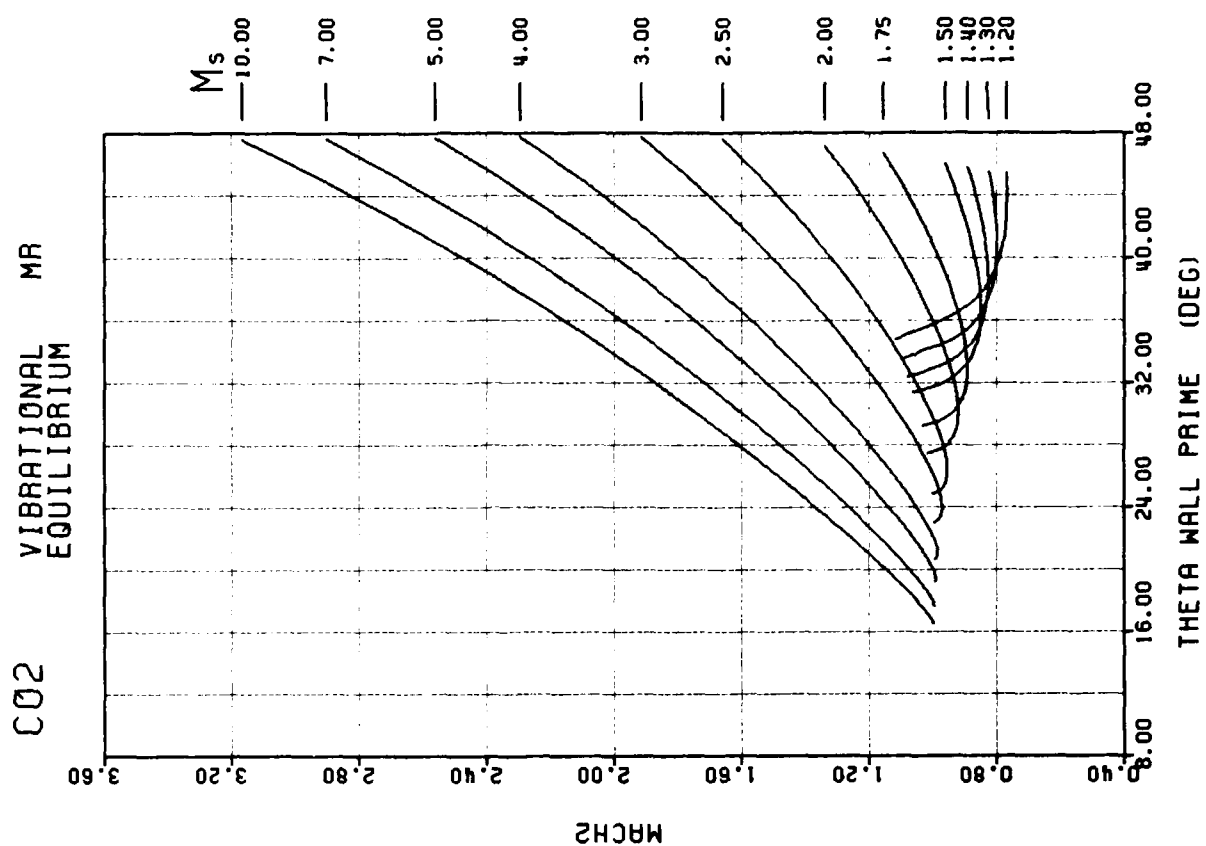
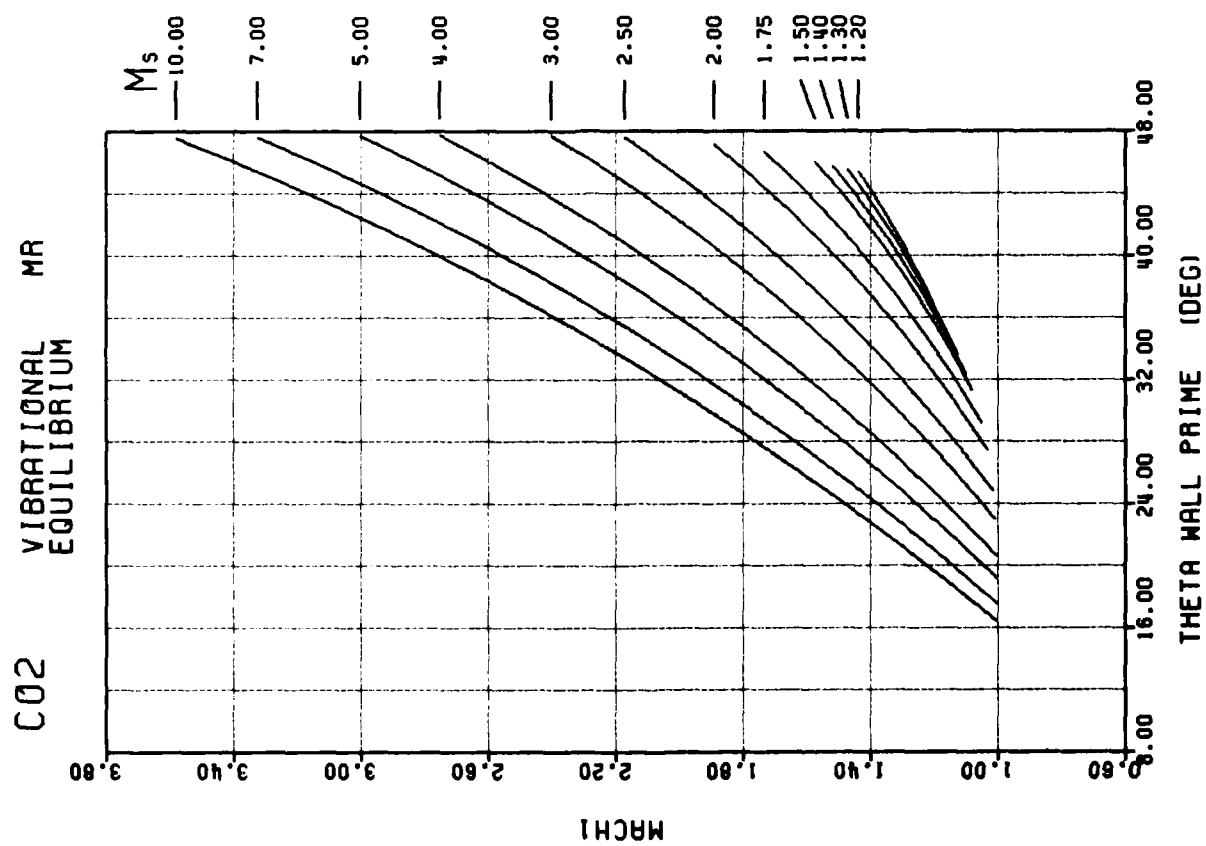


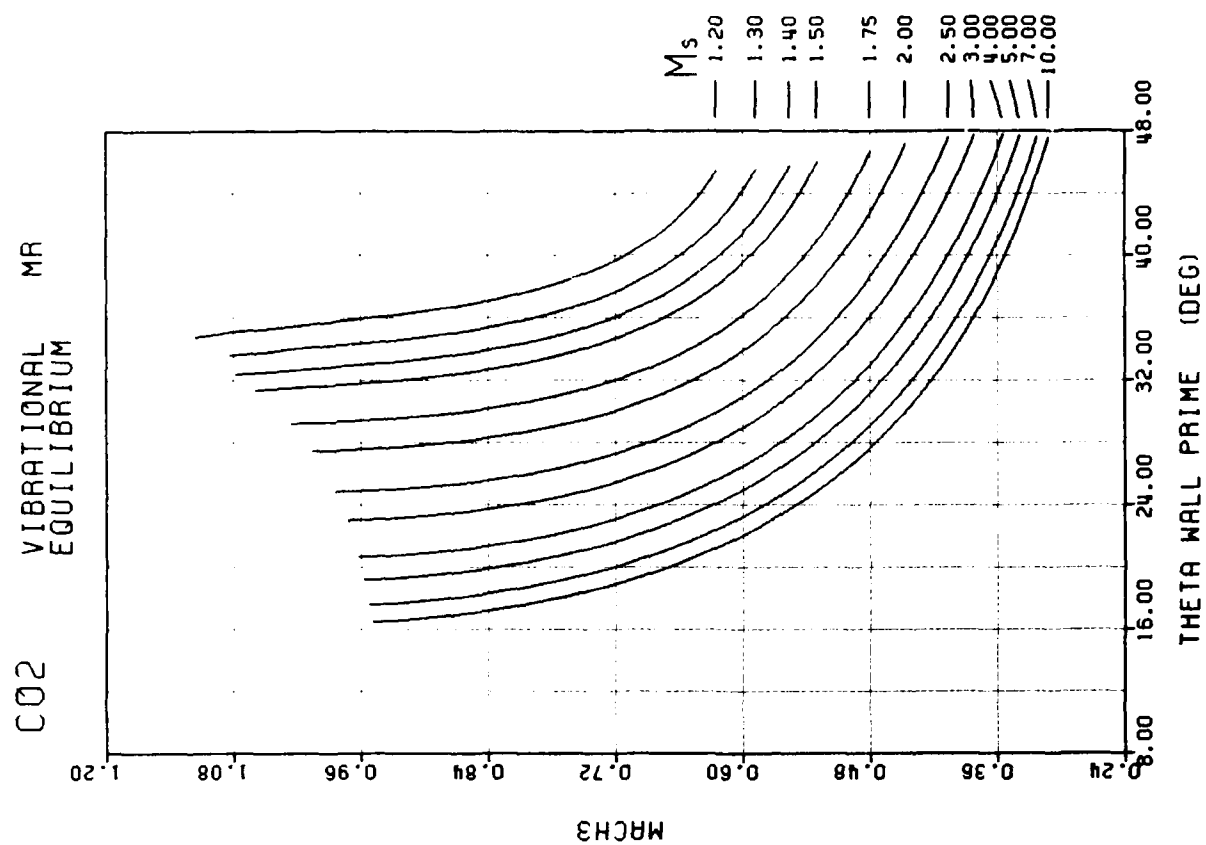
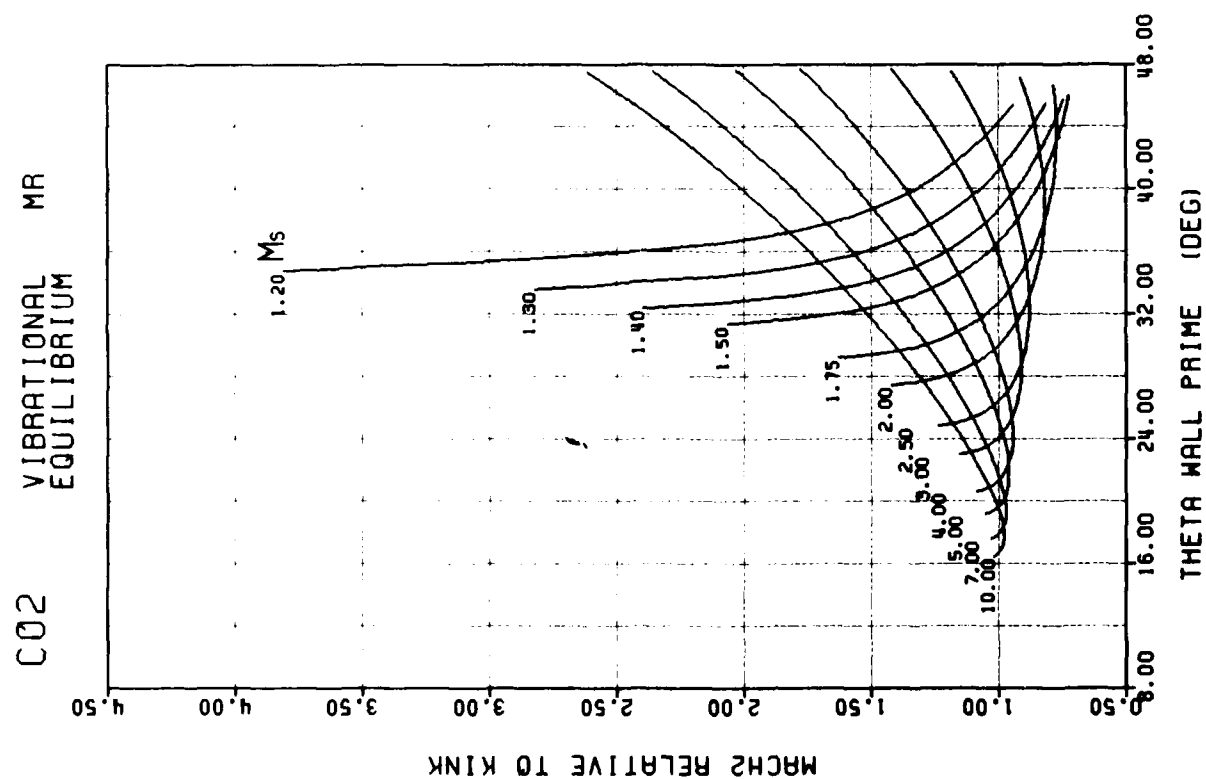
C02 VIBRATIONAL EQUILIBRIUM MR

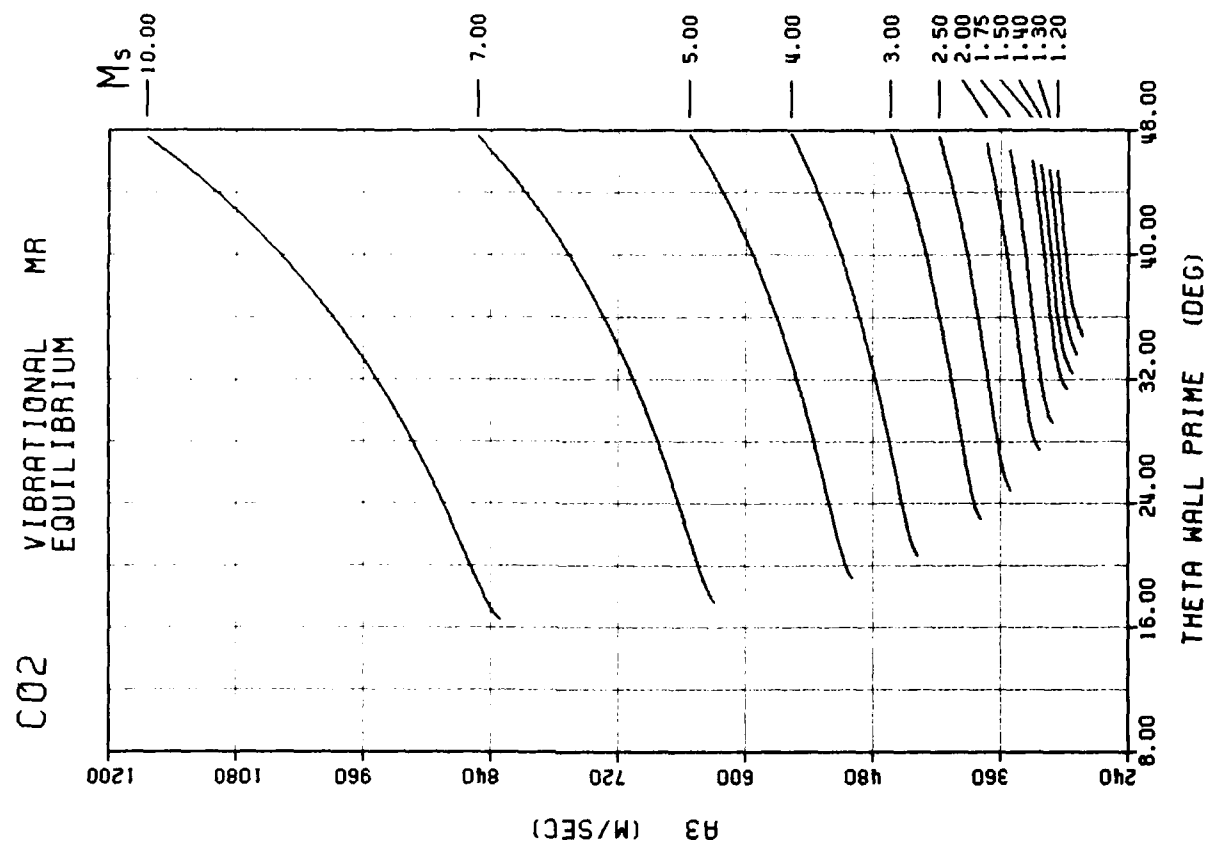
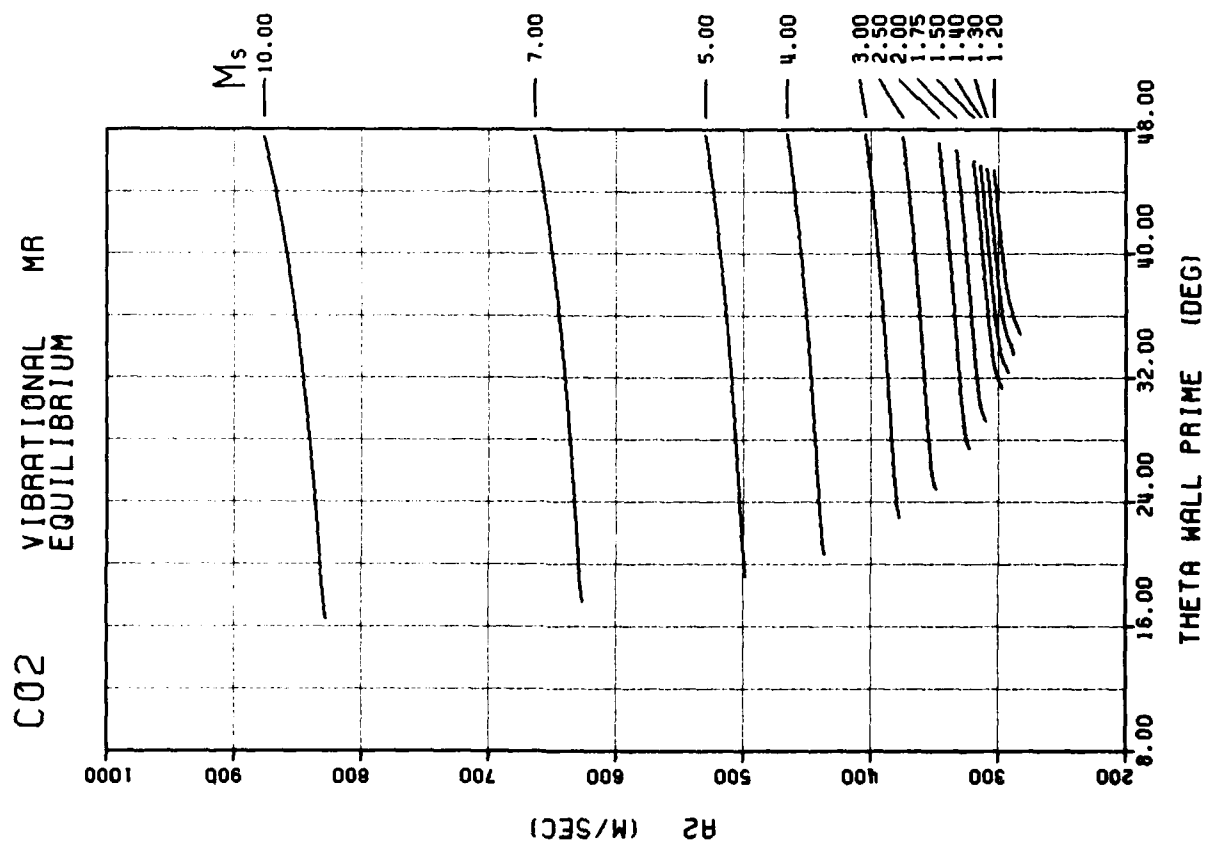


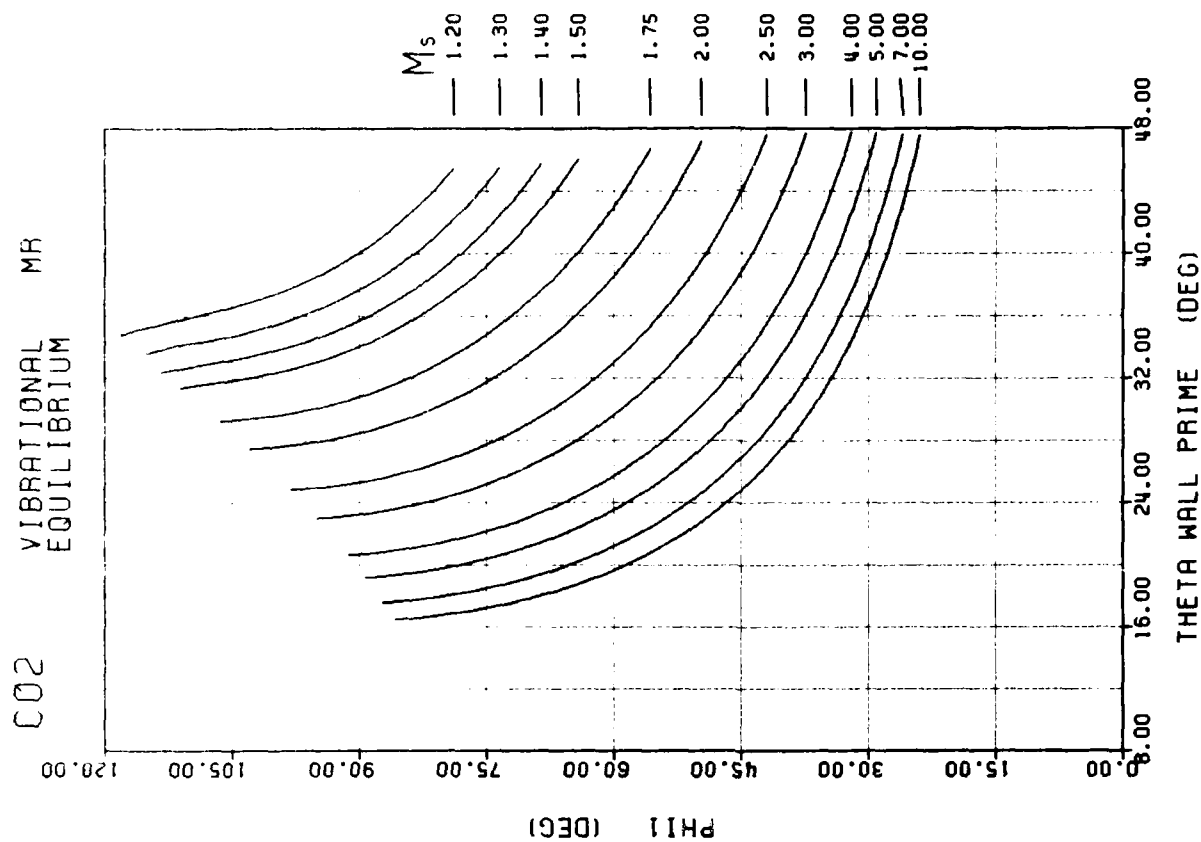
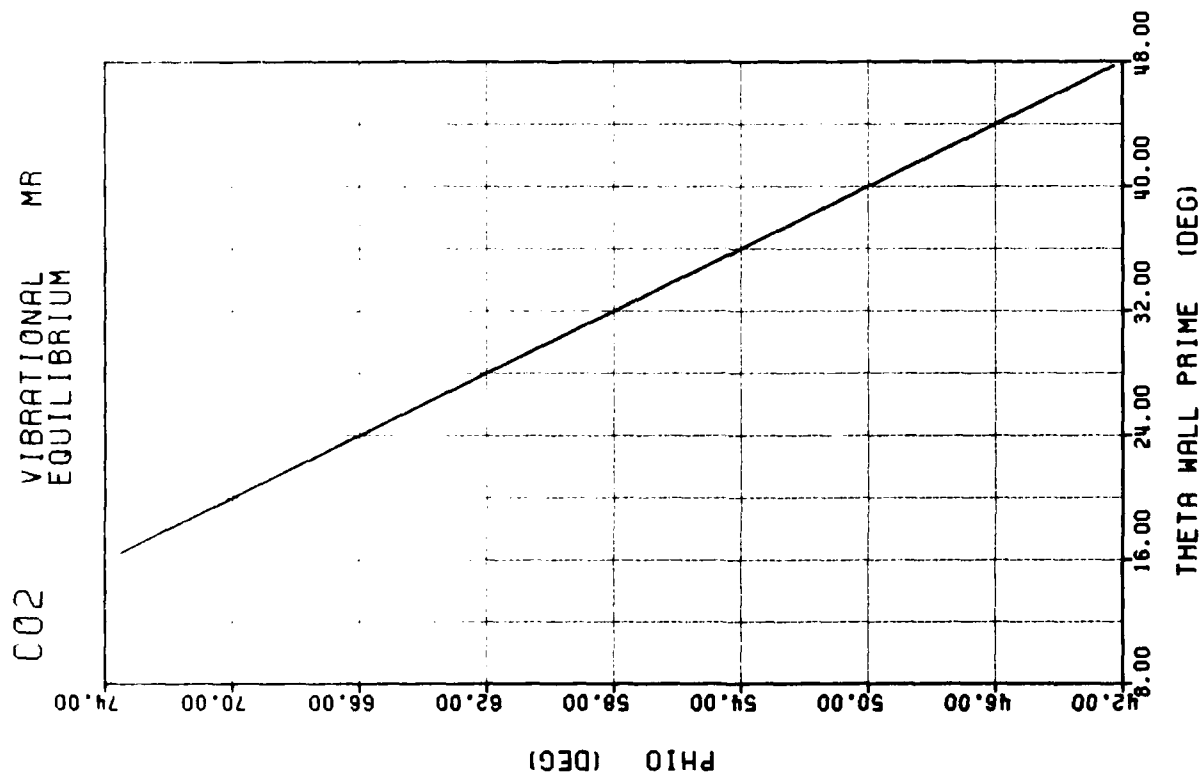


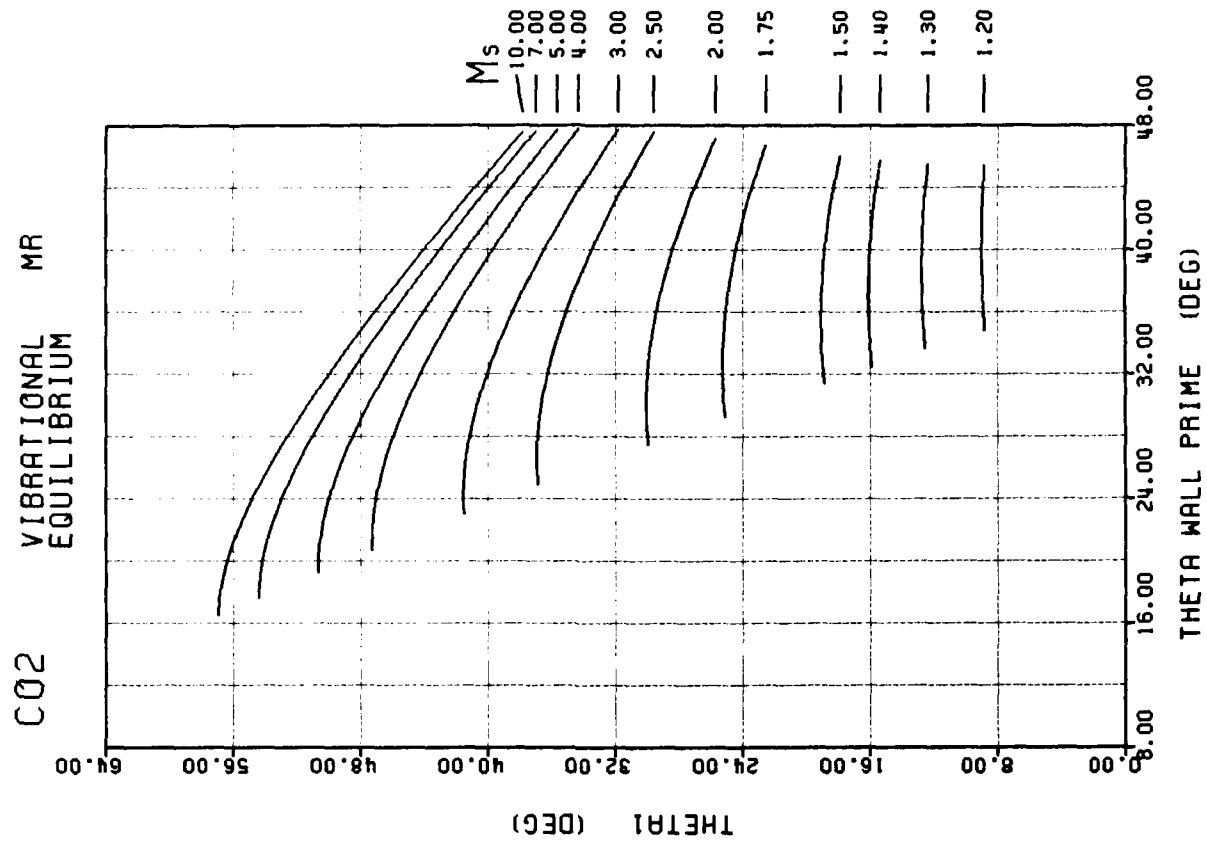
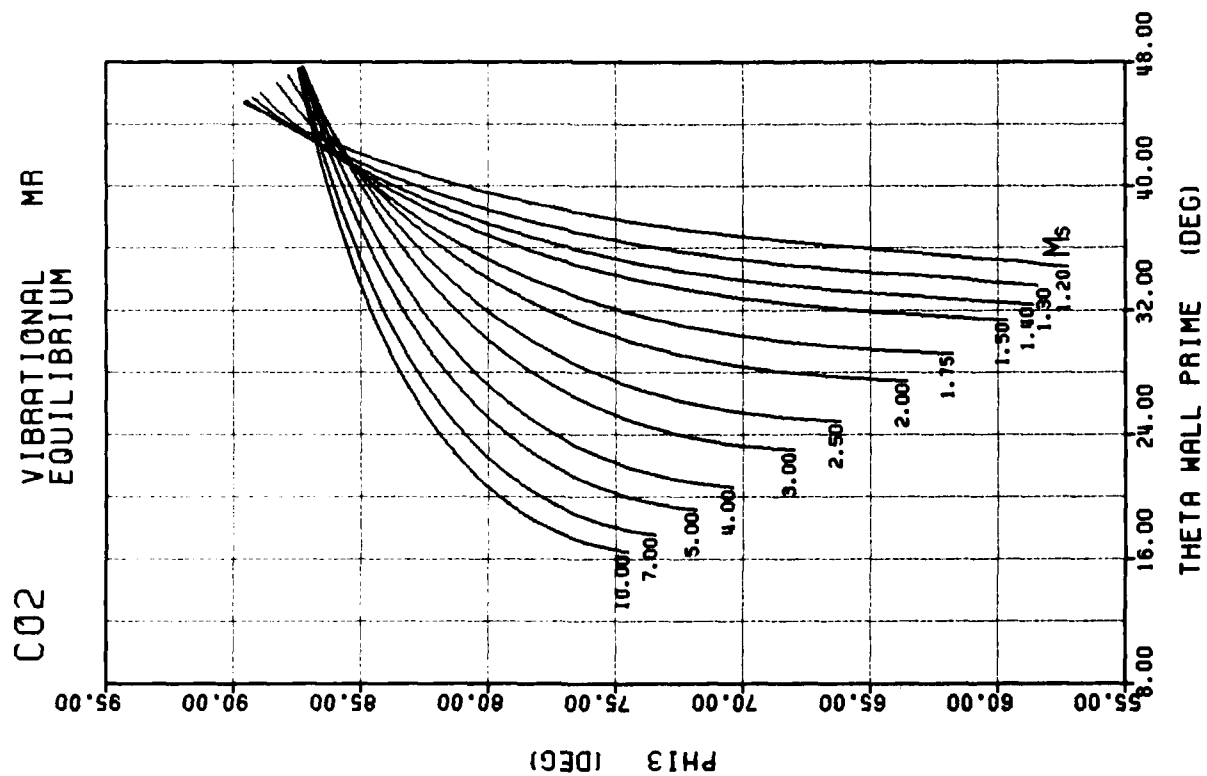




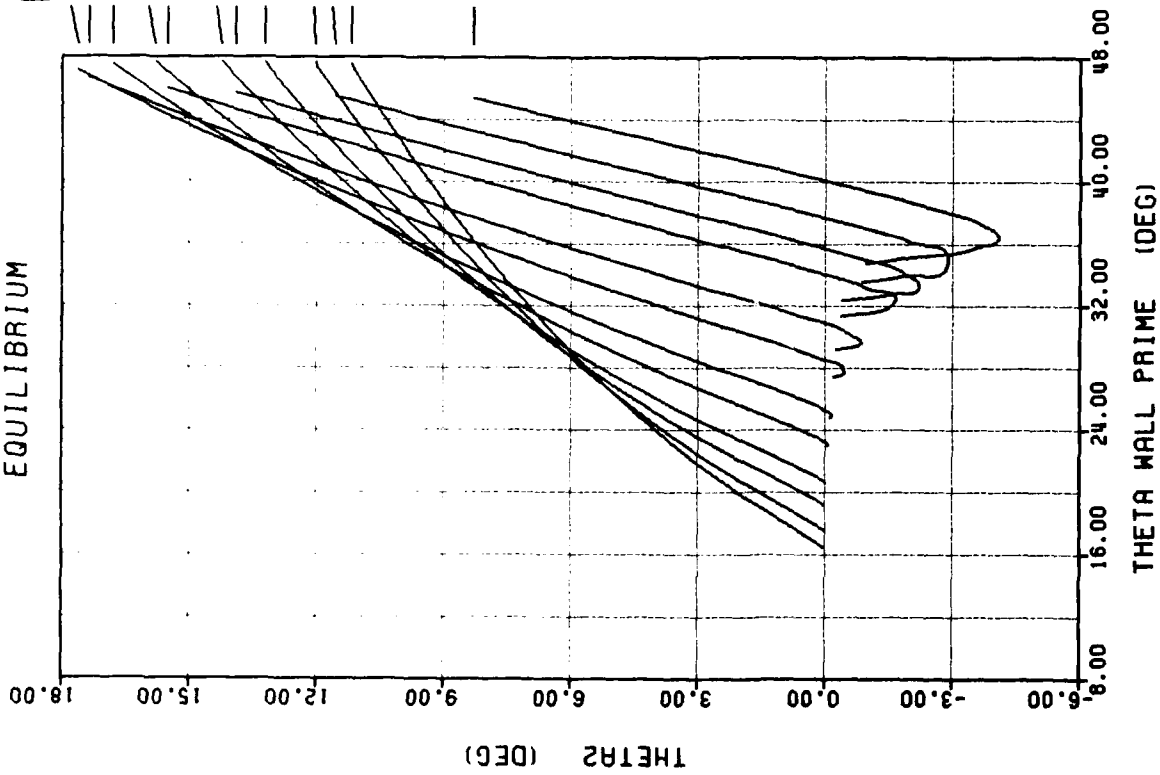




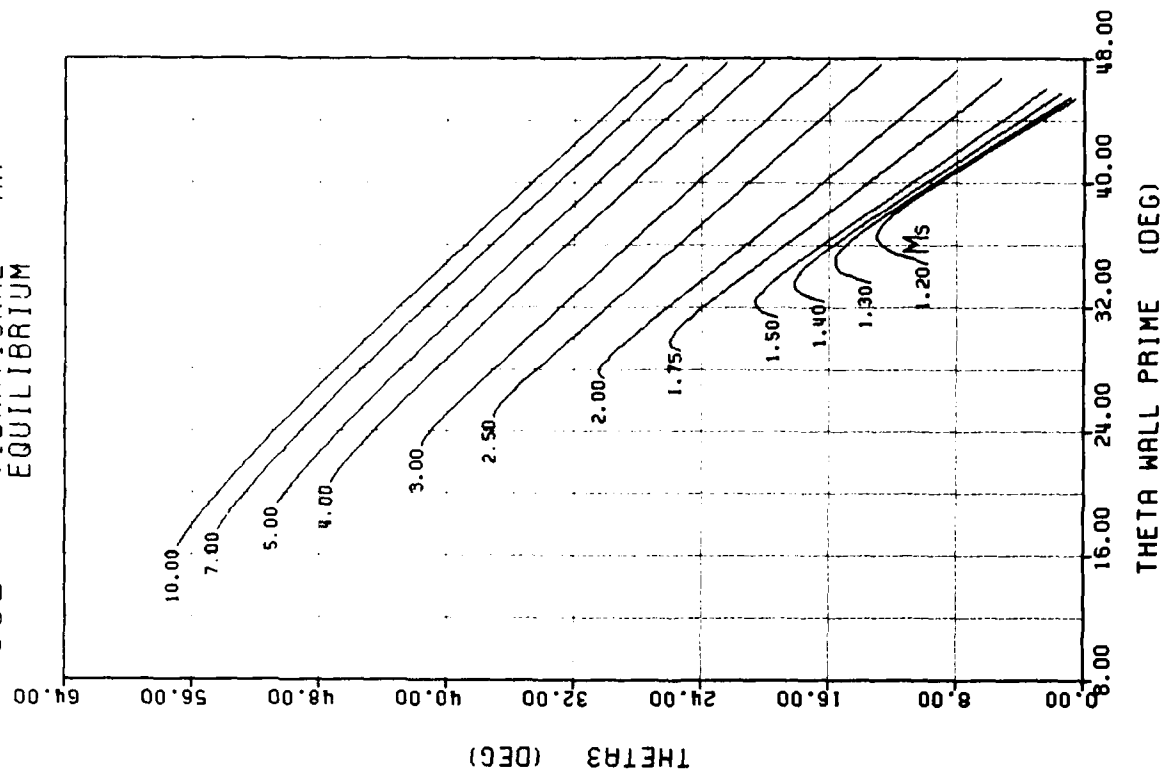


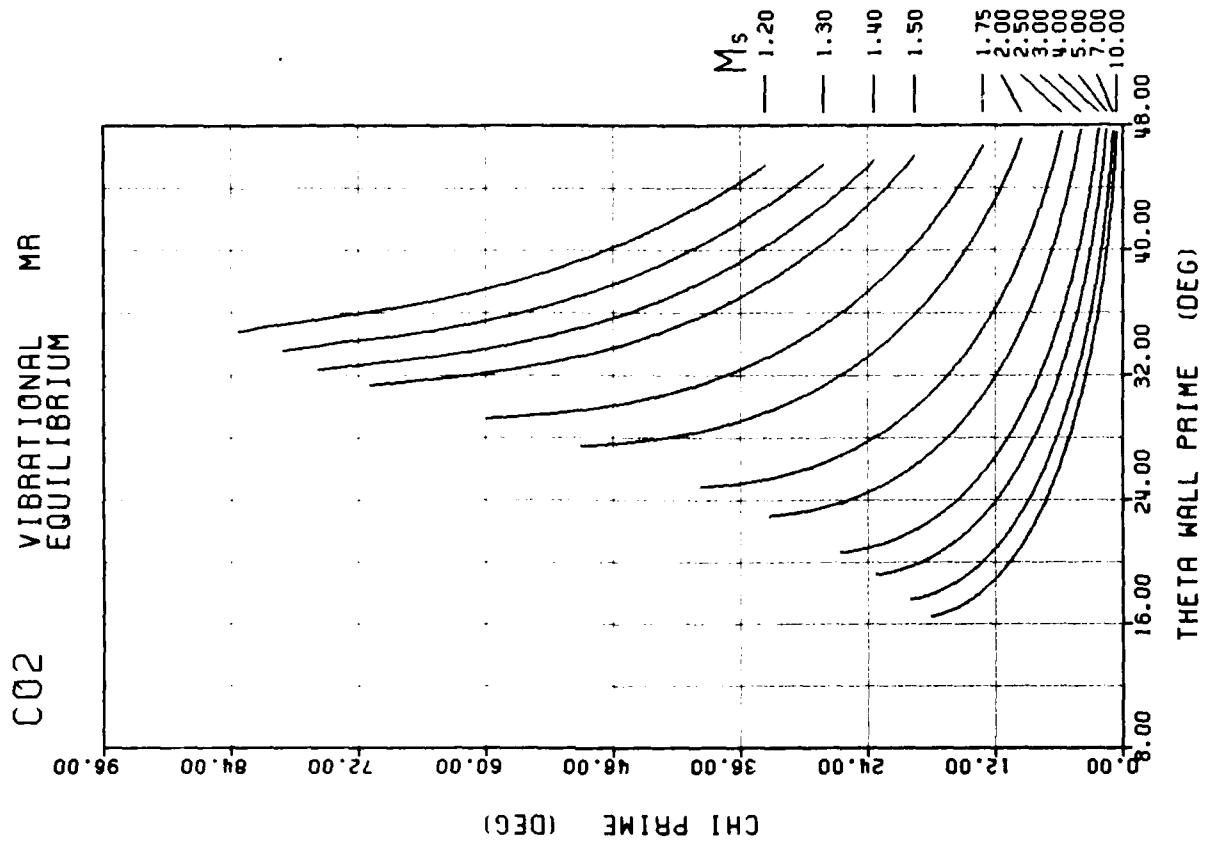
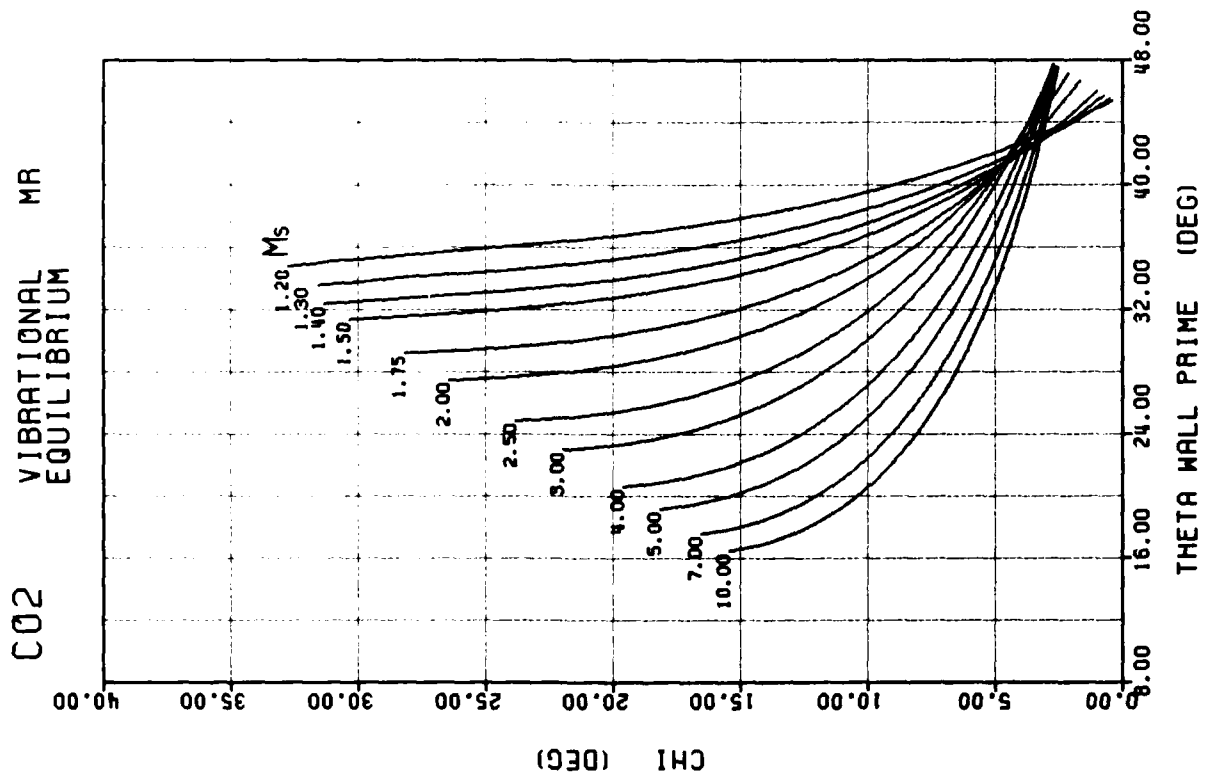


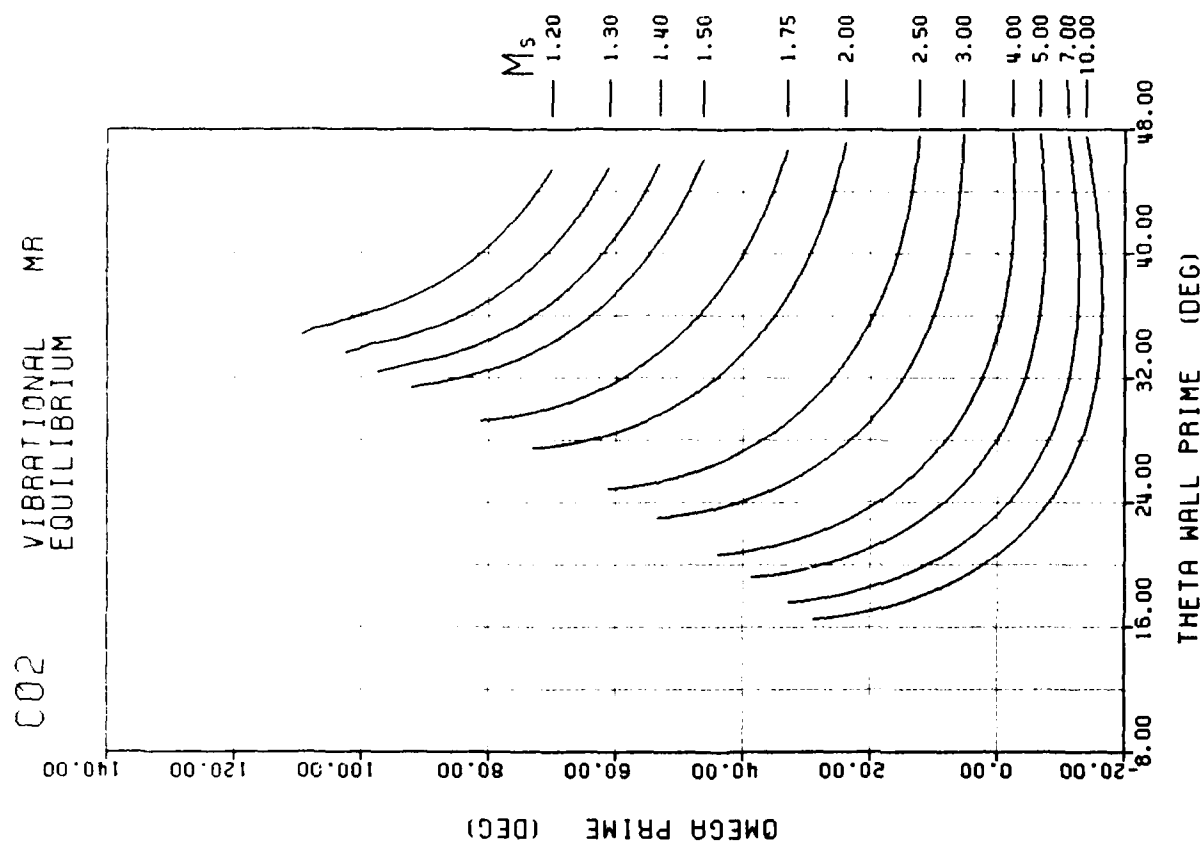
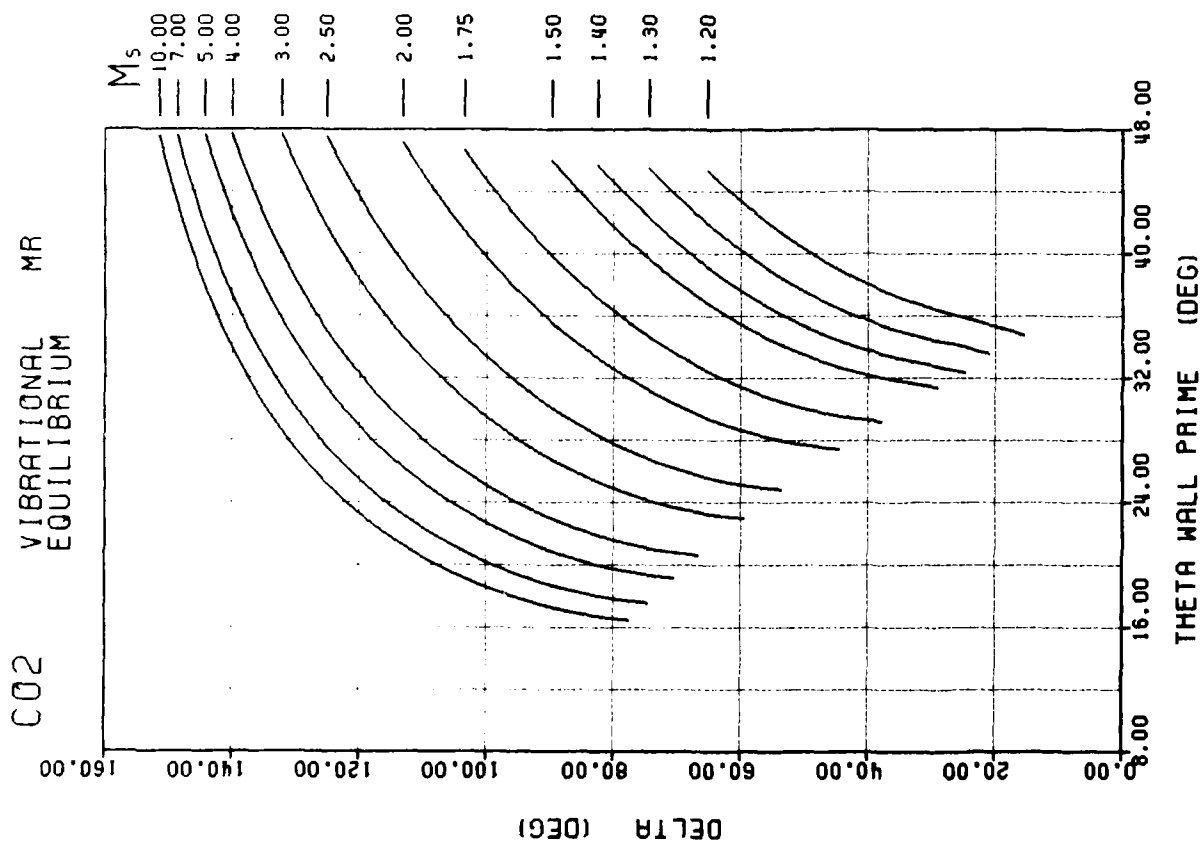
C02 VIBRATIONAL EQUILIBRIUM MR

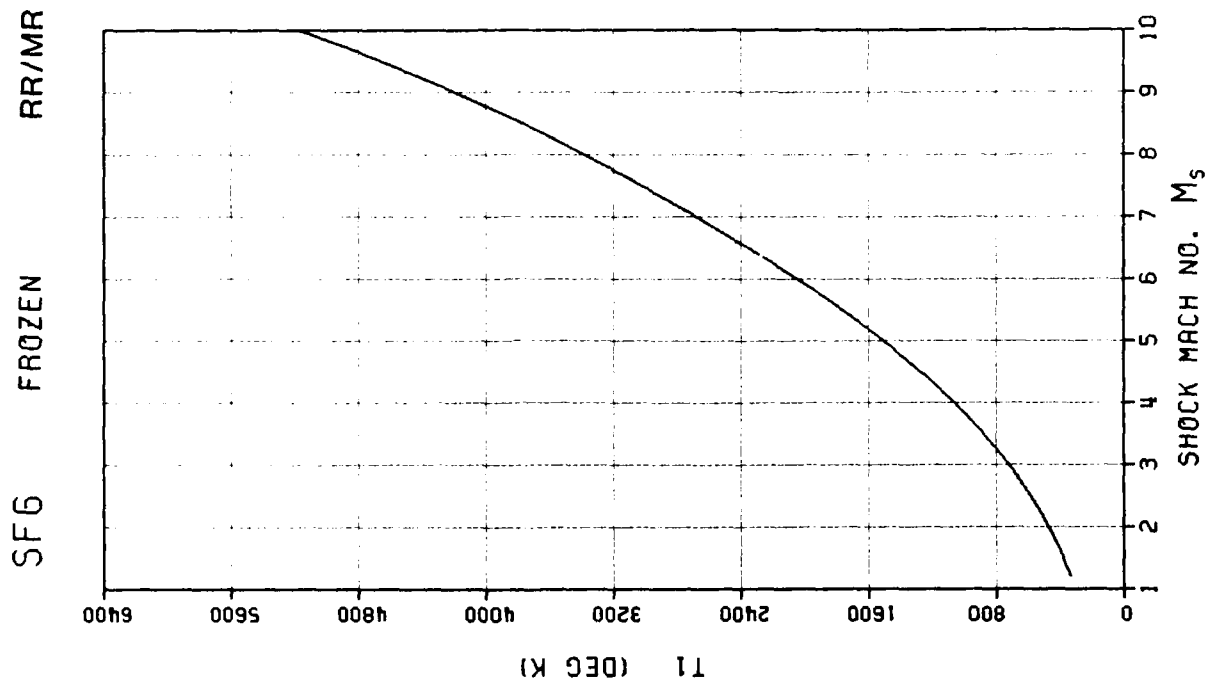
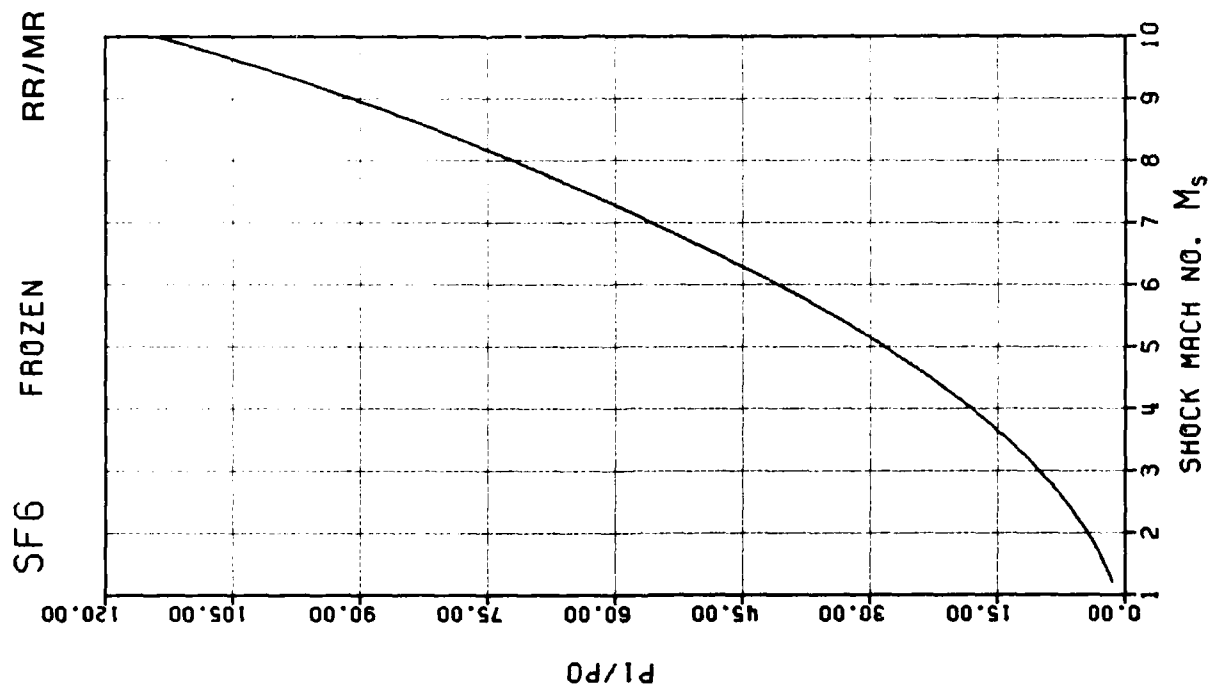


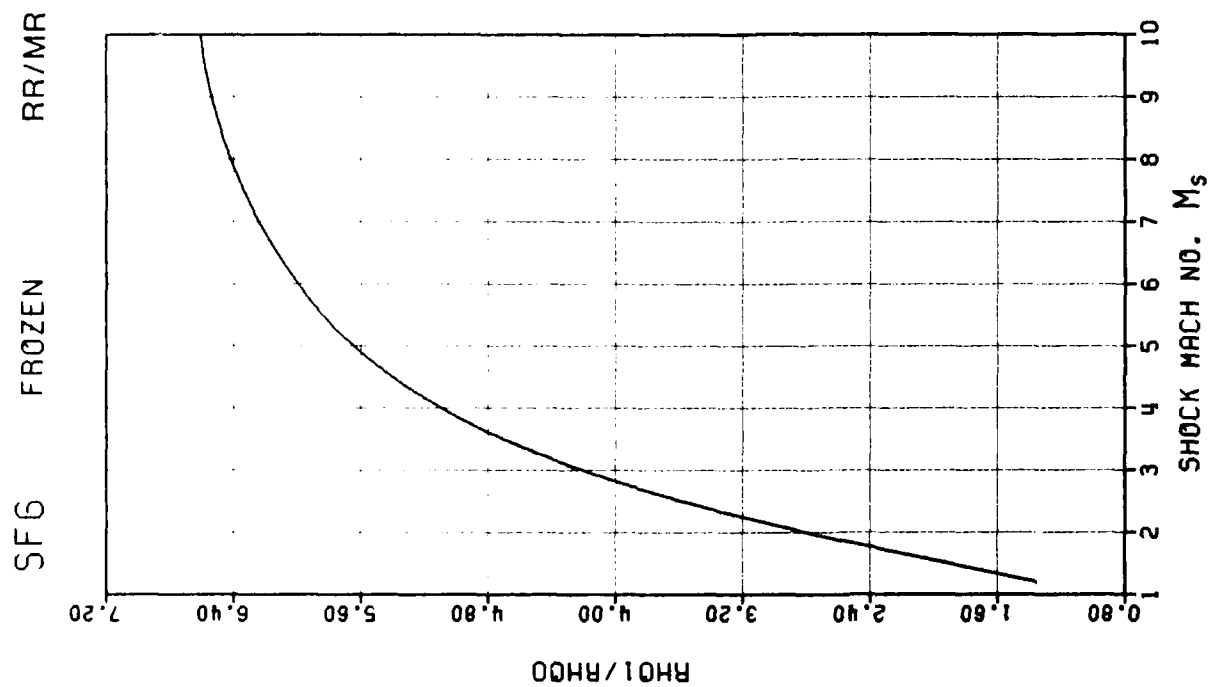
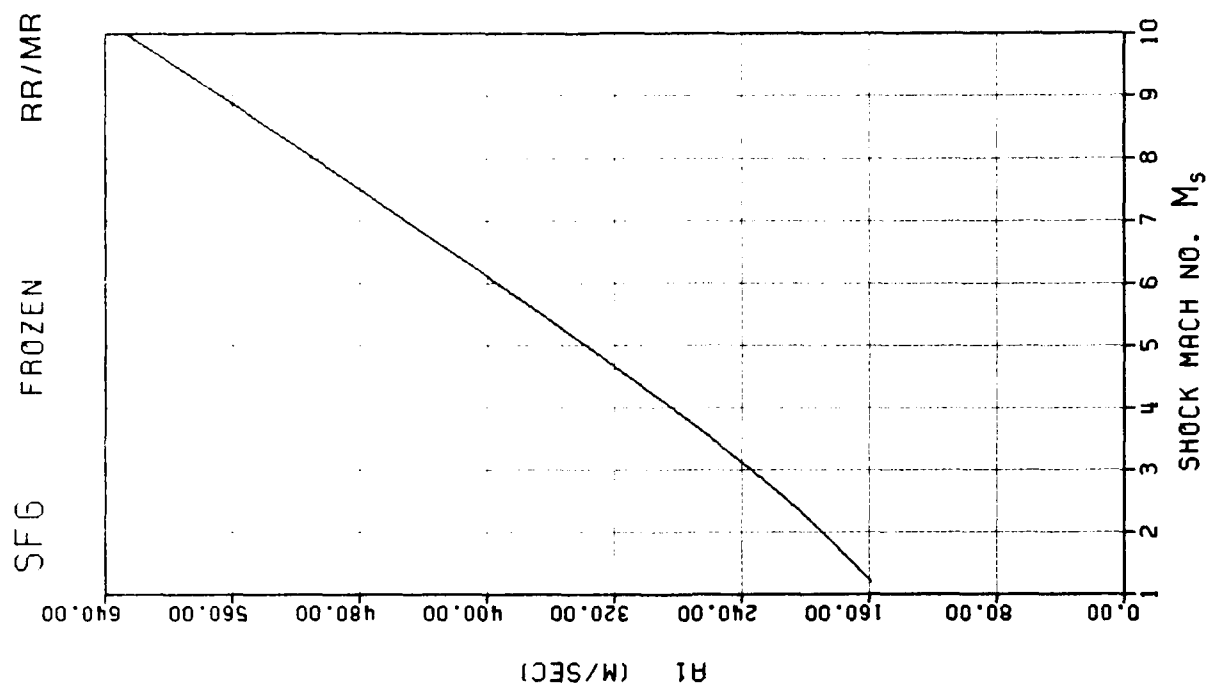
C02 VIBRATIONAL EQUILIBRIUM MR

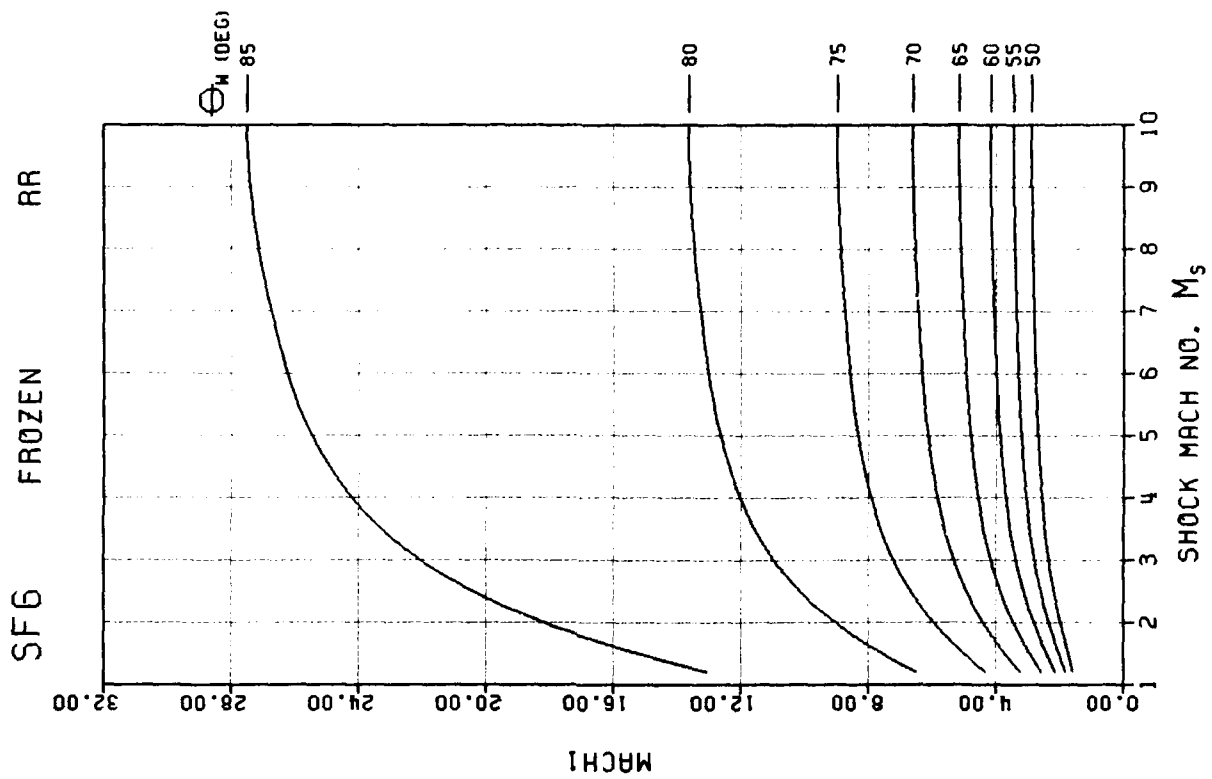
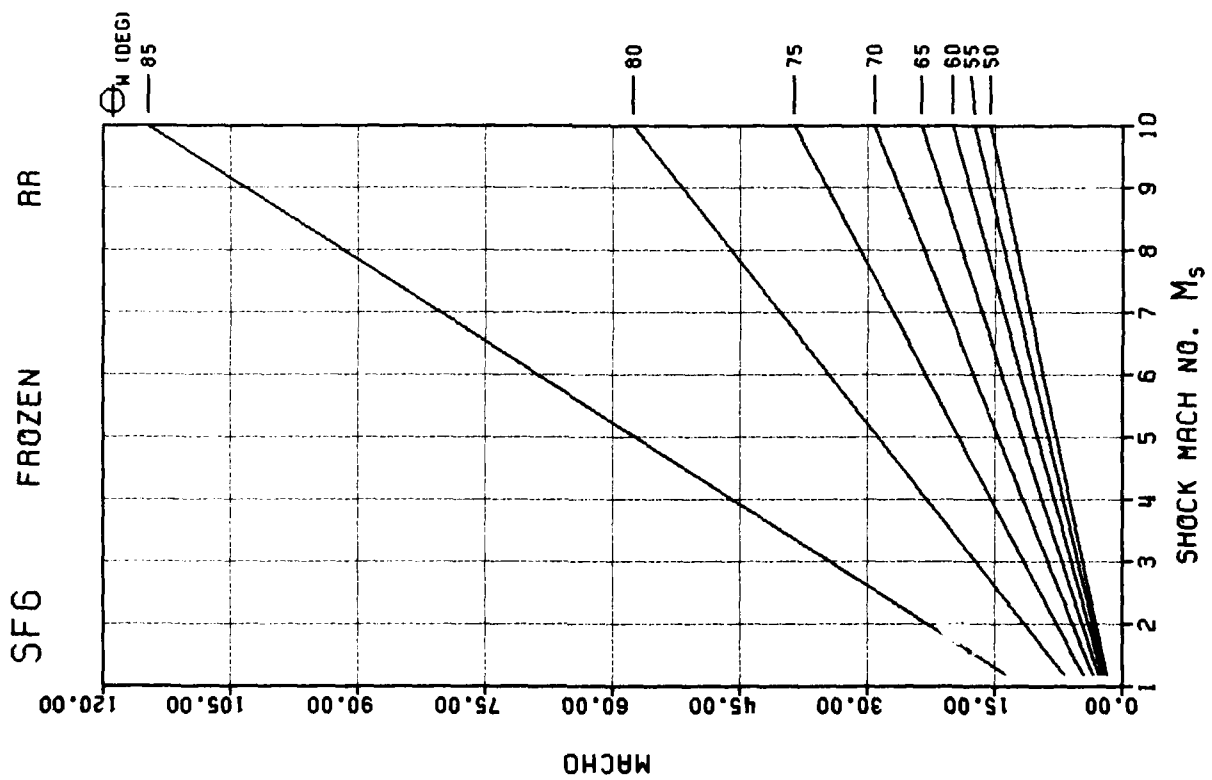


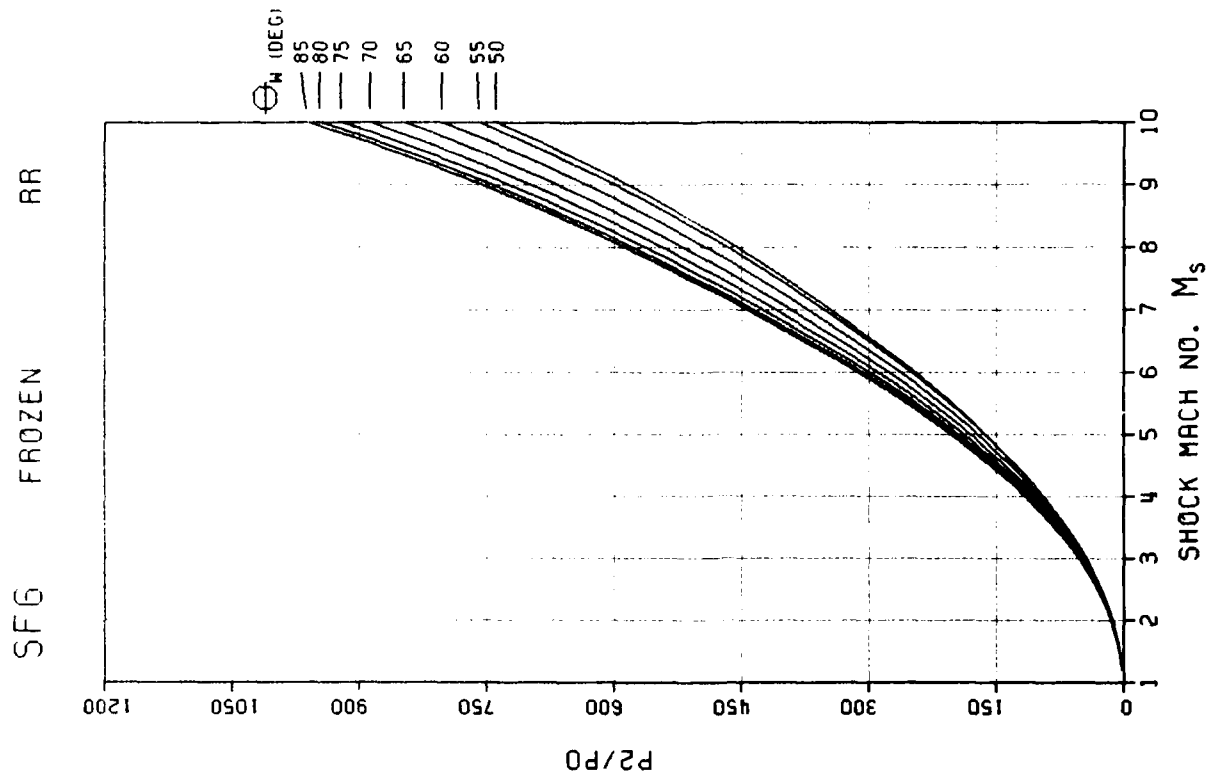
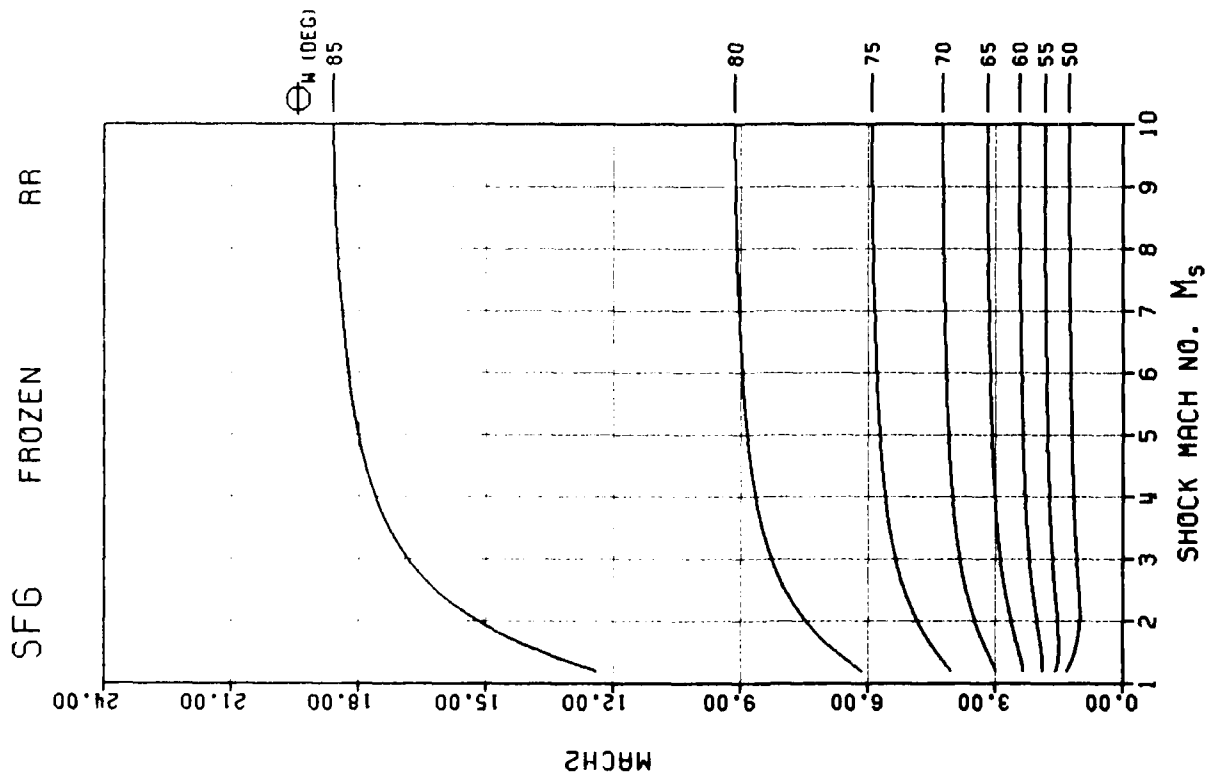


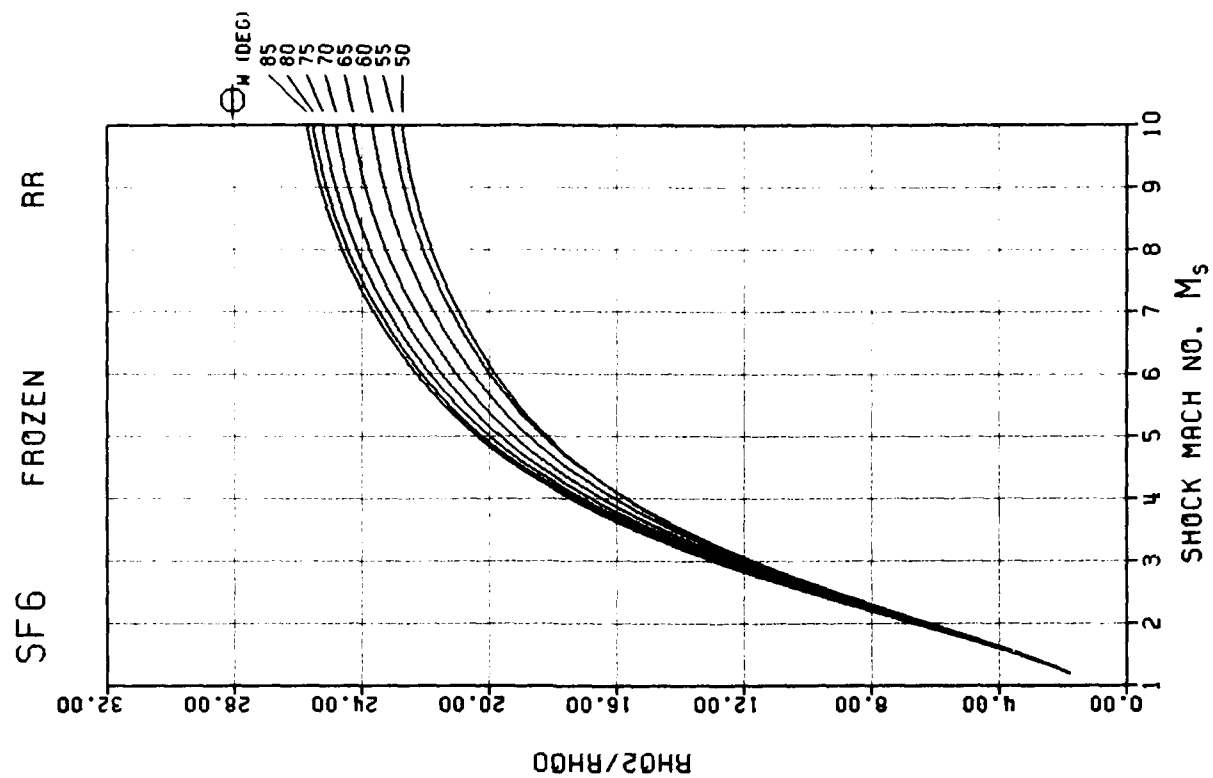
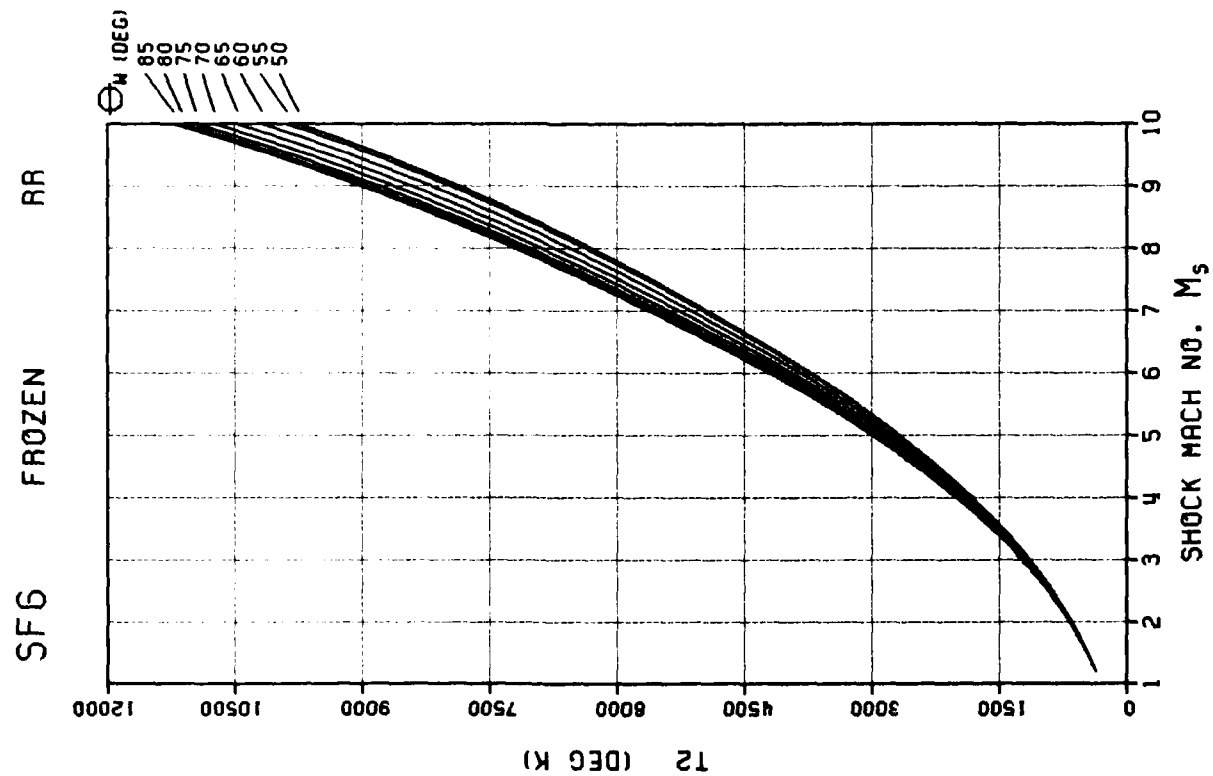


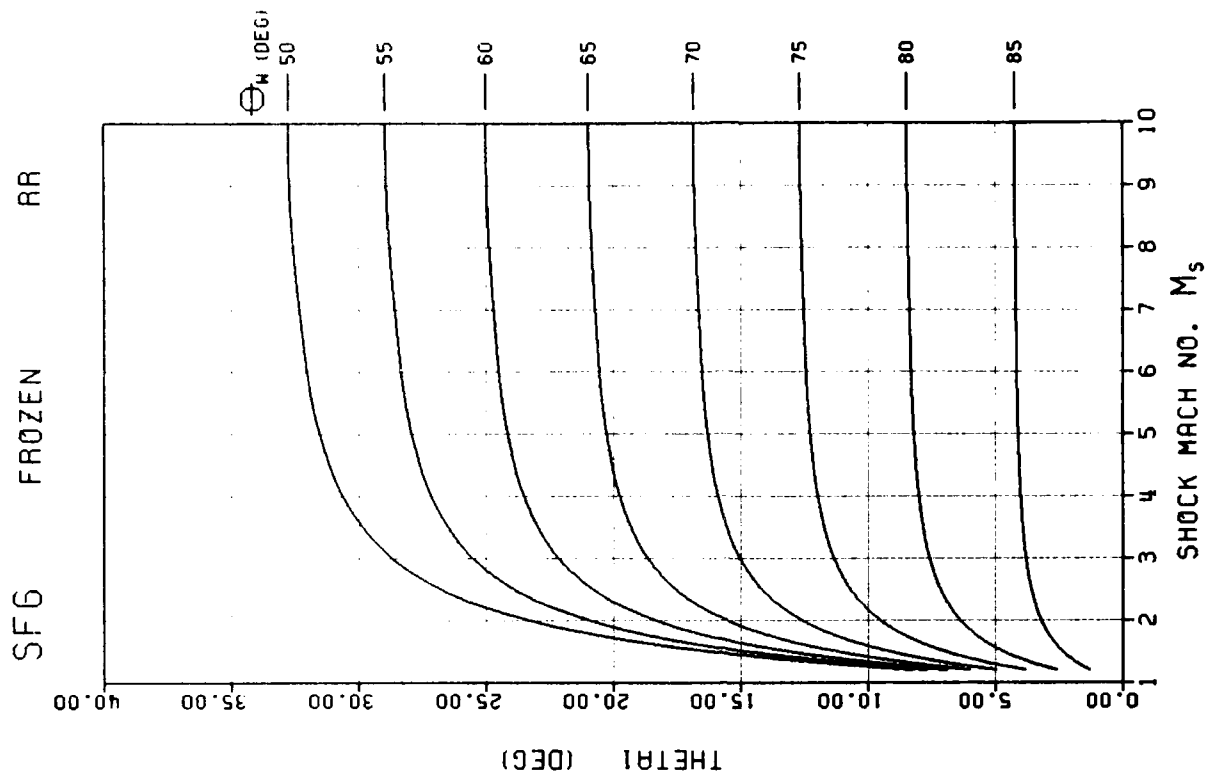
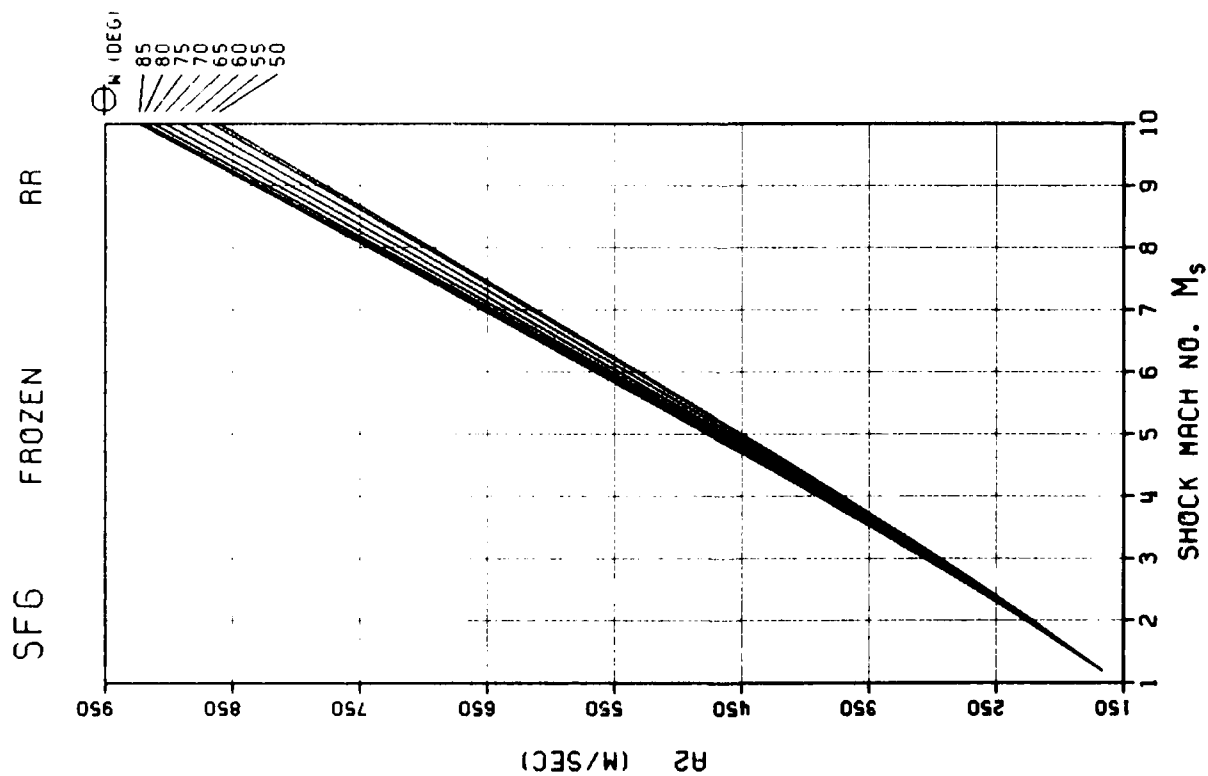


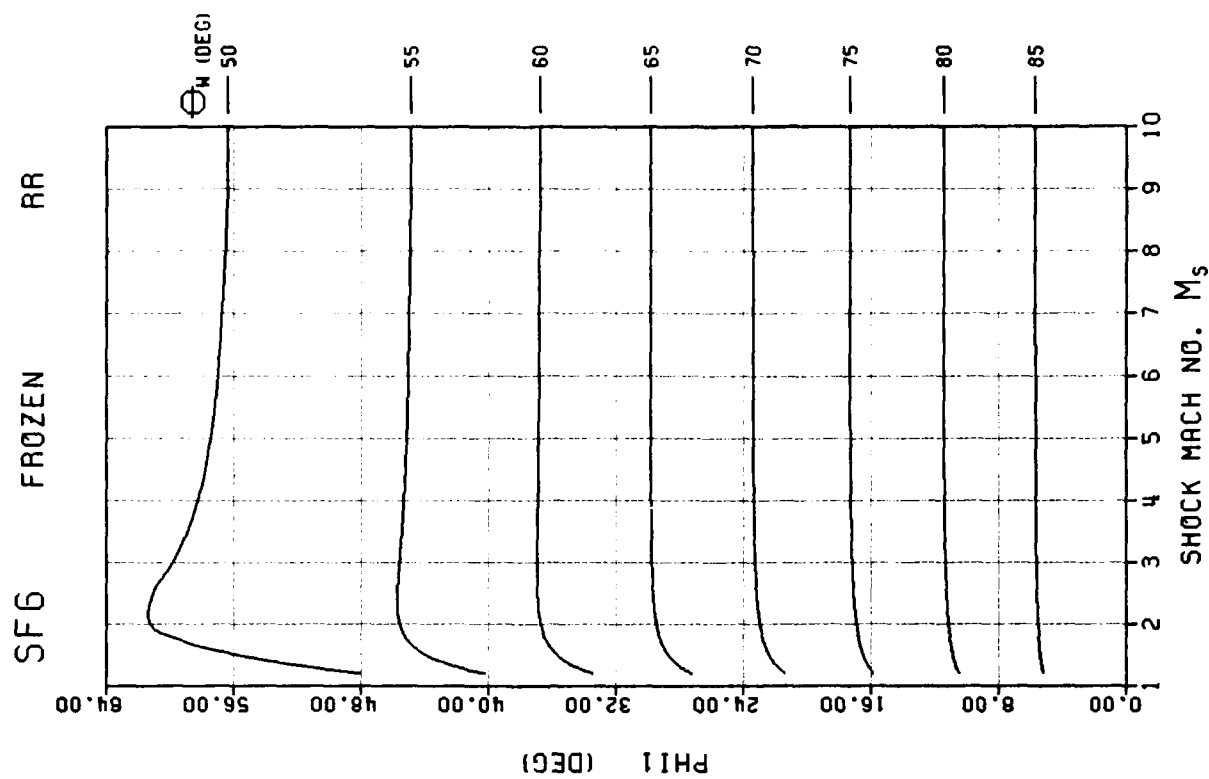
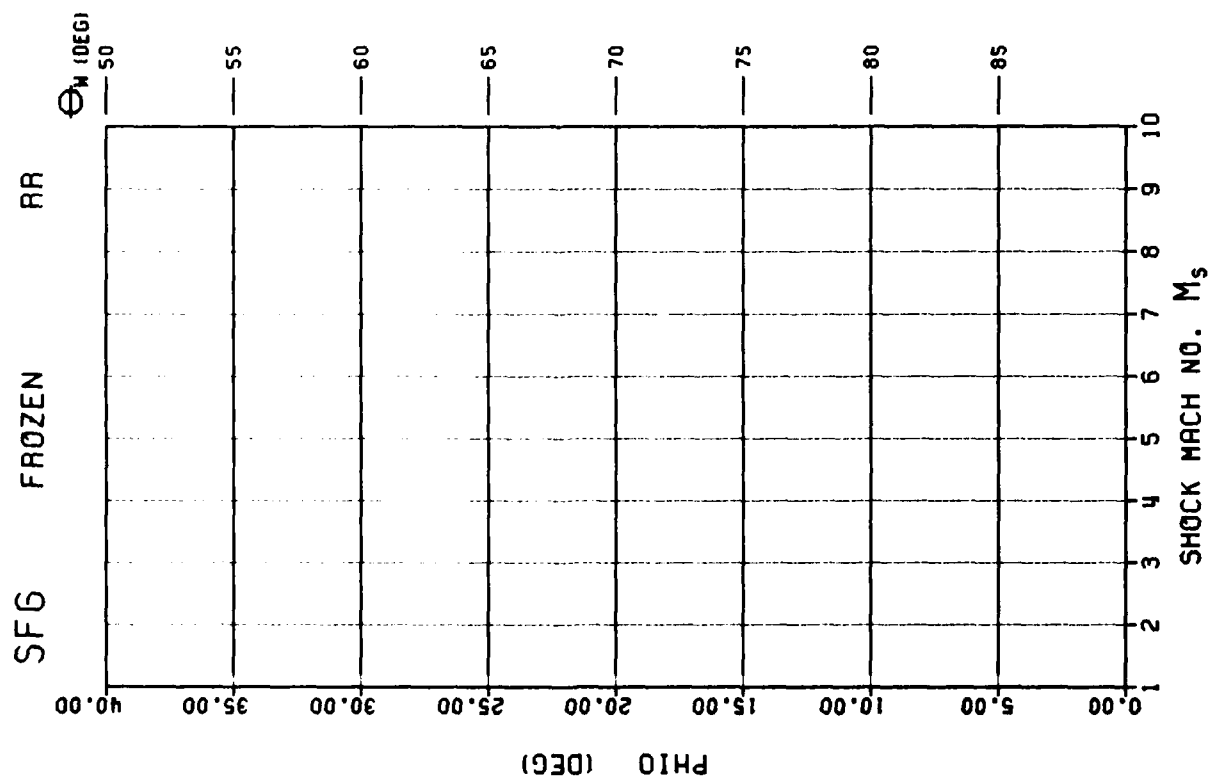


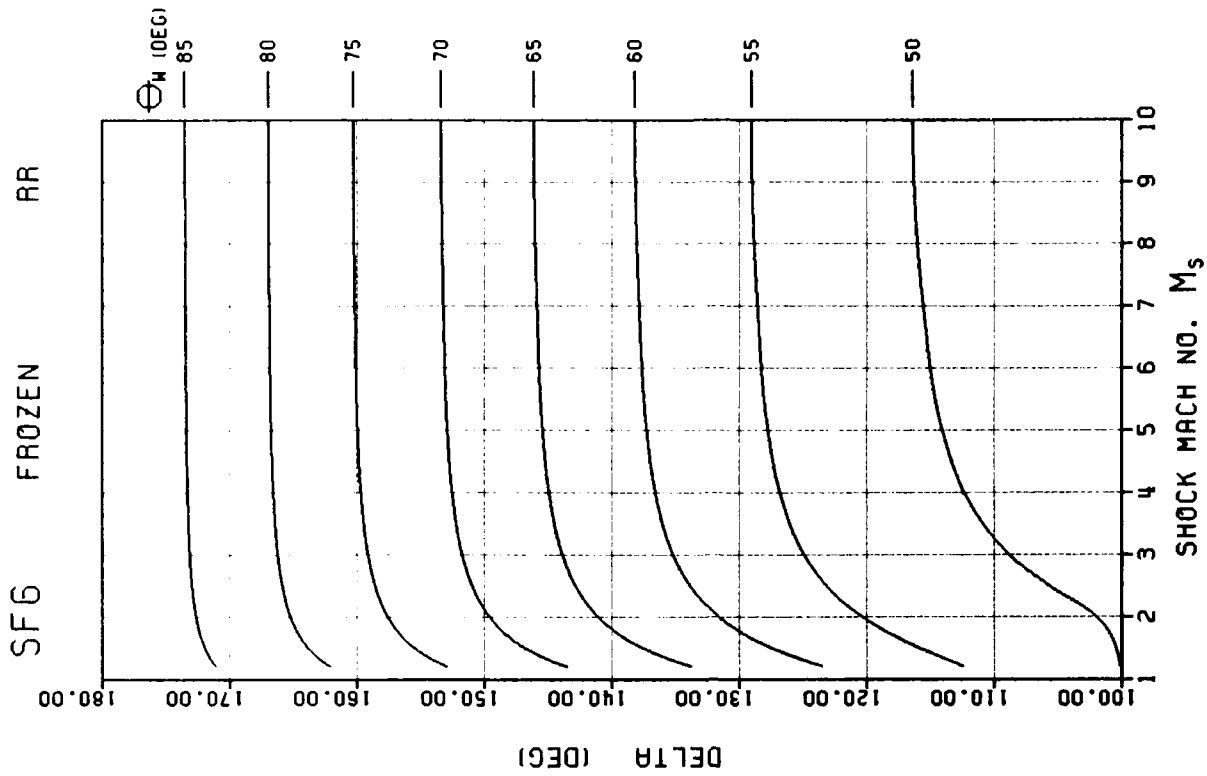
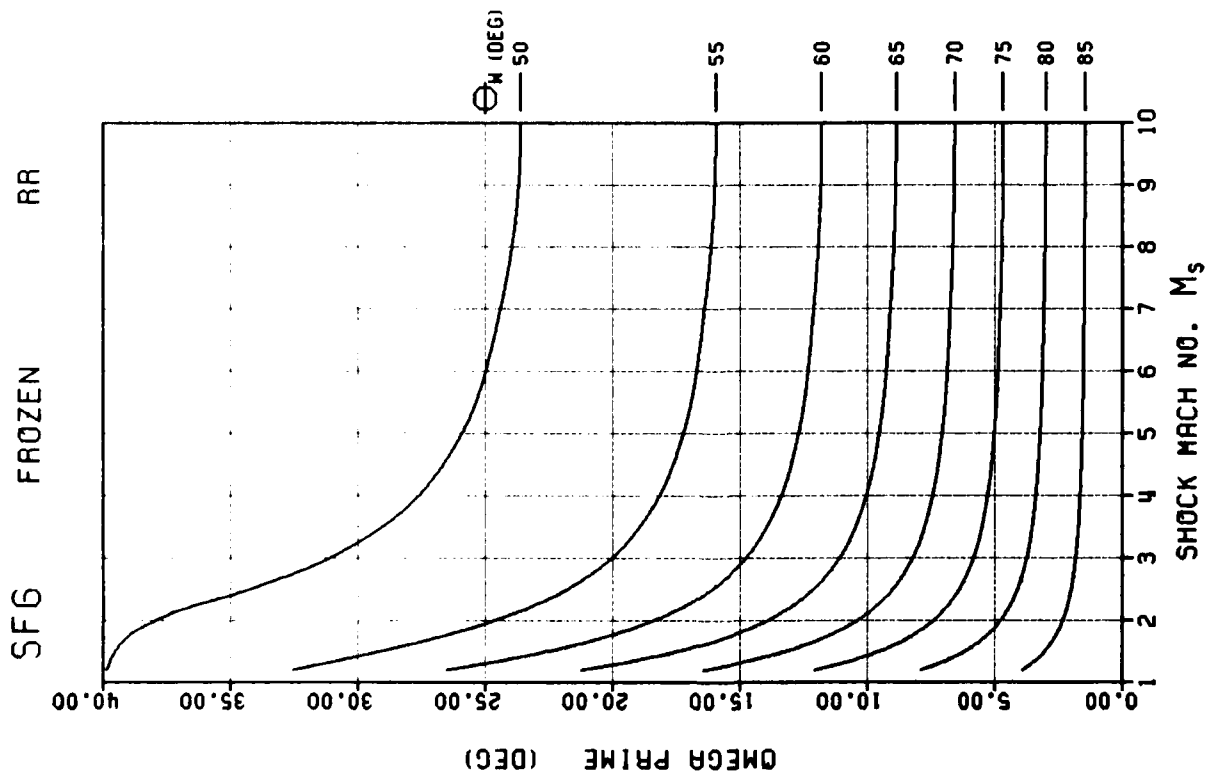


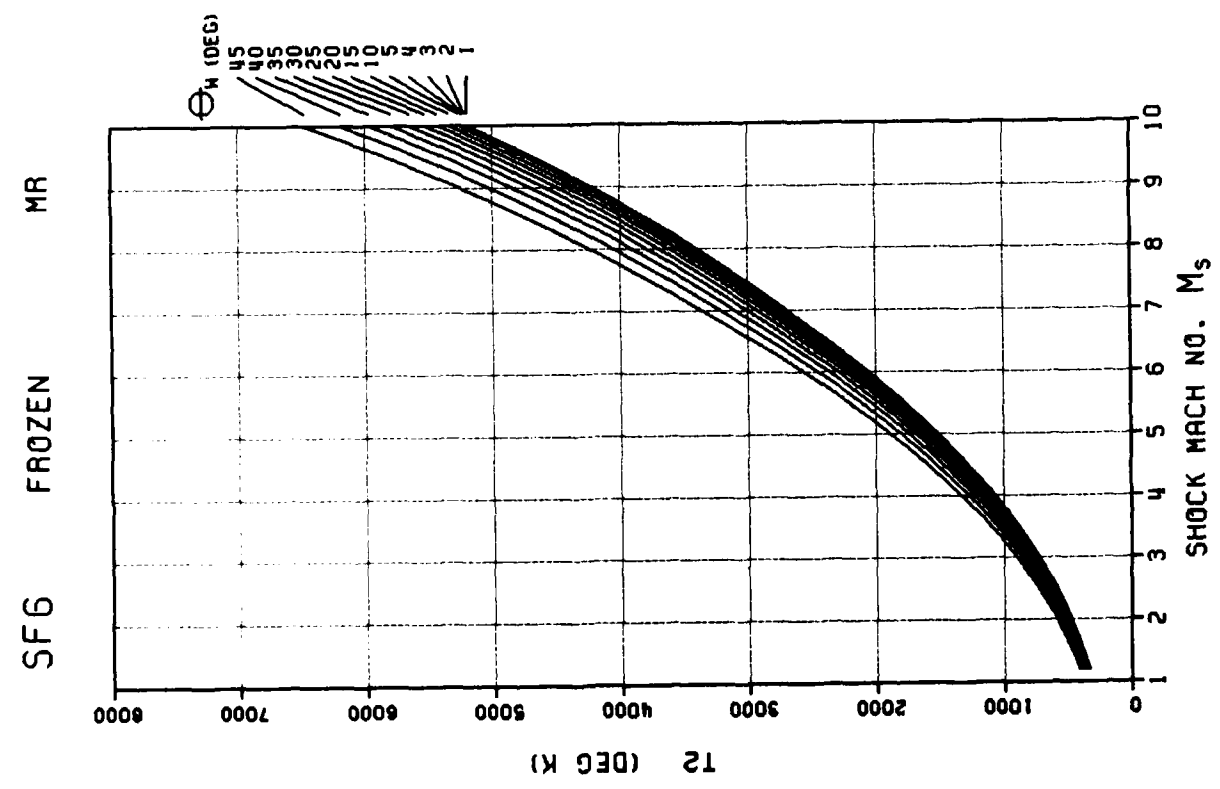
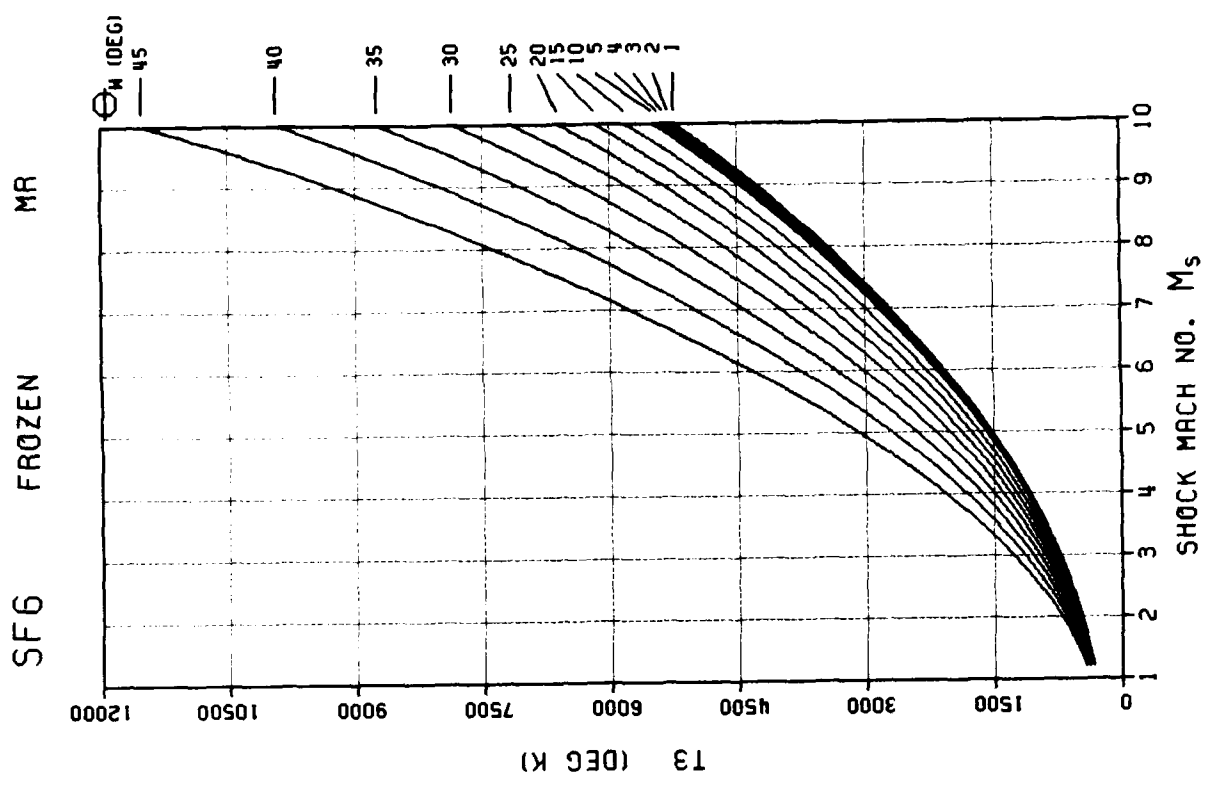


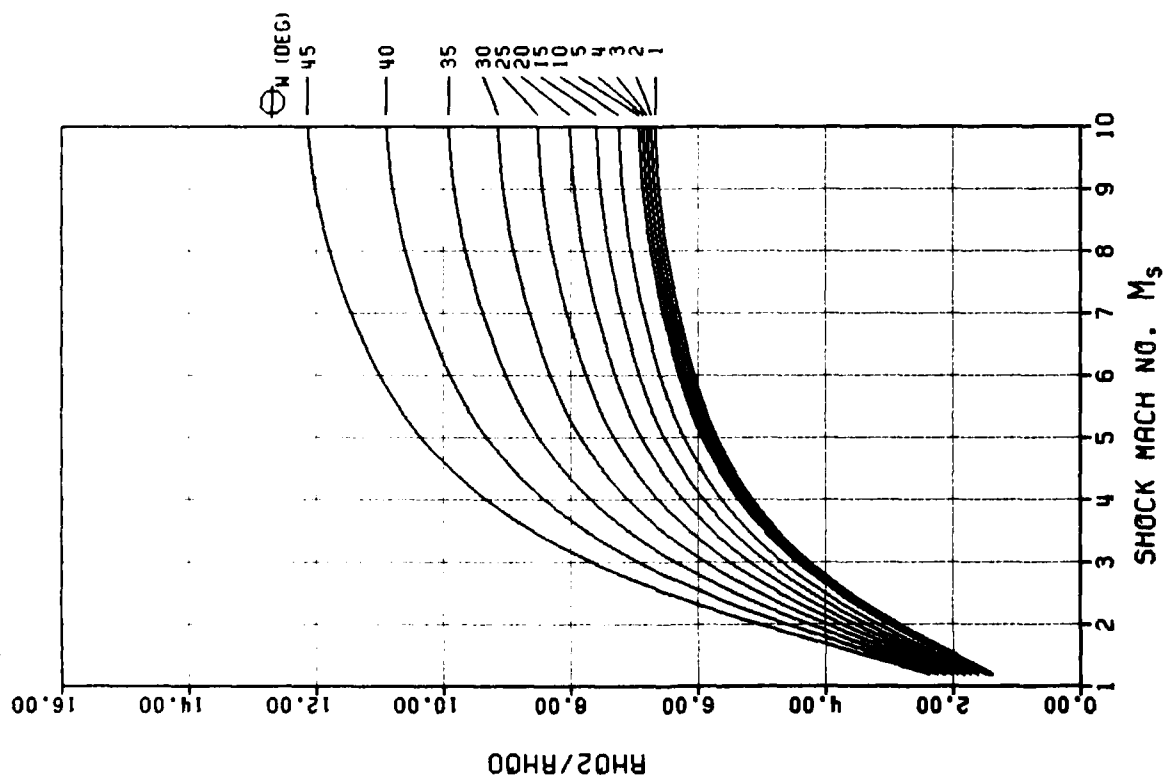
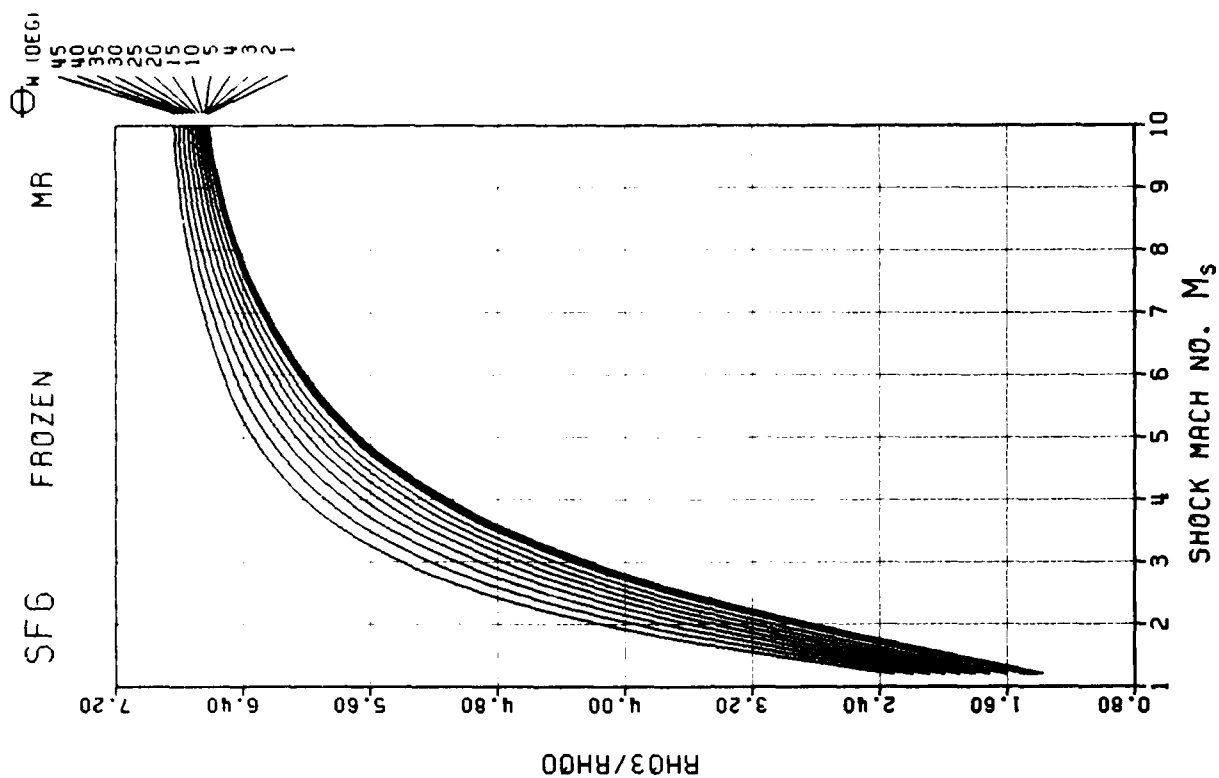


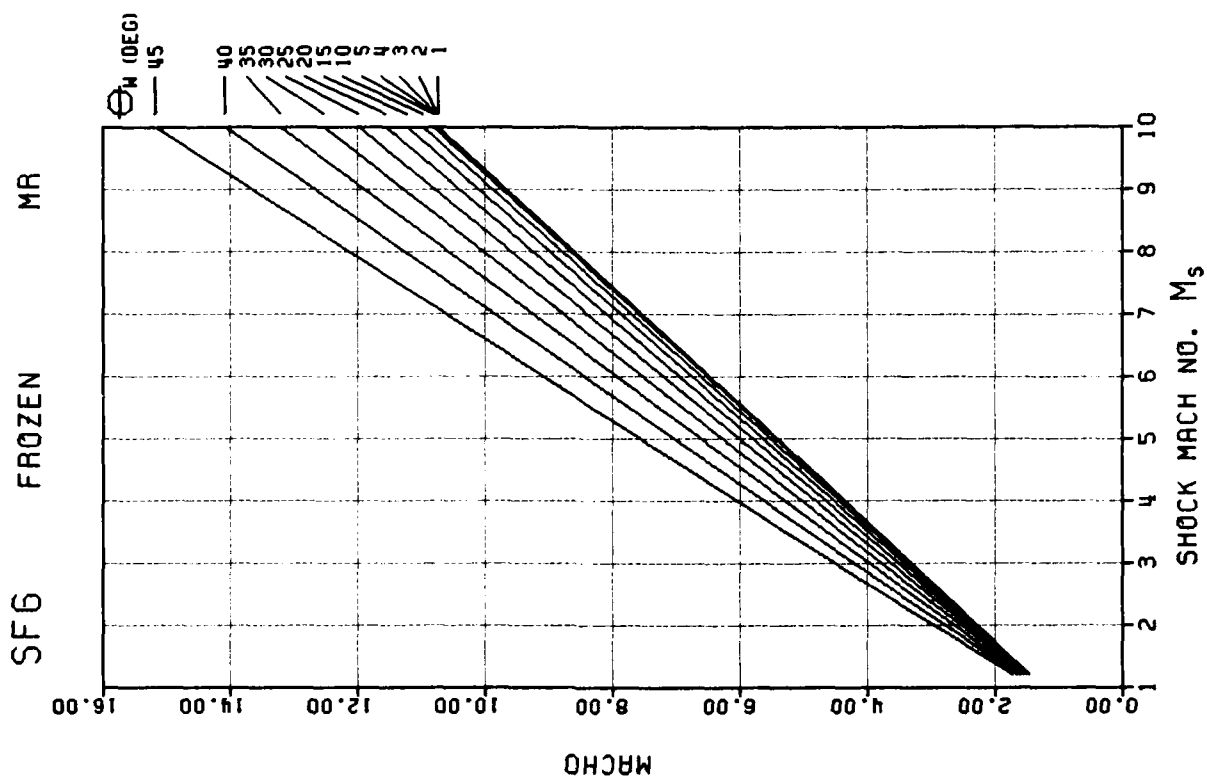
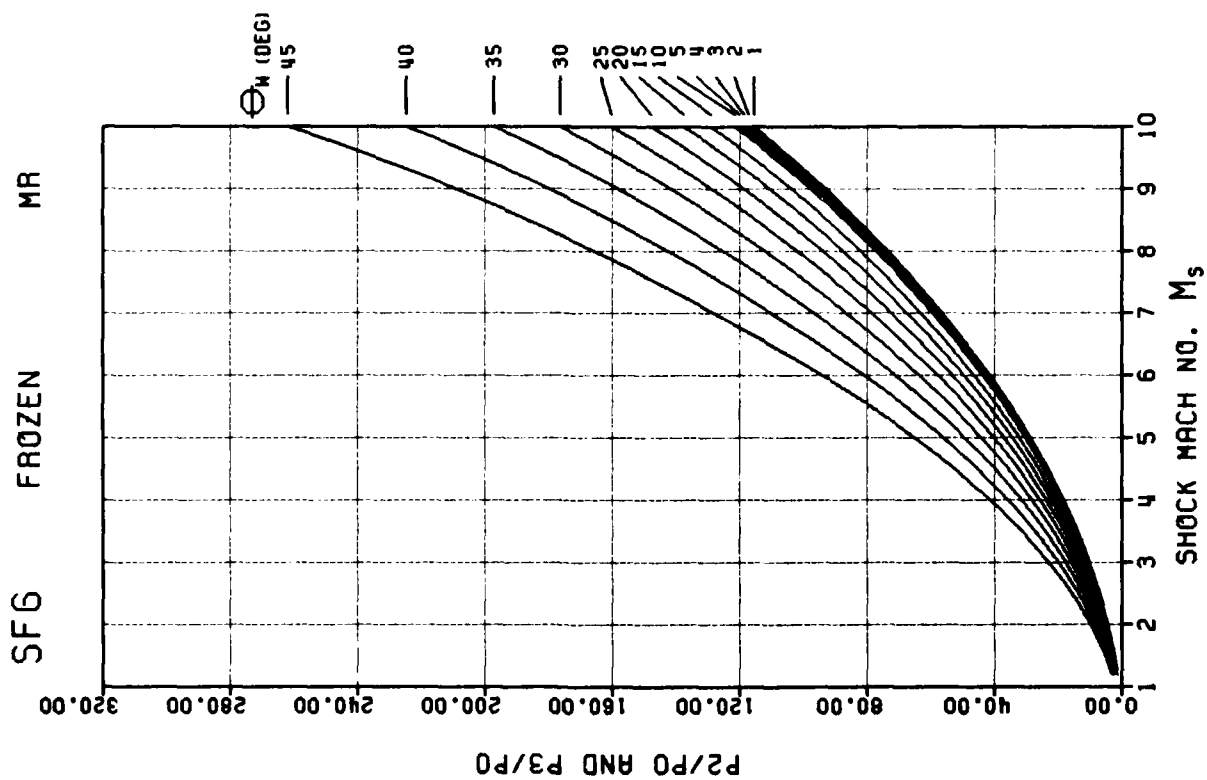


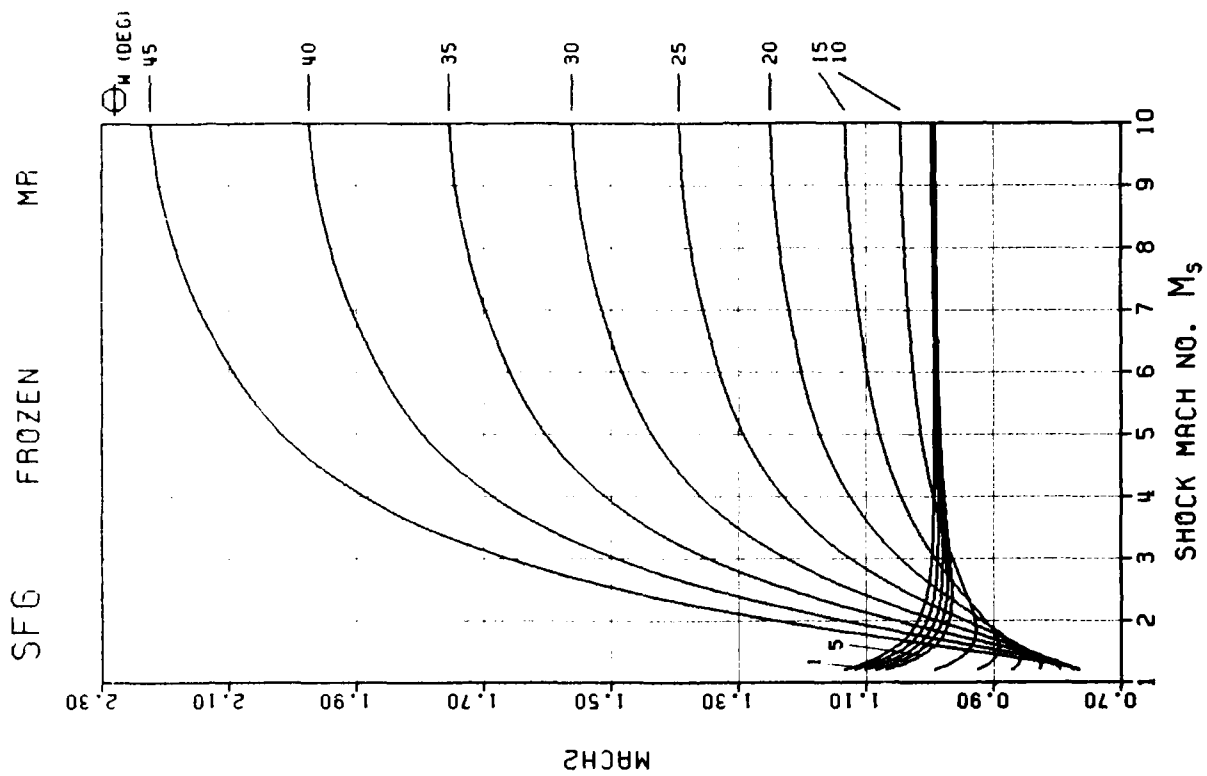
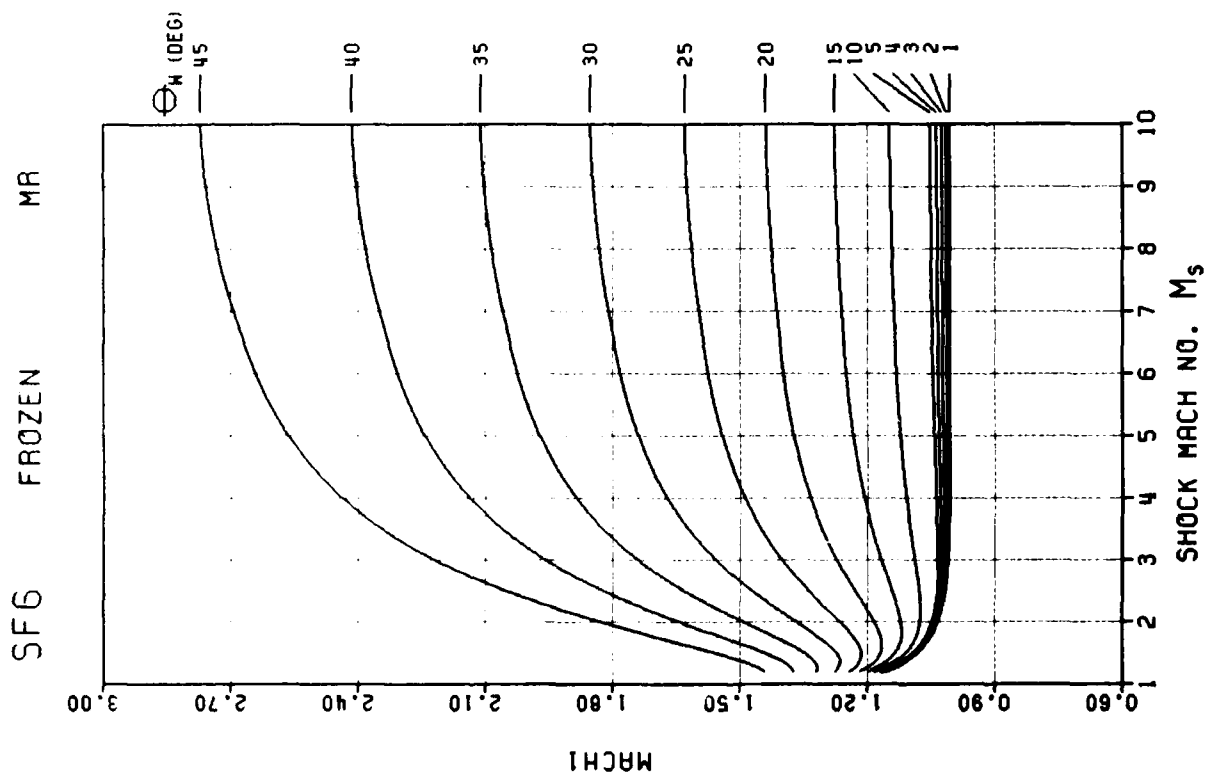


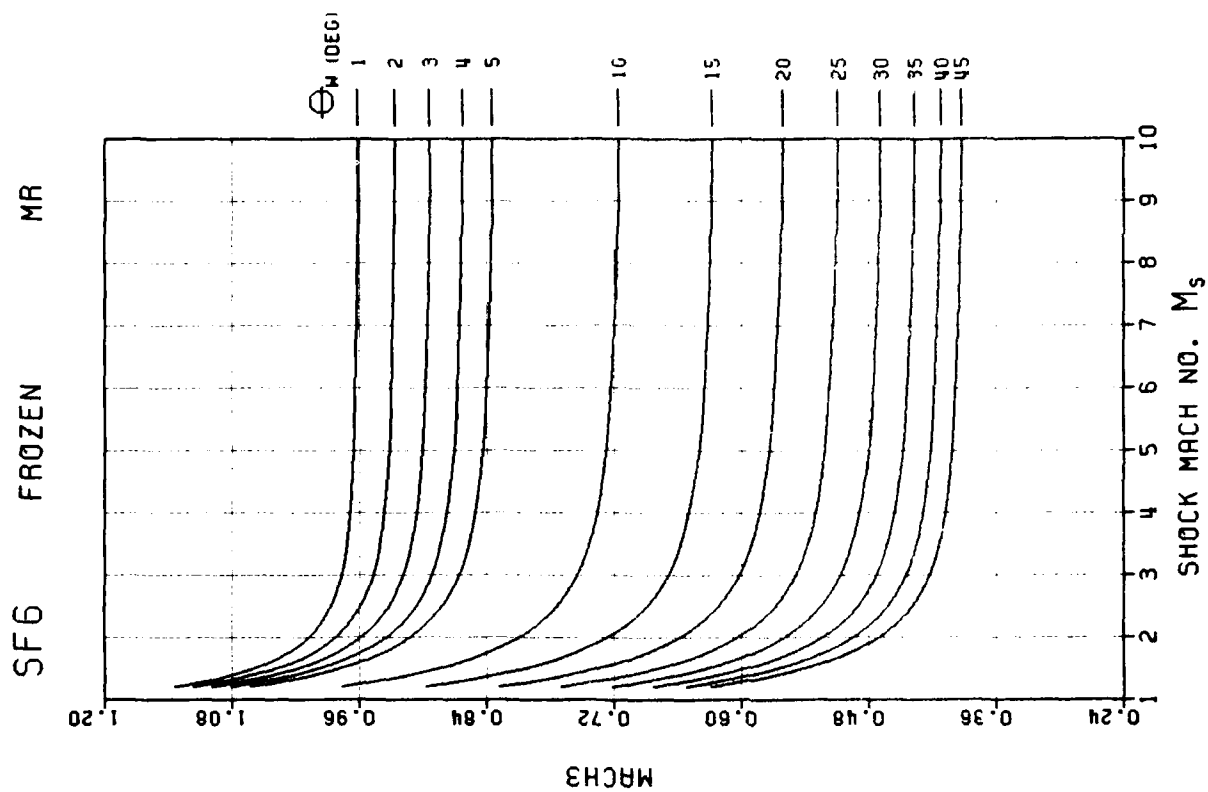
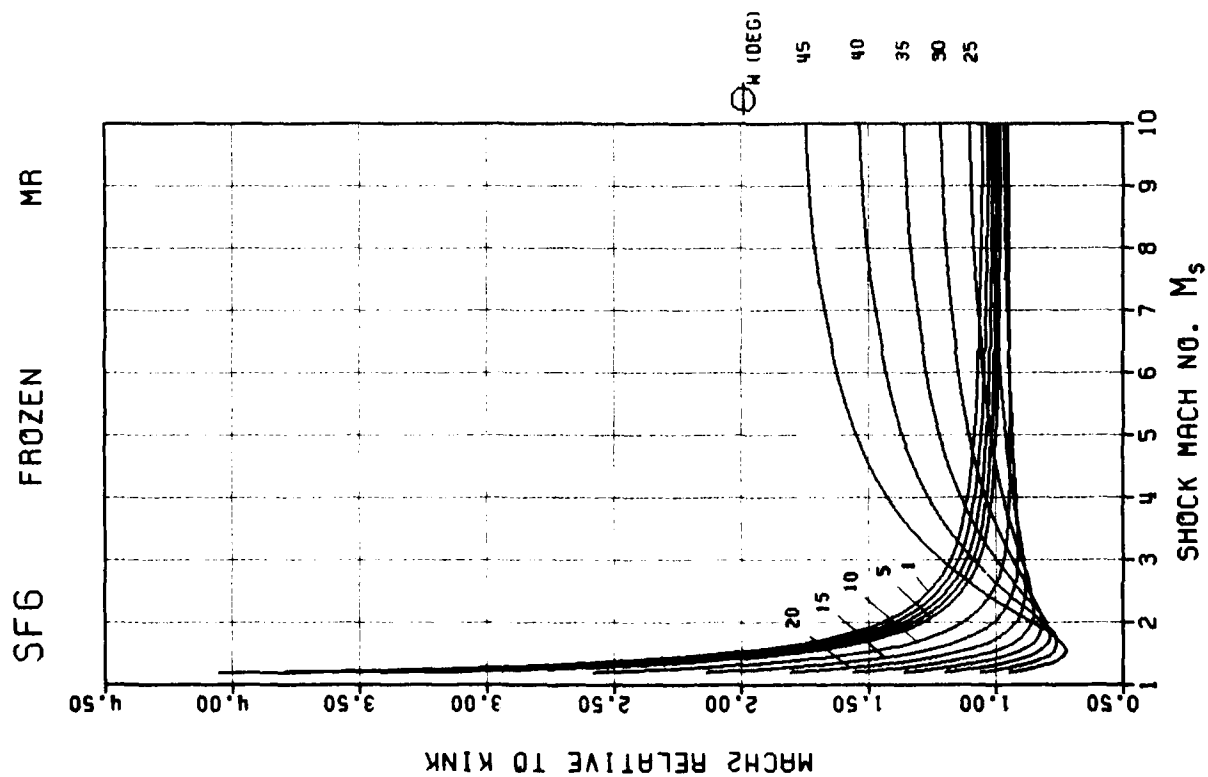


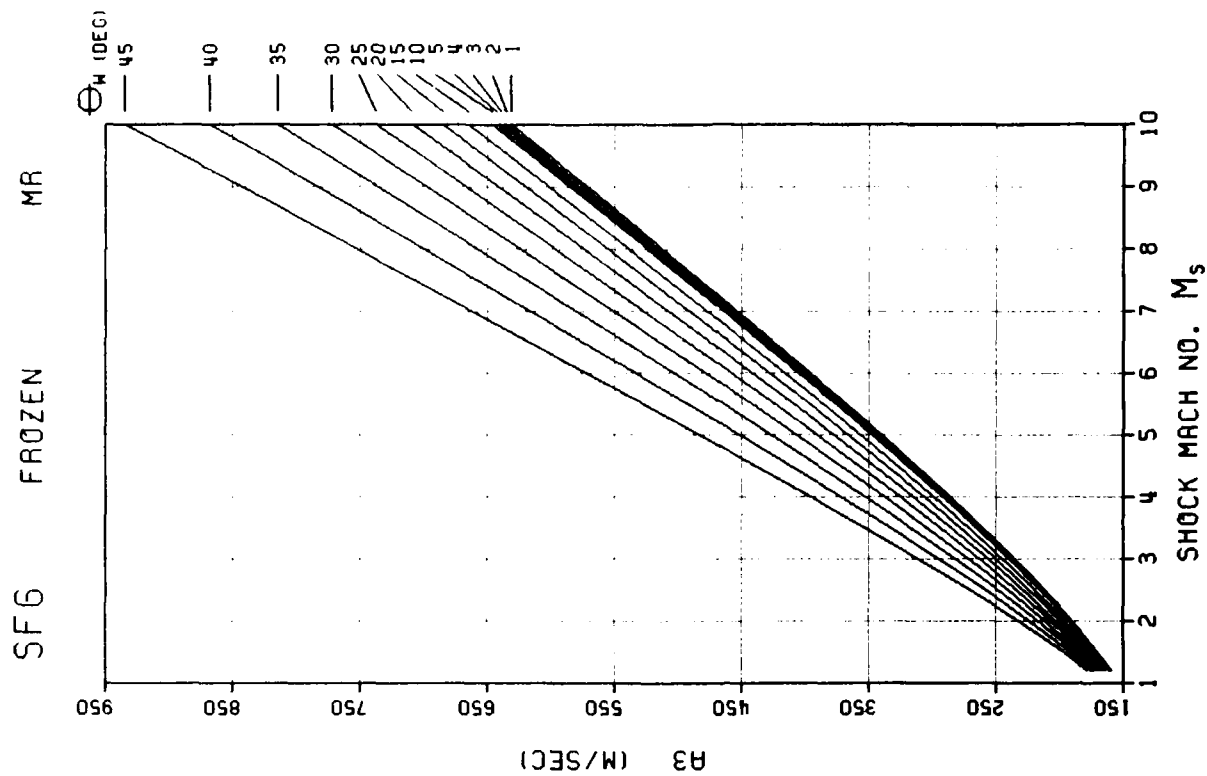
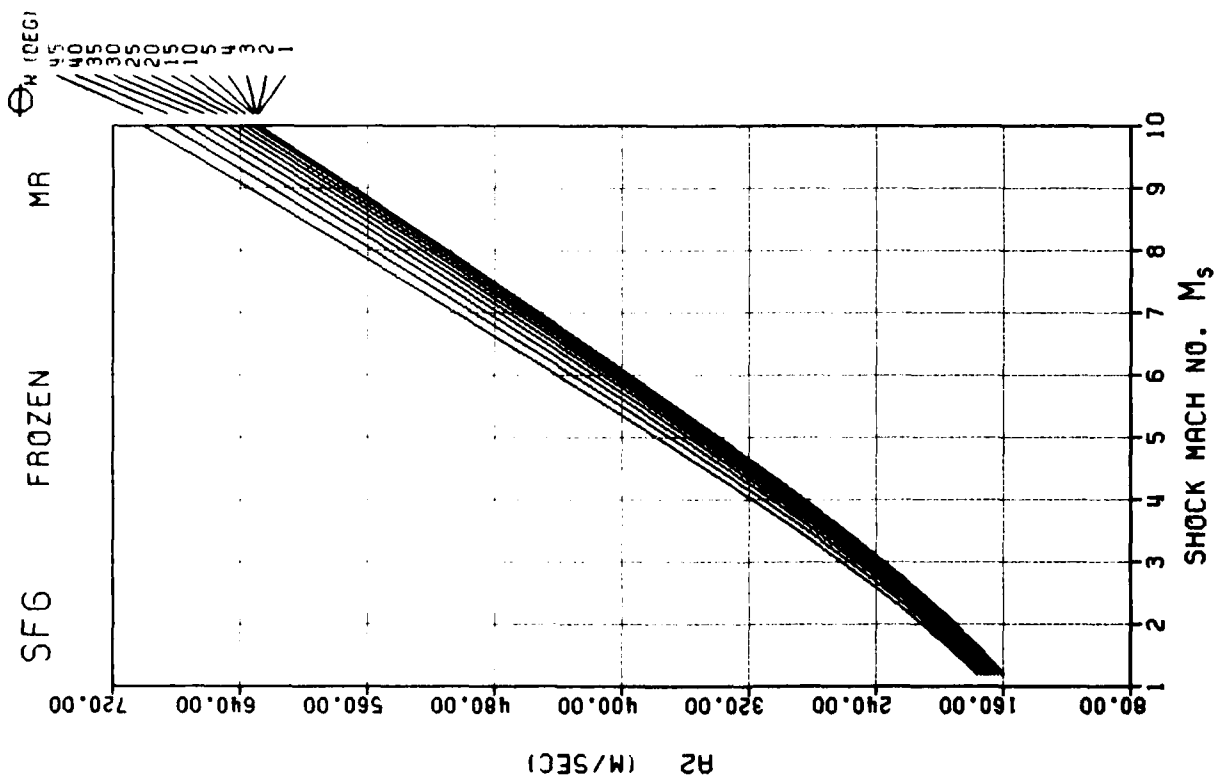


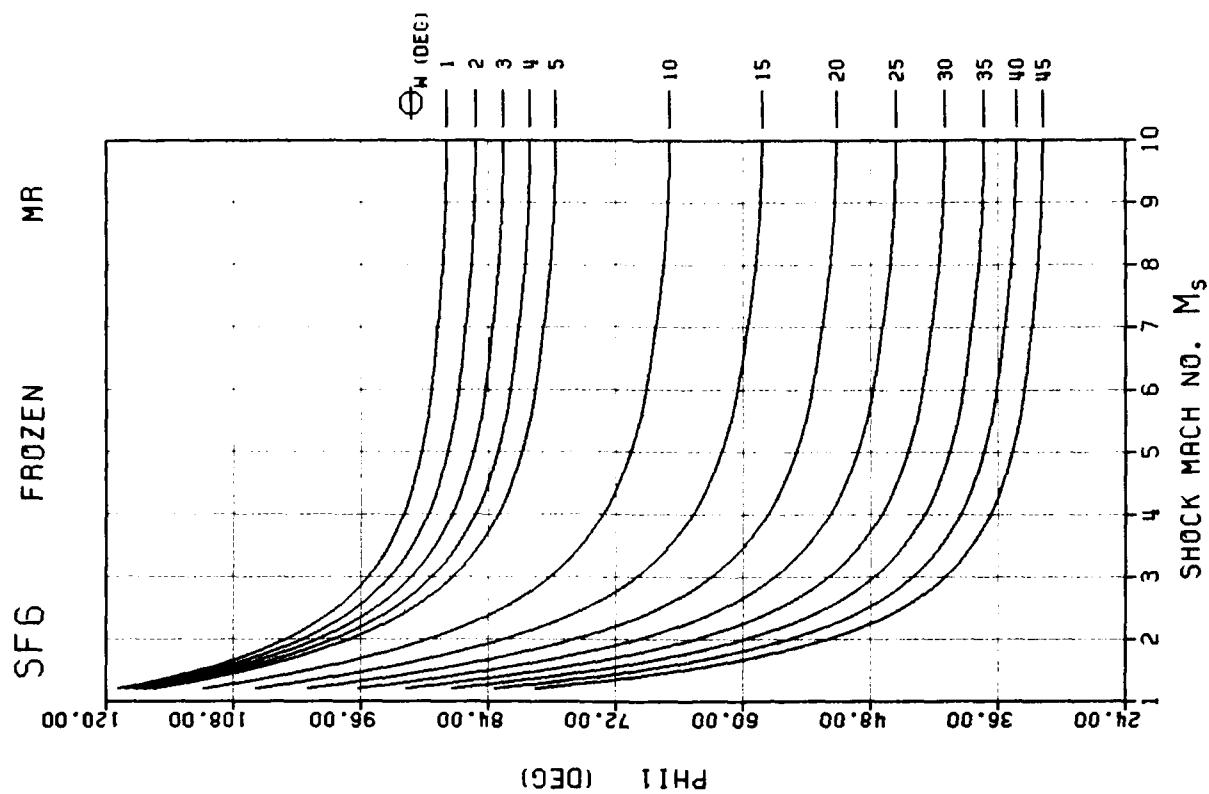
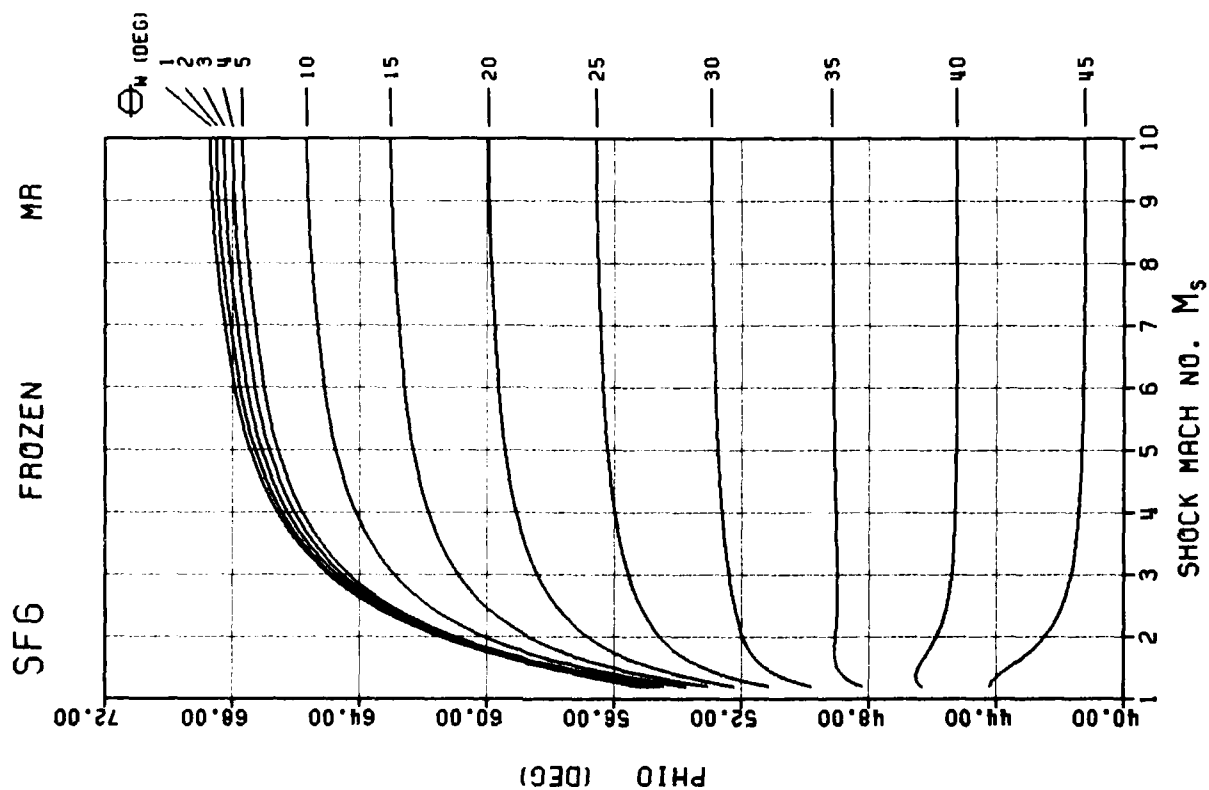


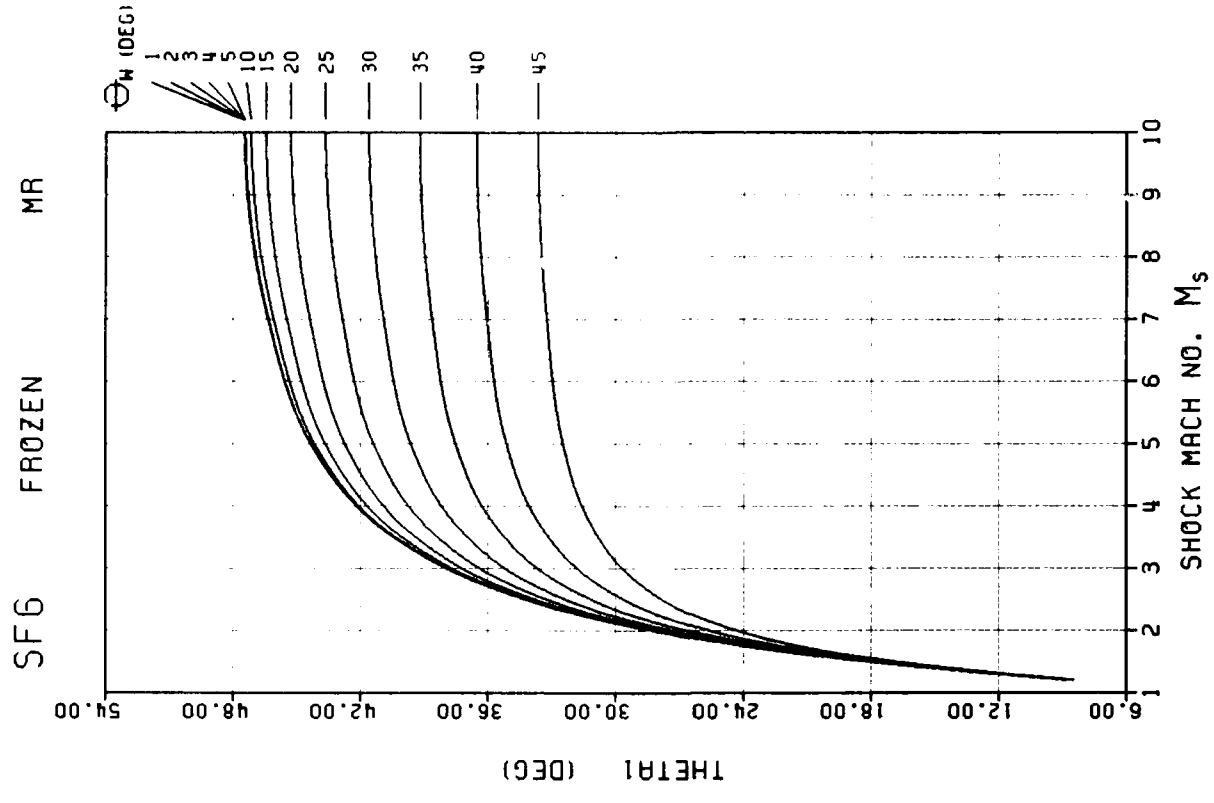
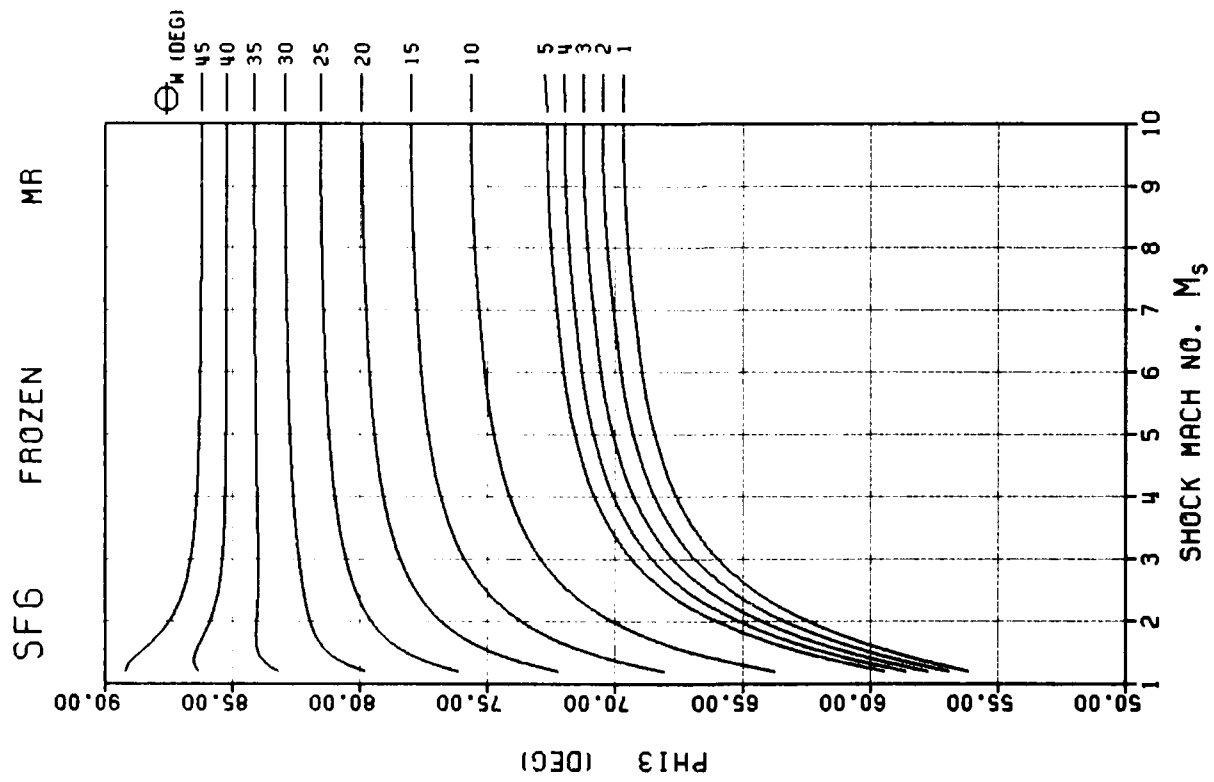


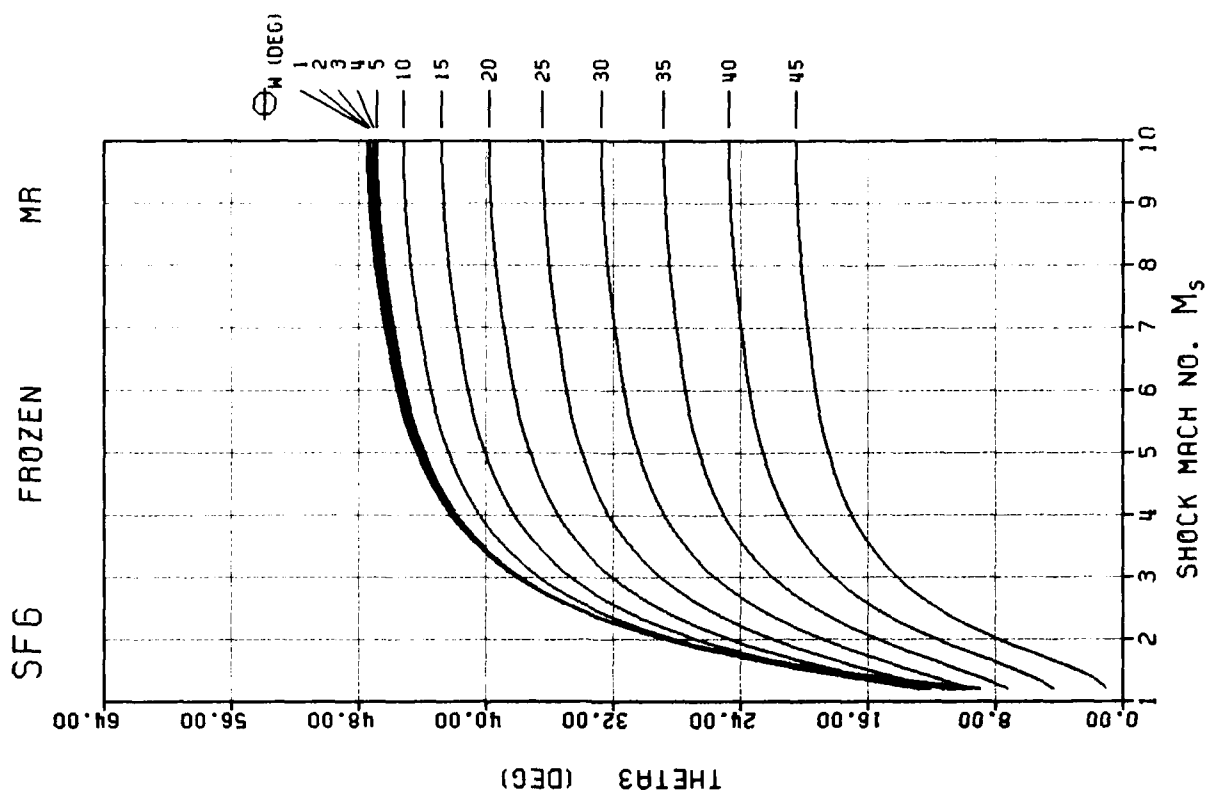
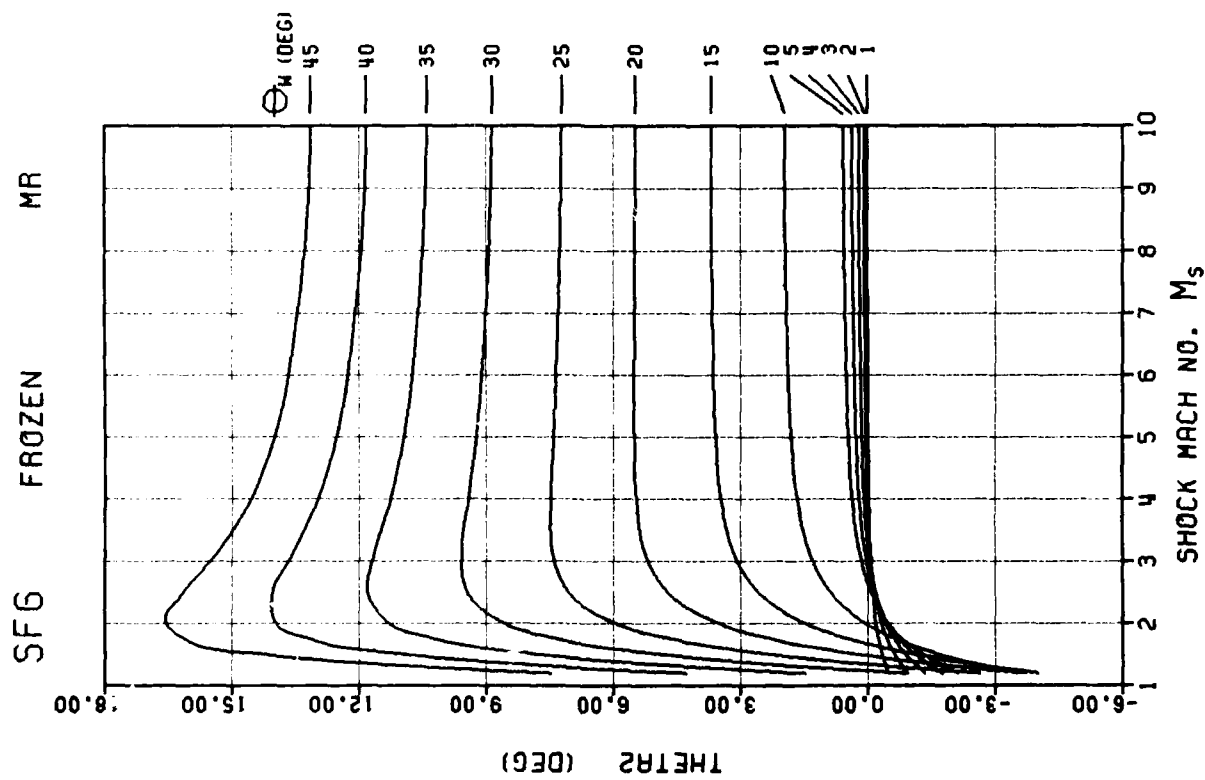


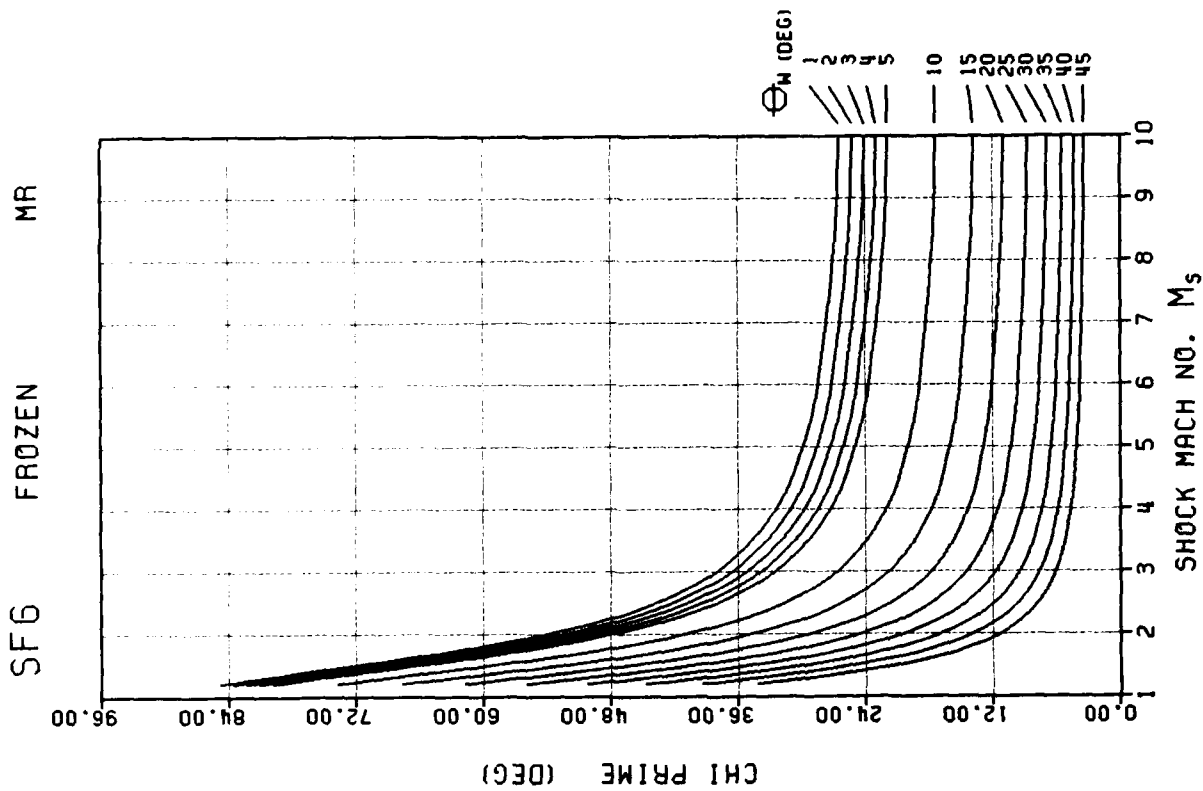
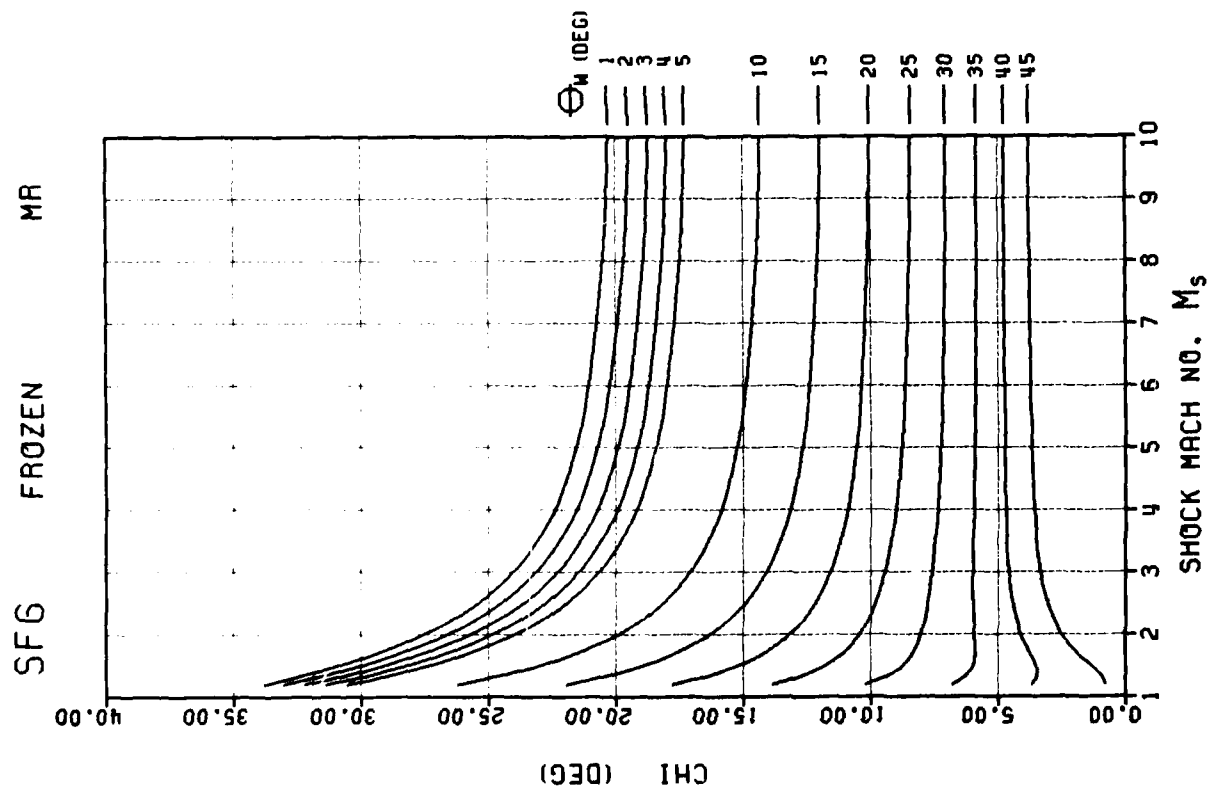


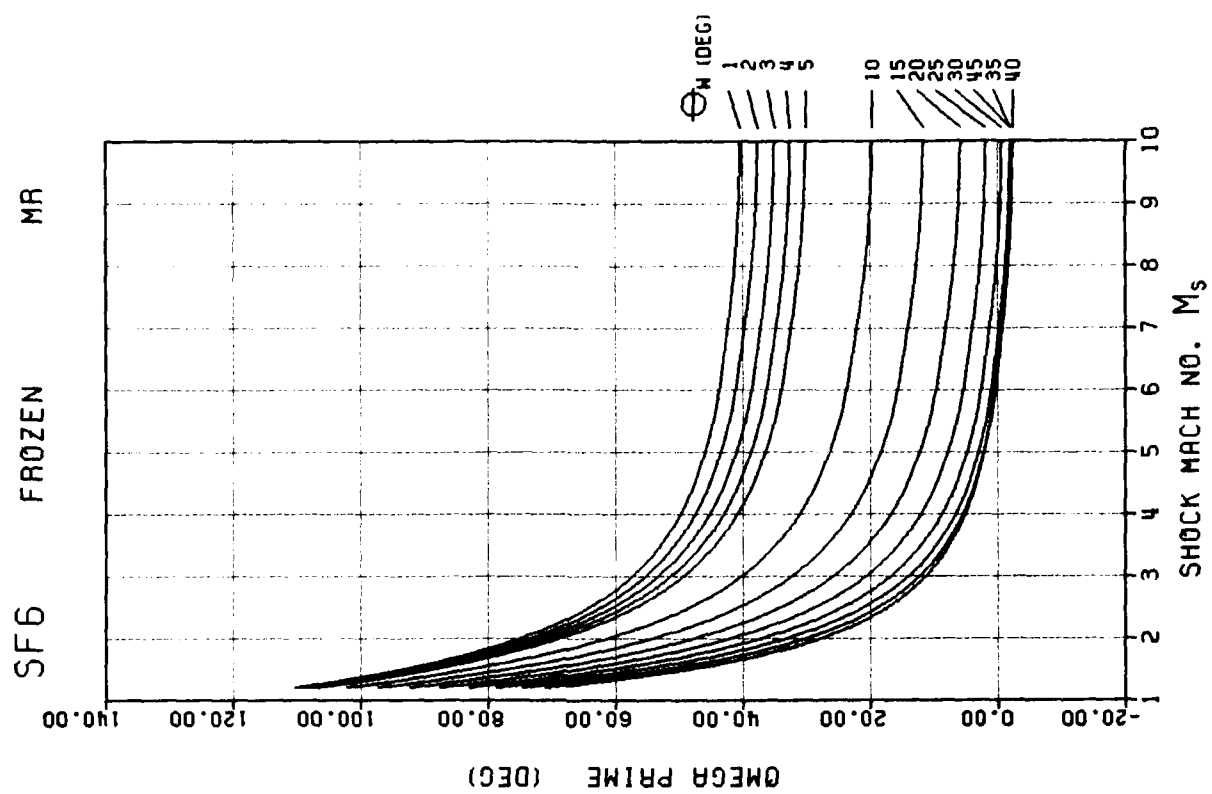
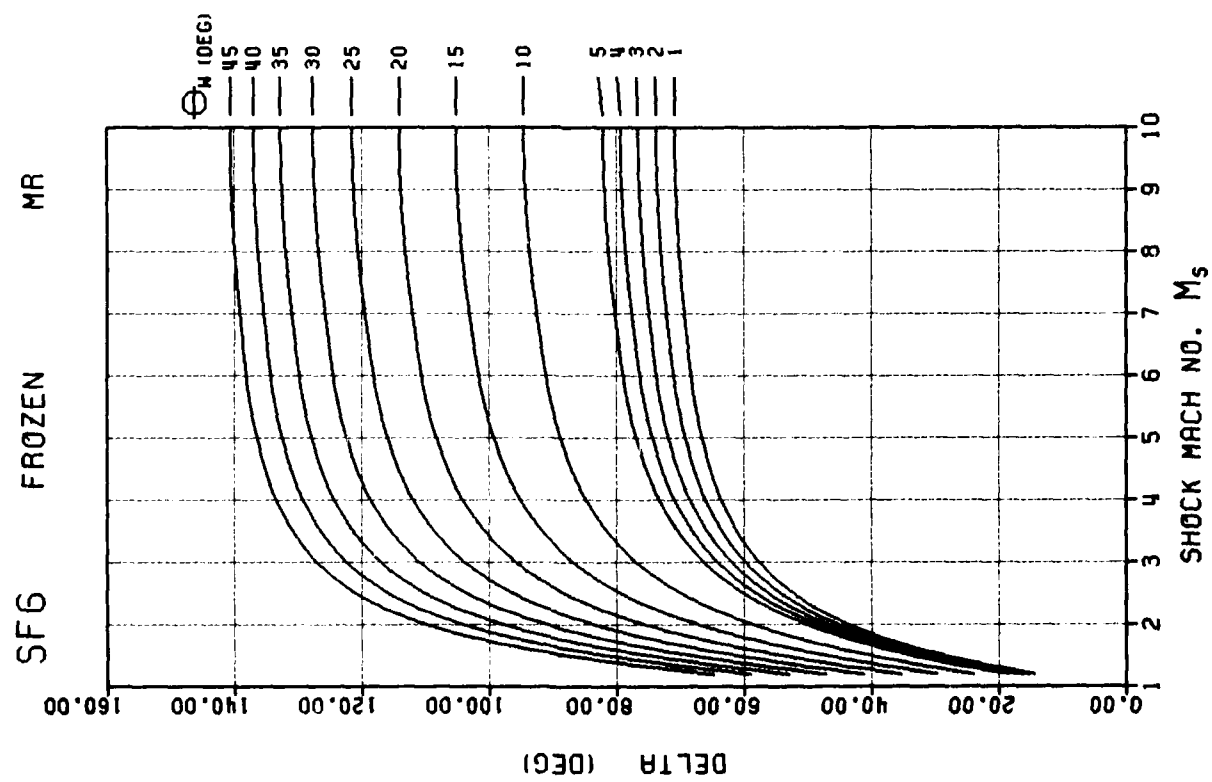


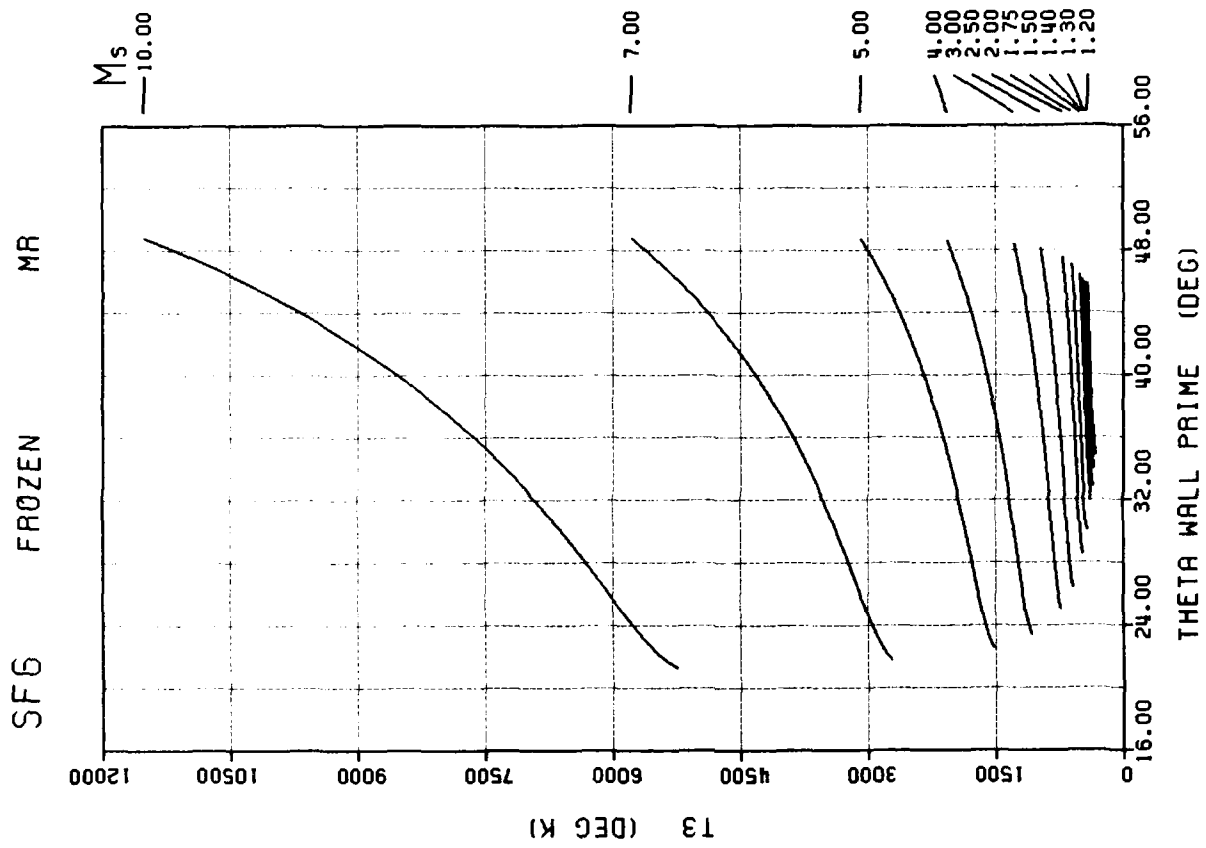
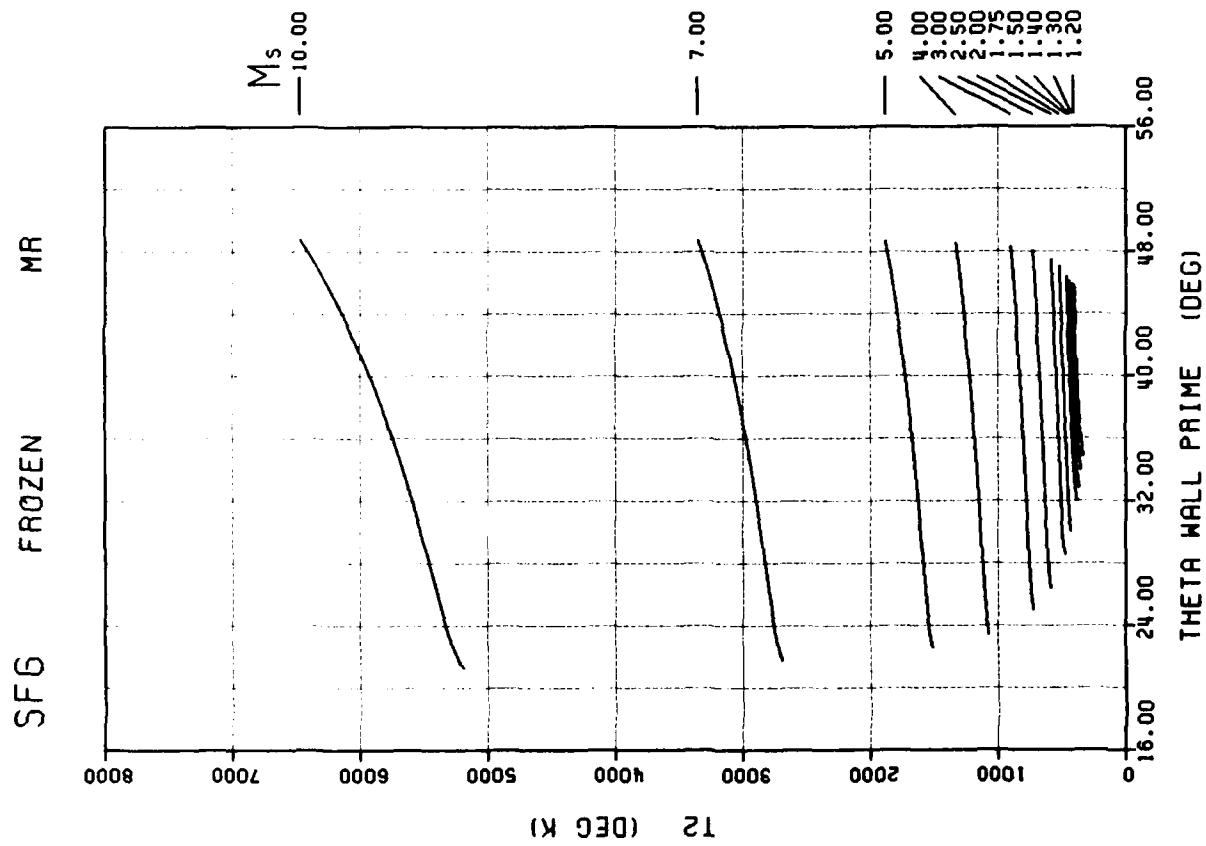


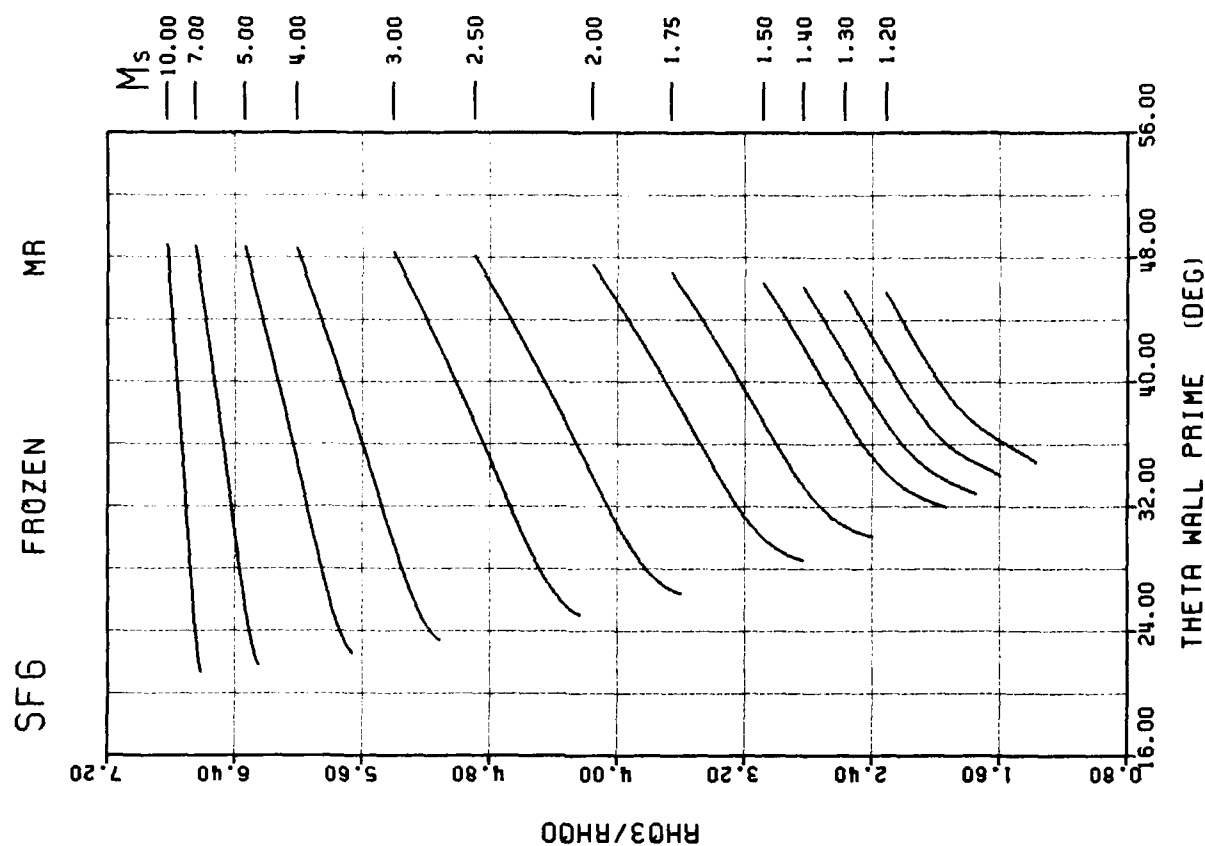
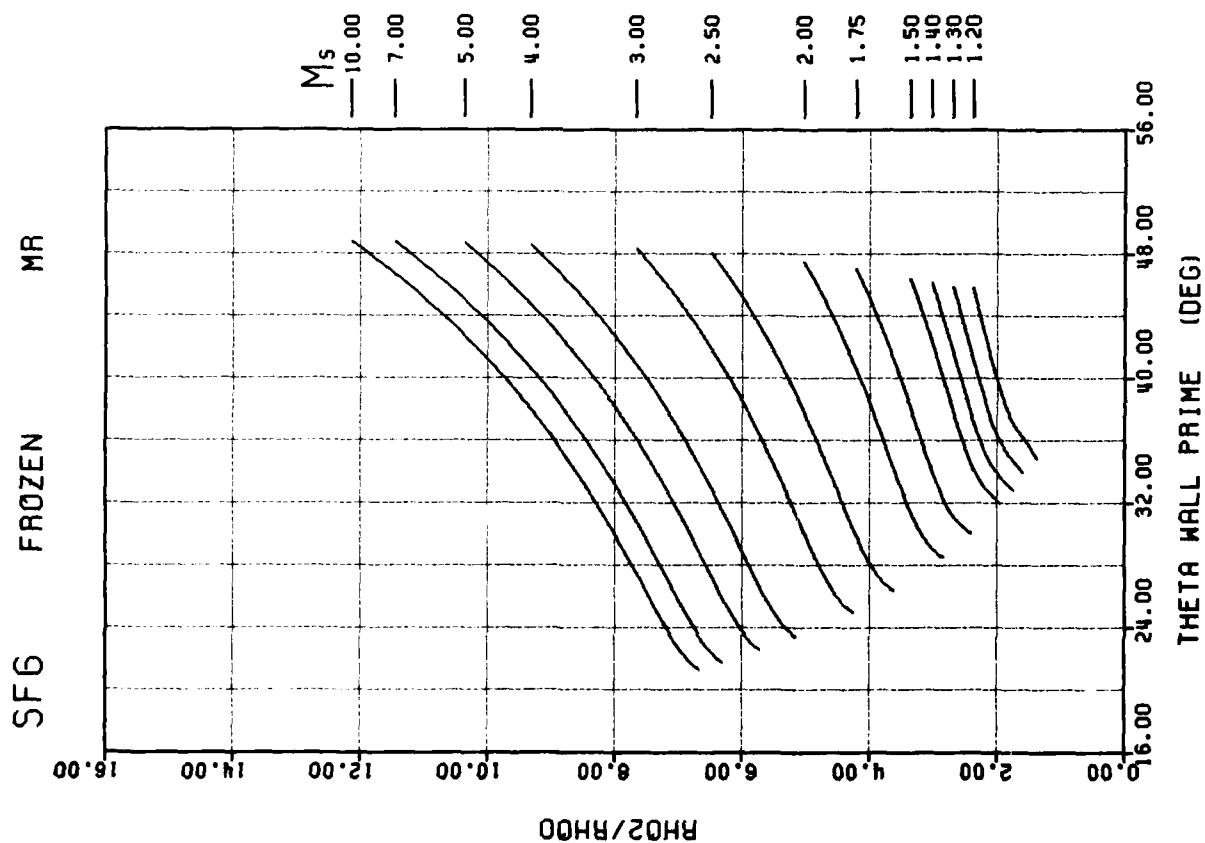


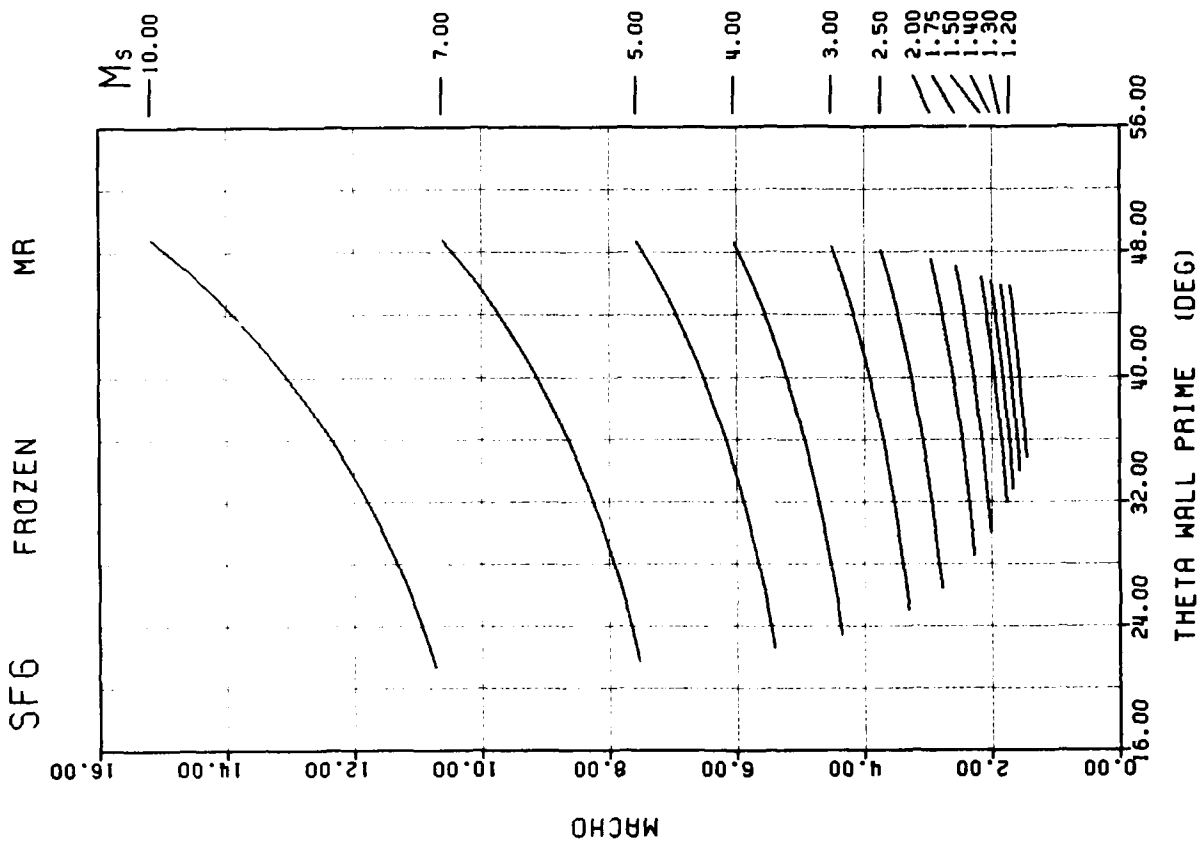
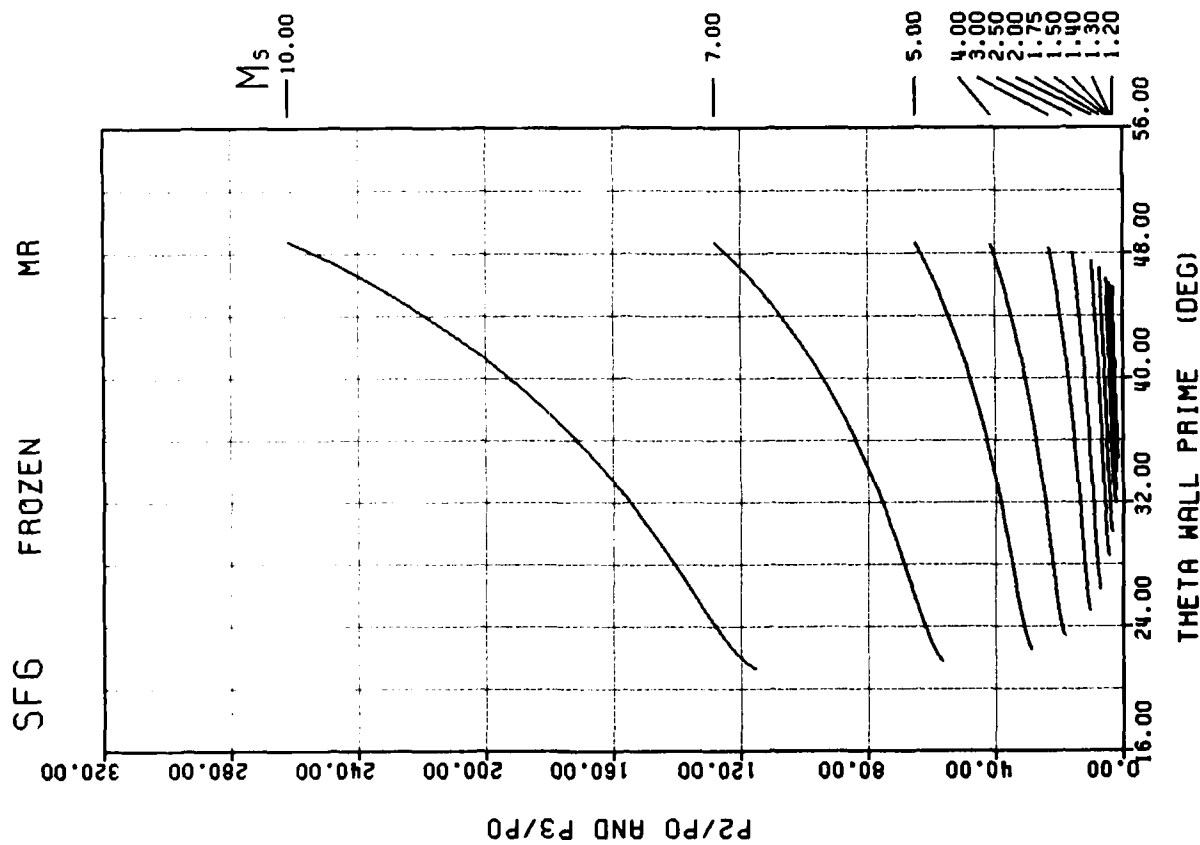


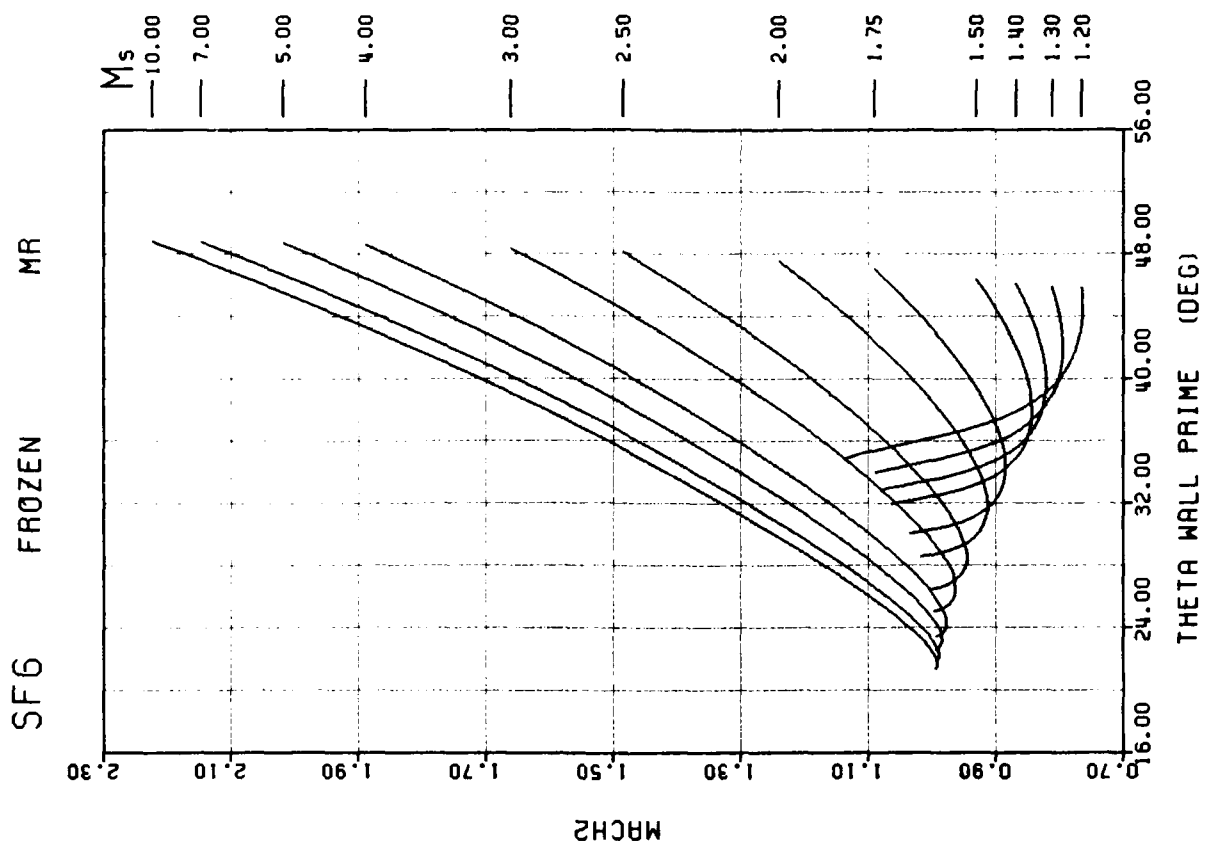
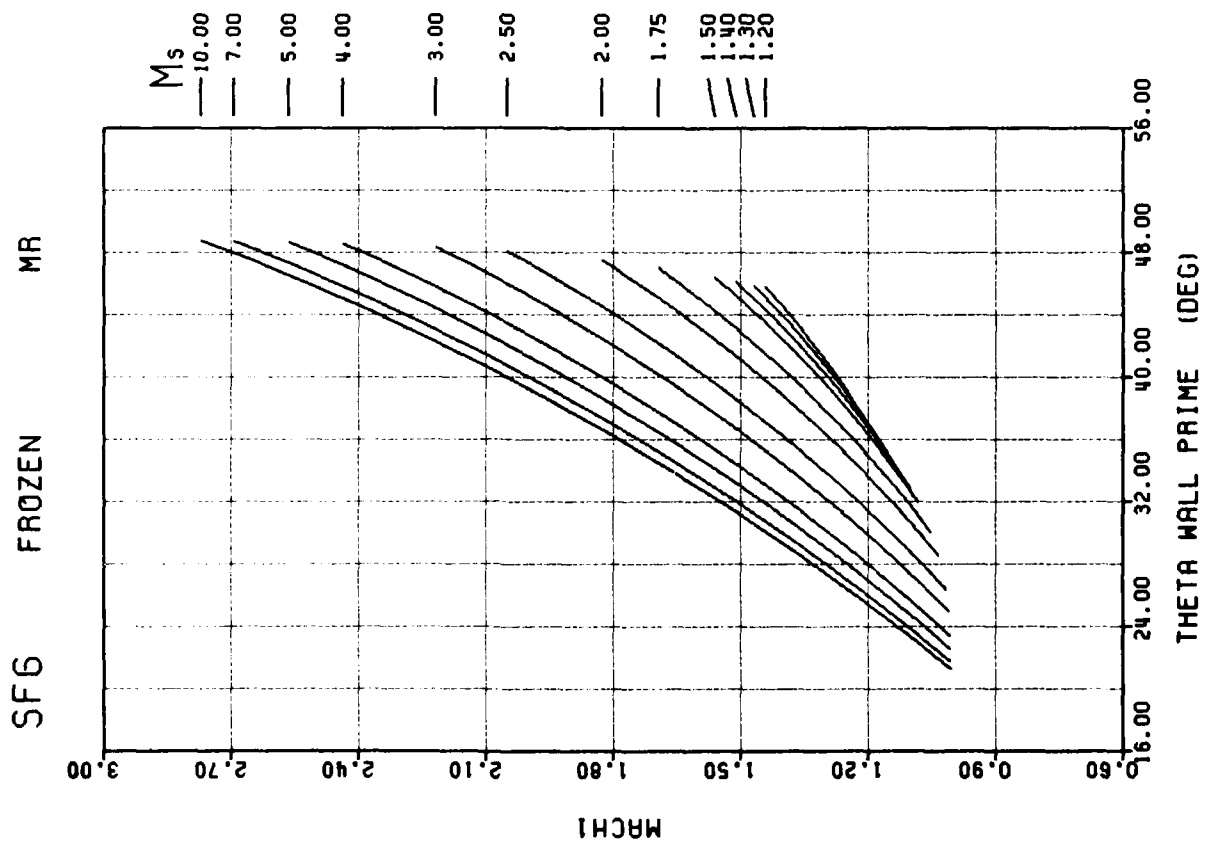


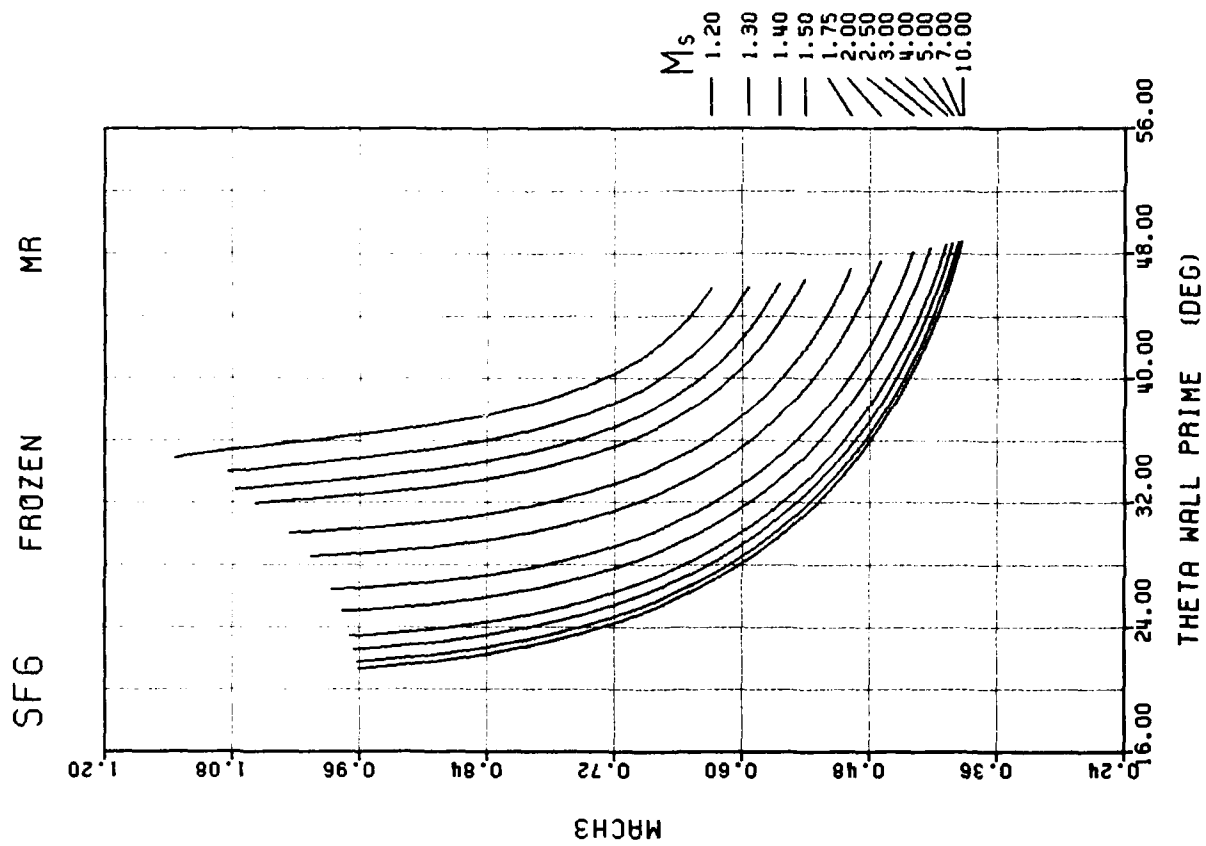
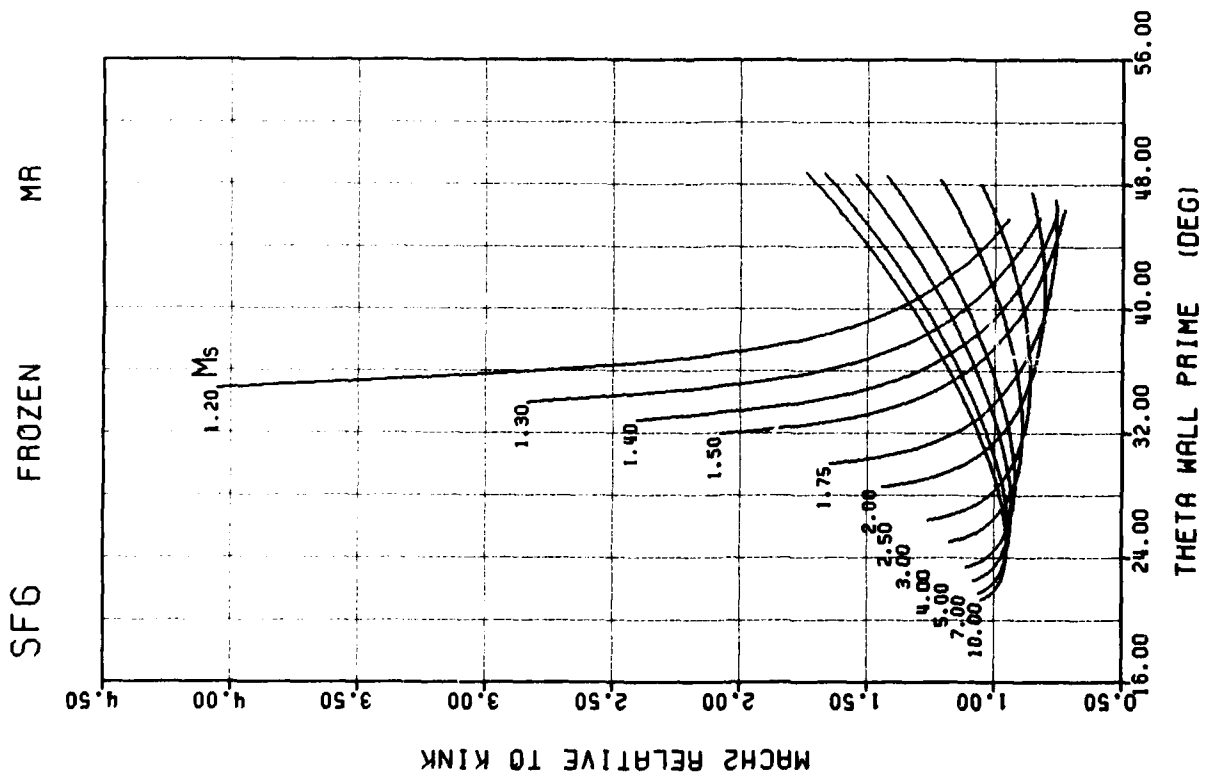


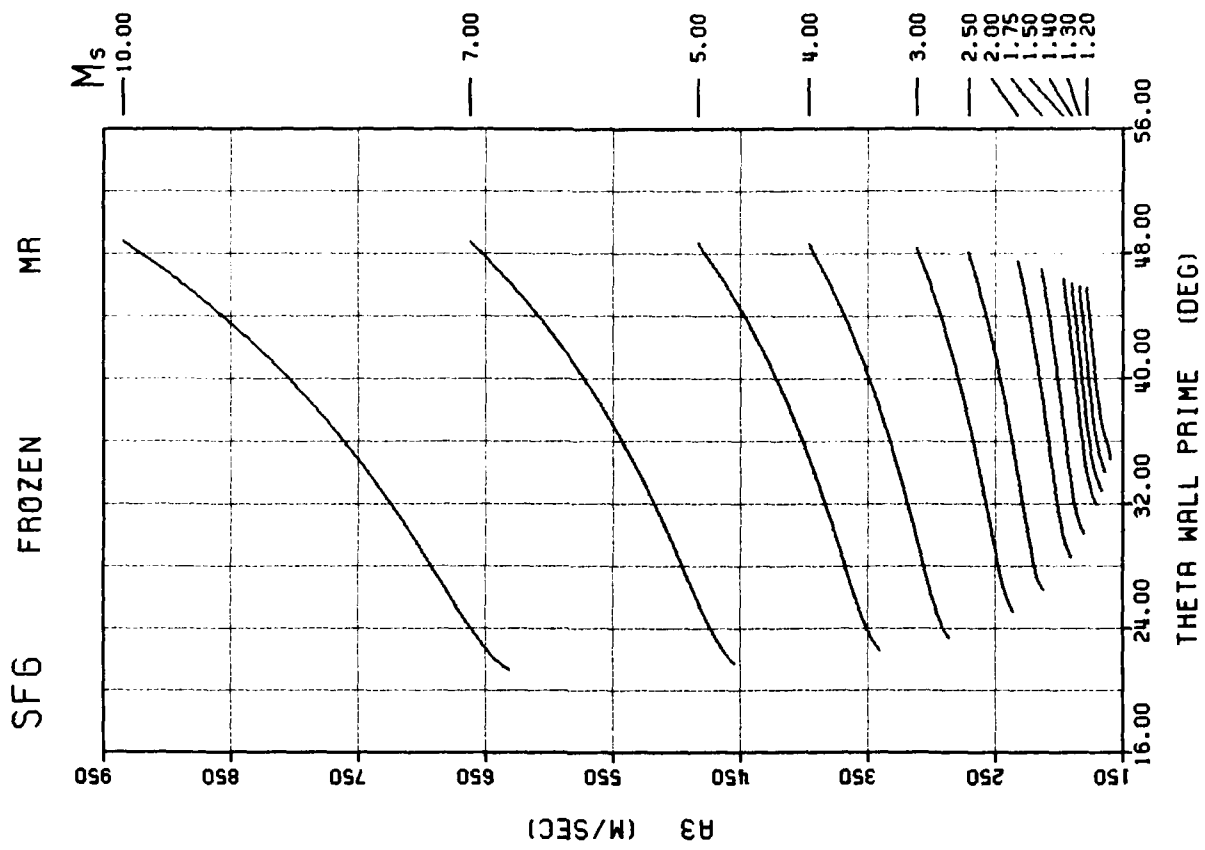
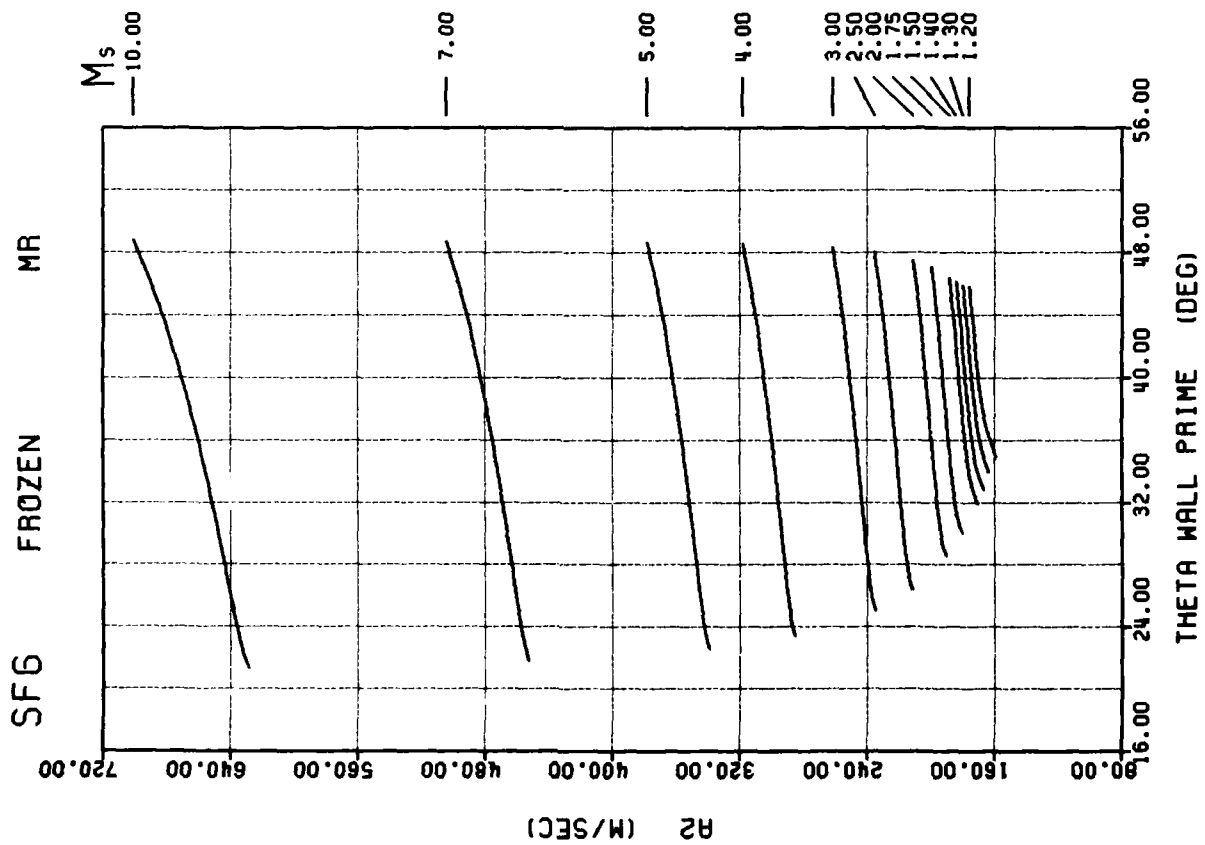


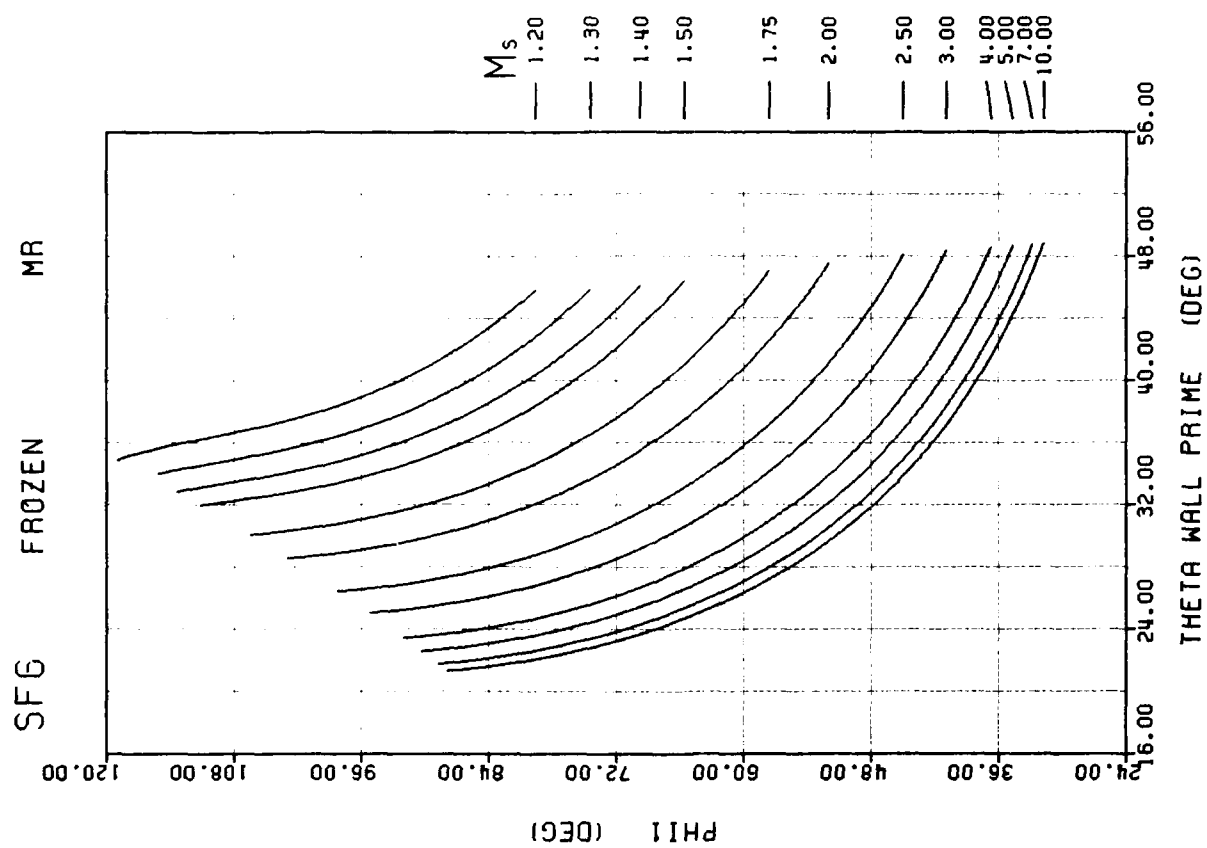
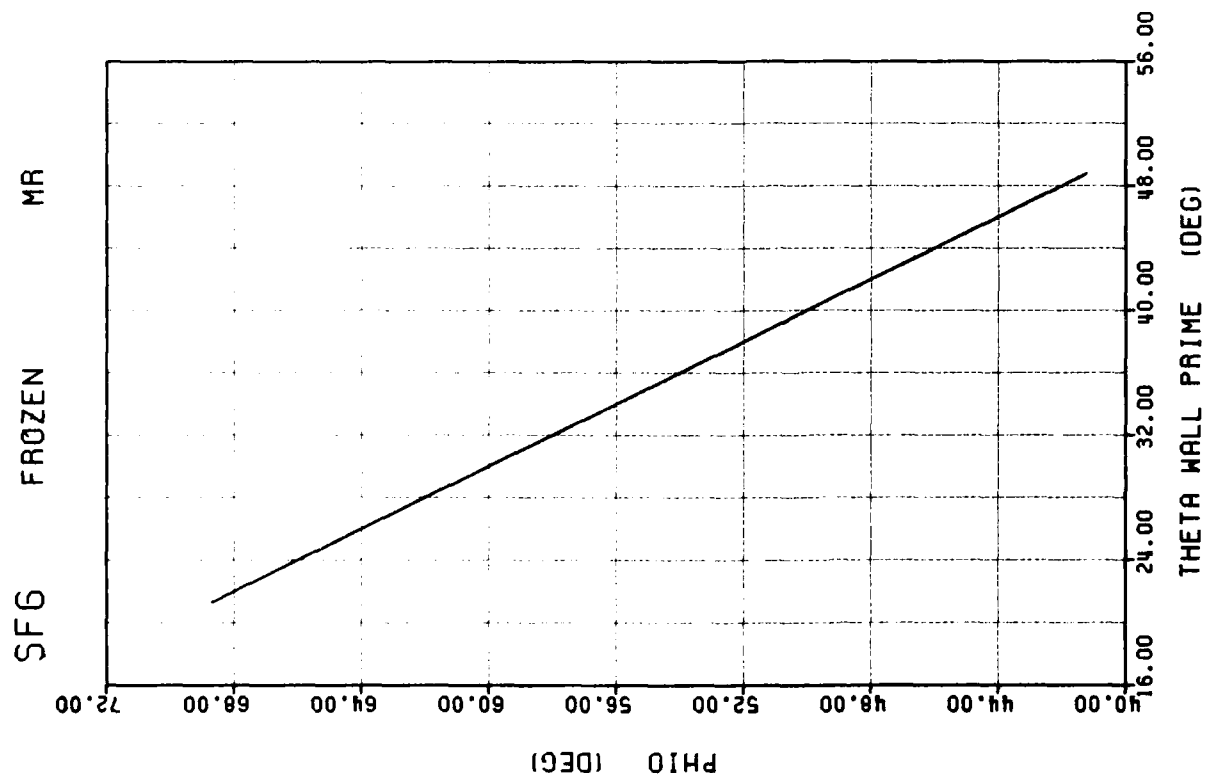


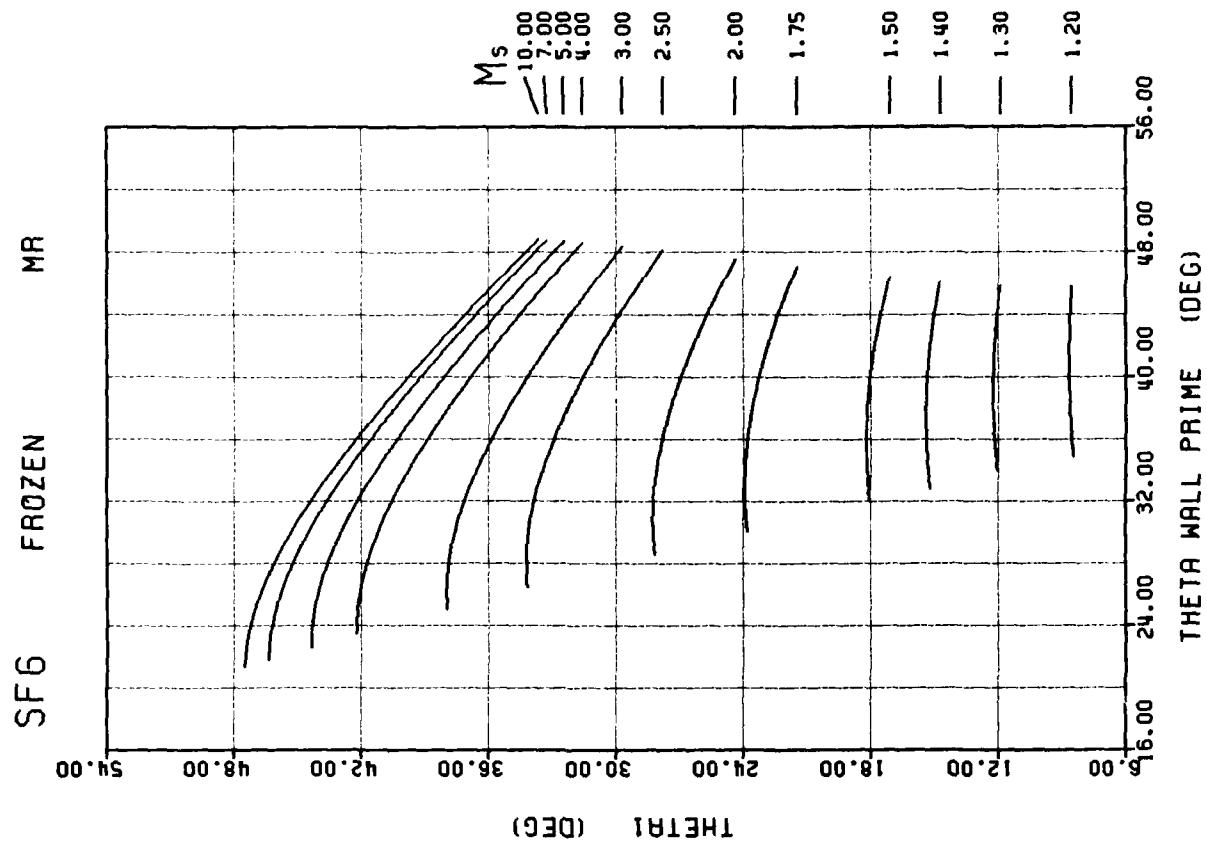
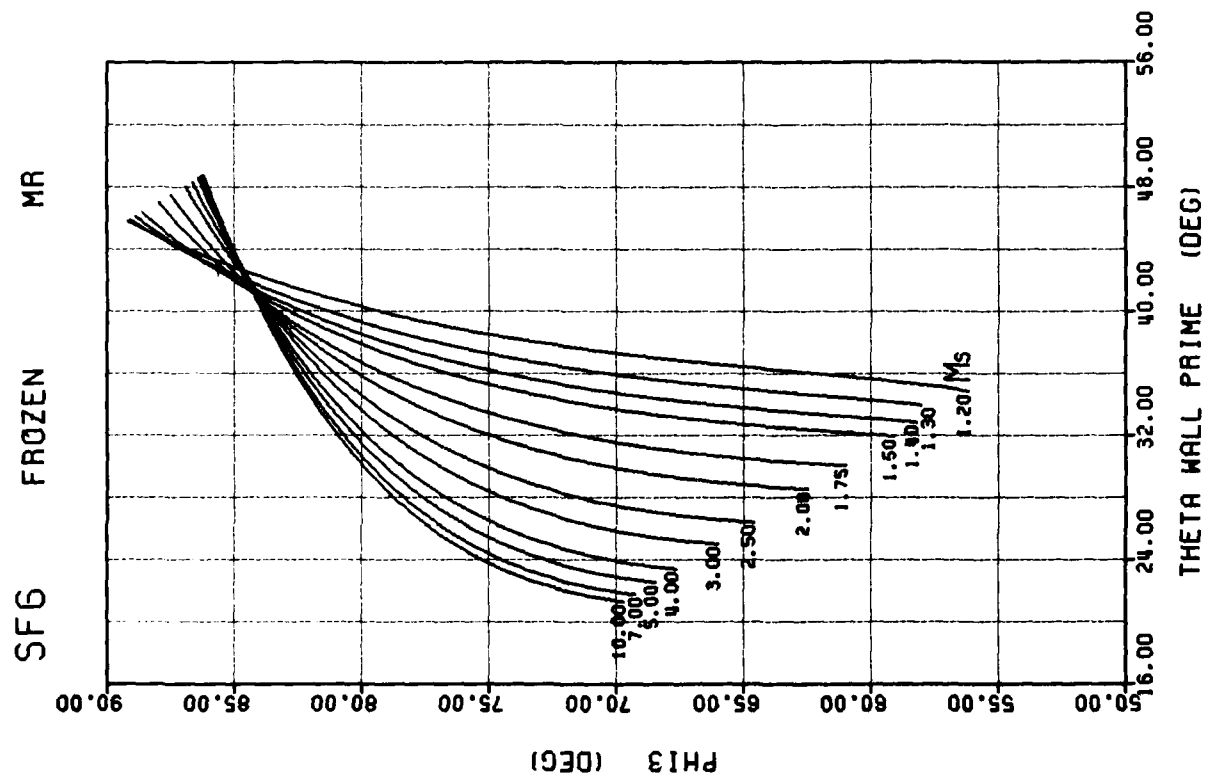


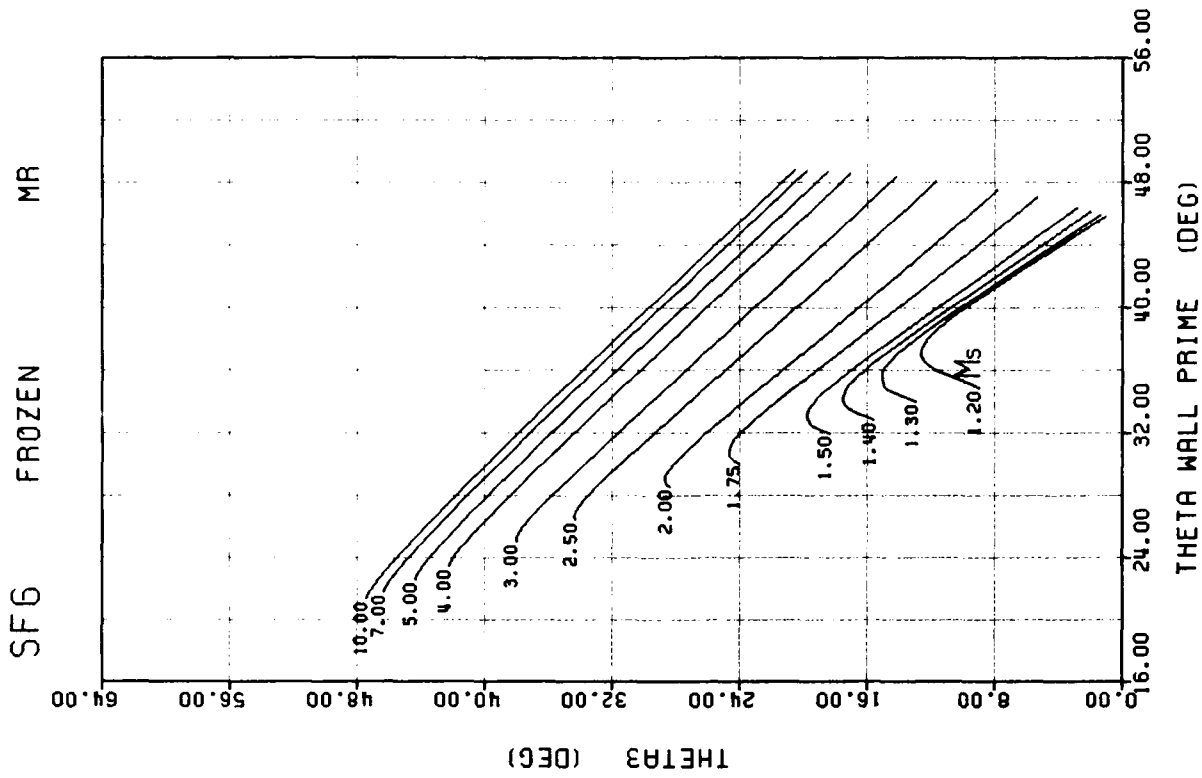
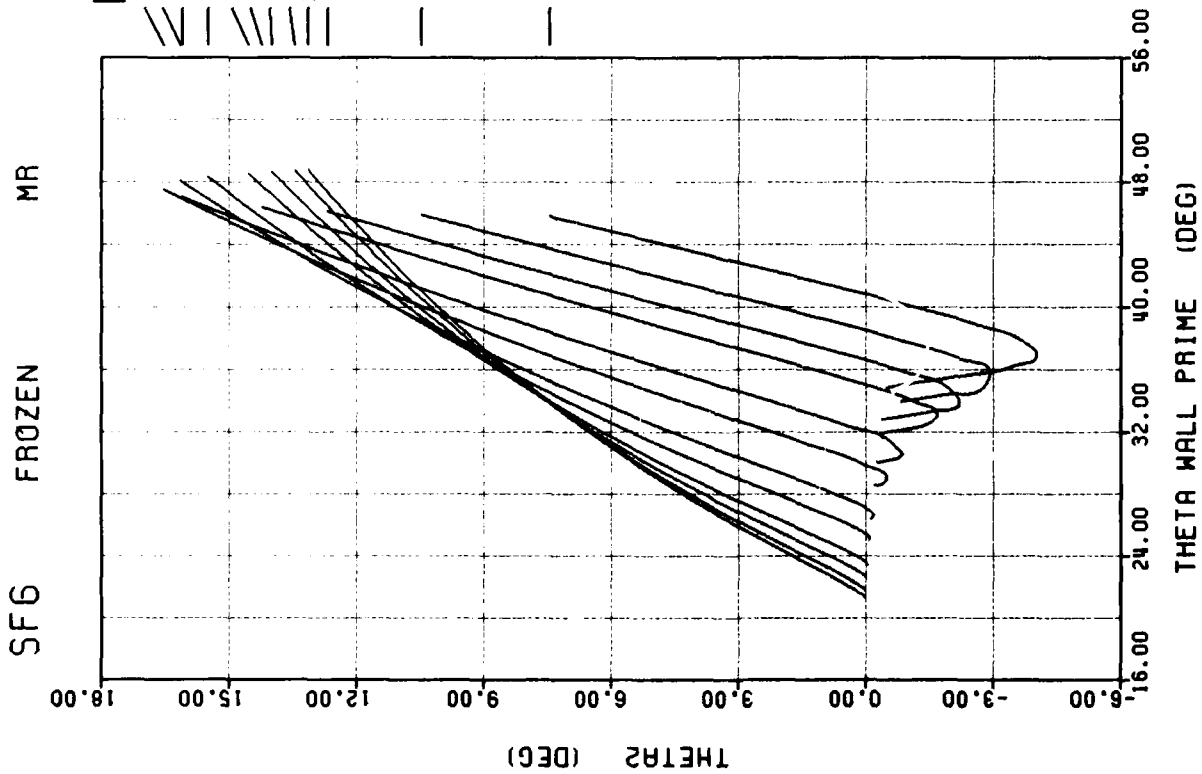


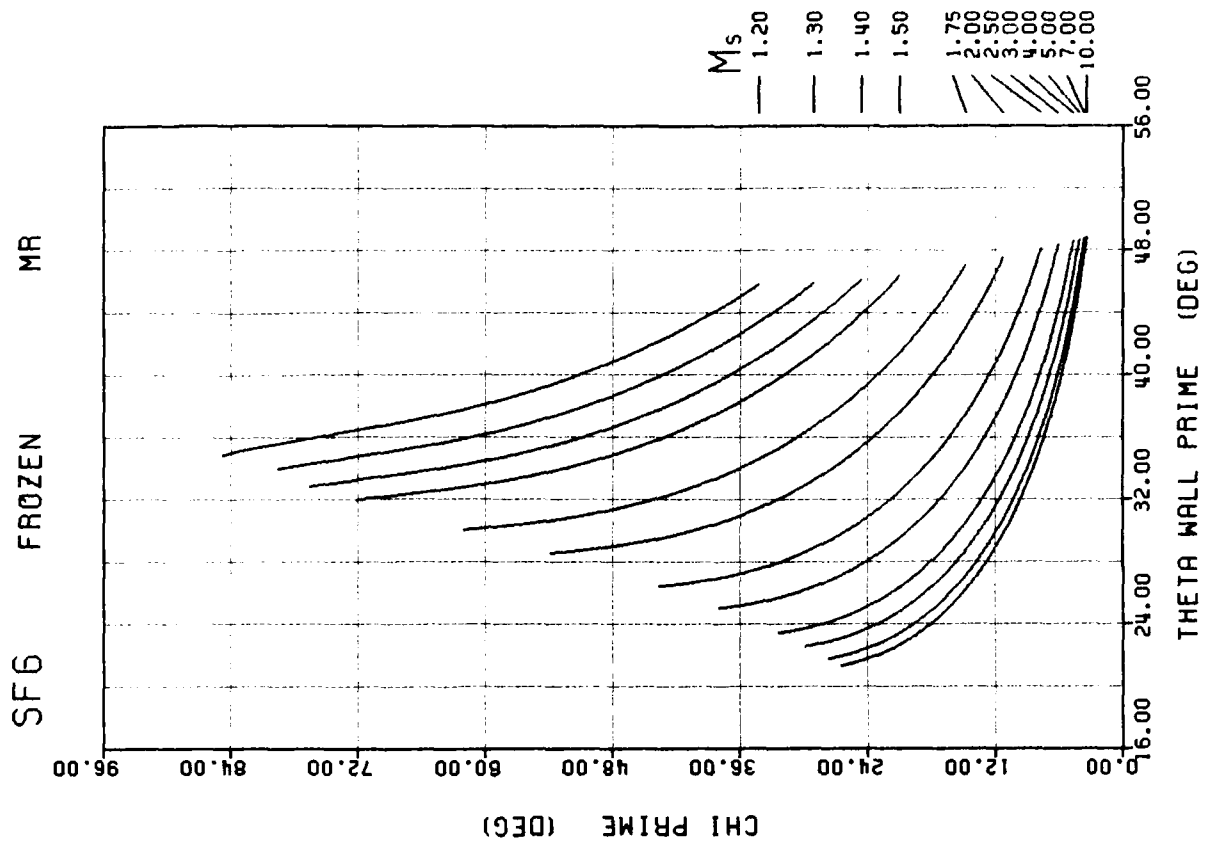
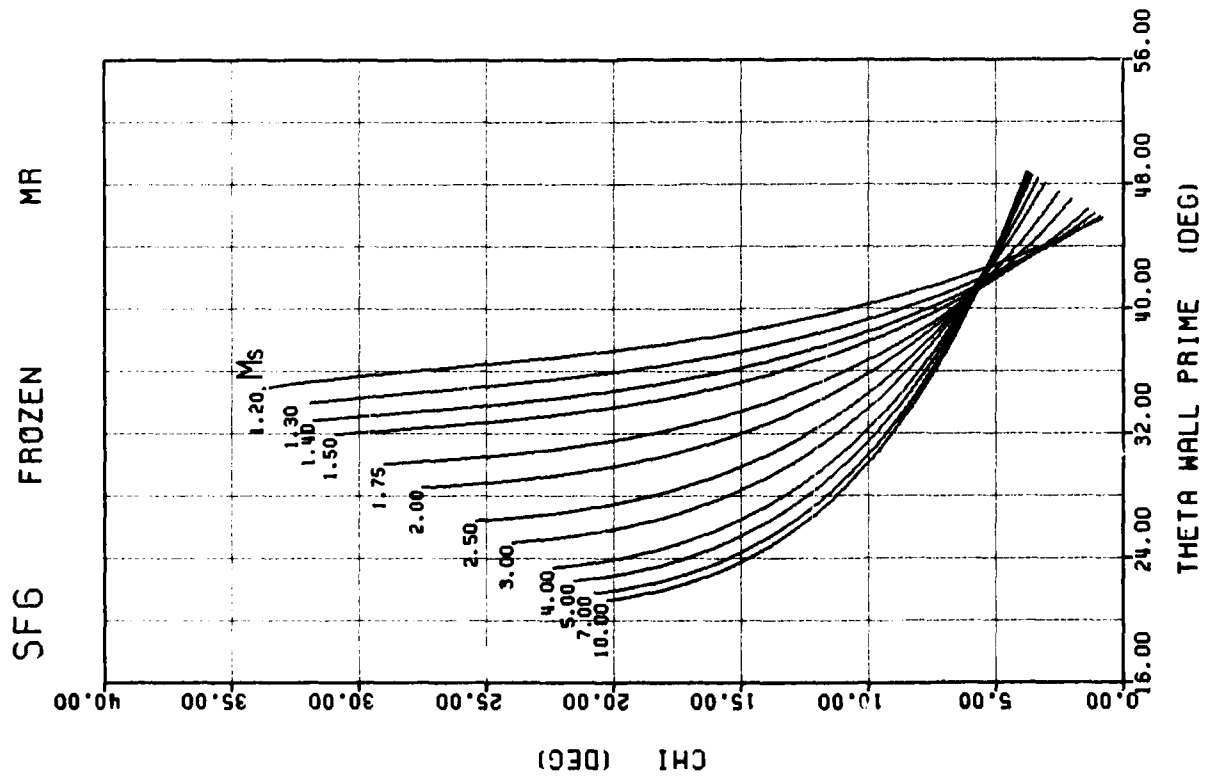


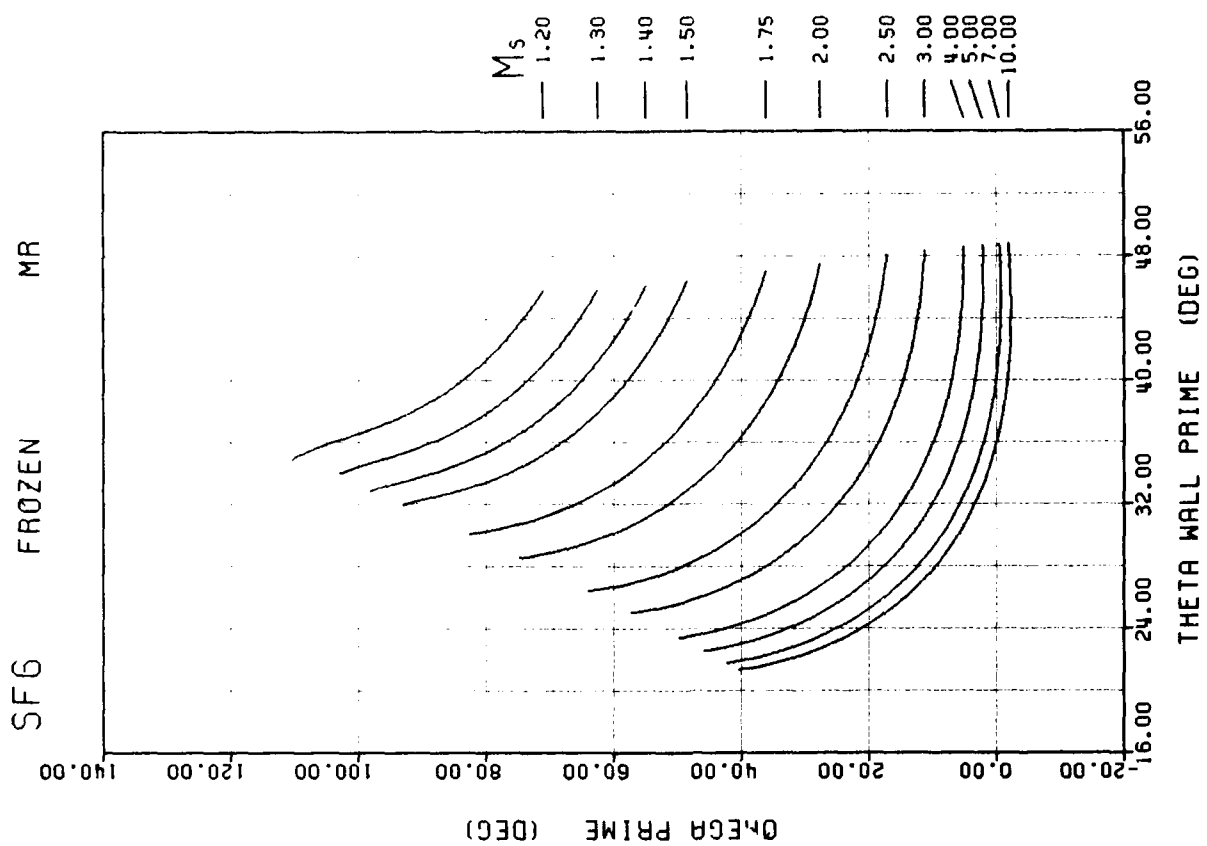
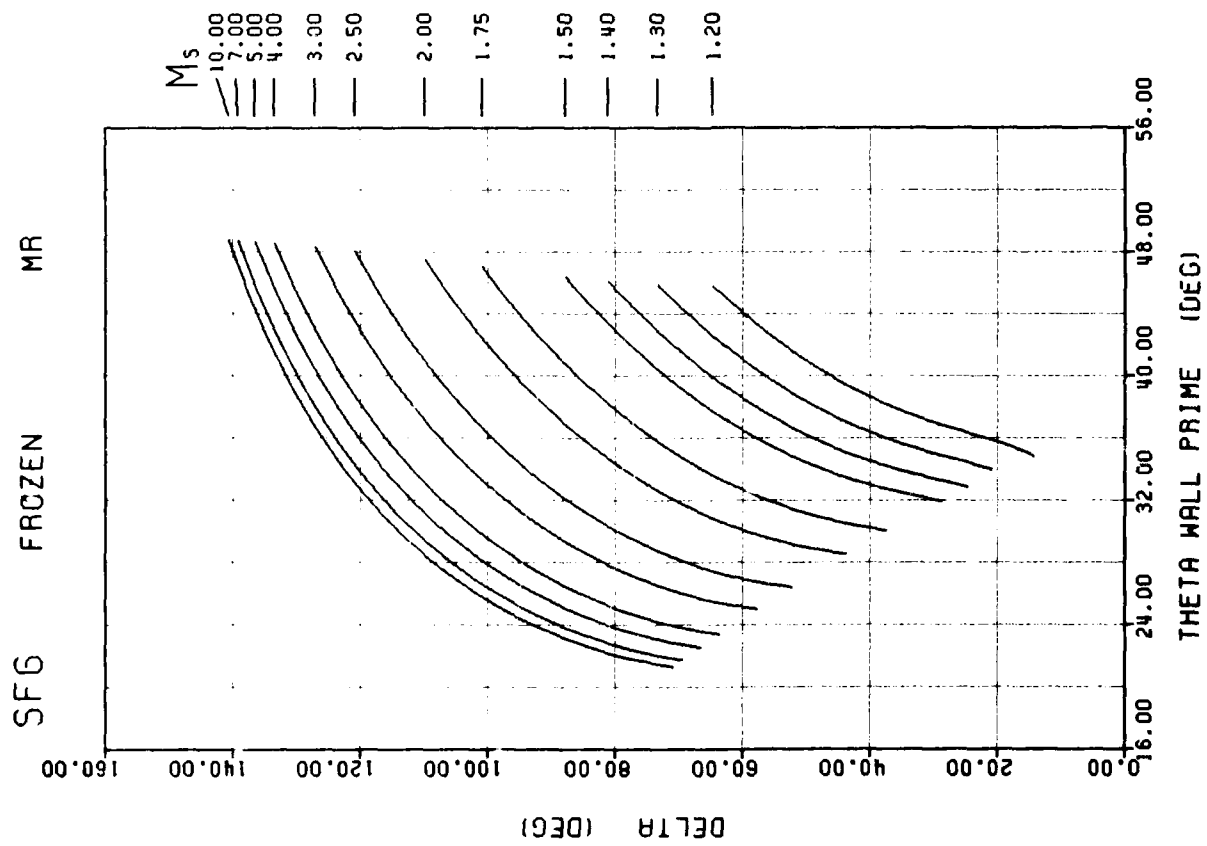












AO-A164 047

TABULAR AND GRAPHICAL SOLUTIONS OF REGULAR AND MACH
REFLECTIONS IN PSEUDO- (U) TORONTO UNIV DOWNSVIEW
(ONTARIO) INST FOR AEROSPACE STUDIES T C MU ET AL.

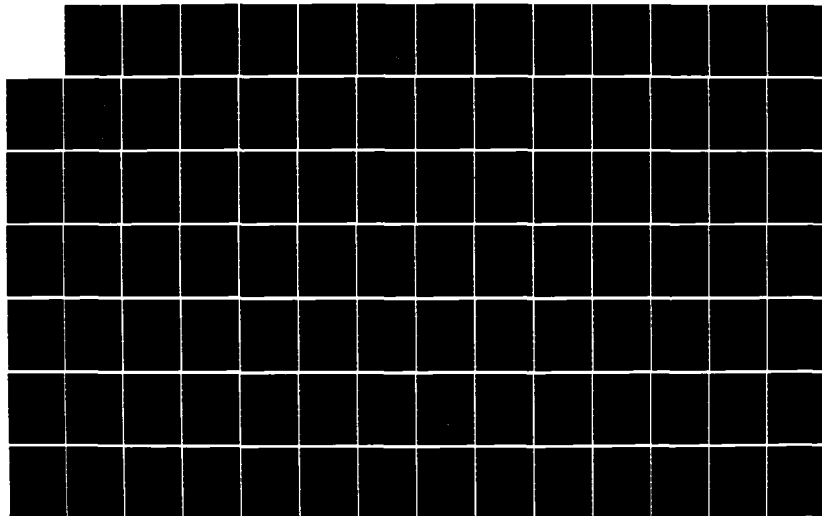
2/3

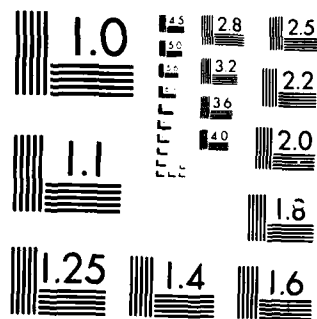
UNCLASSIFIED

JUN 85 UTIAS-283-PT-2 AFOSR-TR-85-1231

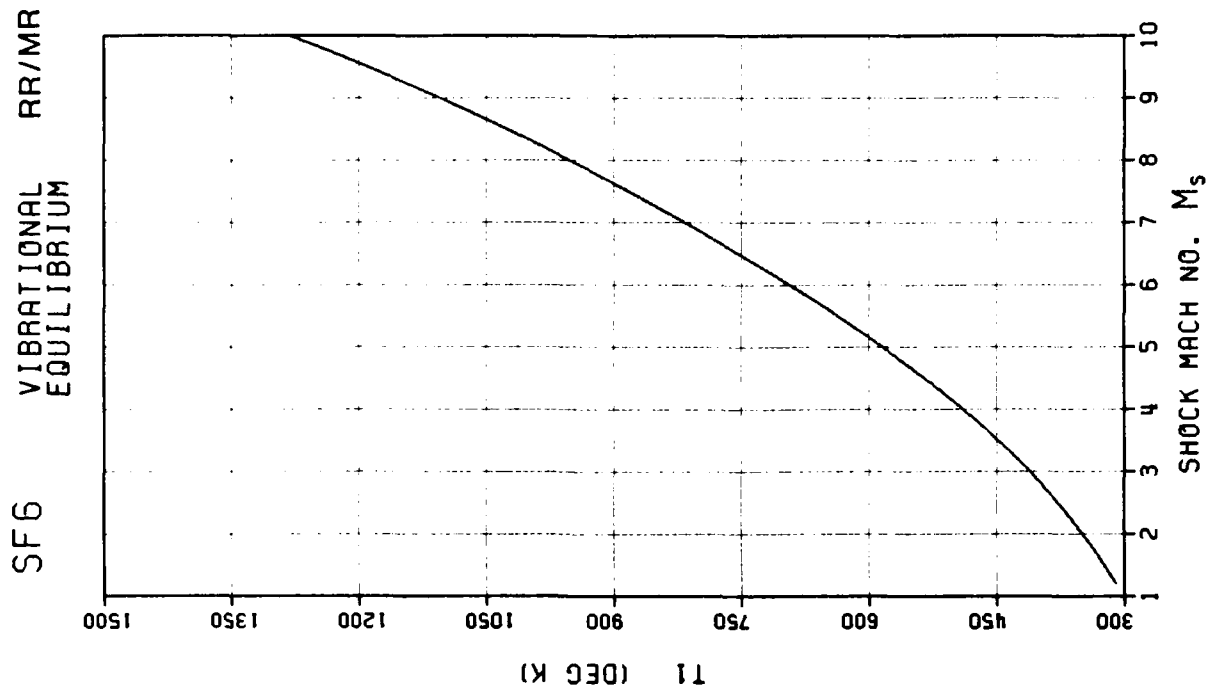
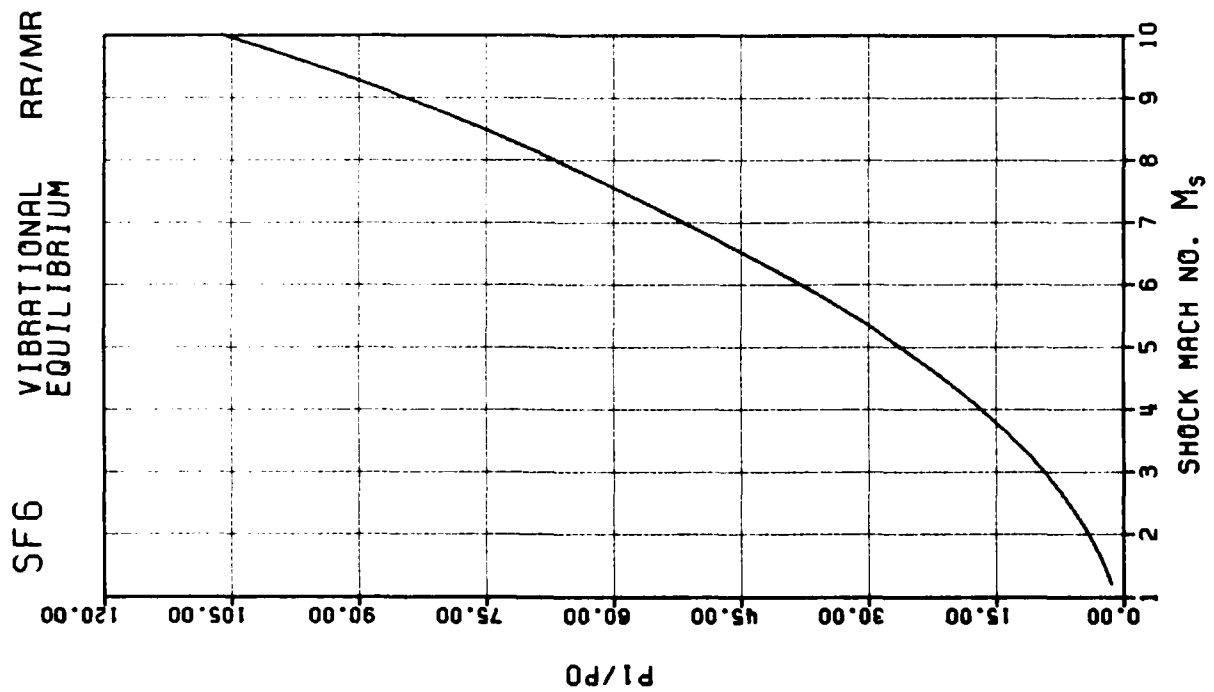
F/G 20/4

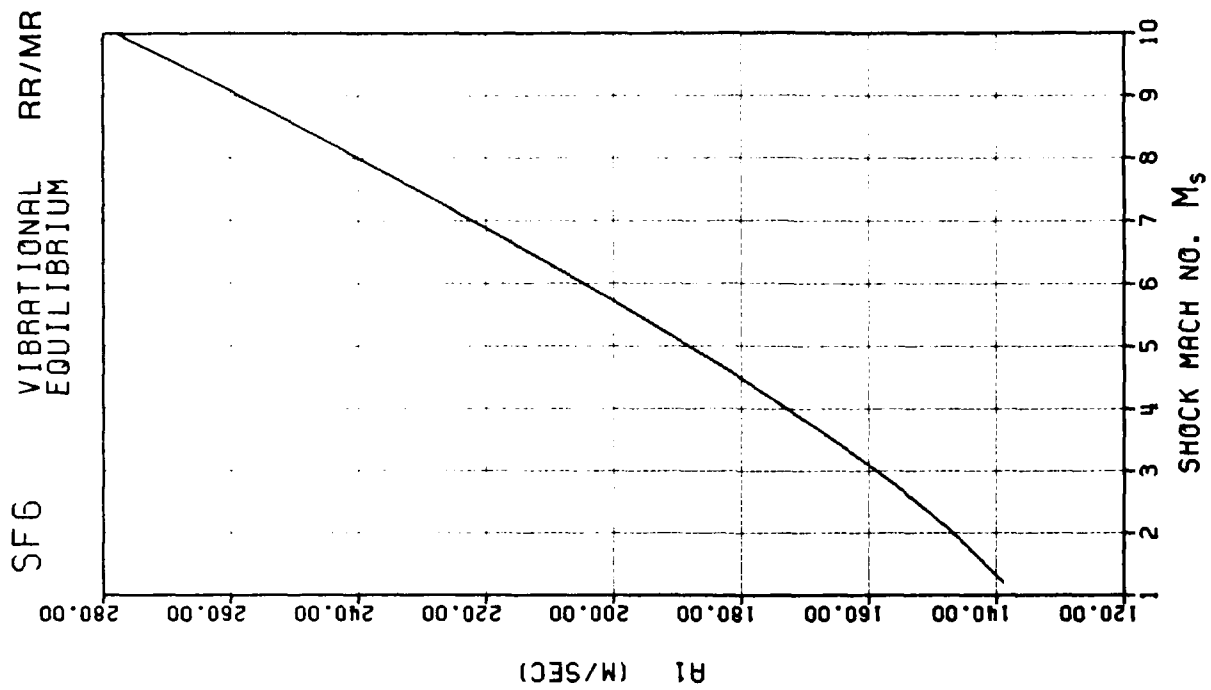
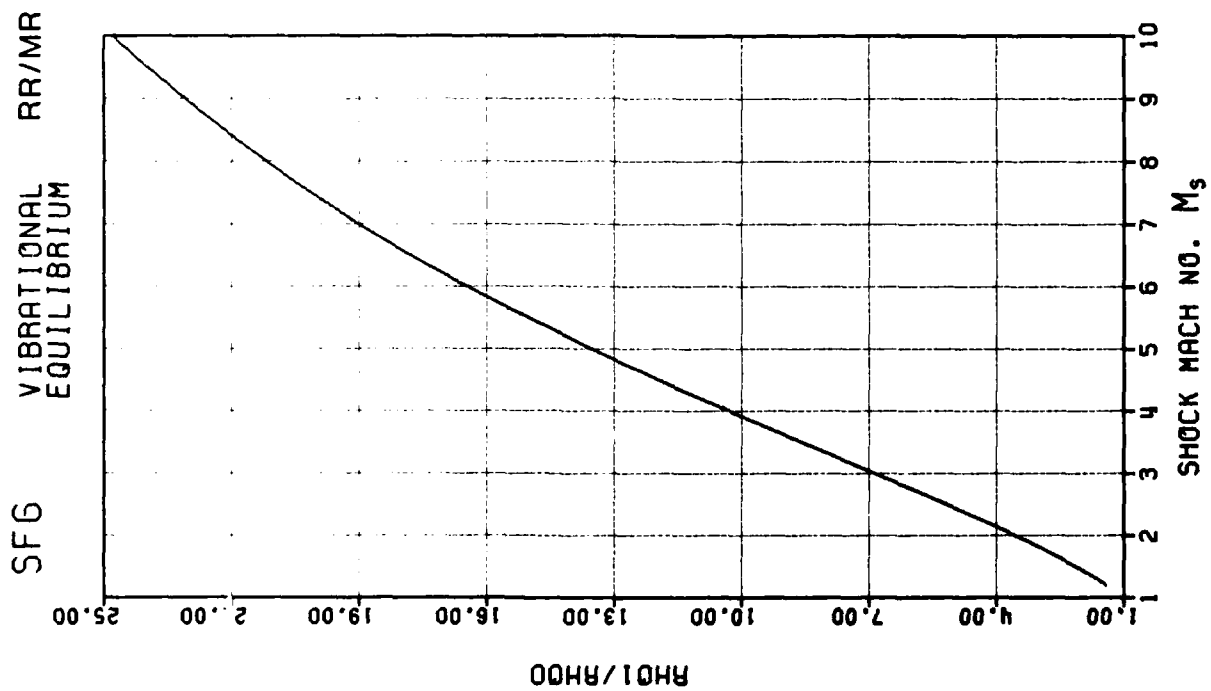
NL

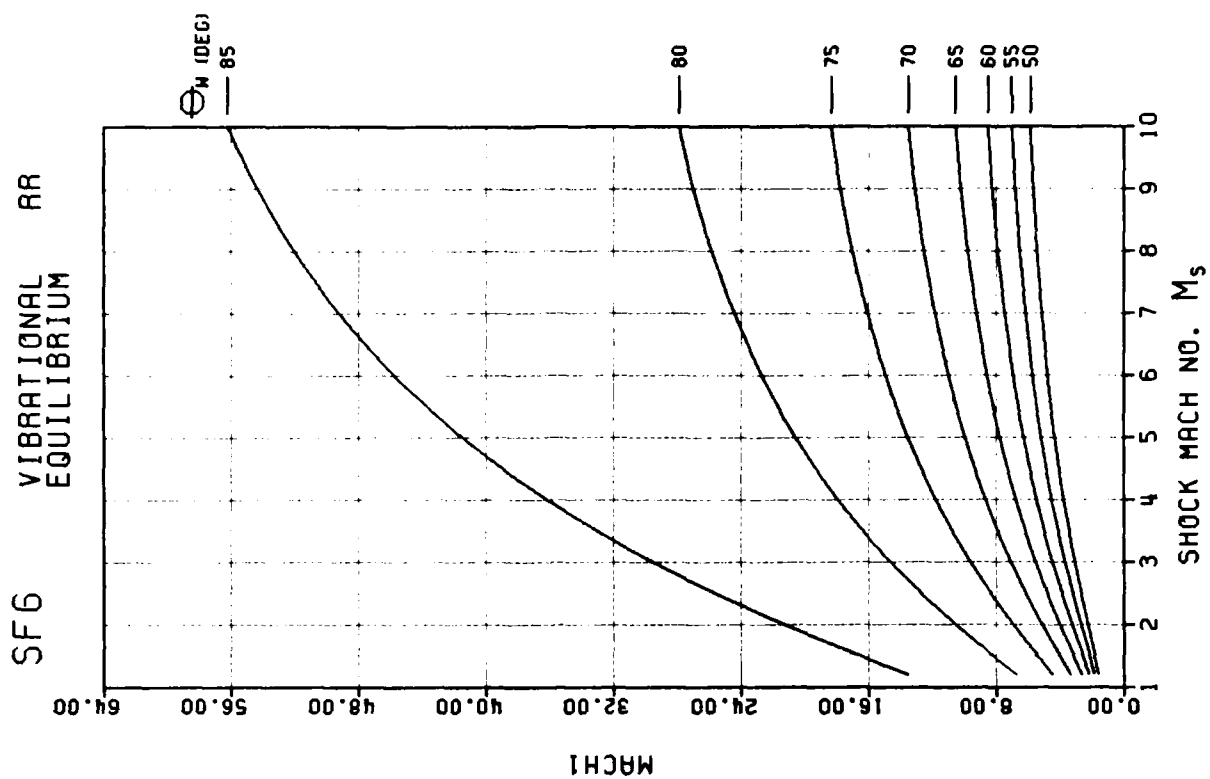
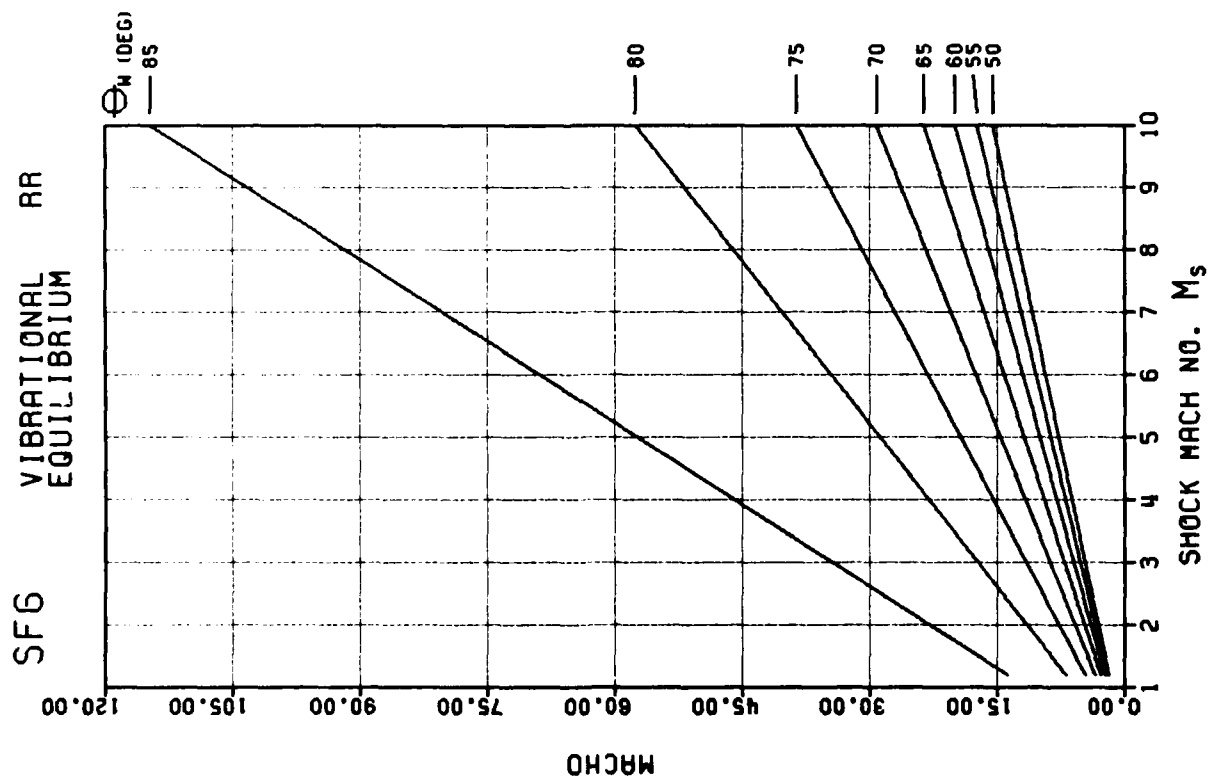


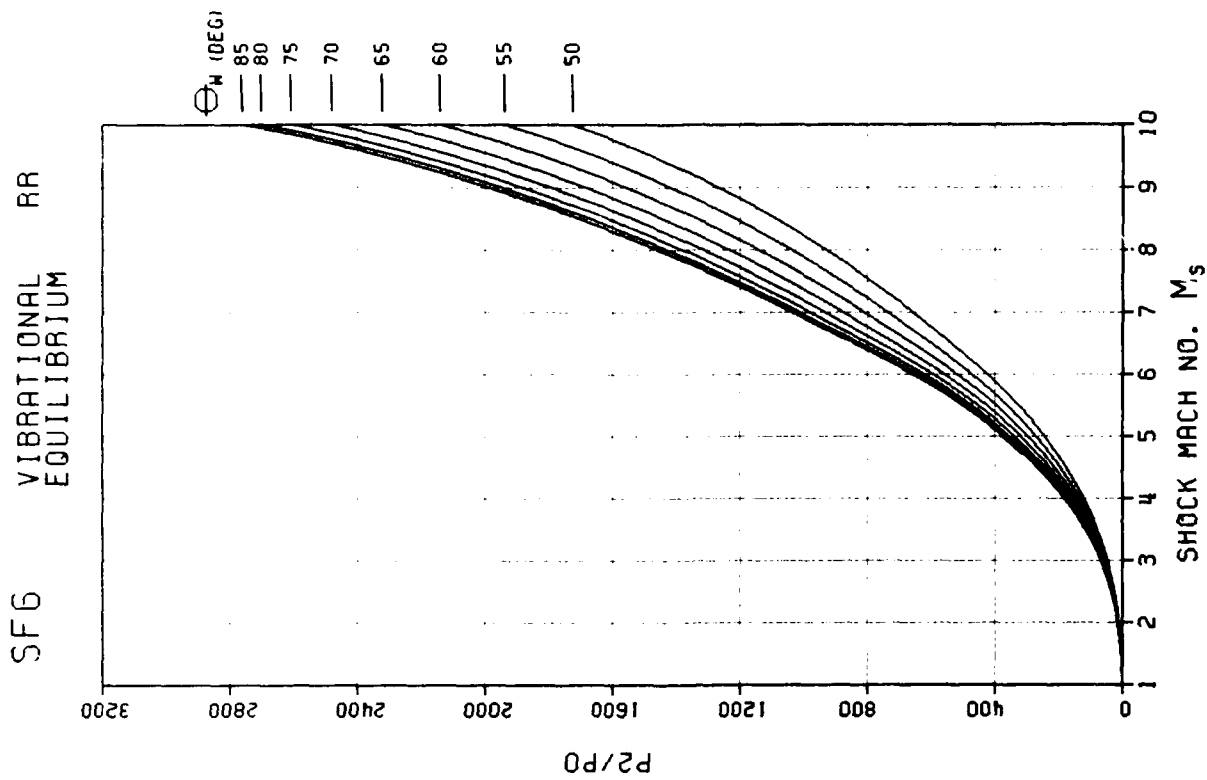
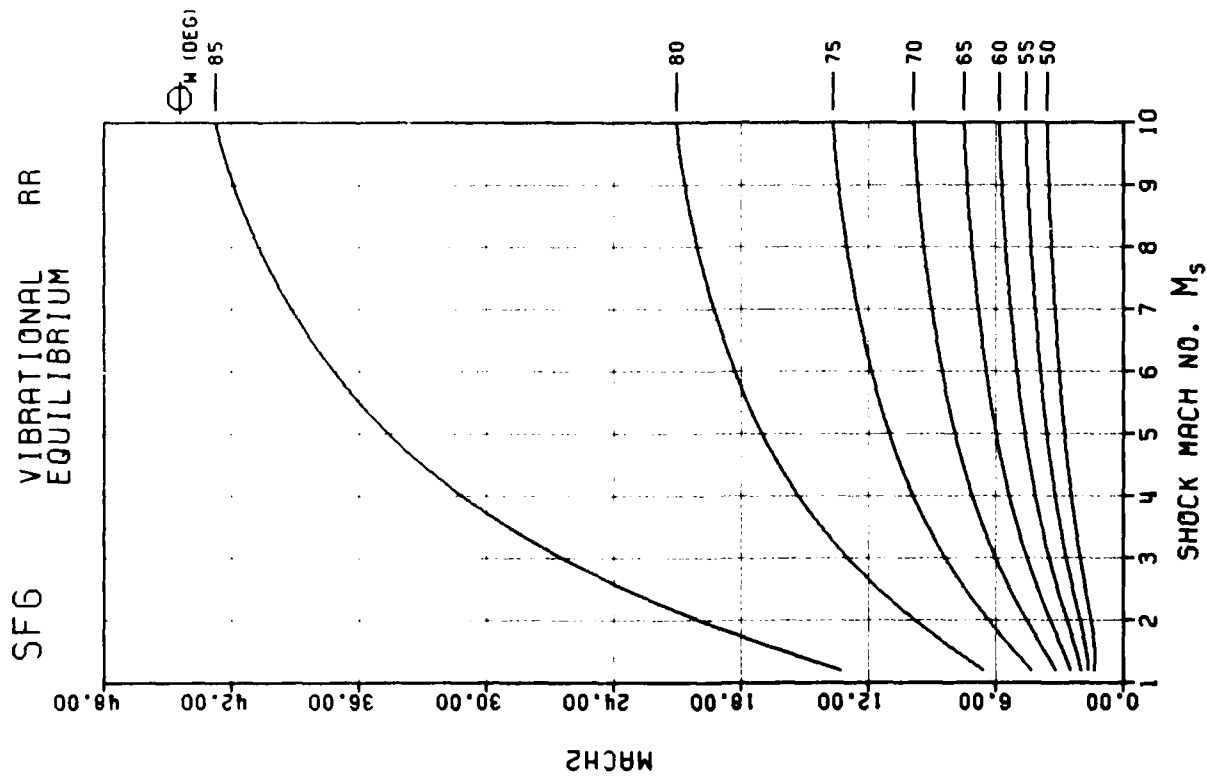


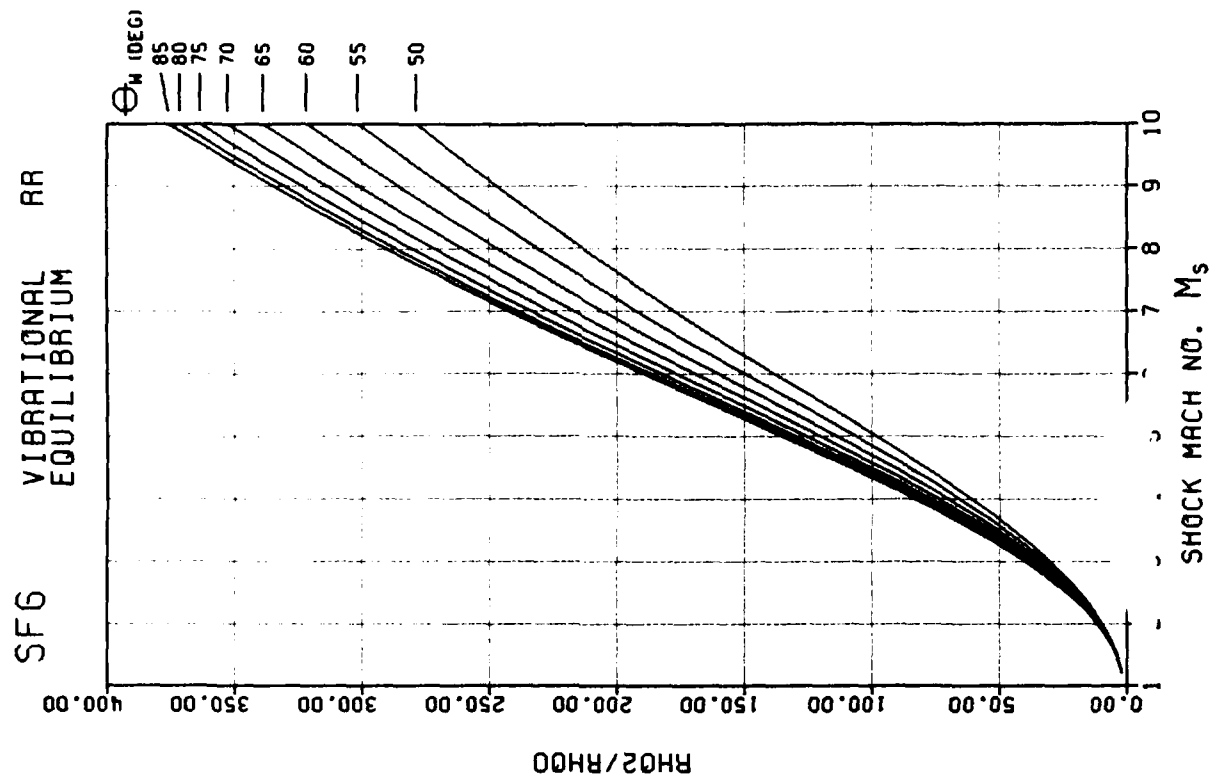
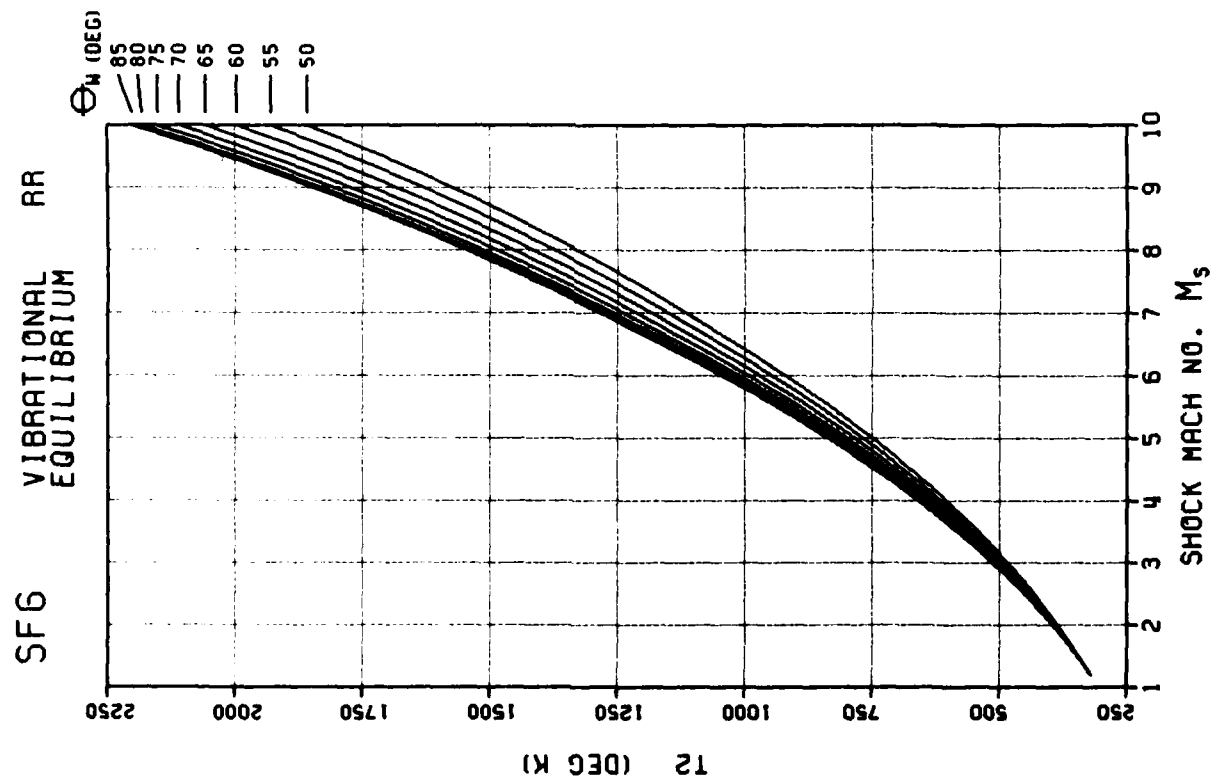
MICROCOPY RESOLUTION TEST CHART
NATIONAL BUREAU OF STANDARDS 1963-A

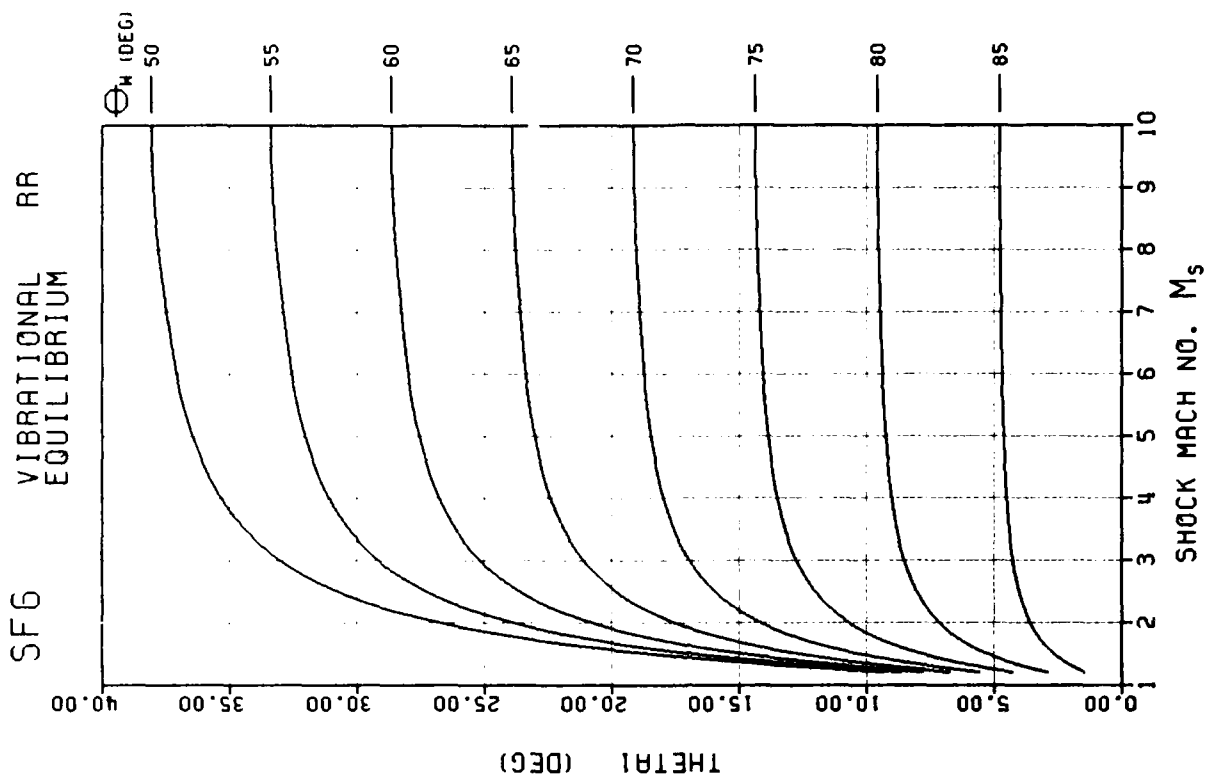
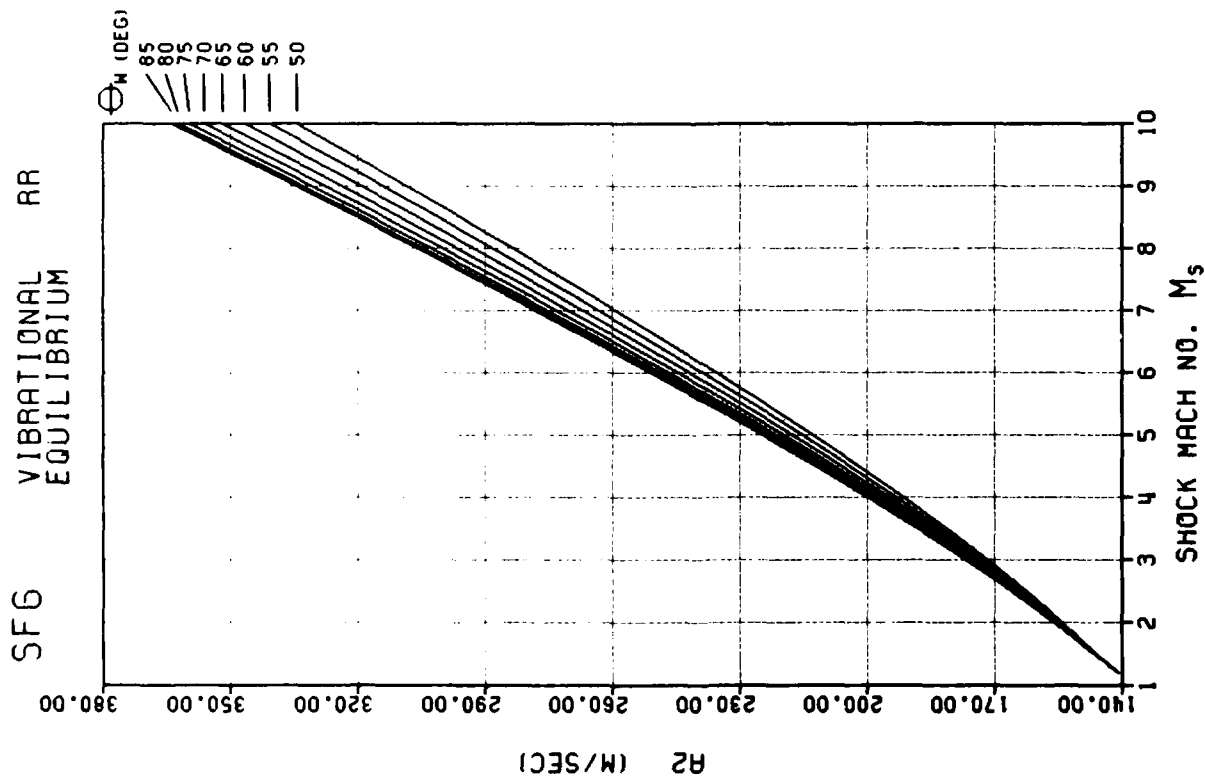


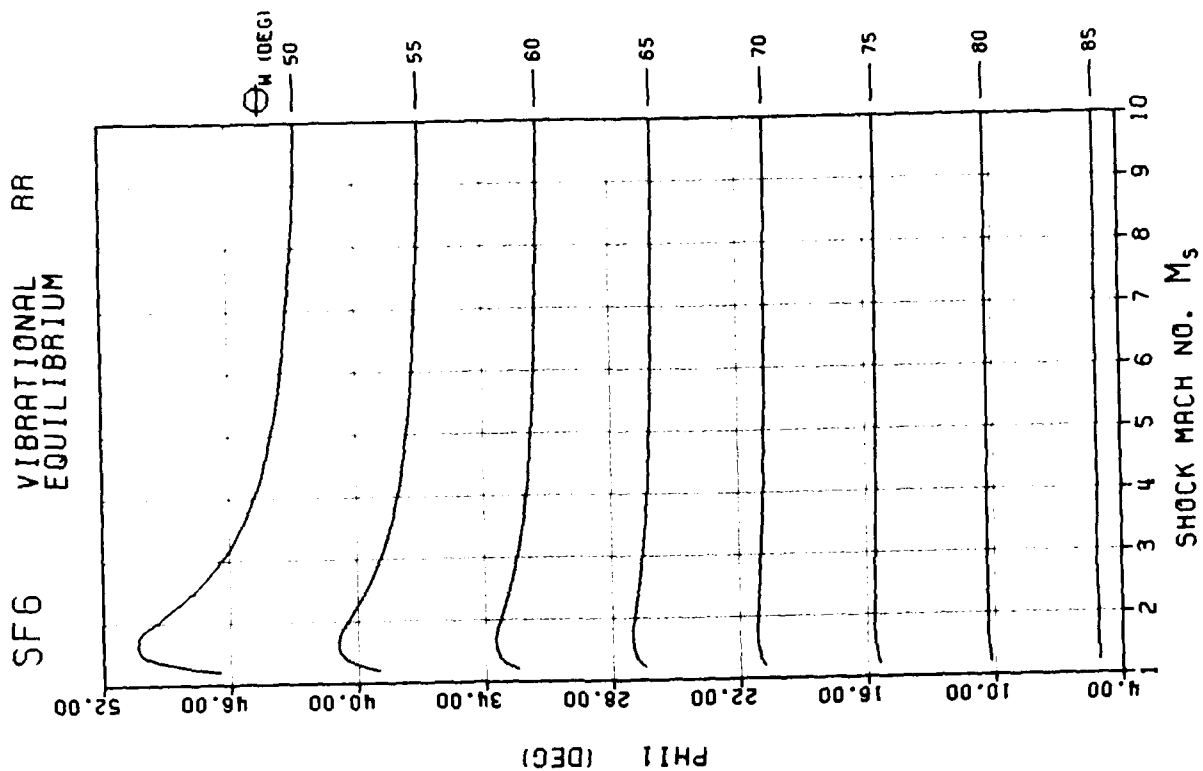
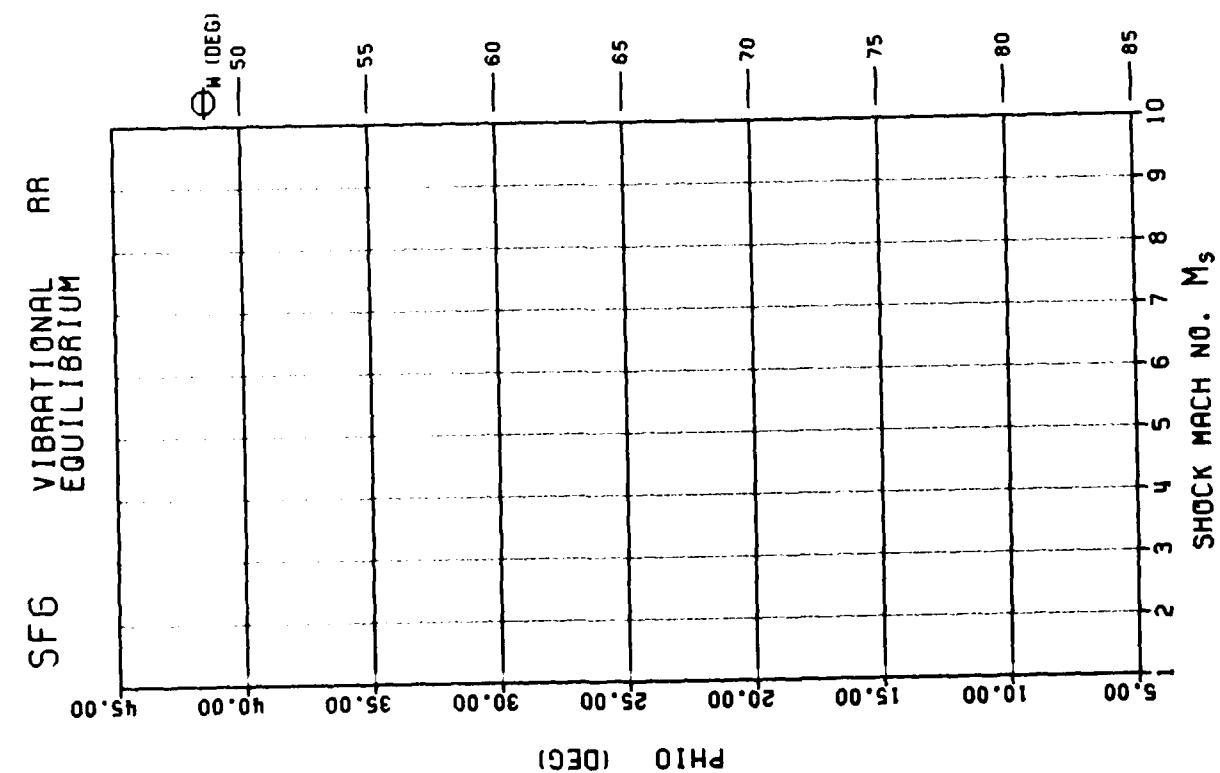


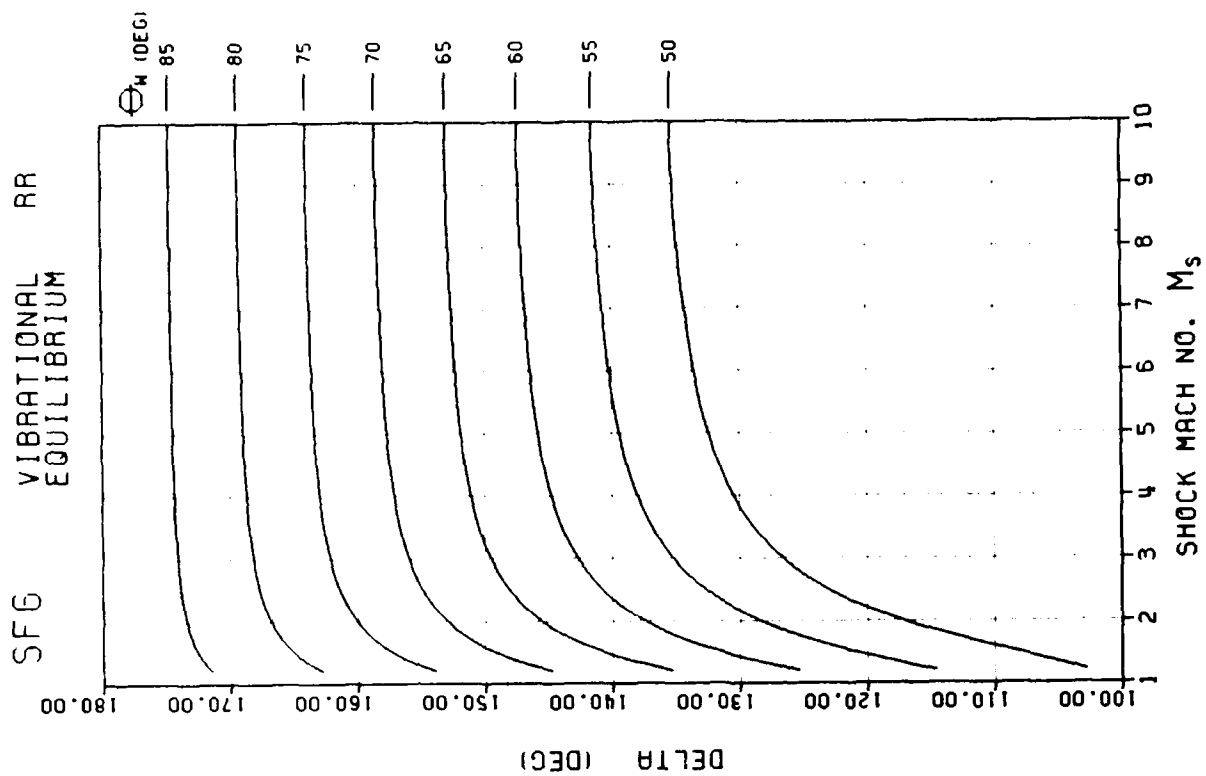
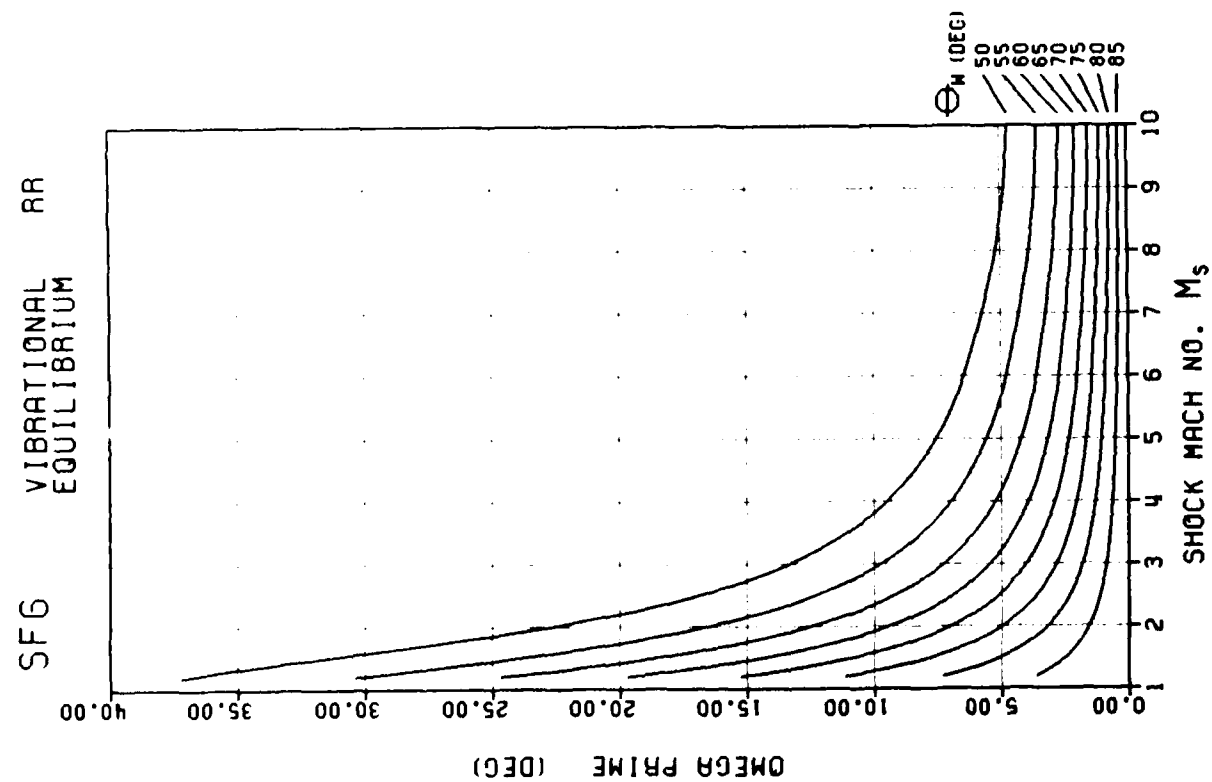


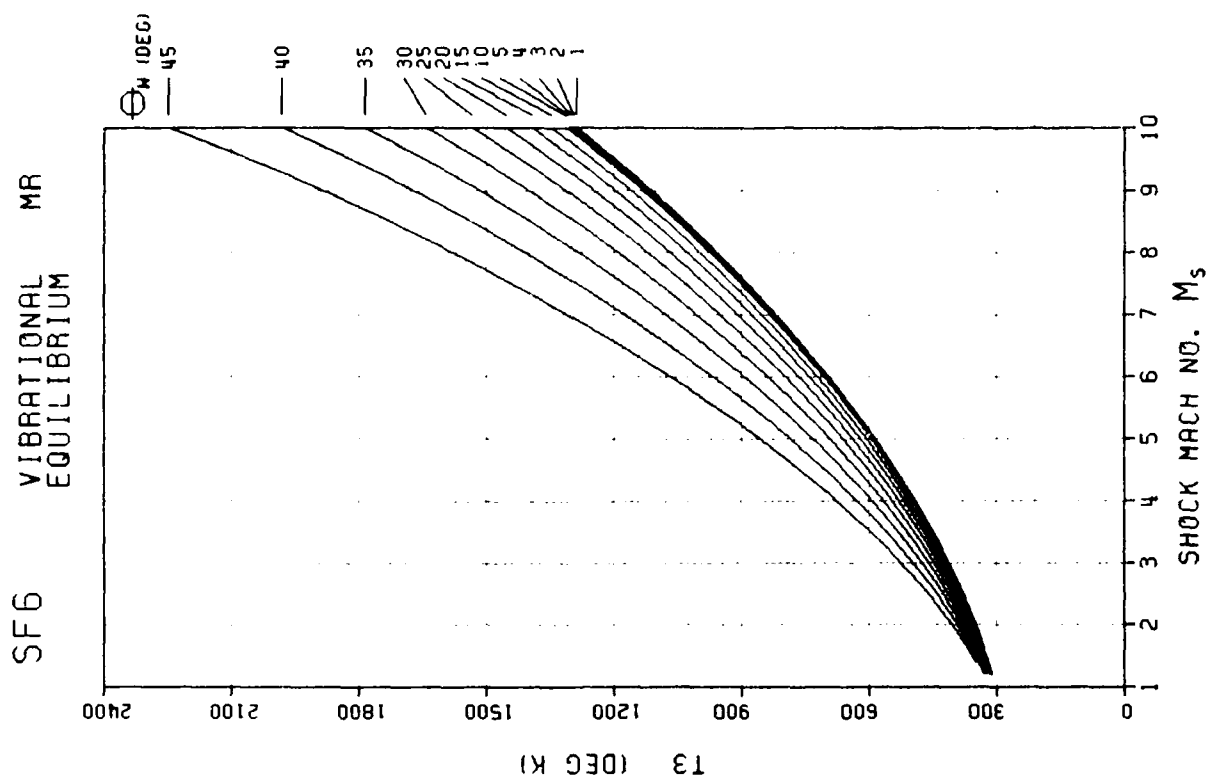
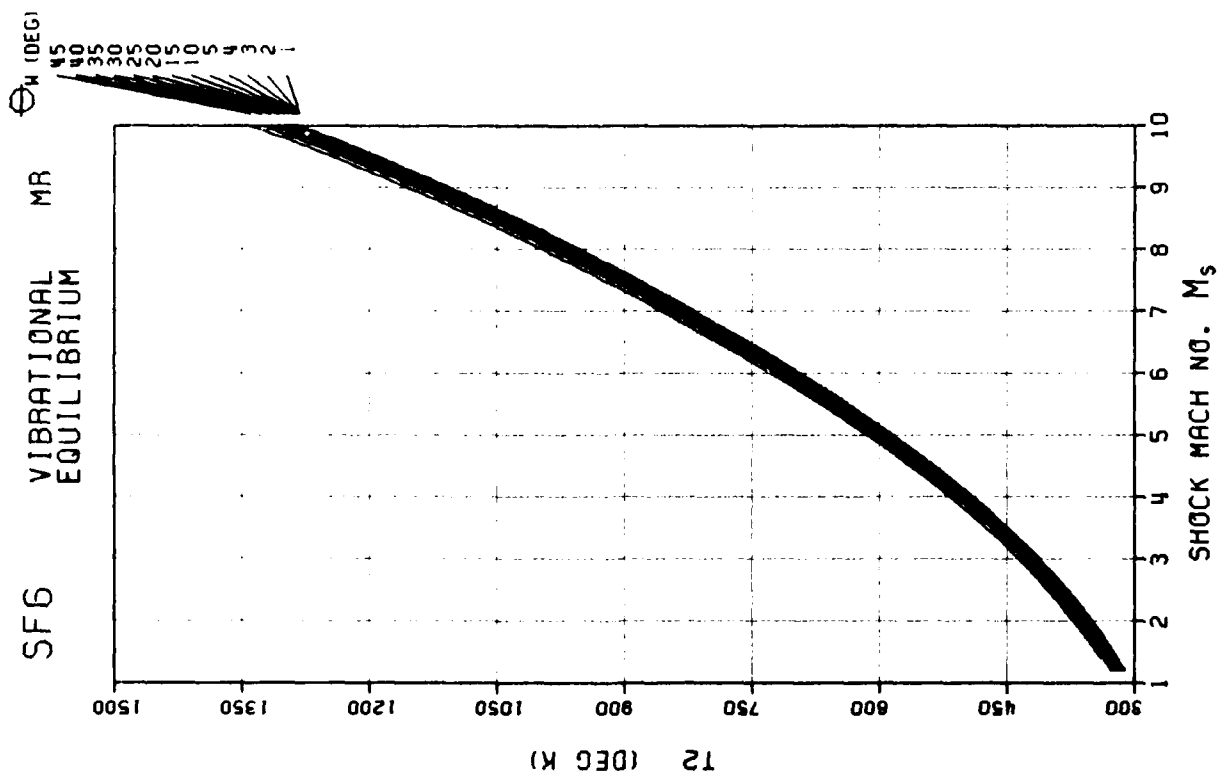


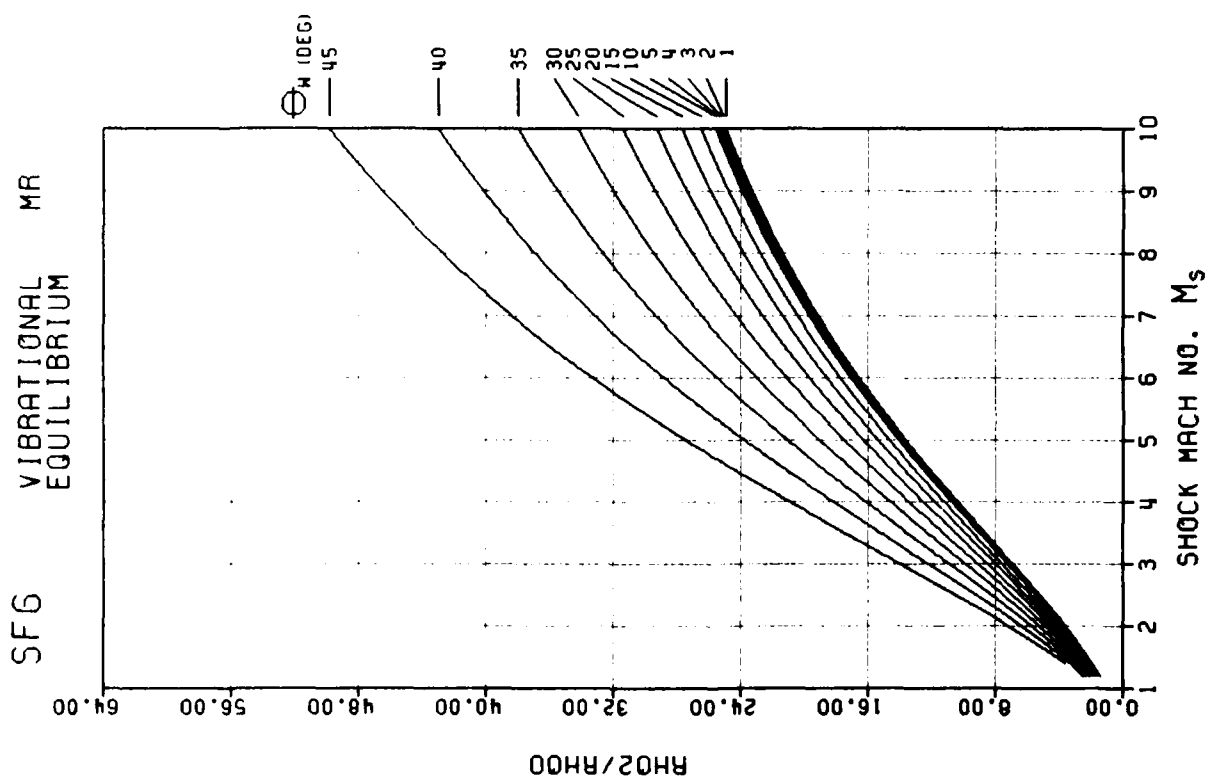
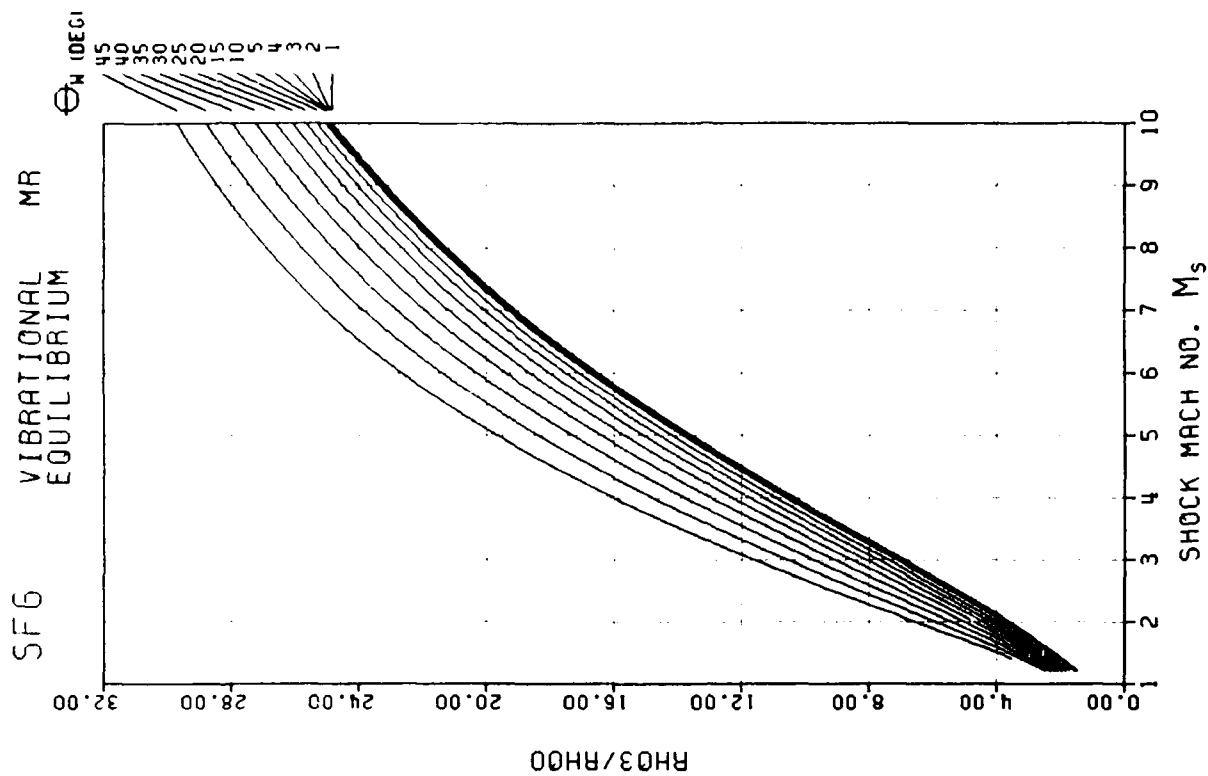




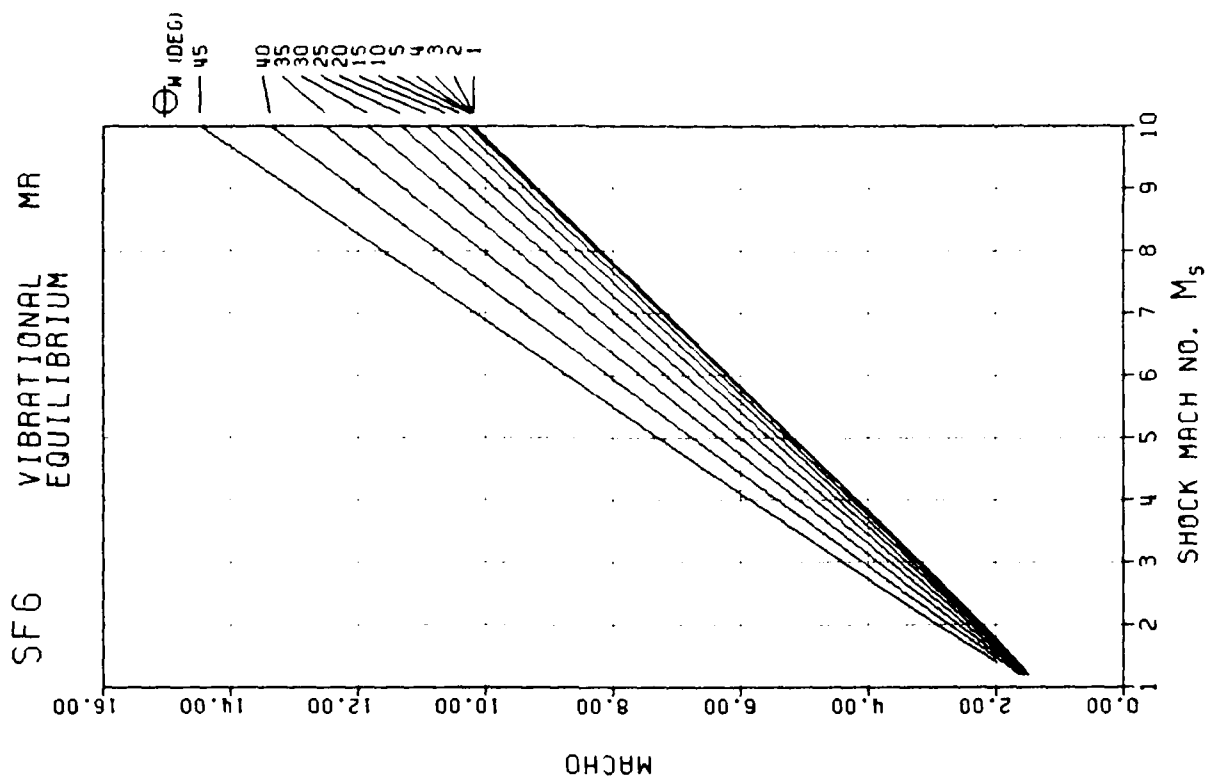
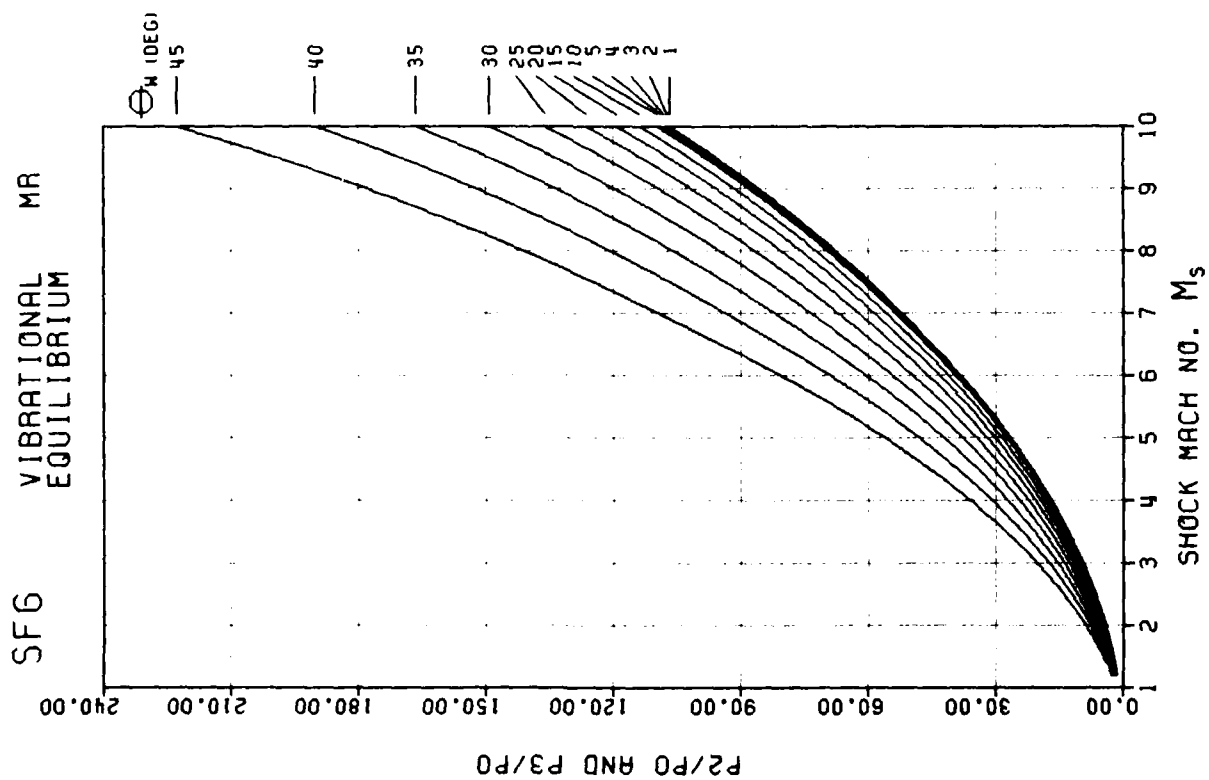


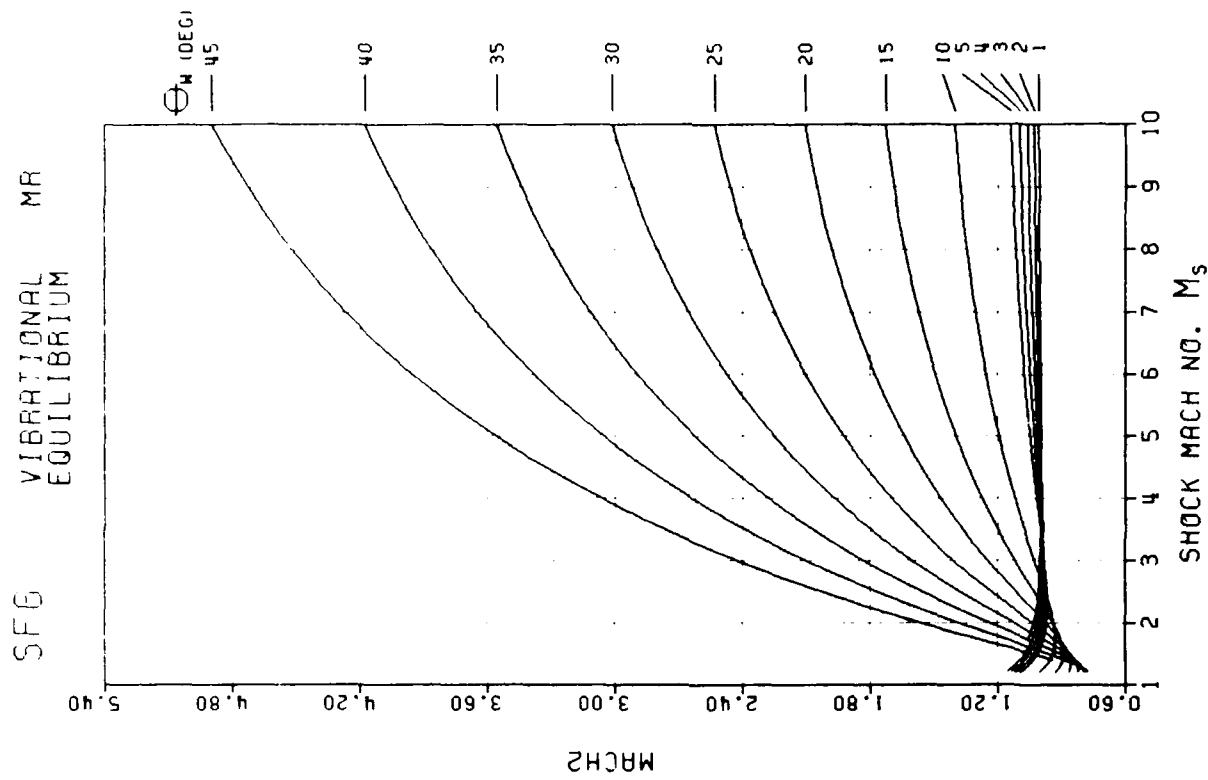
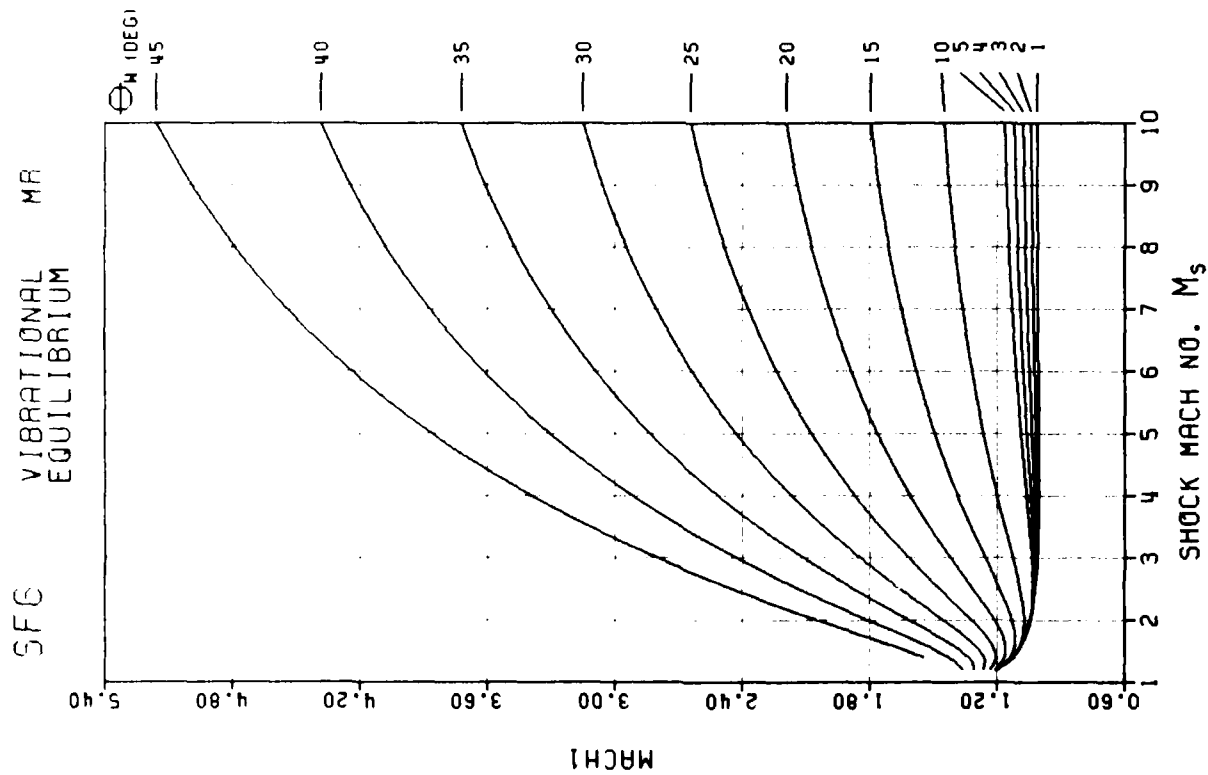


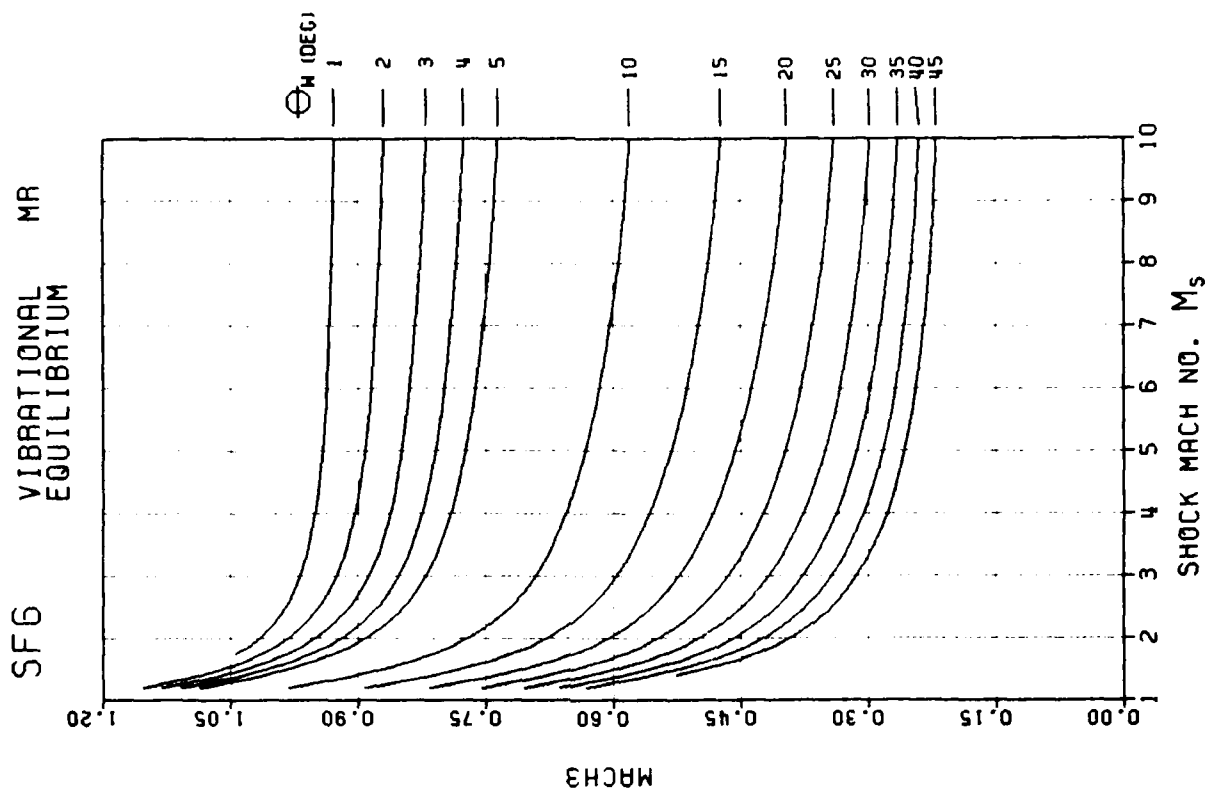
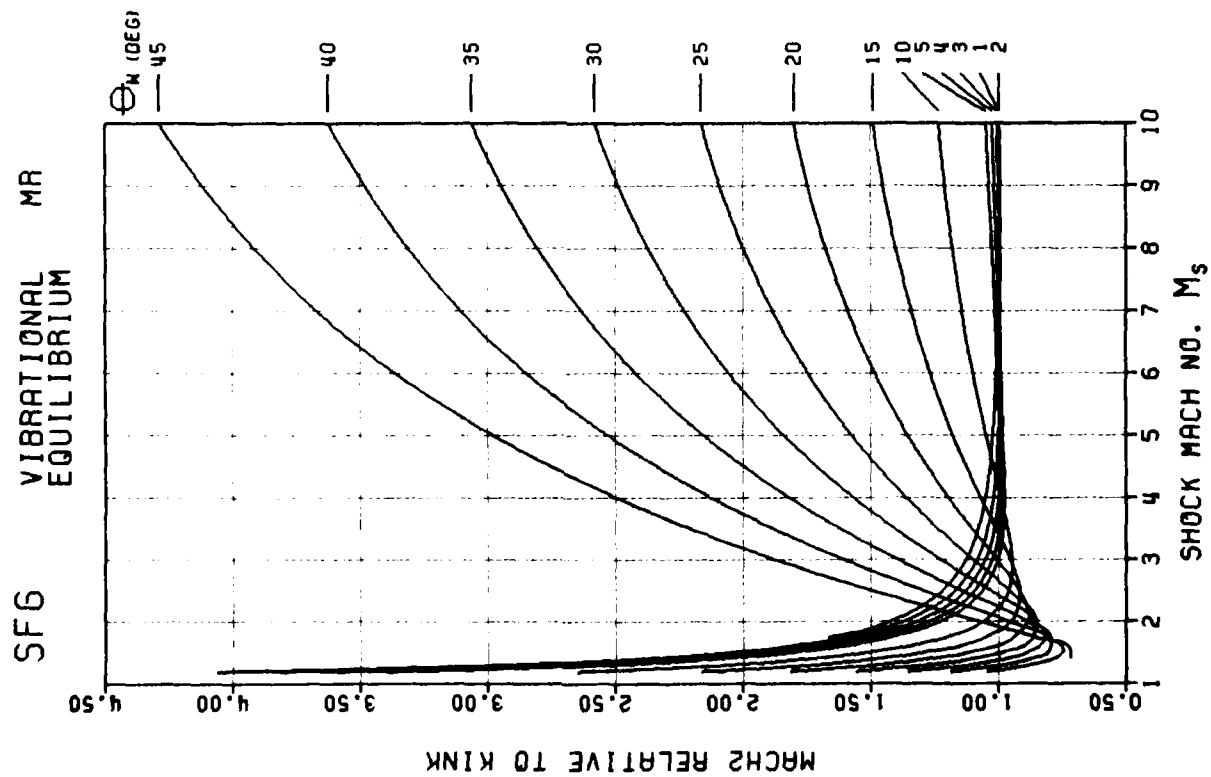


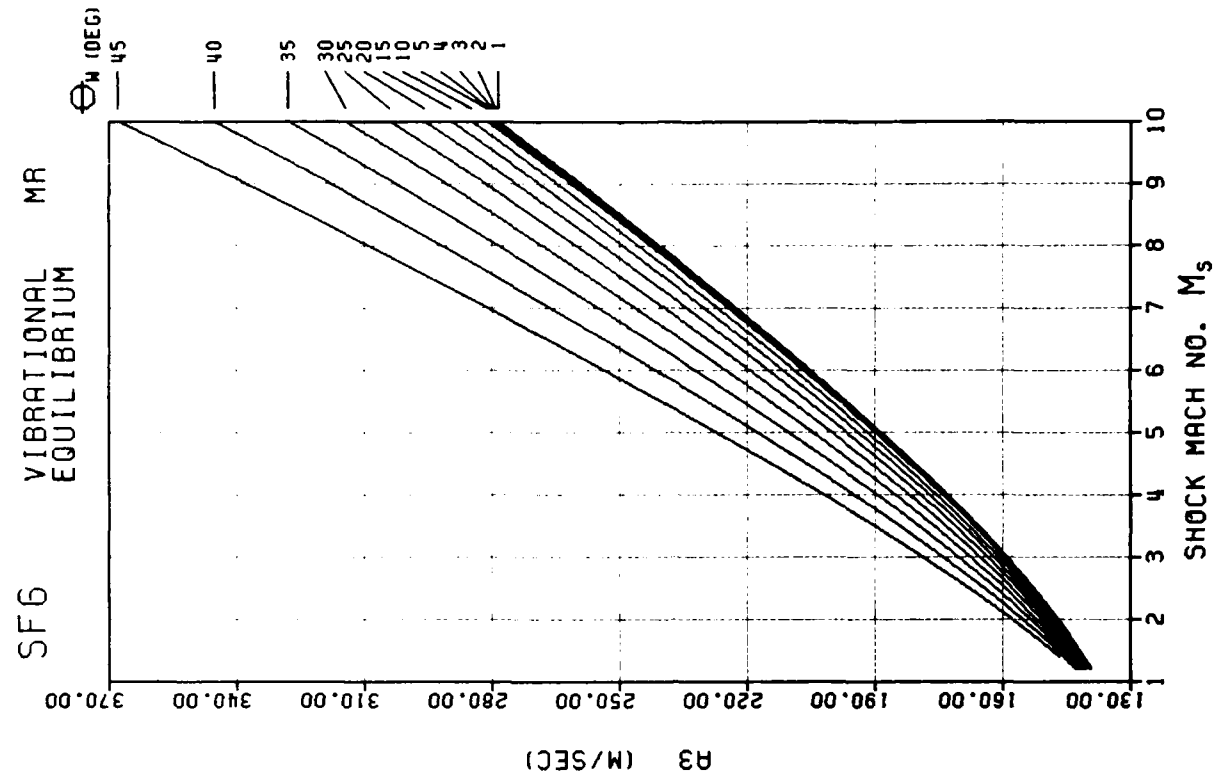
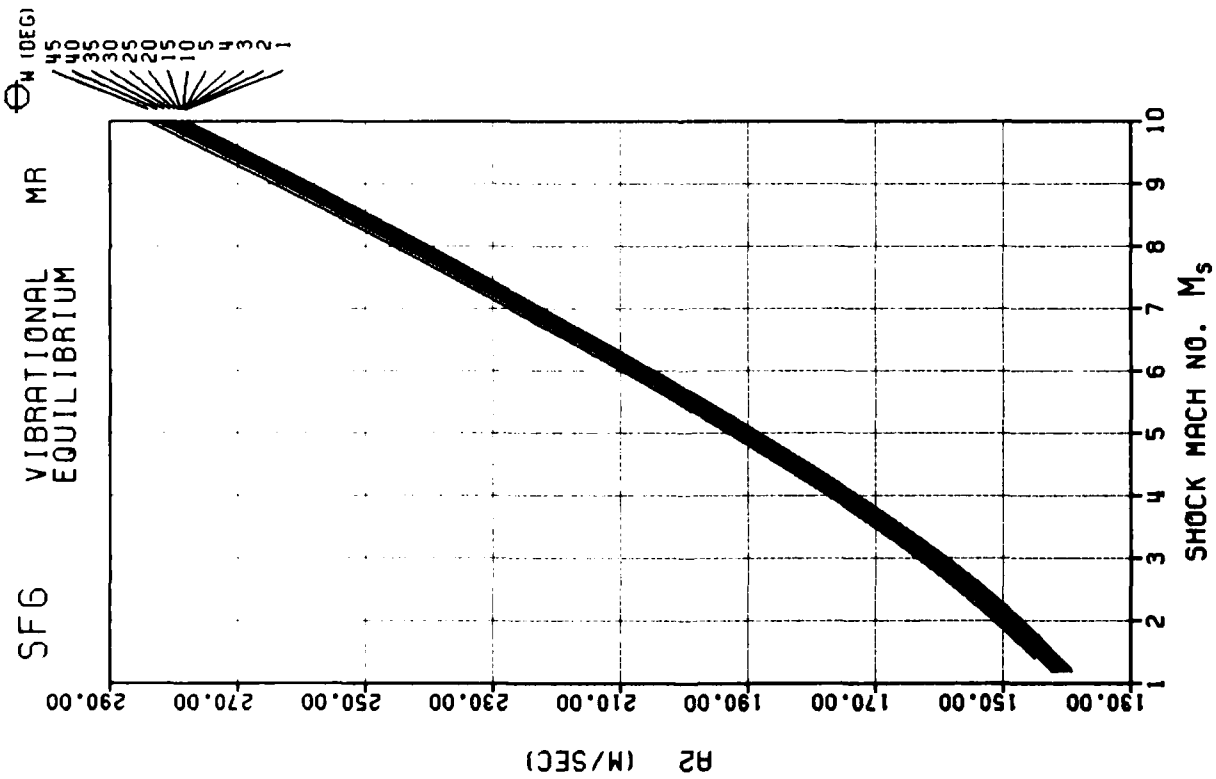


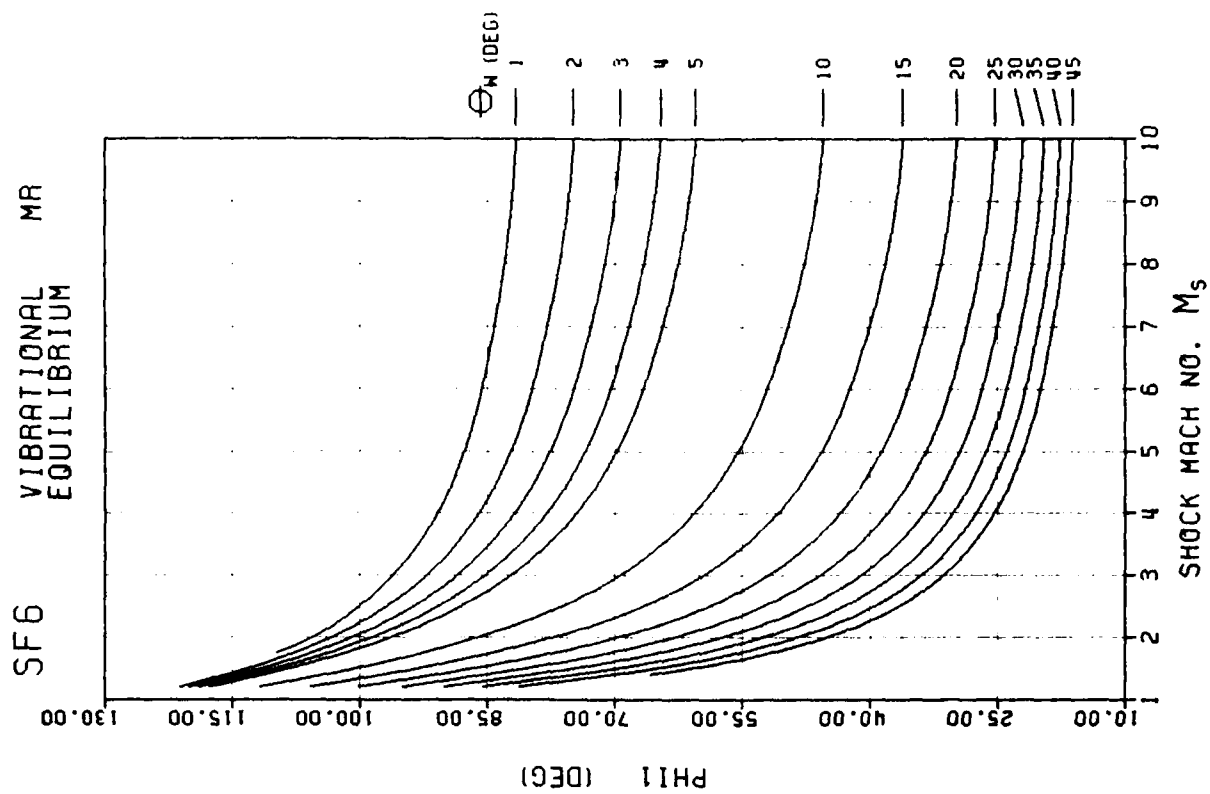
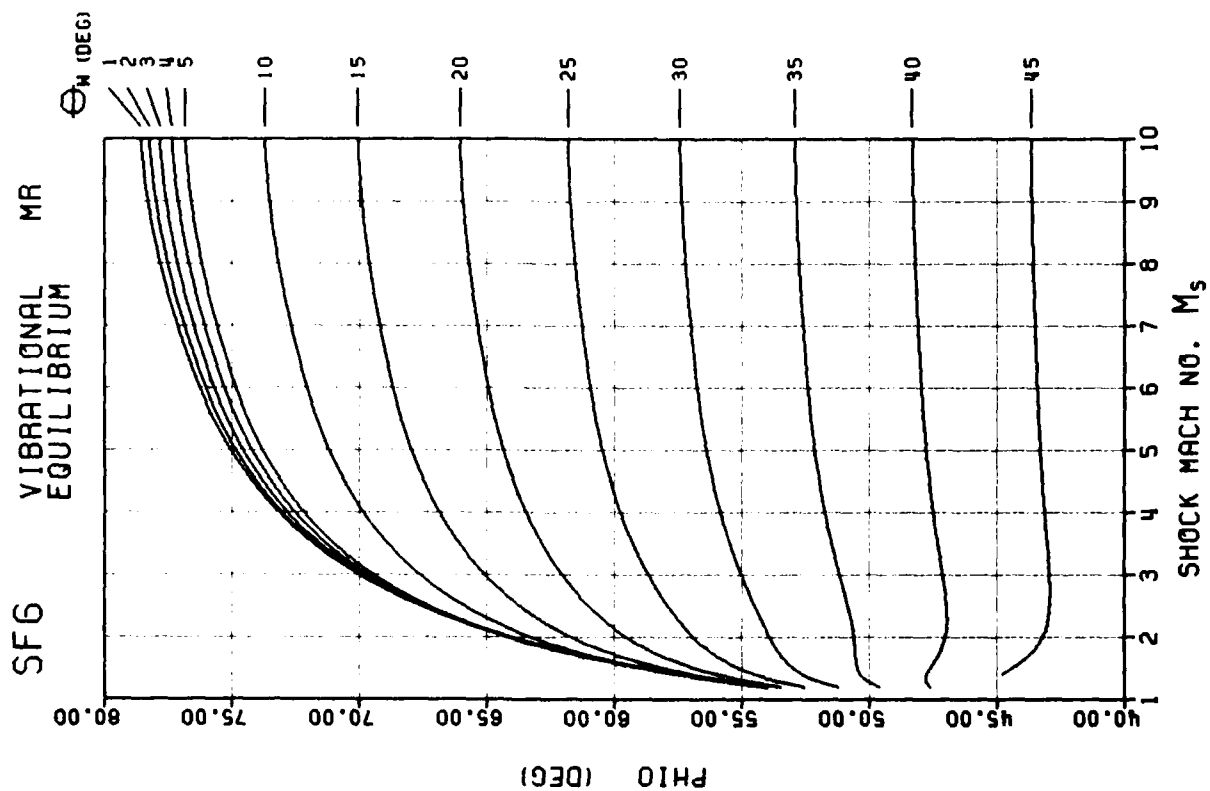
F - 220

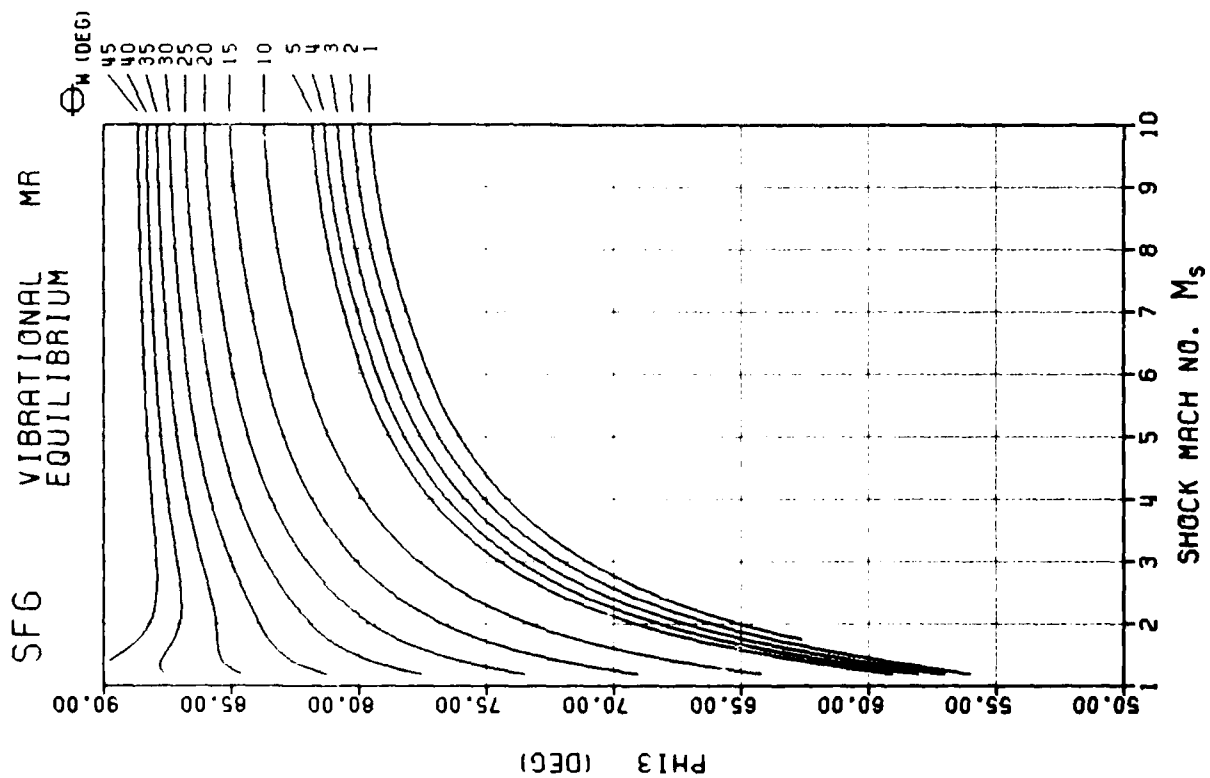
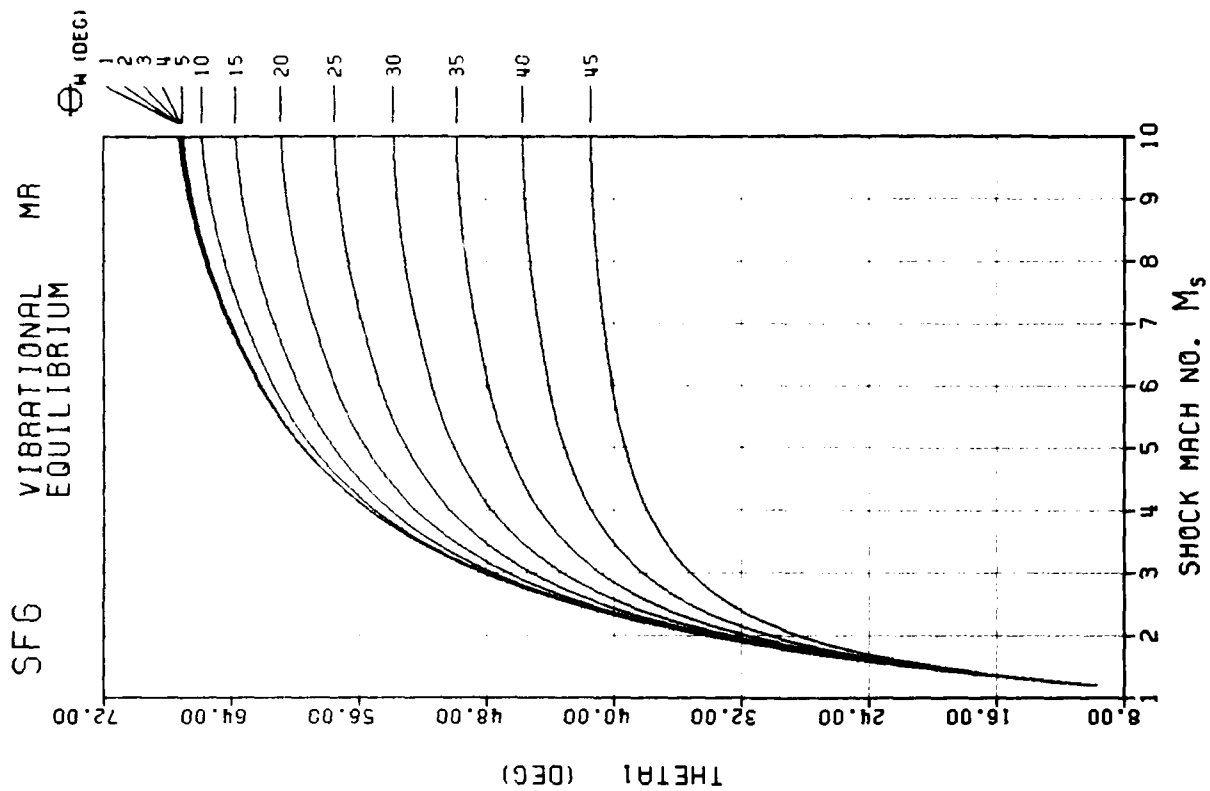


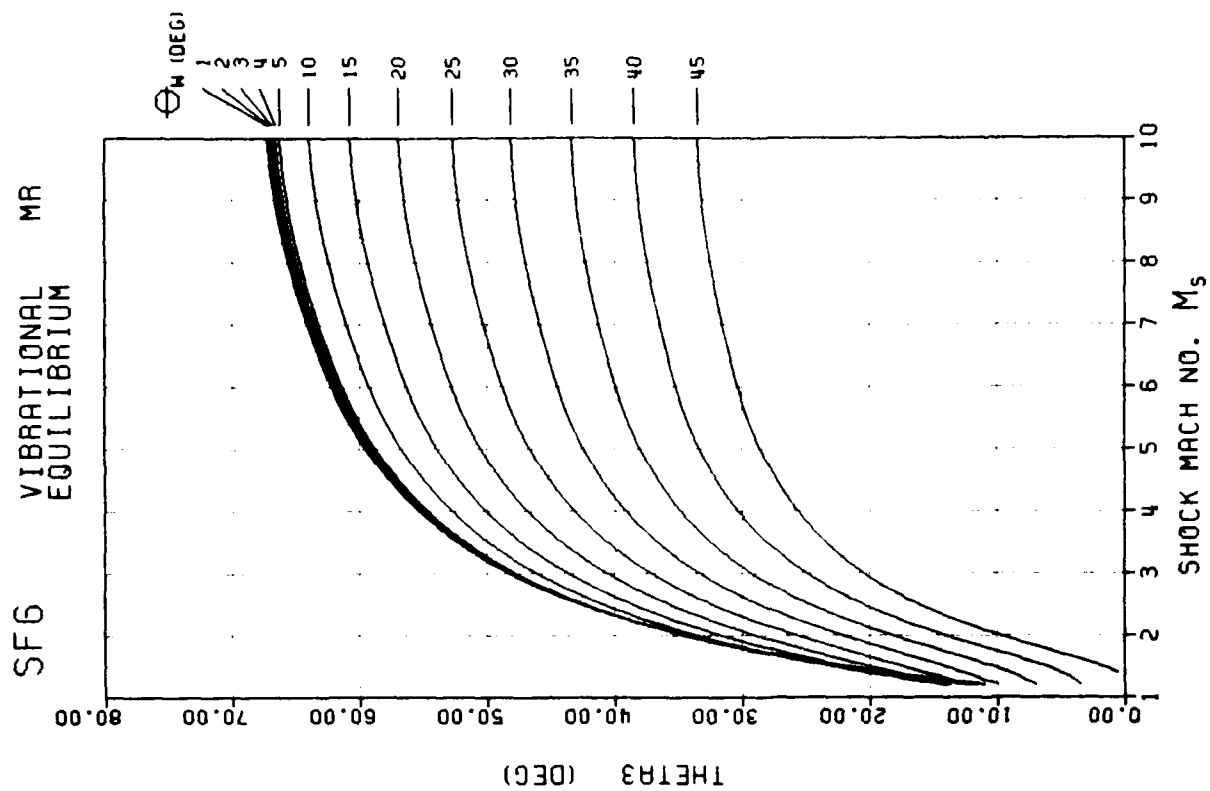
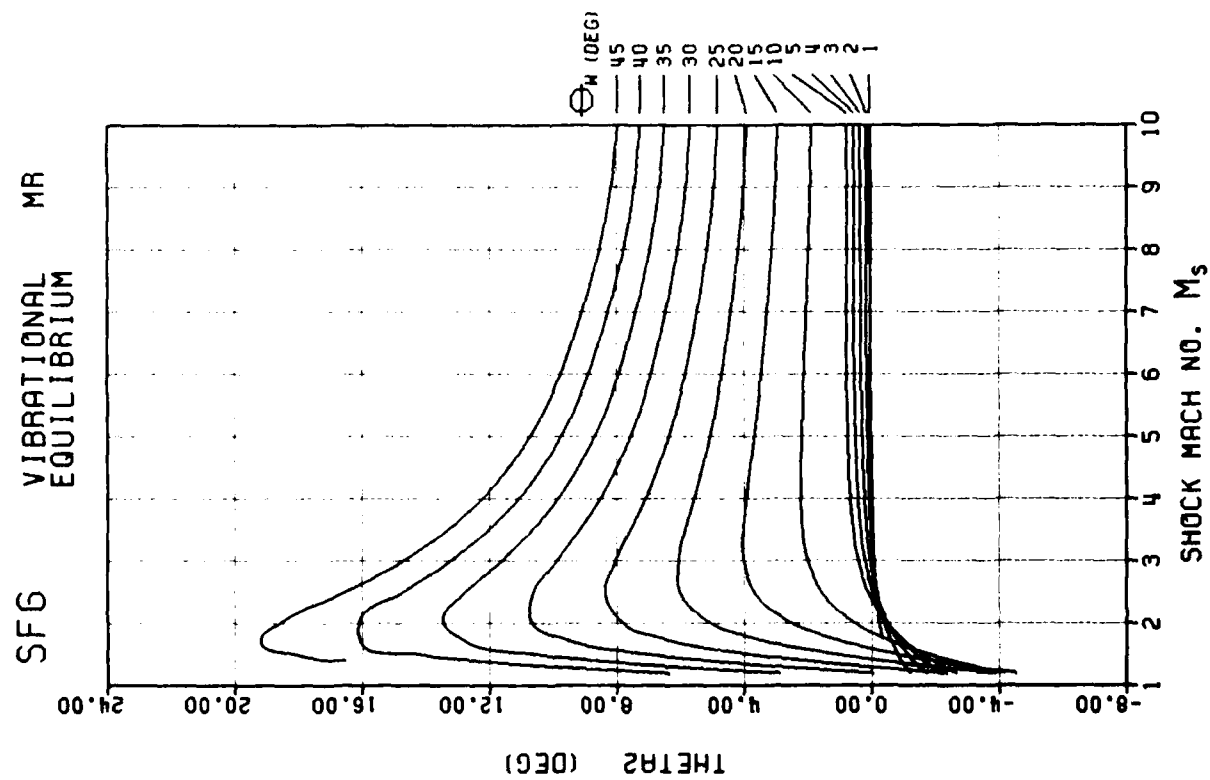


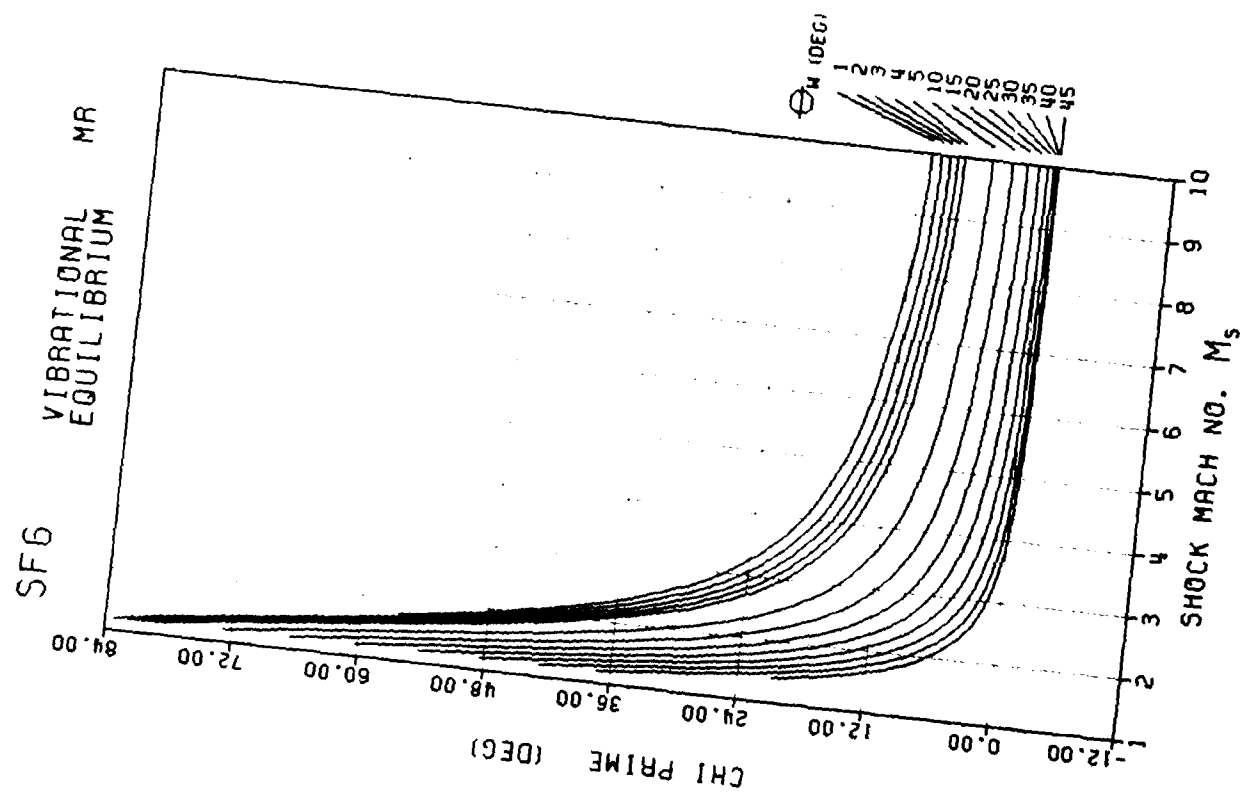
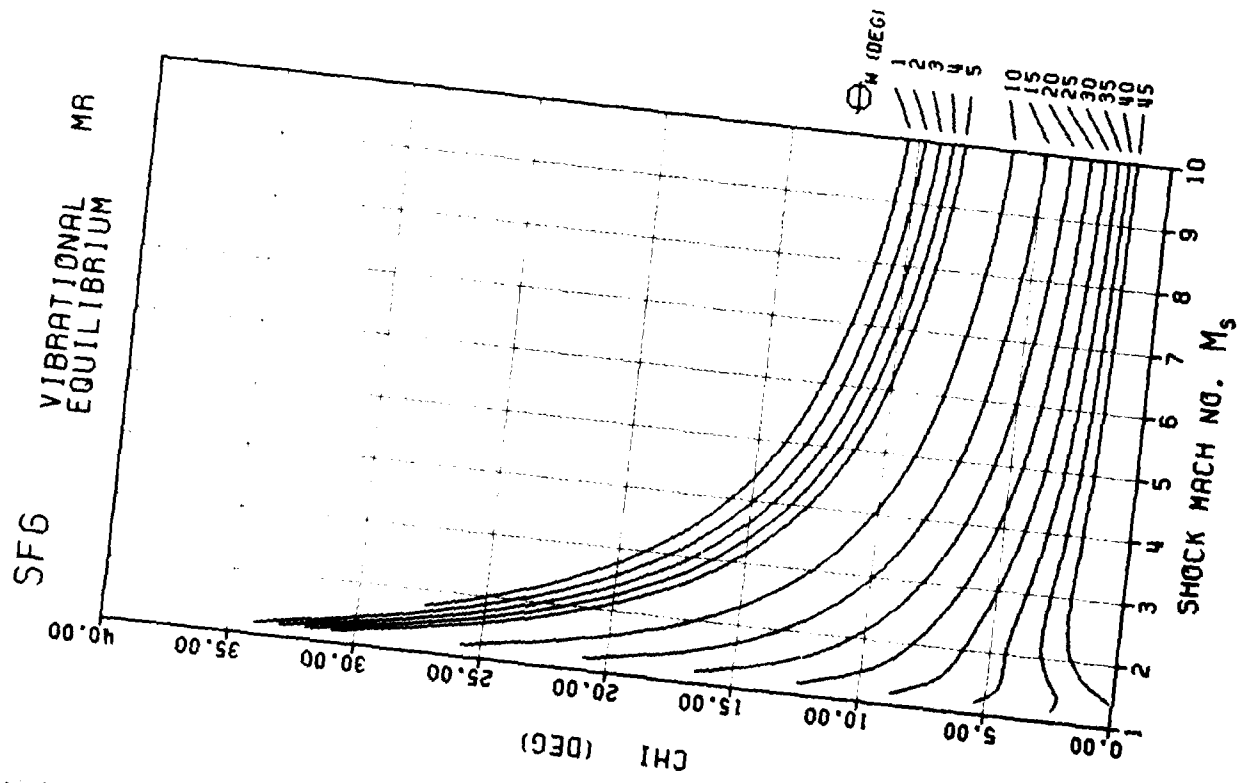


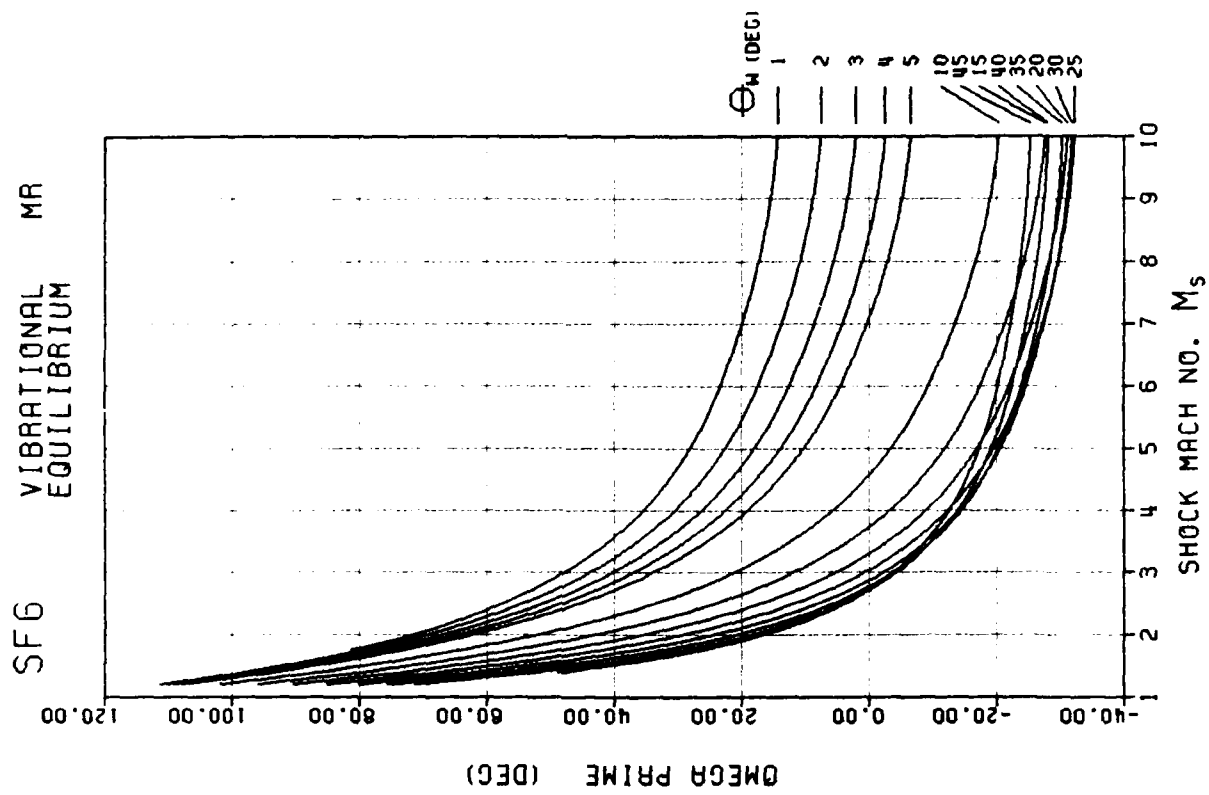
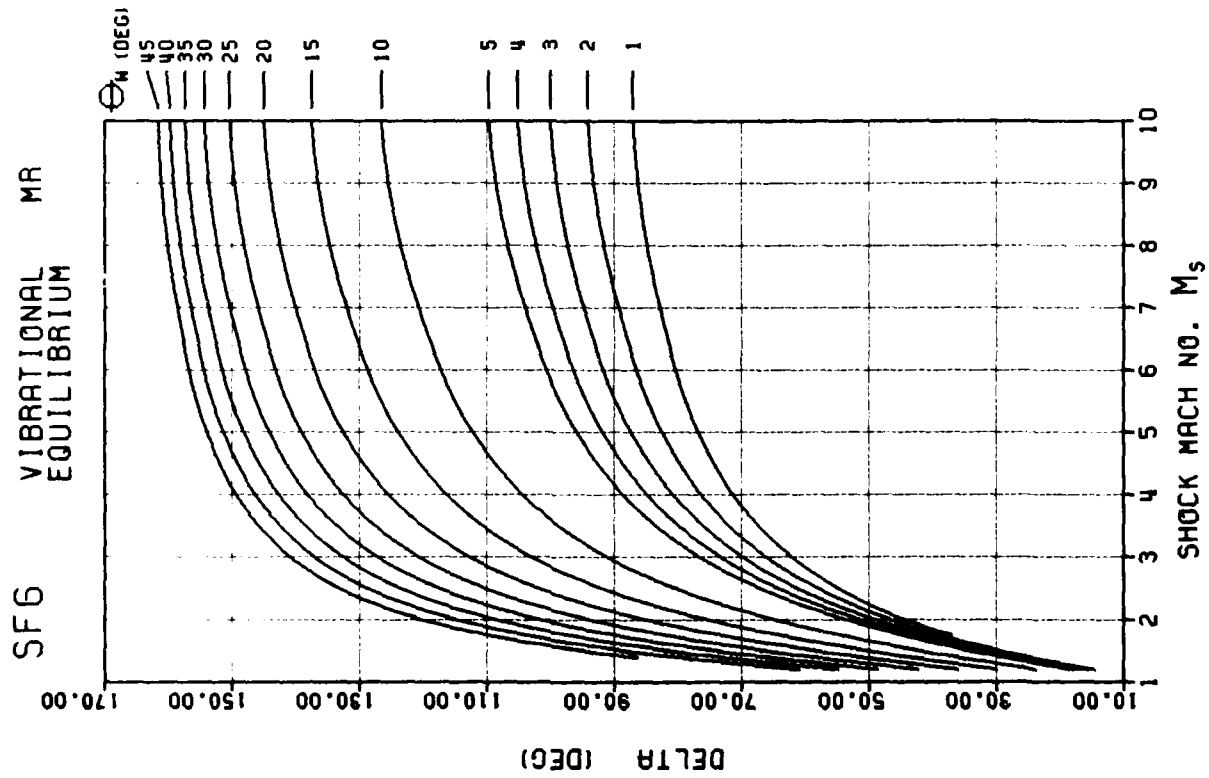


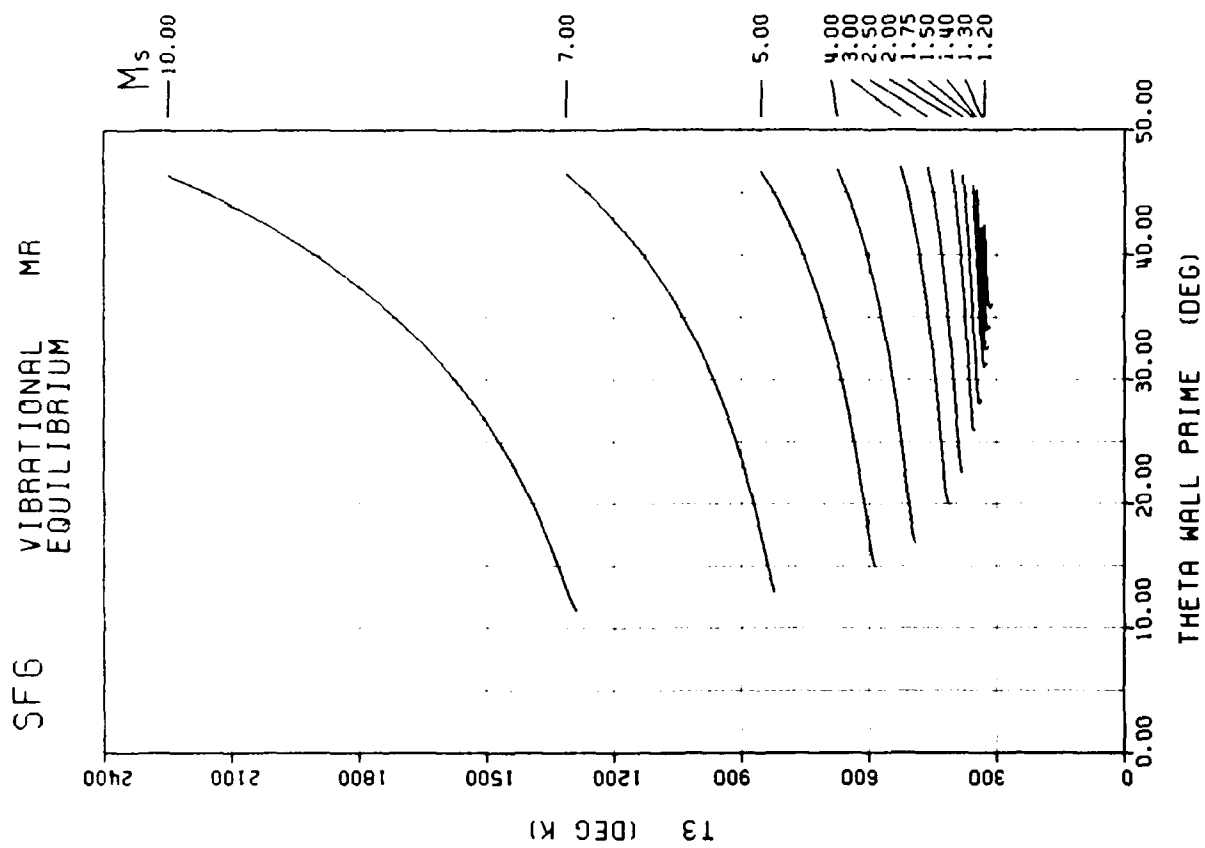
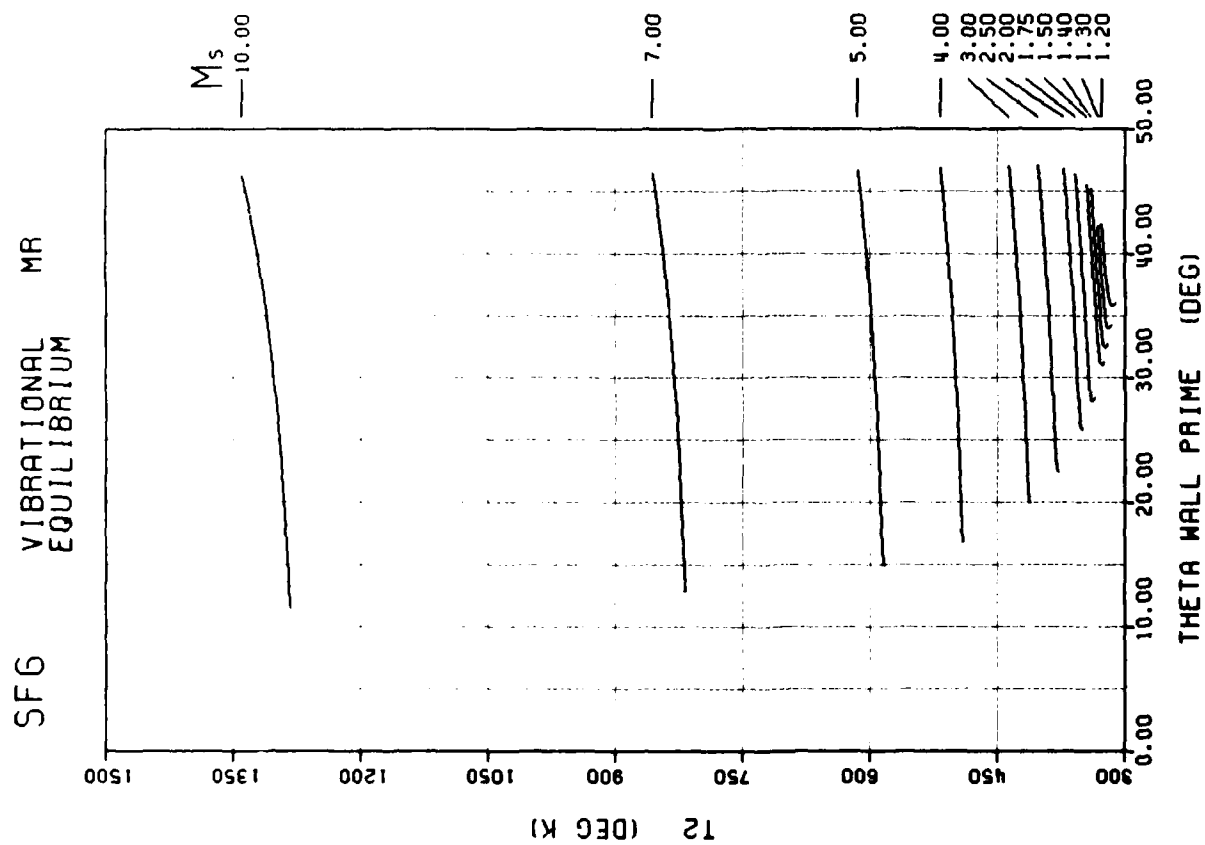


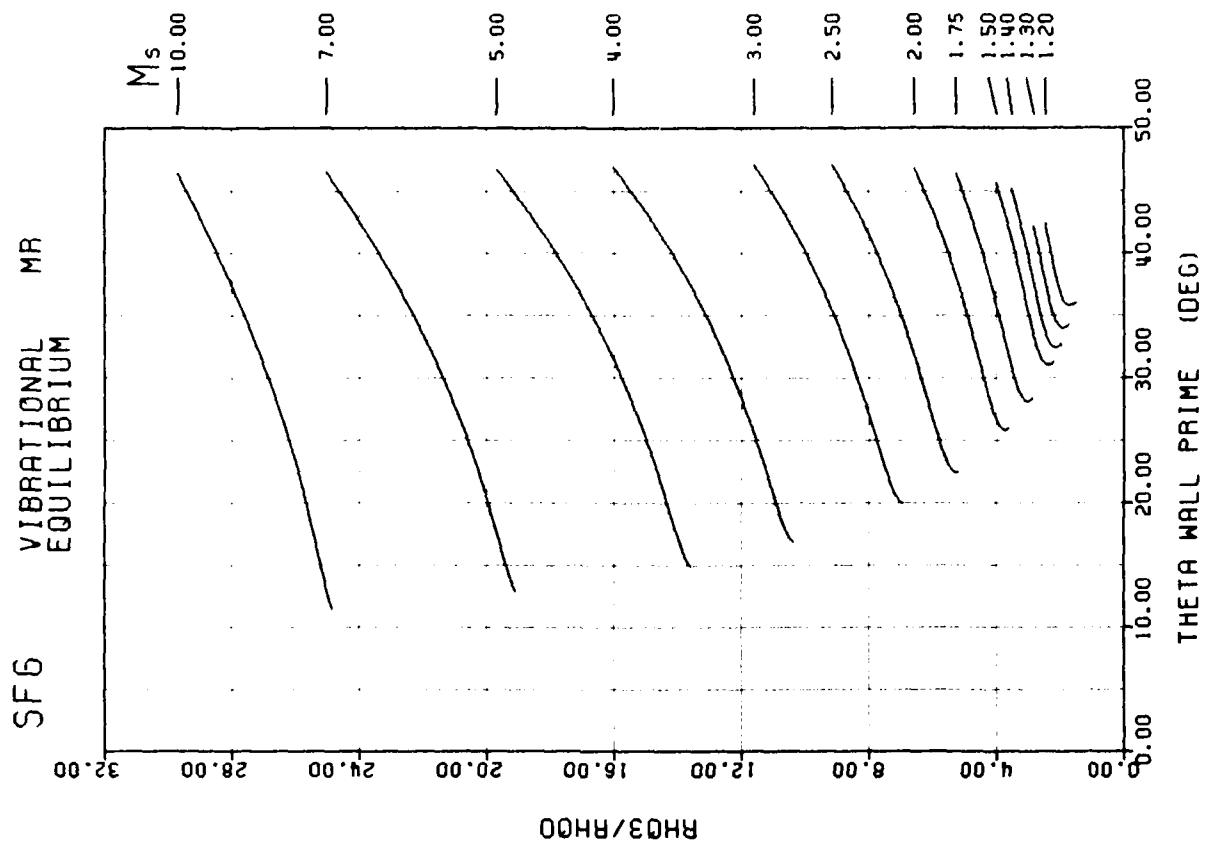
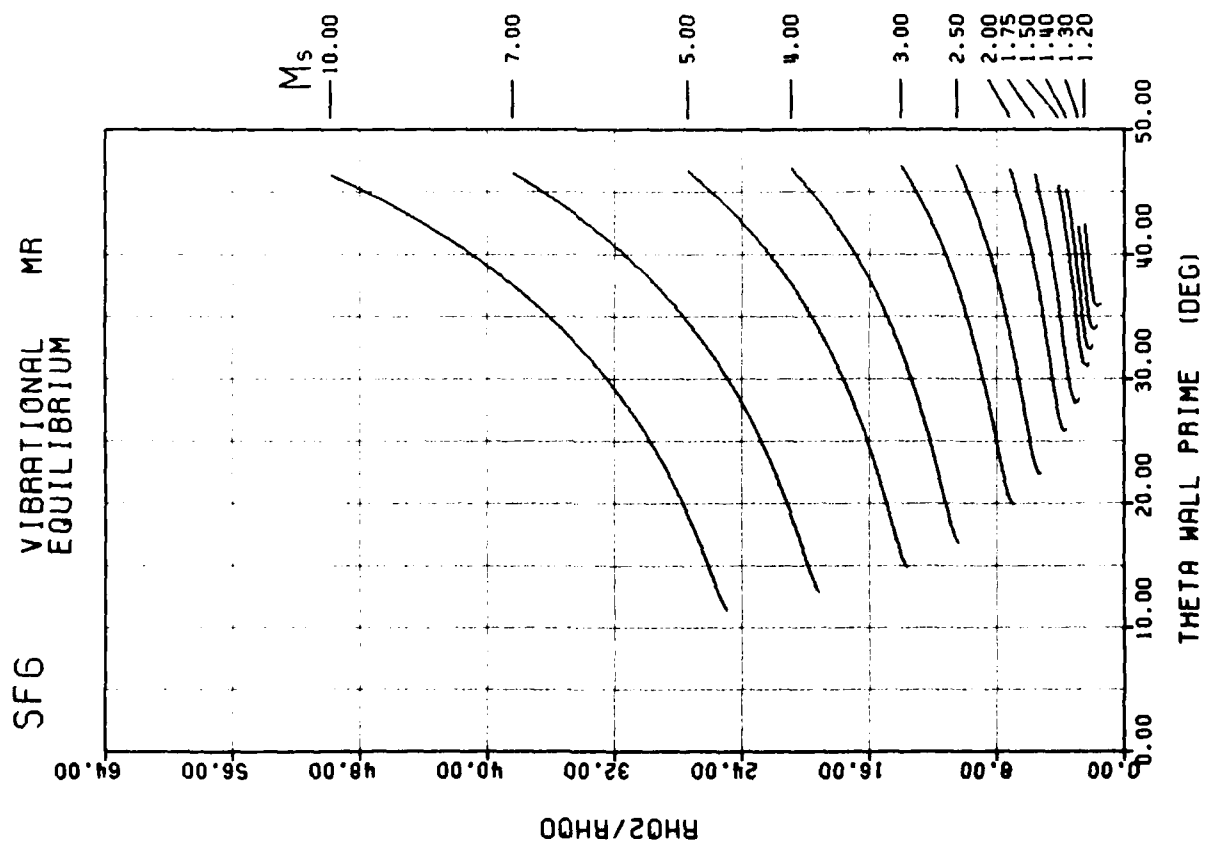


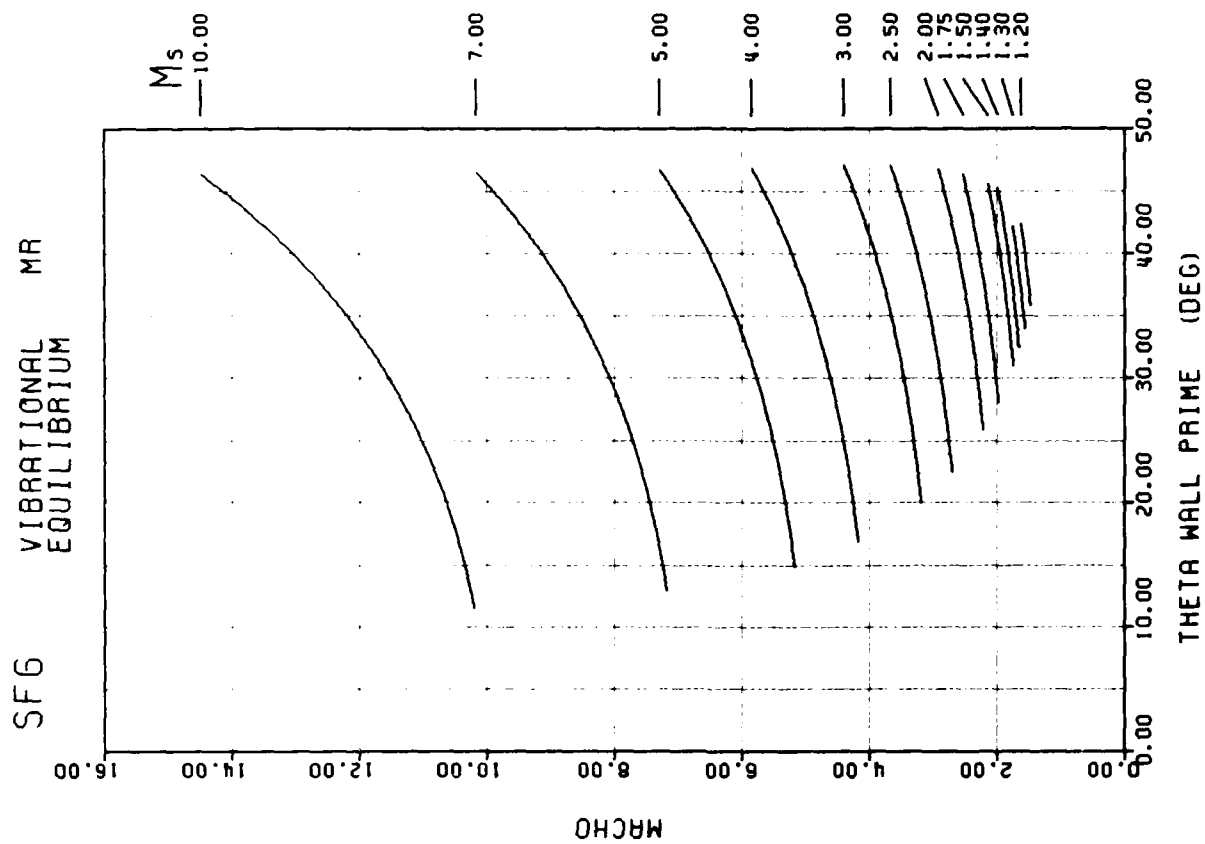
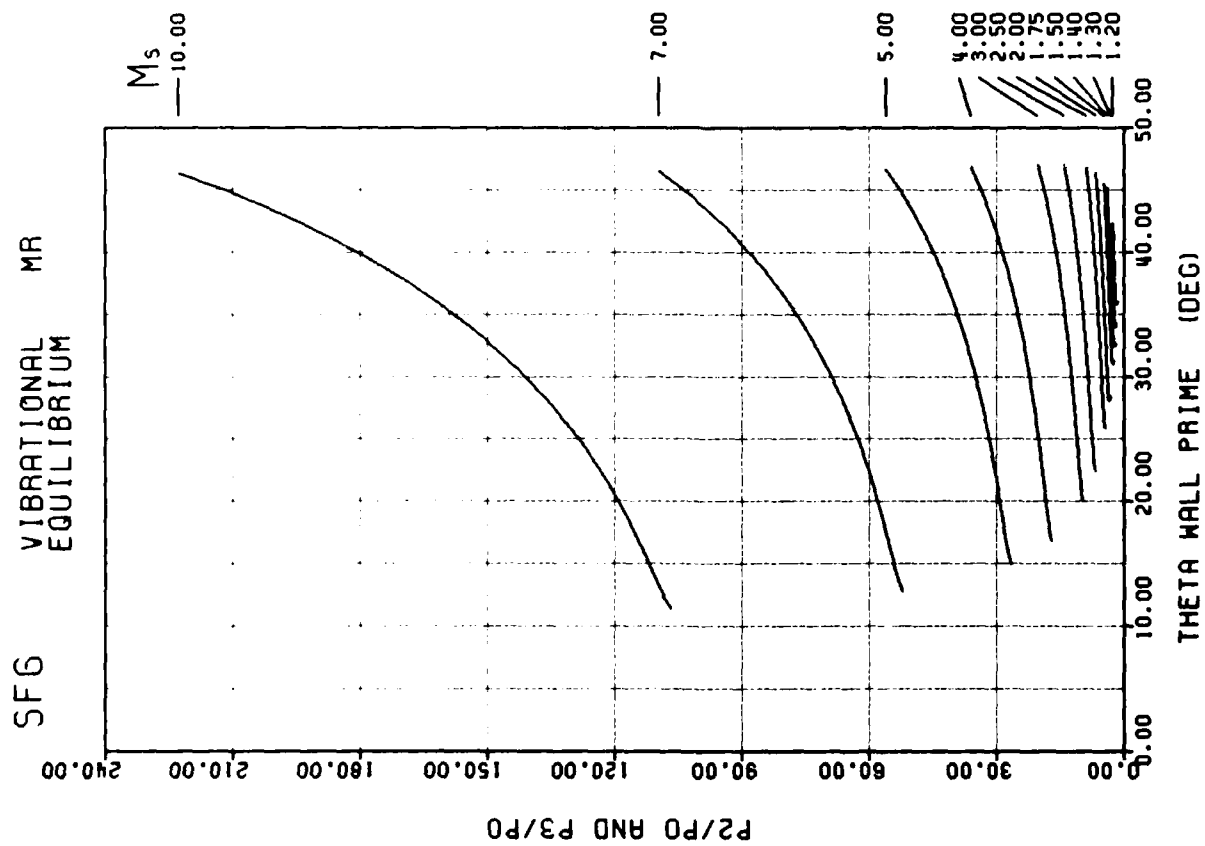


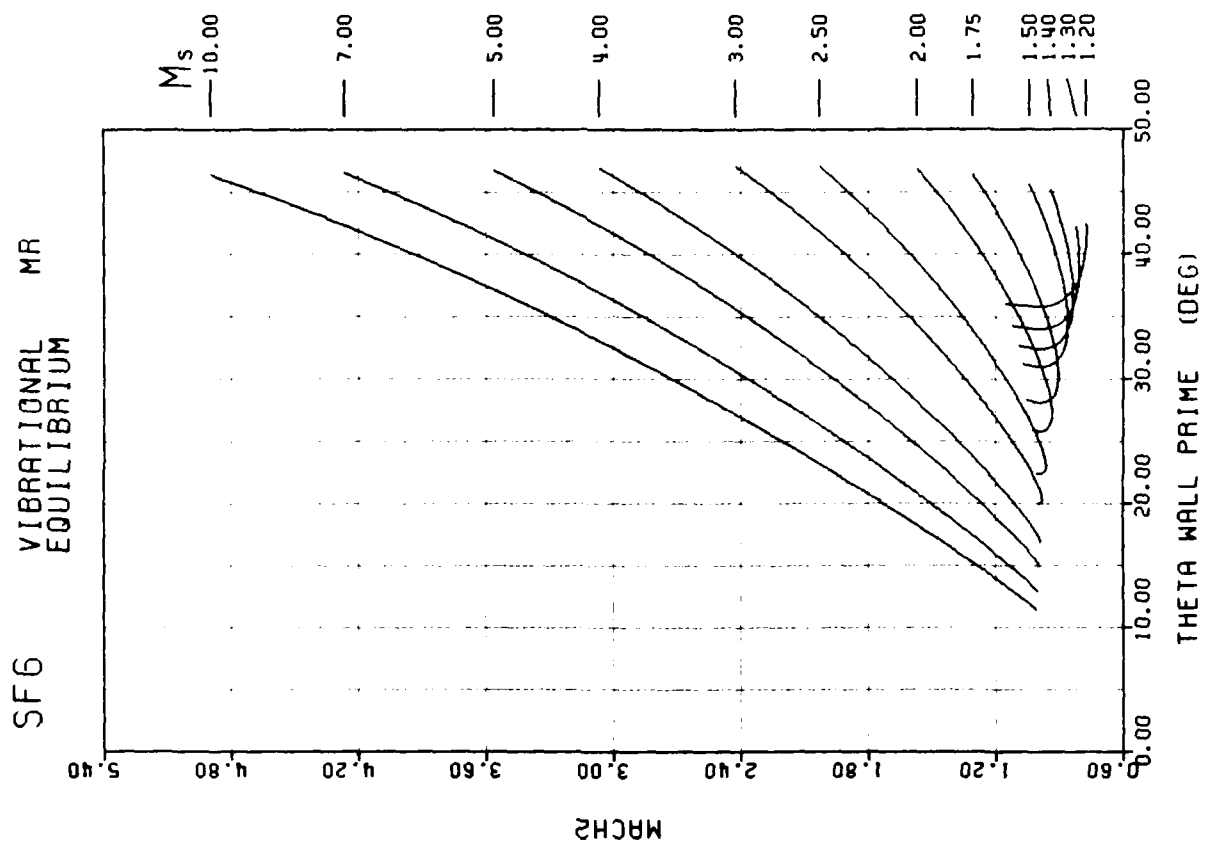
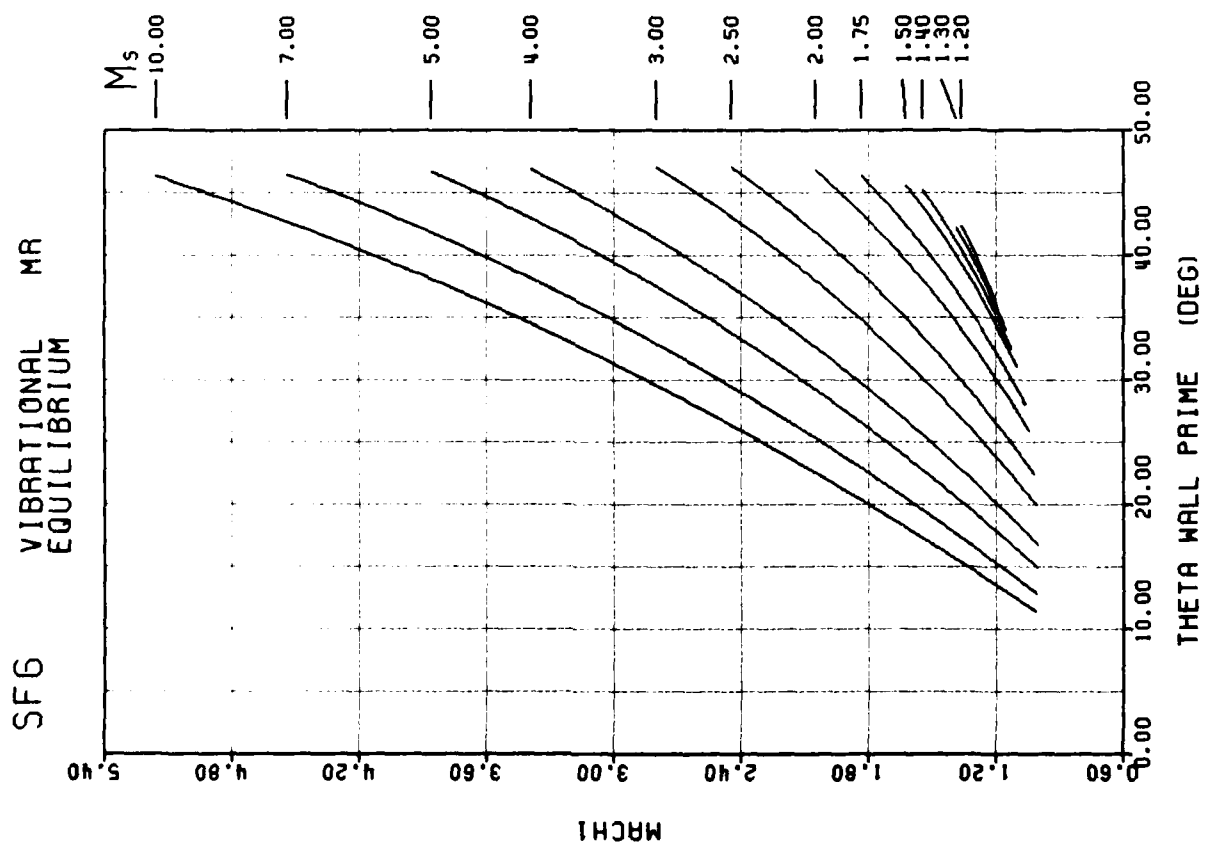


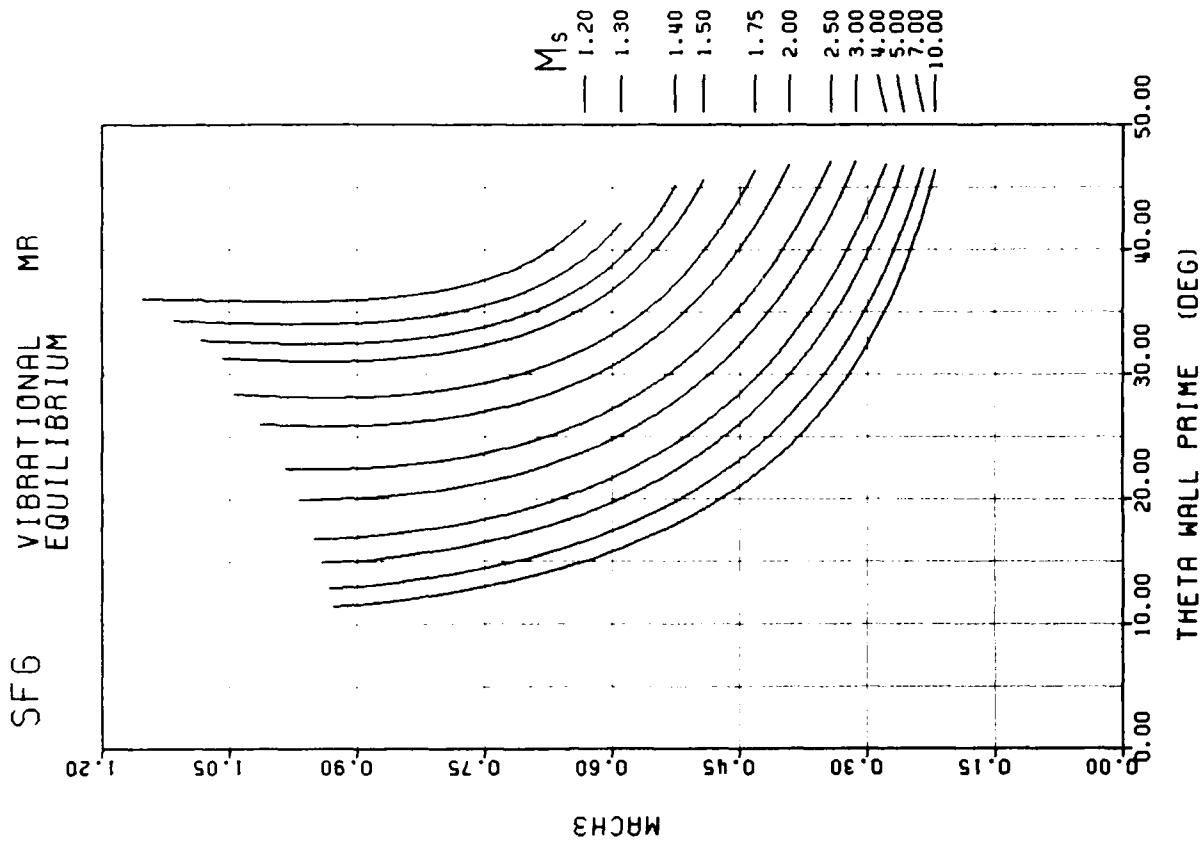
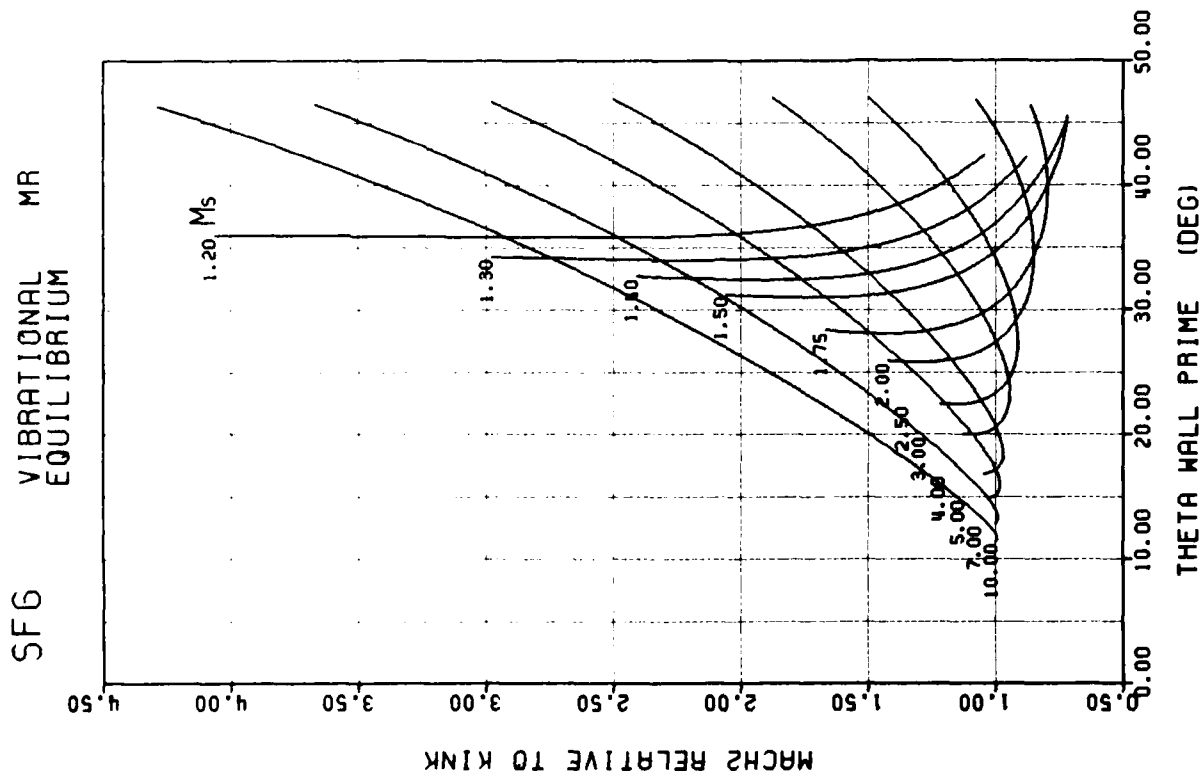


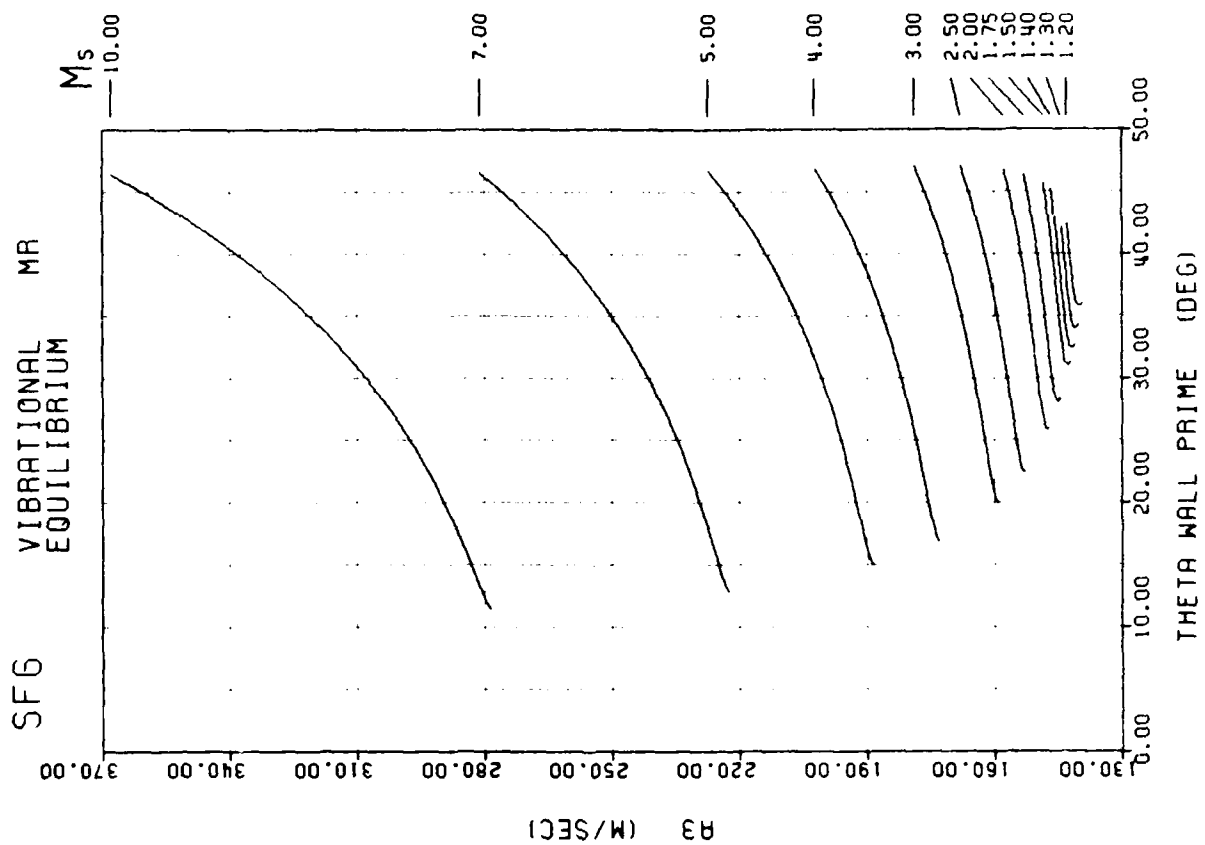
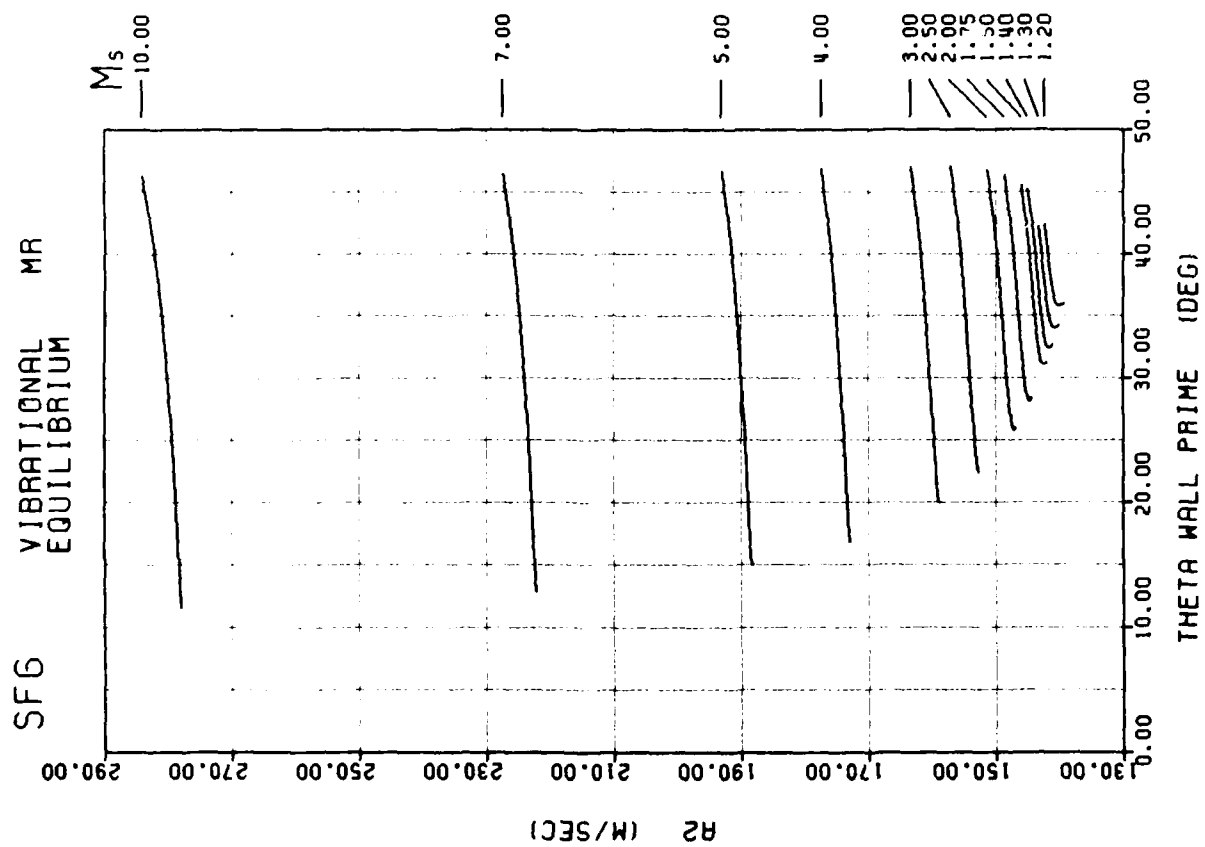


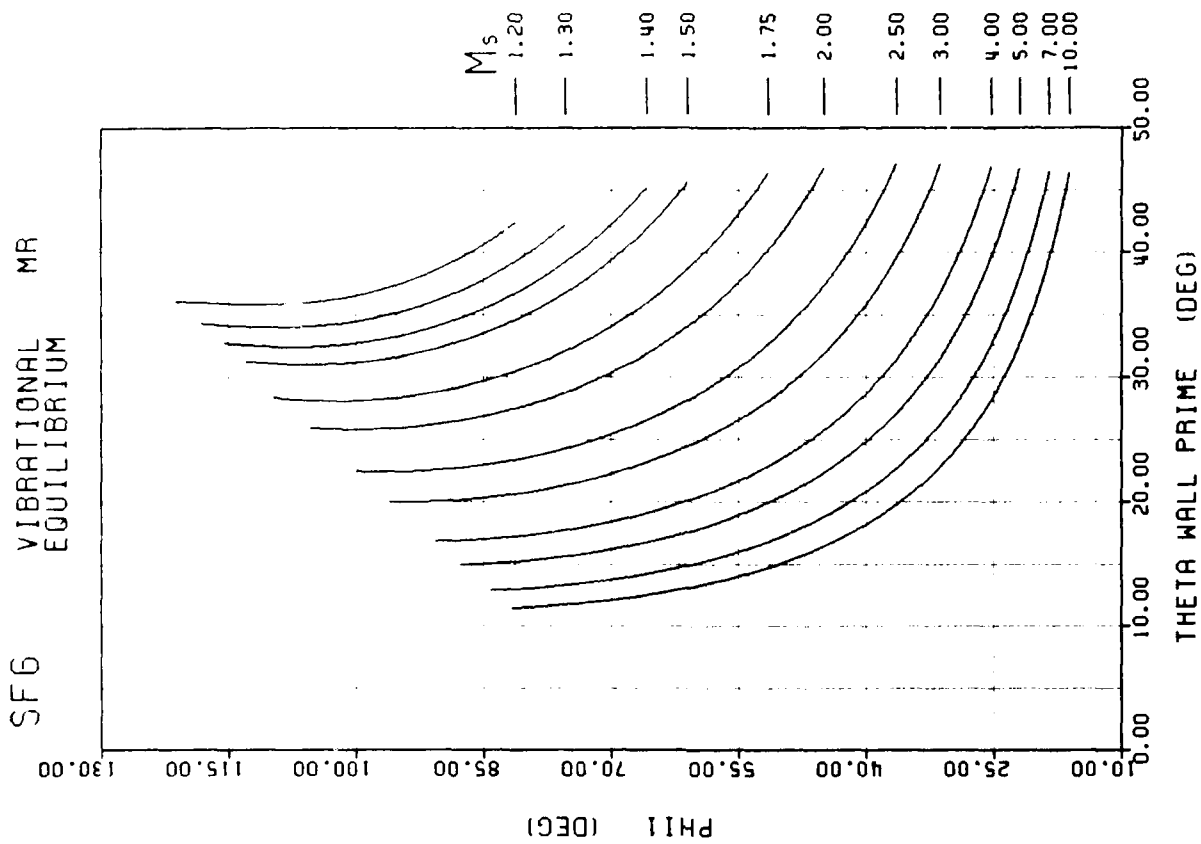
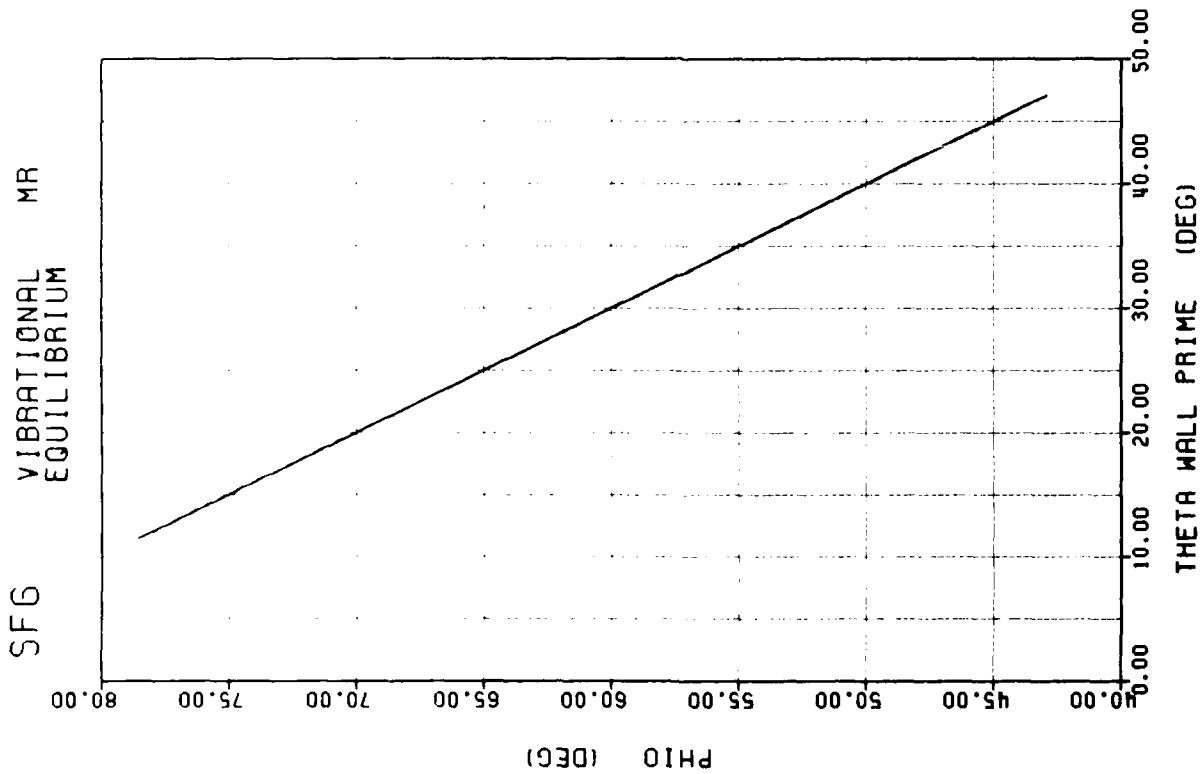


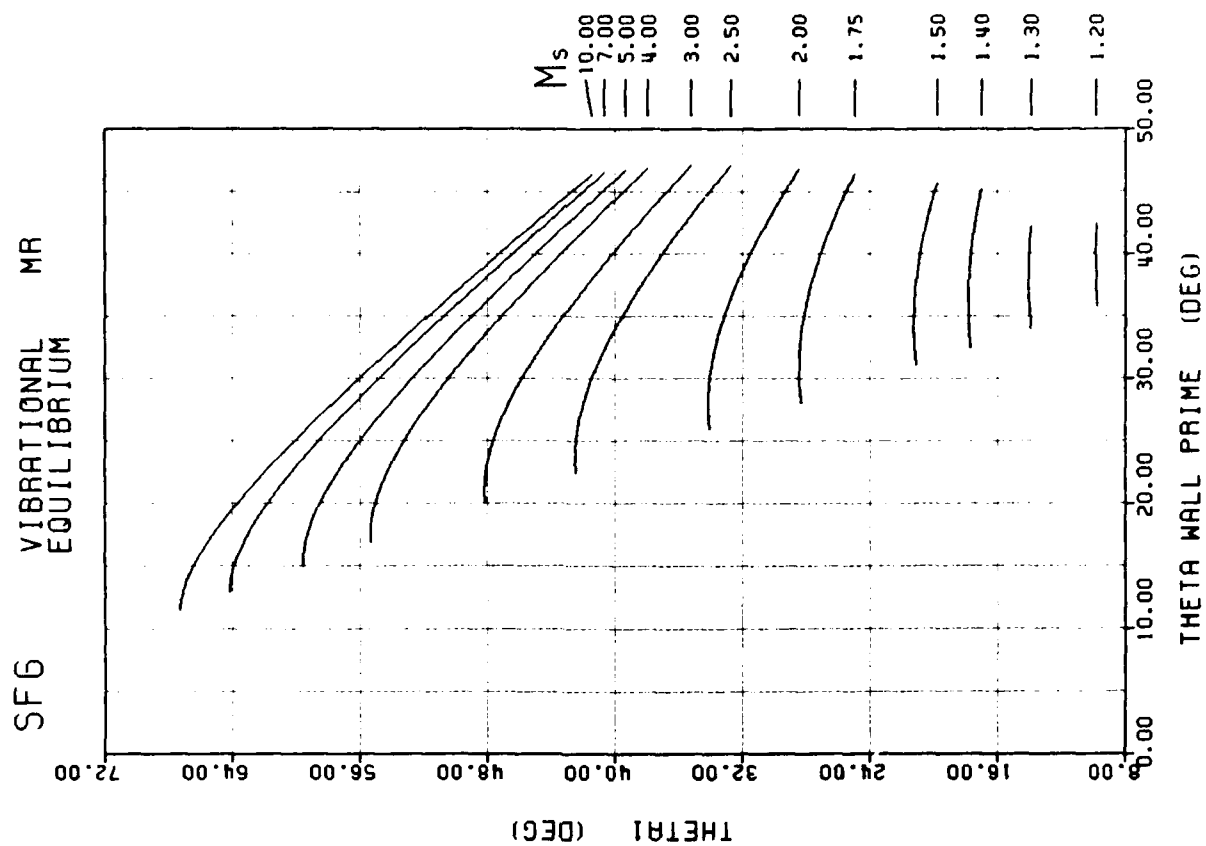
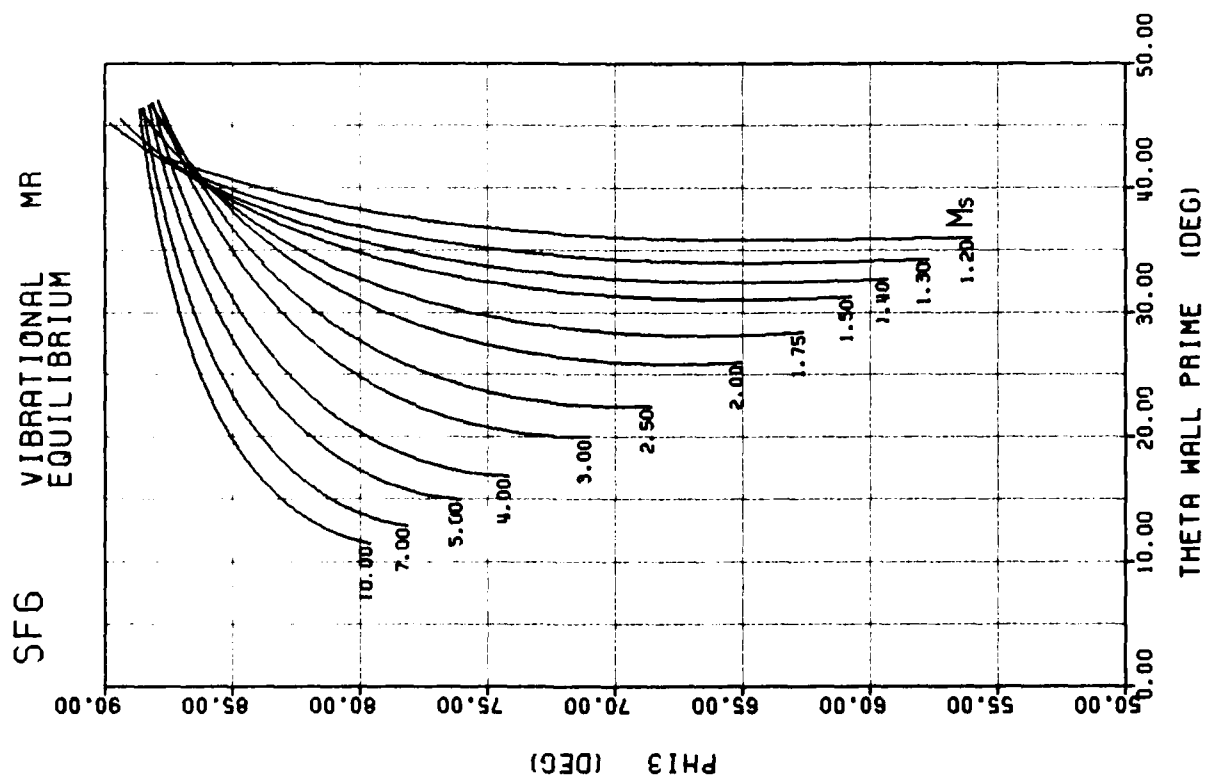


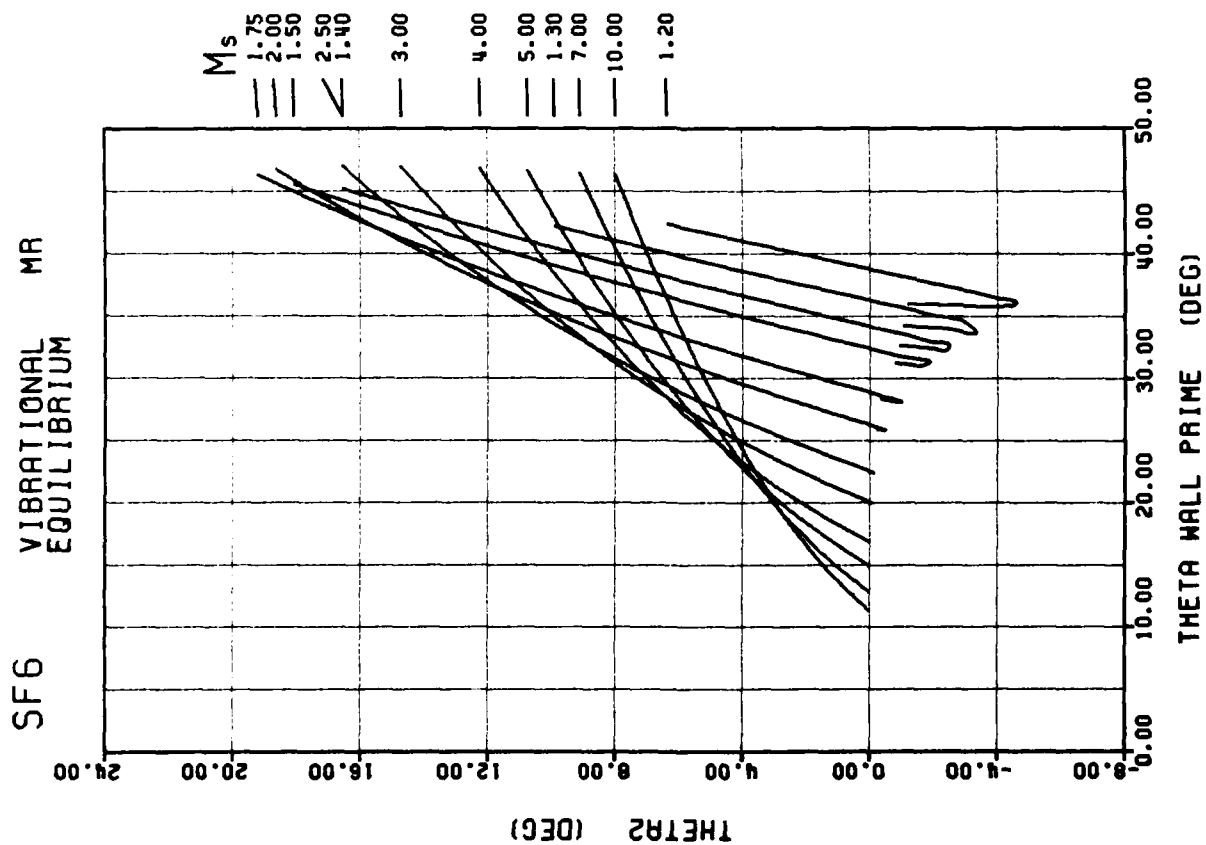
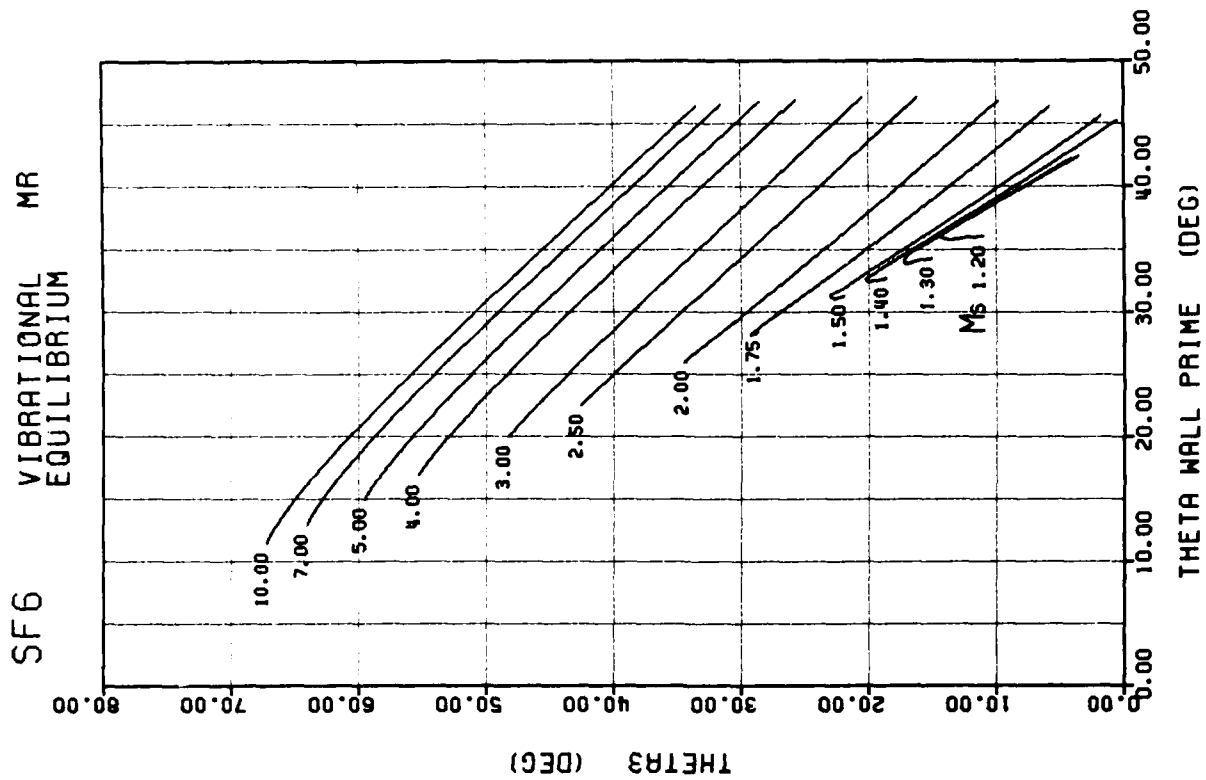


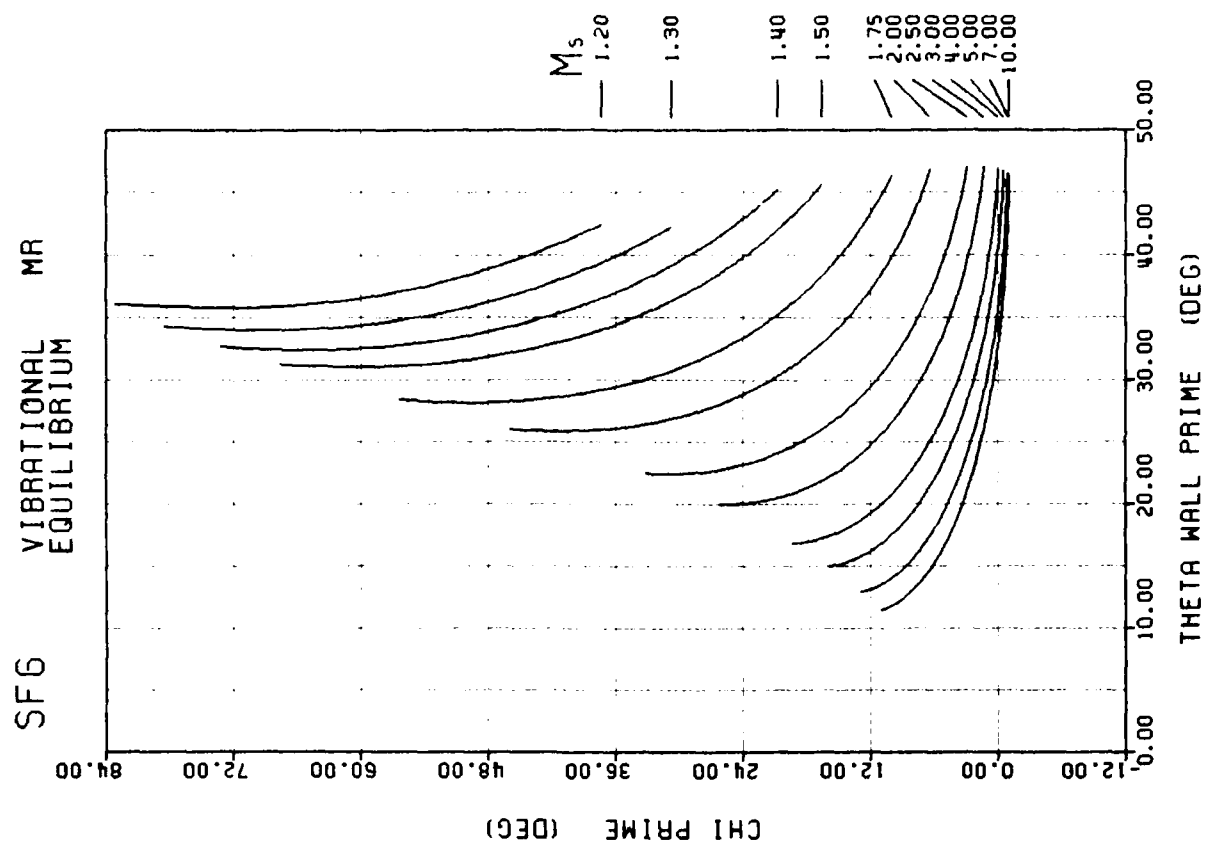
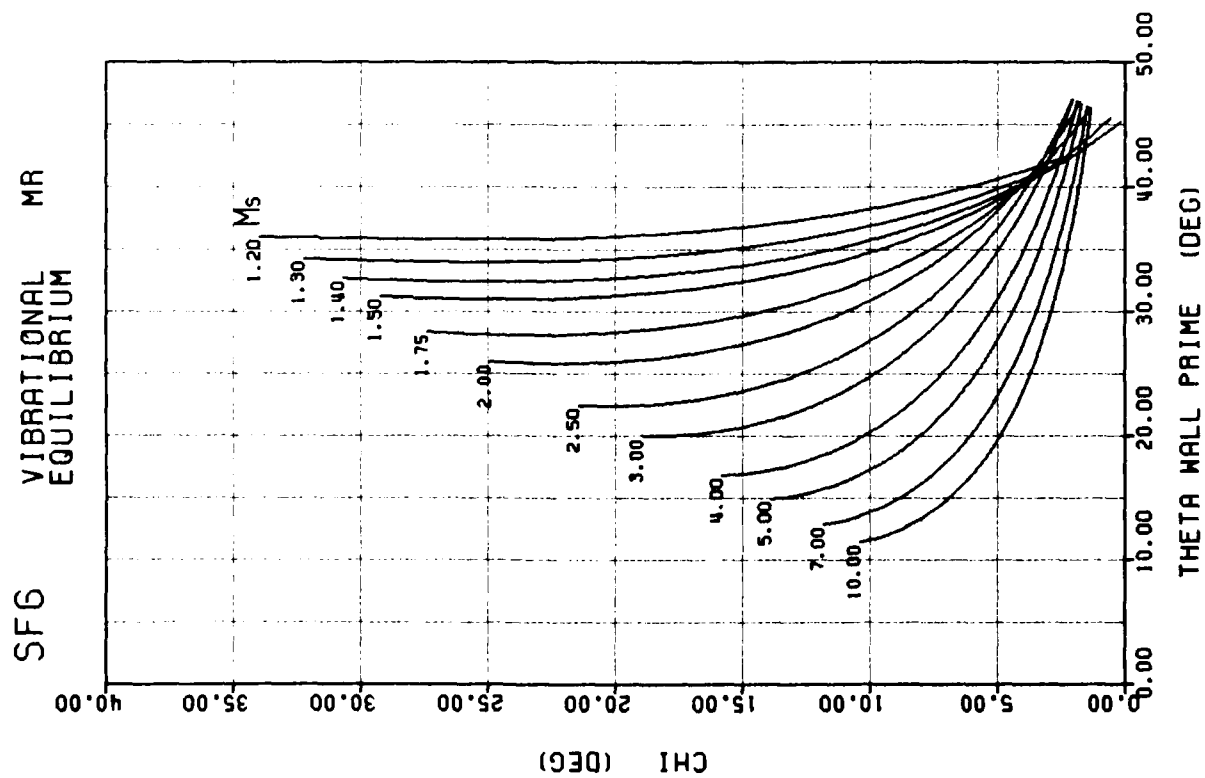


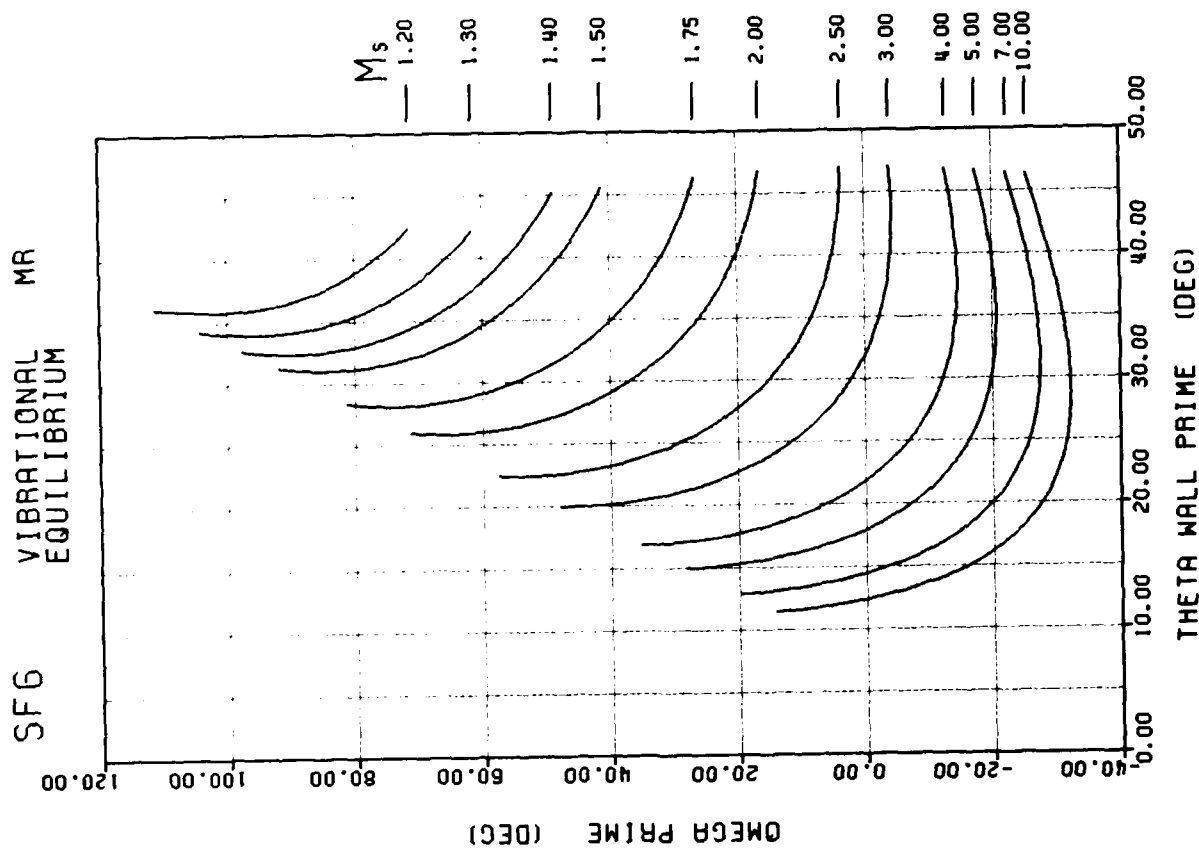
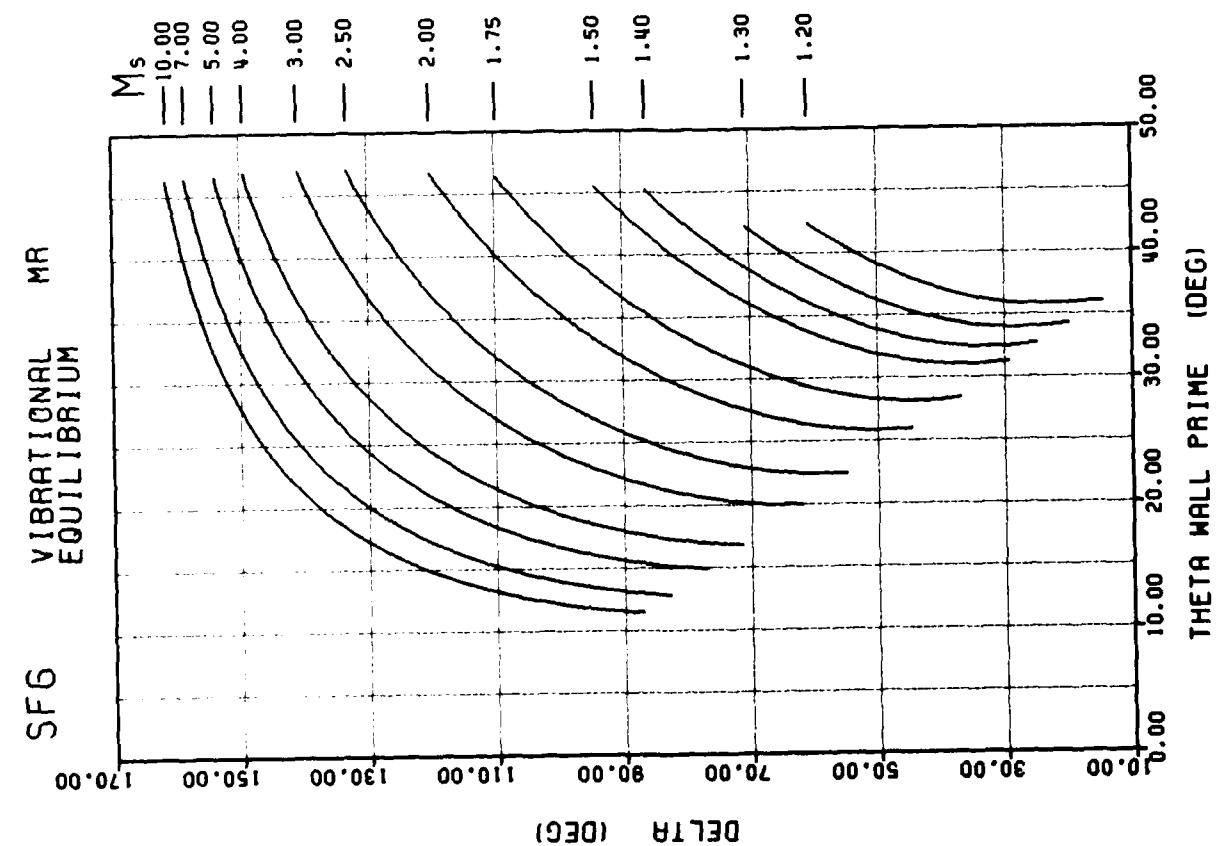


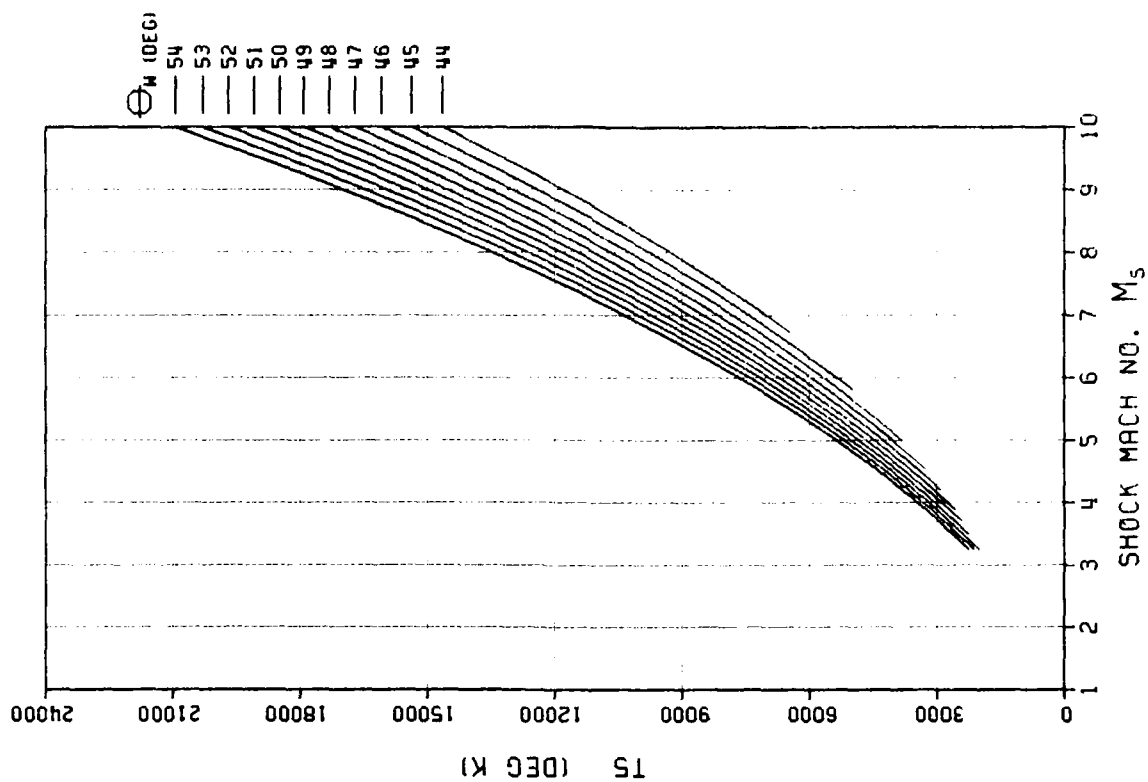
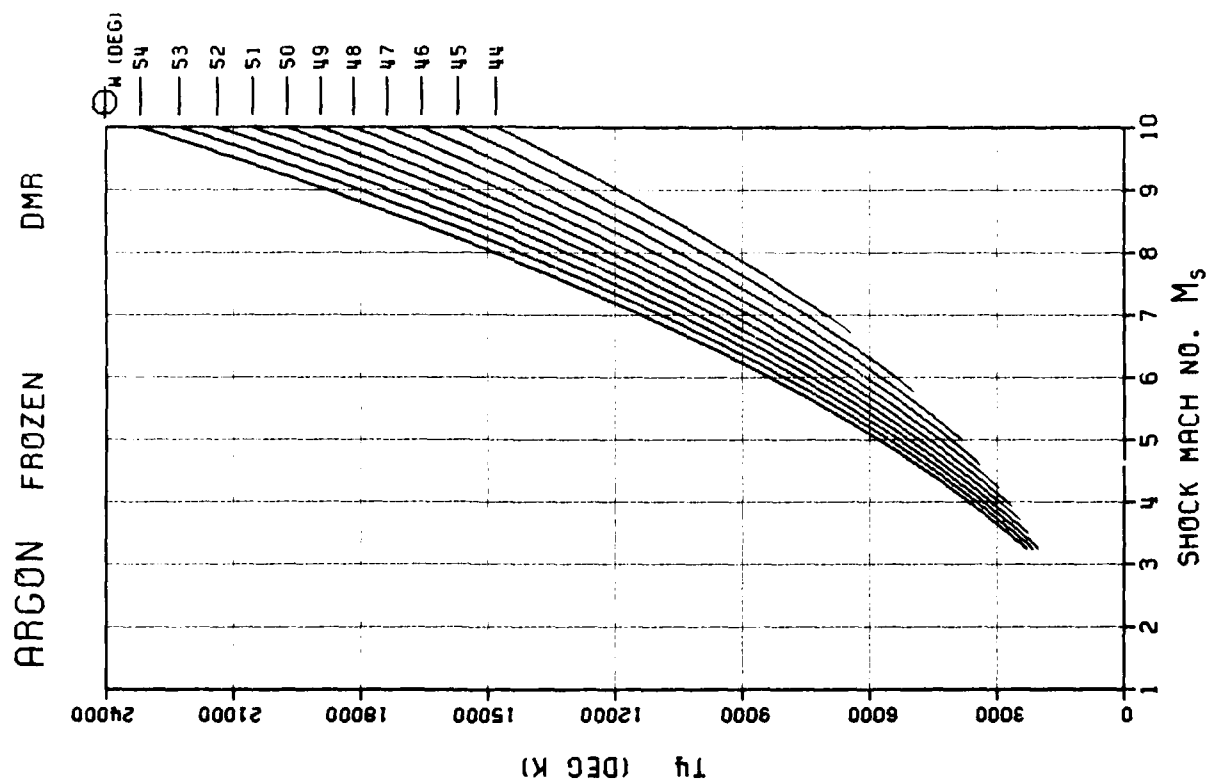


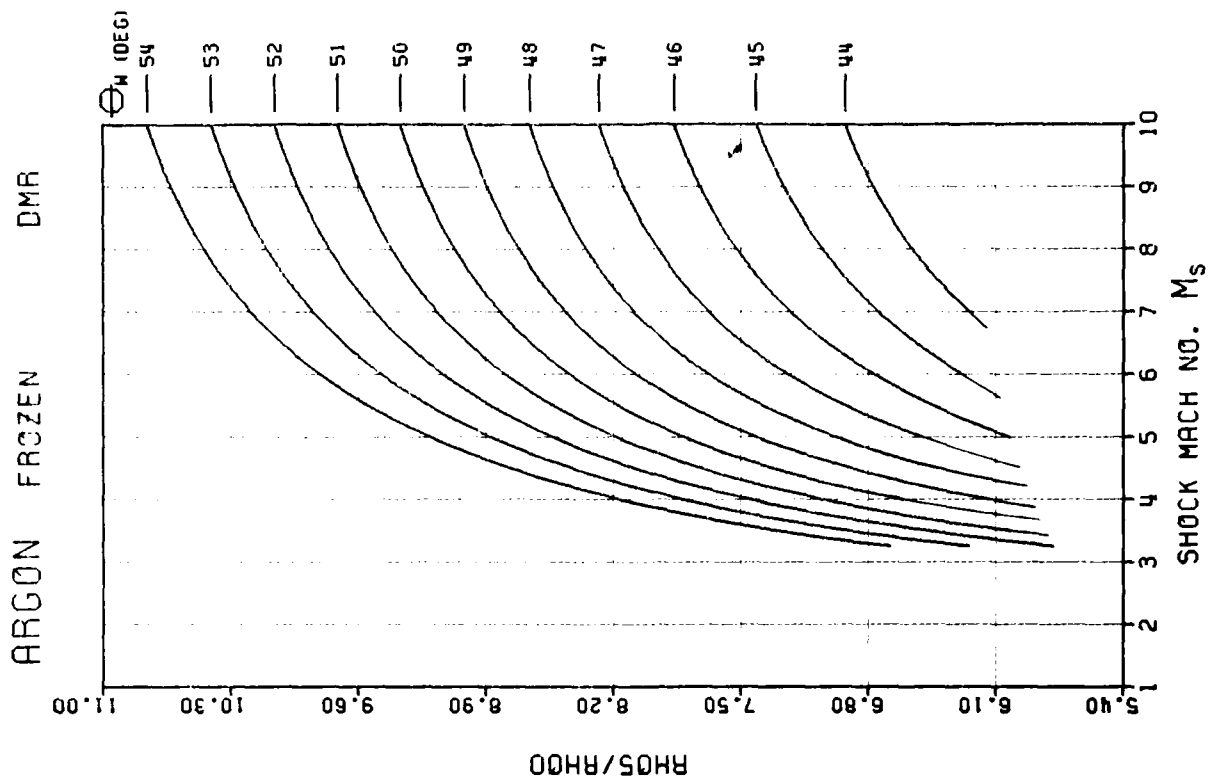
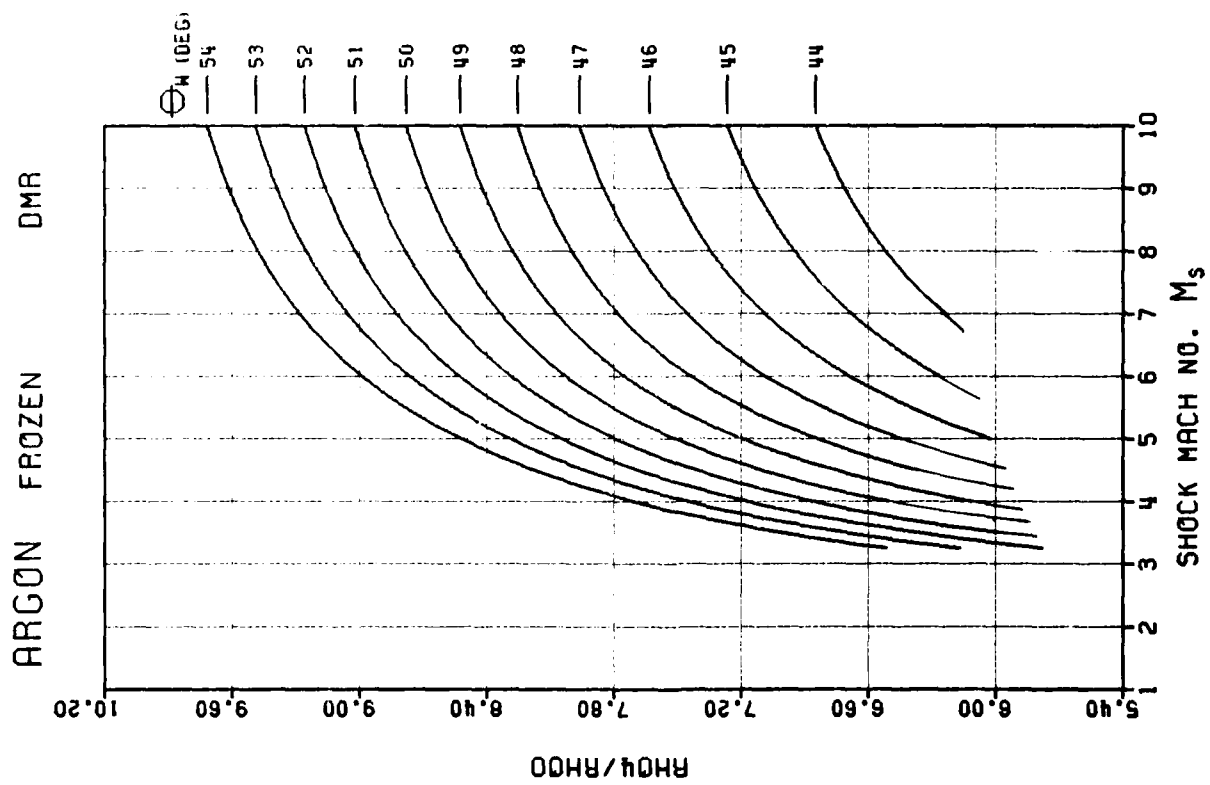


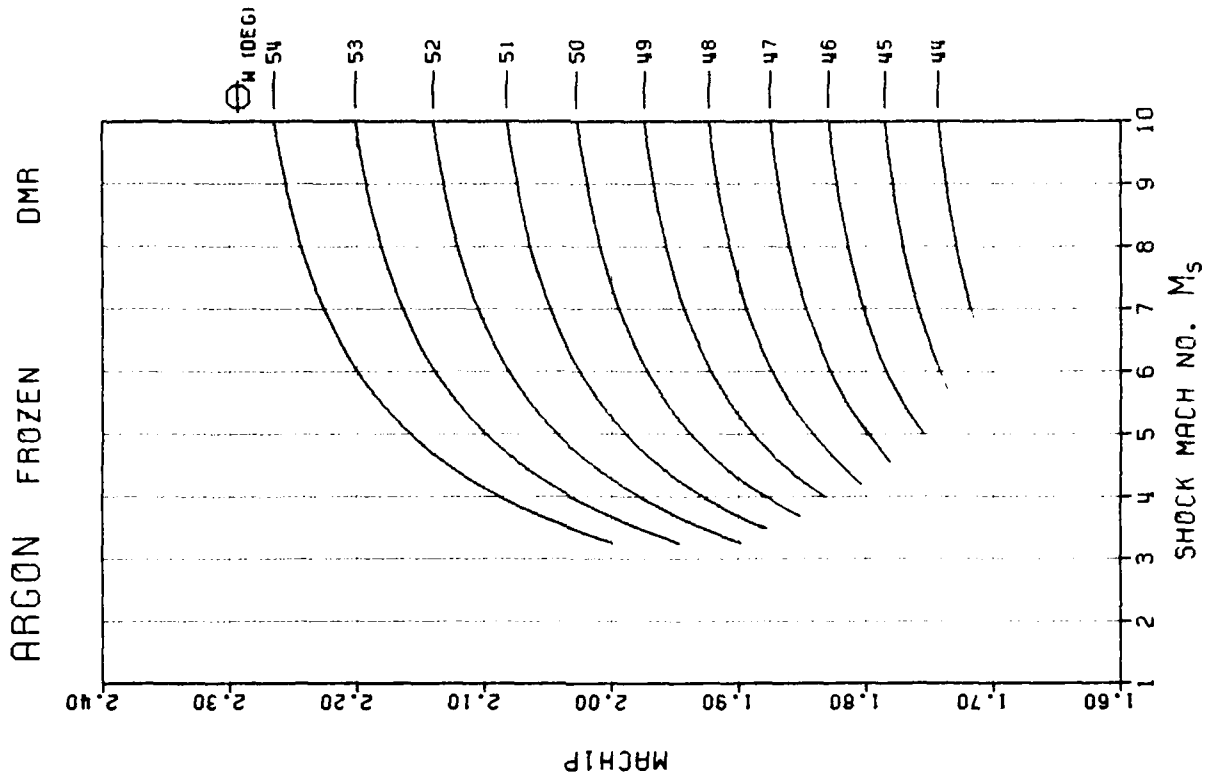
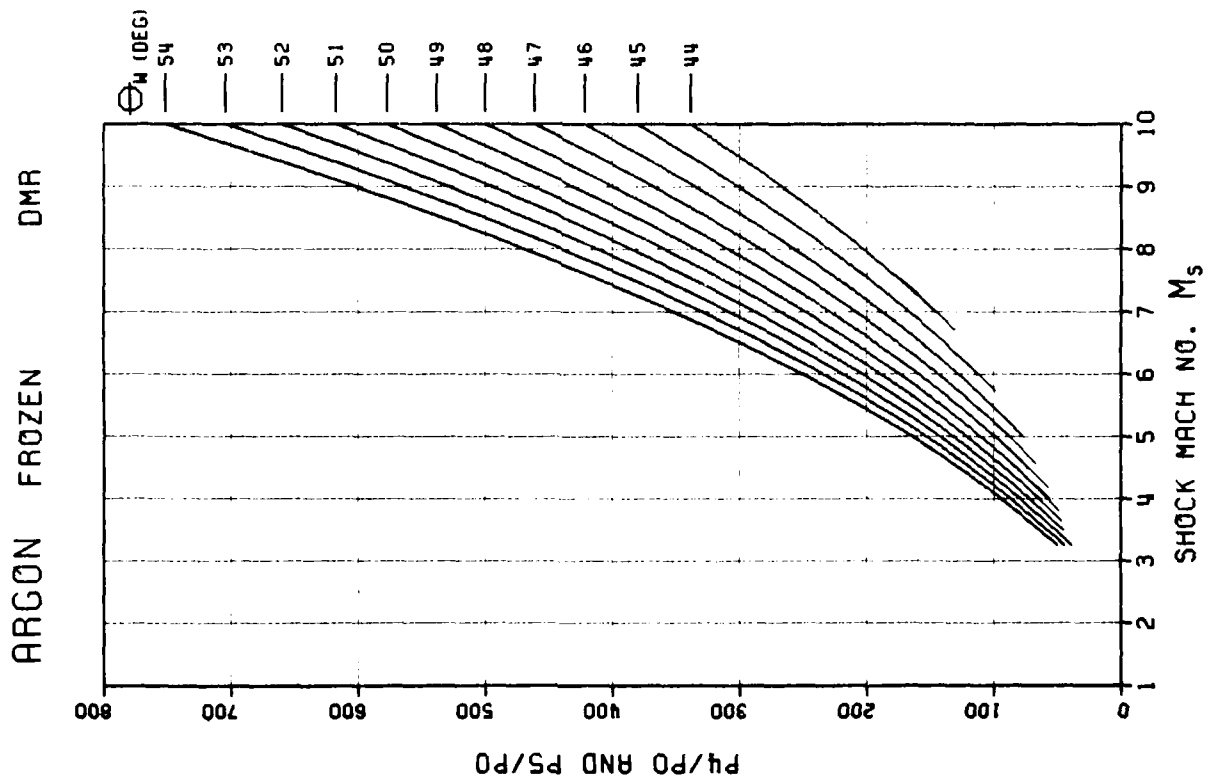


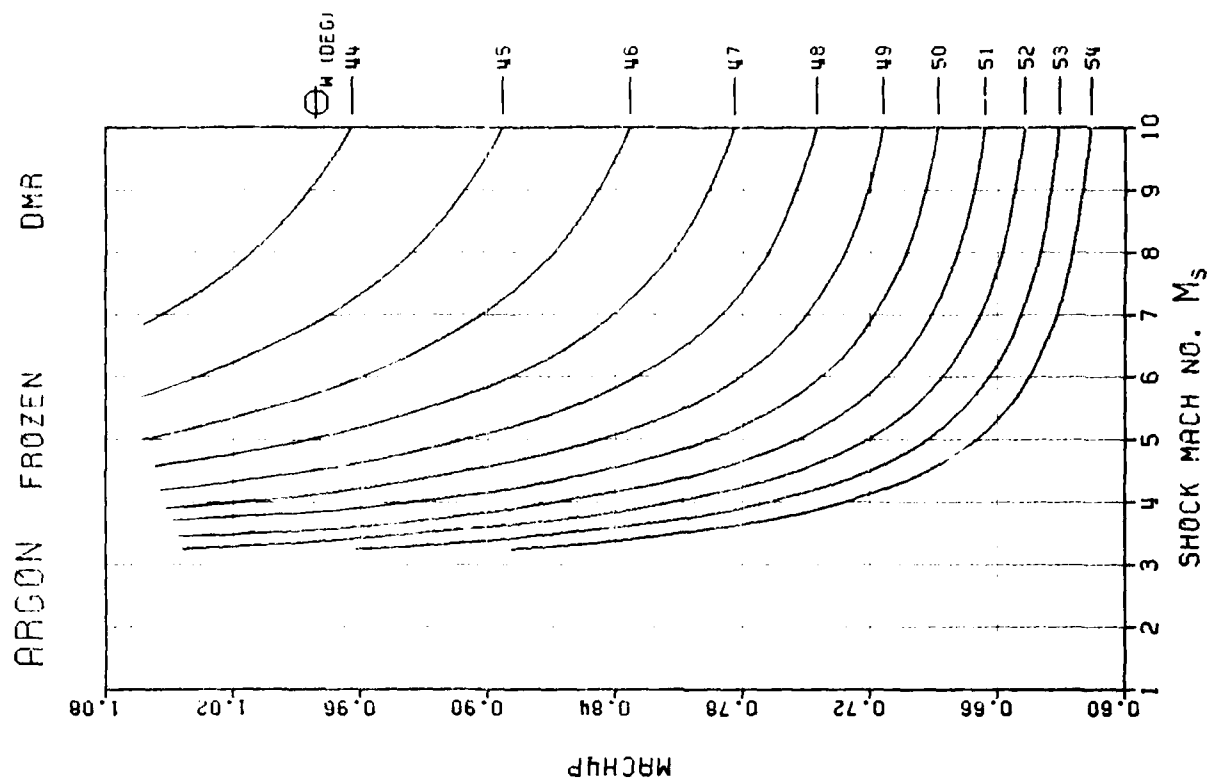
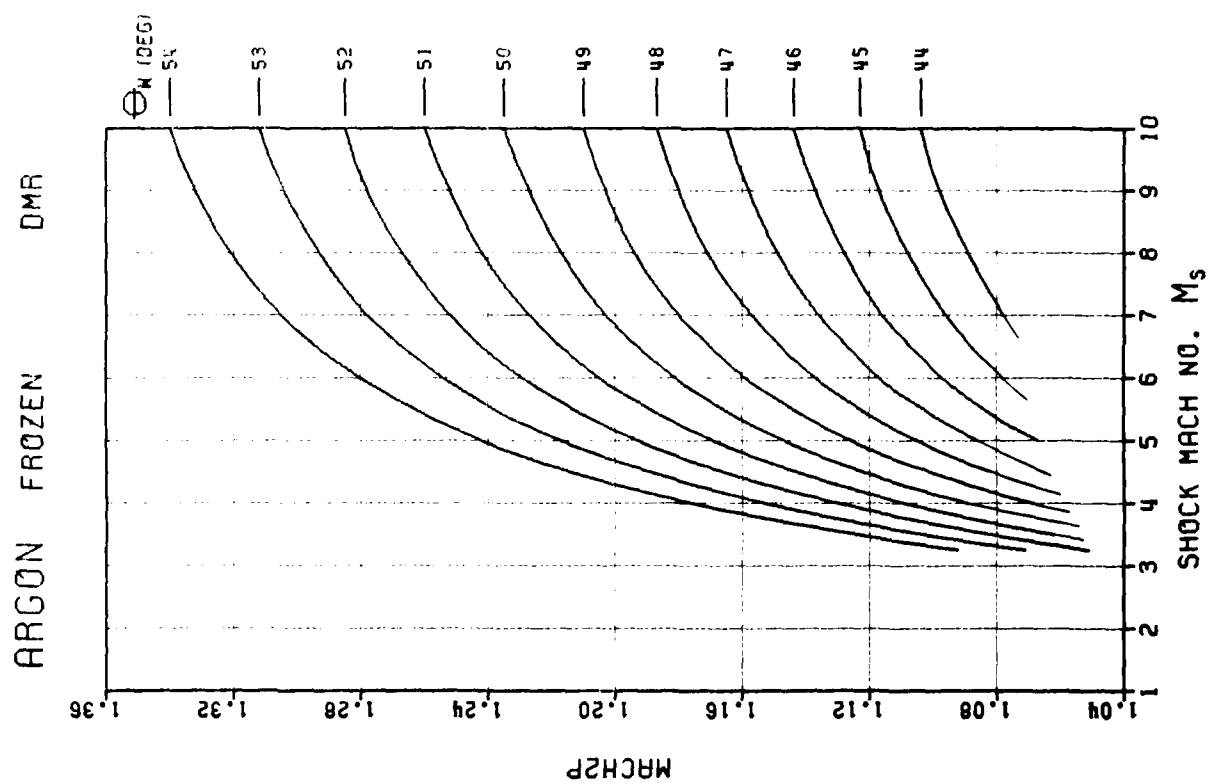


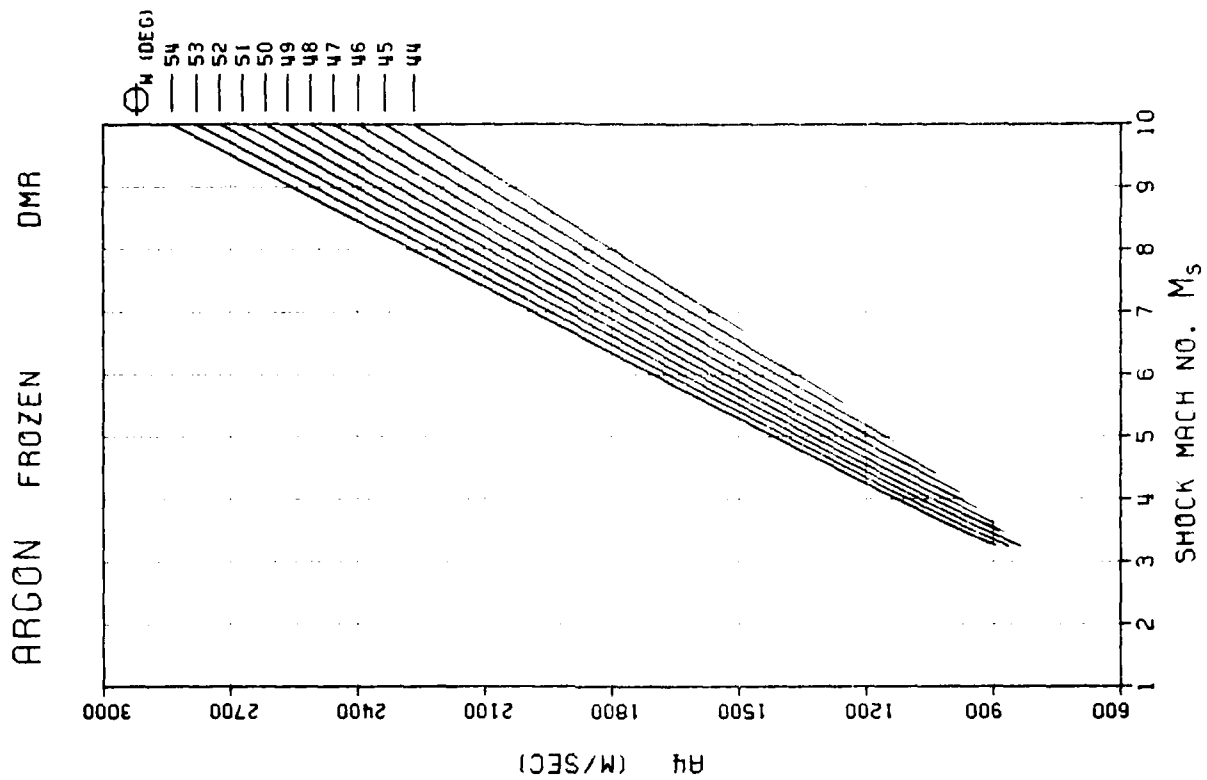
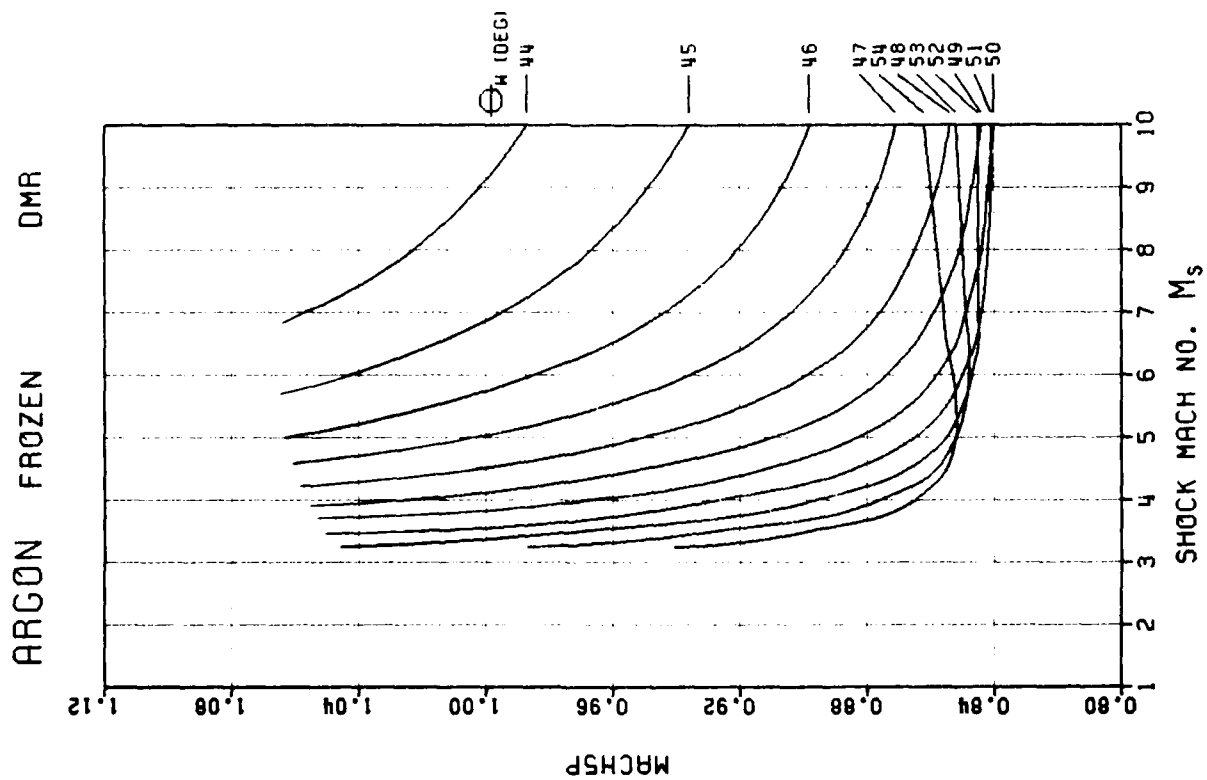


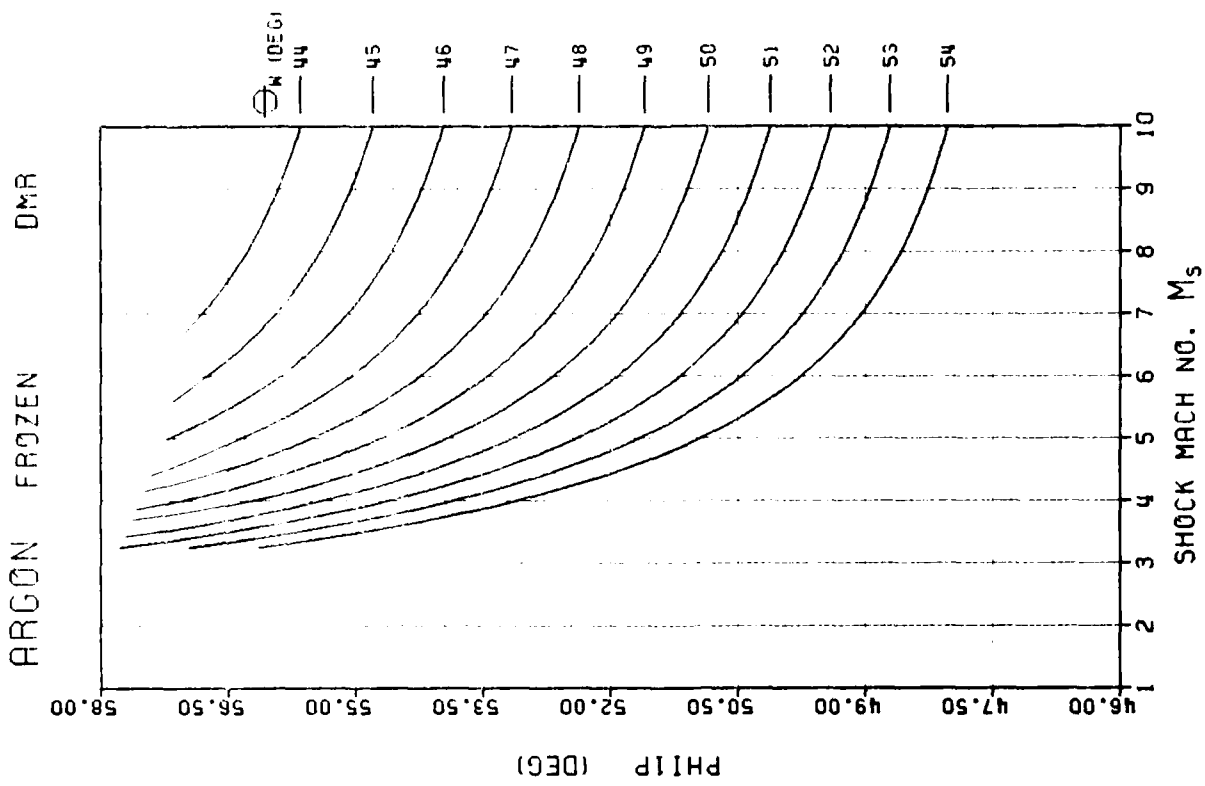
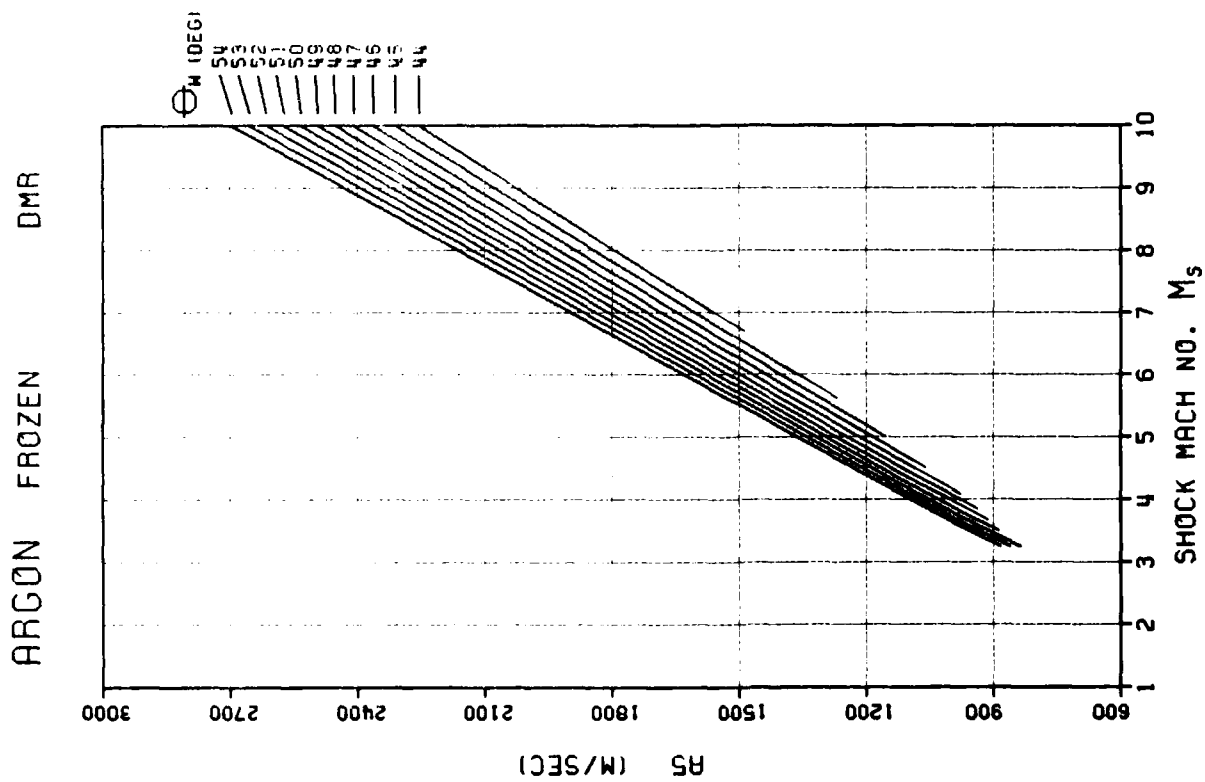


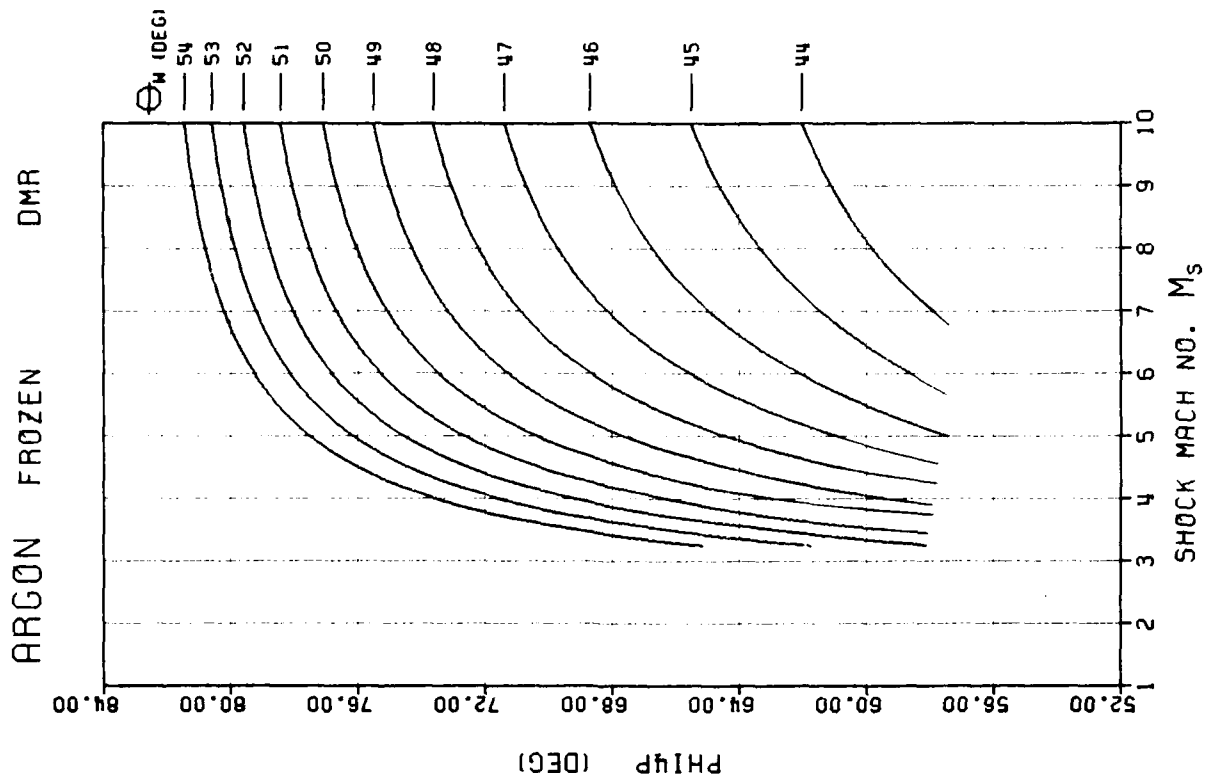
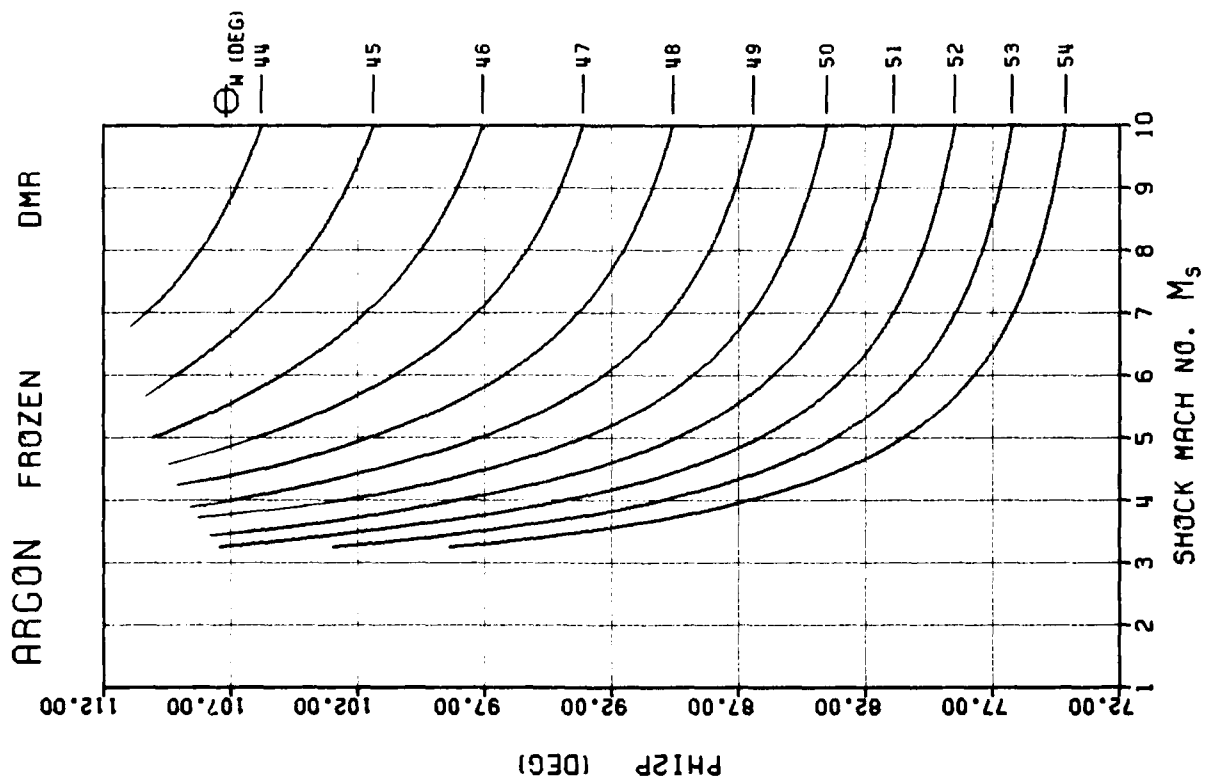




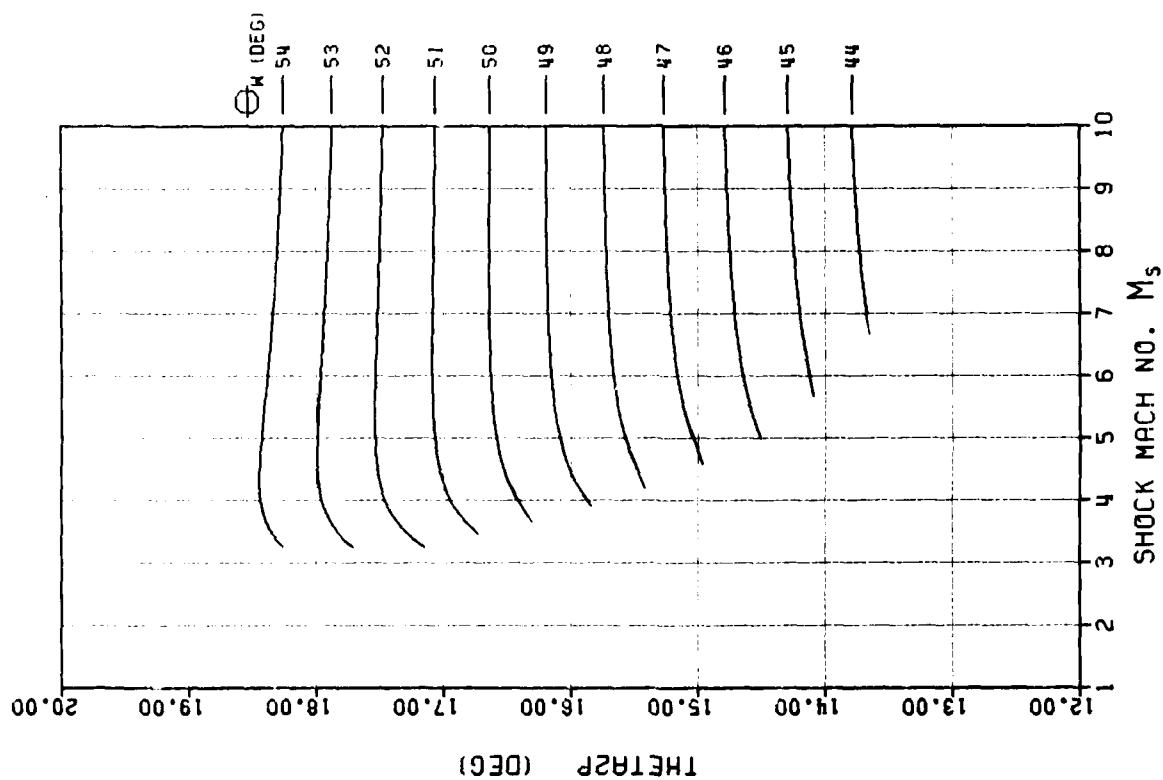




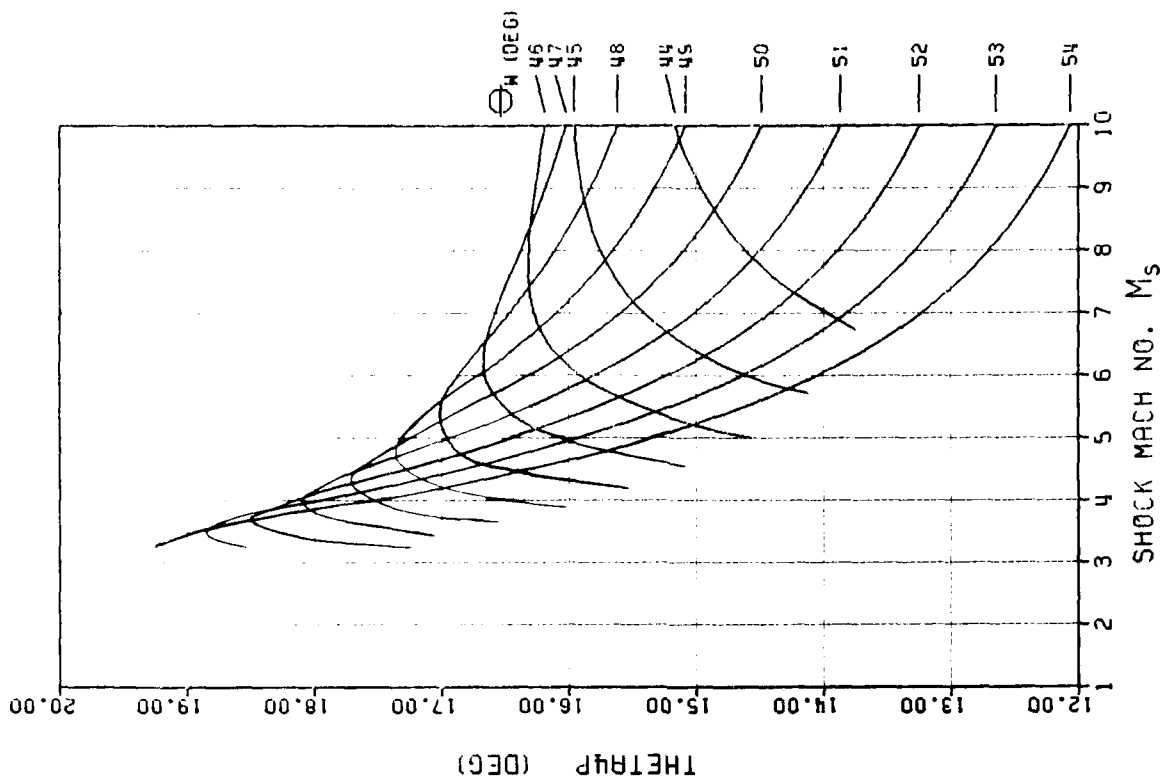


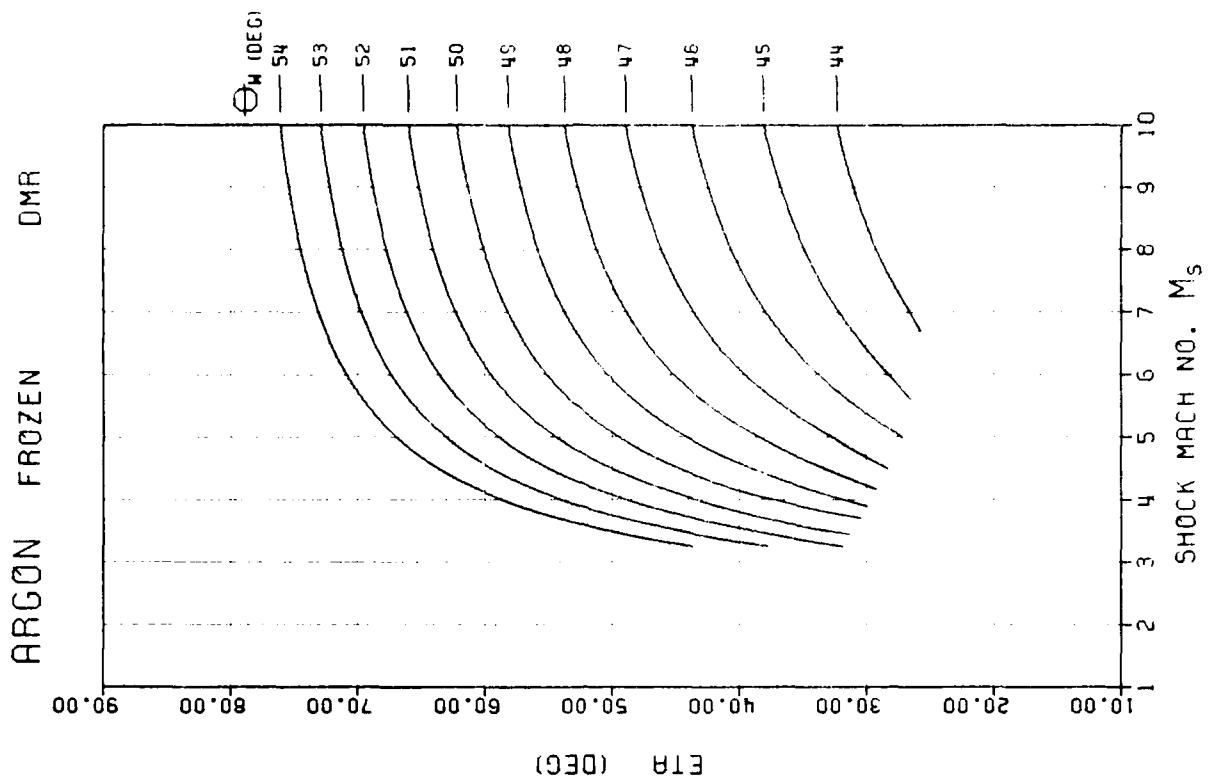
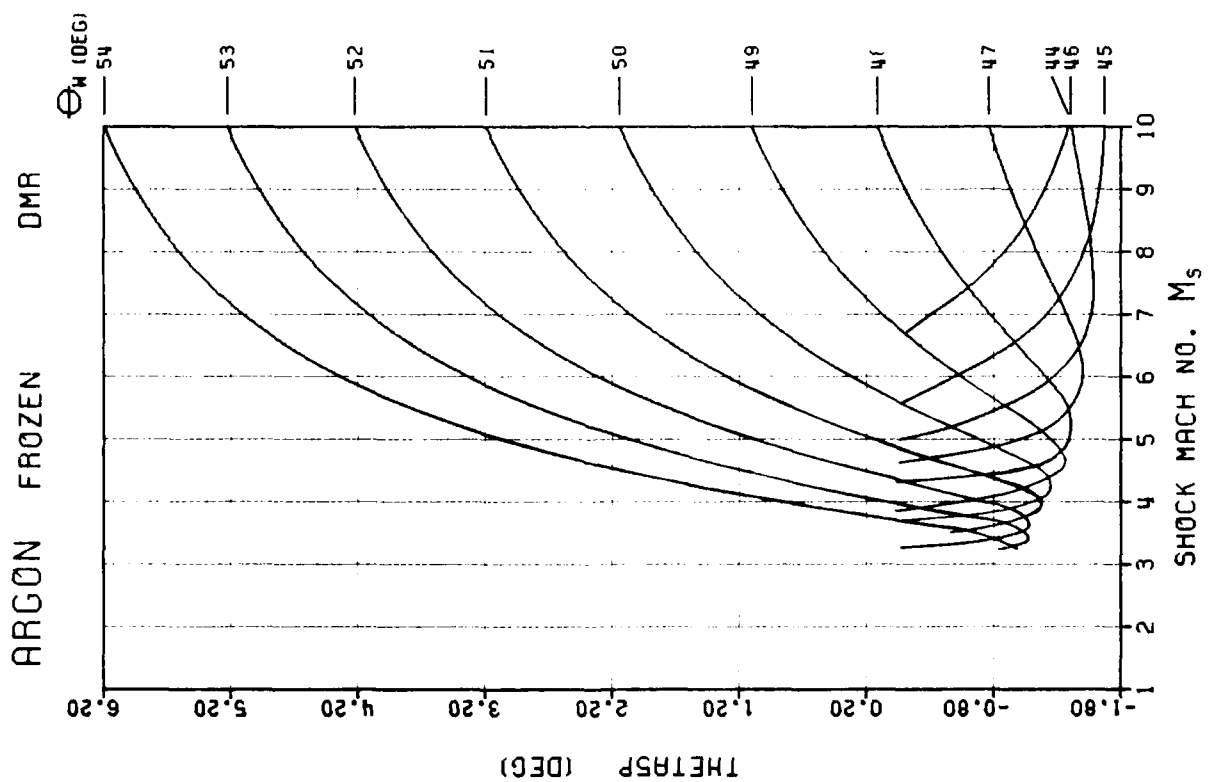


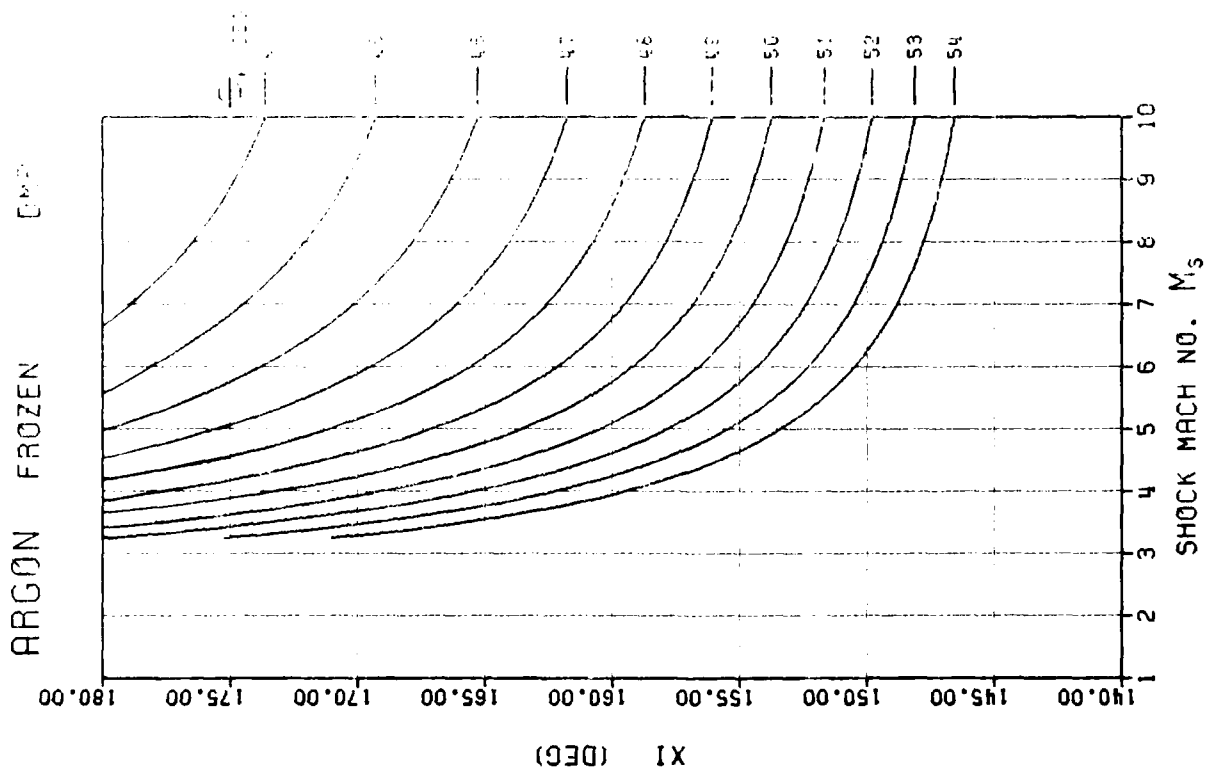
ARGON FROZEN DM2

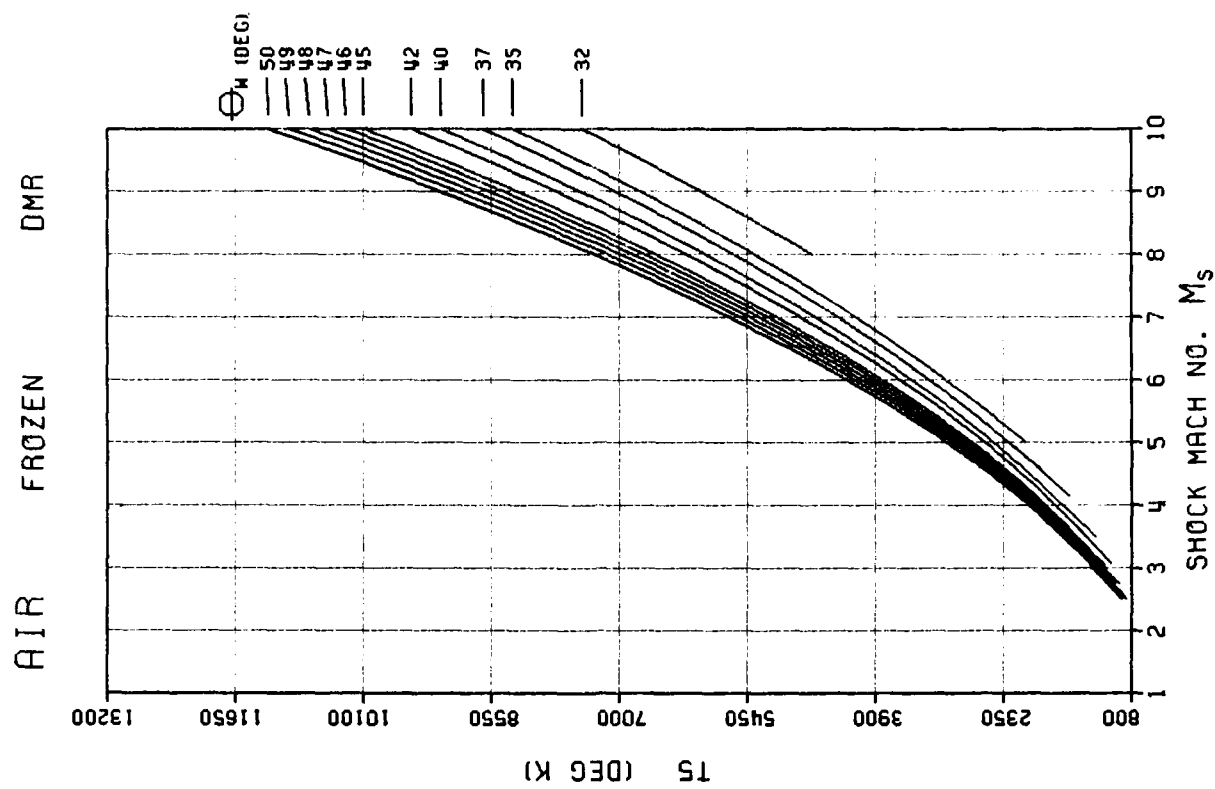
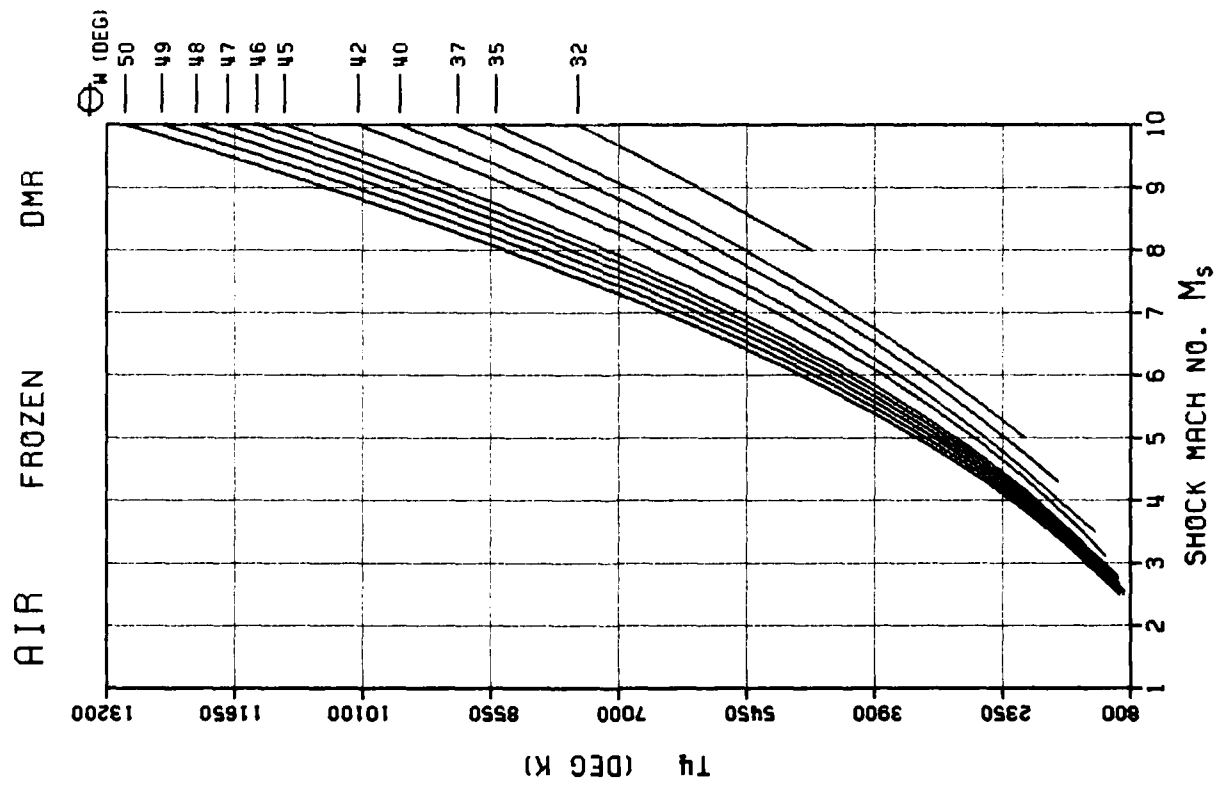


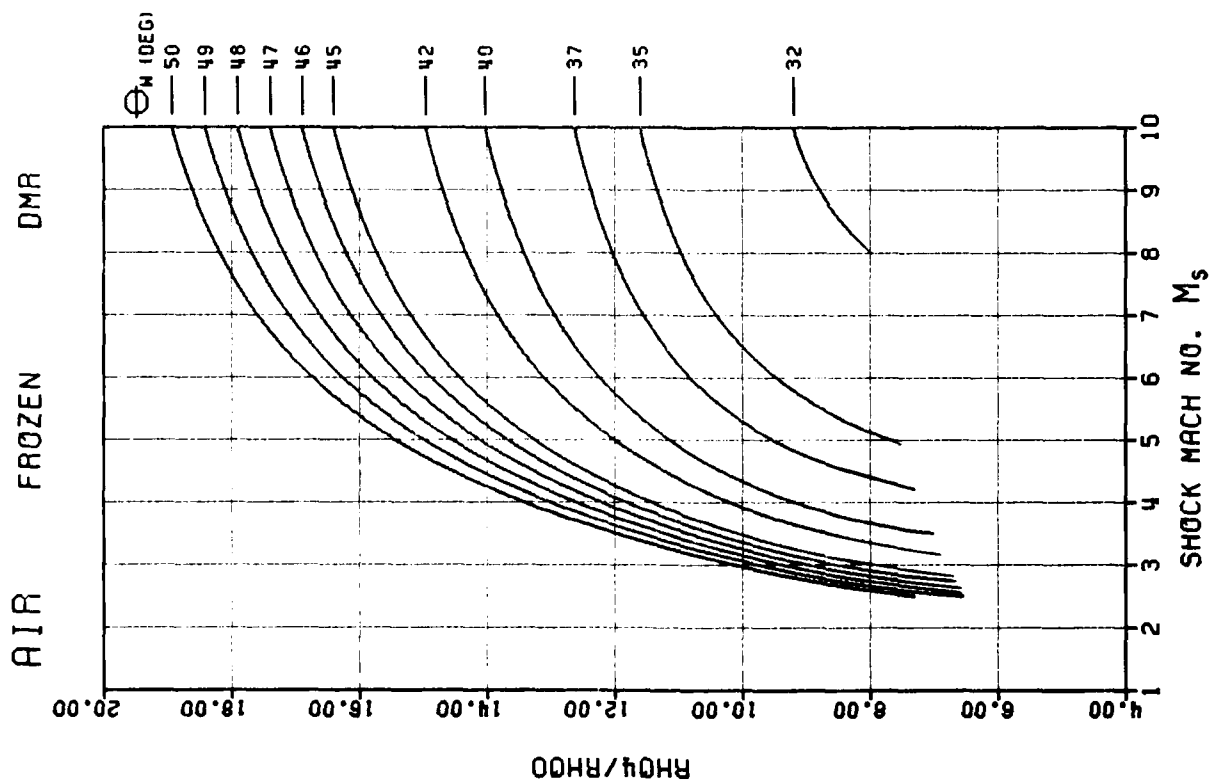
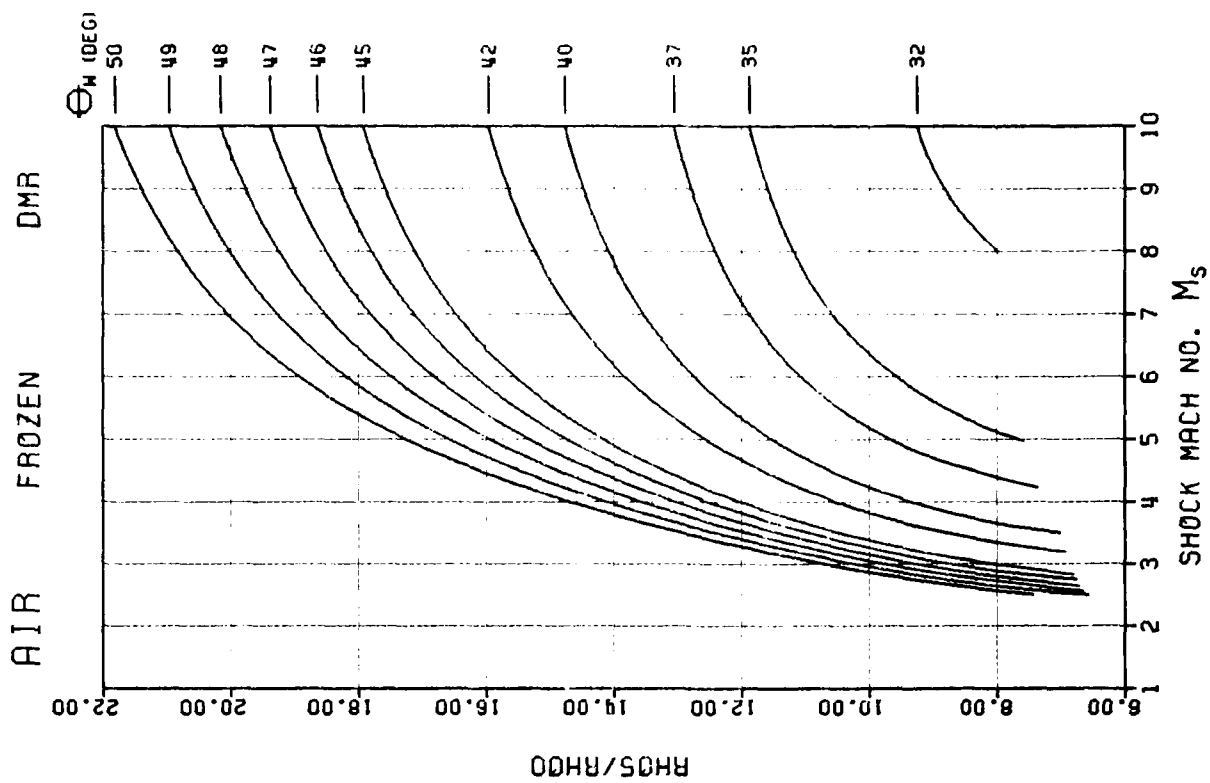
ARGON FROZEN DM2

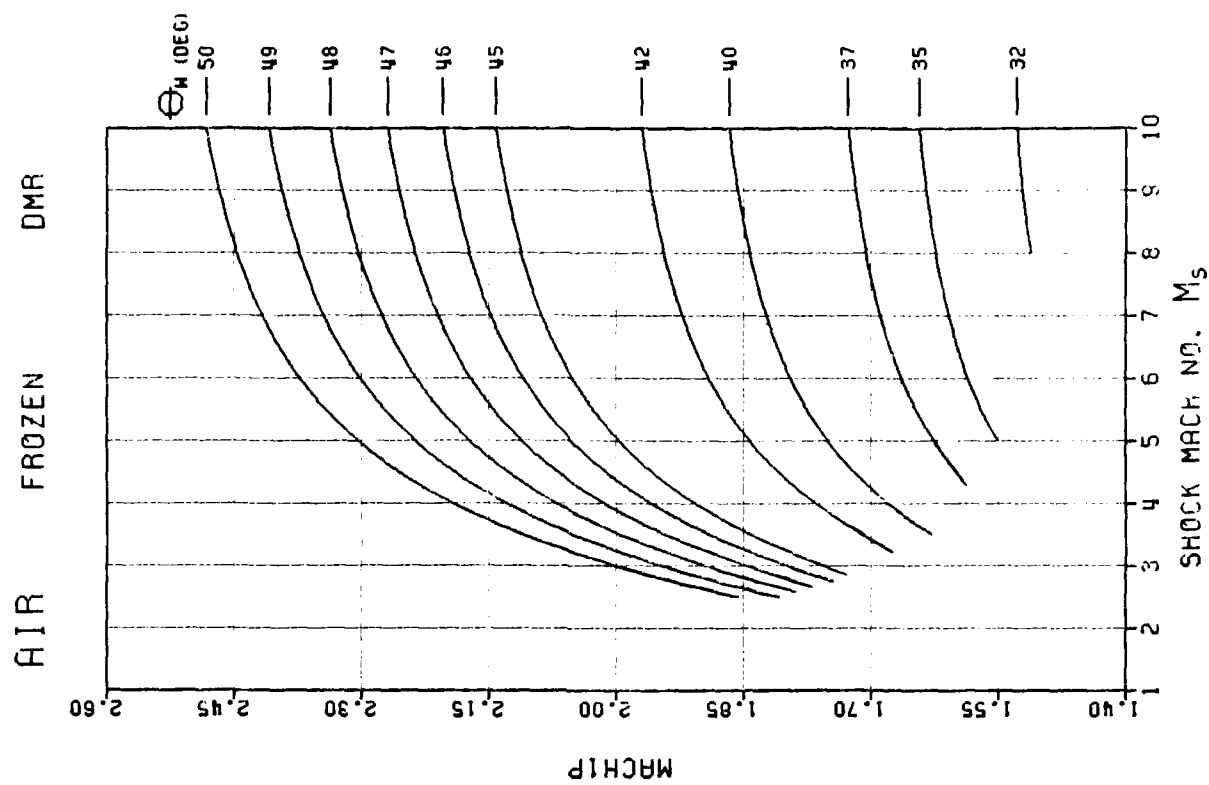
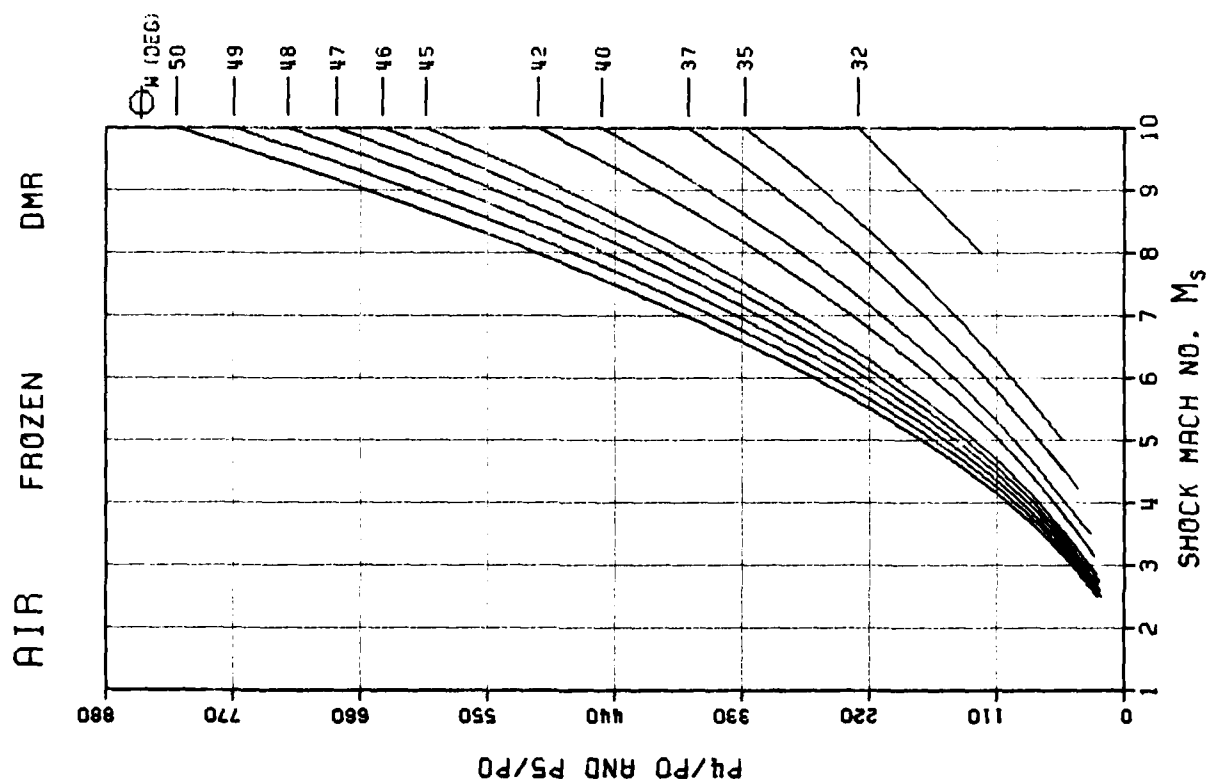


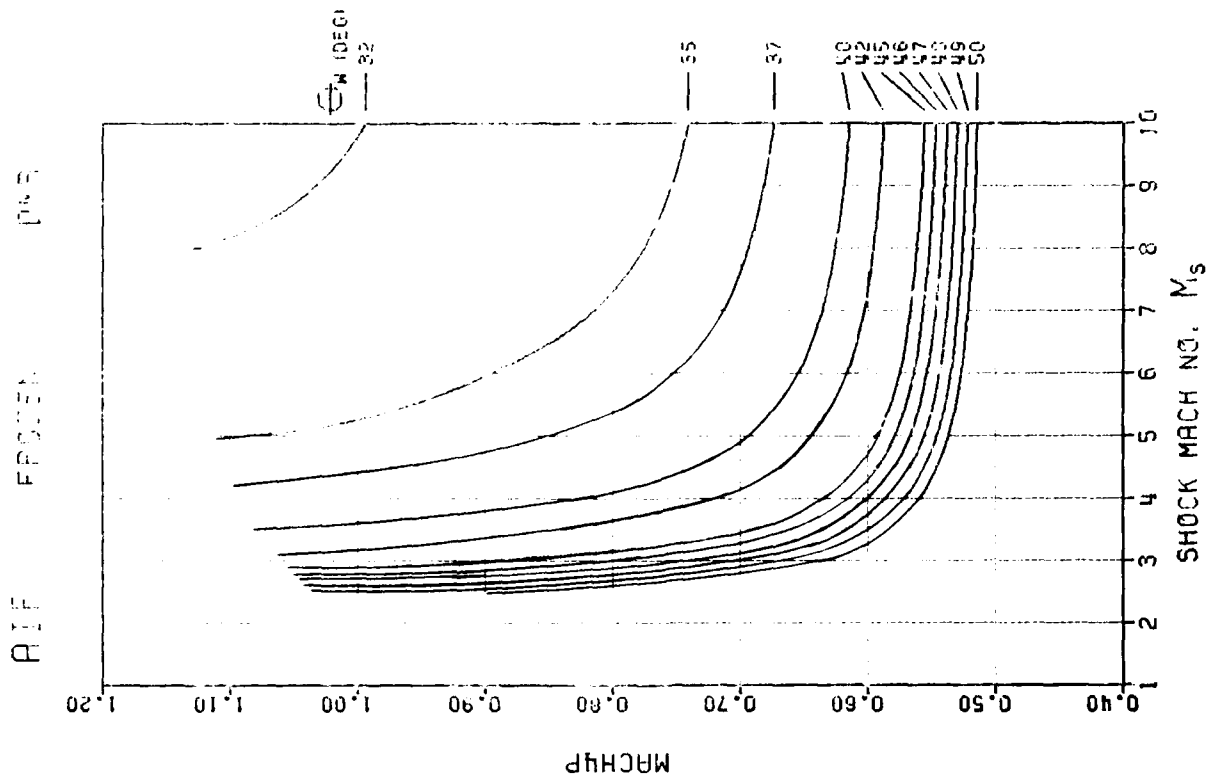
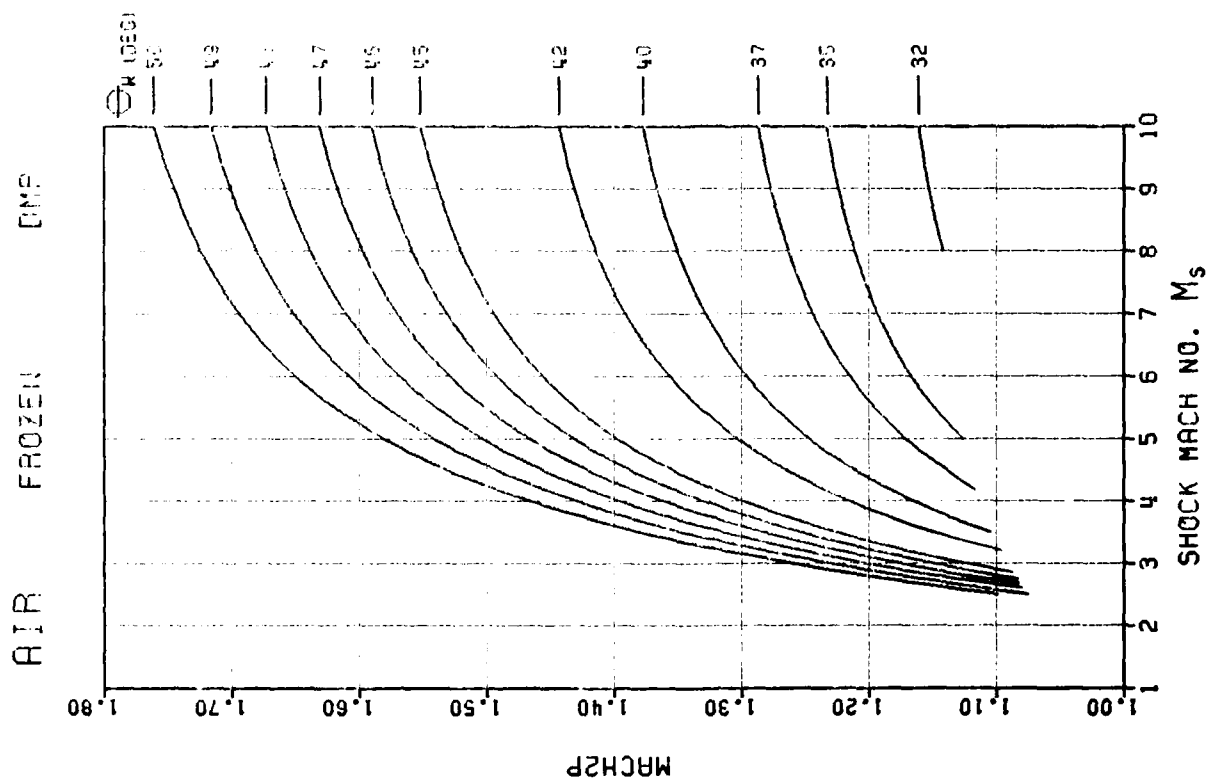


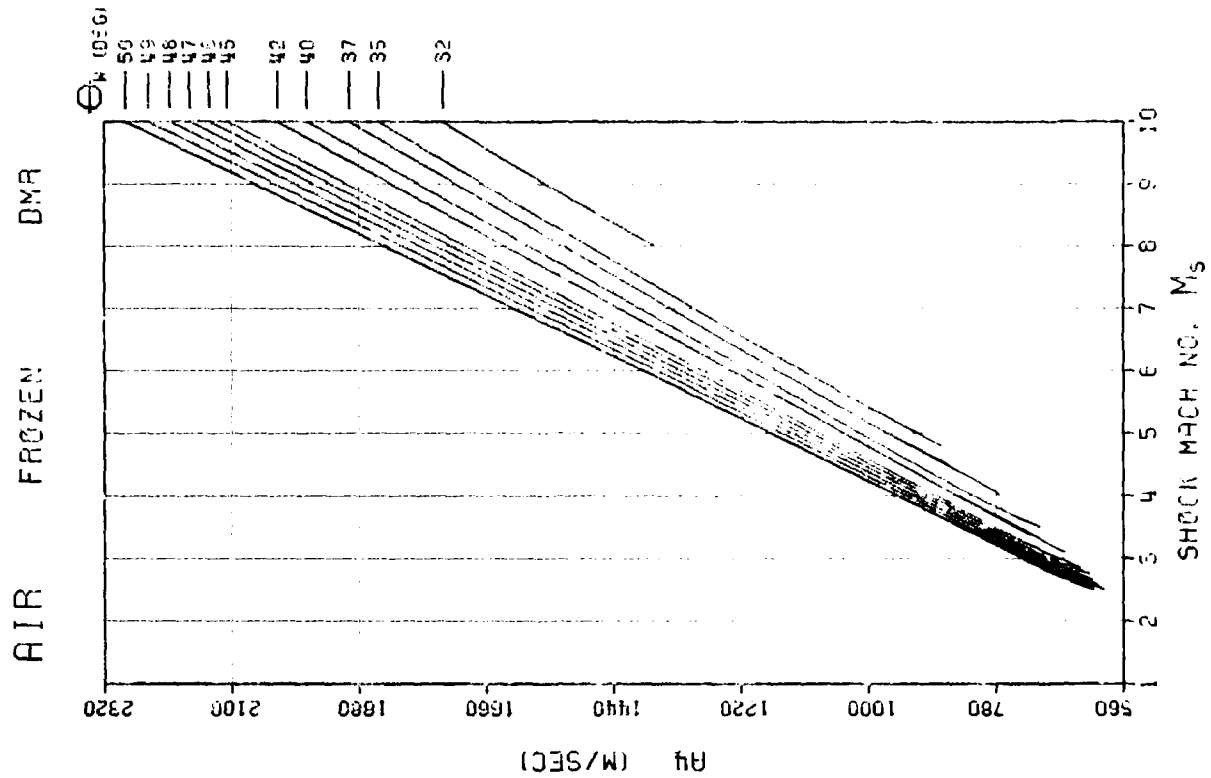
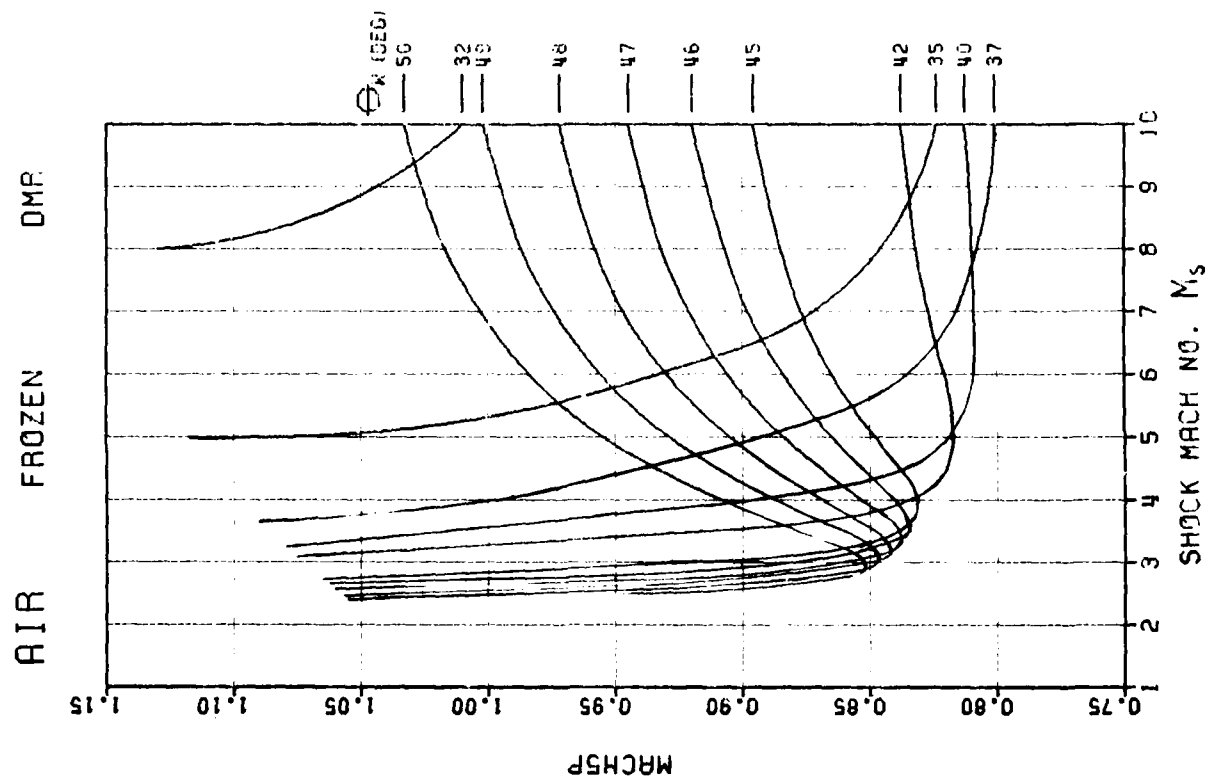


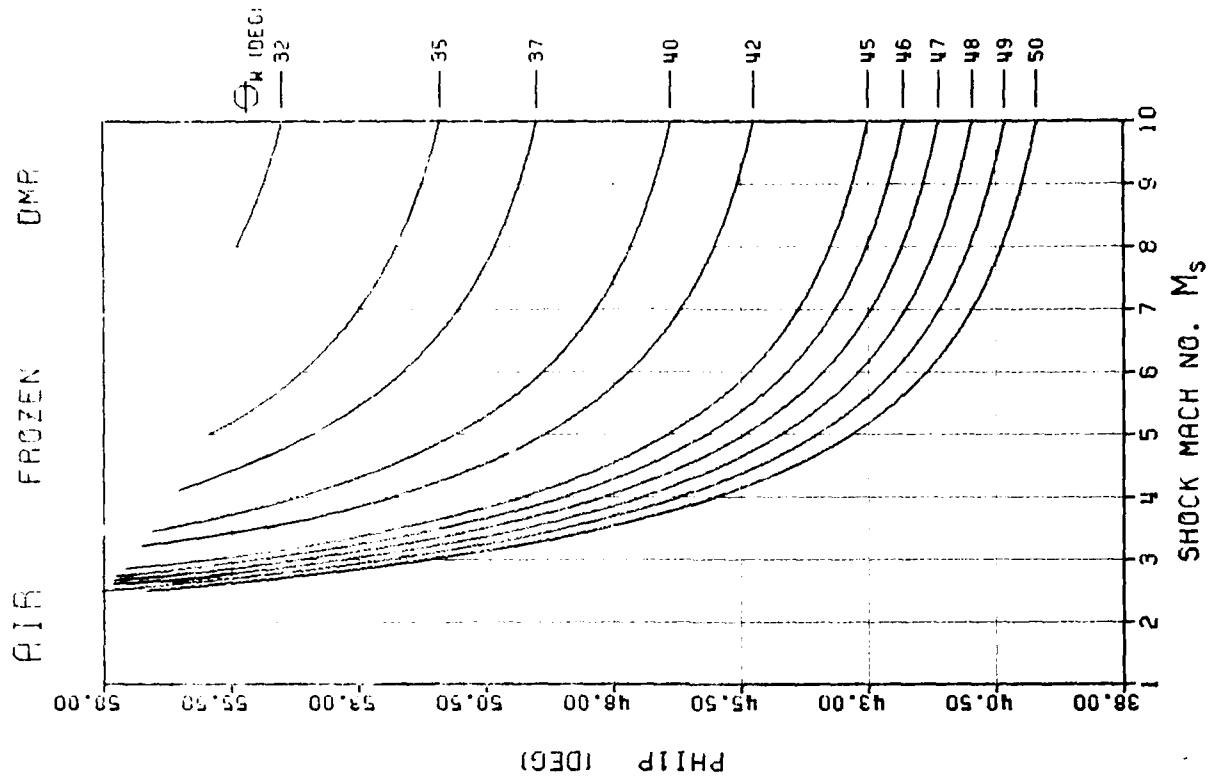
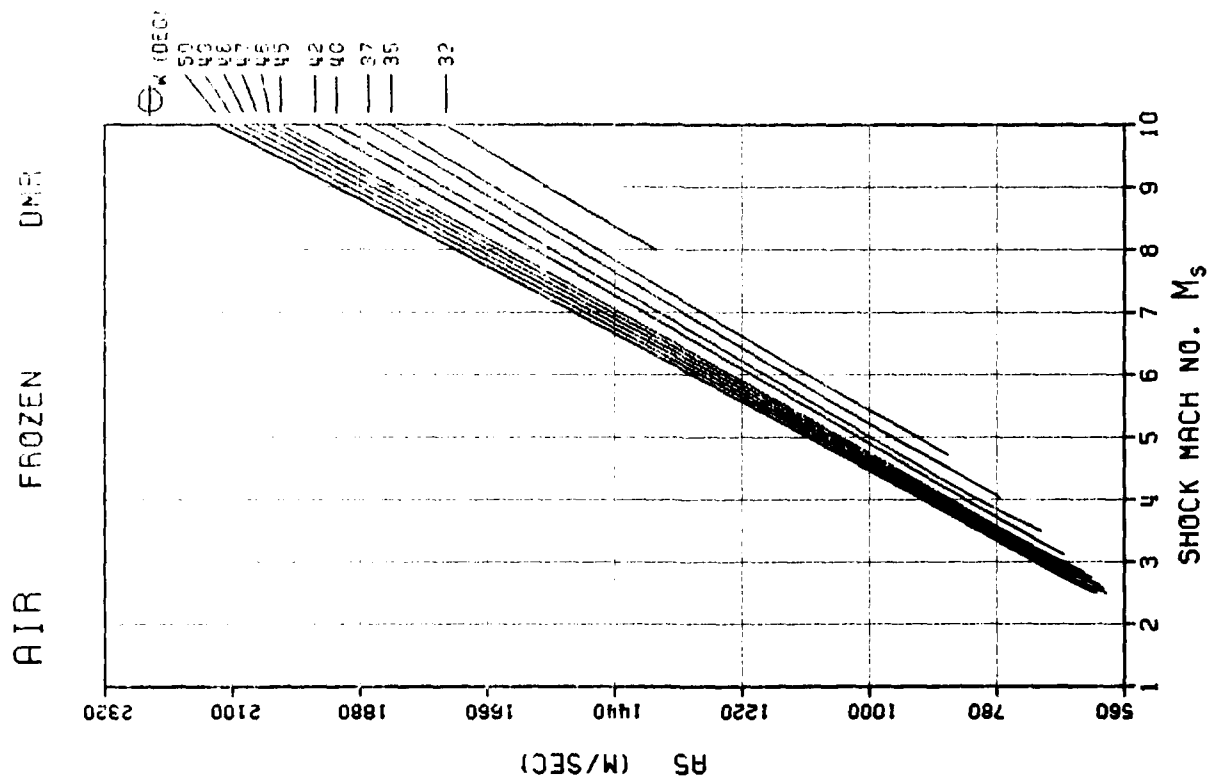


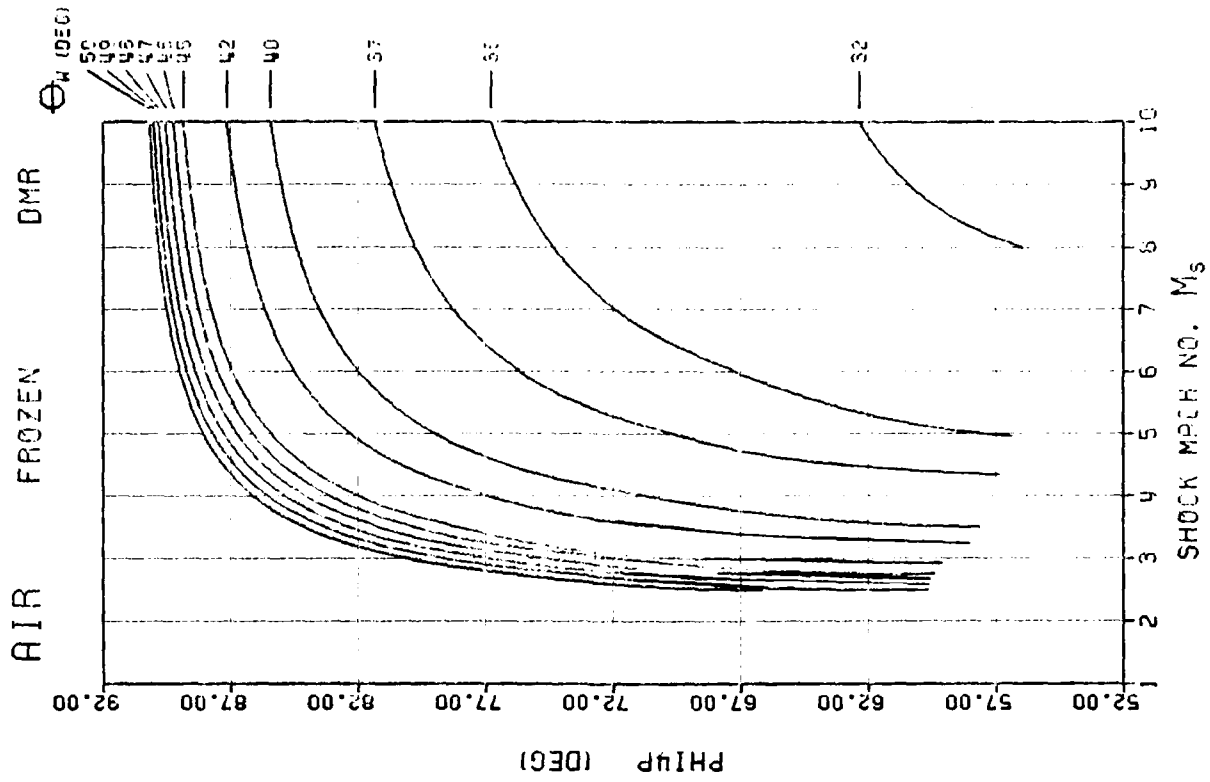
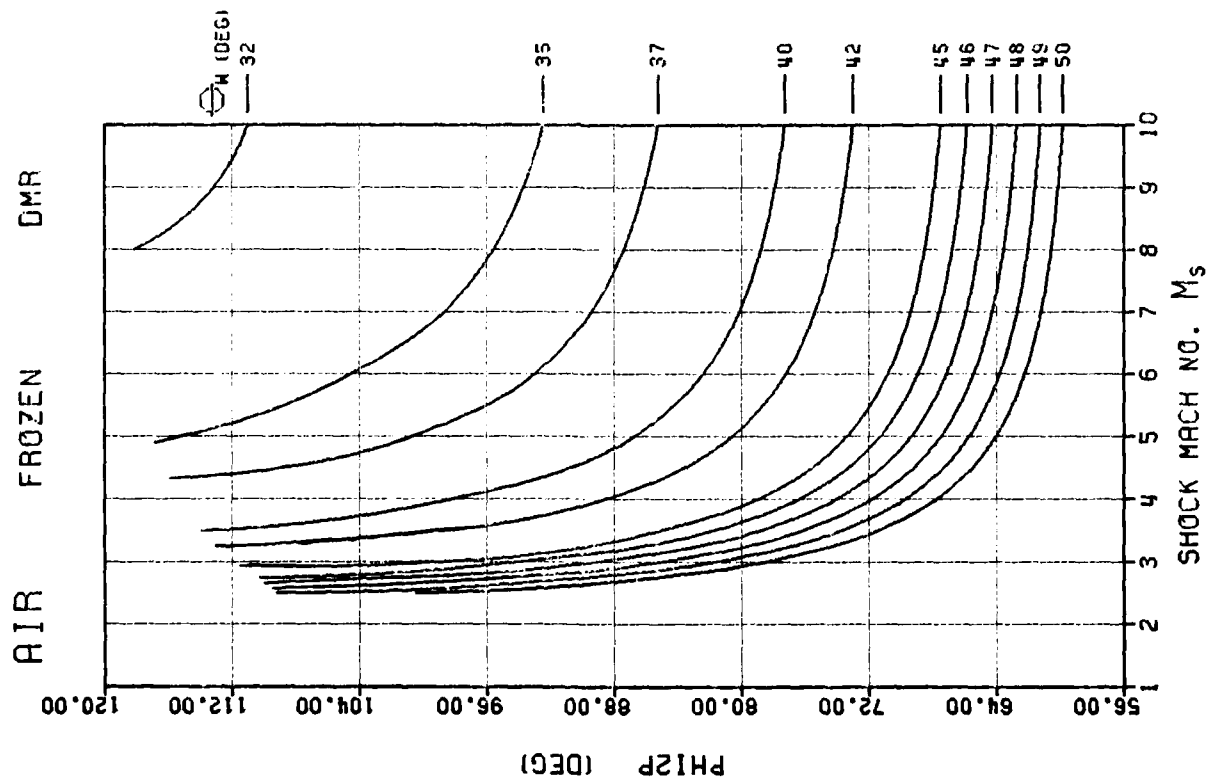


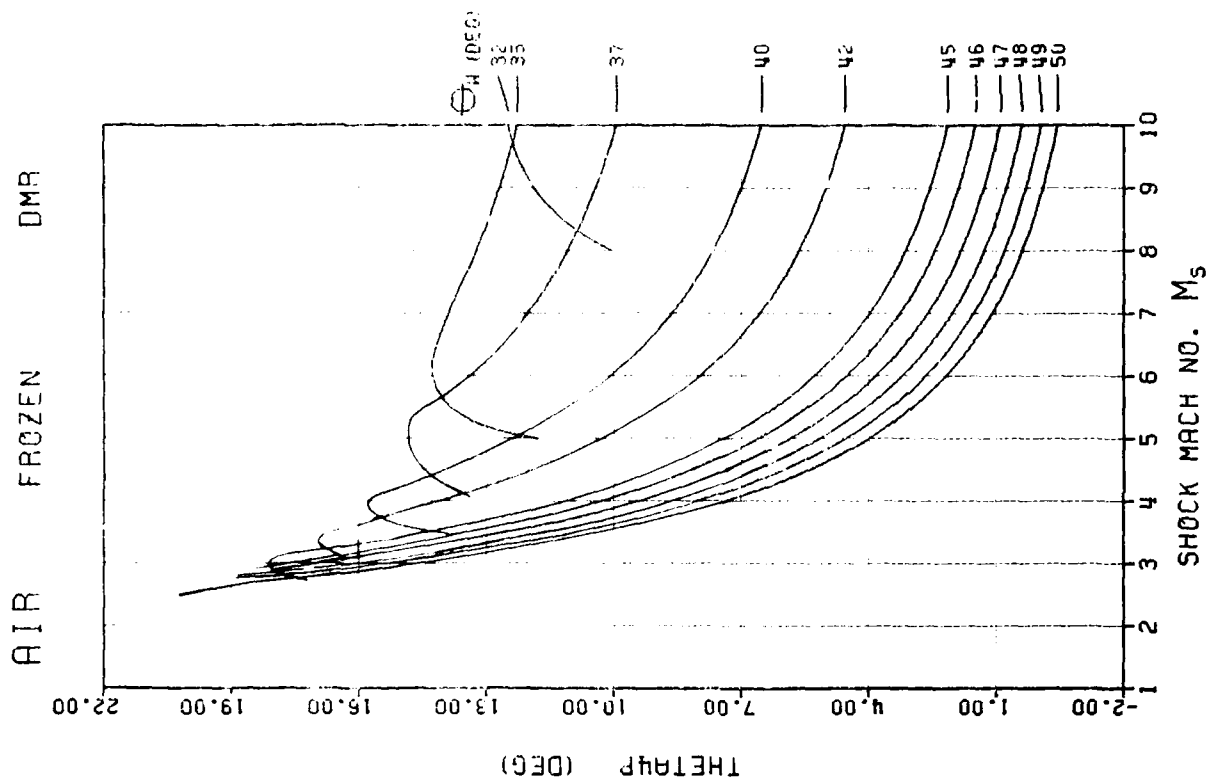
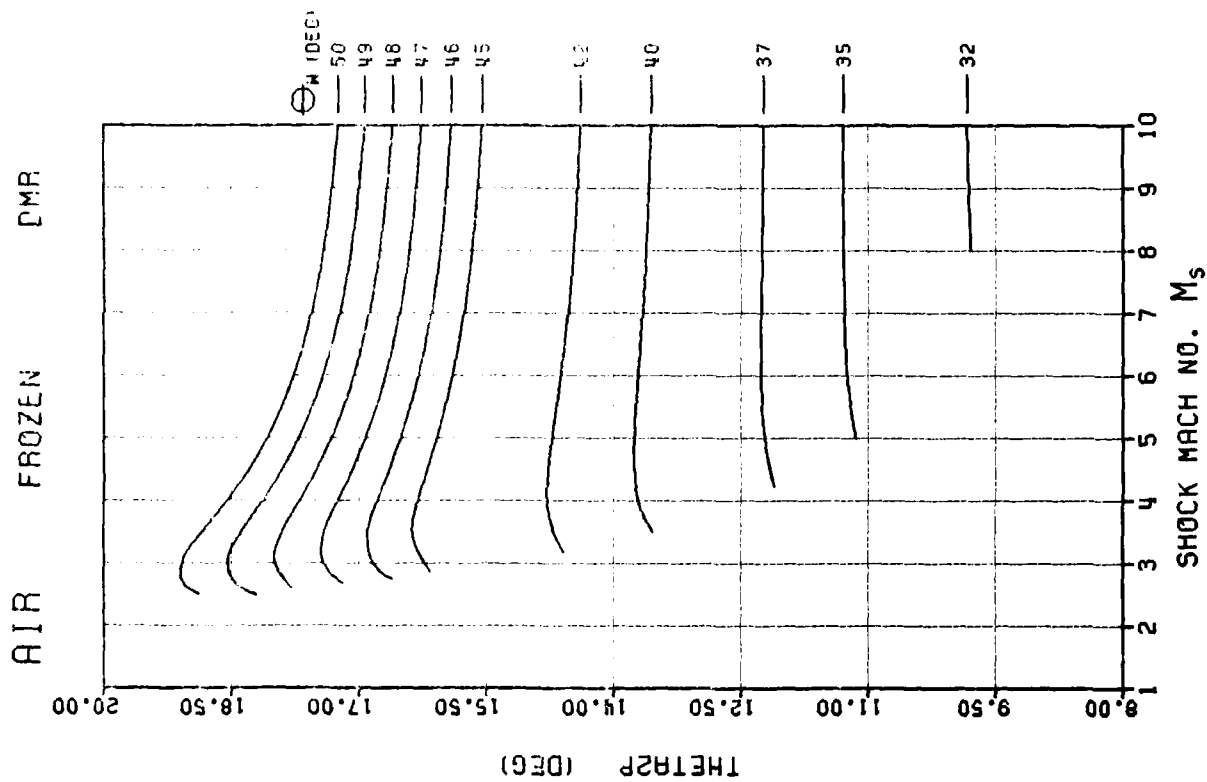


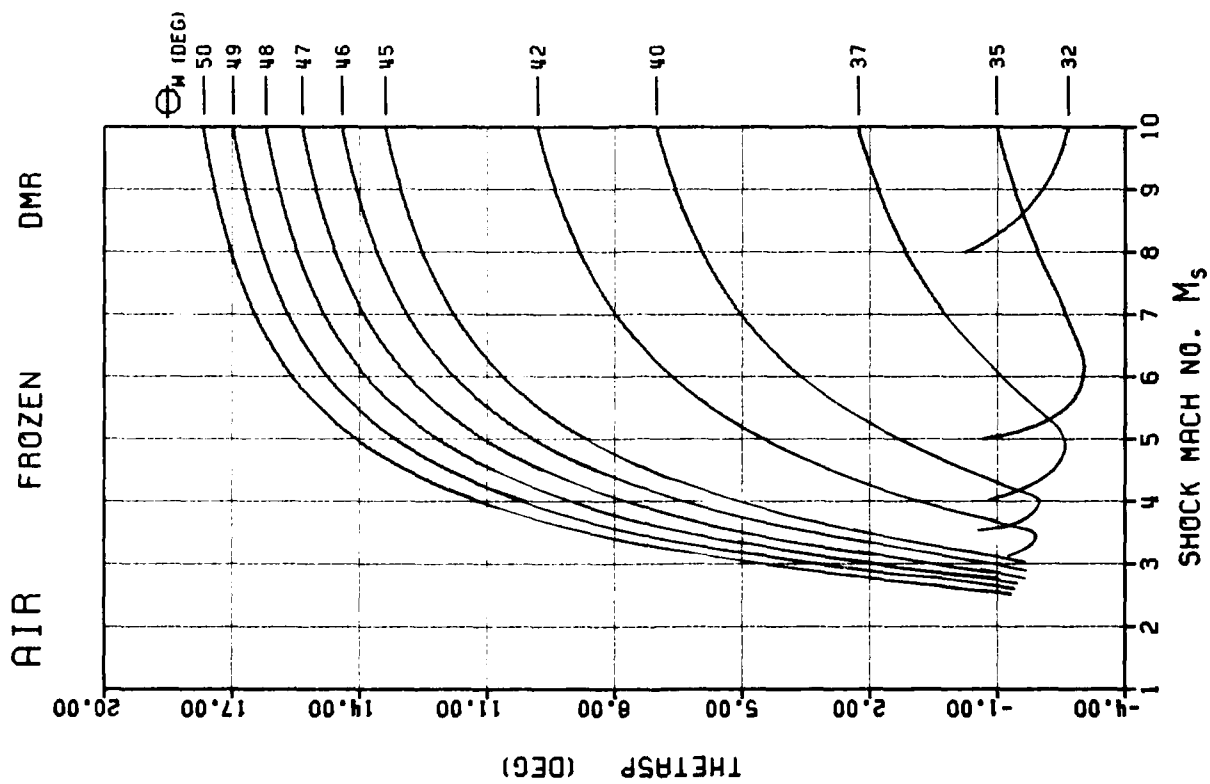
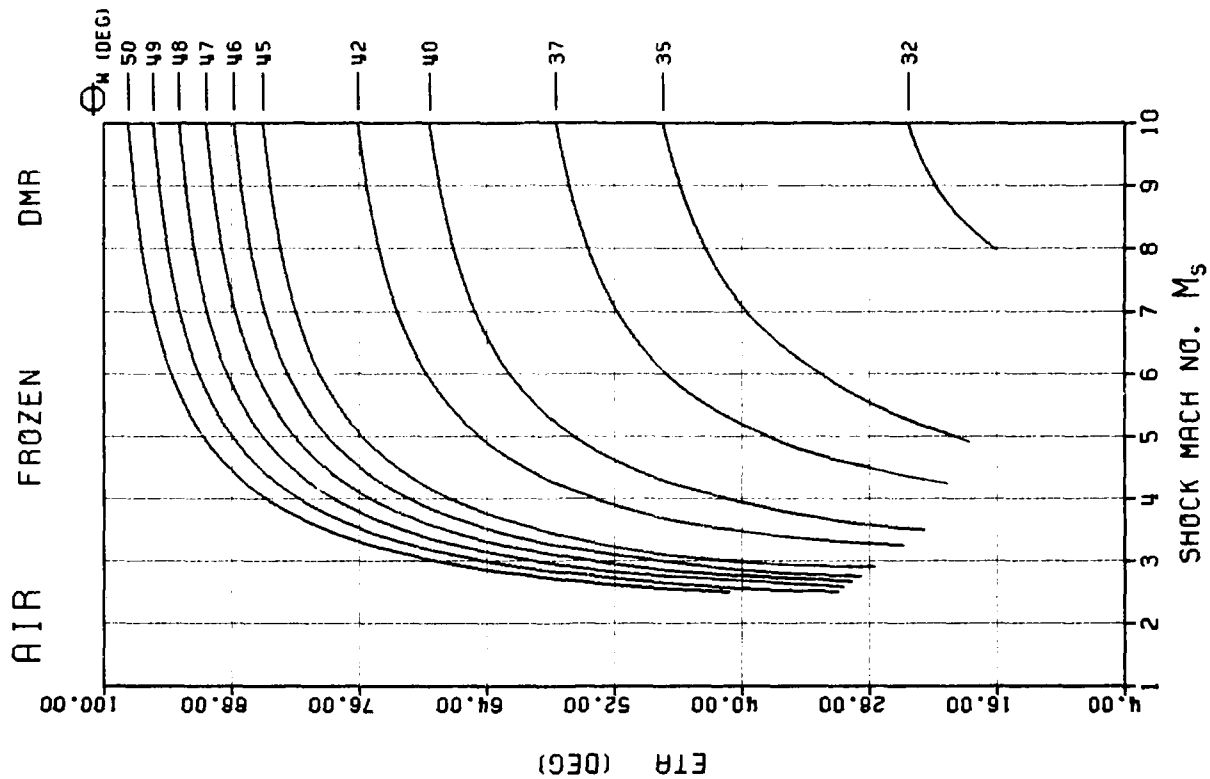


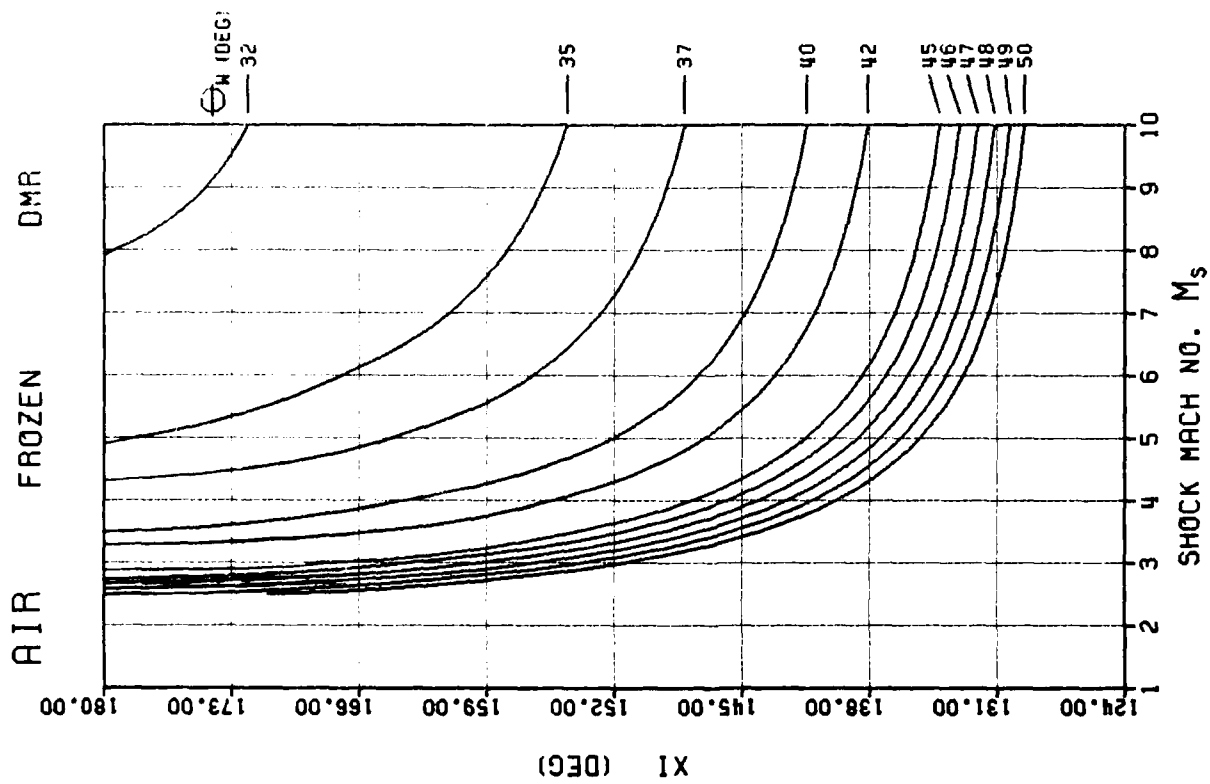




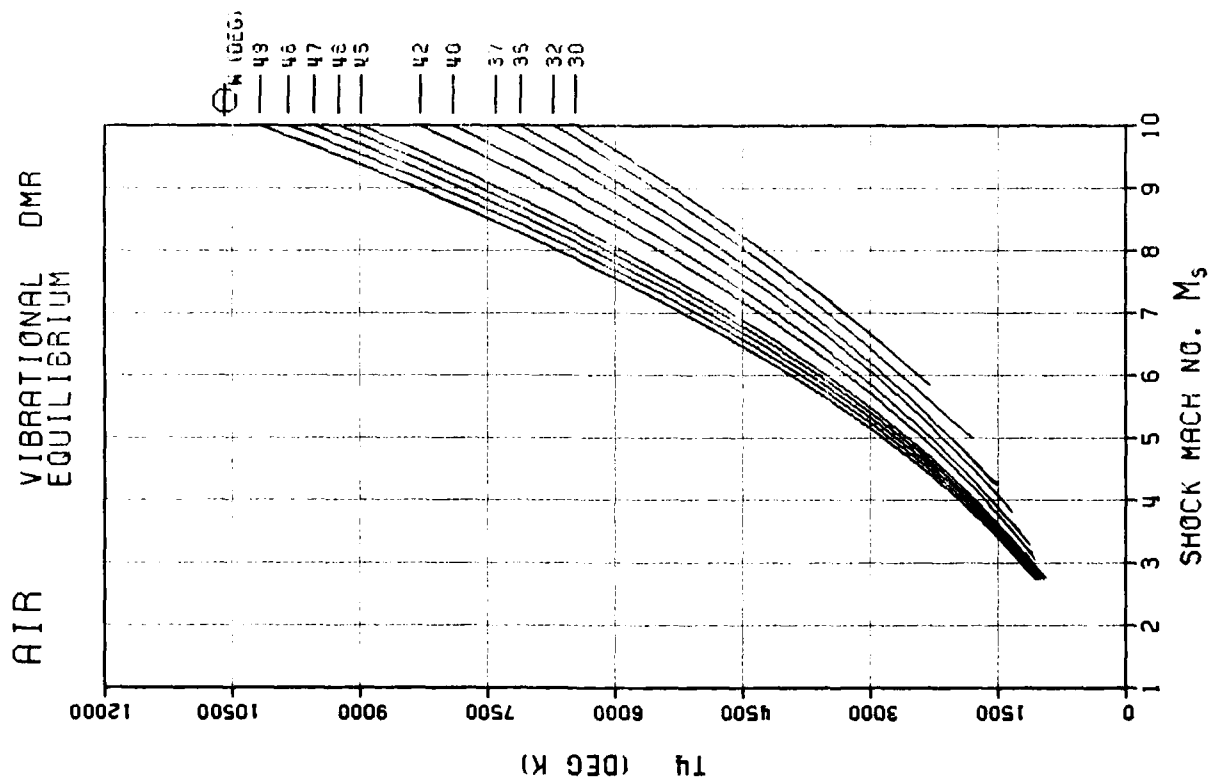
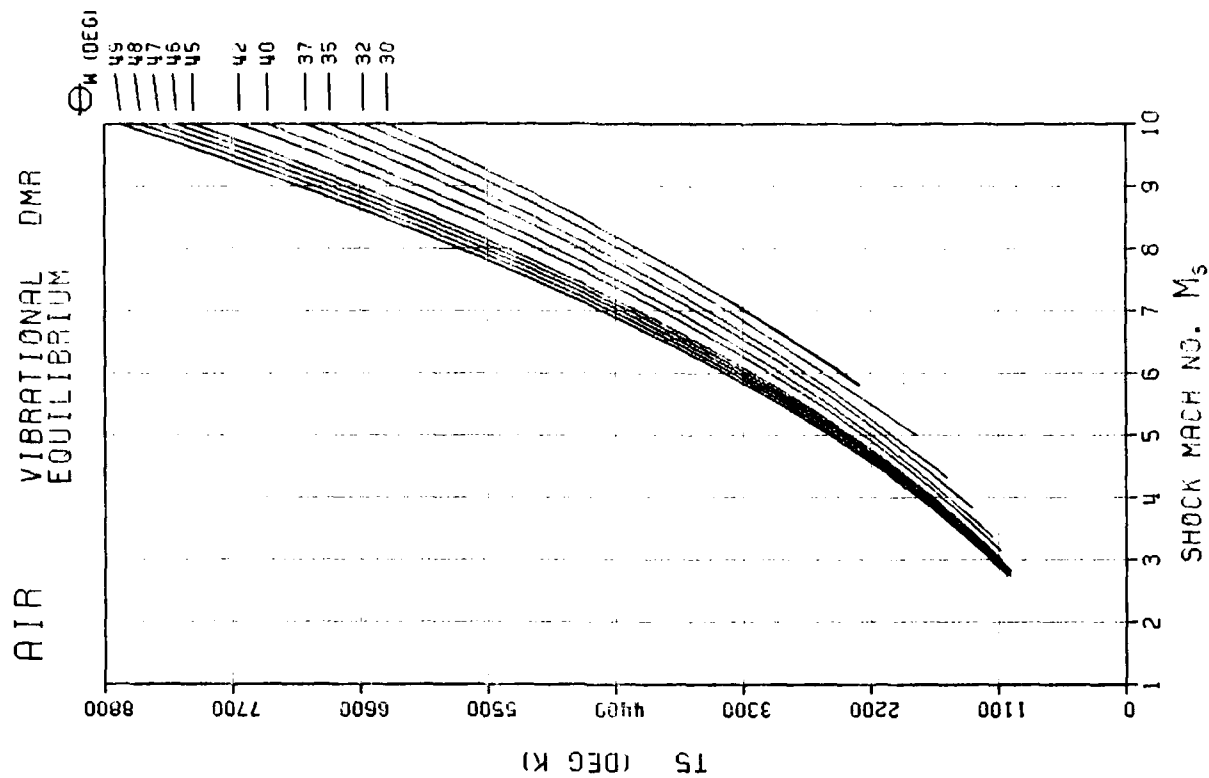


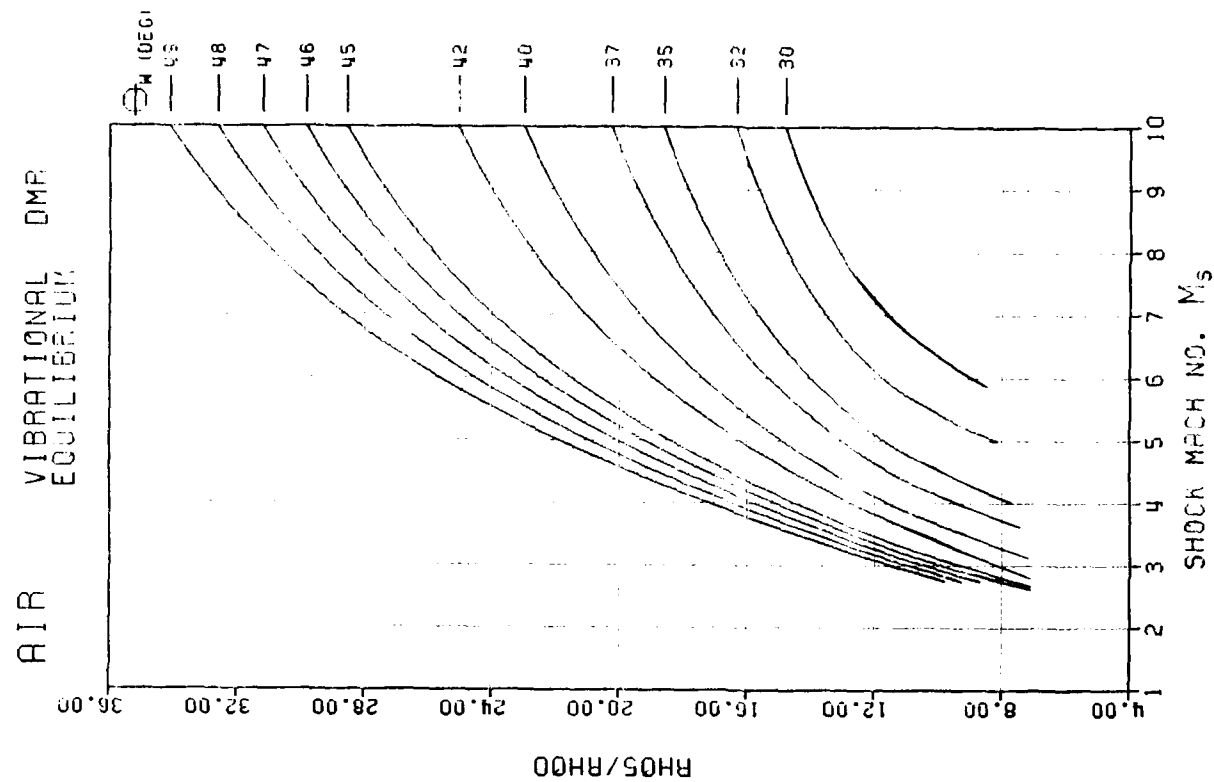
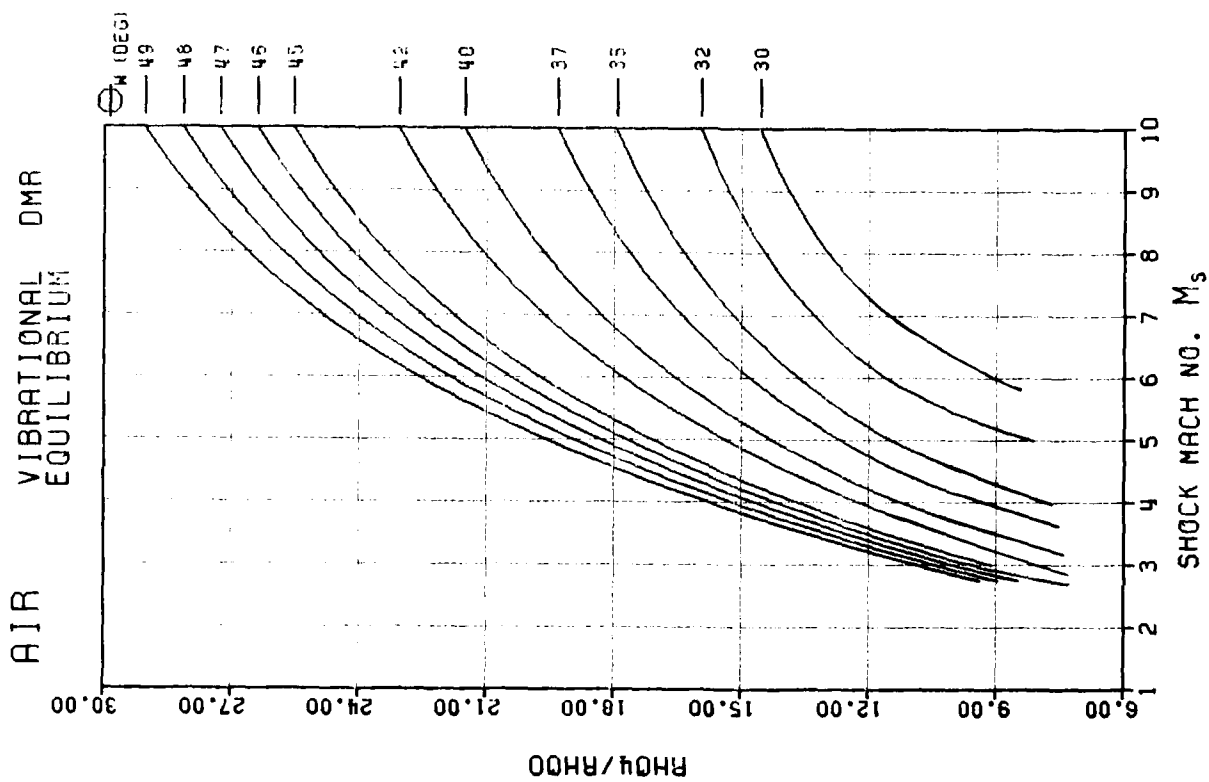


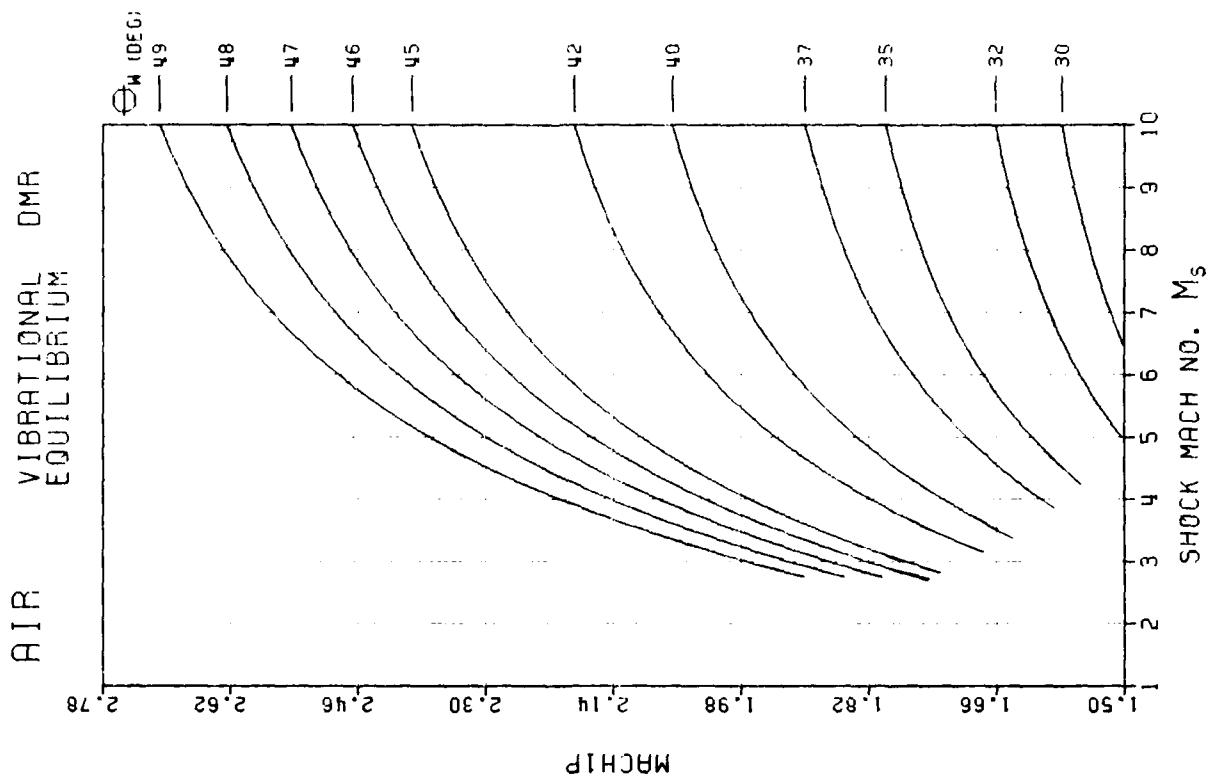
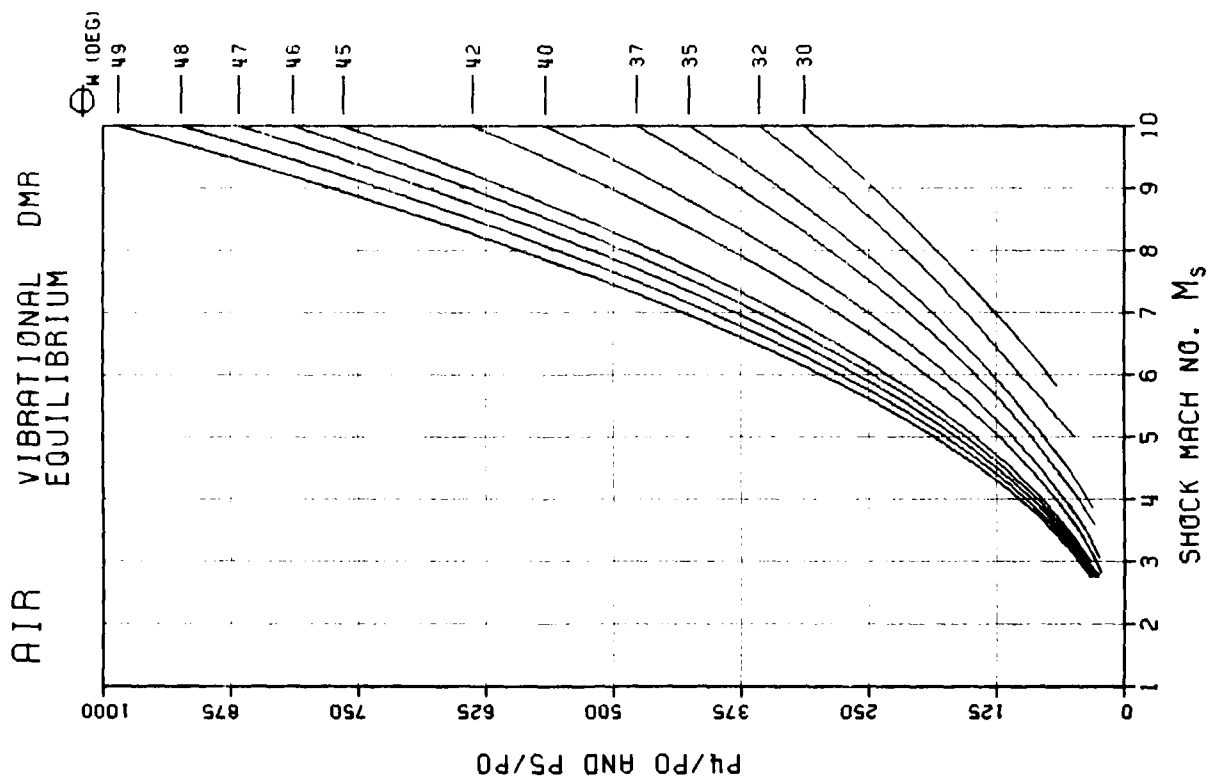


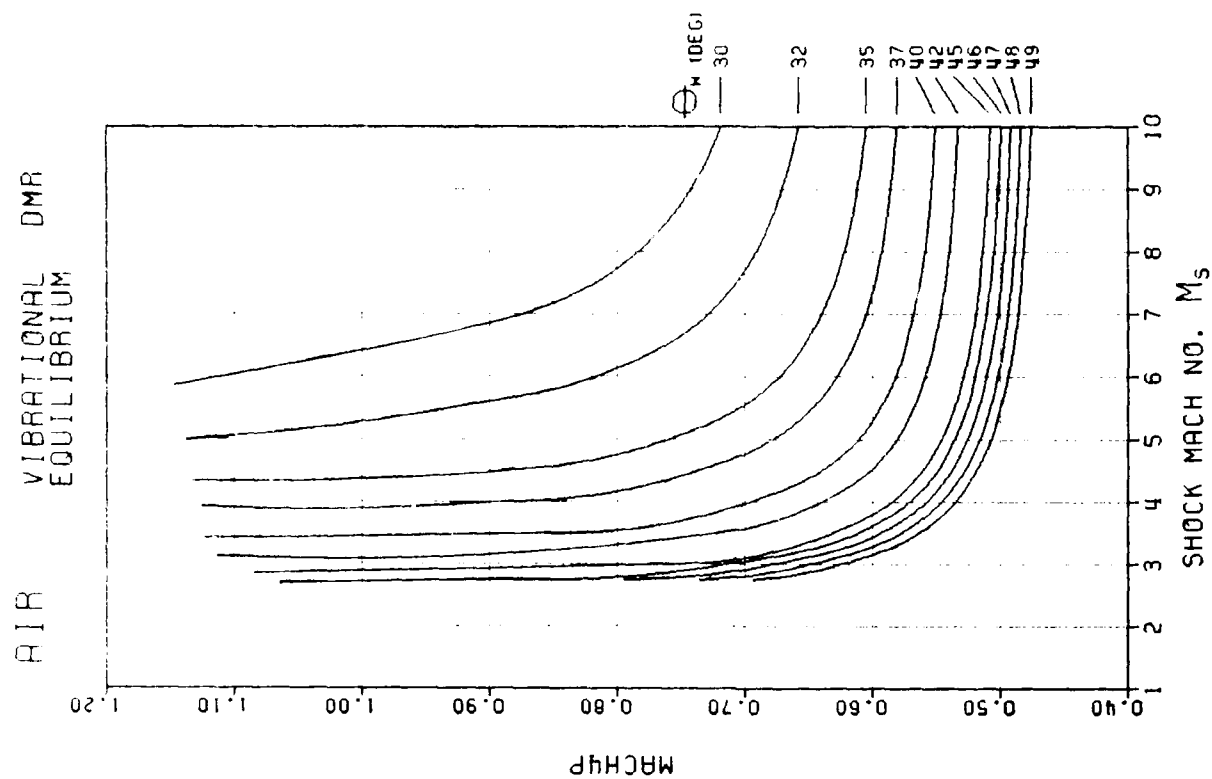
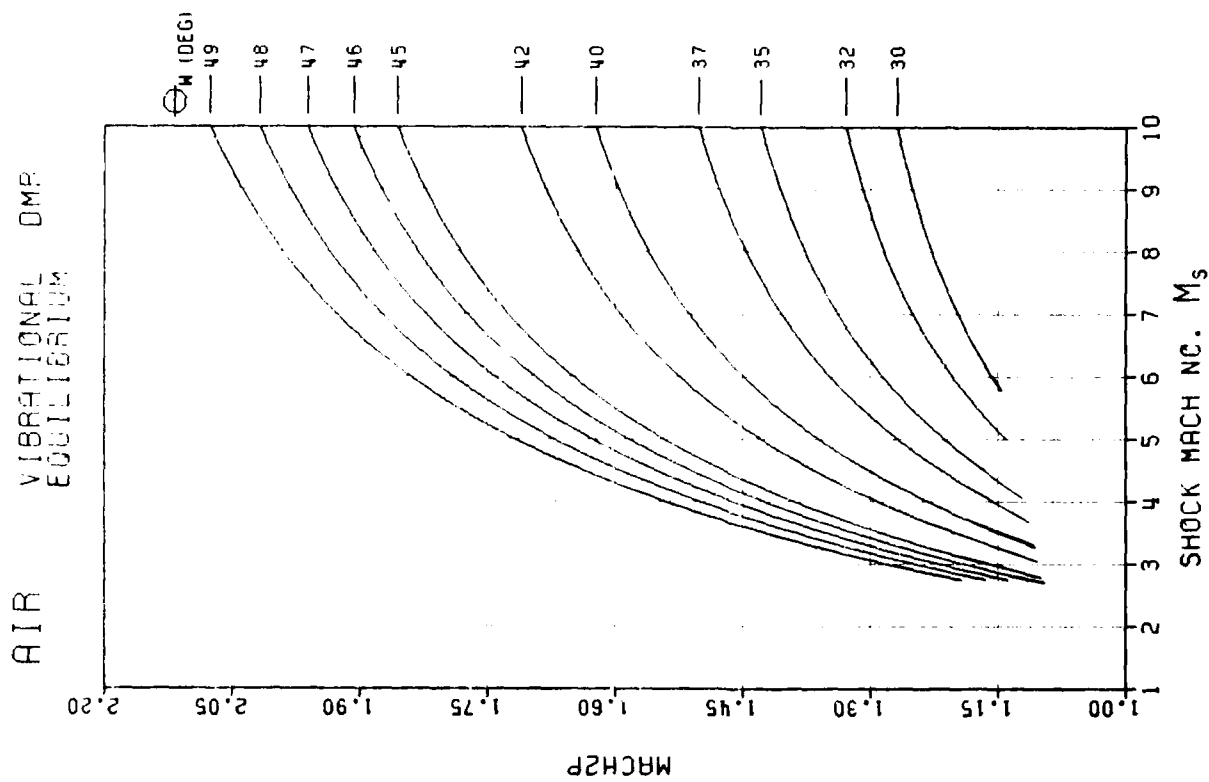


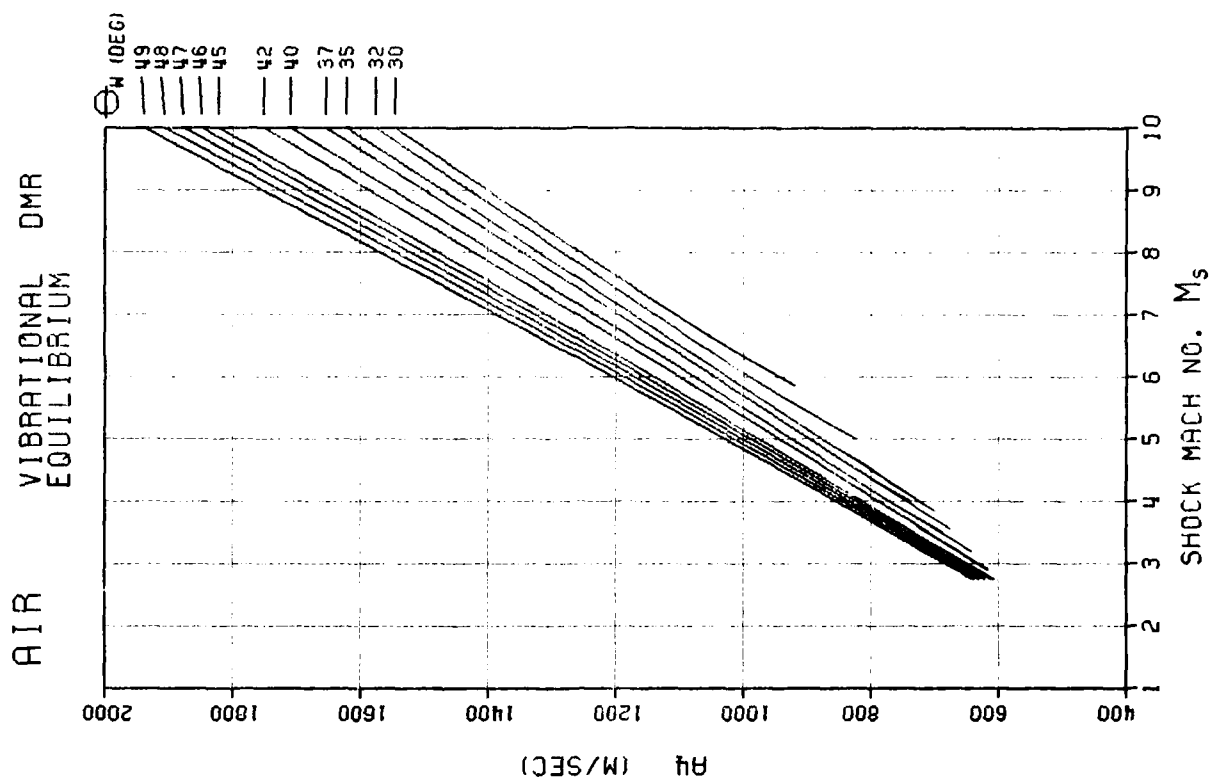
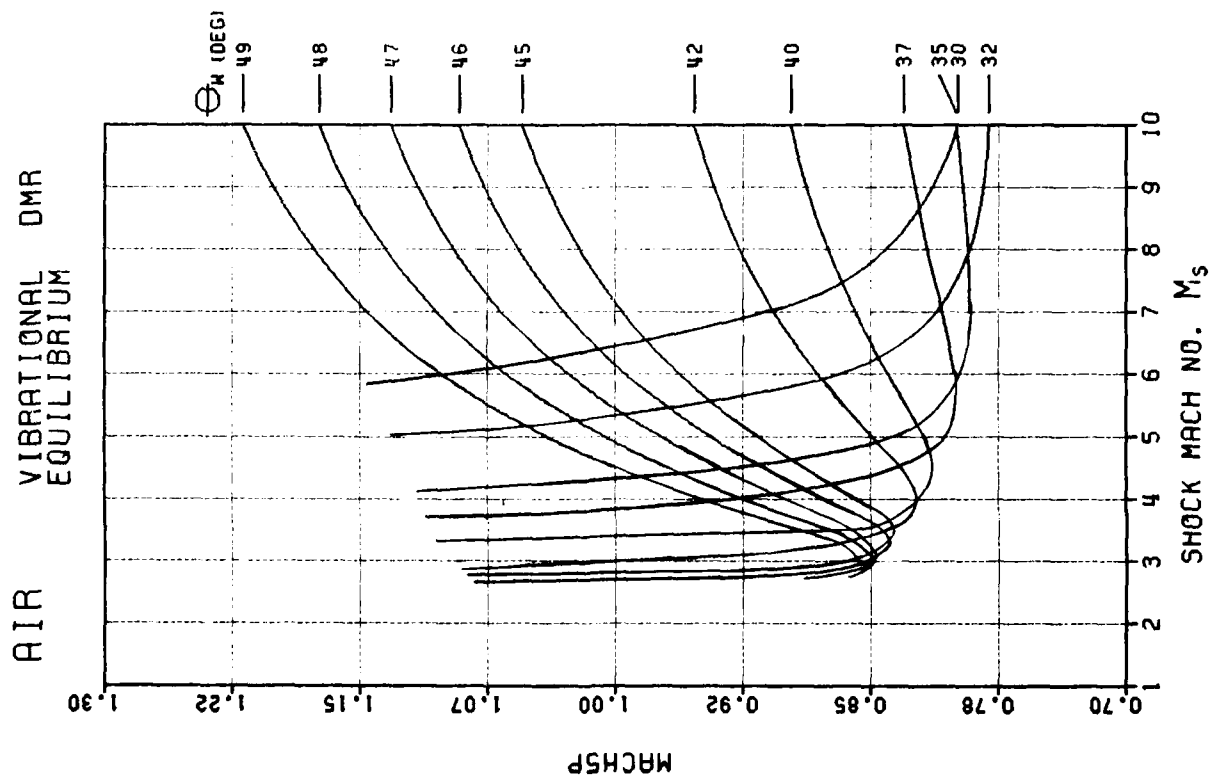
F - 260

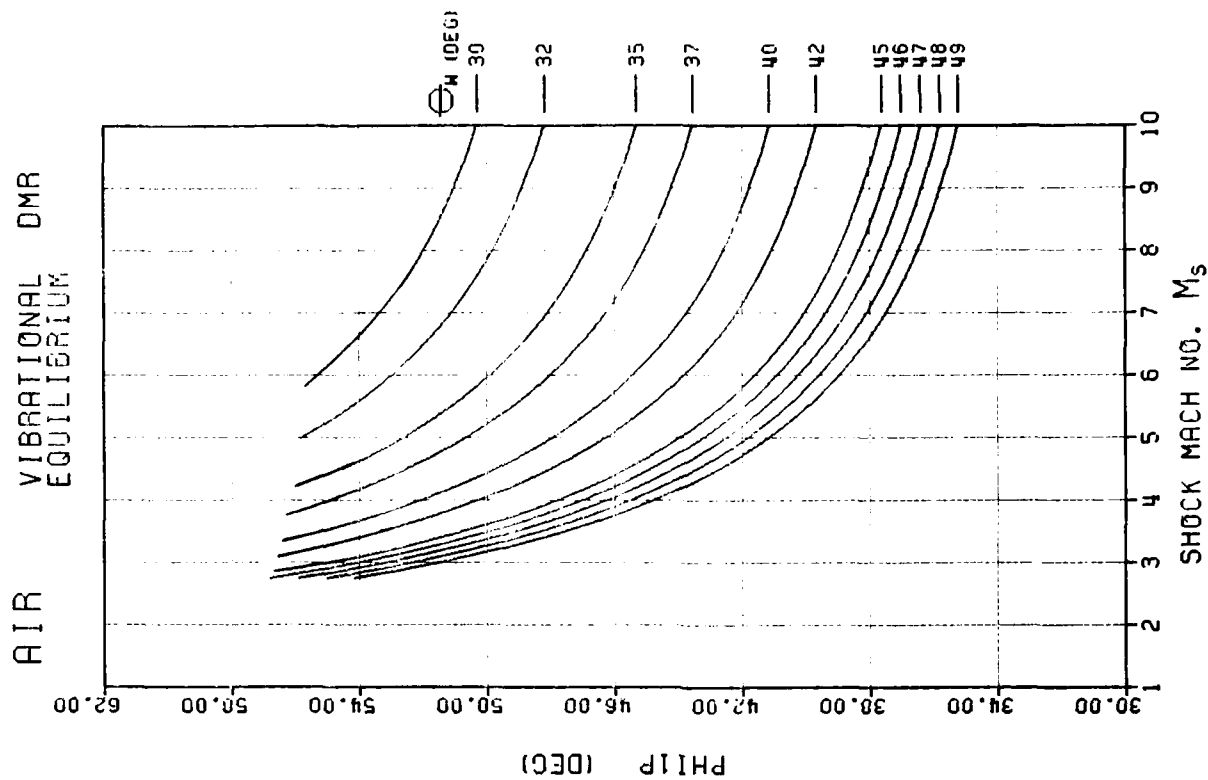
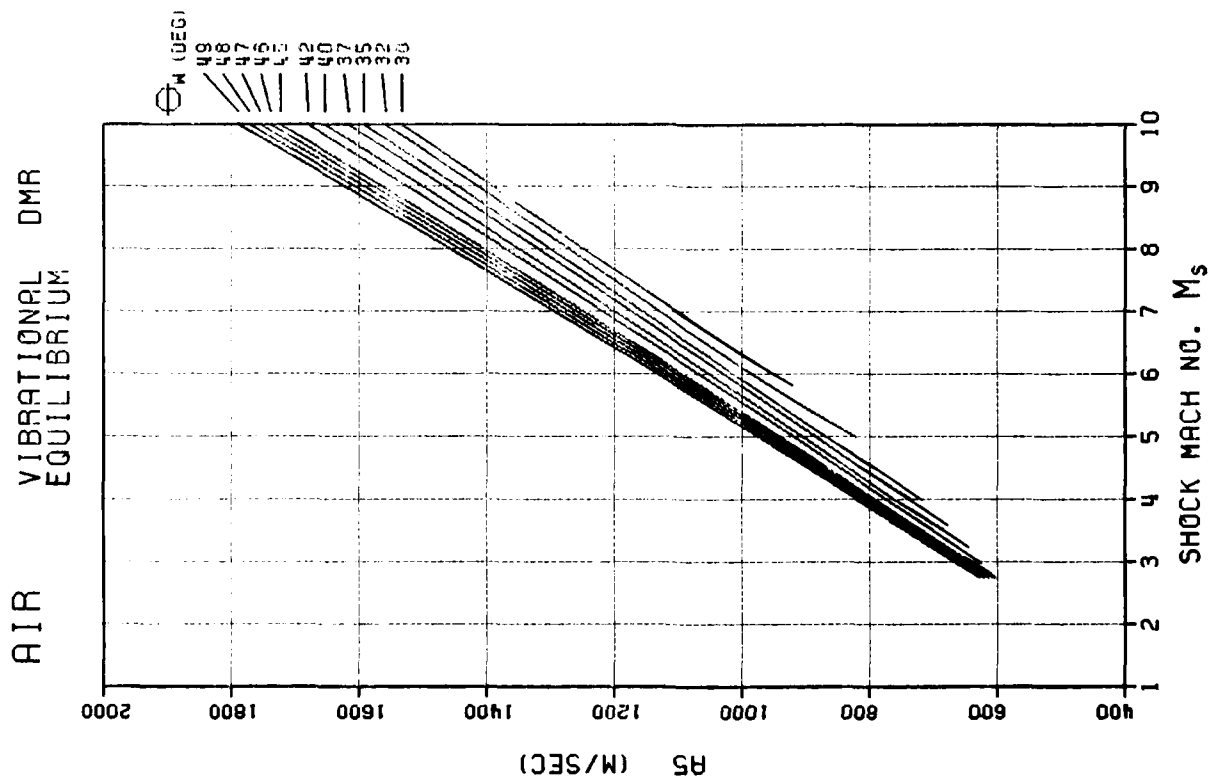


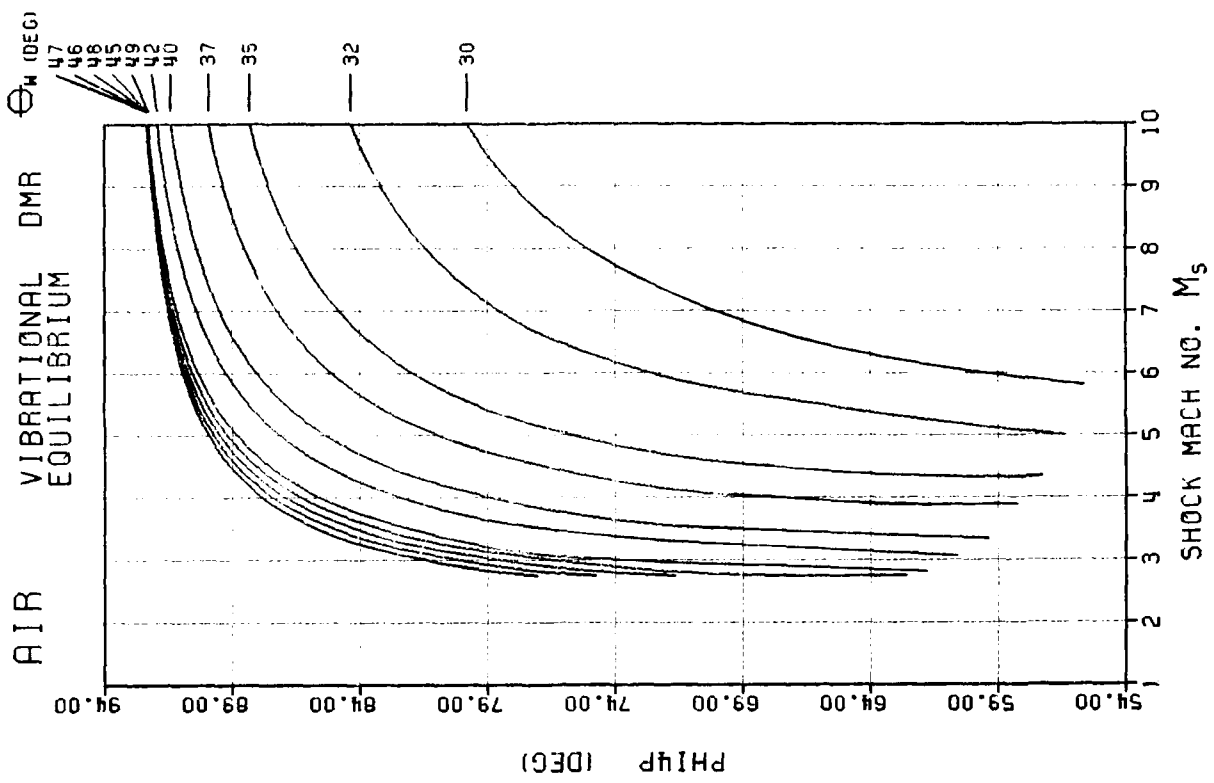
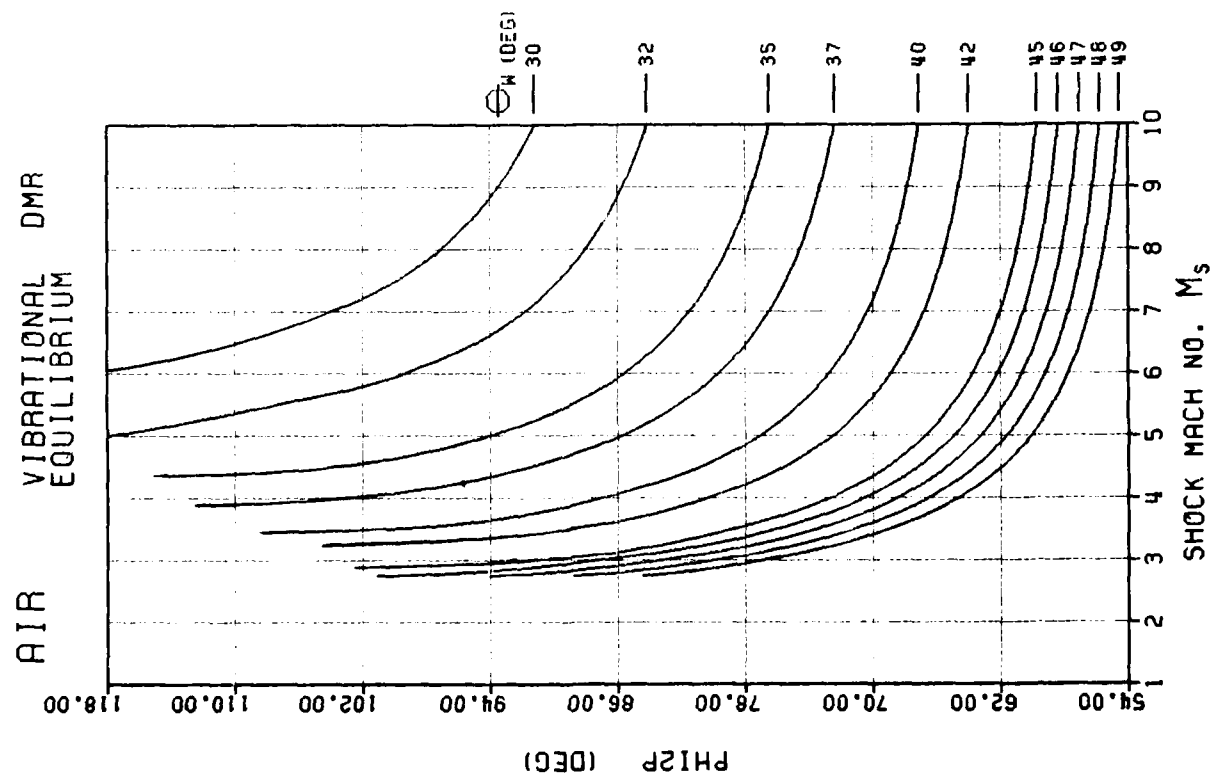


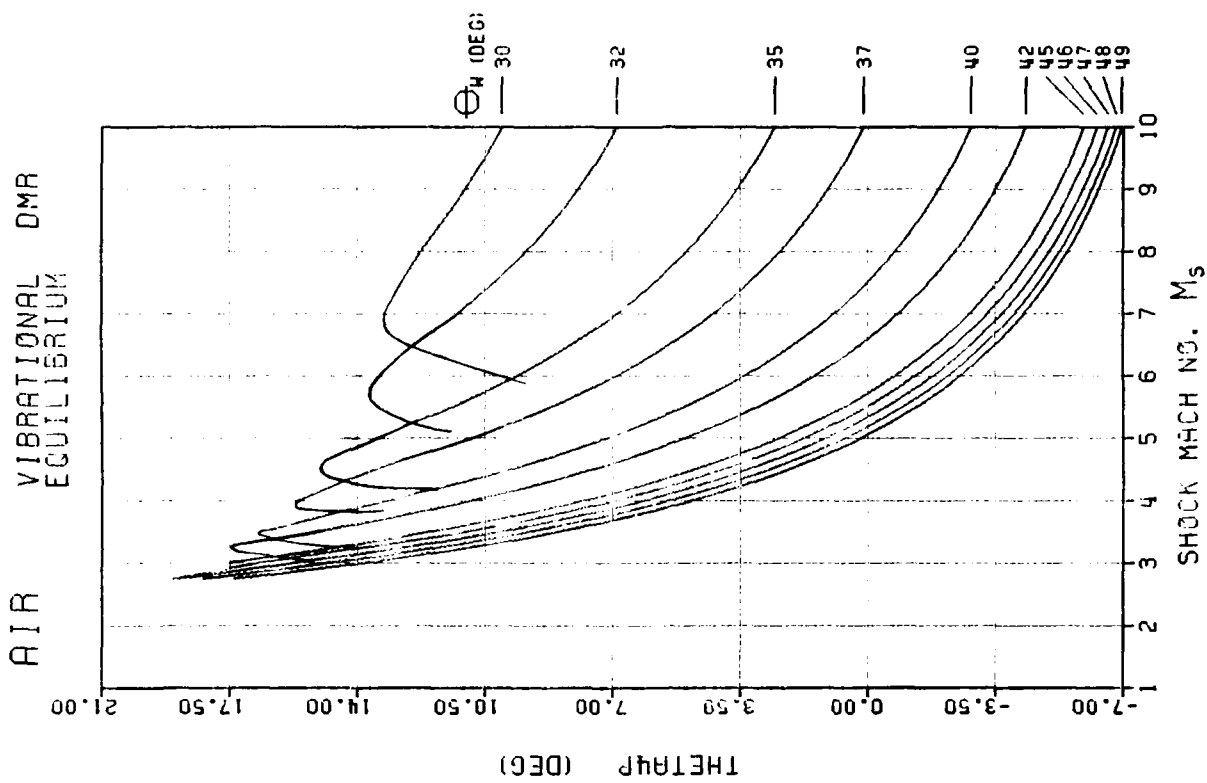
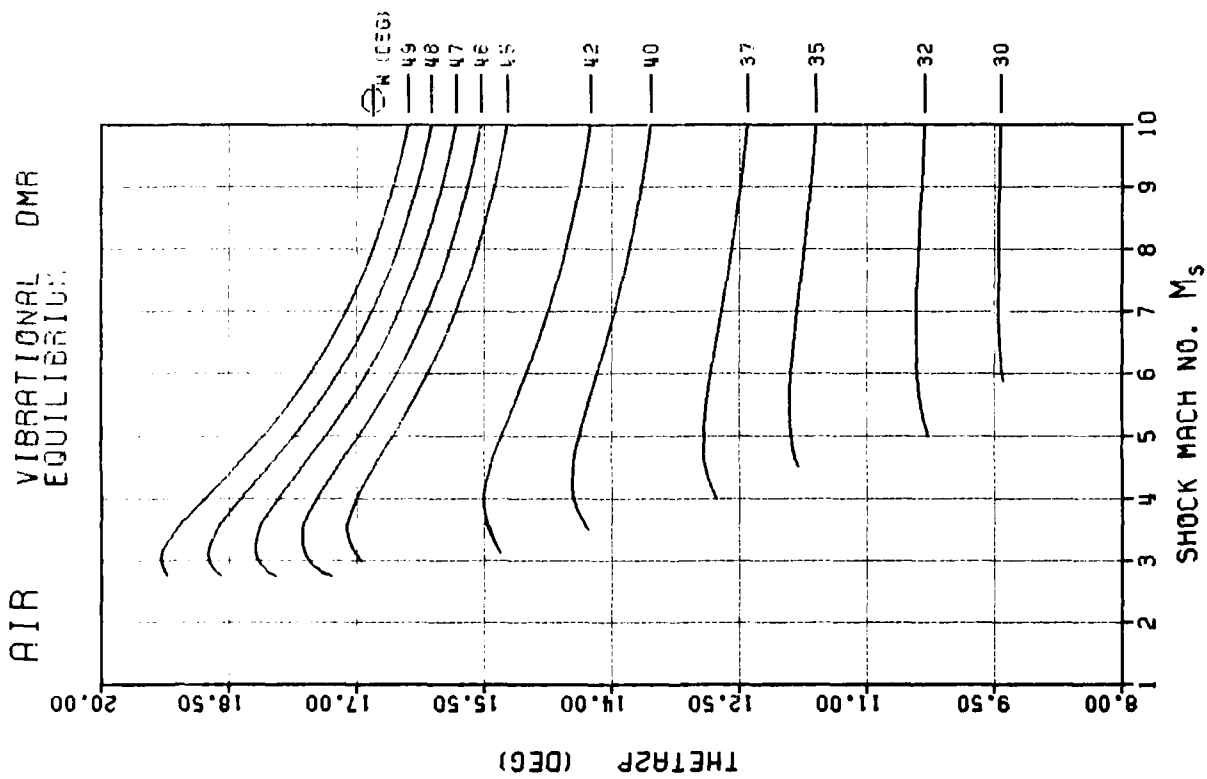


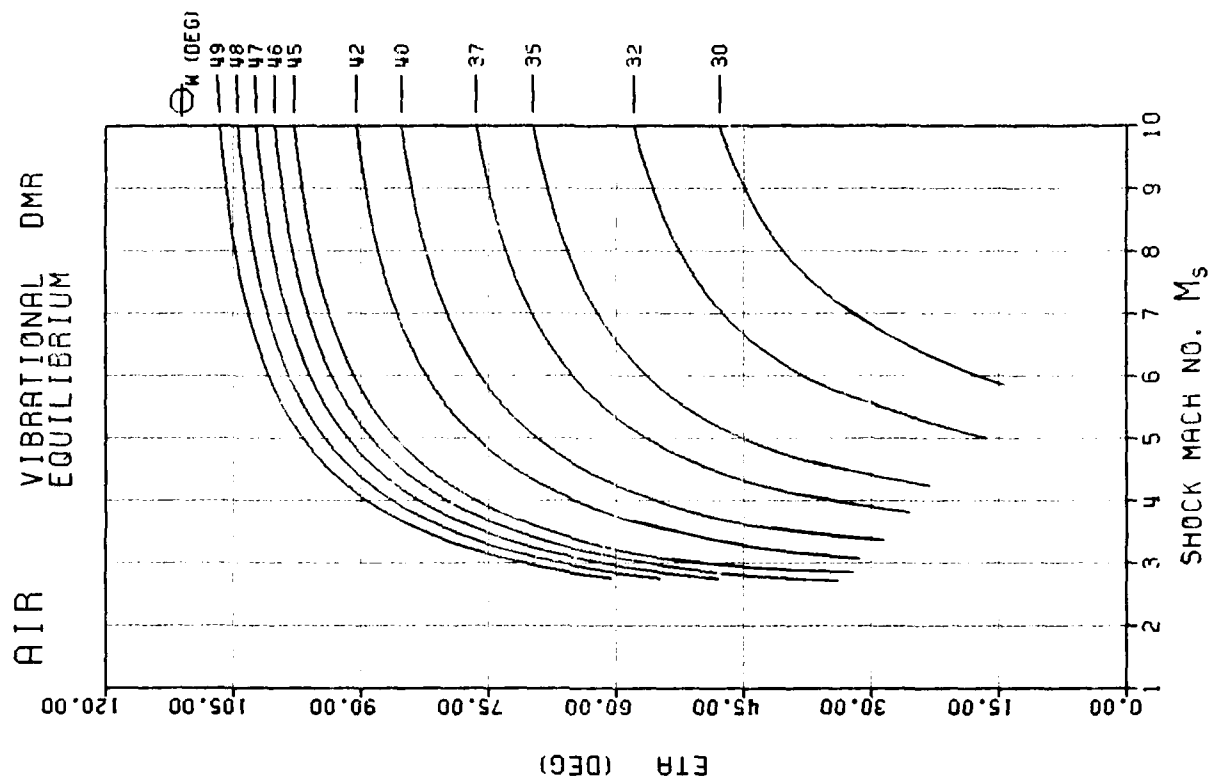
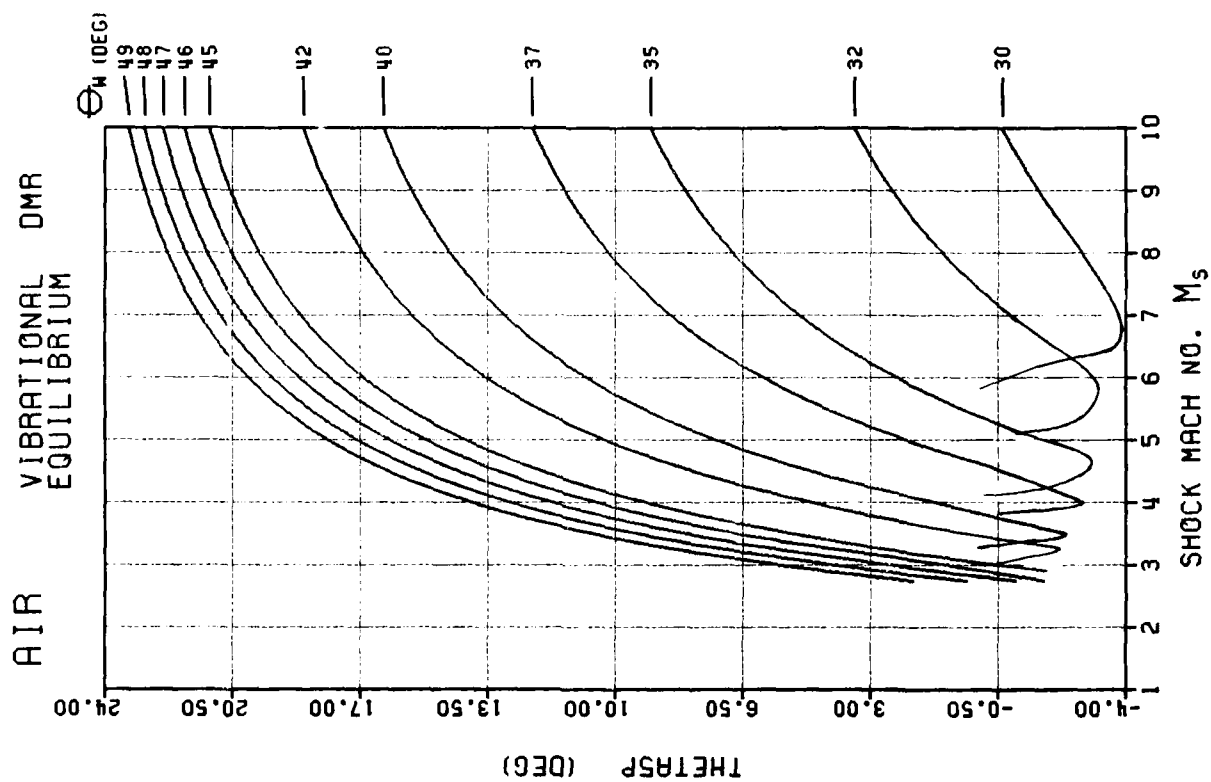


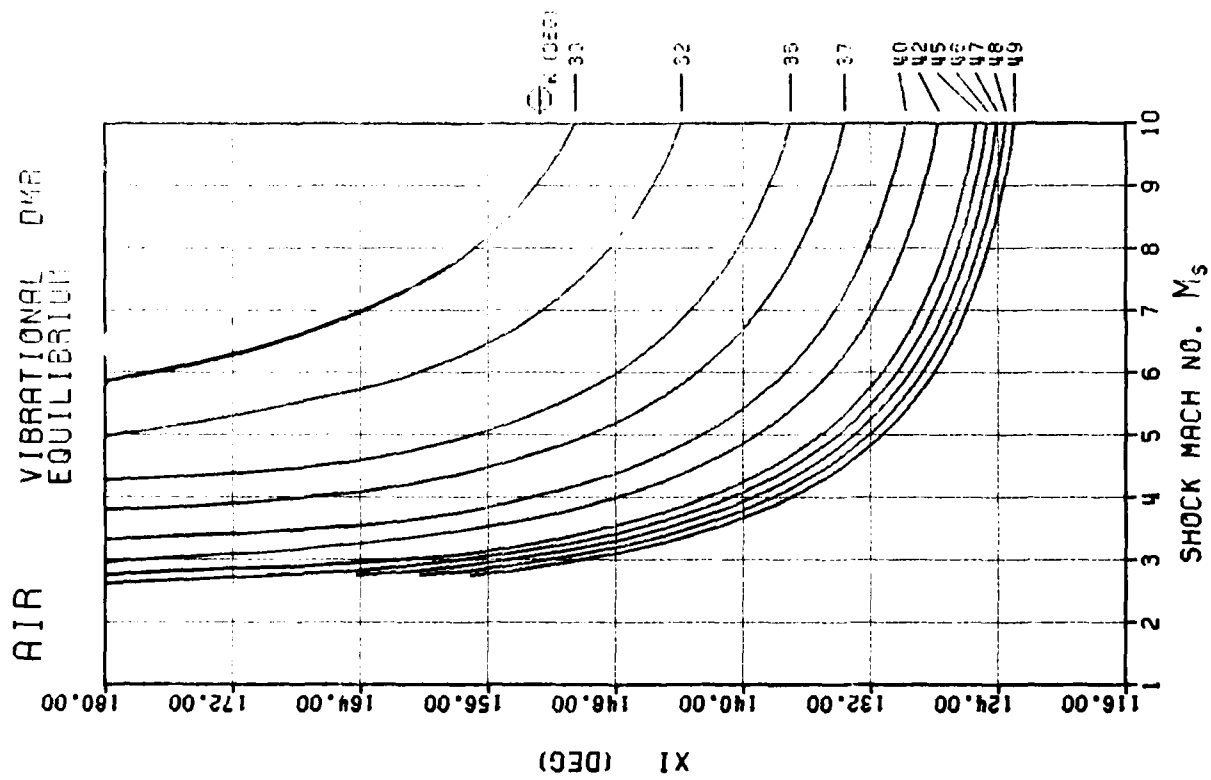




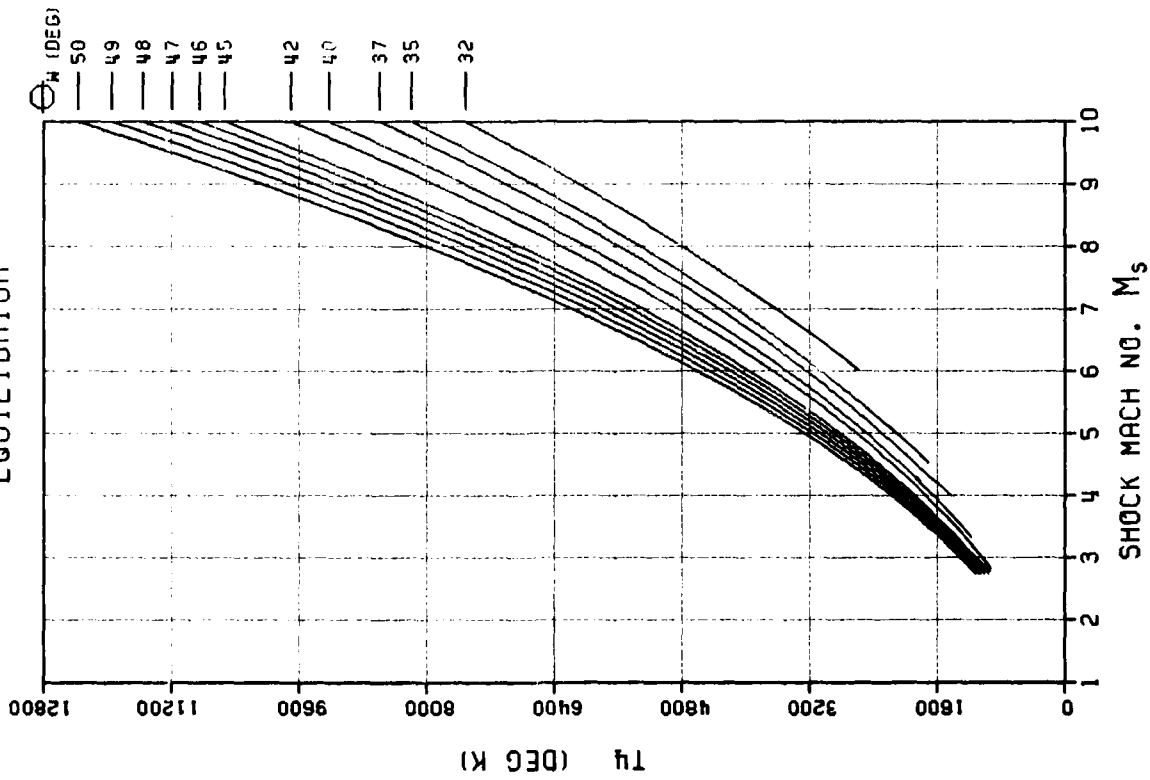




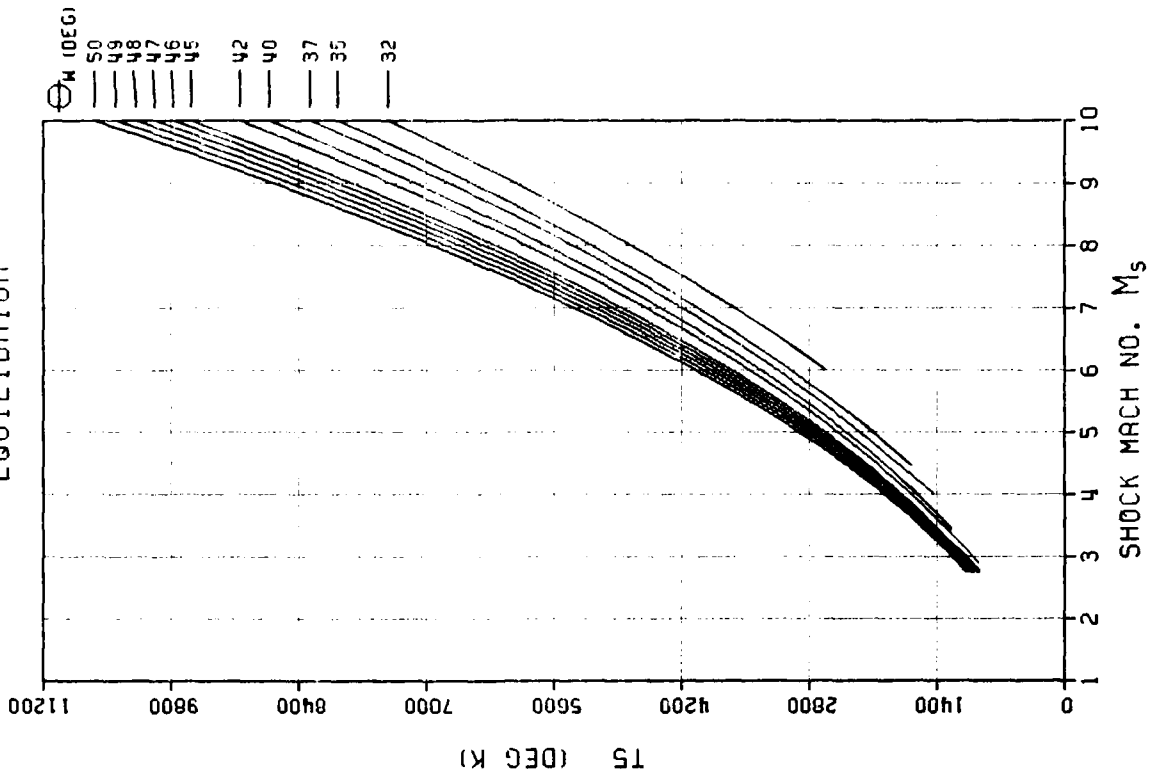




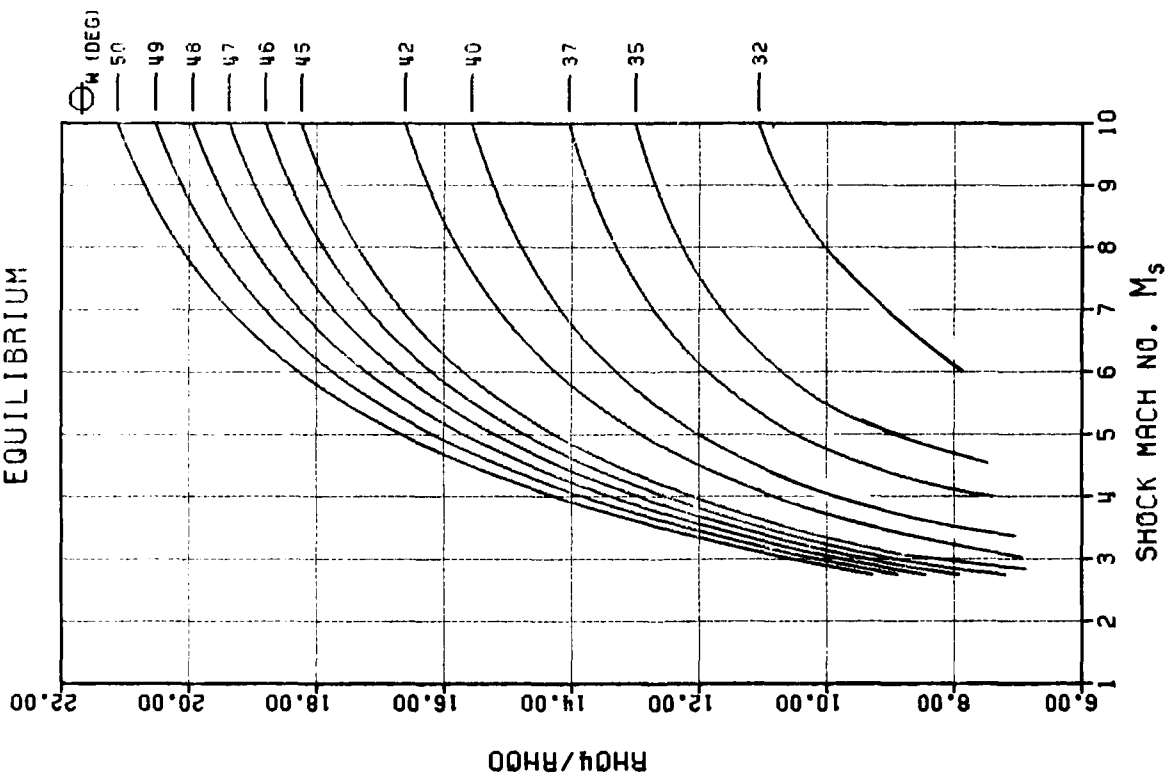
AIR-02 VIBRATIONAL EQUILIBRIUM



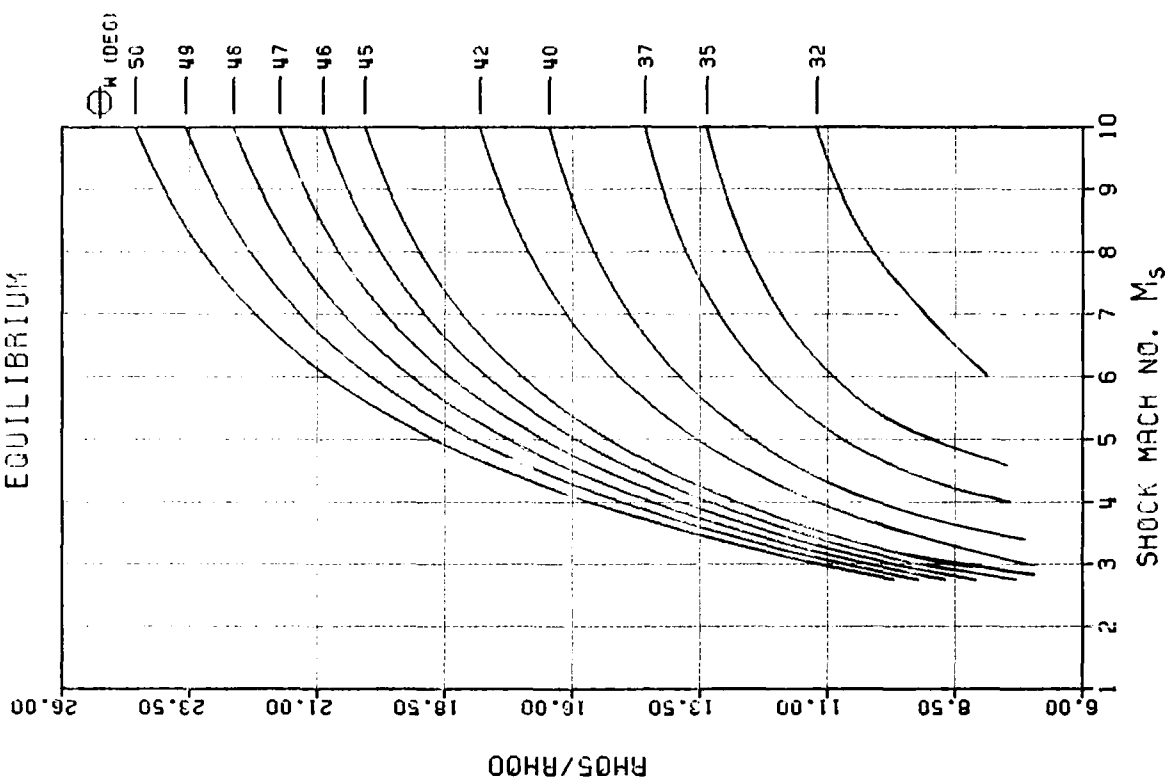
AIR-02 VIBRATIONAL EQUILIBRIUM



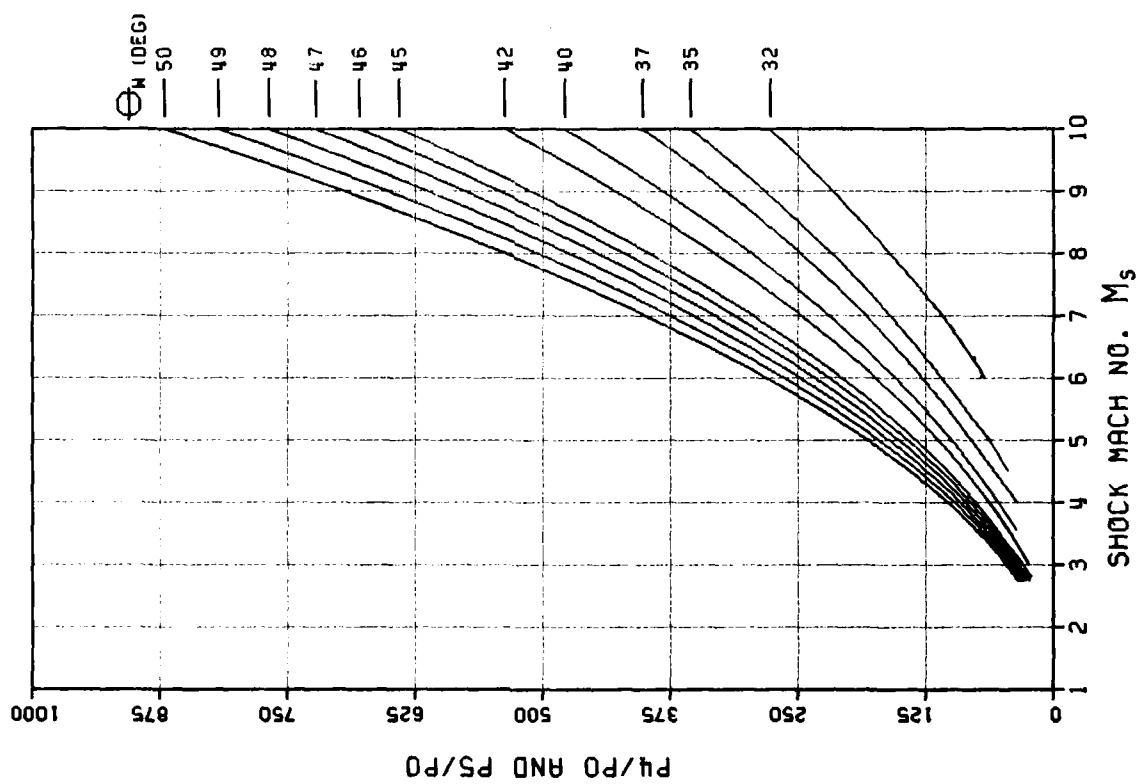
AIR-02 VIBRATIONAL EQUILIBRIUM



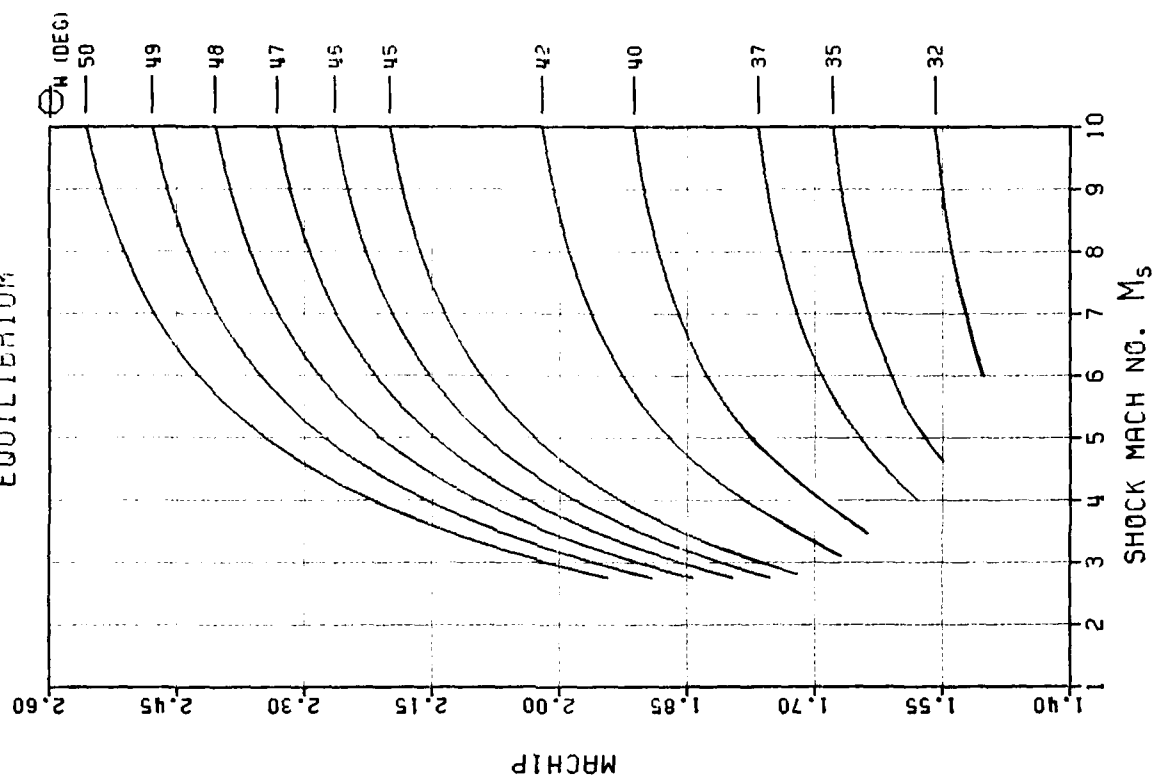
AIR-02 VIBRATIONAL EQUILIBRIUM



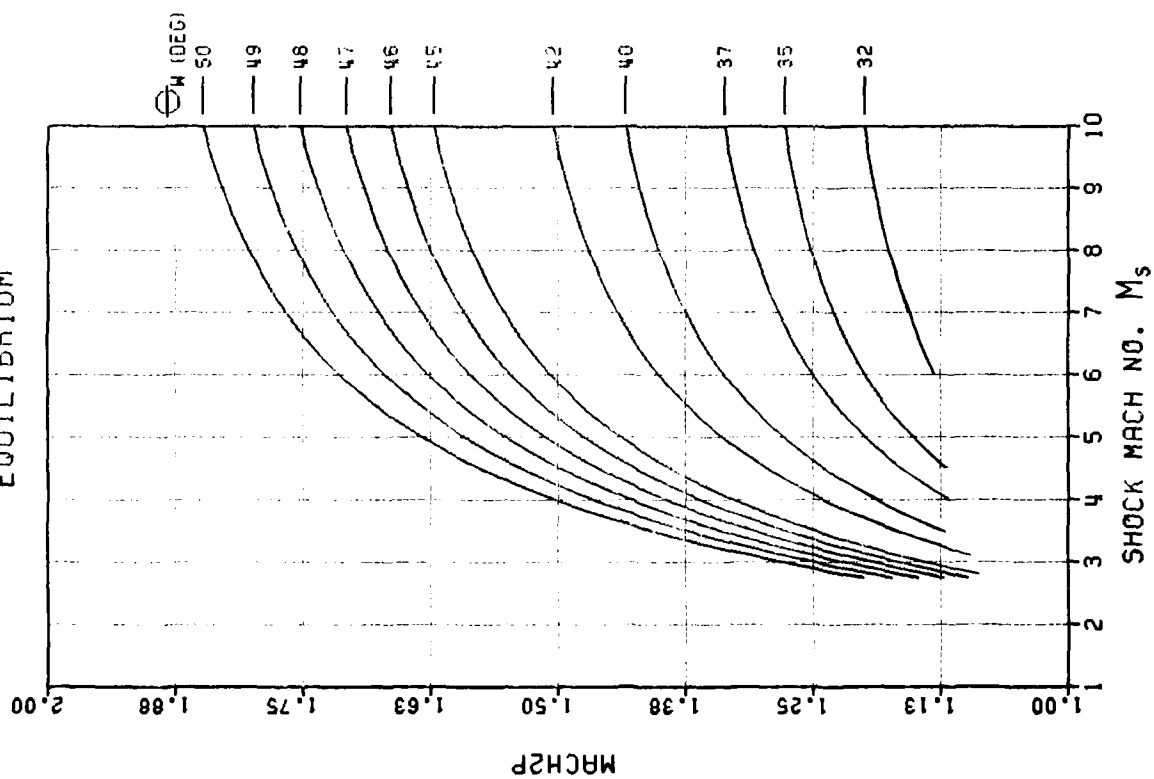
AIR-02 VIBRATIONAL DMR EQUILIBRIUM



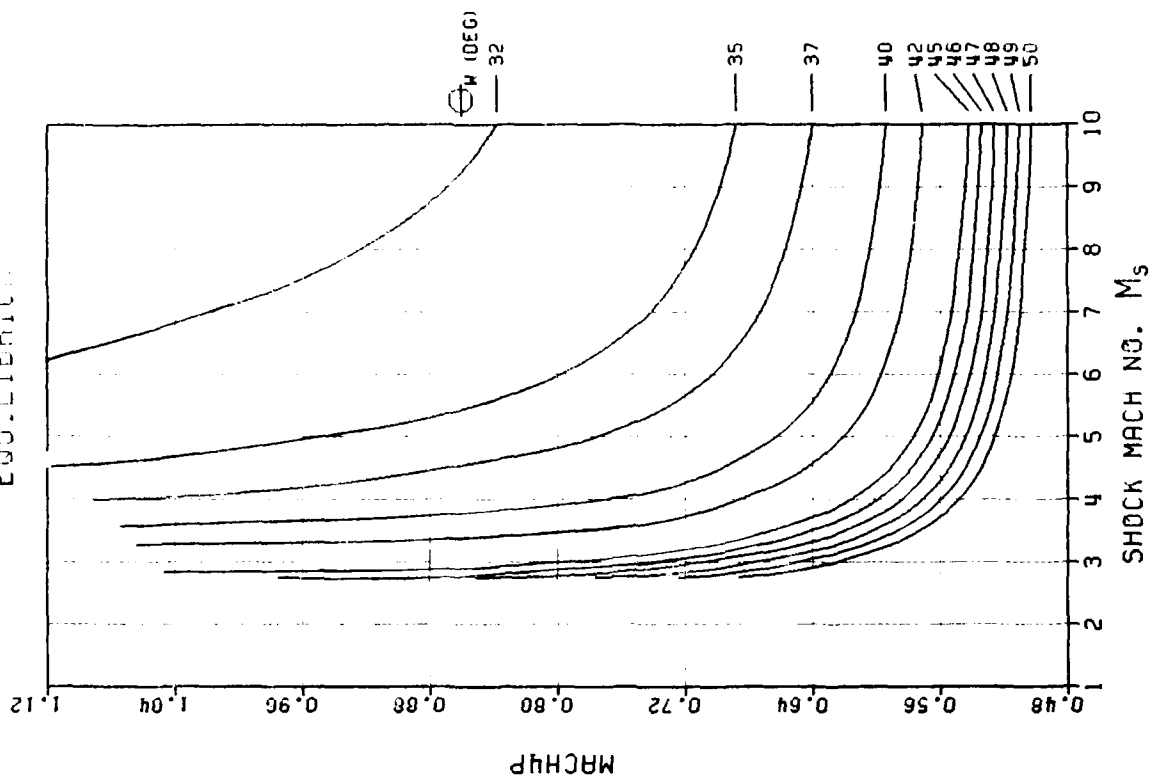
AIR-02 VIBRATIONAL DMR EQUILIBRIUM



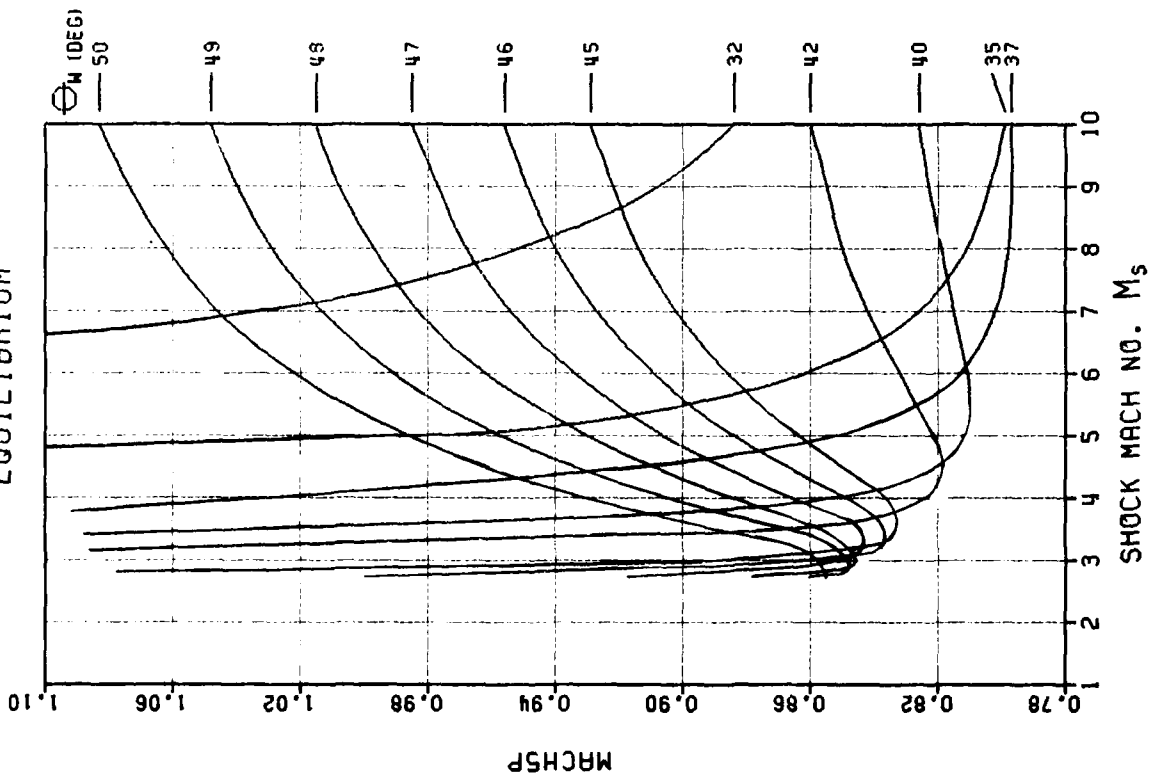
AIR-02 VIBRATIONAL EQUILIBRIUM



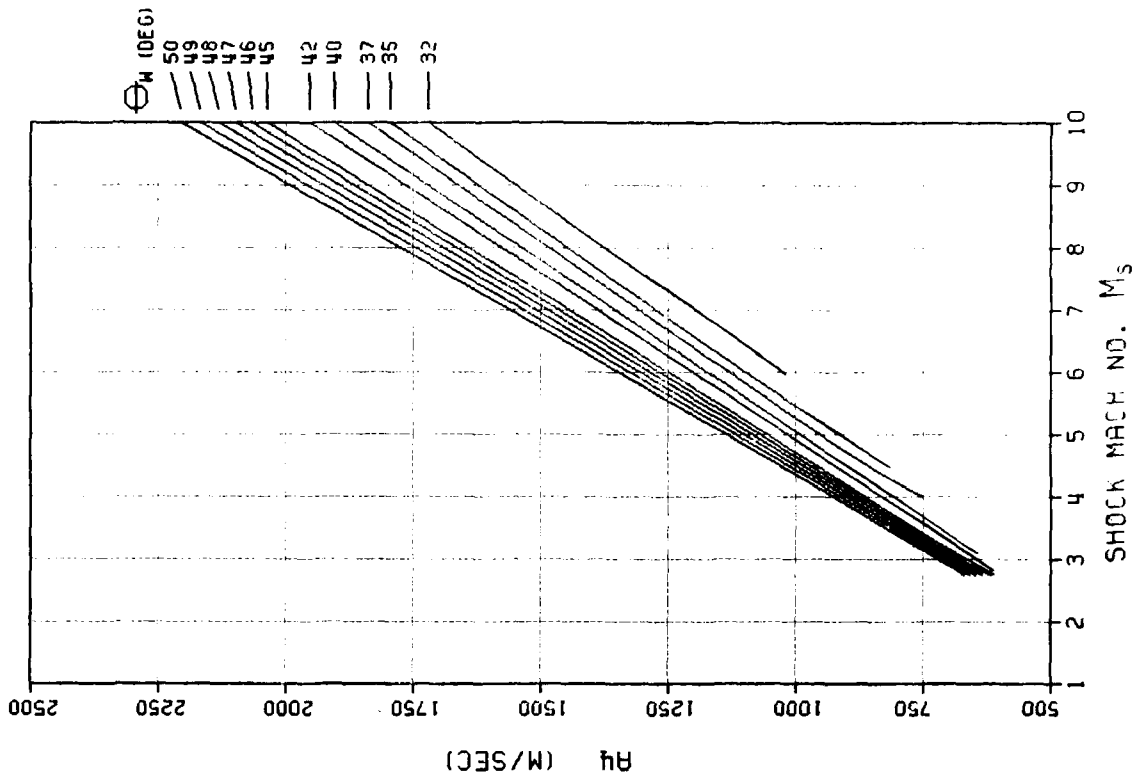
AIR-02 VIBRATIONAL DMR EQUILIBRIUM



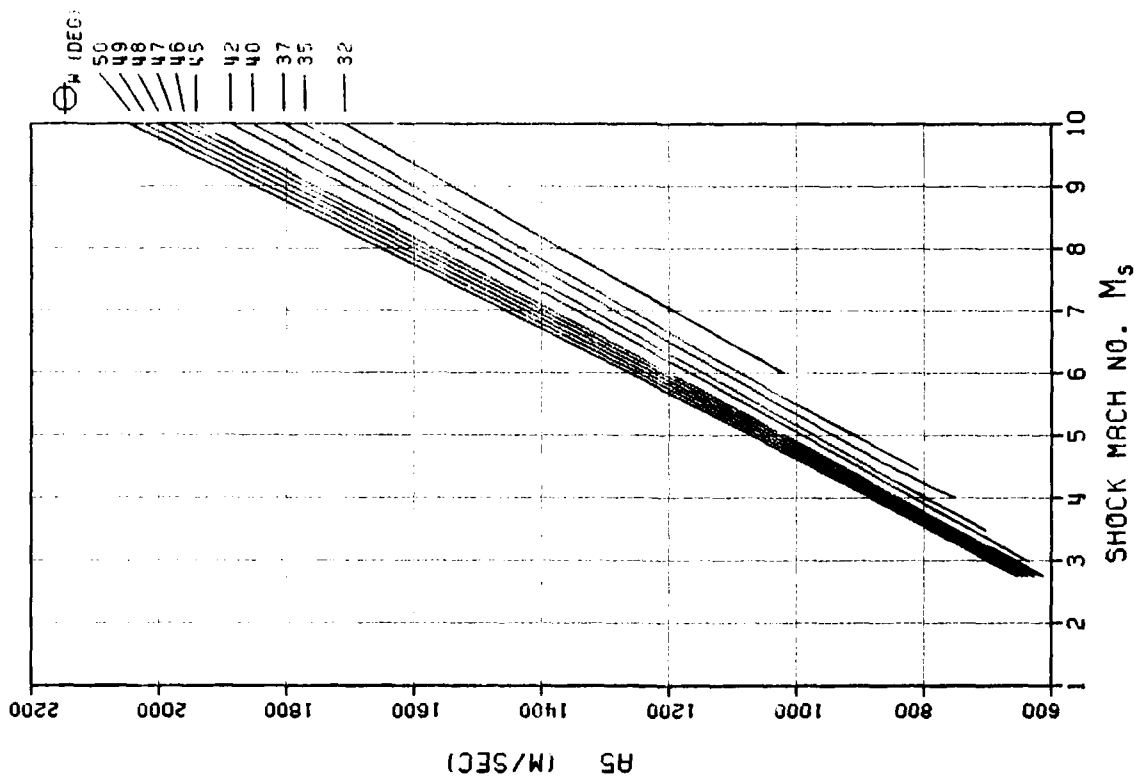
AIR-02 VIBRATIONAL DMR EQUILIBRIUM



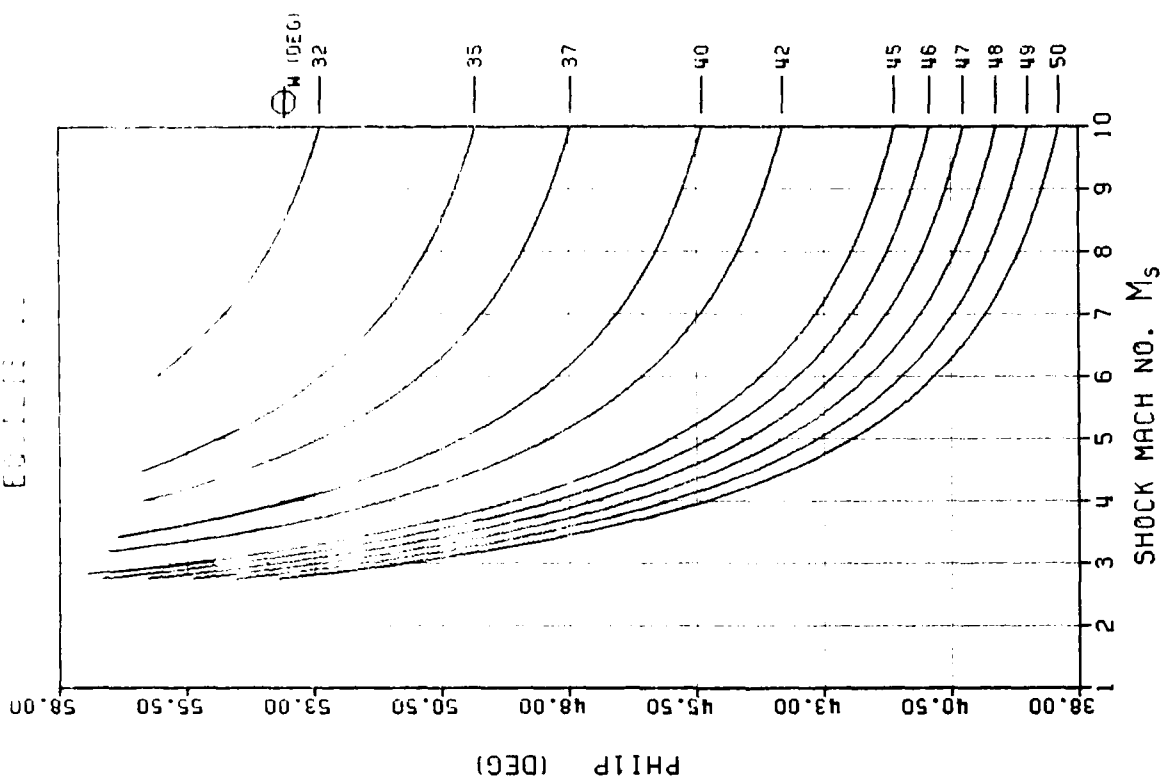
AIR-02 VIBRATIONAL DMR EQUILIBRIUM



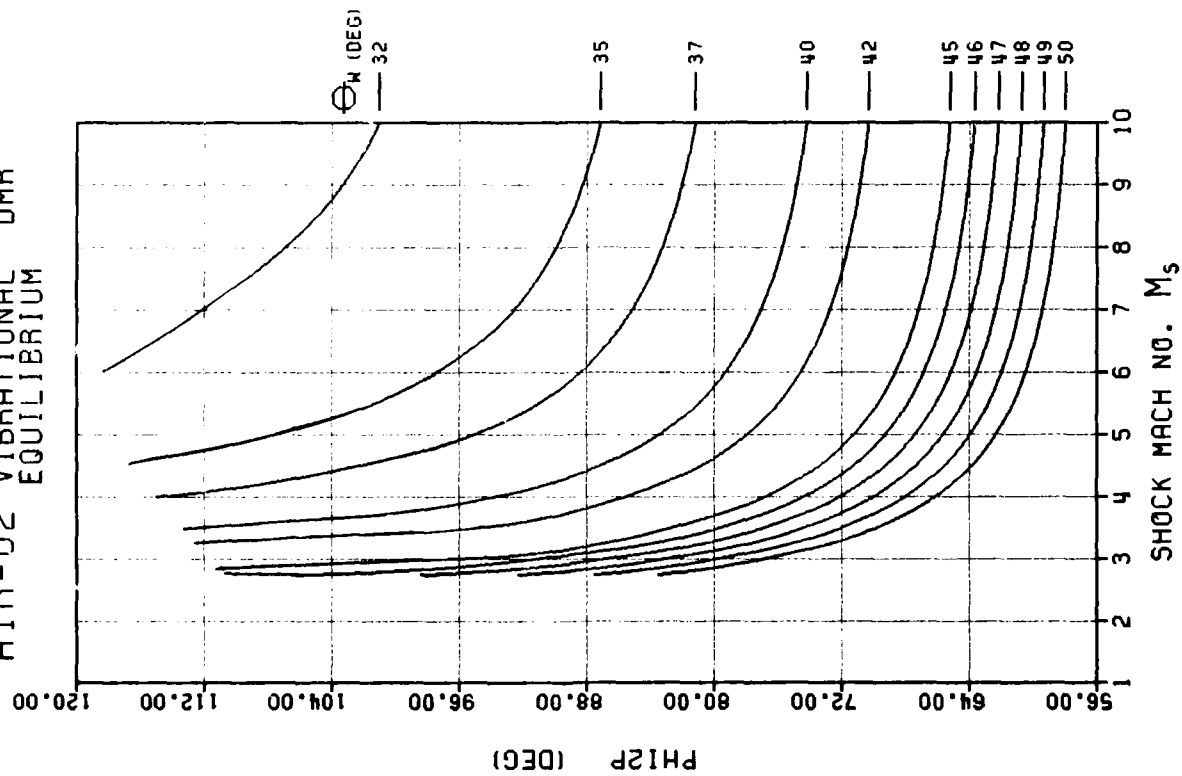
AIR-02 VIBRATIONAL DMR EQUILIBRIUM



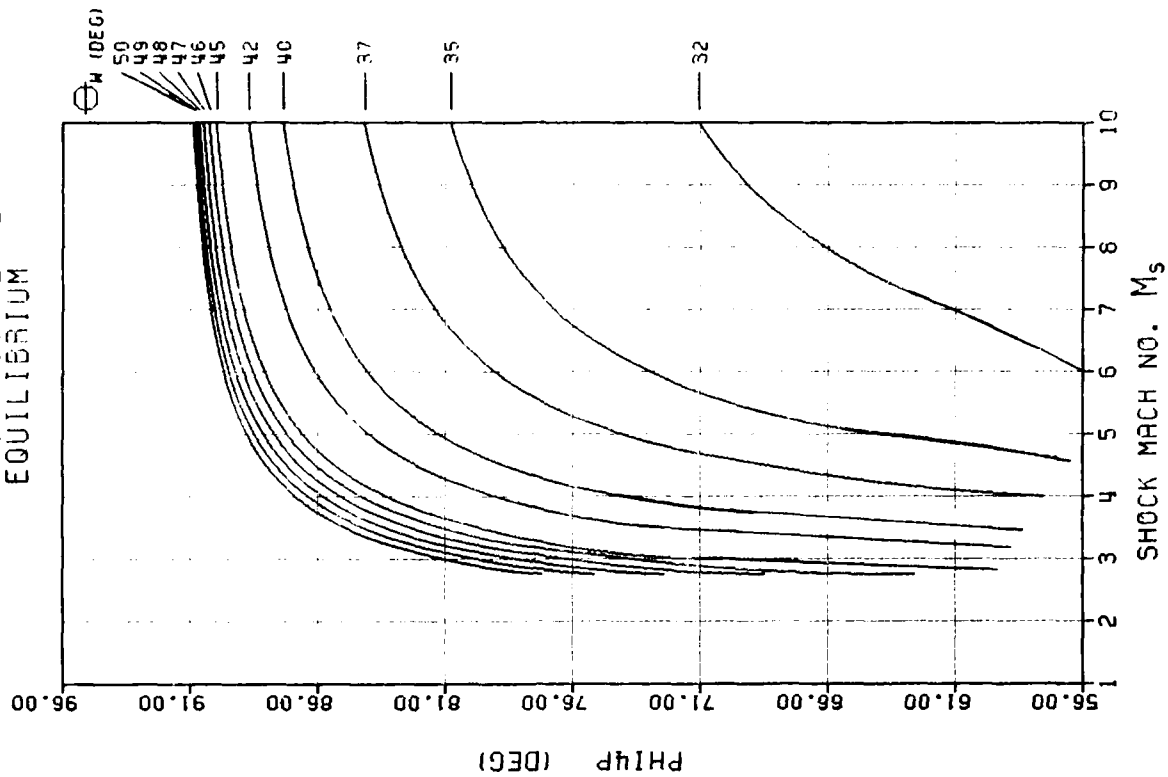
AIR-02 VIBRATIONAL DMR EQUILIBRIUM



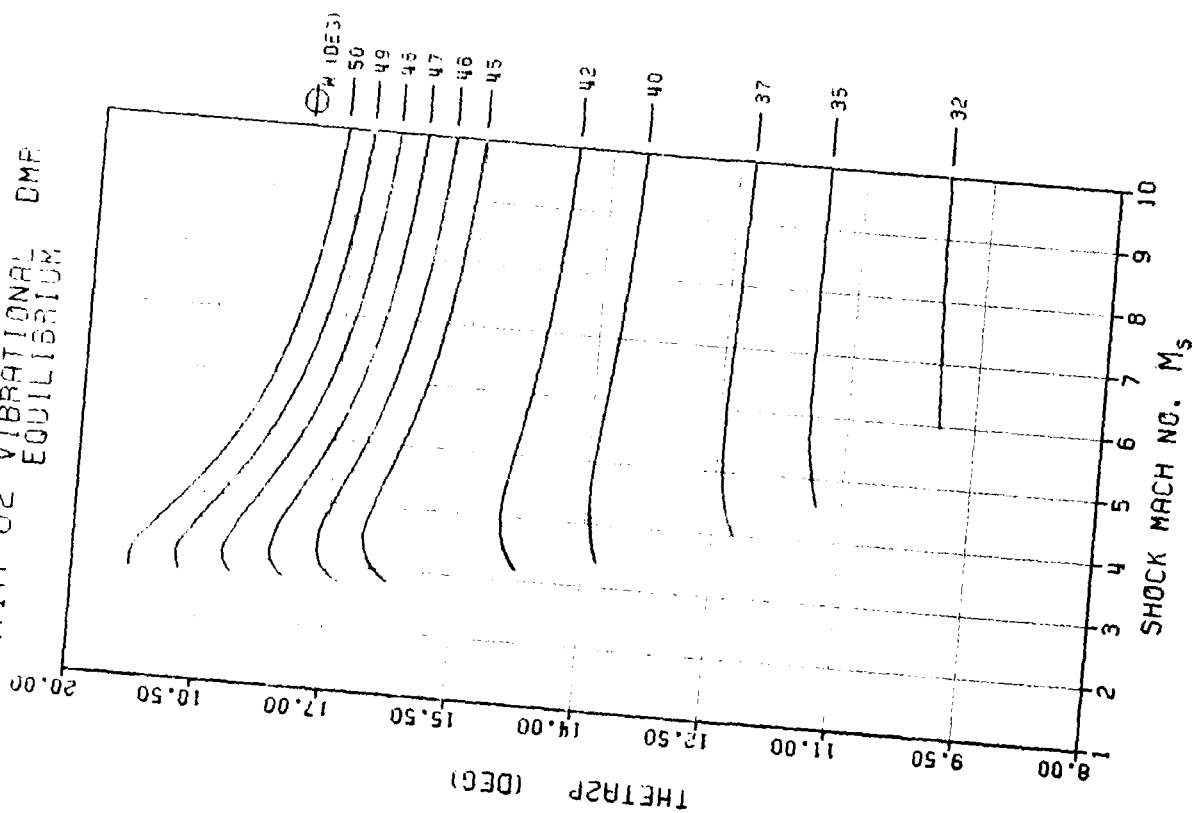
AIR-02 VIBRATIONAL DMR EQUILIBRIUM



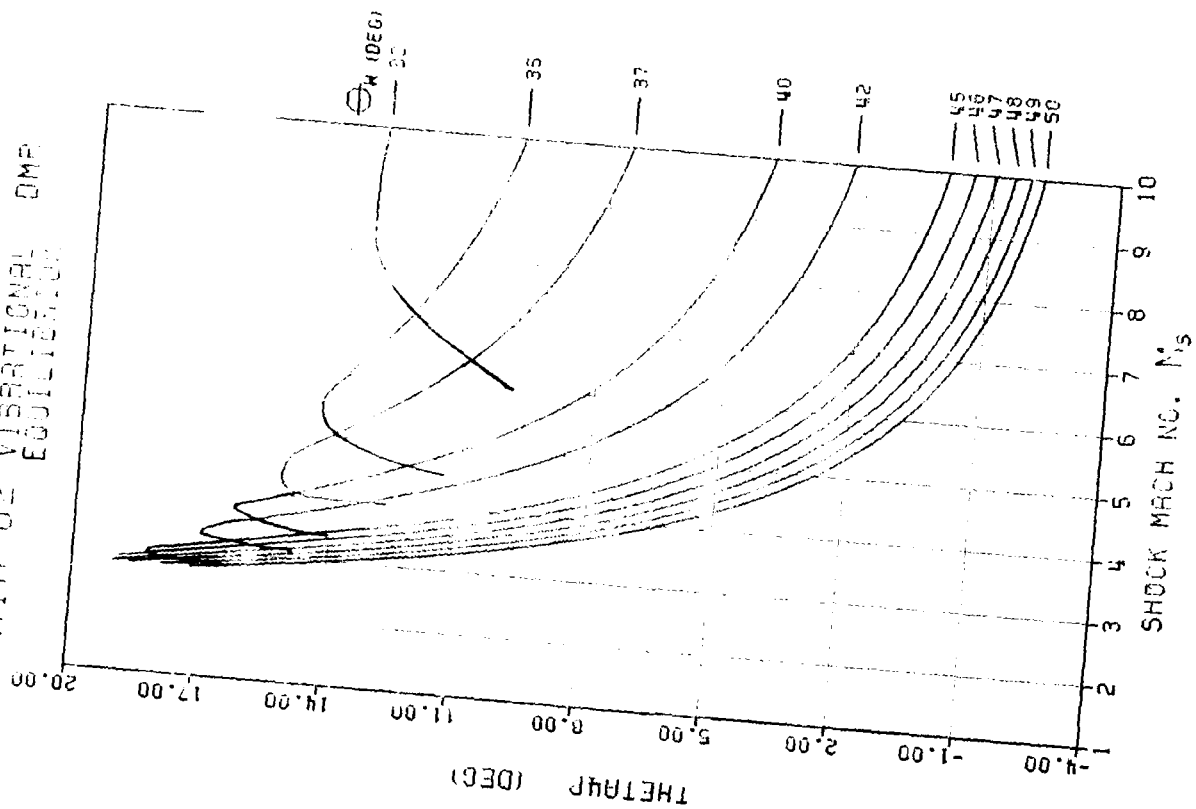
AIR-02 VIBRATIONAL DMR EQUILIBRIUM



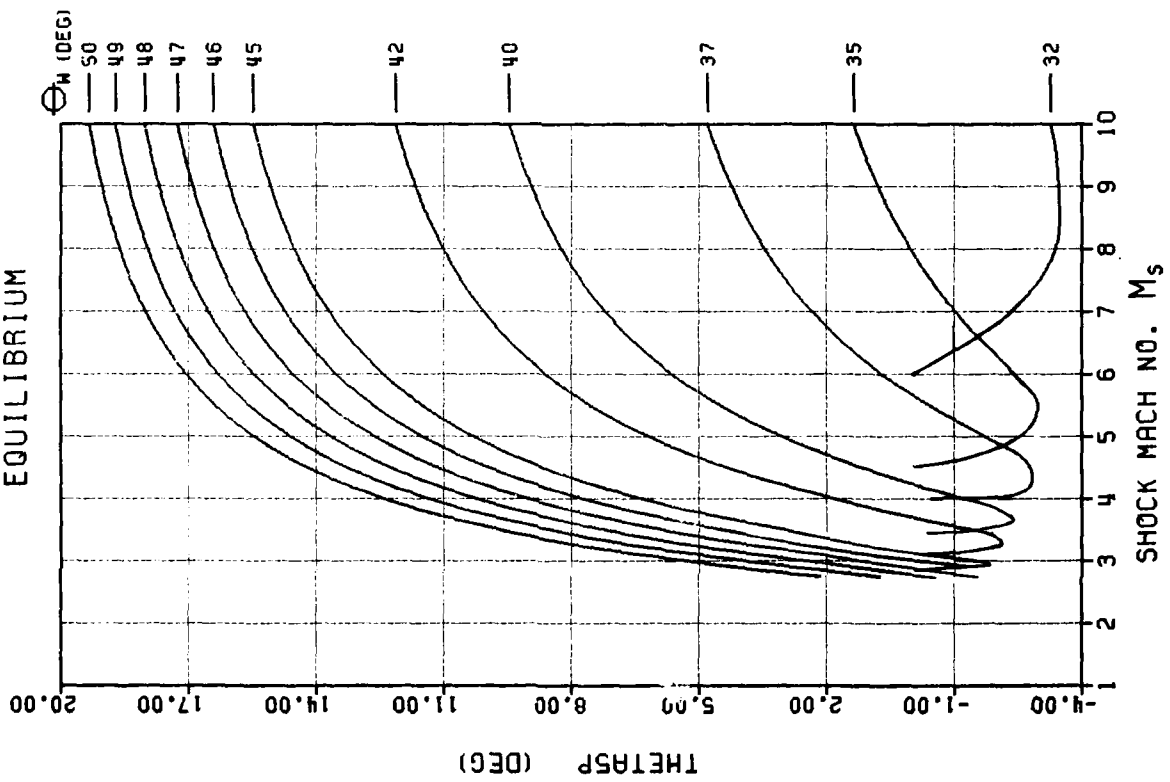
AIR-02 VIBRATIONAL EQUILIBRIUM



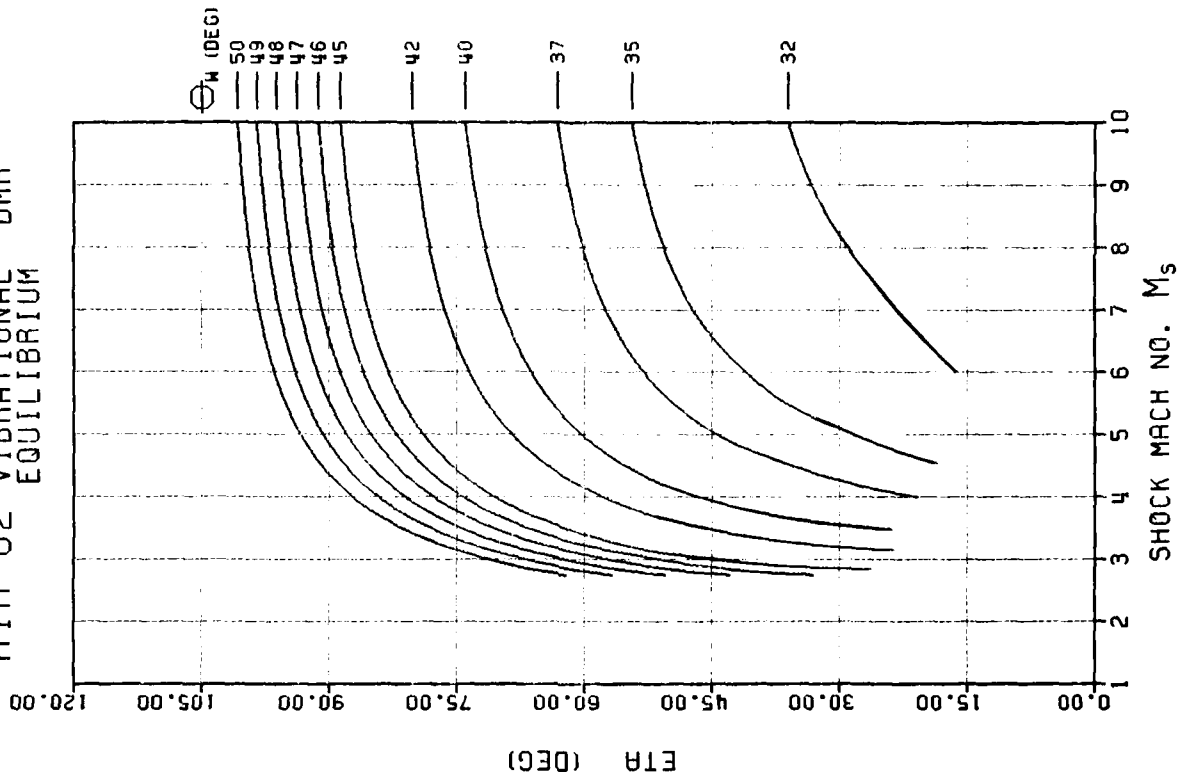
AIR-02 VIBRATIONAL EQUILIBRIUM



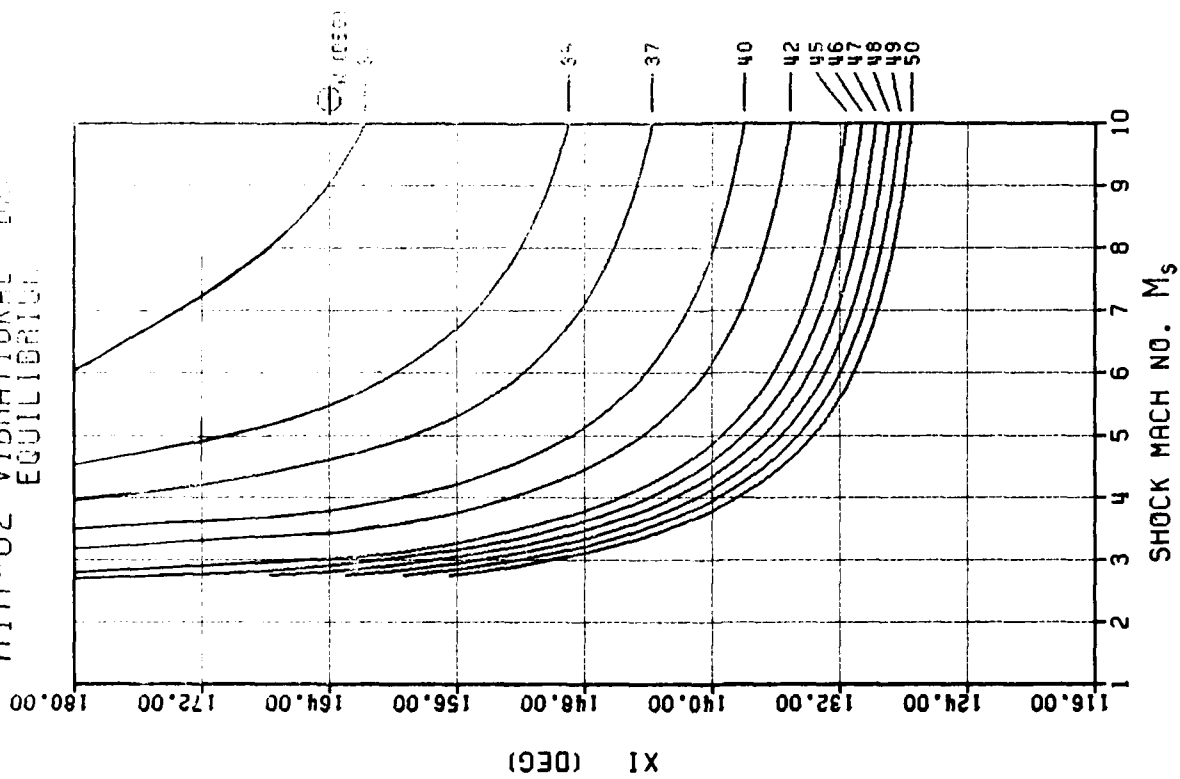
AIR-02 VIBRATIONAL EQUILIBRIUM

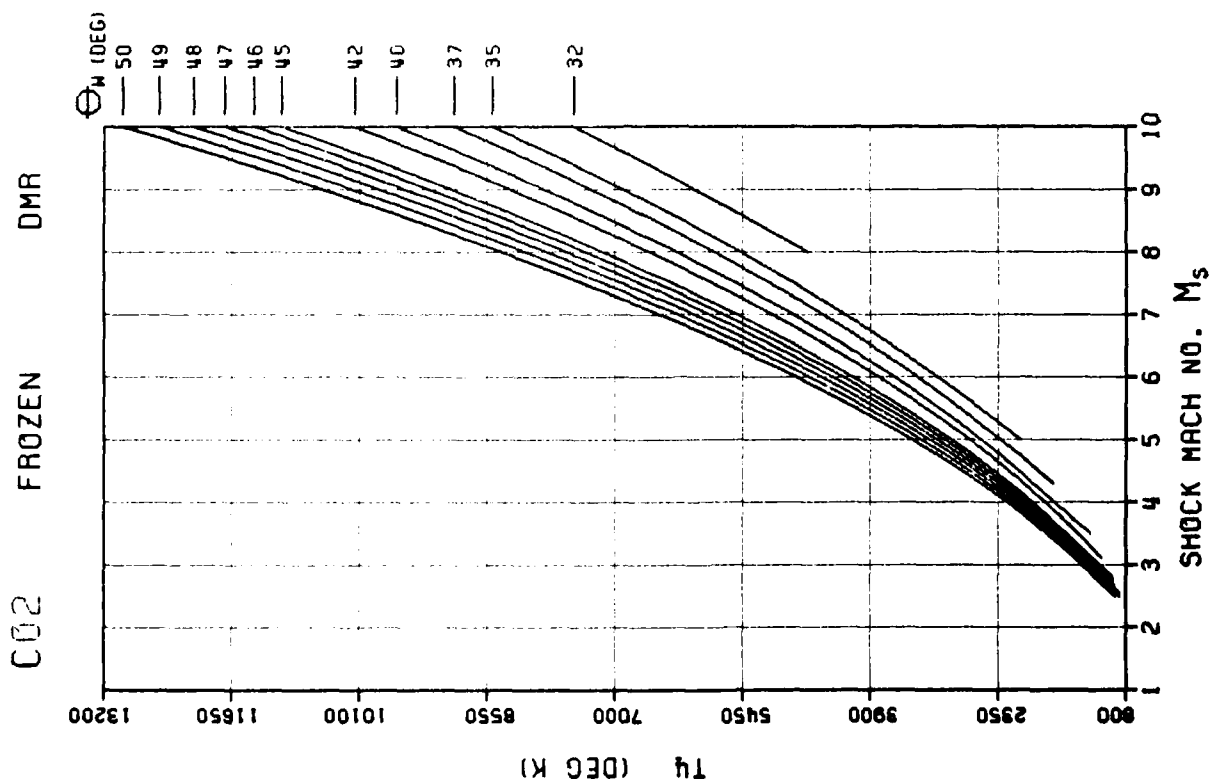
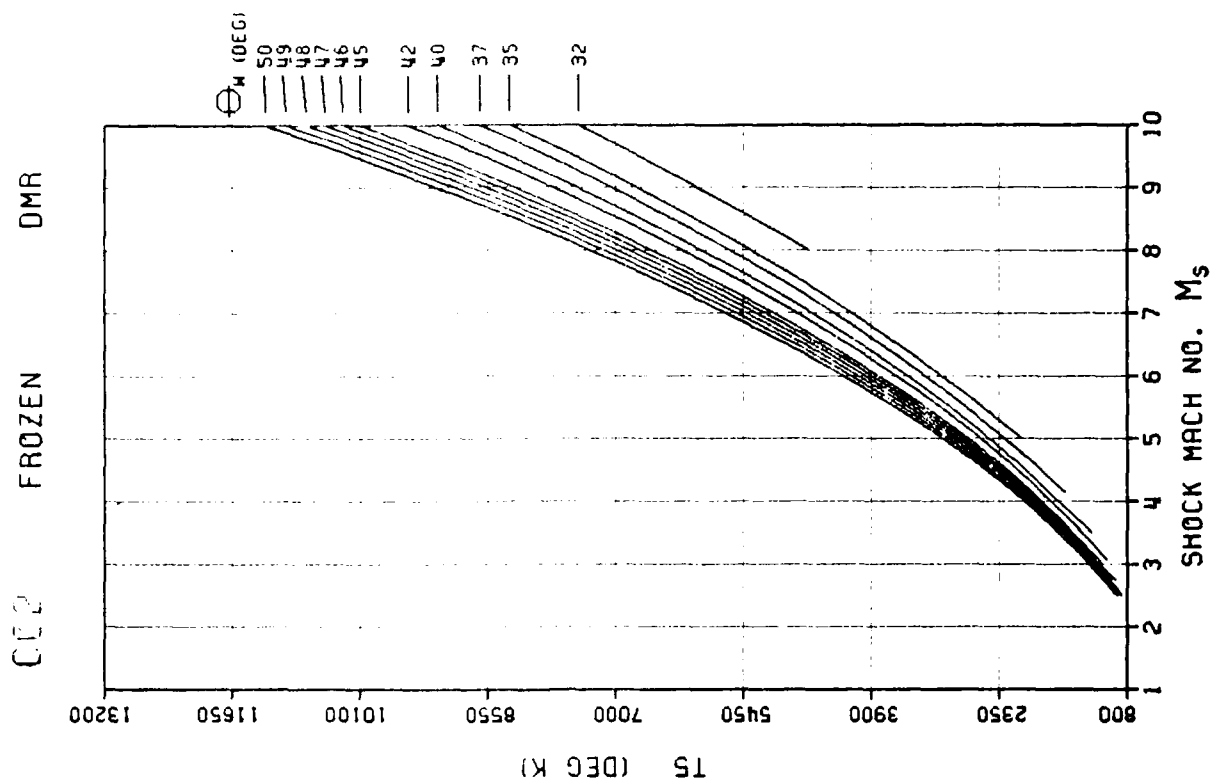


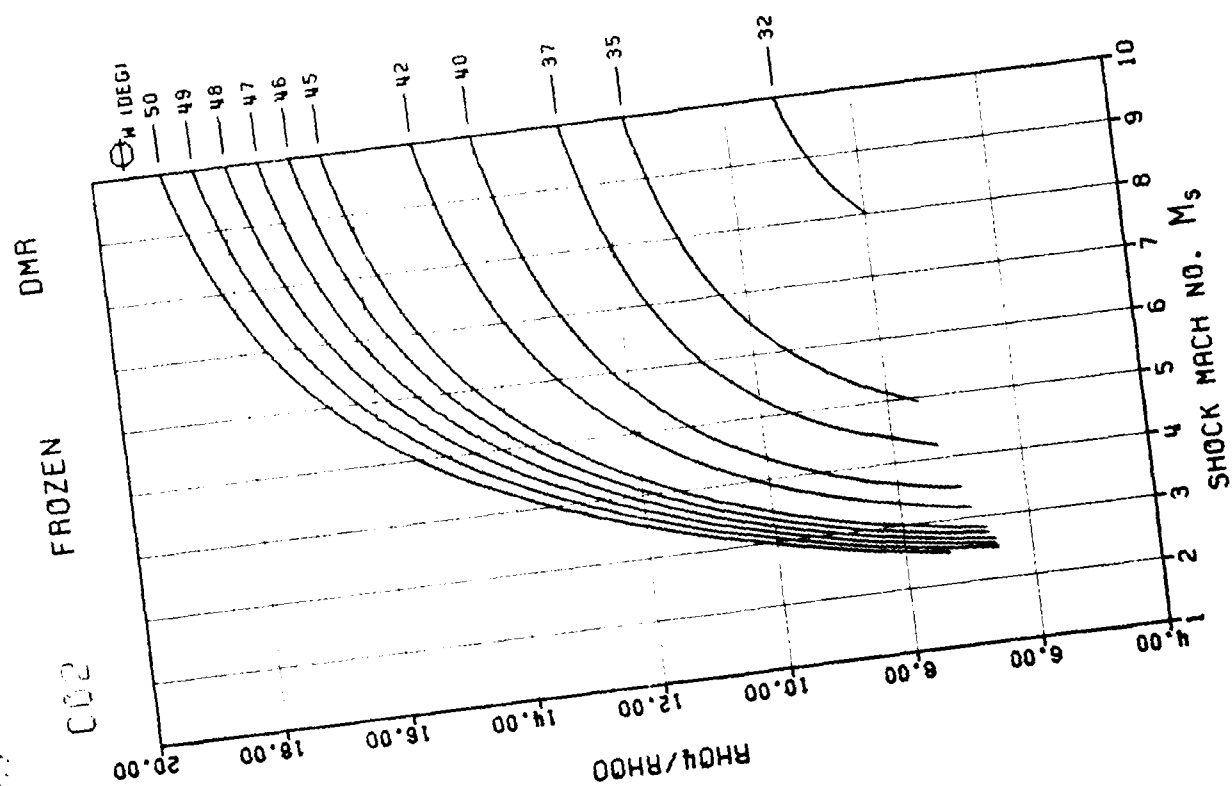
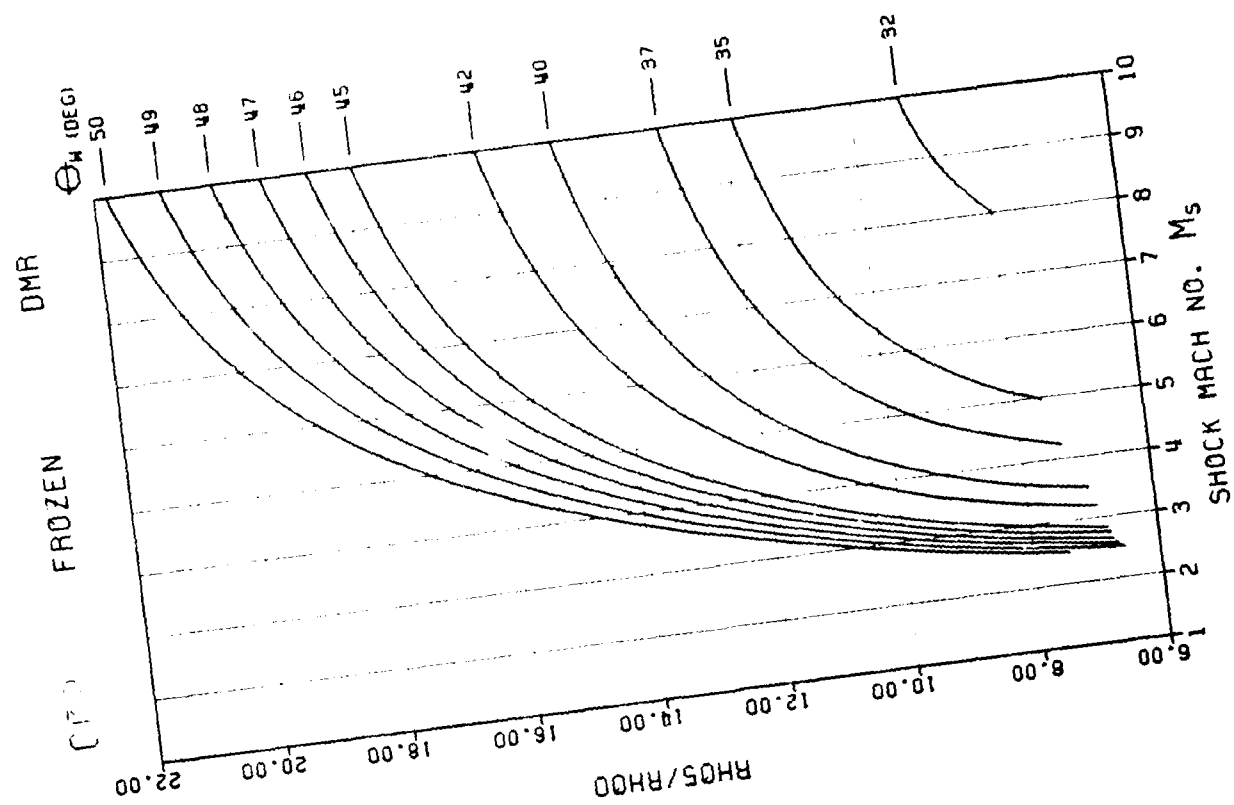
AIR-02 VIBRATIONAL EQUILIBRIUM

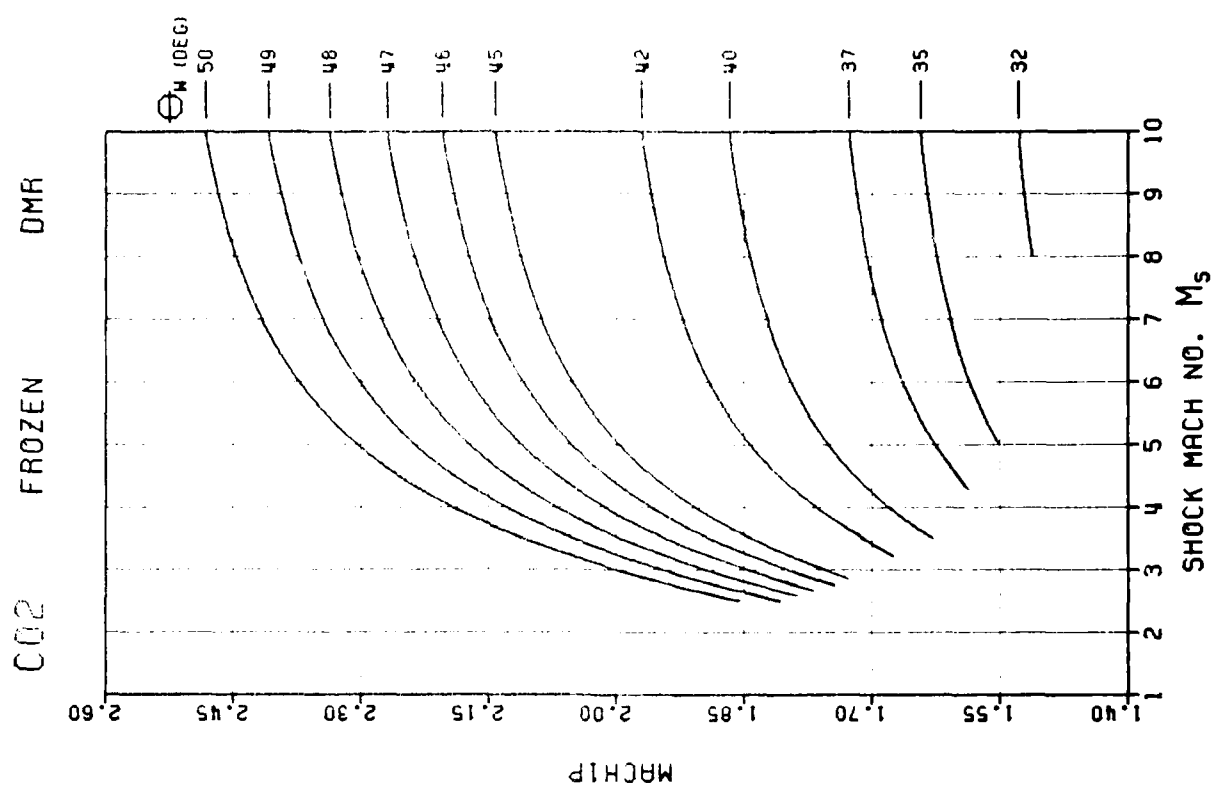
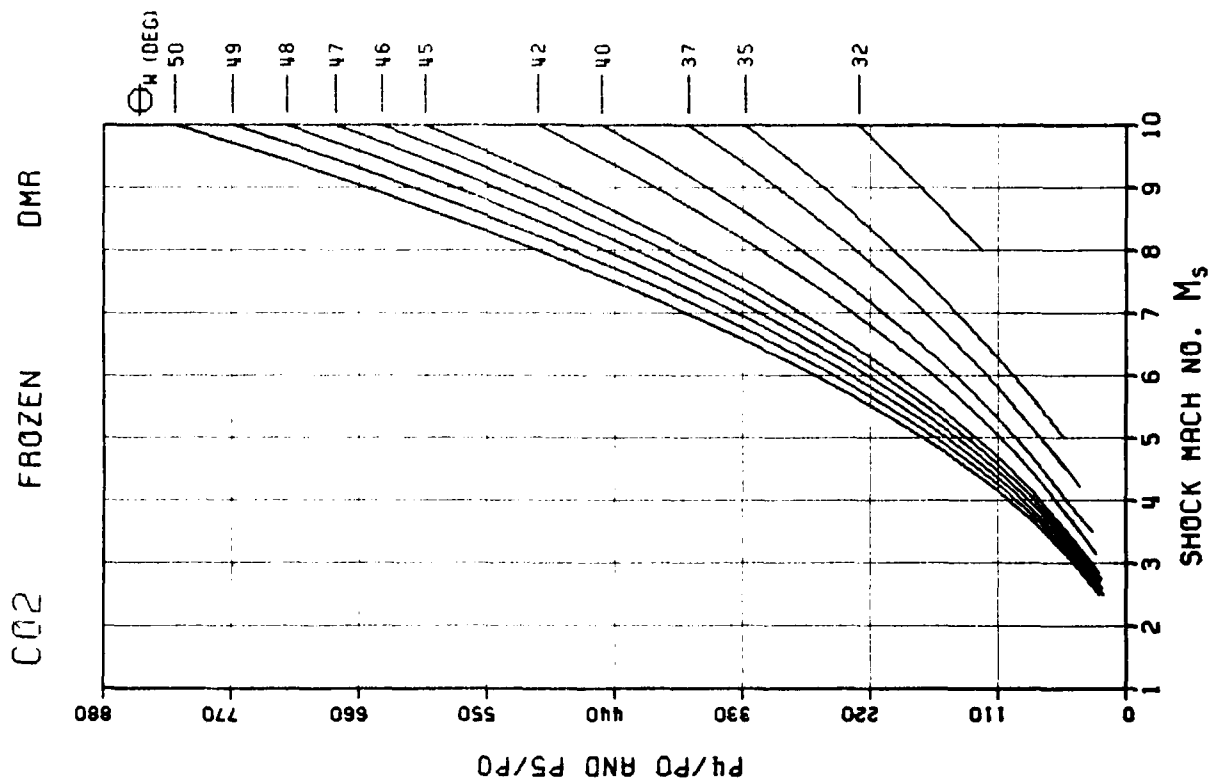


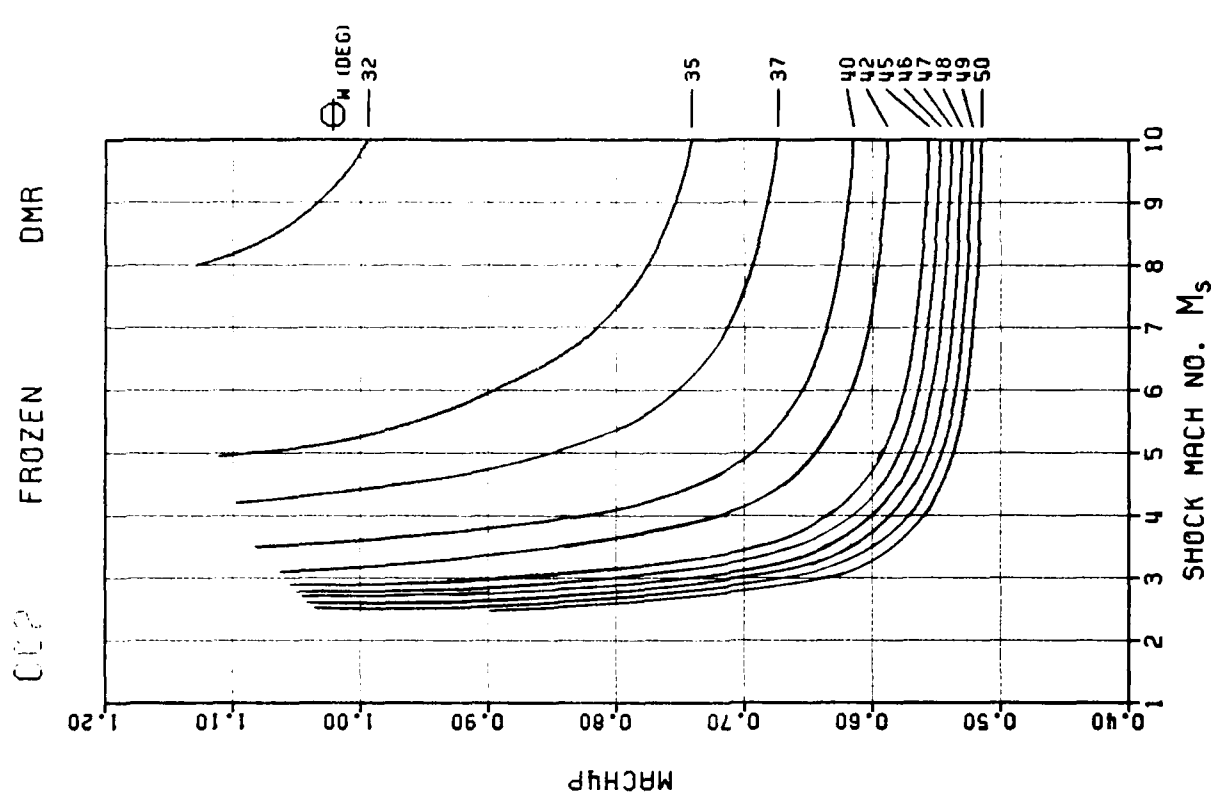
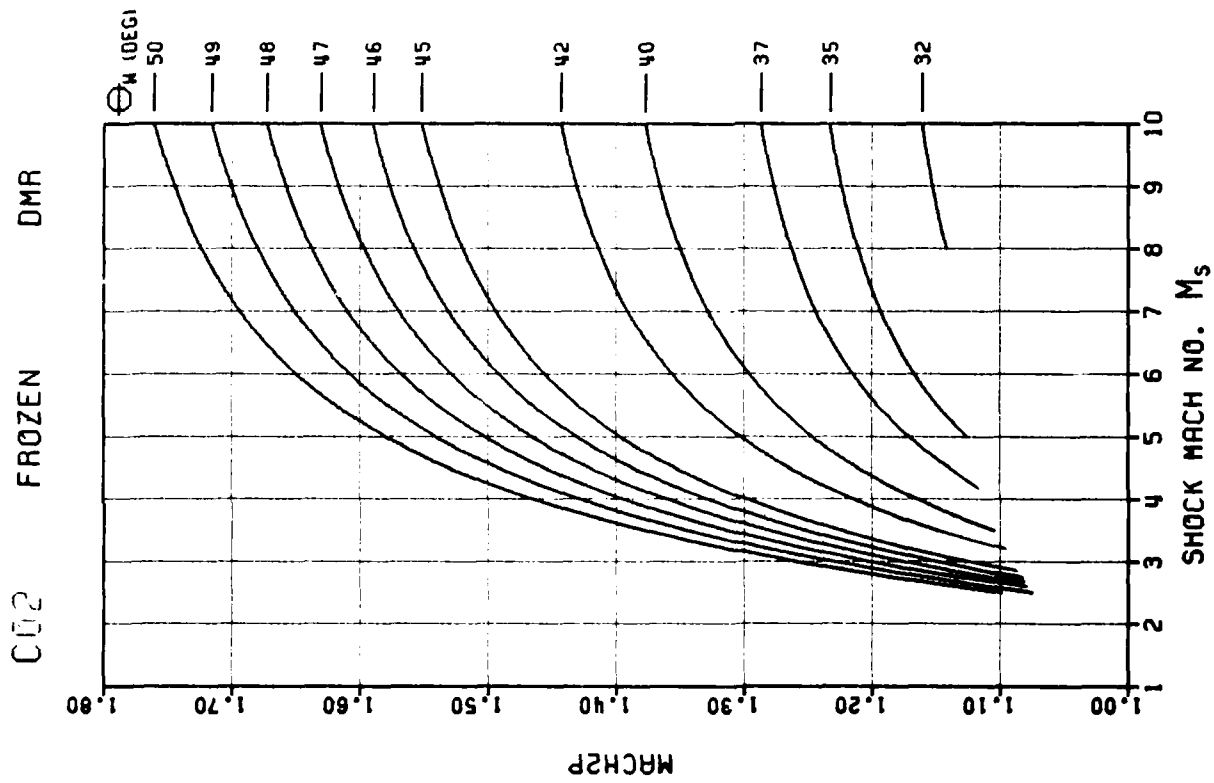
AIR-02 VIBRATIONEL DMS EQUILIBRIUM

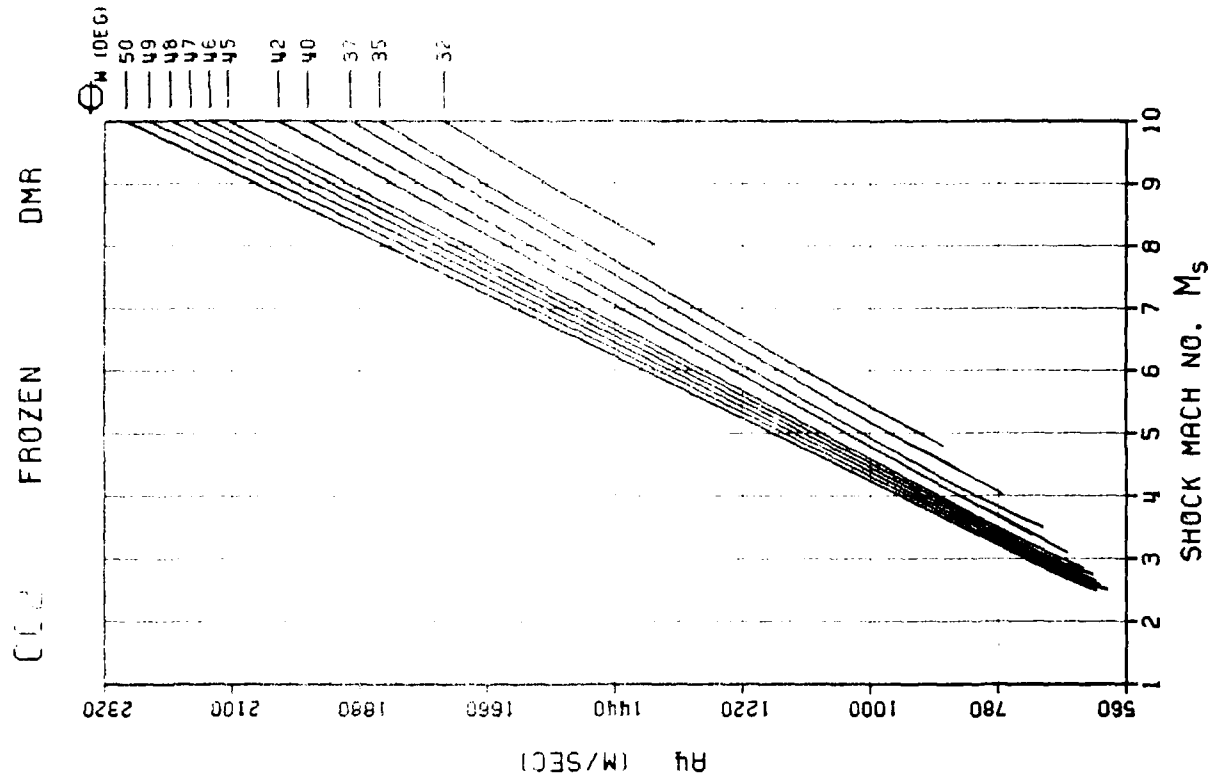
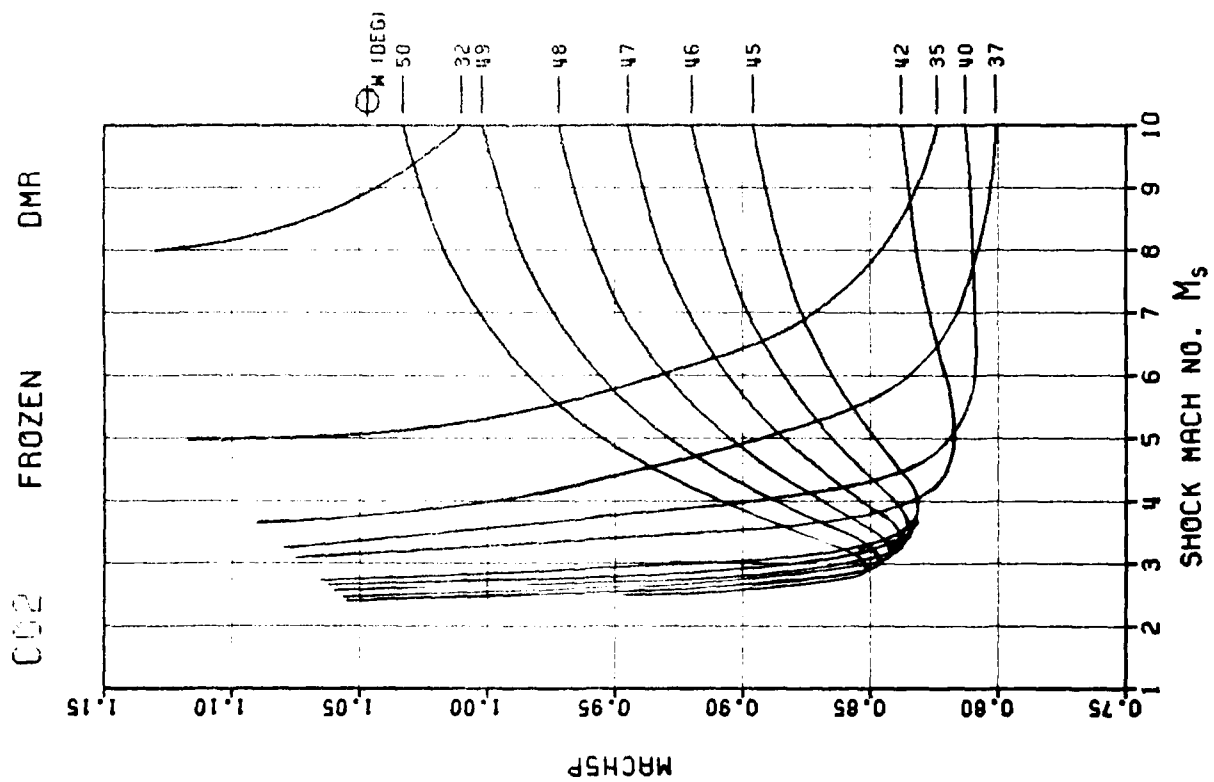


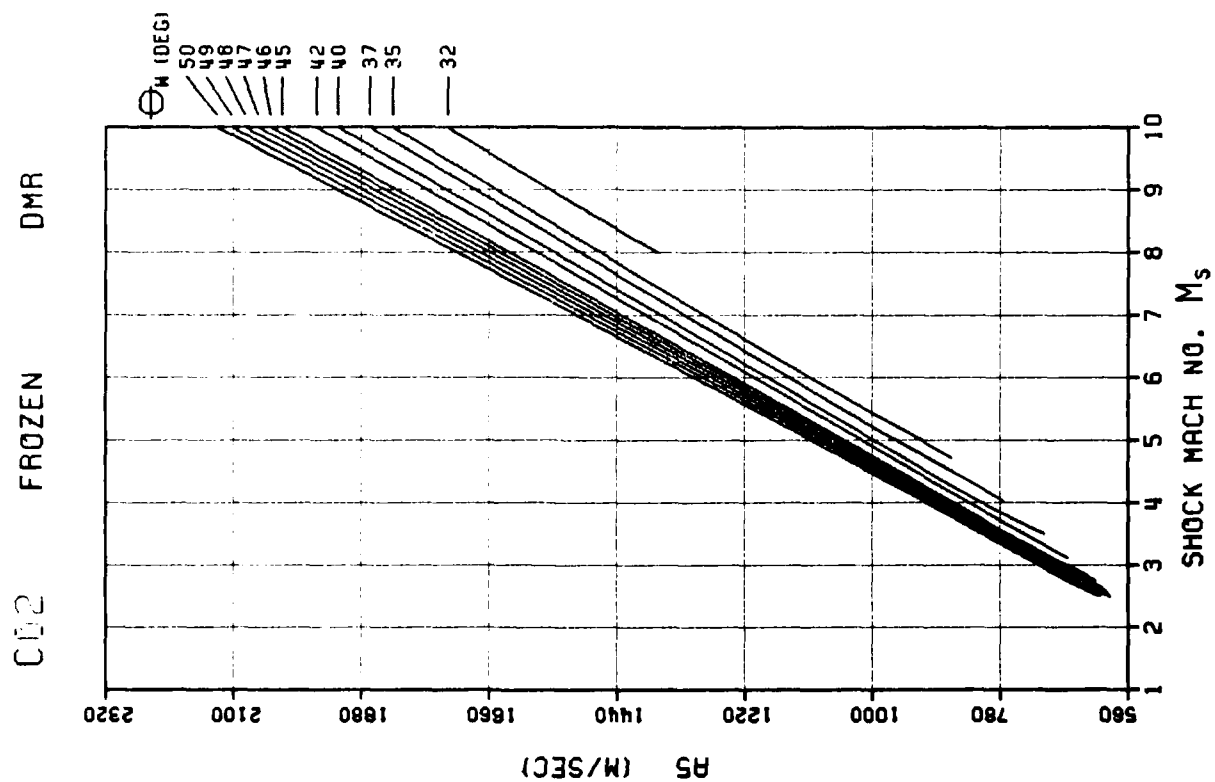
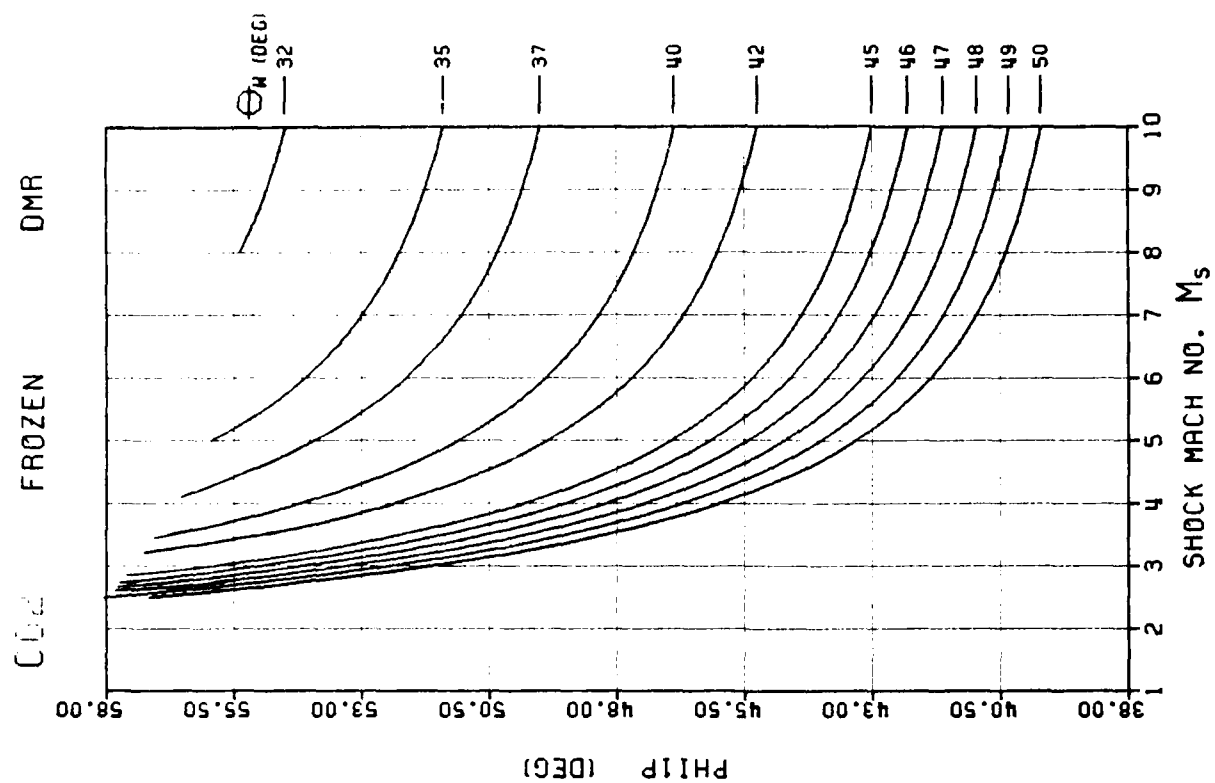


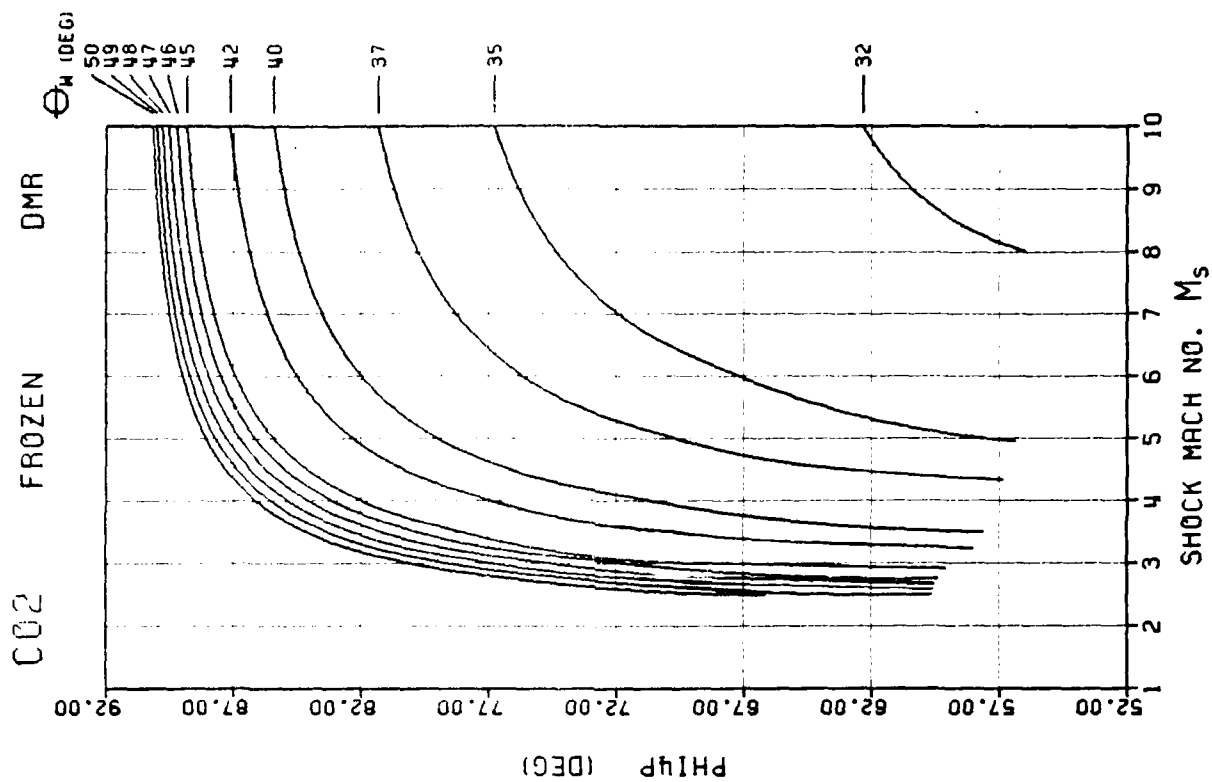
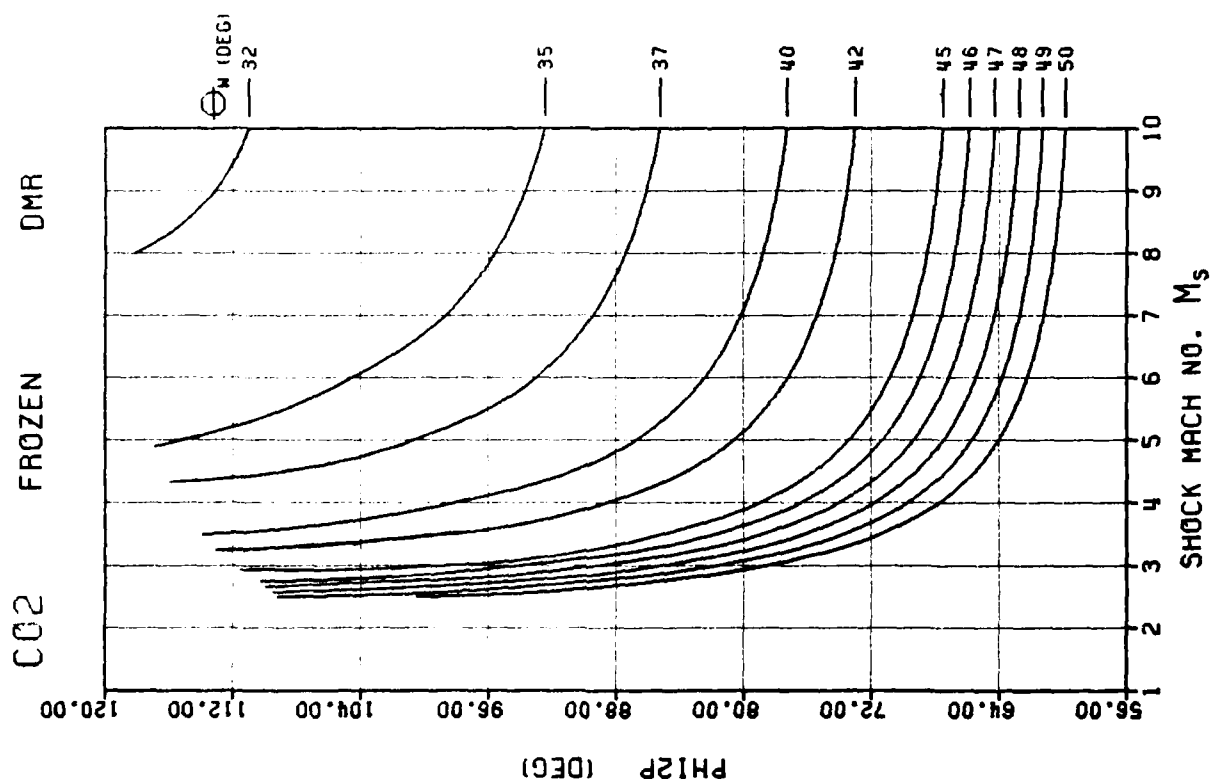


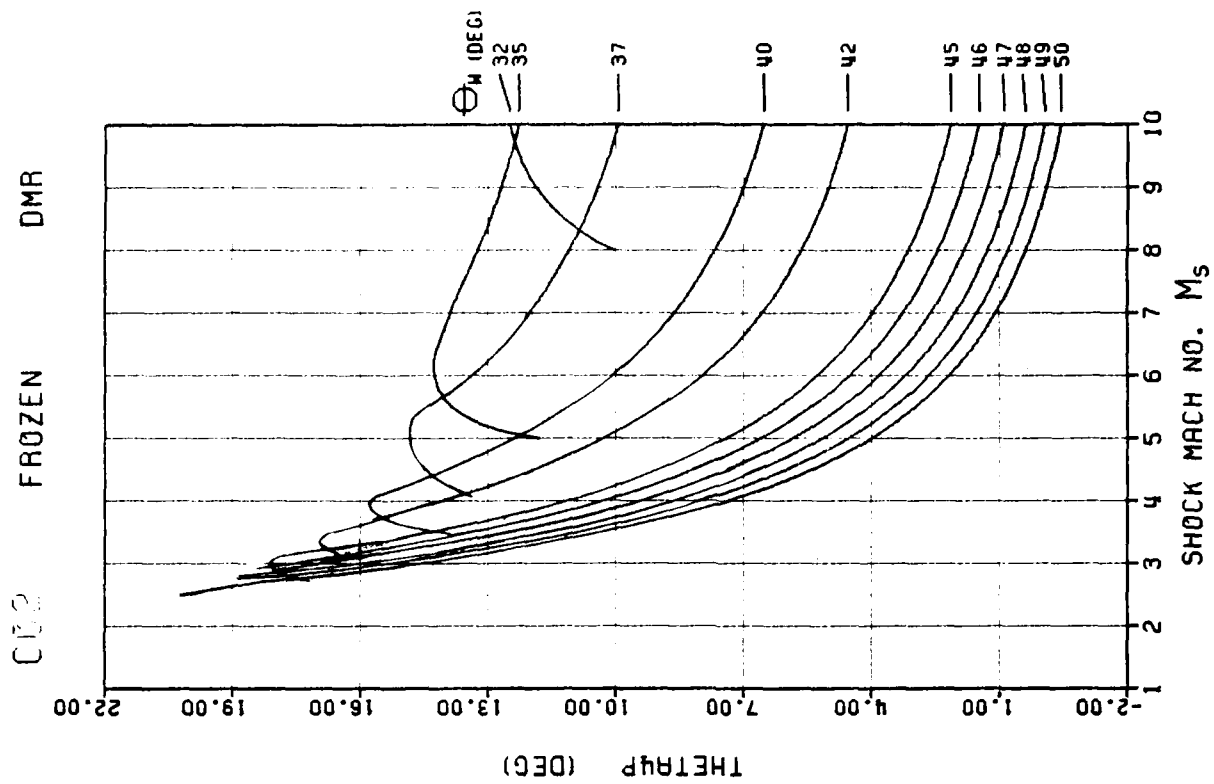
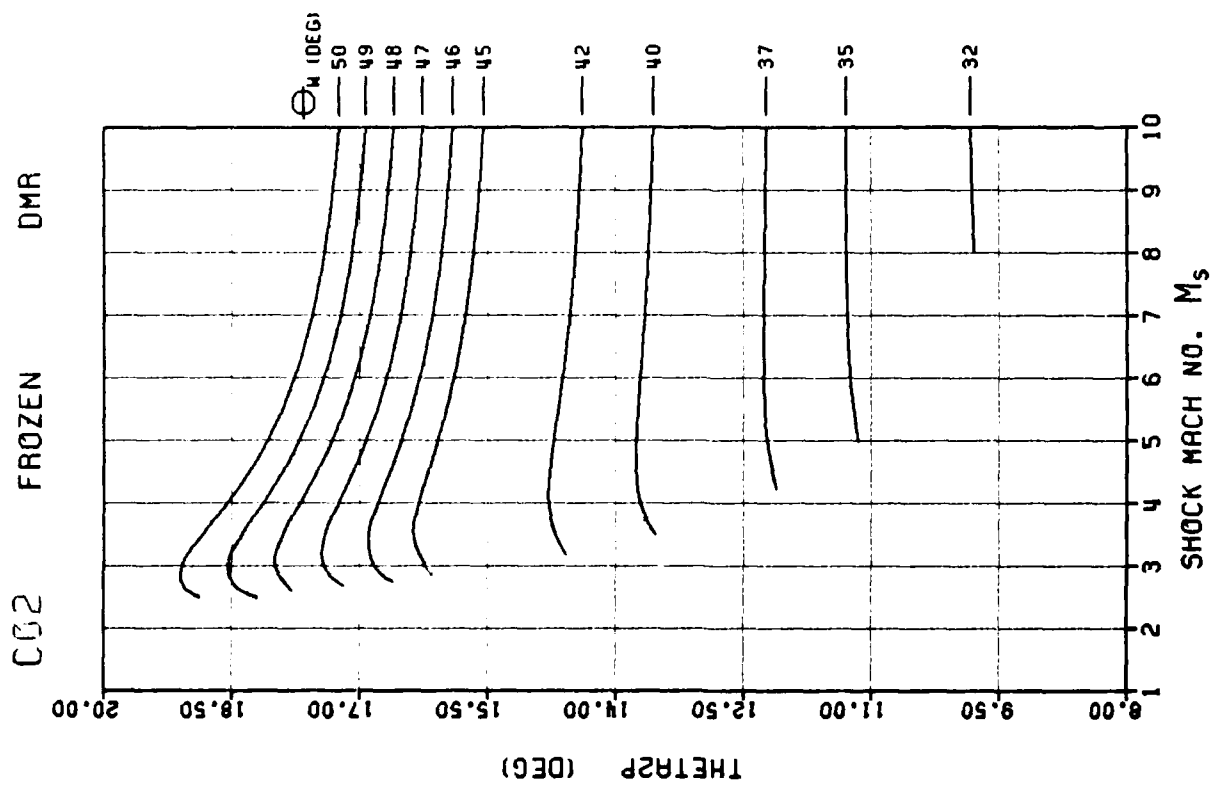


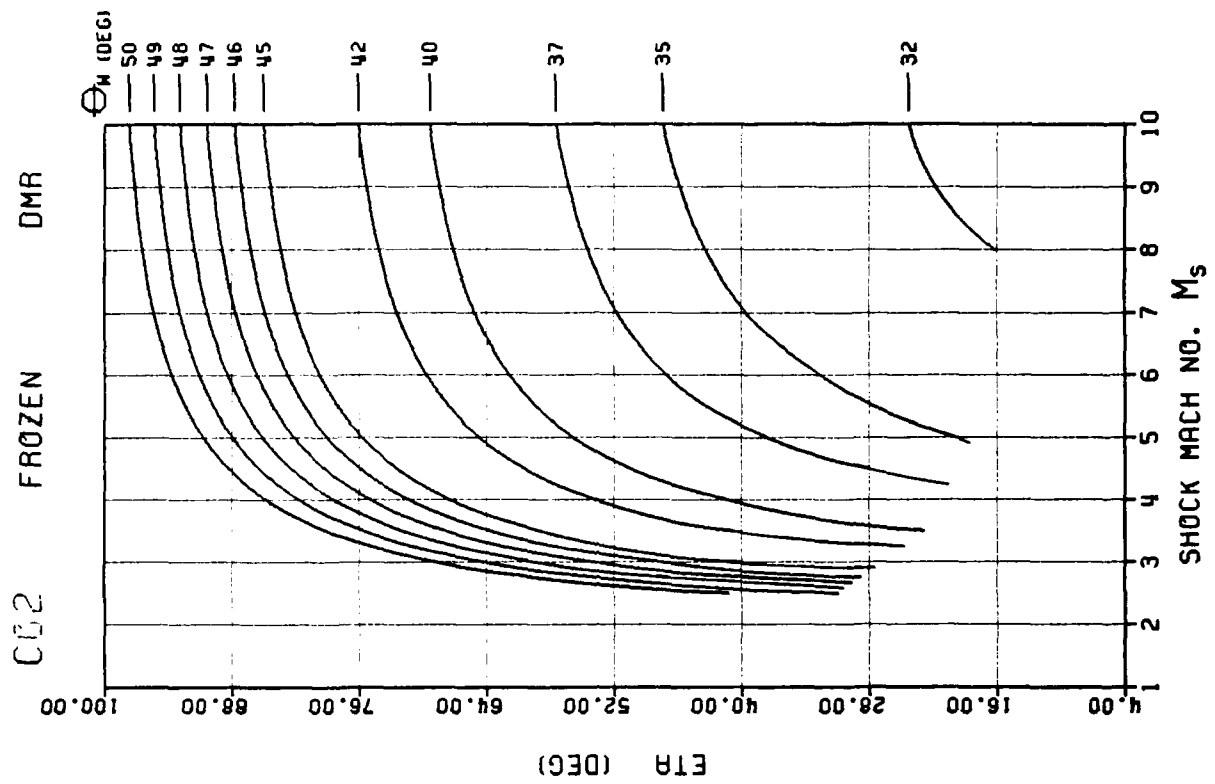
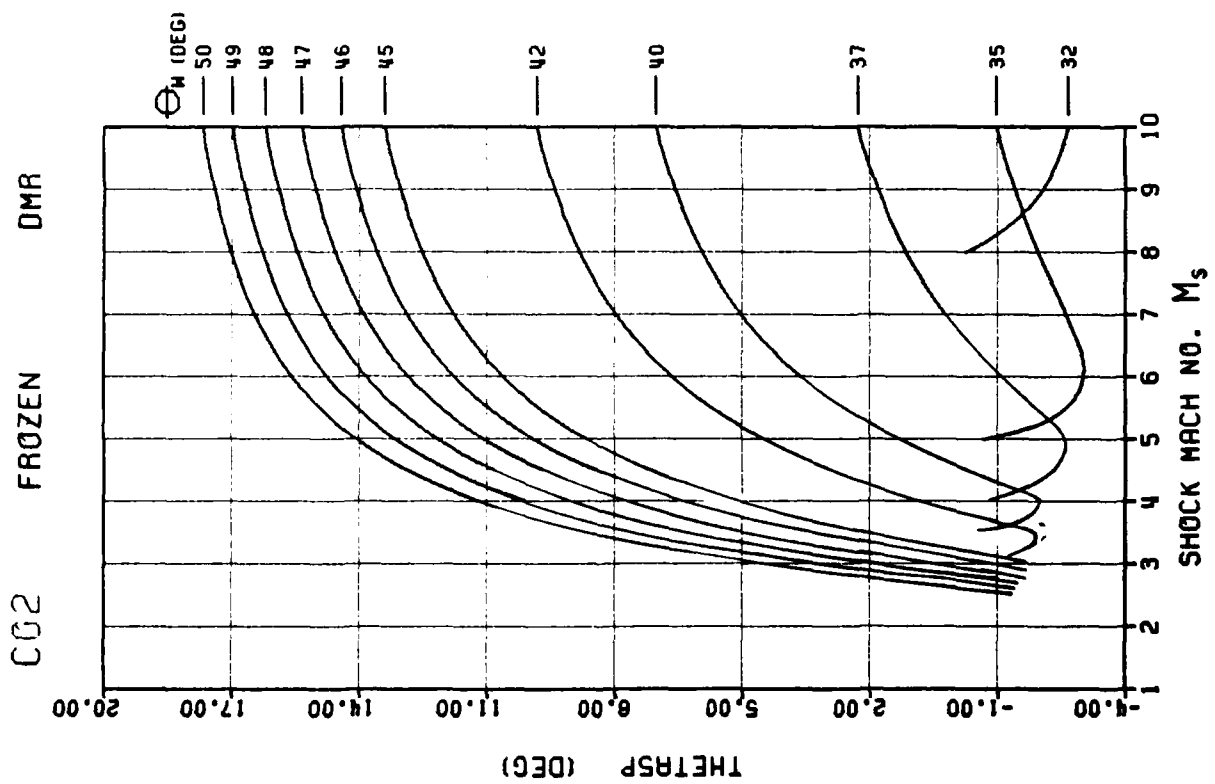


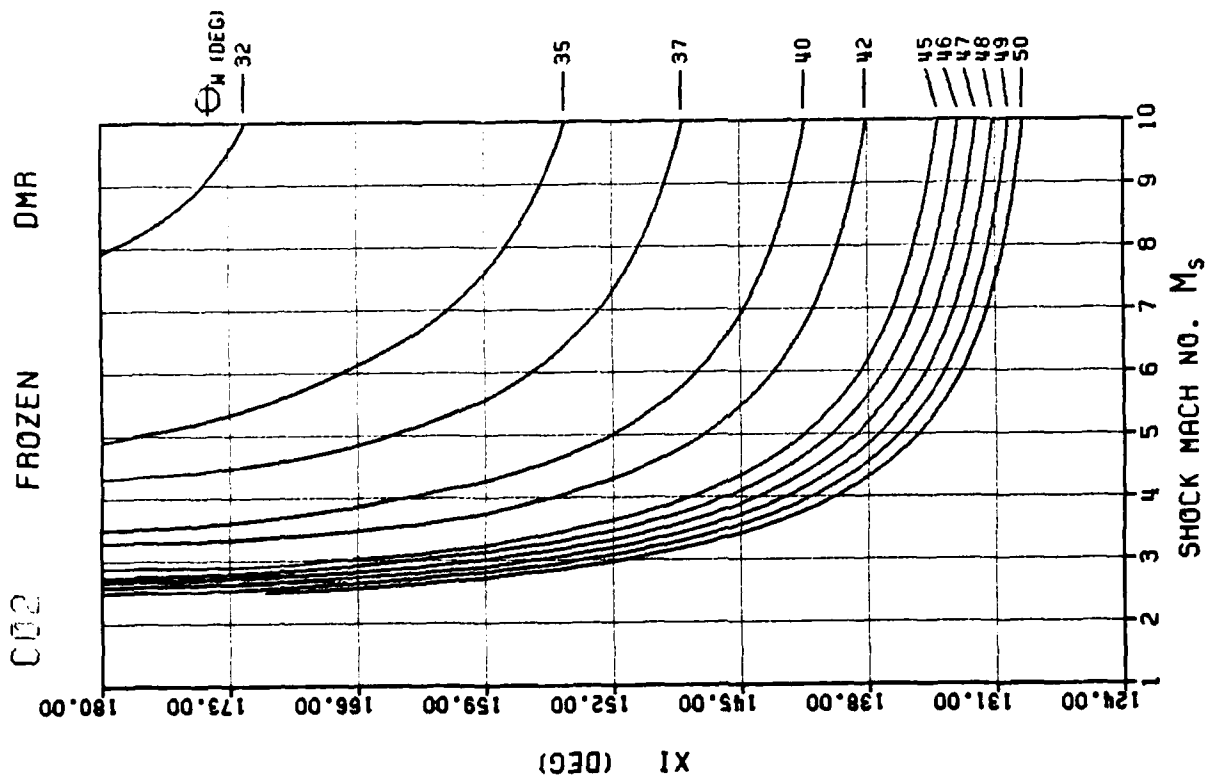




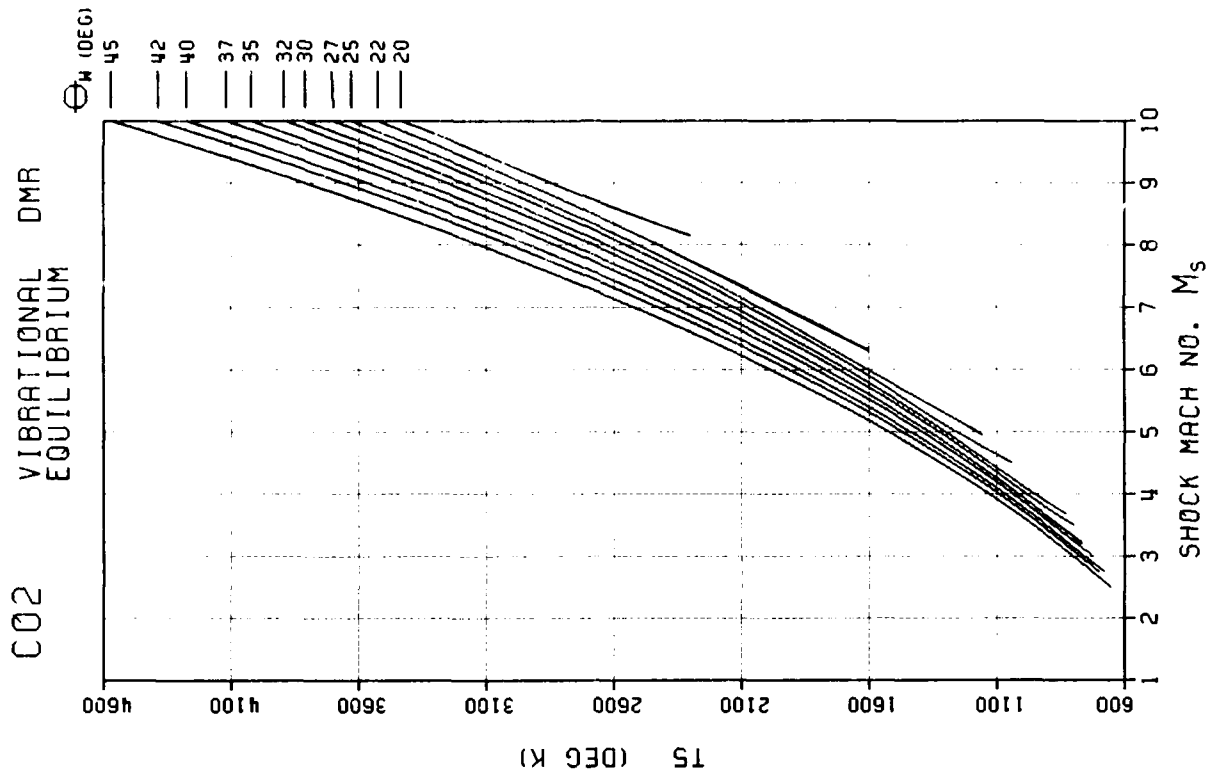
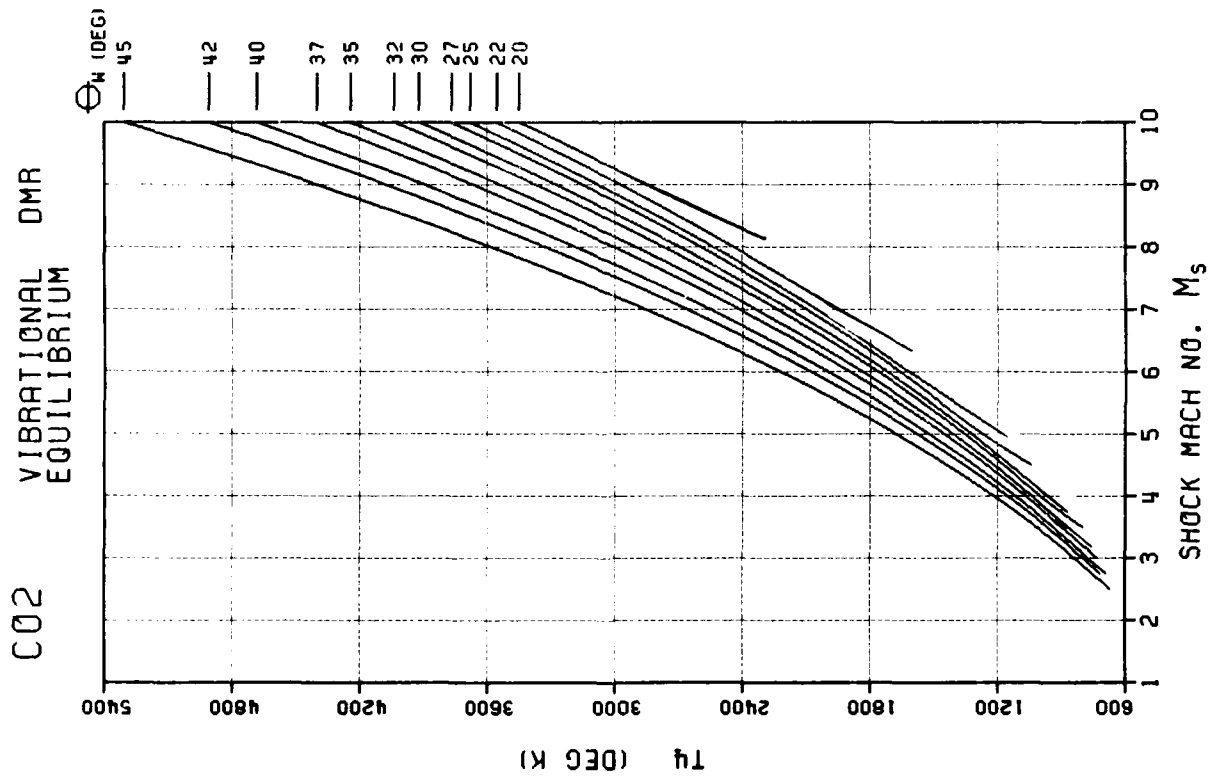


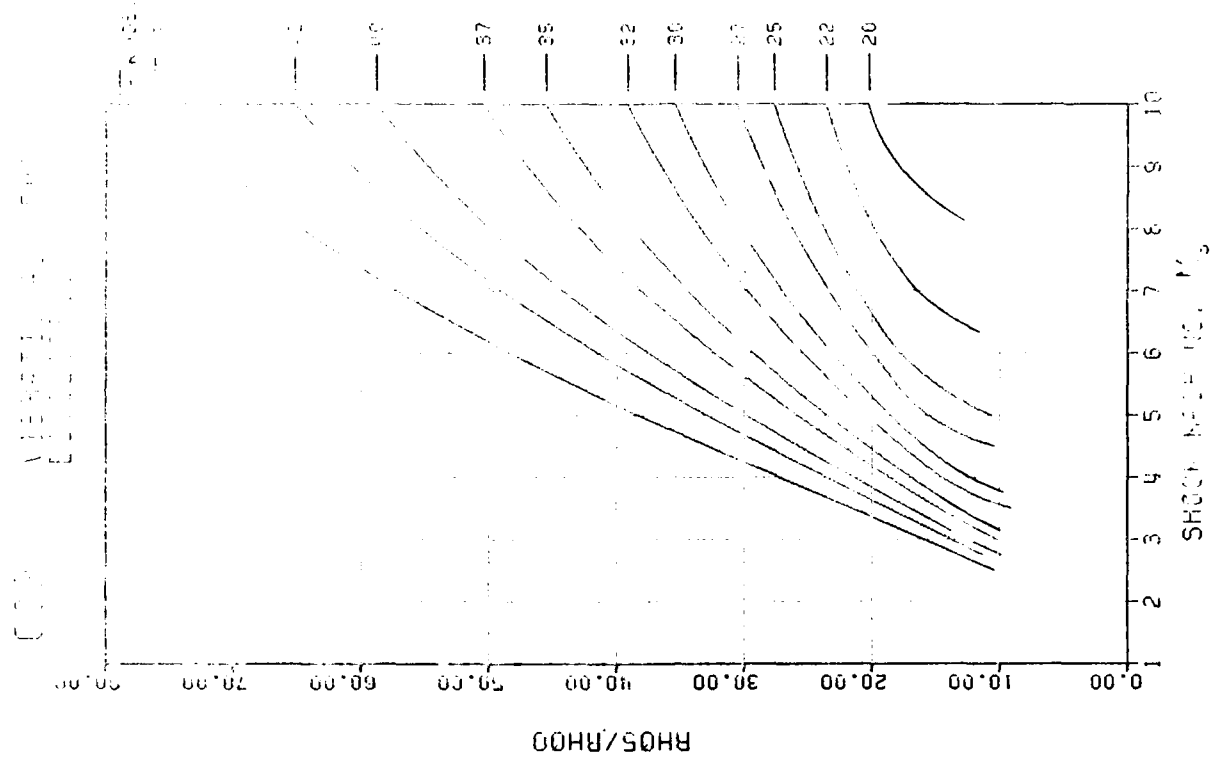
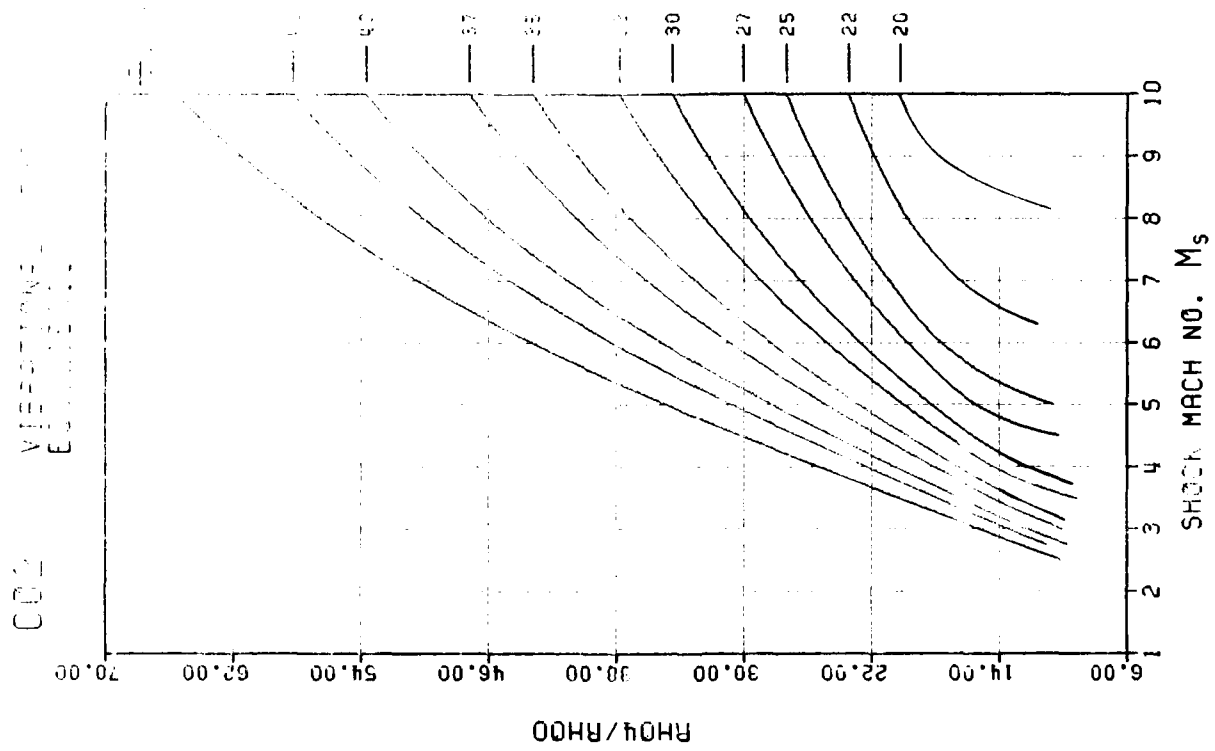


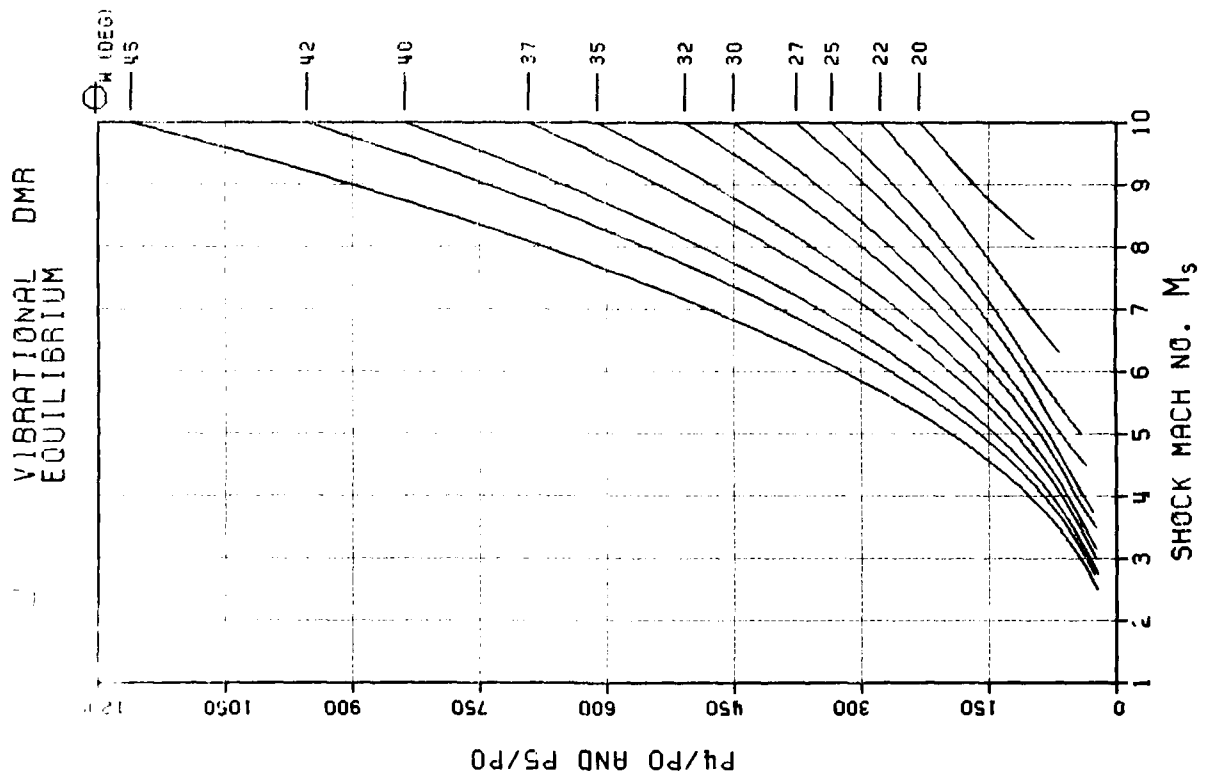
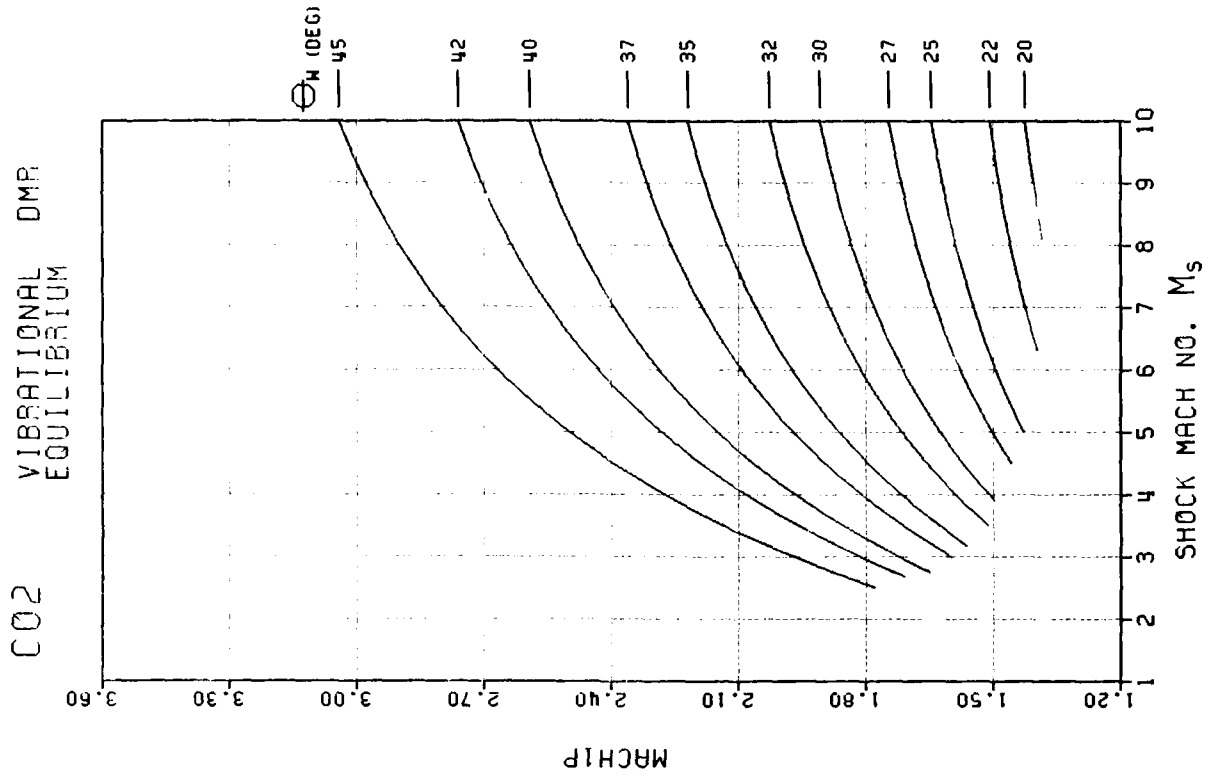


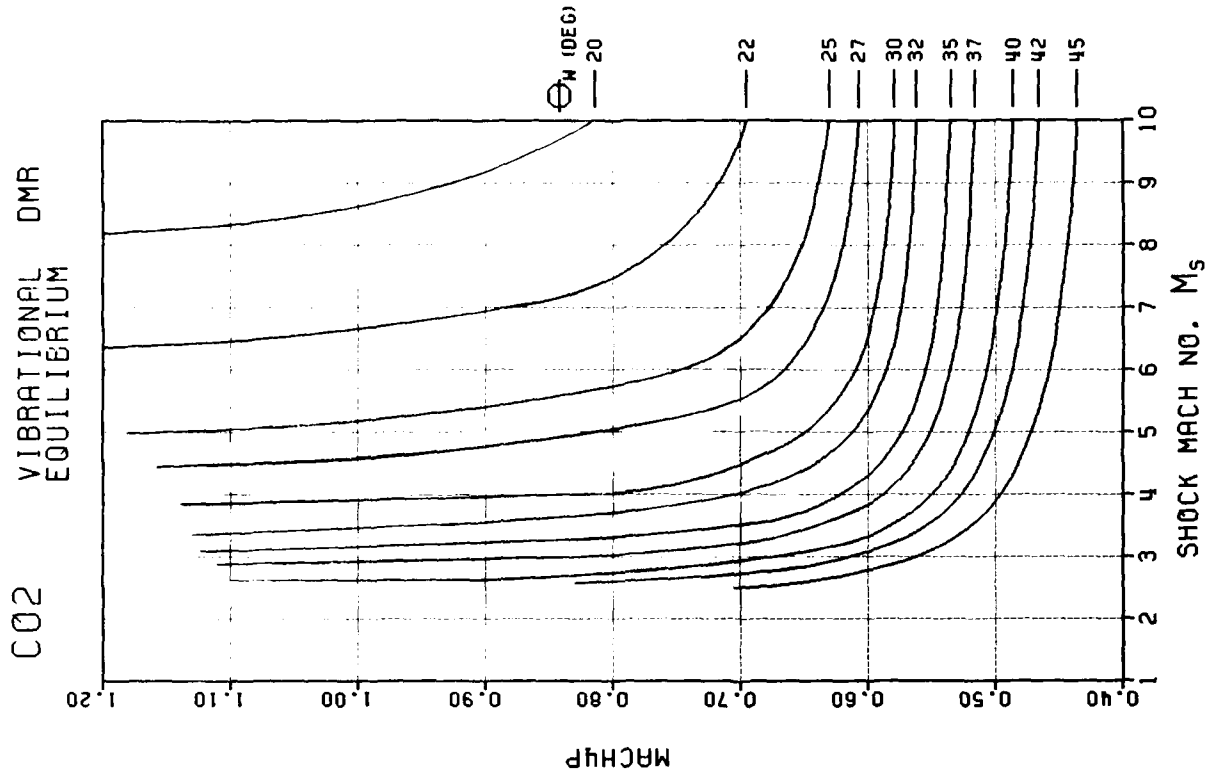
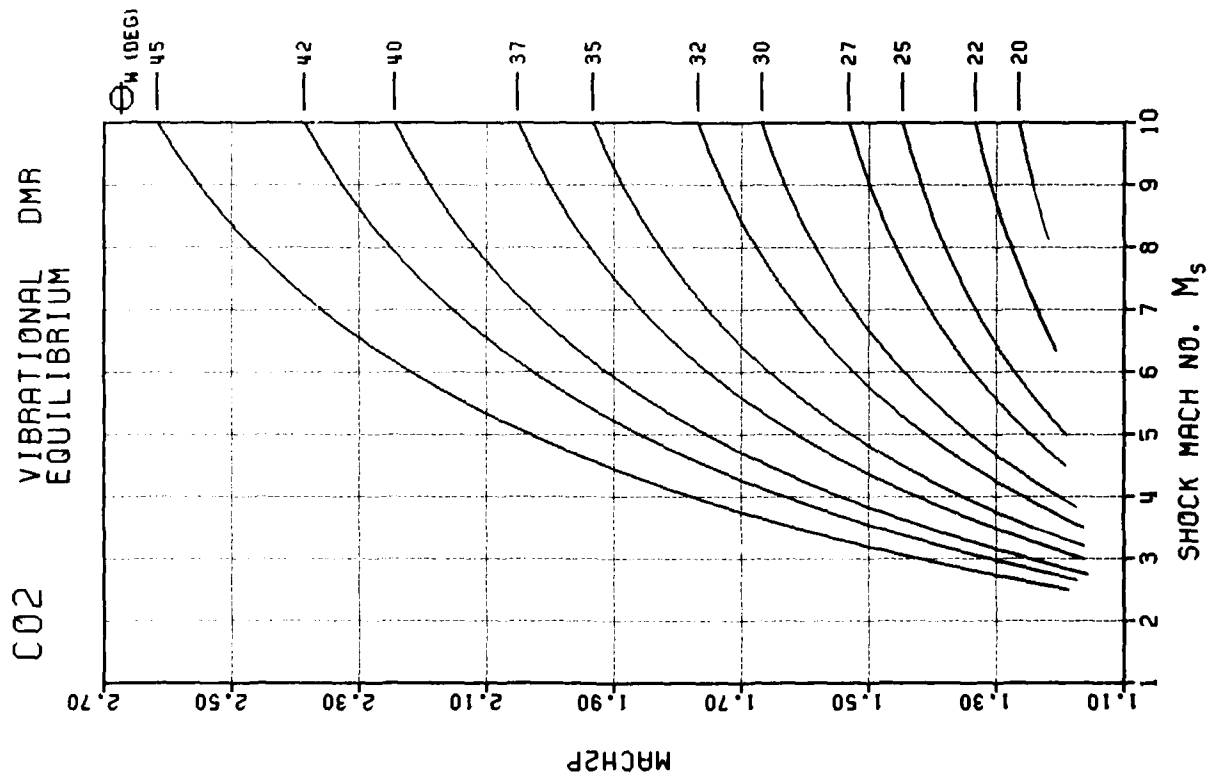


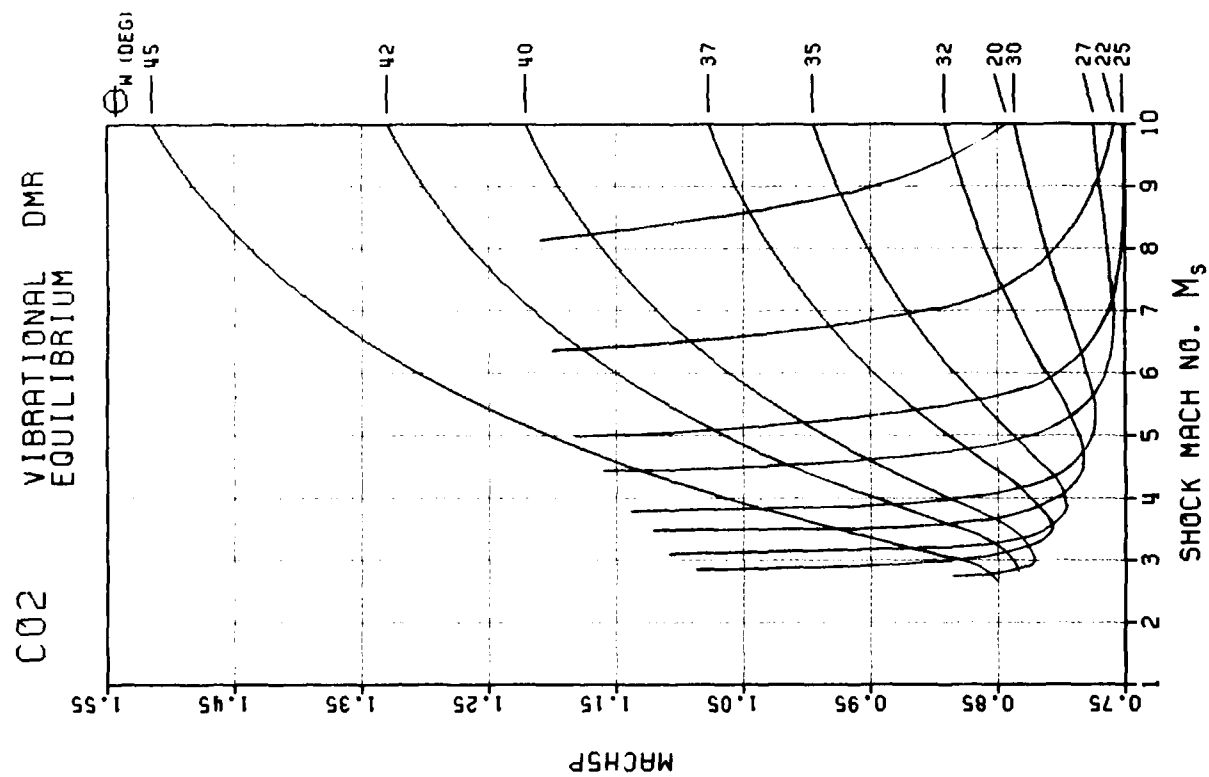
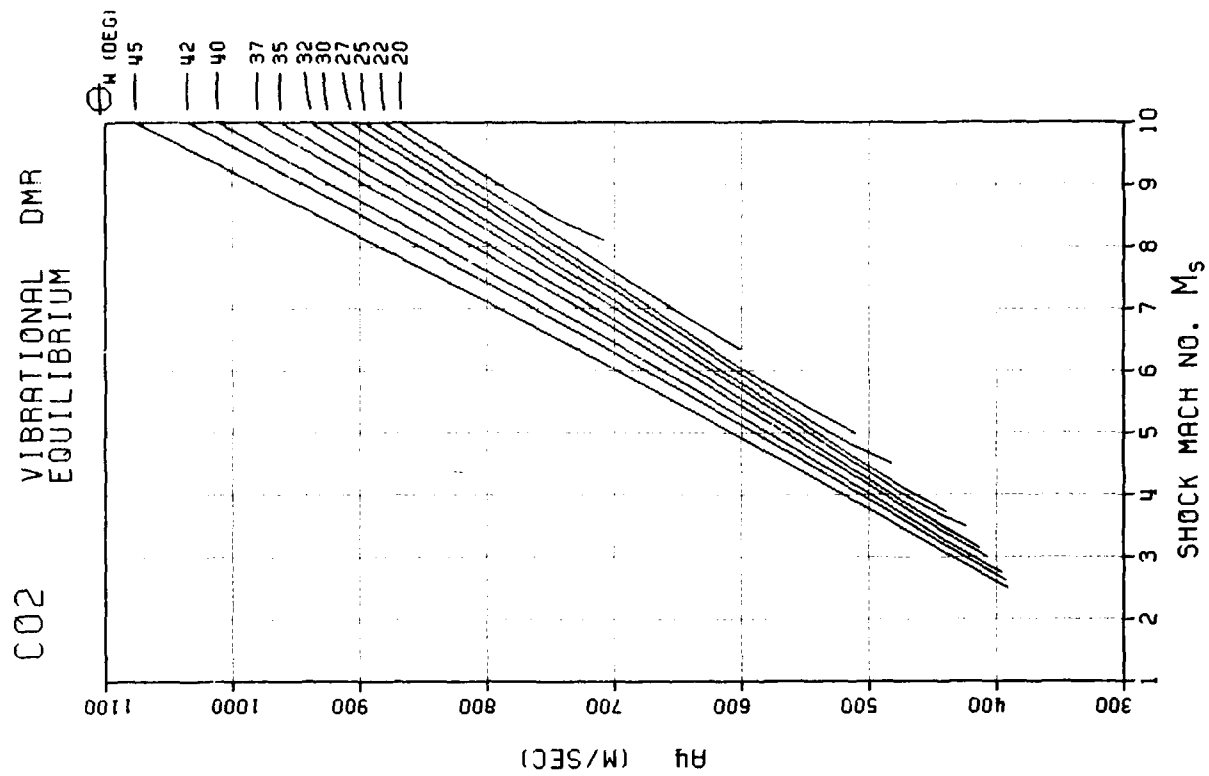
F - 290

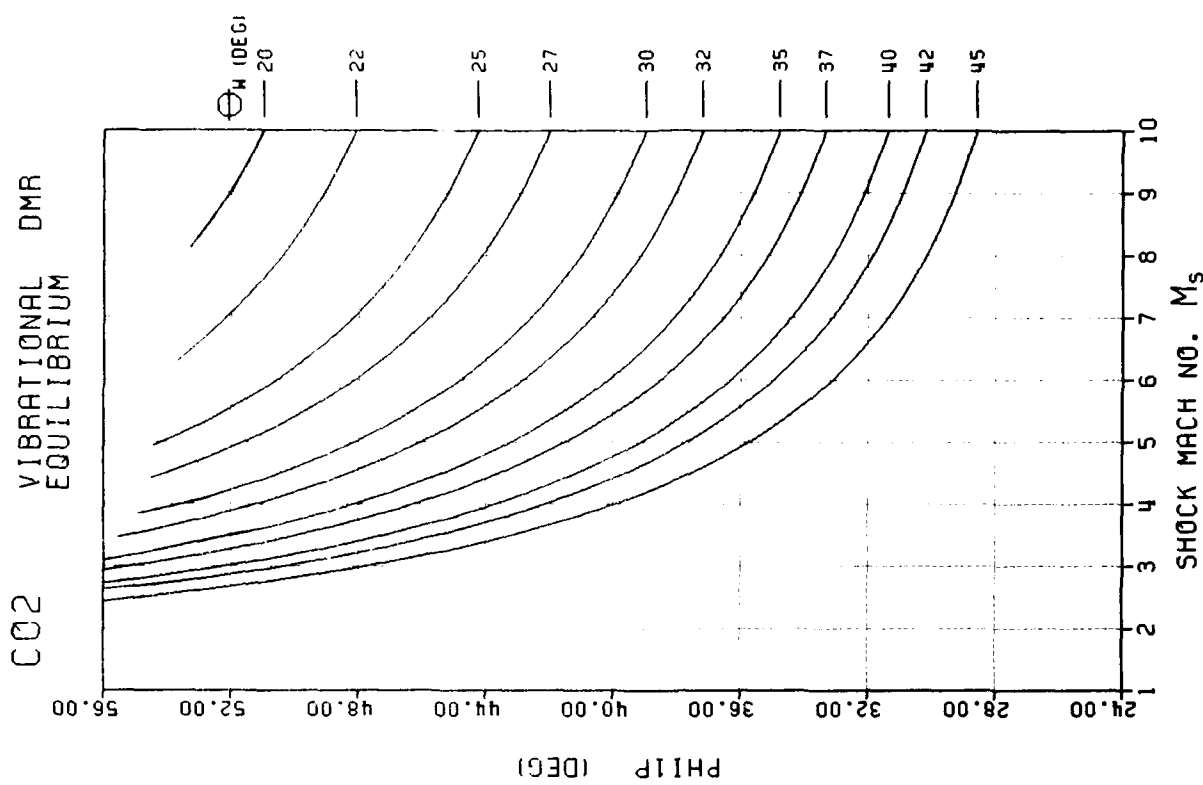
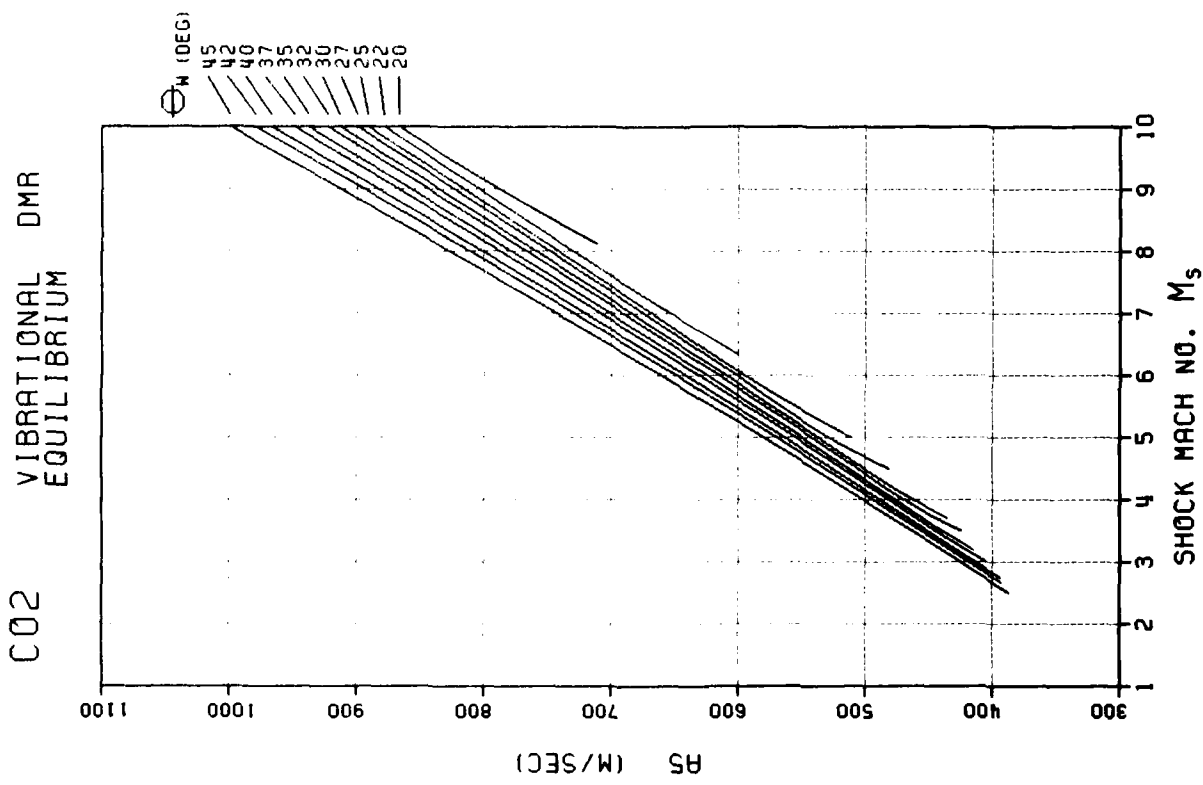


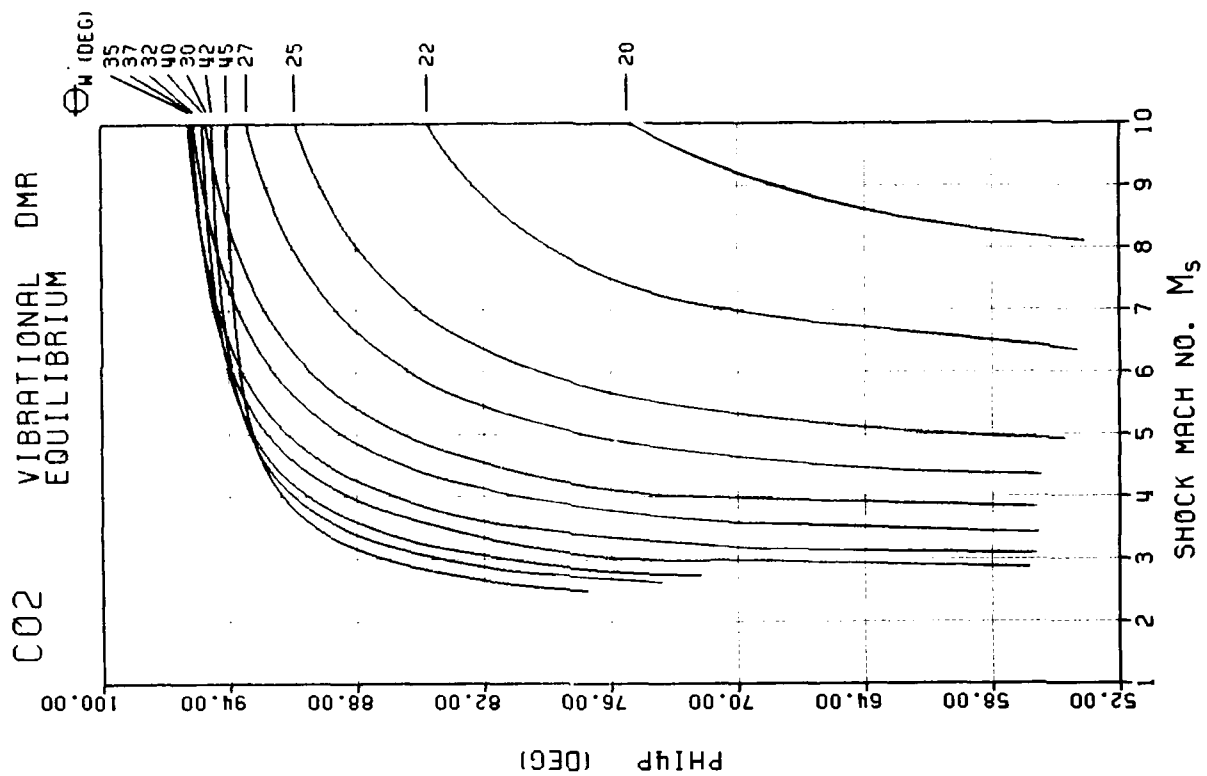
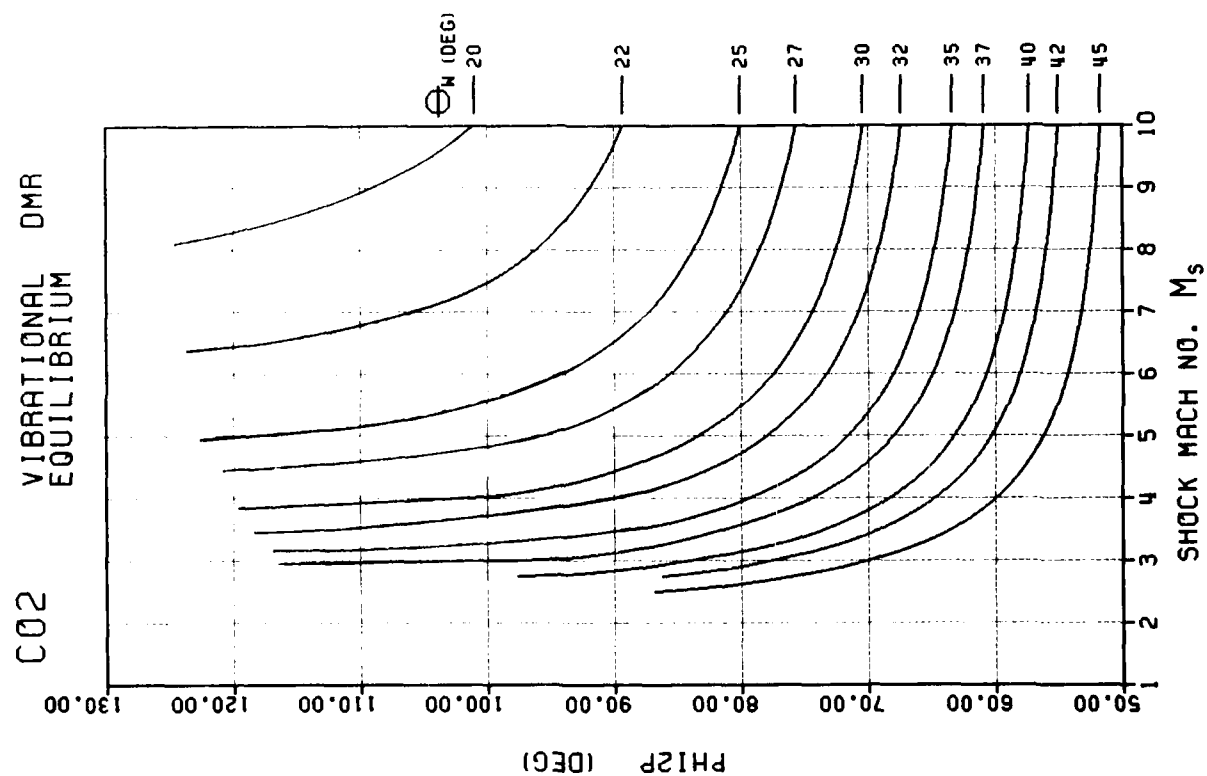


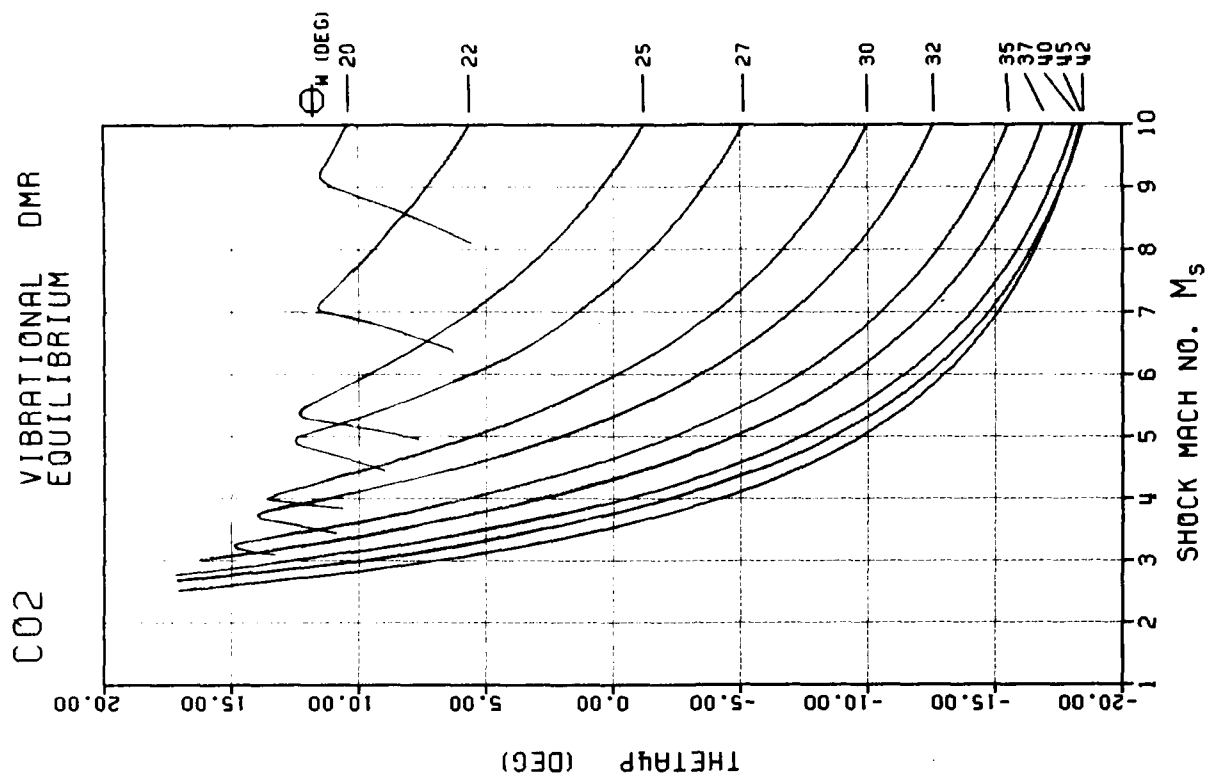
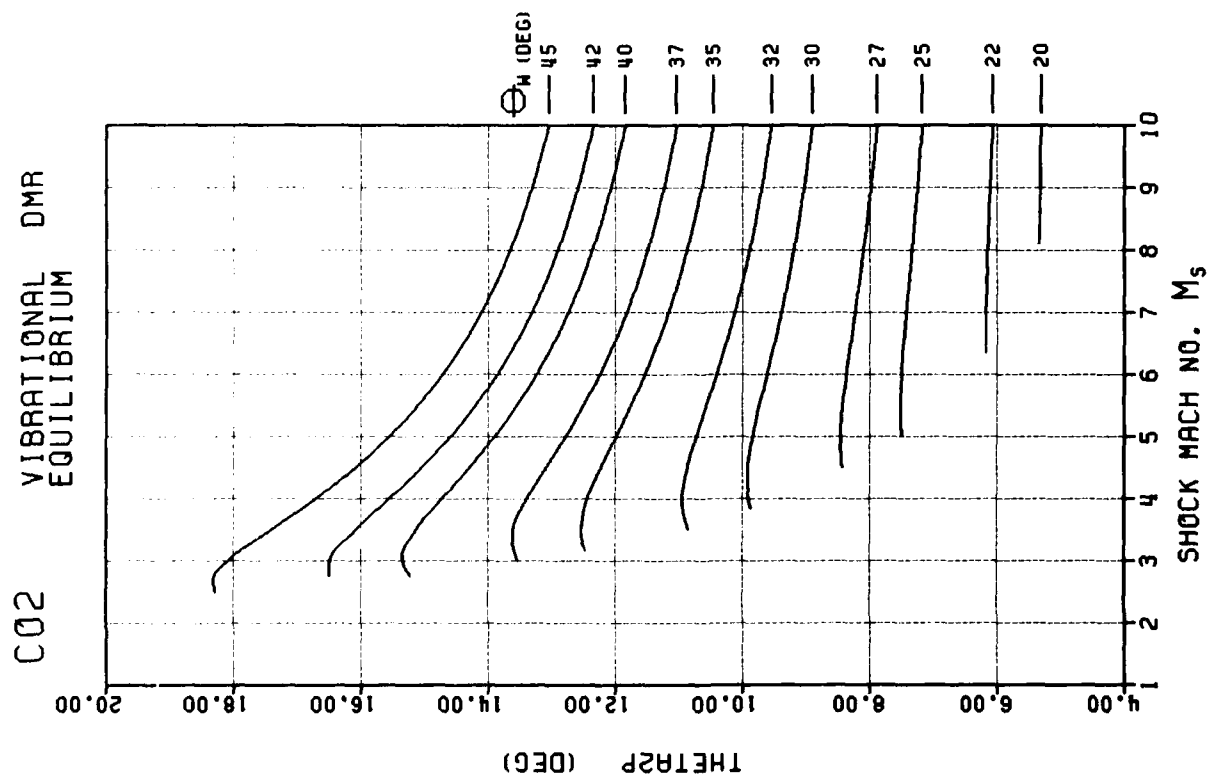


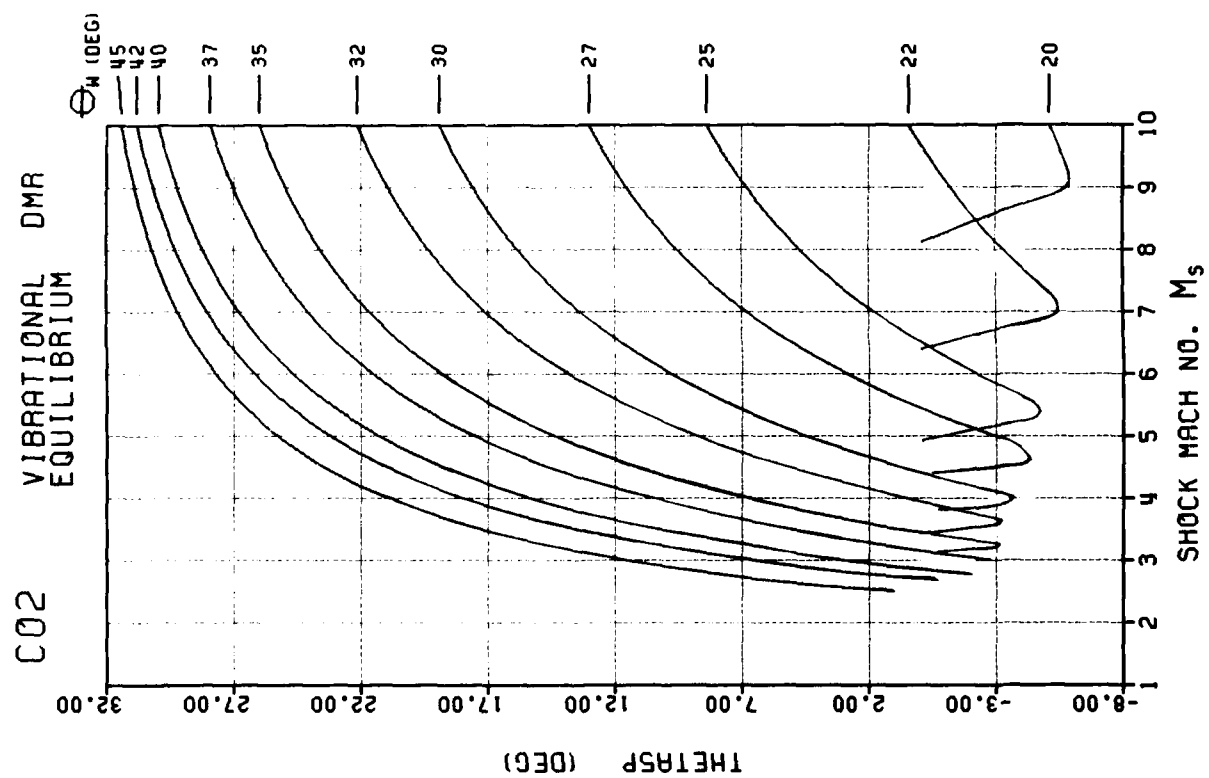
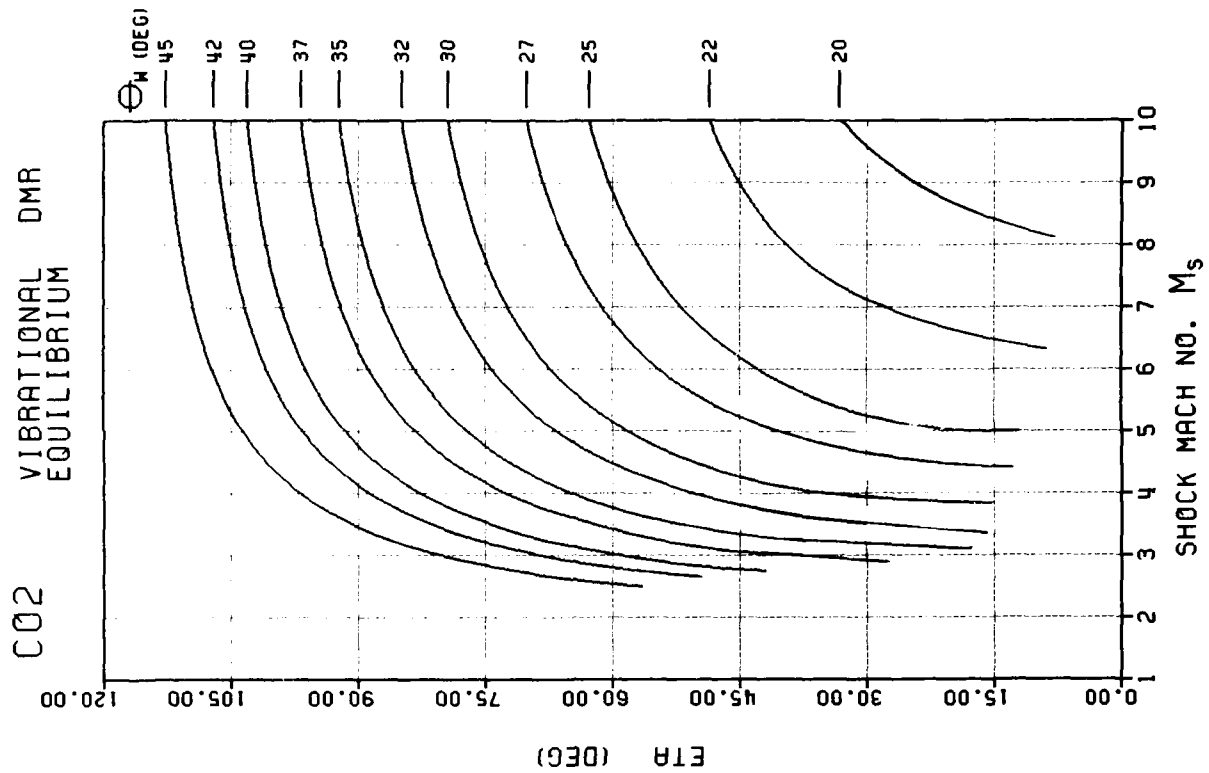


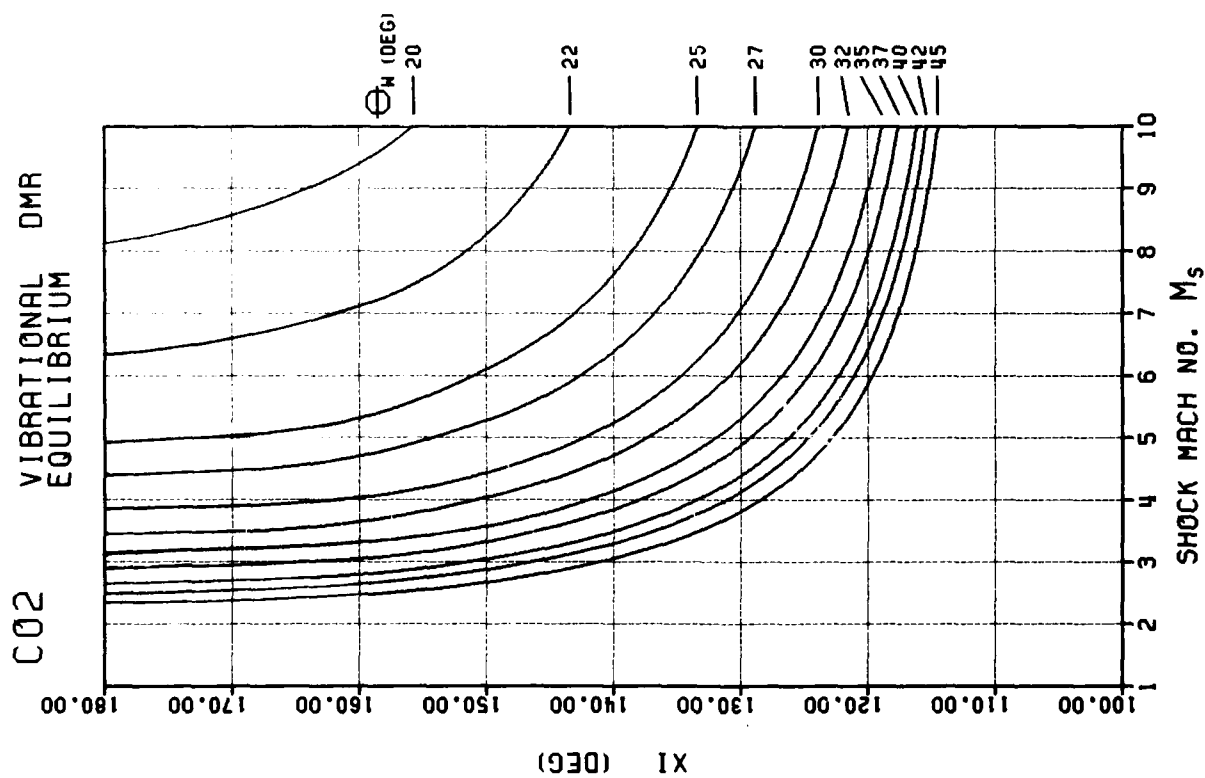




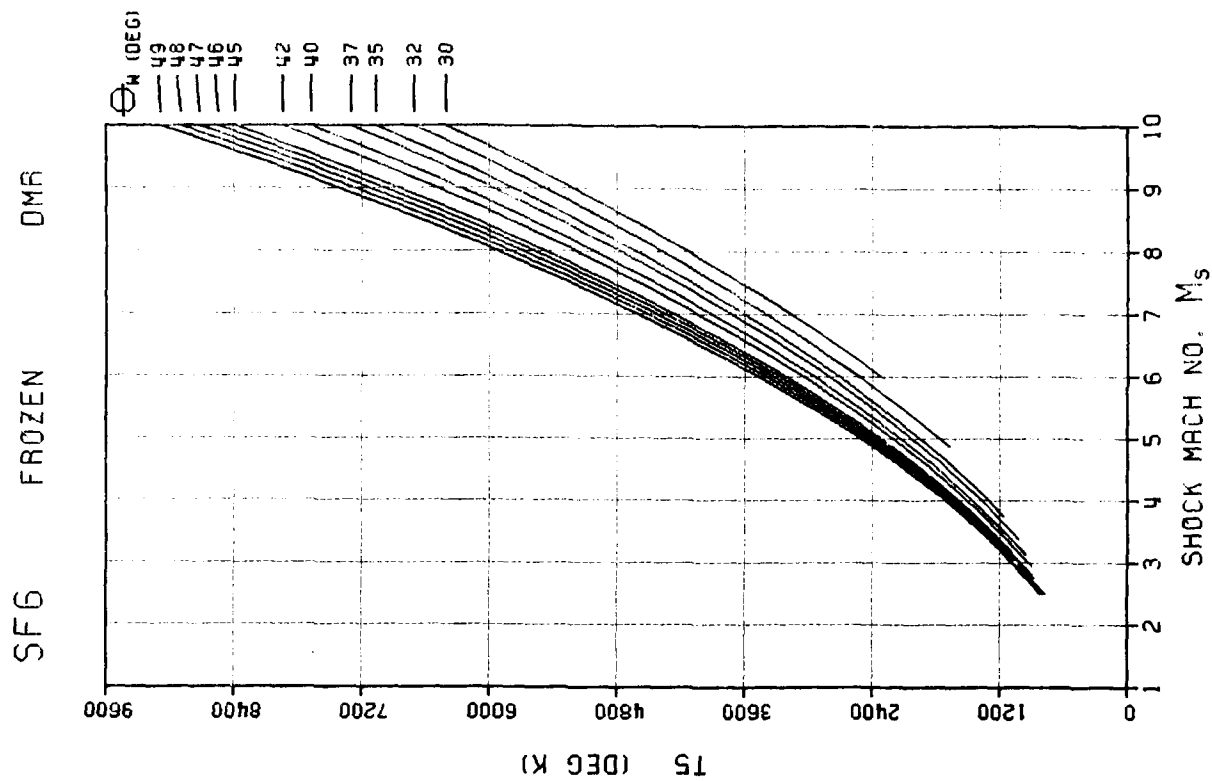
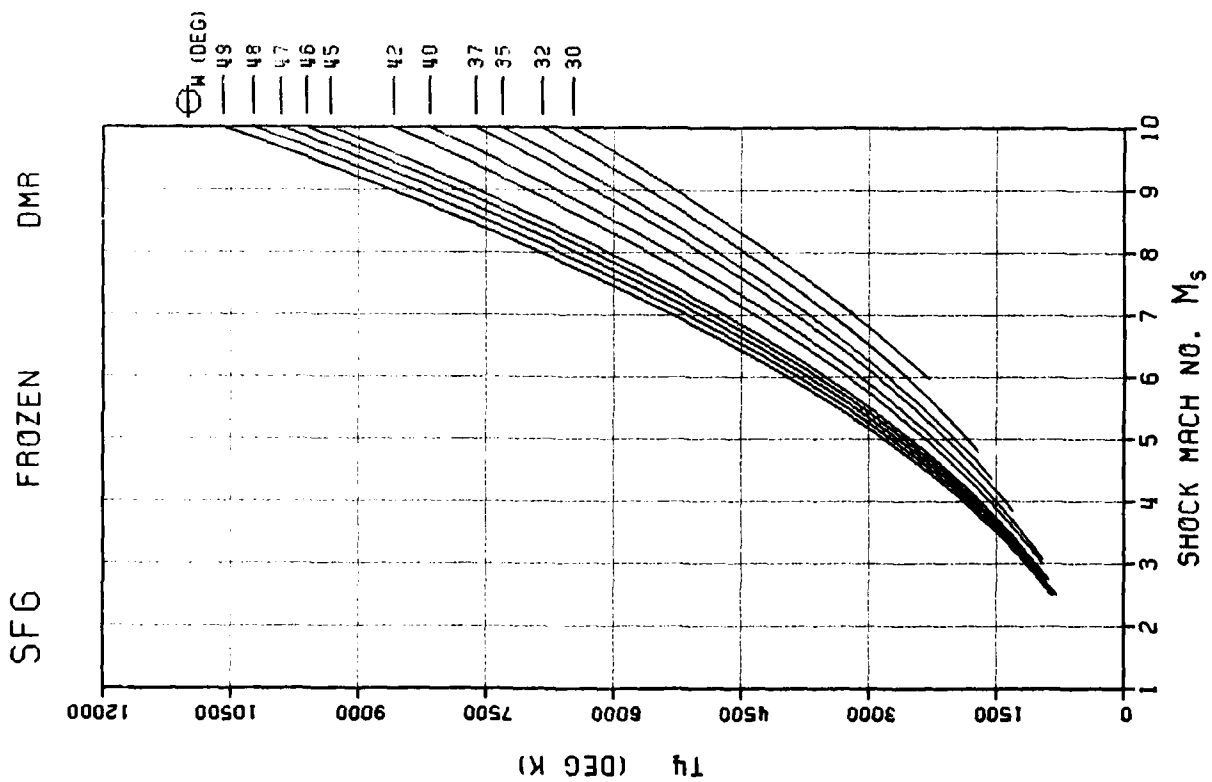


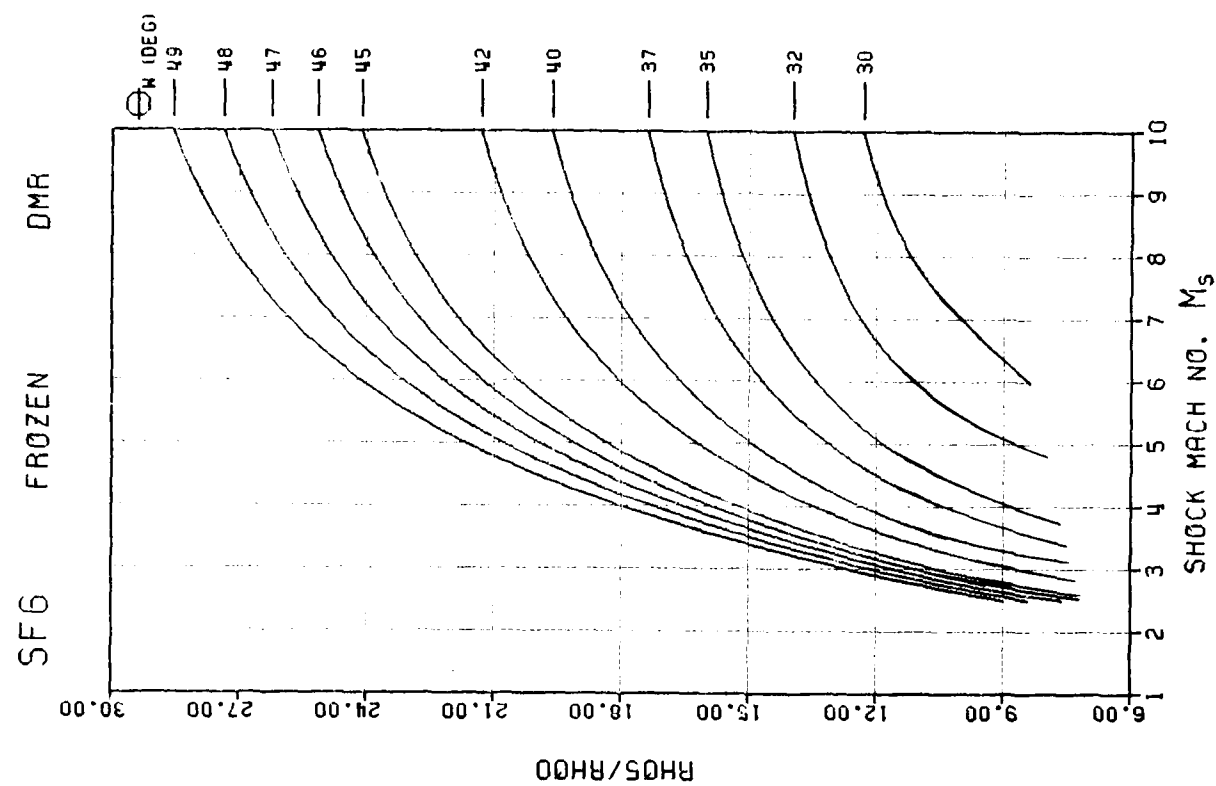
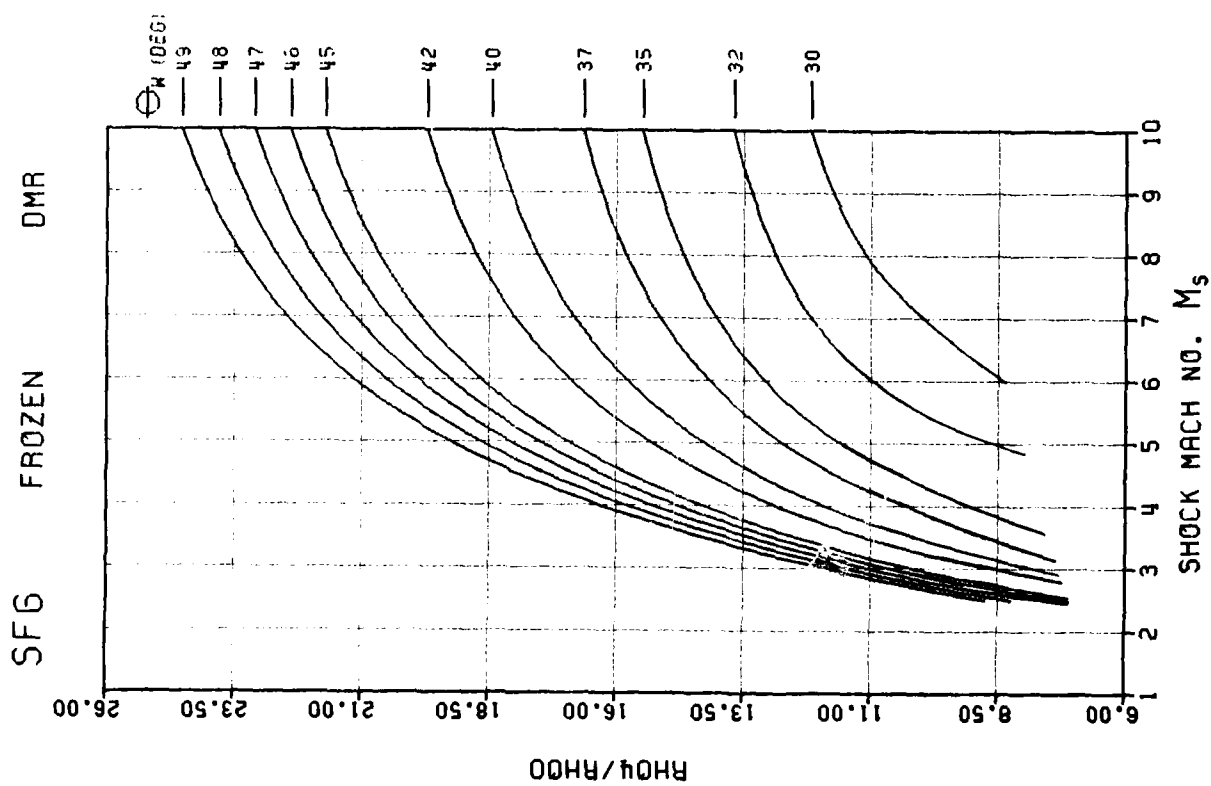


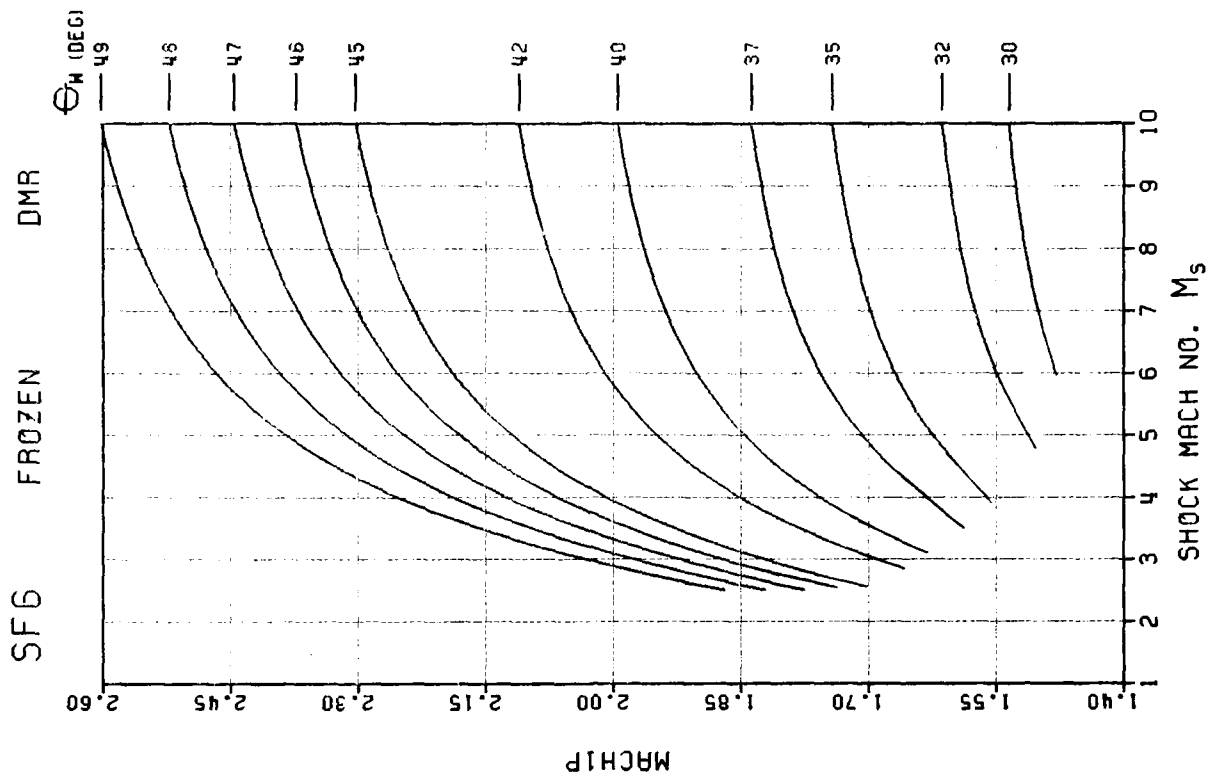
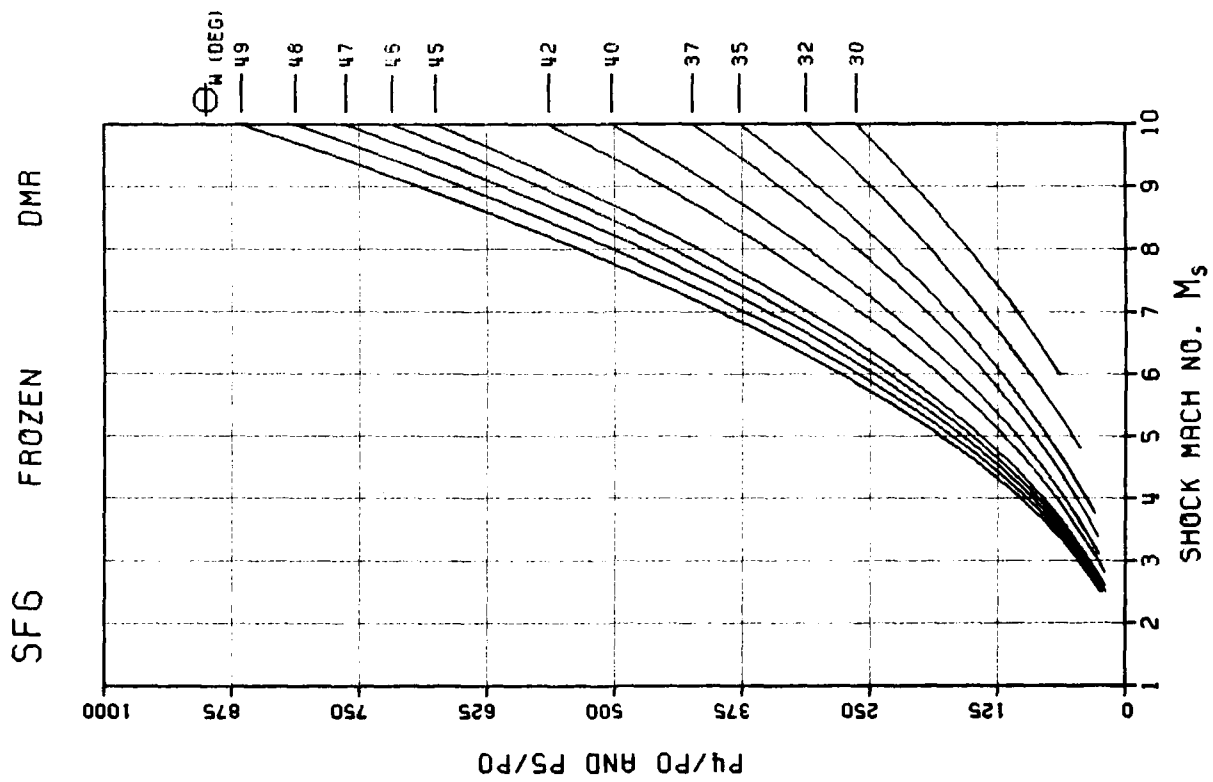


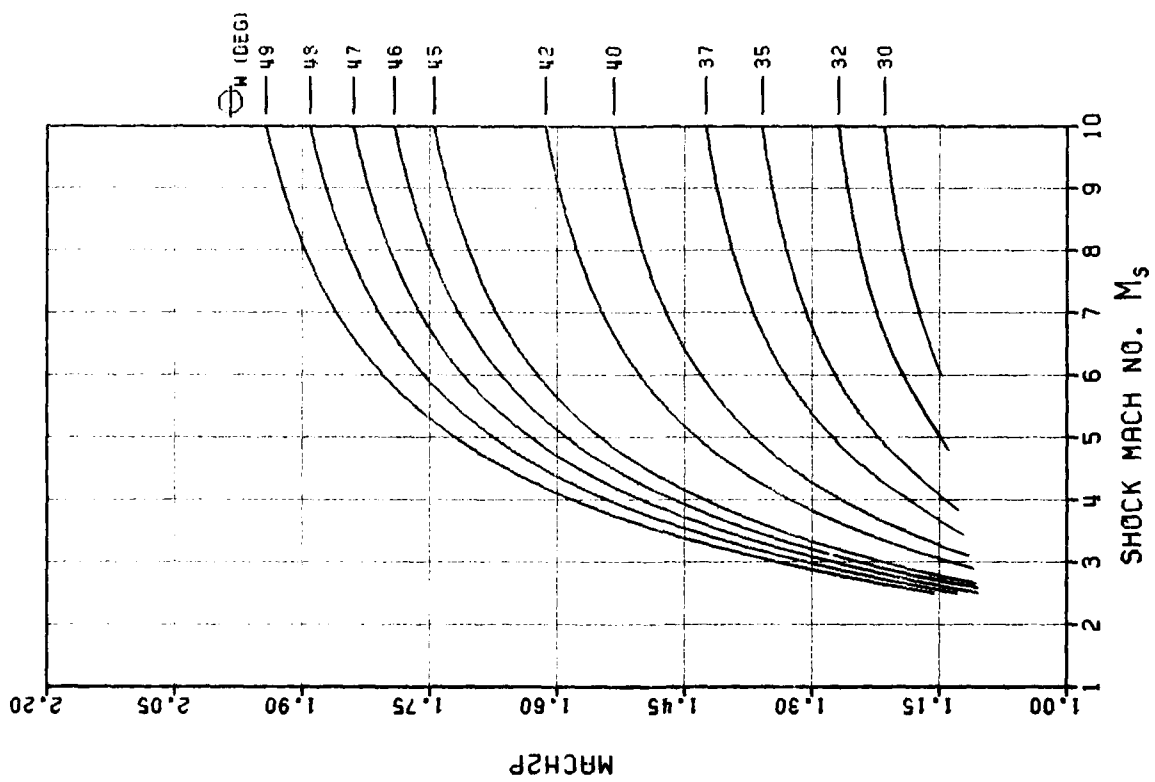
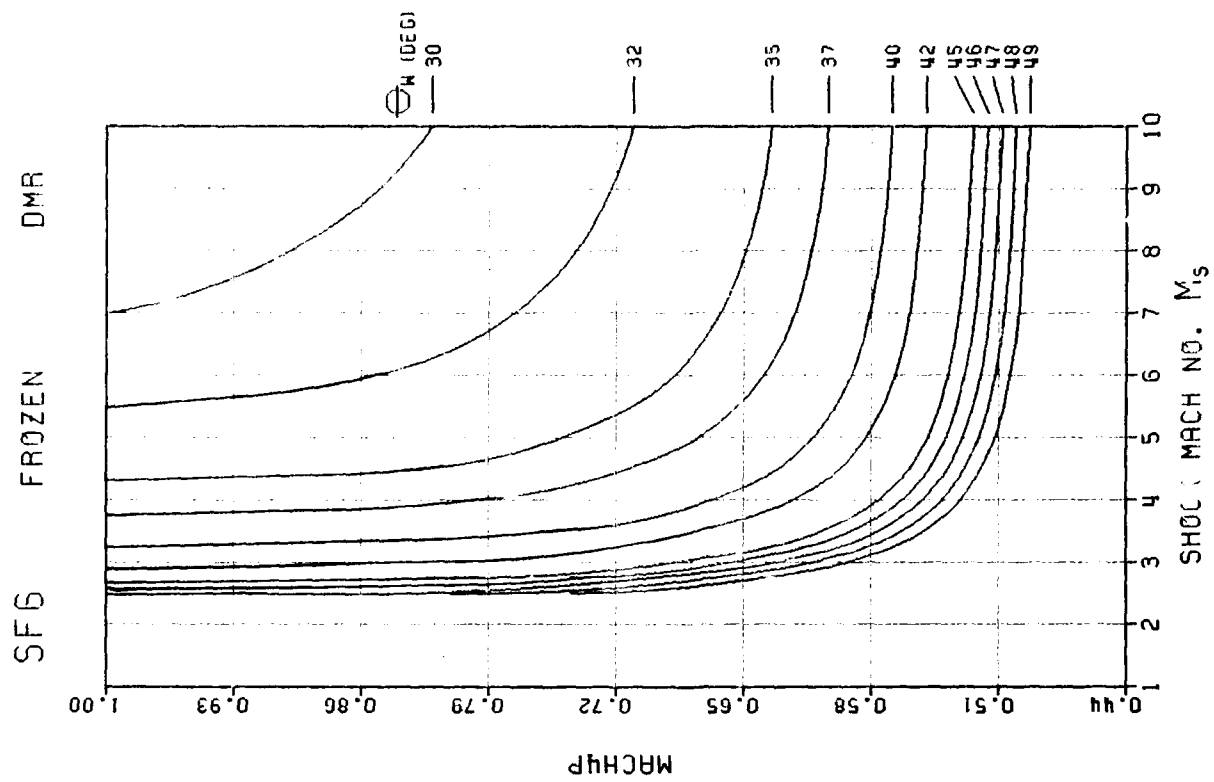


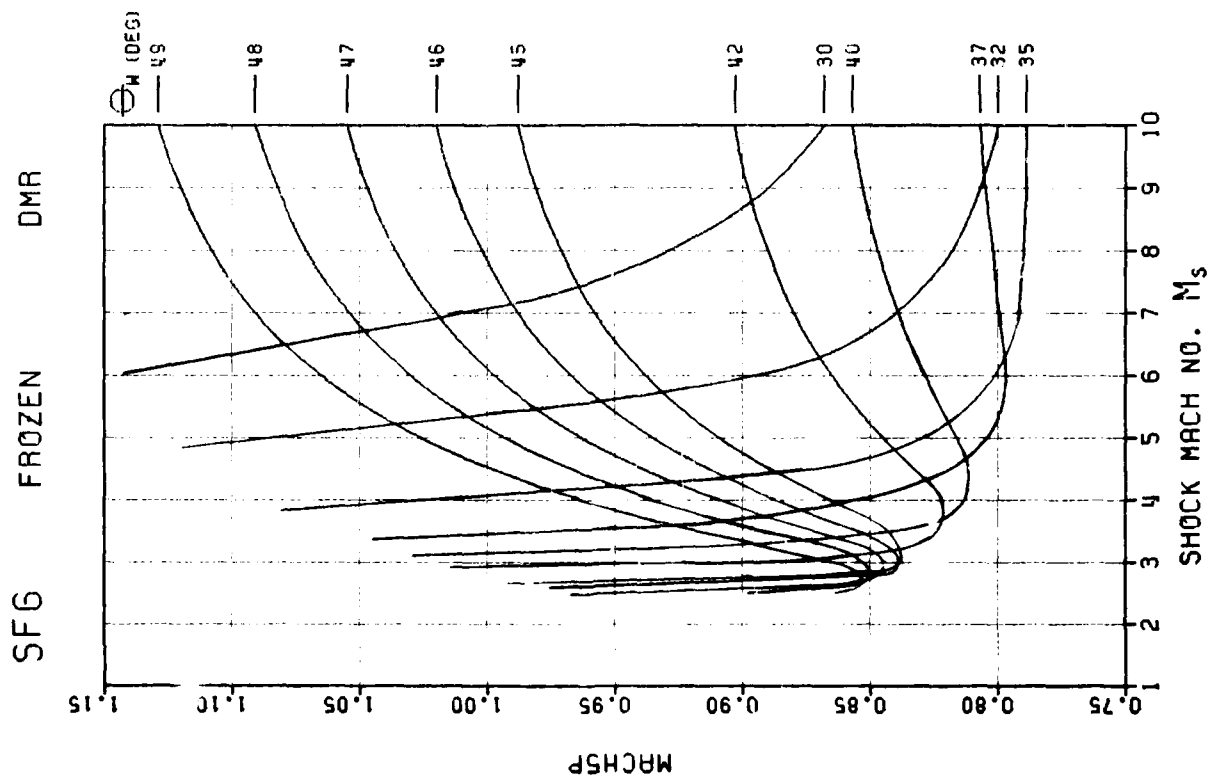
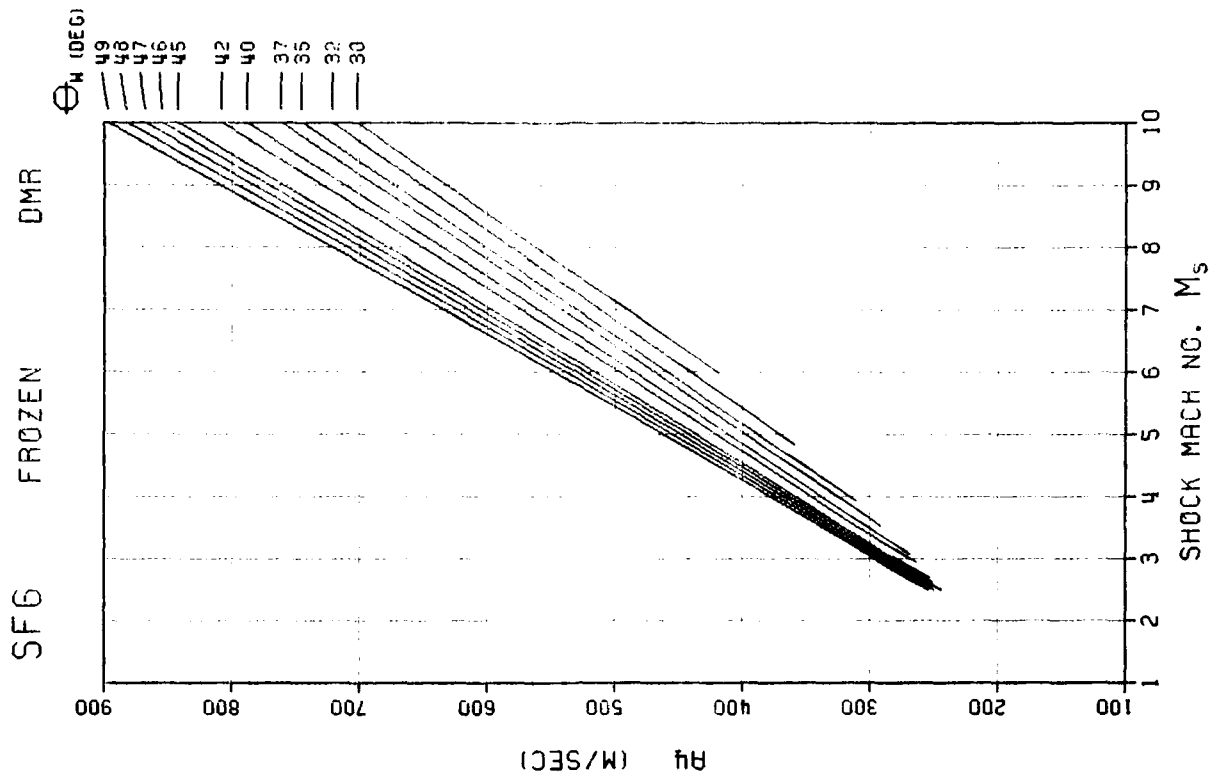
F - 300

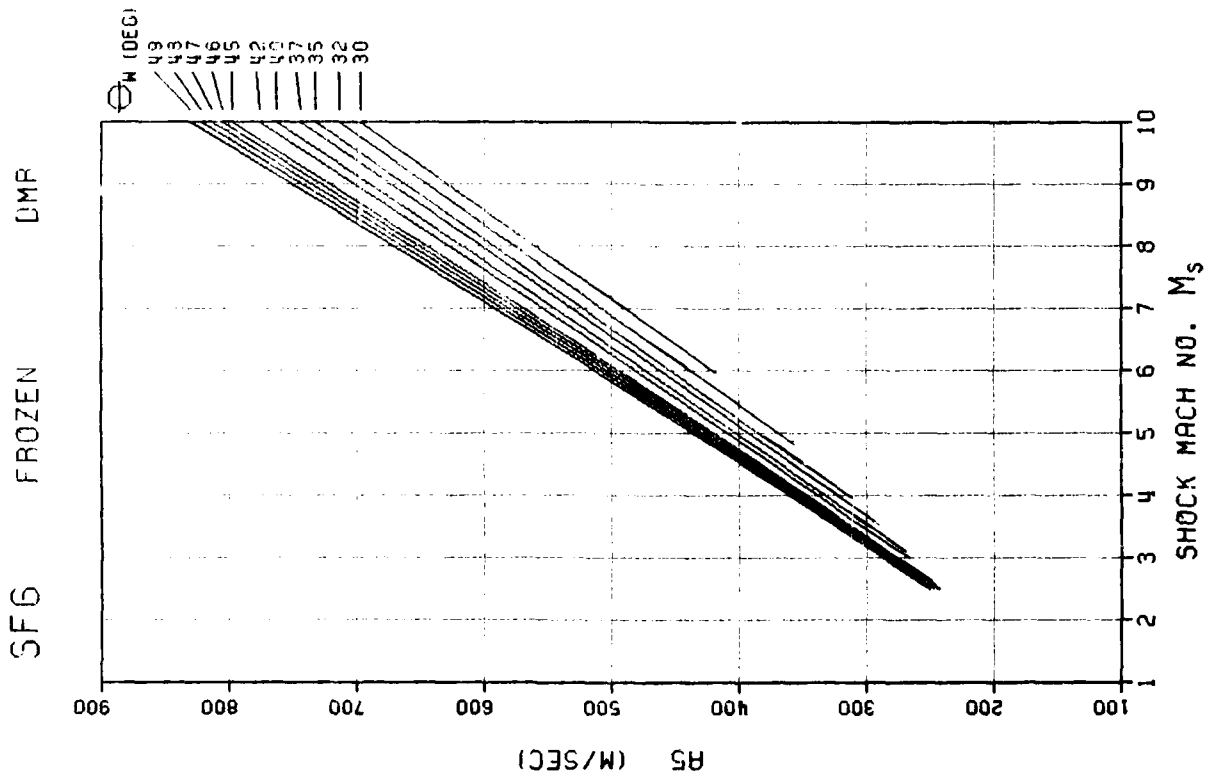
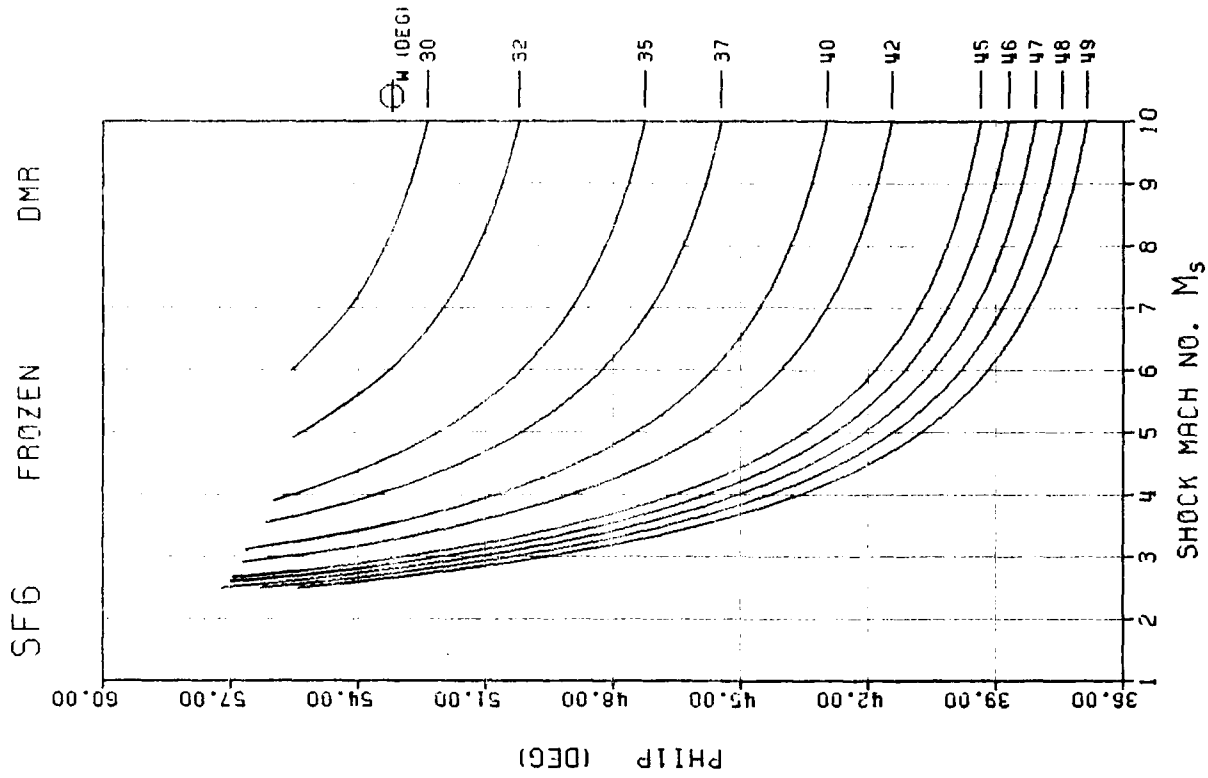












ND-A164 047

TABULAR AND GRAPHICAL SOLUTIONS OF REGULAR AND MACH REFLECTIONS IN PSEUDO- (U) TORONTO UNIV DONMISVIE (ONTARIO) INST FOR AEROSPACE STUDIES T C HU ET AL.

3/3

UNCLASSIFIED

JUN 85 UTIAS-283-PT-2 AFOSR-TR-85-1231 F/G 20/4

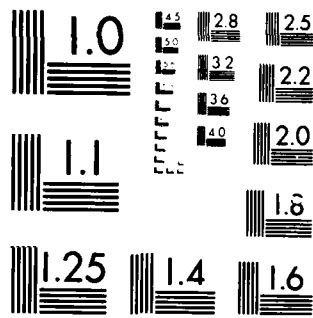
F/G 20/4

NL-

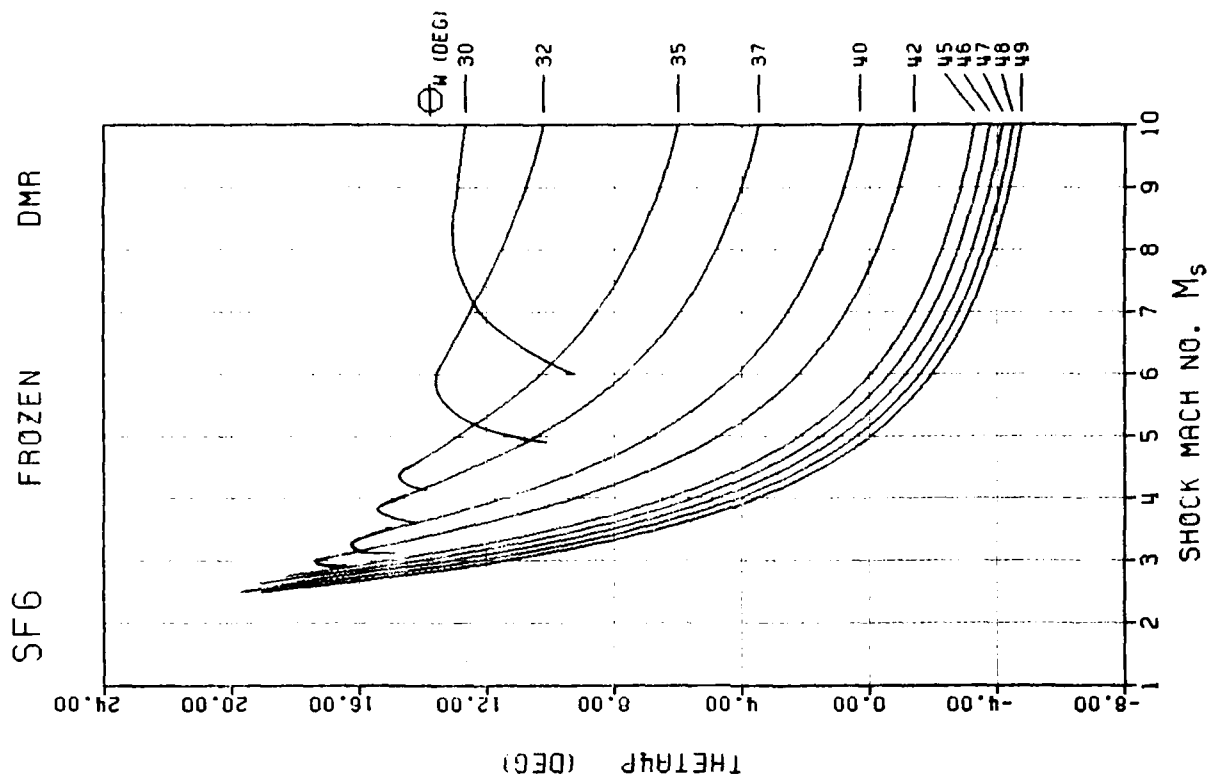
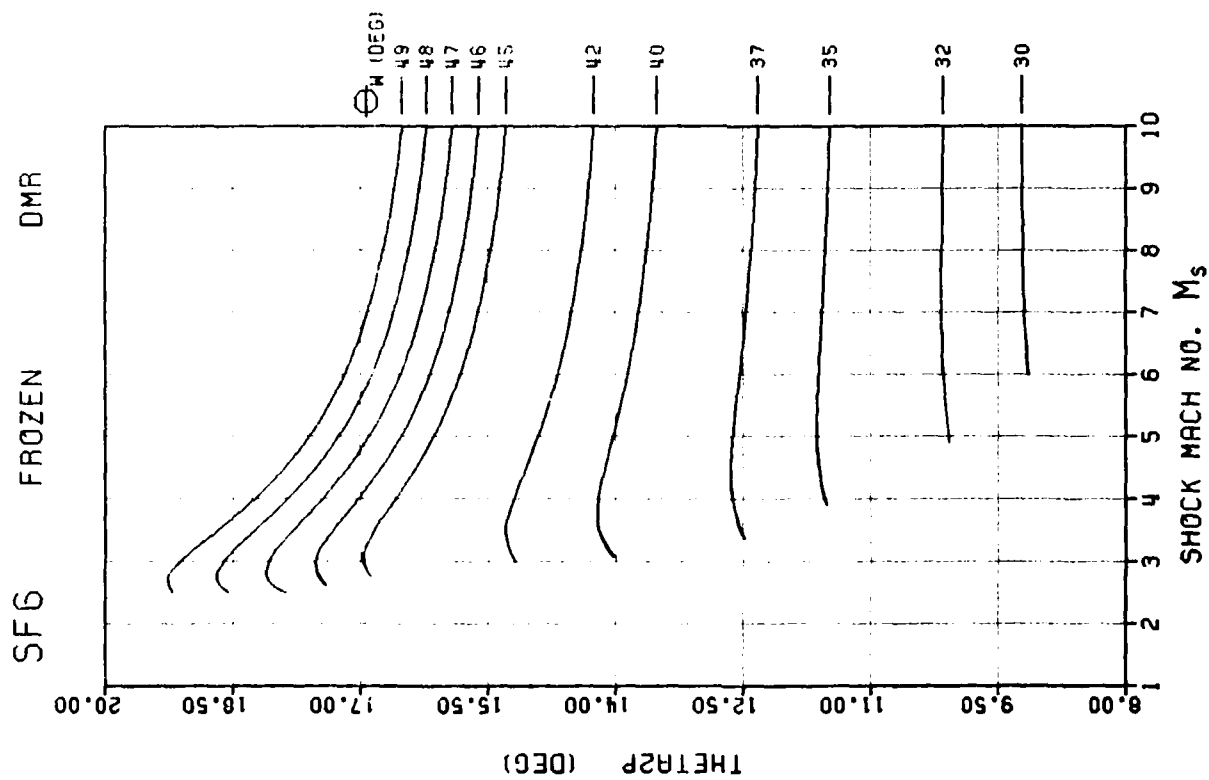
END

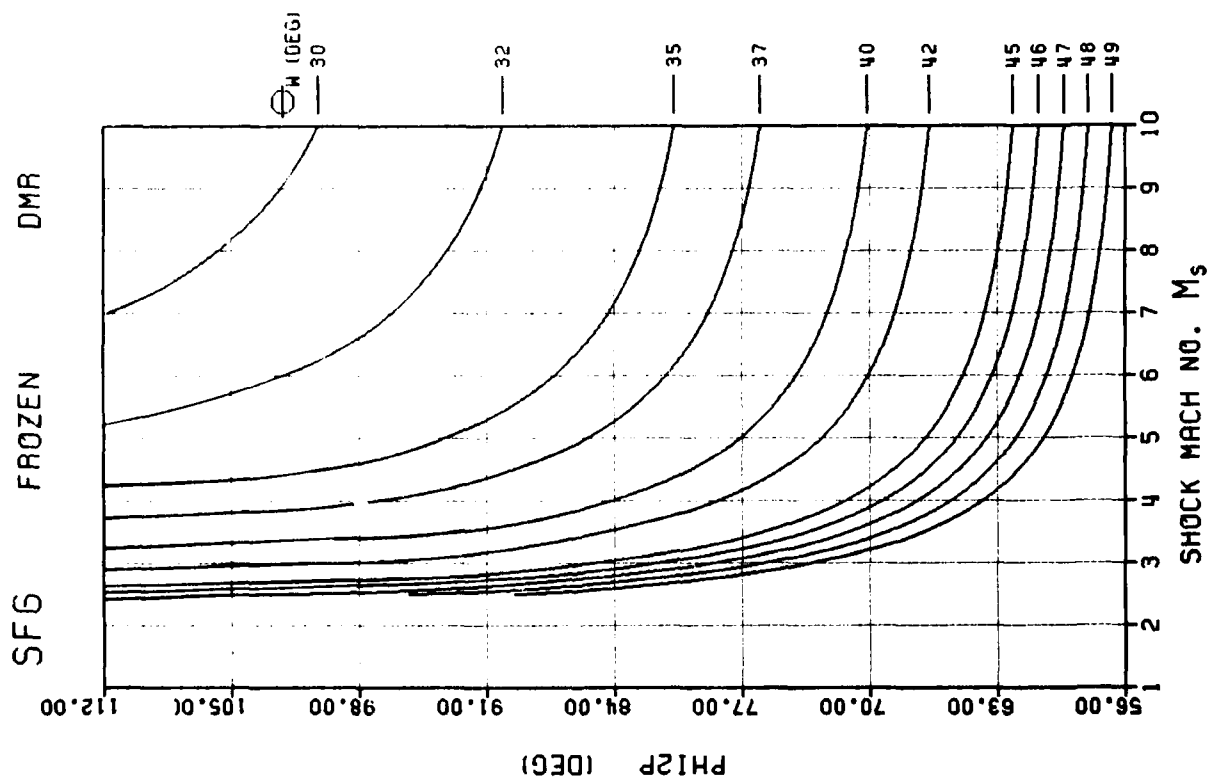
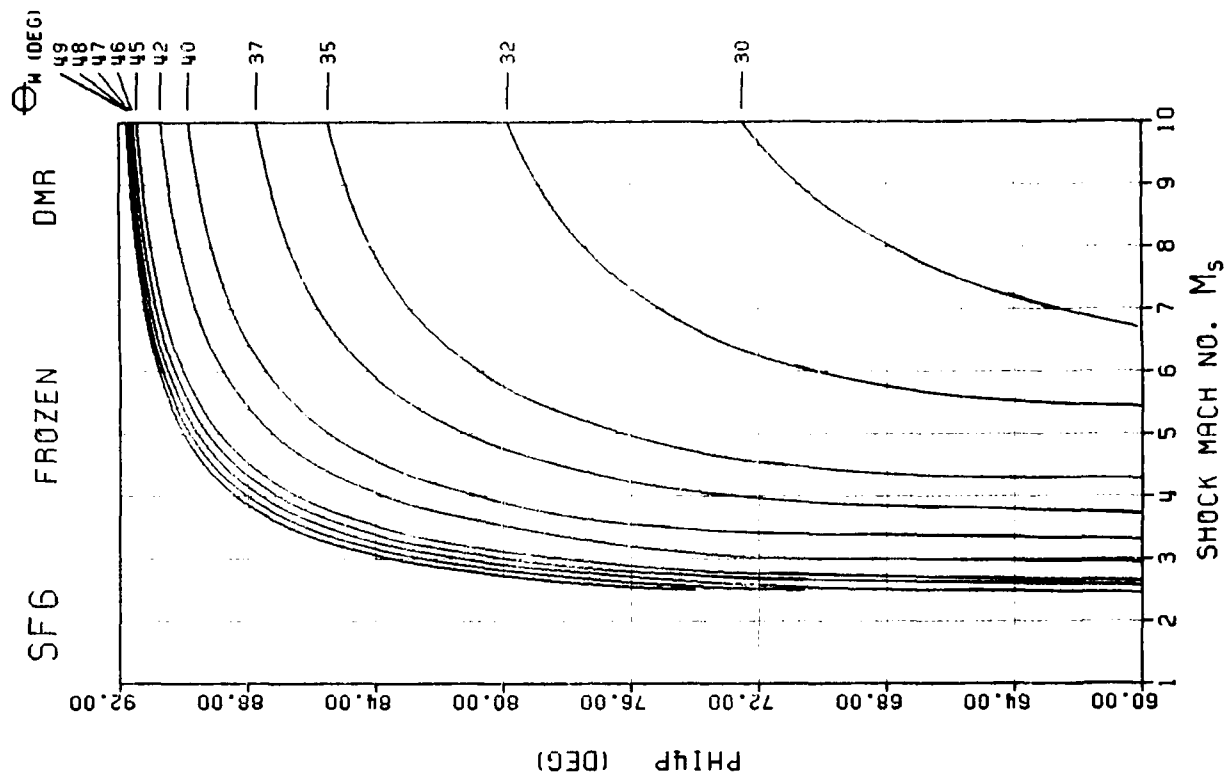
FILMED

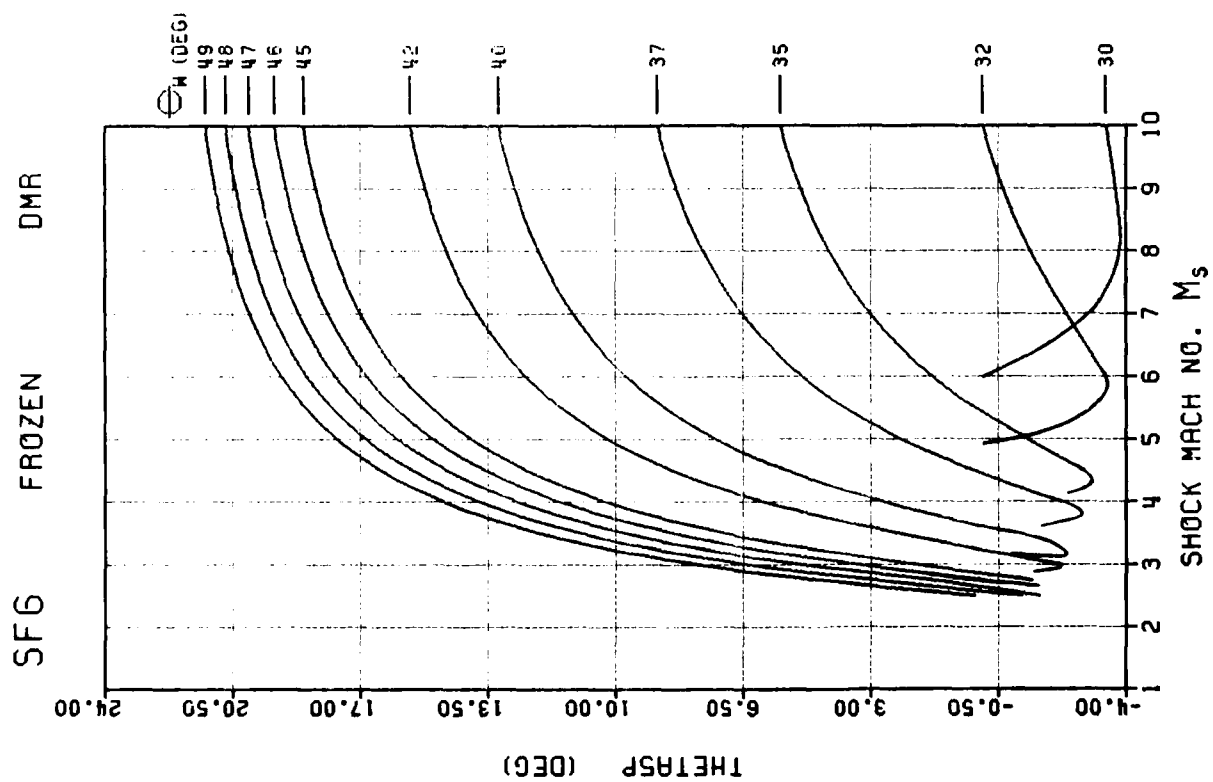
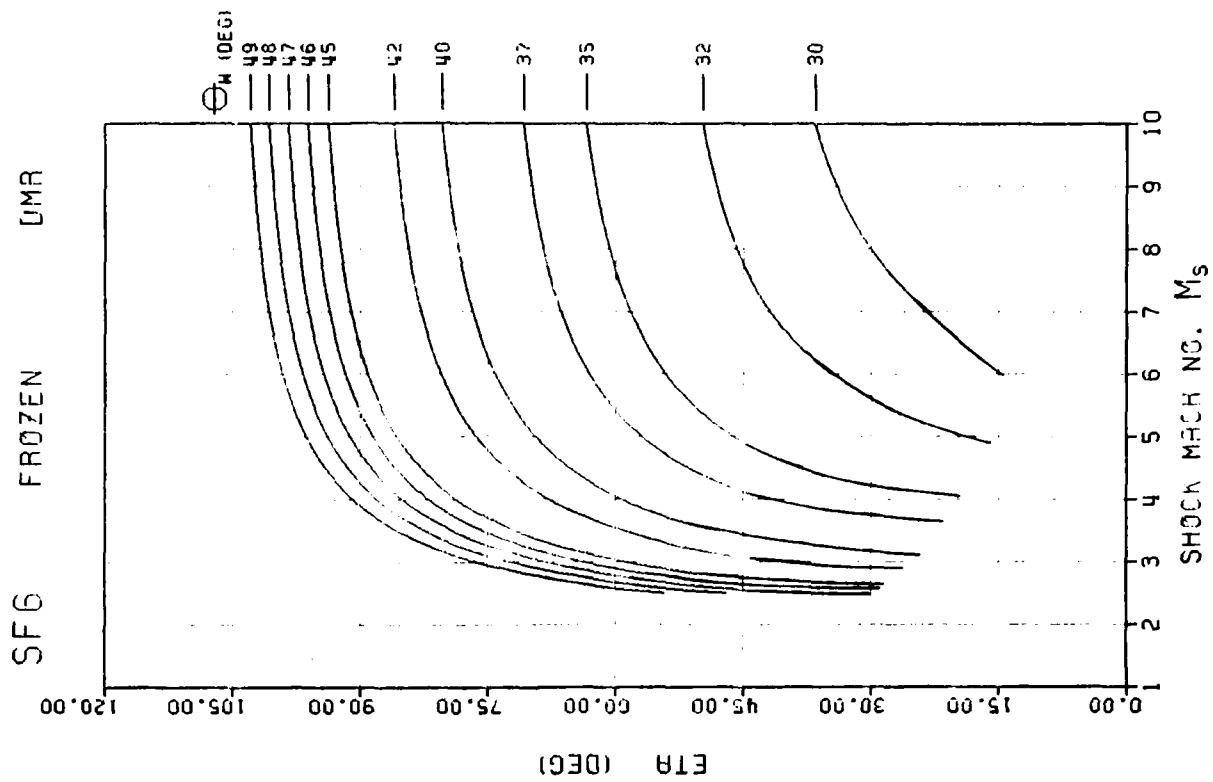
PT-

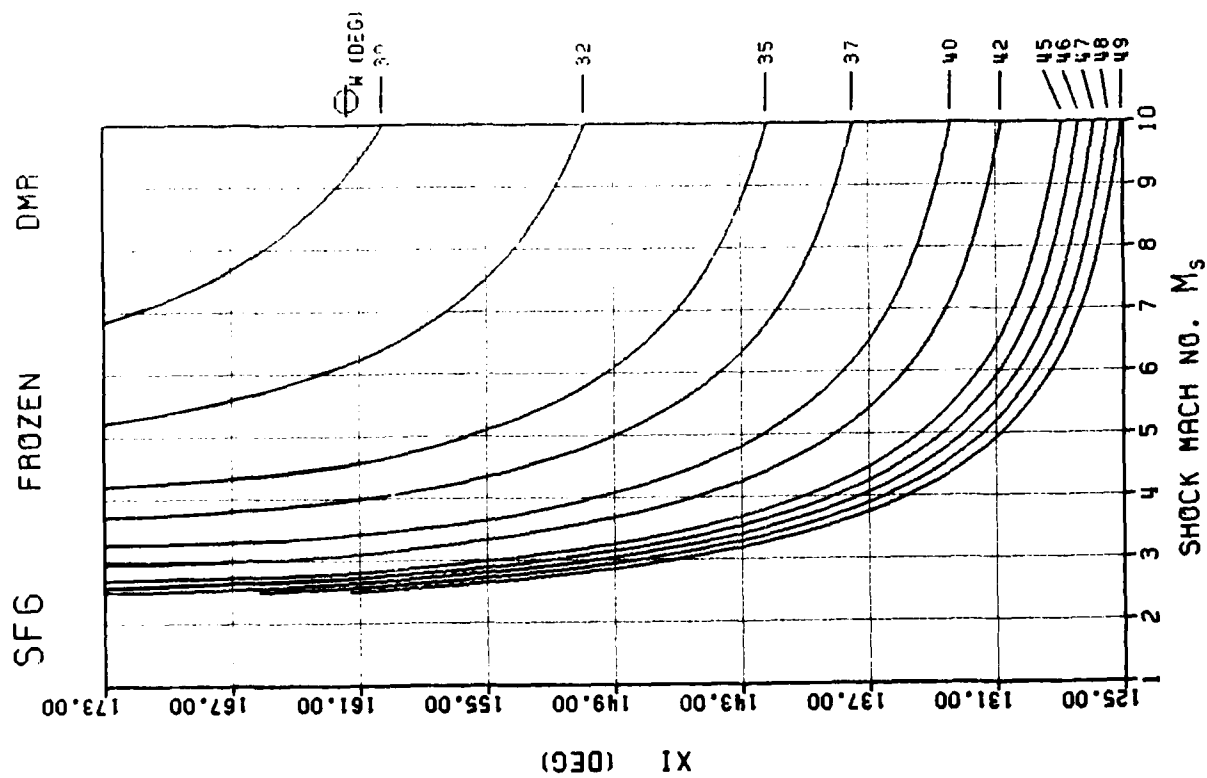


MICROCOPY RESOLUTION TEST CHART
NATIONAL BUREAU OF STANDARDS 1963-A

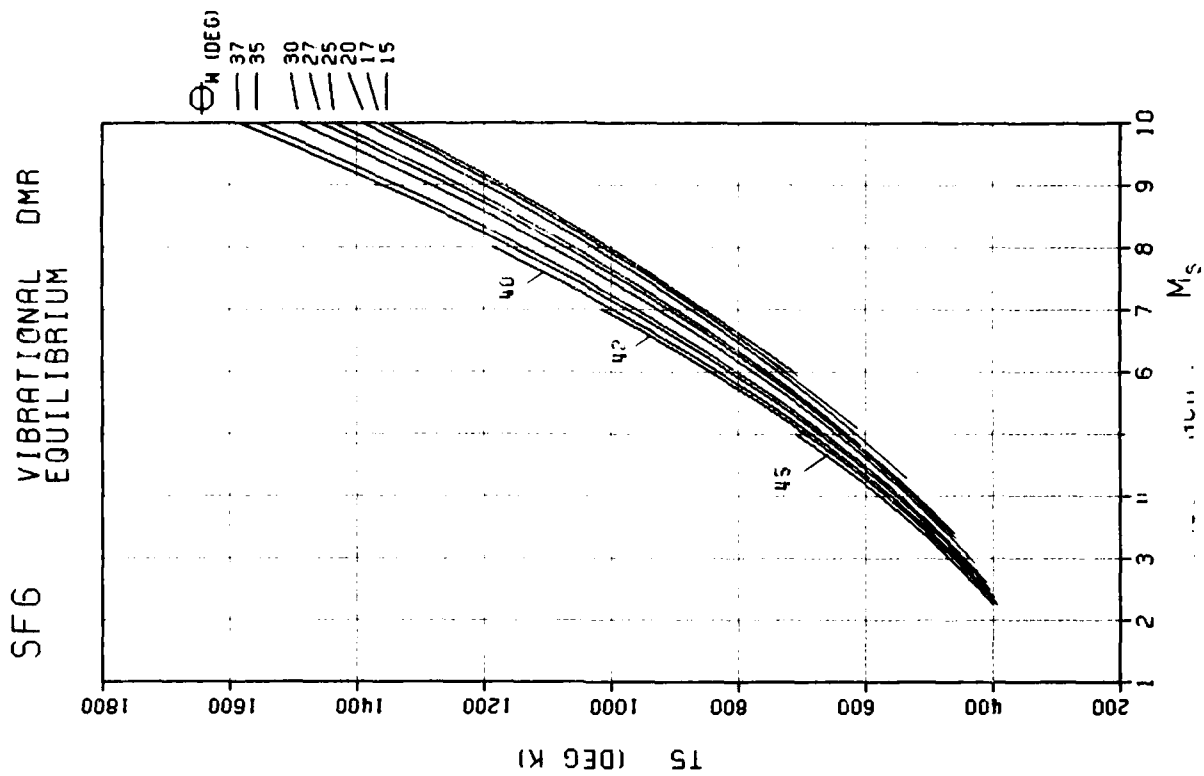
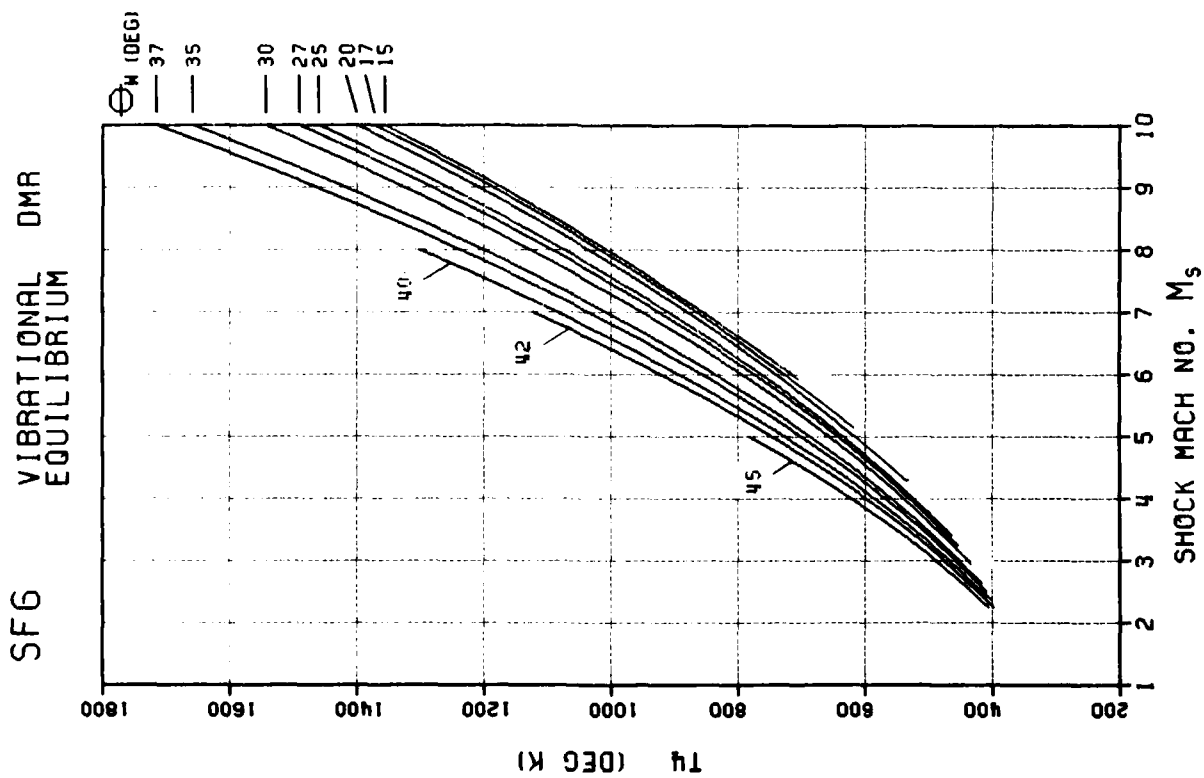


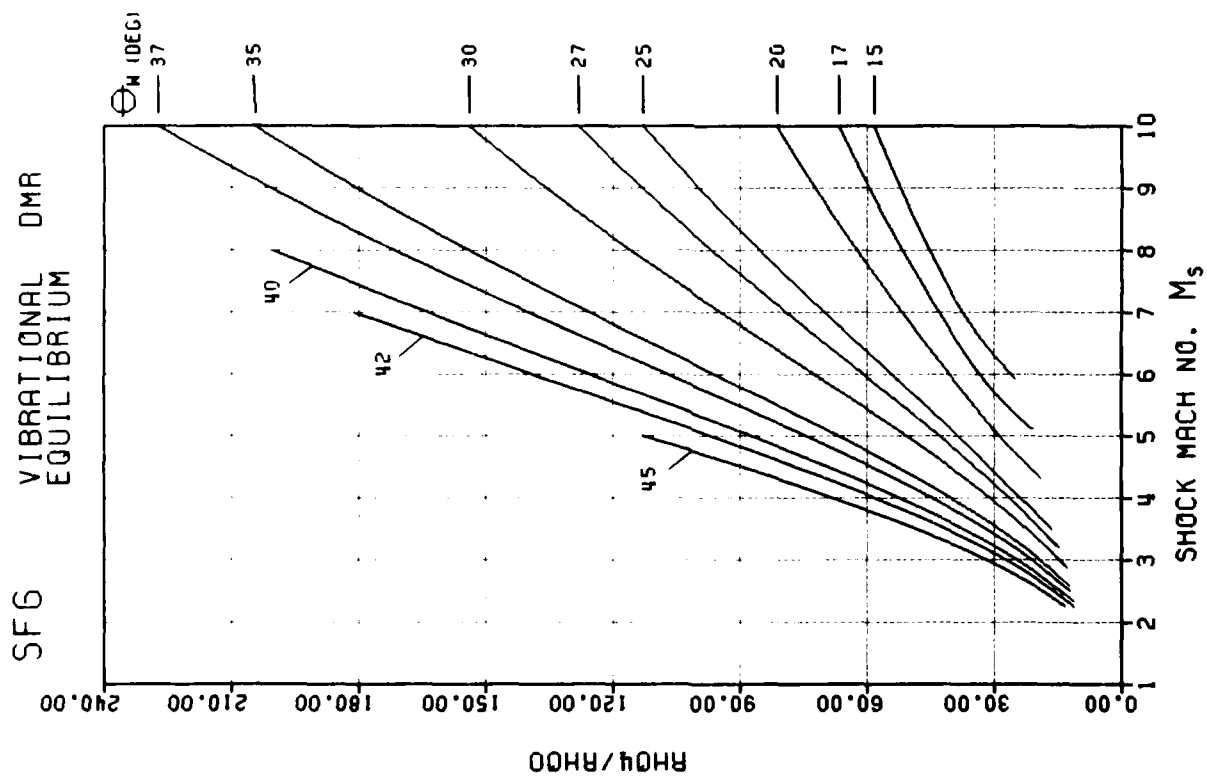
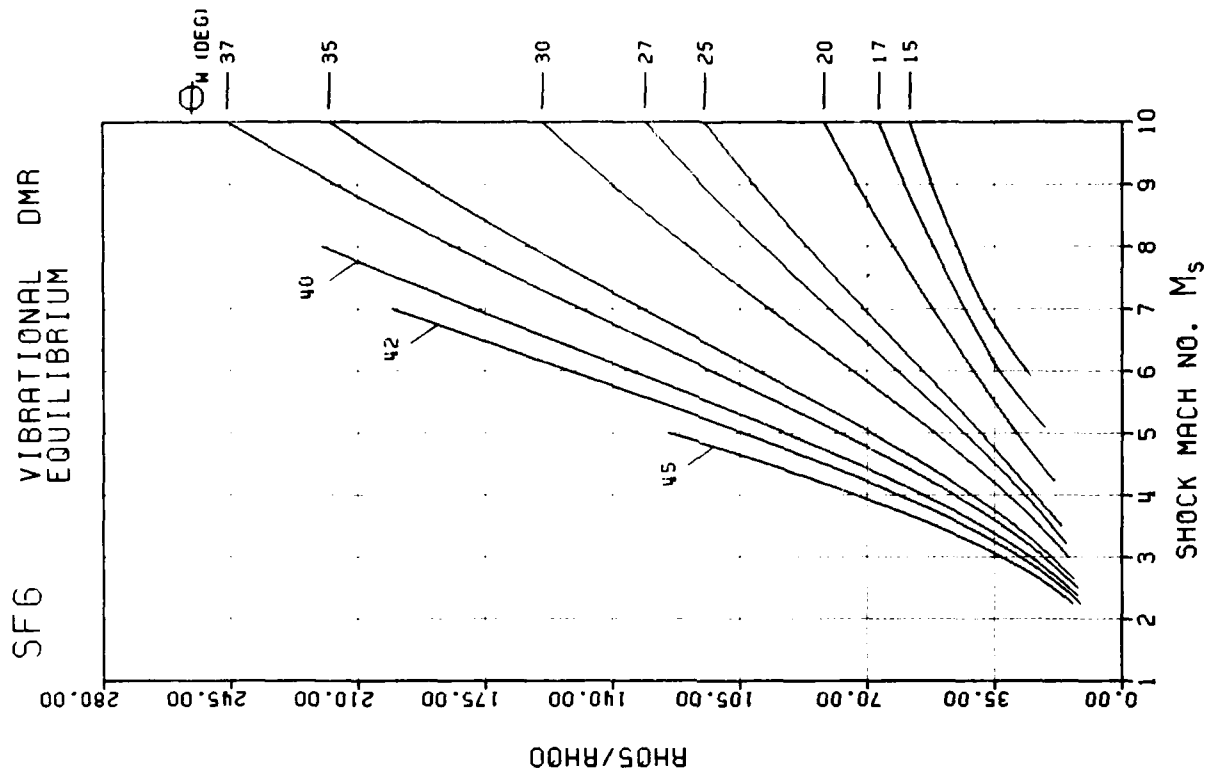


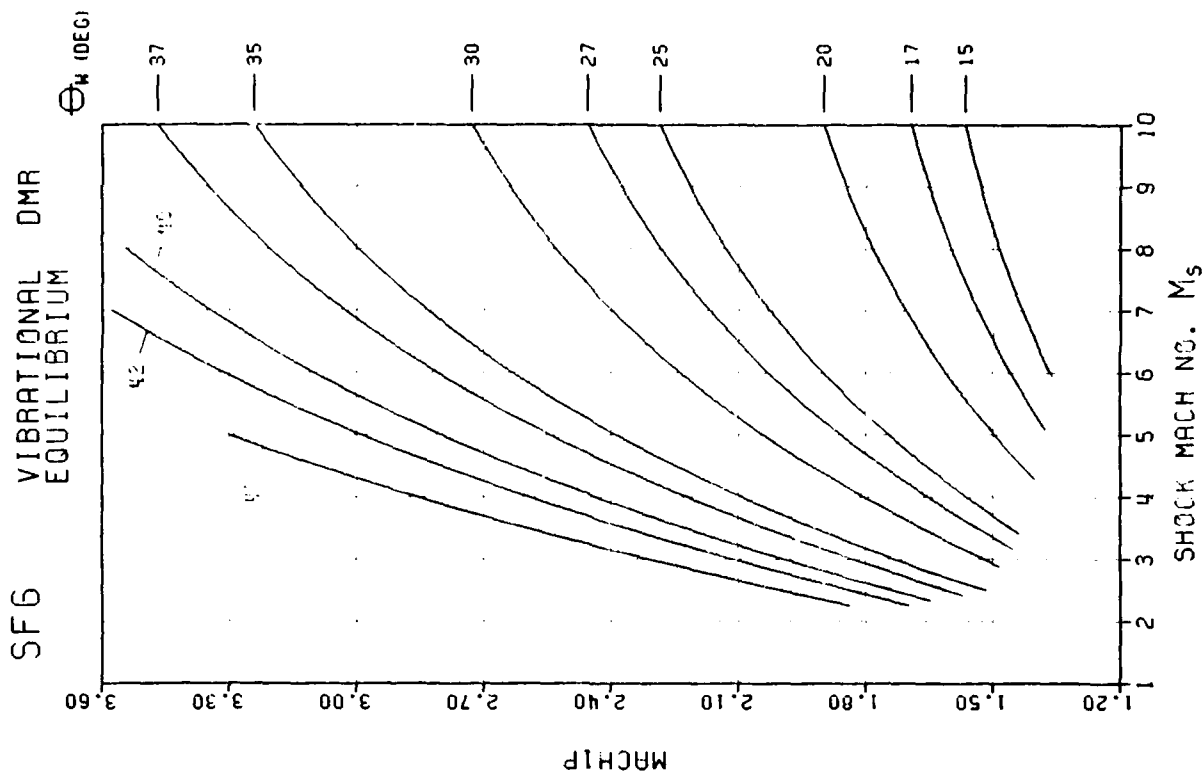
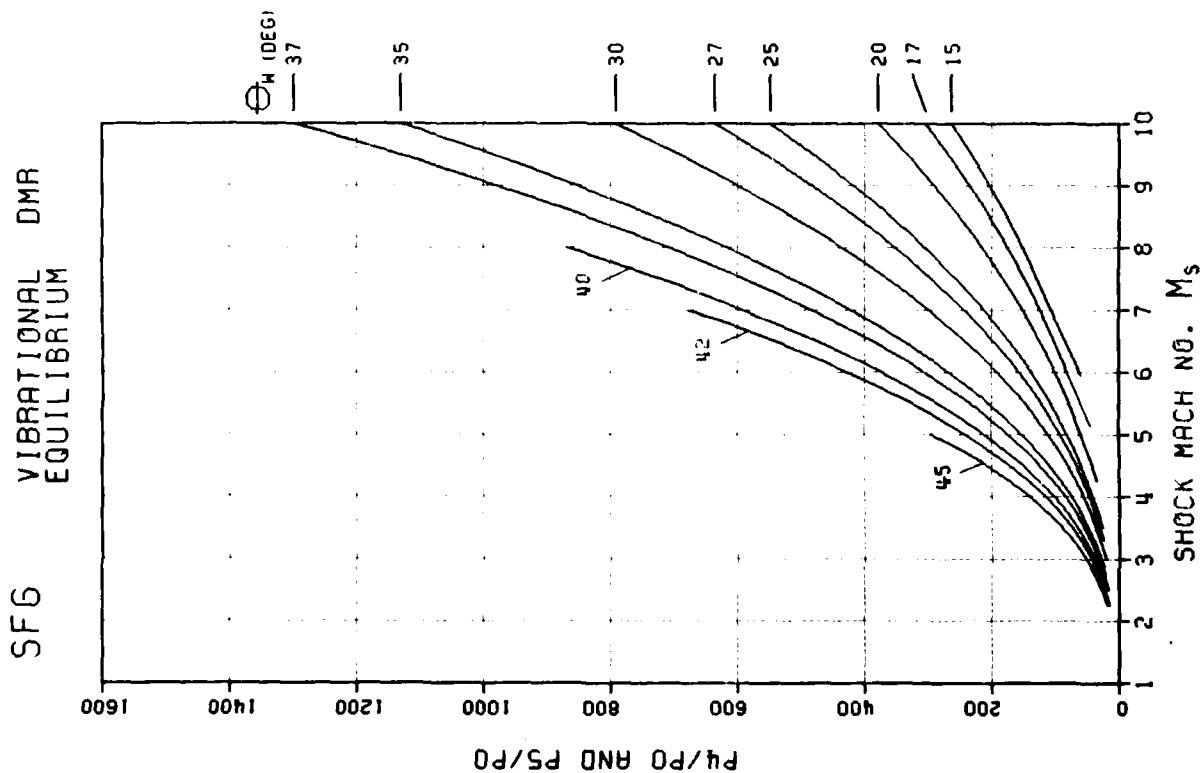


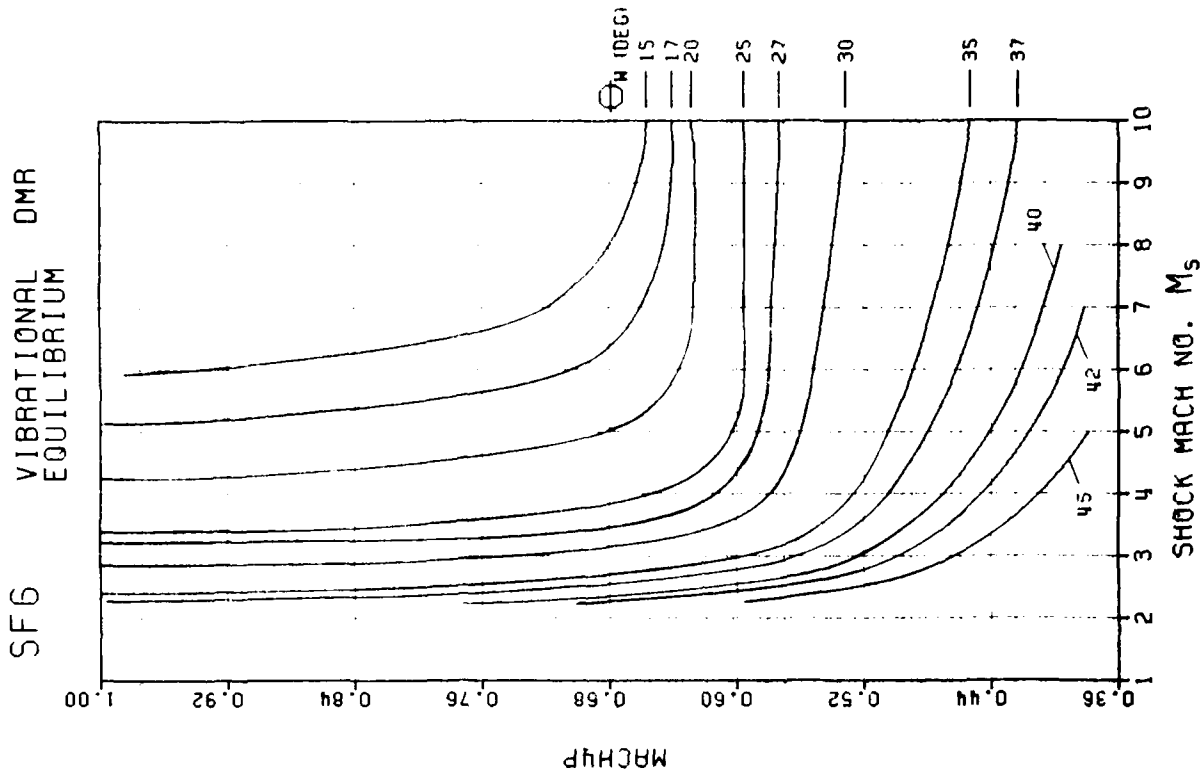
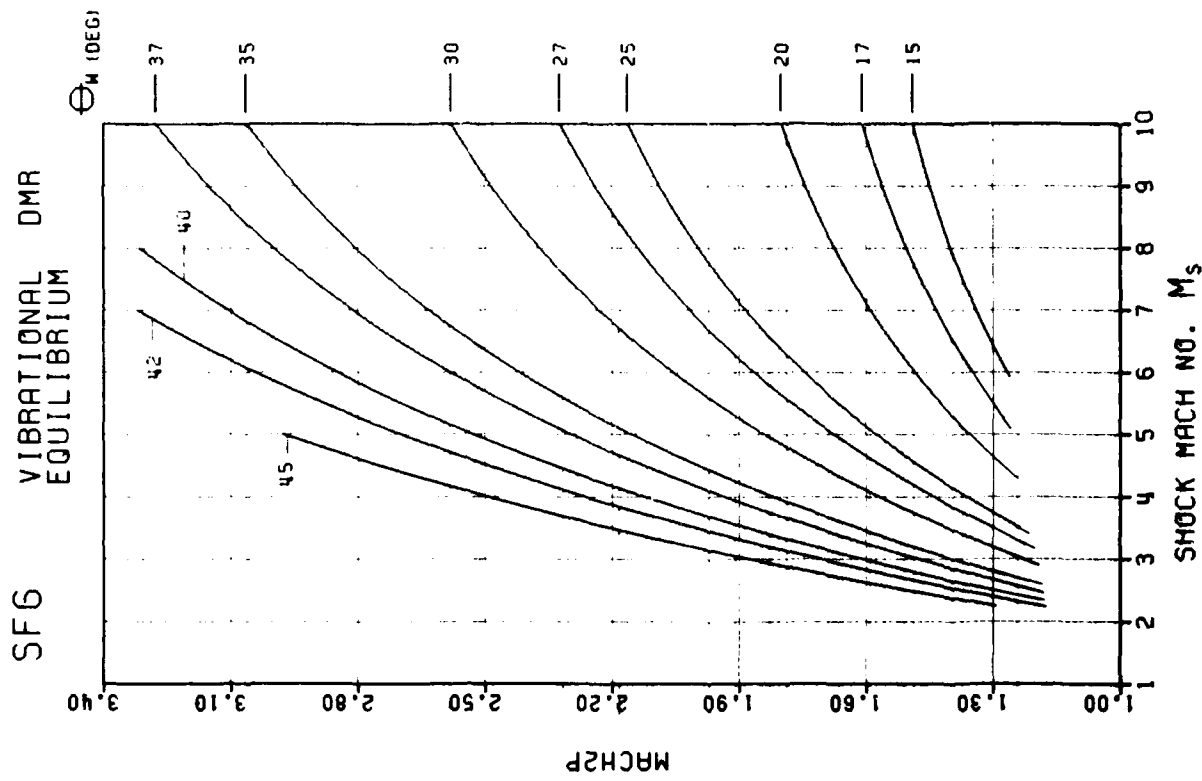


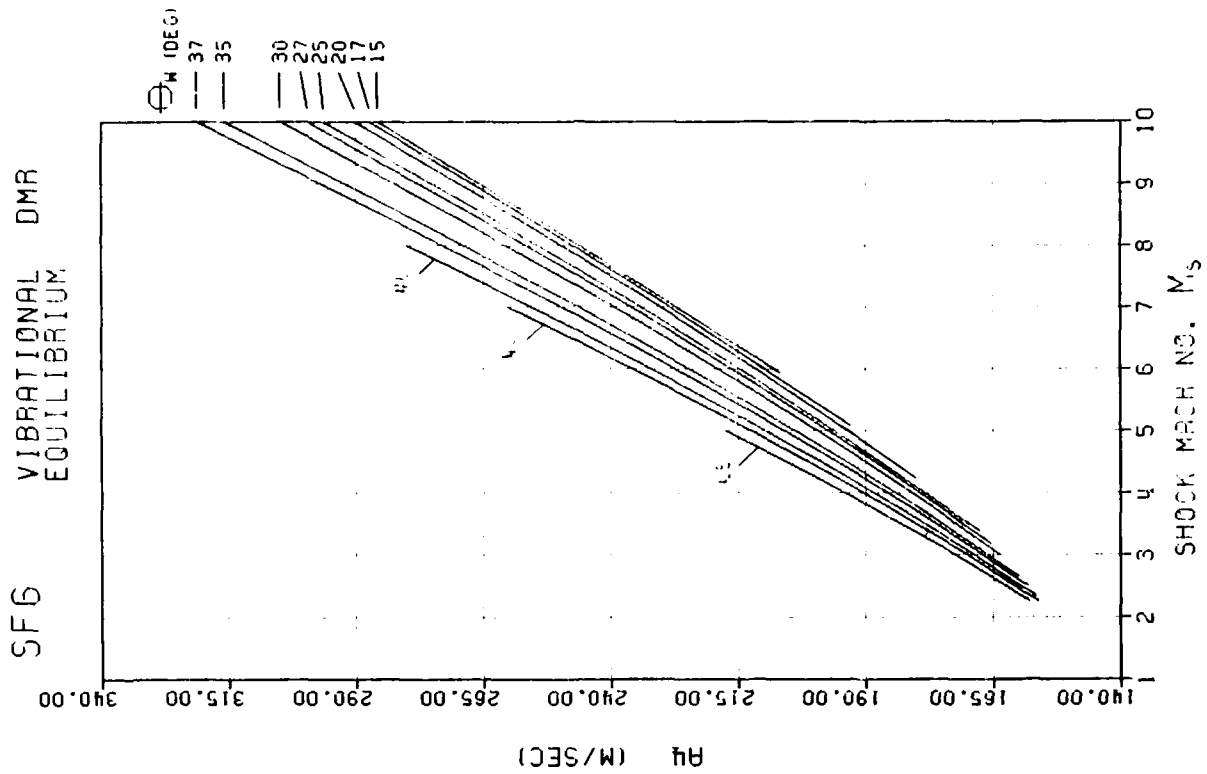
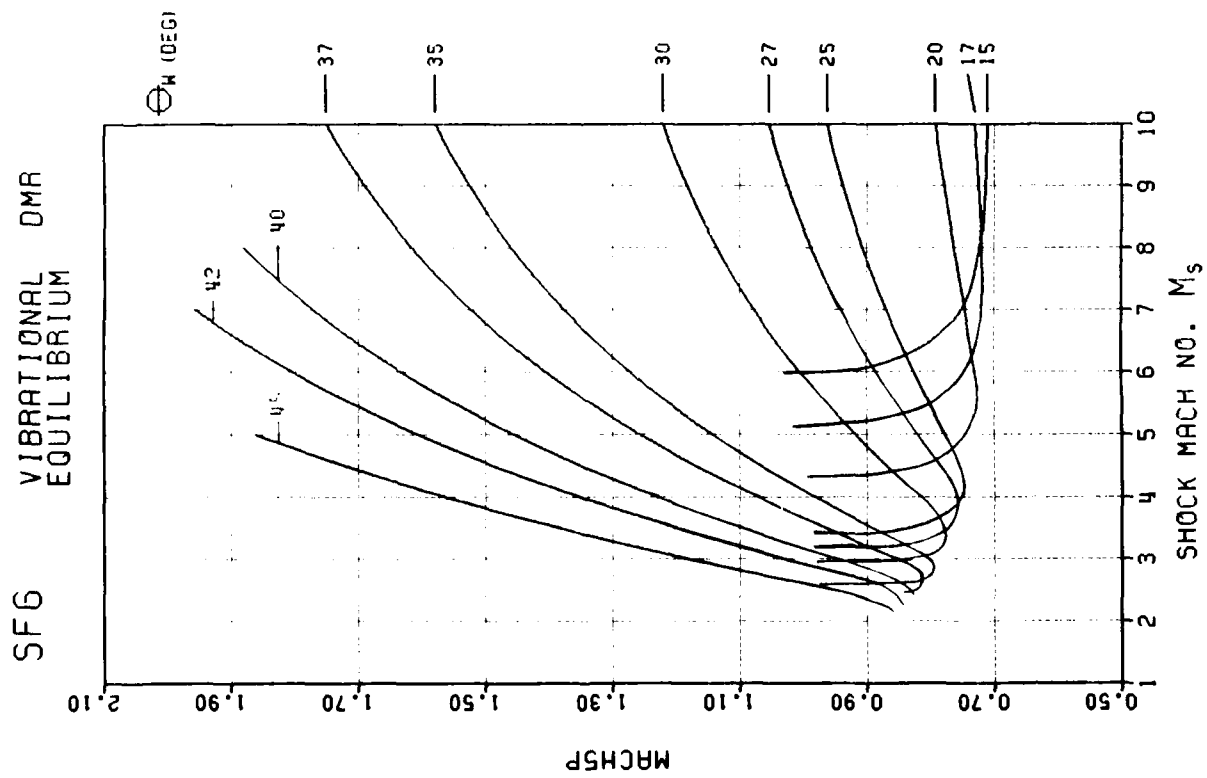
F - 310

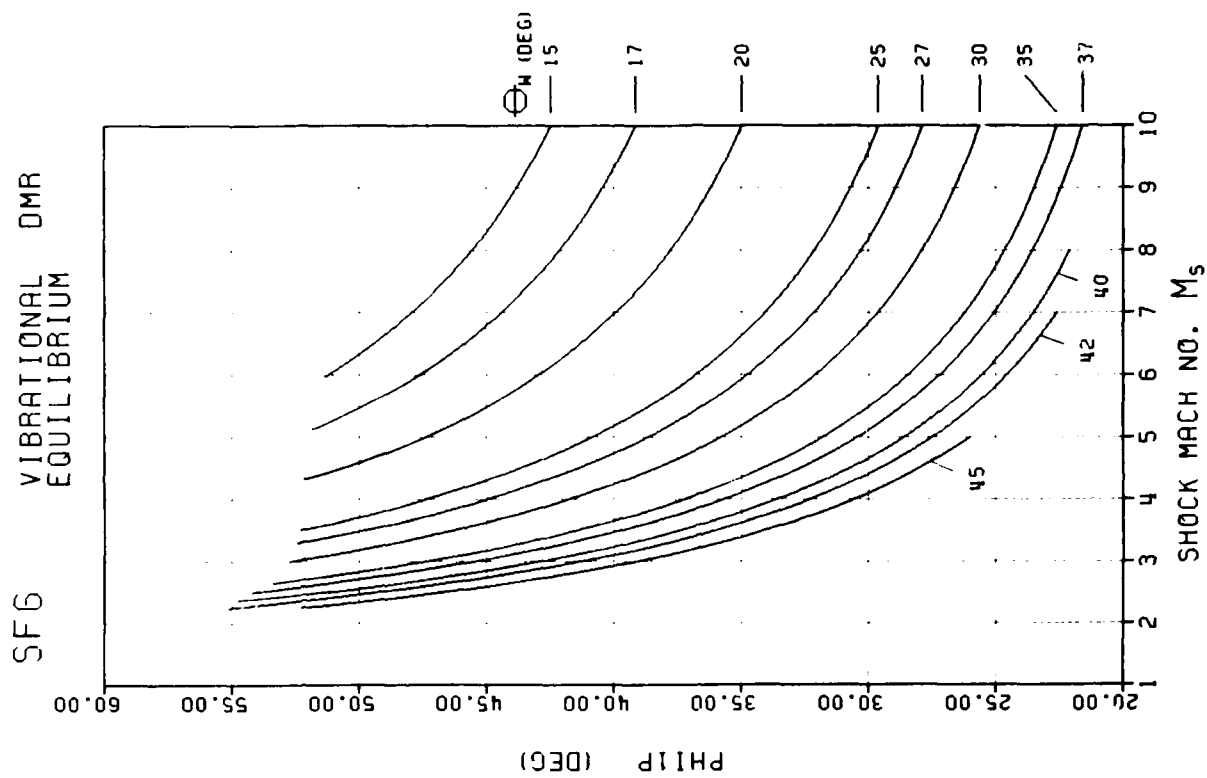
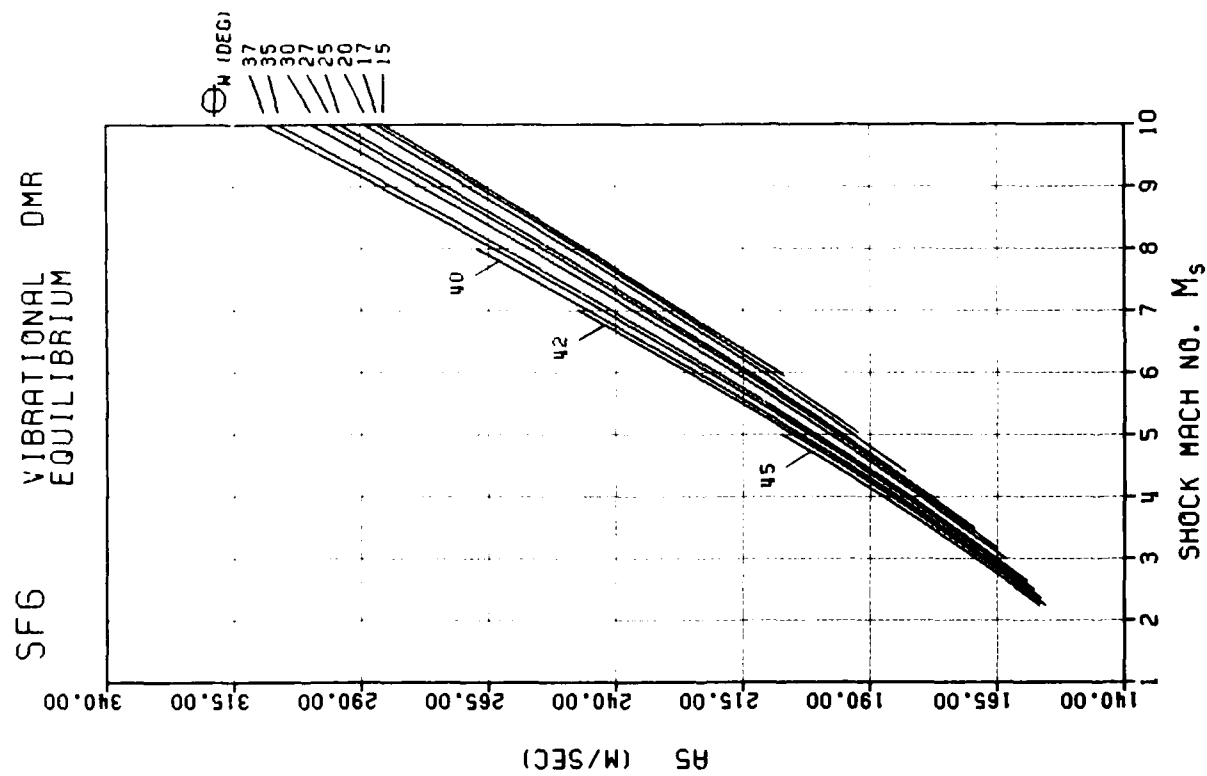


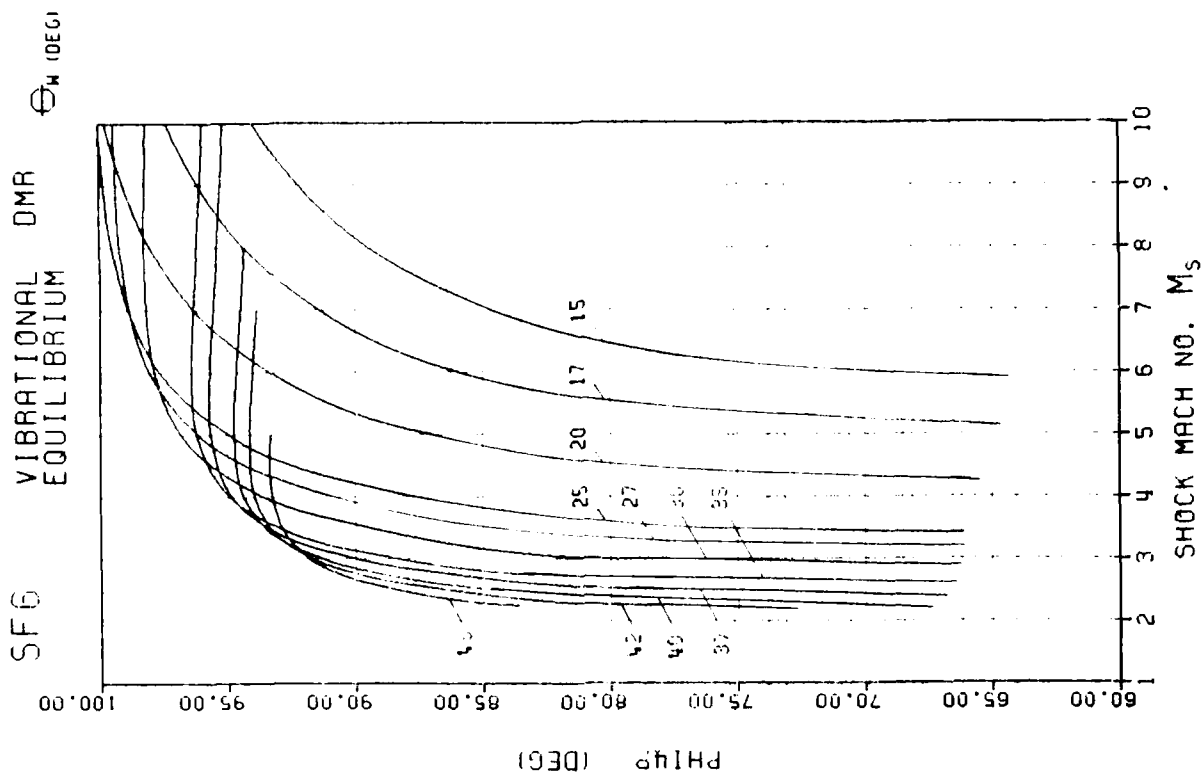
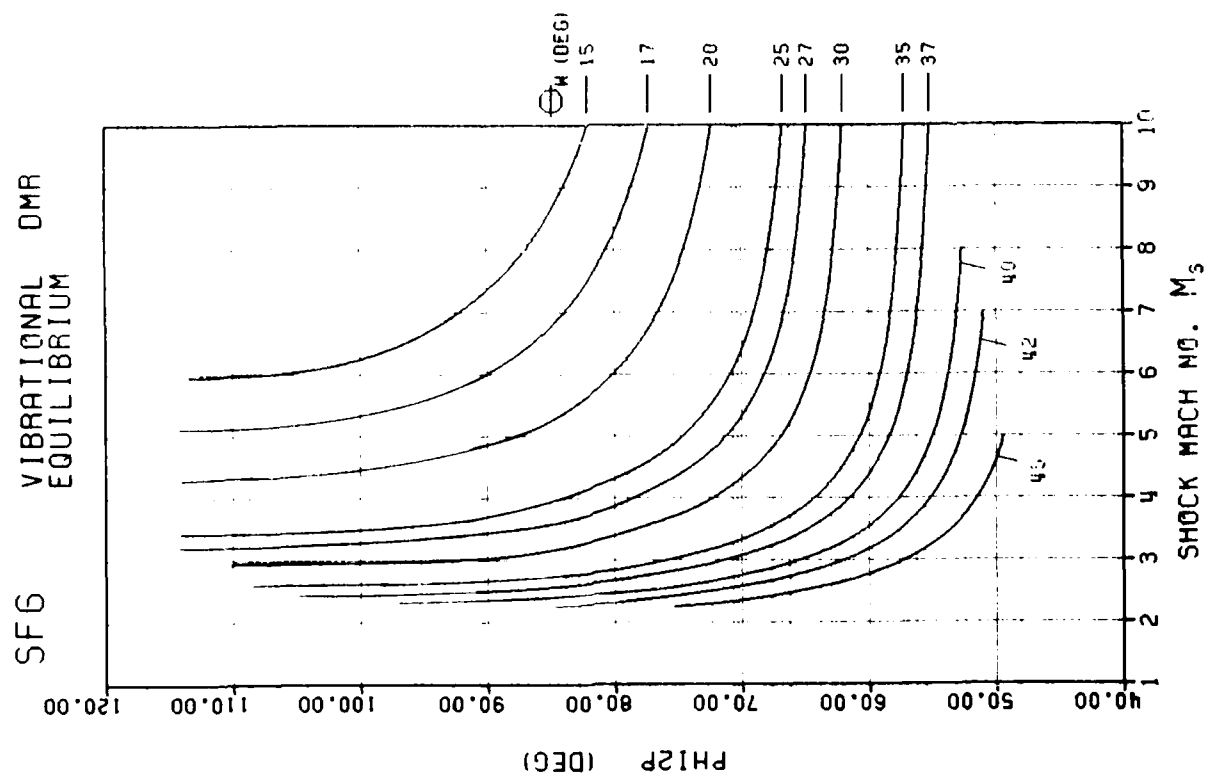


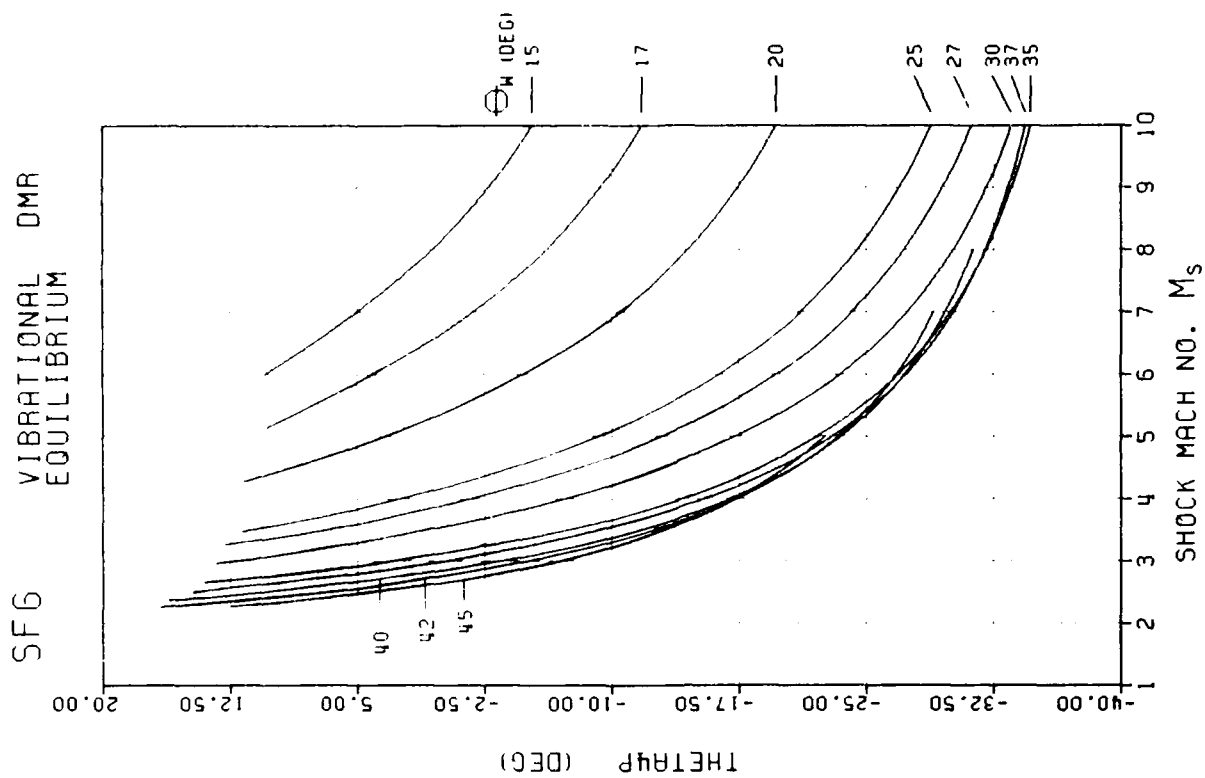
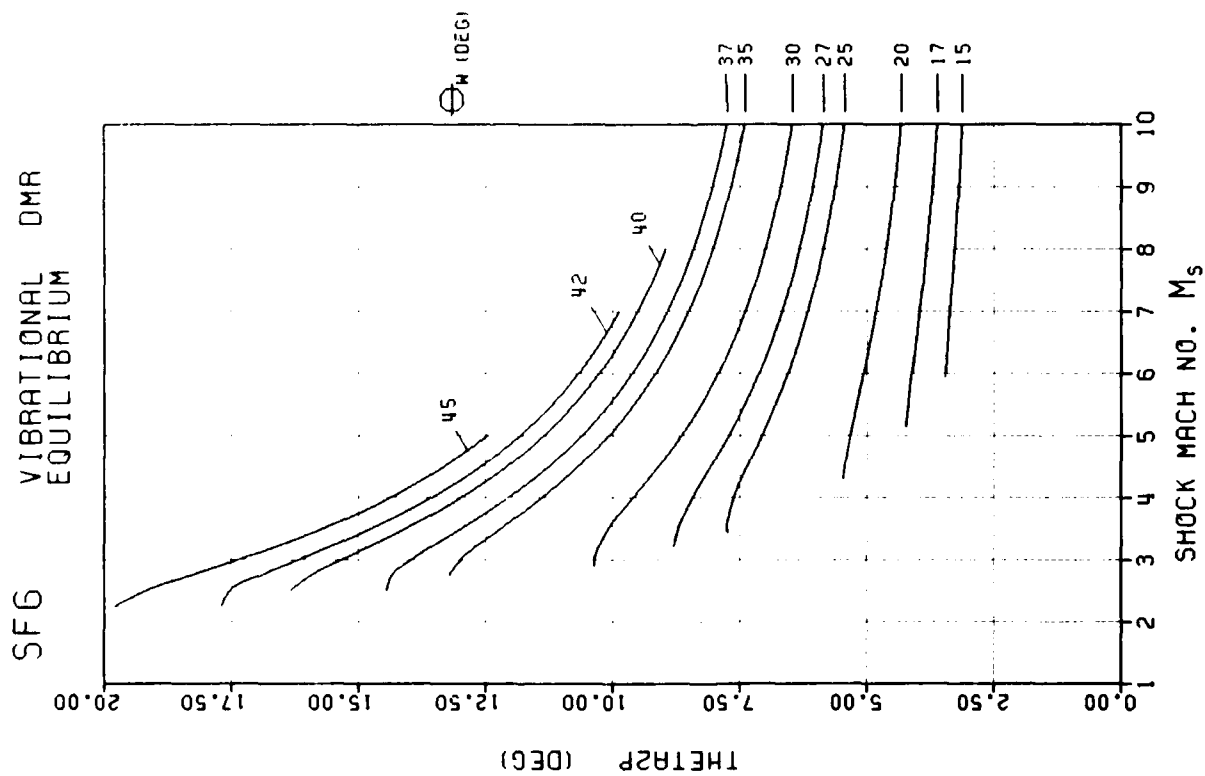


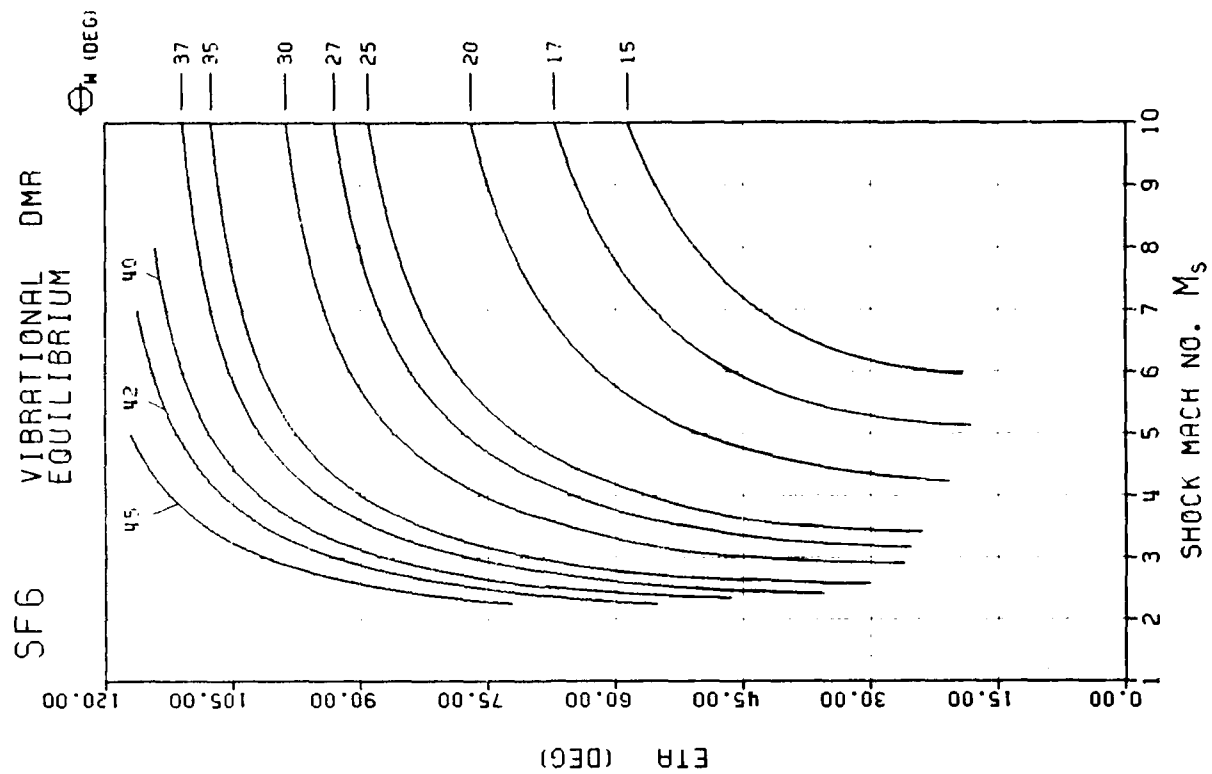
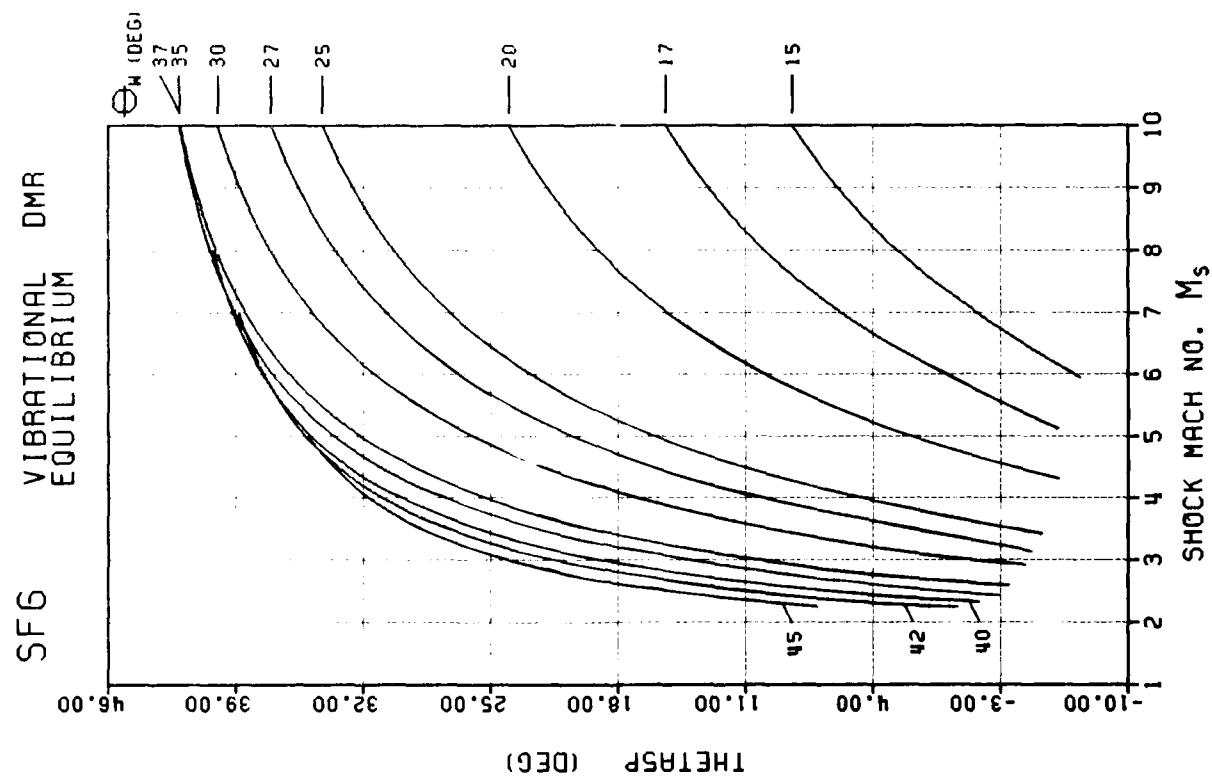


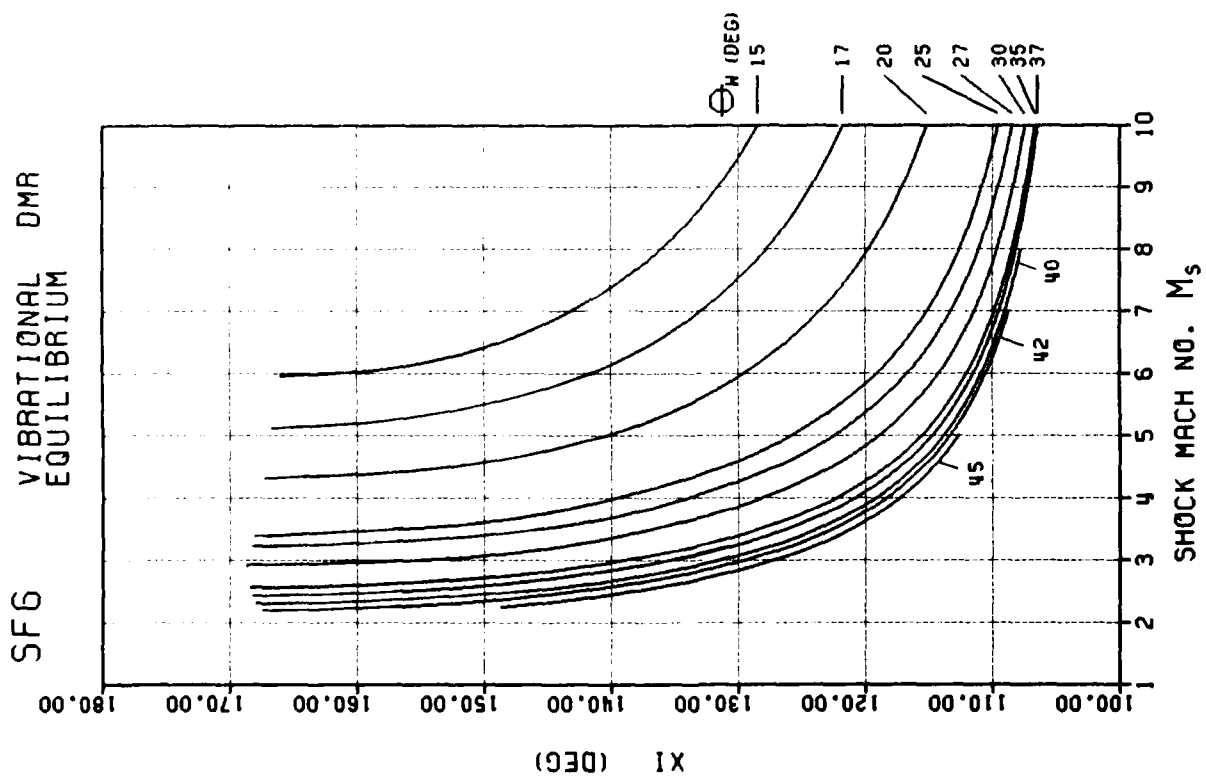












F - 320

APPENDIX A

ACTUAL SIDEWALL PRESSURE HISTORY AND NUMERICAL RESULTS

Recently, Deschambault (Ref. 11) measured the pressure history on and above a 40° wedge for the four types of pseudo-stationary oblique-shock-wave reflection in air. The numerical results generated by the present work are compared with the experimental pressure histories recorded by Deschambault and the results from the numerical simulation done by Glaz (Ref. 12) for a case of DMR in air. The comparison is applied only to the regions around the two triple points due to the limitations of the three-shock theory. Hence, only the sidewall pressure histories are considered. The wedge surface and sidewall pressure histories can be found in Ref. 11. Figure A-1 illustrates the sidewall pressure gauge positions used in the experiments by Deschambault.

Initial conditions : $M_s = 3.72$, $\theta_w = 40^\circ$, $P_0 = 45$ torr (6 kPa) and
 $T_0 = 21.94^\circ\text{C}$

The infinite-fringe interferogram is presented in Fig. A-2. Since the flow is self-similar, the position of the gauge "path" across the wave system can be traced by superimposing Fig. A-1 onto Fig. A-2. The traced positions of the gauges in the reflection system are shown schematically in Fig. A-3. In this run, both gauges 6 and 7 were below the first triple-point trajectory. Gauge 6 measured the pressure jumps across the Mach stem M from state (0) to state (3) close to the wedge surface, across the rolled up slipstream and across the tip of the second Mach stem M' to state (5). Gauge 7 is located slightly above gauge 6 and it recorded the pressure across the primary Mach stem M, across the upper portion of the rolled up slipstream S and across the second Mach stem M' from state (2) to state (5). Gauge 8 was located above the first triple-point trajectory but below the second triple-point trajectory. Gauge 8 was able to measure the pressure jumps across the incident shock wave I to state (1), across the primary reflected shock wave R to state (2), and across the second triple point T' to state (5). Gauge 9 was positioned above the first and second triple-point trajectories. It recorded the pressure jumps across the incident shock wave I to state (1) and across the second reflected shock wave R' to state (4) just behind the second triple point T'. The experimental sidewall pressure histories are shown in Fig. A-4. The measured pressures of the various flow states are indicated in Fig. A-4 and the various states in Fig. A-7.

The corresponding pressure histories at the four gauge locations given by the numerical simulation of Glaz (Ref. 12) are presented in Fig. A-5. Since each station is merely a mesh point on the numerical grid network, the time resolution of the numerical simulation is much greater than that of the pressure gauge. In addition, the numerical records have infinite rise times, whereas physically the gauge has a finite dimension and rise times limited to about $4 \mu\text{s}$. The pressure histories generated by the numerical code trace the local and instantaneous pressure variations ideally at a point station. Experimentally, a pressure gauge provides the average pressure over its finite recording area and the peak signals are

smoothed out because of the limited transient response time. The pressure jump across each shock wave is indicated in torr and kPa units on the plots. The lower pressure experienced at station 6 than at station 7 across the rolled up slipstream is clearly shown in Fig. A-5 by the sharp dip immediately behind the jump across the primary Mach stem M at station 6 here. The pressure jumps recorded by gauge 8 across the incident shock, first reflected shock and the second Mach stem are not as sharp and definite as shown by the simulated results. In the measured pressure history, the rise from P_2 to P_5 are continuous. However the simulation has a pressure peak at P_2 , then the pressure dips slightly before rising up to P_5 . Gauge 8 and 9 both measured about the same P_1 , but gauge 9 has a longer record of P_1 than gauge 8 because gauge 9 went from state (1) to state (4) above T' , whereas gauge 8 went from state (1) through state (2) to state (5) below T' . Due to the limited time record of the simulated pressure history given at station 9, the shape of the pressure history and the value of P_4 cannot be read and compared with the measured value. However P_4 can be read out from the isobaric contours of the entire reflection configuration (Fig. A-6).

The isobaric contours of the entire flow field (Ref. 12) and the enlargement of the flow regions around the two triple points are presented in Fig. A-6. From Fig. A-6(b), both P_2 and P_3 behind the first triple point are 2×10^6 dynes/cm² or 200 kPa (1500 torr), and both P_4 and P_5 behind the second triple point are 3×10^6 dynes/cm² or 300 kPa (2250 torr). Besides extracting the pressure information from the isobaric contour plots, several reflection angles can also be measured from this figure for comparing with the experimental values. The angles of interest are: (1) angle between incident shock wave and reflected shock wave at the first triple point δ , (2) angle between first reflected and second reflected shock η , (3) angle between first reflected shock and second Mach stem ξ , (4) first triple-point trajectory angle χ , and (5) second triple-point trajectory angle χ' . Refer to Fig. A-7 for the definition of these angles.

The computer program that calculates the various thermodynamic states was modified so that a unique thermodynamic of state could be specified for each flow region. This is seen to be important for doing analysis in air where several flow regions may still be frozen while the rest of the flow regions may be in equilibrium. Concerning equilibrium flow in air, there may be some circumstances where only the oxygen molecules are in vibrational equilibrium, or in some other cases, both oxygen and nitrogen molecules are in vibrational equilibrium. Since the incident shock Mach number is low in this case, no dissociation needs to be included in the analysis. To determine whether the flow is frozen or in equilibrium, relaxation length concepts are used. If the relaxation length of an internal degree of freedom is considerably shorter than a characteristic length, the state is considered to be in equilibrium. Otherwise, it is assumed to be frozen. The vibrational relaxation length of N_2 is calculated according to the data reported by White and Millikan (Ref. 13) which shows that below a temperature of 3000 K at a pressure of one atmosphere, N_2 is excited more rapidly in air than in pure N_2 . The vibrational relaxation length of O_2 in air is calculated using the relation given by Lutz and Kiefer (Ref. 14) for pure O_2 . Also included is the correction factor introduced by Vincenti (Ref. 15). This takes into

account the experimental findings of Blackman (Ref. 16) that O_2-N_2 collisions in air are only 40% as effective as O_2-O_2 collisions in transferring energy for vibrational readjustment of O_2 . According to this analytical model, states (0), (1) and (2) are frozen, whereas the flow in states (3), (4) and (5) are in O_2 vibrational equilibrium. The vibrational relaxation length calculated by the present program is 38 mm in state (1), 16 mm in state (2), 3 mm in state (3), 7 mm in state (4) and 9 mm in state (5). Results of this model are listed in Table A-1 under present analysis (A).

Glaz used in his simulation the real-gas equation of state for air by Deschambault (Ref. 17), which was originally developed by Hansen (Ref. 18). Glaz's results indicated that all flow regions of the reflection system should be in equilibrium and a frozen gas assumption would not be valid. Another run was done using the present program based on the assumption that all five flow regions are in vibrational equilibrium and the results are listed in Table A-1 under present analysis (B). The pressure of each flow region and the reflection angles measured or calculated from experiment, numerical simulation and analysis are all tabulated in Table A-1. Both the numerical simulation (Ref. 12) and the analysis from the present work give extremely good results for pressures in the flow regions (1) to (3) with a maximum discrepancy of 2.5%. The measured P_3 of gauge 7 was used for comparison since gauge 6 gave a lower value because the vortical flow of the rolled up primary slipstream went past gauge 6. Behind the second triple point T', the pressures P_4 and P_5 given by Glaz are consistently higher than the measured values by 13.6% and 10.5%, respectively. However, the numerical results from the present study gave similar results to the experimental P_4 and P_5 values with the maximum deviation only 3.6% for set (A) and 7.1% for set (B).

The pressures predicted by the present analysis (A) agree very well with the measured pressures from the experiment. However, the pressures predicted by the present analysis (B) agree better with the numerical simulation results than with the measurements from experiment.

The first triple-point-trajectory angle χ was predicted very well by Glaz and the present work with a maximum deviation of 0.5° . The second triple-point-trajectory angle χ' was very well predicted by the present analysis (A). Numerical simulation and present analysis (B) give slightly smaller values of χ' than the measured experimental value. The present analyses (A) and (B) give values of the reflection angles δ , ξ and η to within 1.6° and 3.5° respectively that of the experimental value for this case. Glaz predicted the angles δ and η being 4° and 3.5° respectively too high, whereas the angle ξ had a value of 9.5° too low. Present analysis (A) agrees best with experiment on physical quantities. Present analysis (B) give very reasonable physical angles except the value of χ' is slightly low. Numerical simulation predicts triple point trajectory angles well but not so for the reflection angles.

A comparison of the values of δ shows how well the numerical work from the present study can predict the orientation of the reflected shock wave R at the first triple point T relative to the incident shock wave I. Similarly, comparisons of the angle ξ and η indicates the accuracy of the numerical work in predicting the orientation of the second reflected shock

wave R' and the second Mach stem M' relative to the primary reflected shock wave R . The numerical simulation by Glaz predicts a smaller angle ξ and a larger angle η than the experimental and analytical values, and it gives larger values of P_4 and P_5 . This is because decreasing ξ will place the second reflected shock R' more normal to the incoming flow, subsequently increasing the pressure P_4 behind it in region (4). Similarly, as the second Mach stem M' becomes stronger, the angle η gets larger and the incoming flow in region (2) is now more normal to the second Mach stem M' , thus resulting in a higher pressure P_5 in region (5).

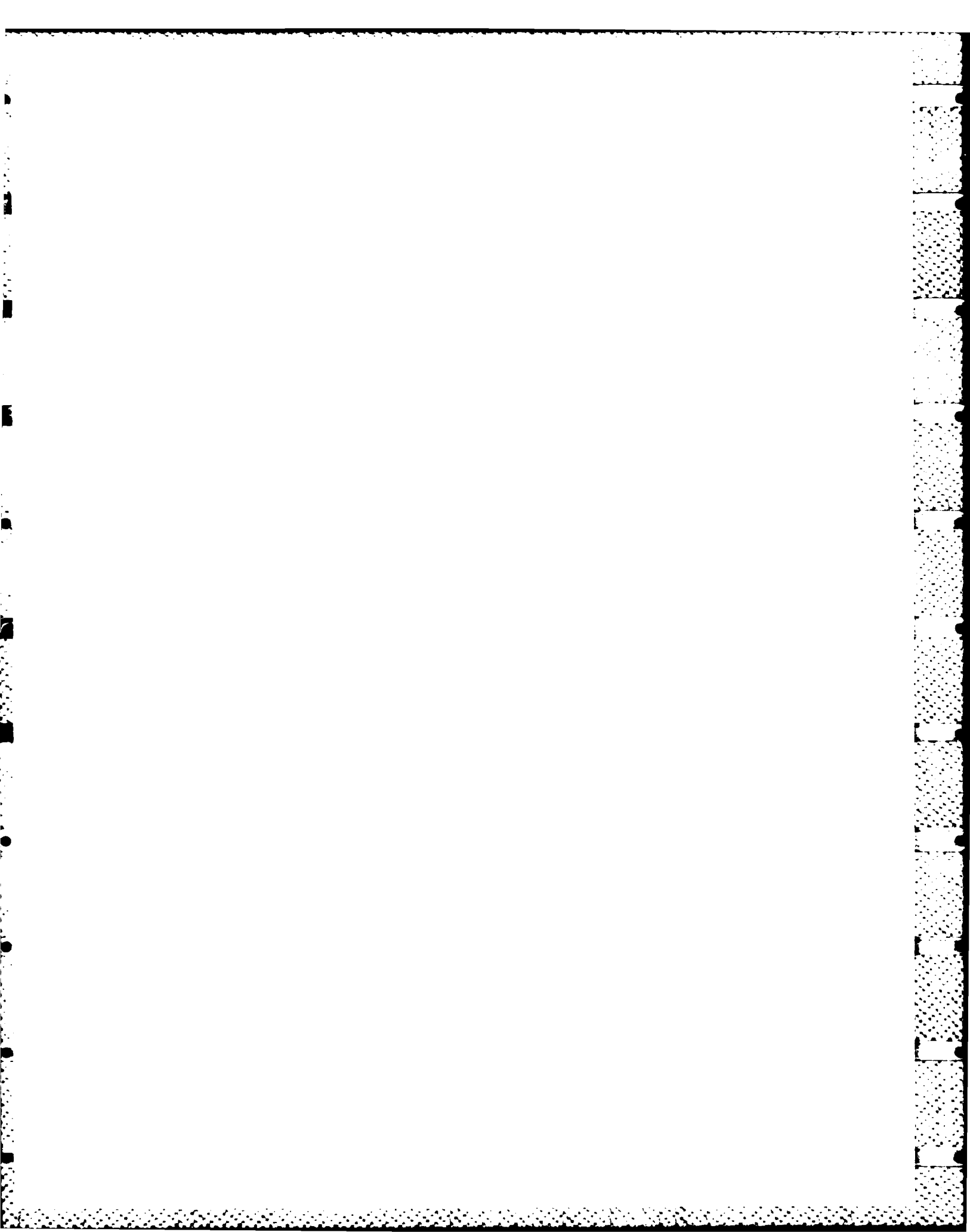
Present analysis (A) has given results for the pressure at all five states (1) to (5) showing good agreement with experiment. It can predict accurately the orientations of the shock waves around the two triple points. The good agreement indicates that the application of different equations of state to each region is justified based on relaxation length concepts. The numerical simulation by Glaz provides more detailed information about the entire flow field in contrast to the present work. However, his results show larger deviations in the pressures behind the second triple point and in the reflection angles when compared to the experimental results.

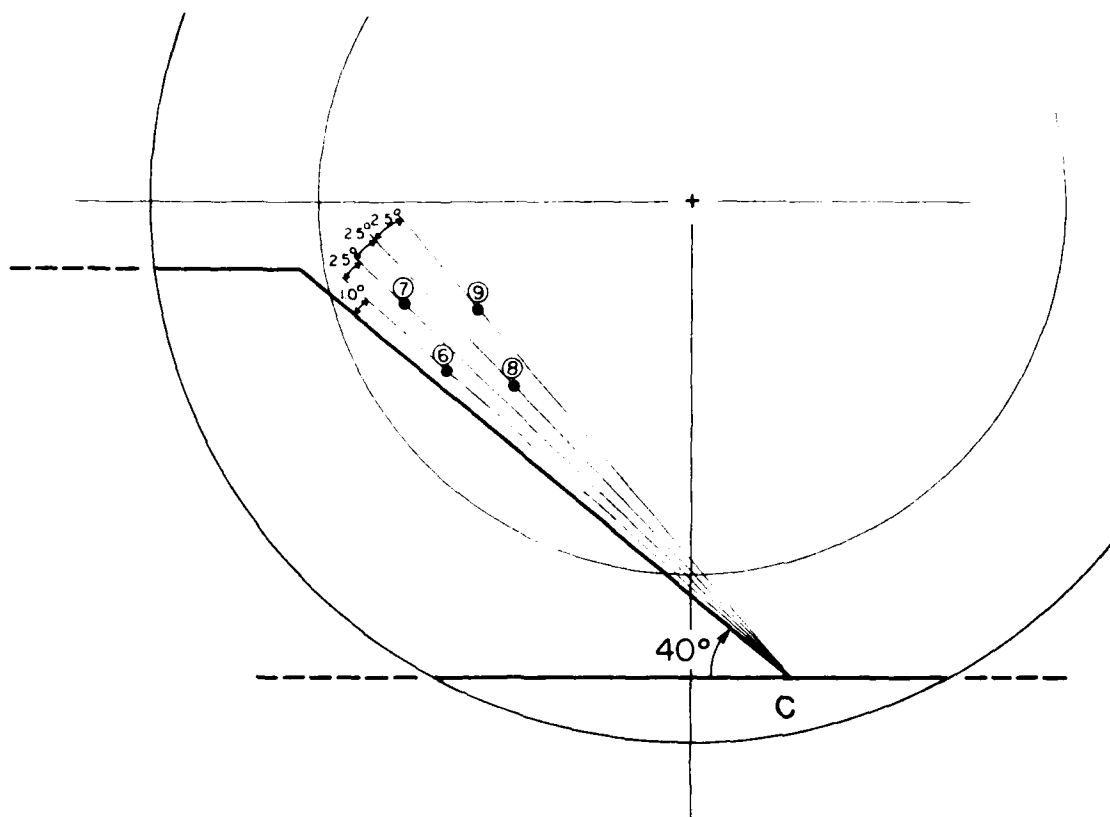
TABLE A-1

Comparison of Pressures and Physical Angles between
Experiment and Numerical Results for a DMR in Air.

$M_s = 3.72$, $\theta_w = 40^\circ$, $P_0 = 45$ torr (6 kPa), $T_0 = 21.94^\circ\text{C}$.

| Parameter | Experiment (Ref. 11) | | Numerical Simulation (Ref. 12) | | Present Analysis | | | |
|-----------|----------------------|-------|-----------------------------------|--------|------------------|----------|-------------|------------|
| | Torr | kPa | Gauge | Torr | kPa | Station | (A) Torr | (B) kPa |
| P_1 | 716 | 95.5 | 8 | 728 | 97.1 | 8 | 719 | 95.9 |
| | 722 | 96.3 | 9 | 728 | 97.1 | 9 | 730 | 97.3 |
| P_2 | 1456 | 194.1 | 8 | 1455 | 194.0 | 8 | 1439 | 191.9 |
| P_3 | 1476 | 196.8 | 7 | 1506 | 200.8 | 7 | 1439 | 191.9 |
| | 1396 | 186.1 | 6 | 1542 | 205.6 | 6 | 1449 | 193.2 |
| P_4 | 1981 | 264.1 | 9 | 2250 | 300.0 | Fig. A-5 | 2052 | 273.6 |
| P_5 | 2045 | 272.6 | 8 | 2259 | 301.2 | 8 | 2052 | 273.6 |
| χ | 5.0° | | | 5.5° | | | 4.8° | 4.5° |
| χ' | 7.8° | | | 7.0° | | | 7.4° | 6.5° |
| δ | 123.0° | | | 127.0° | | | 124.0° | 126.2° |
| ξ | 162.5° | | | 153.0° | | | 160.9° | 159.0° |
| η | 46.5° | | | 50.0° | | | 45.4° | 47.7° |





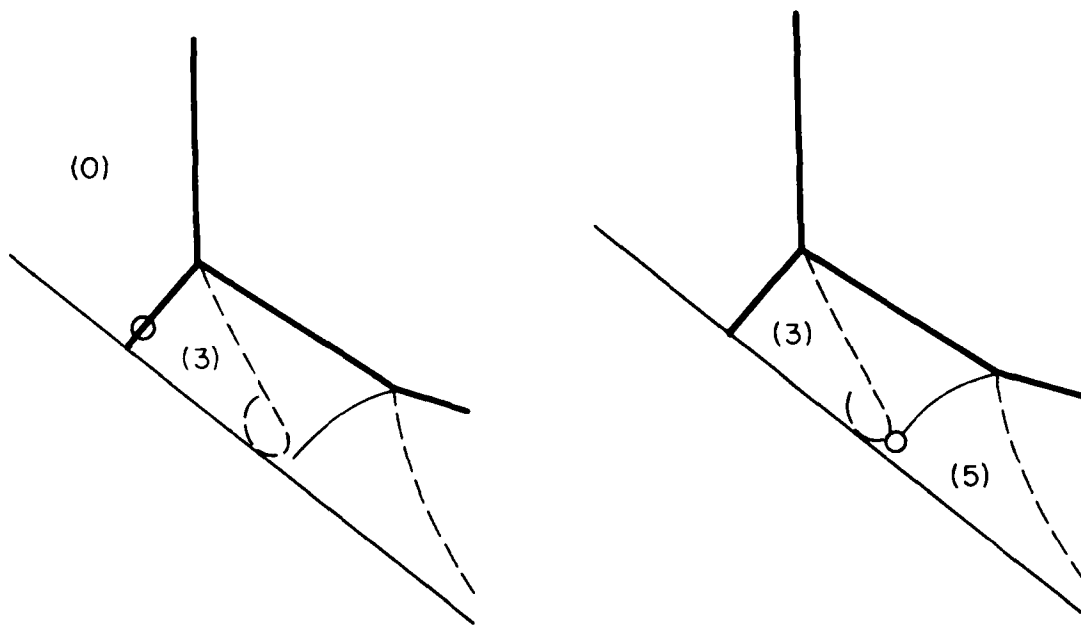
Gauge 6 is 8.56 cm from C
 Gauge 7 is 9.65 cm from C
 Gauge 8 is 7.75 cm from C
 Gauge 9 is 8.76 cm from C

Fig. A-1 Schematic diagram of gauge positions on the specially constructed steel window.



Fig. A-2 Infinite-fringe interferogram of double-Mach reflection in air (Ref. 11). $M_s = 3.72$, $\theta_w = 40^\circ$, $P_0 = 45$ torr (6 kPa), $T_0 = 21.94^\circ\text{C}$ and $\lambda = 6943 \text{ \AA}$.

Gauge 6



Gauge 7

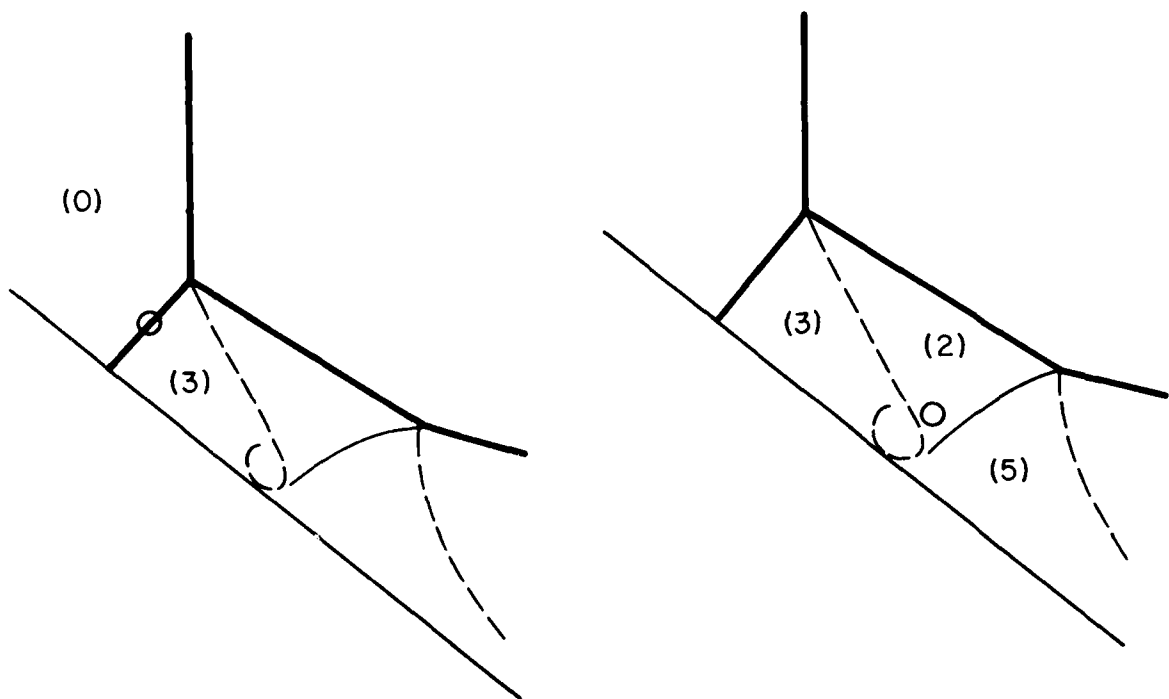
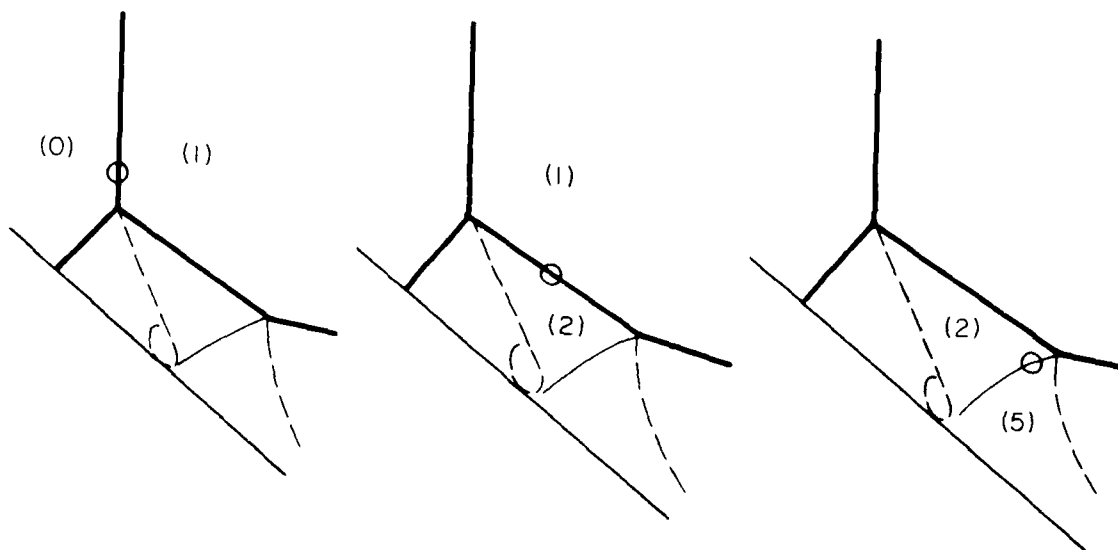


Fig. A-3 Positions of the gauge path across the reflection system traced by superimposition.

Gauge 8



Gauge 9

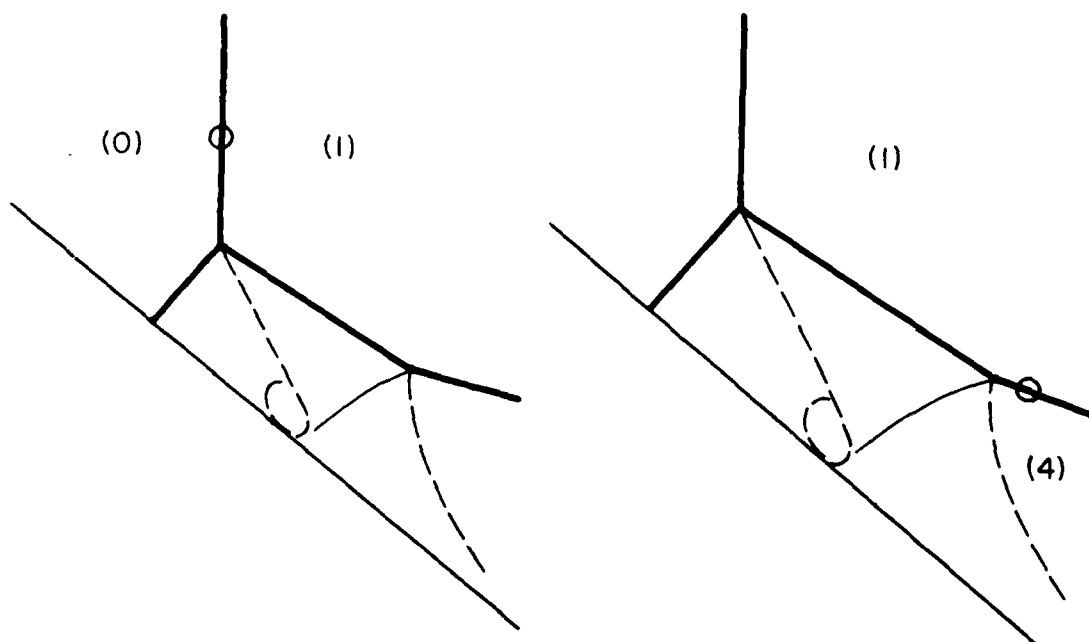
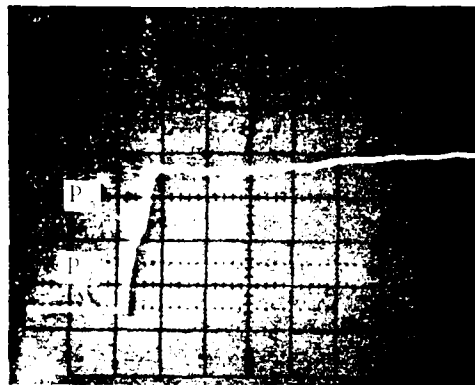


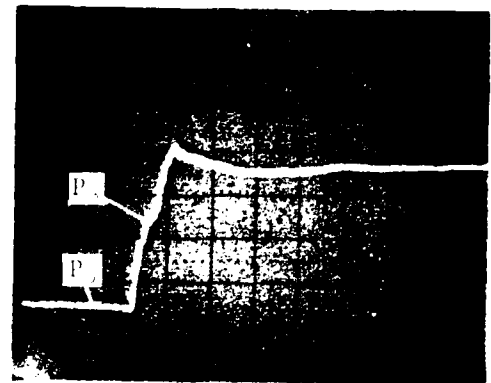
Fig. A-3 (Continued) Positions of gauge path across the reflection system by superimposition.

GAUGE 6



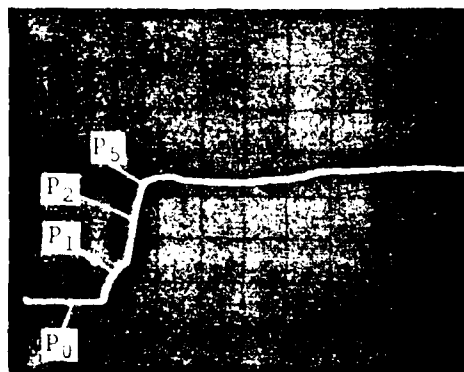
90.80 kPa/div (vertical)
 20 μ s/div (horizontal)
 P_0 45 torr (6 kPa)
 P_3 1396 torr (186.1 kPa)

GAUGE 7



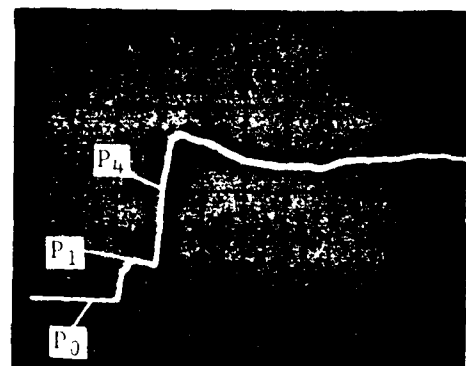
95.42 kPa/div (vertical)
 20 μ s/div (horizontal)
 P_0 45 torr (6 kPa)
 P_3 1476 torr (196.8 kPa)

GAUGE 8



98.80 kPa/div (vertical)
 20 μ s/div (horizontal)
 P_0 45 torr (6 kPa)
 P_1 716 torr (95.55 kPa)
 P_2 1456 torr (194.1 kPa)
 P_5 2045 torr (272.6 kPa)

GAUGE 9



98.18 kPa/div (vertical)
 20 μ s/div (horizontal)
 P_0 45 torr (6 kPa)
 P_1 722 torr (96.3 kPa)
 P_4 1981 torr (264.1 kPa)

Fig. A-4 Pressure history measurements along the sidewall above the wedge surface for the case of double-Mach reflection in air by Deschambault (Ref. 11). $M_S = 3.72$, $\alpha_w = 40^\circ$, $P_0 = 45$ torr (6.11 kPa), $T_0 = 21.94^\circ \text{C}$.

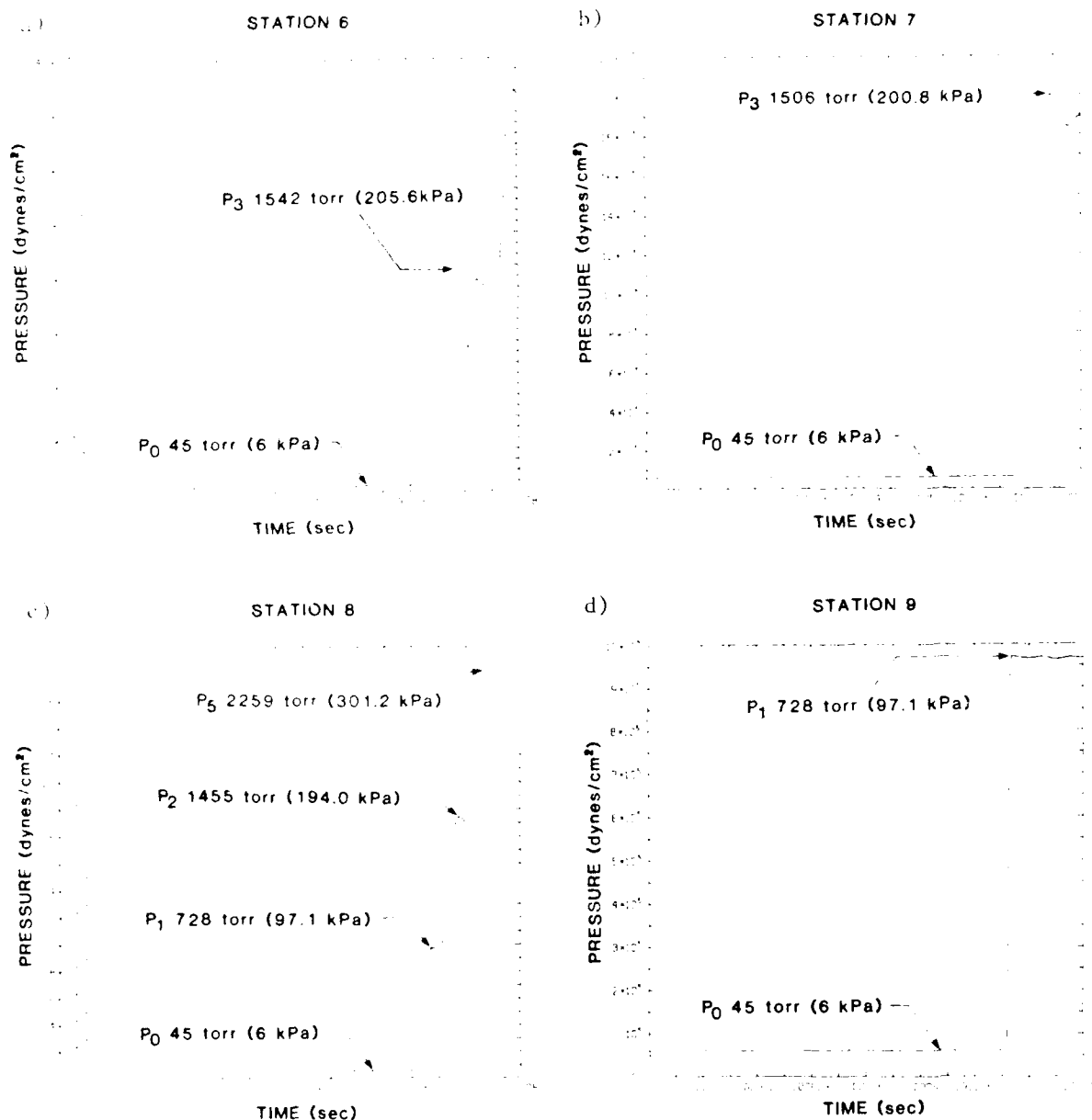
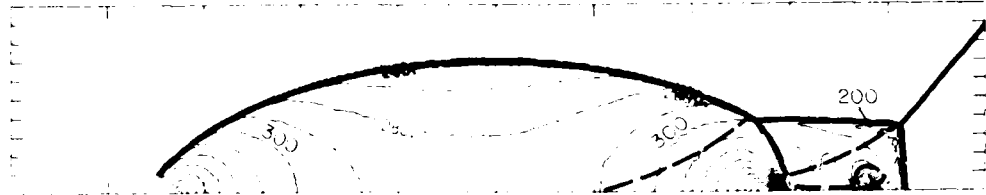


Fig. A-5 Numerical simulation of pressure history by Glaz (Ref. 12).
for the case of double-Mach reflection in air. $M_s = 3.72$,
 $\theta_w = 40^\circ$, $P_0 = 45$ torr (6 kPa), $T_0 = 21.94^\circ \text{C}$.

a) Isobaric contours of the entire flow field



b) Isobaric contours of the flow regions around the two triple points

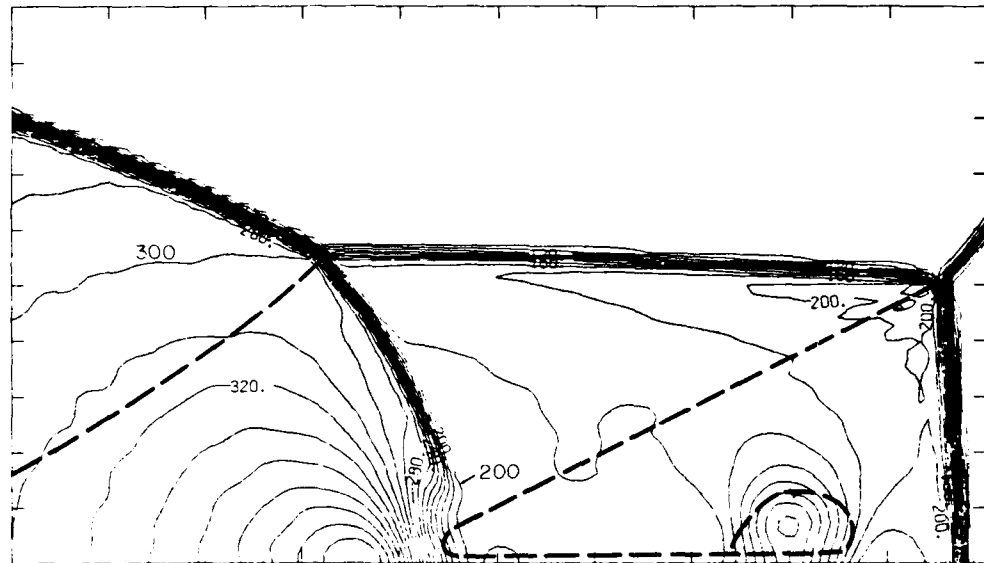


Fig. A-6 Numerical simulation of pressure contours by Glaz (Ref. 12) for the case of double-Mach reflection in air. $M_s = 3.72$, $\theta_w = 40^\circ$, $P_0 = 45$ torr (6 kPa), $T_0 = 21.94^\circ\text{C}$ and $\gamma = 1.4$. Contours are shown from 0.0 to 3.8×10^6 dynes/cm² with an interval of 1.0×10^5 and labels are scaled by 1.0×10^{-4} .

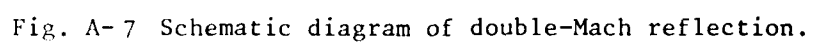


Fig. A-7 Schematic diagram of double-Mach reflection.

APPENDIX B

COMPUTER-PROGRAM LISTING FOR THE ANALYTICAL SOLUTION OF REGULAR AND MACH REFLECTIONS

The computer program listed here follows the method of calculation discussed in Section 2. The program is very general and is used for argon, nitrogen, air, carbon dioxide and sulfur hexafluoride. It allows a choice of frozen, perfect or vibrational equilibrium thermodynamic states. It can be easily modified to include any other gas by changing SUBROUTINE GAS.

The program will first check whether the input flow conditions can give regular reflection by calling SUBROUTINE RR. If it fails to obtain a solution, the program will proceed to call SUBROUTINE SIMMR to calculate Mach reflection case. If the actual wedge angle has been chosen as the parameter, the program will predict a trajectory angle for the first triple point. However, if the effective wedge angle has been chosen as the parameter, the program will iterate the wedge angle until the calculated effective wedge angle is the same as the input one. After solving for the first triple-point system, a check of the flow Mach number in region (2) with respect to the kink is done. If that is a supersonic flow, the second triple-point system will be solved by calling SUBROUTINE TRPL2. The subroutines are listed following the main program alphabetically. Input data are explained in the main program. The program is run on the Perkin Elmer 3250 Computer System at UTIAS.

```
C-----
C-----
C-----
C-----
C-----
C-----
C-----
C-----
C-----
C-----
```

.....

| IQ | CHOICES OF PARAMETER | GENERATION LEVEL |
|----------|---|------------------|
| GT2,GT4 | 1 - THETA WALL, 2 - THETA WALL, PRIME | |
| IST(0-5) | INITIAL GUESSES FOR PHI2P AND PHI4P (DEG.) | |
| NUM | EQUATION OF STATE FOR FLOW REGIONS (0) TO (5) | |
| MACHS | EXPERIMENT NUMBER | |
| PRSTOT | INCIDENT SHOCK MACH NUMBER | |
| THPO | INITIAL PRESSURE (TORR) | |
| PTPW | INITIAL TEMPERATURE (DEG. CELSIUS) | |
| CHI | WEDGE ANGLE THETA WALL (DEG.) | |
| | FIRST TRIPLE-POINT-TRAJECTORY ANGLE (DEG.) | |

—

B.2


```

606 FORMAT(1H ,/,15X,'PHI0=',F8.4,' (DEG) THETA1=',F8.4,' (DEG)  

ITAM=',F8.4,' (DEG)',/,15X,'PHI1=',F8.4,' (DEG) THETA2=',F8.4,' (DEG)  

2' (DEG) OMEGA=',F8.4,' (DEG)'),  

607 FORMAT(1H ,7X,' DENSITY (KG/M**3)',7X,4(F10.7,6X),/  

608 FORMAT(1H ,7X,' S. SPEED (M/SEC)',6X,4(F8.1,8X),/  

609 FORMAT(1H ,/,9X,'** STATE **',16X,11,15X,11,15X,11,/  

610 FORMAT(7X, VIB, R.L. (NM) IN REGIONS 1 & 2 =',2F10.6),  

85 STOP  

END  

-----  

C *** SUBROUTINE SUB-PROGRAM GAS ***  

-----  

SUBROUTINE GAS(P,T,G,RHO,H,A,MASS,ISTATE)  

C -- THIS SUBROUTINE IS DOUBLE-PRECISION --  

C  

C IMPLICIT REAL*8(A-H,M,O-Z)  

C DIMENSION AMASS(7),AG(7),TCO2(4),TSF6(6),AG1(7)  

C COMMON IREAL,IGAS,G0,ALPHA,BETA  

C DATA AMASS/28.967D0,28.0134D0,39.944D0,44.010D0,146.06D0,146.06D0,/  

128.967D0/  

C DATA AG1/1.4D0,1.4D0,1.667D0,1.29D0,1.093D0,1.333D0,1.4D0/  

C DATA AG/1.4D0,1.4D0,1.667D0,1.4D0,1.333D0,1.021D0,1.4D0/  

C DATA TSF6/1114.5D0,954.8D0,1380.5D0,884.4D0,752.5D0,522.0D0/  

C DATA TCO2/960.2D0,960.3D0,1932.2D0,3380.3D0/  

C IREAL=0 FROZEN  

C IREAL=1 PERFECT (CONSTANT GAMMA)  

C IREAL=2 EQUILIBRIUM (INCL. VIB.)  

C IGAS=1 AIR  

C IGAS=2 NITROGEN  

C IGAS=3 ARGON  

C IGAS=4 CO2  

C IGAS=5 SF6  

C IGAS=6 GAMMA=1.333  

C IGAS=7 ONLY OXYGEN IS EXCITED IN AIR  

C ISTATE=0 FLOW IS AT CHOSEN STATE  

C ISTATE=1 FLOW IS AT VIB. EQUILIBRIUM  

C  

C RR = 8.3201D3  

C MASS = AMASS(IGAS)  

C TOX = 2230.0  

C TN = 3340.0  

C G0 = AG(IGAS)  

C IF(IREAL.EQ.1) G0=AG1(IGAS)  

C  

C MASS = MASS*(1.0+ALPHA)  

C G = (G0+ALPHA*BETA)/(1.0+ALPHA*BETA)  

C H = G/(G-1.0)*RR/MASS*T  

C  

C IF(ISTATE.EQ.1) GOTO 5  

C IF(IREAL.NE.2) GO TO 200  

C GO TO(10,20,30,40,50,60,70),IGAS  

5

```

B.3

```

P1 = PRS1/Q1
P2 = PRS2/Q1
WRITE(6,601) NUM,MACHS,PTHW,ISOL,ISOL,IREAL,IGAS
WRITE(6,609) ISTAT0,ISTAT1,ISTAT2
WRITE(6,602)
WRITE(6,603) MACH0,MACH1,MACH2
WRITE(6,604) P0,P1,P2
WRITE(6,605) TMP0,TMP1,TMP2
WRITE(6,607) DRH00,DRH01,DRH02
WRITE(6,608) DAO,DAI,DA2
P0 = 90.0-THETA0/Q2
T1 = P0-PHI01/Q2
P1 = PHI1/Q2
T2 = (PHI1-PHI12)/Q2
W = P1-T1
D = PTHWP+90.-W
C P0 (PHI0) / T1 (THETA1) / P1 (PHI1) / T2 (THETA2) / W (OMEGA) /
C D (DELTA)
WRITE(6,606) P0,T1,D,P1,T2,W
MA(1)=MACH1
MA(2)=MACH2
PR(1)=PRS1
PR(2)=PRS2
TH(1)=THP1
TH(2)=THP2
PH(1)=P0
PH(2)=P1
TH(1)=T1
TH(2)=T2
IST(1)=ISTAT1
IST(2)=ISTAT2
DO 80 I=1,2
CALL VIB(IGAS,PR(1),TH(1),TAU)
DPR=PR(1)
DTH=TH(1)
CALL GAS(DPR,DTH,DUM,DUM,AS,DUM,IST(1))
V2=MA(1)*AS*SWN((PH(1)-TH(1))*3.14159/180.)
VEL(1)=TAU*V2*1.E-06*1000.
CONTINUE
WRITE(6,610) (VEL(I),I=1,2)
IF(MACHS.EQ.0)GOTO 85
GOTO 1
80
C
501 FORMAT(4I2,2X,2F6.1)
502 FORMAT(15,5F10.3)
503 FORMAT(3X,'NO SOLUTION FOR RR')
504 FORMAT(3X,'SOLUTION DID NOT CONVERGE')
505 FORMAT(1H1)
506 FORMAT(6I2)
601 FORMAT(1H ' , , , , ' EXP= , I4,3X, '***** RE-SOLUTION AT MACHS= , F7.3,
13X 'THETA= , F6.2, ' (DEG) ISOL= , I2,3X, 'IREAL= ,
1,12,3X, 'IGAS= , I2)
602 FORMAT(1H ' , 9X, '*** REGION ** , I6X, '0' , 15X, '1' , 15X, '2')
603 FORMAT(1H ' , 9X, 'MACH' , I8X, 4(F8.4,8X))
604 FORMAT(1H ' , 7X, 'PRESSURE (TORR)' , 9X, 4(F8.2,8X))
605 FORMAT(1H ' , 6X, 'TEMPERATURE (DEG K)' , 6X, 4(F8.2,8X))

```

```

C
10 V = (TOX/T)**2*DEXP(TOX/T)/(DEXP(TOX/T)-1.0)**2*0.21*(TN/T)**2*
1DEXP(TN/T)/(DEXP(TN/T)-1.0)**2*0.79
H = (3.5*T+TOX)/(DEXP(TOX/T)-1.0)*0.21*IN/(DEXP(TN/T)-1.0)*0.79*
12.5*ALPHA*BETA*T)*RR/MASS
G1 = (3.5*V)/(2.5*V)
GO TO 100

C
20 V = (TN/T)**2*DEXP(TN/T)/(DEXP(TN/T)-1.0)**2
H = (3.5*T+IN/(DEXP(TN/T)-1.0)*2.5*ALPHA*BETA*T)*RR/MASS
G1 = (3.5*V)/(2.5*V)
GO TO 100

C
30 GO TO 200

C
40 V = 0.0
H = 3.5*T
DO 41 I = 1,4
V = V+(TCU2(I)/T)**2*DEXP(TCU2(I)/T)/(DEXP(TCU2(I)/T)-1.0)**2
H = H+TCU2(I)/(DEXP(TCU2(I)/T)-1.0)
41 CONTINUE
H = (H+2.5*ALPHA*BETA*T)*RR/MASS
G1 = (3.5*V)/(2.5*V)
GO TO 100

C
50 V = 0.0
H = 4.0*T
DO 51 I = 1,6
IFACT = I
IF(1.GT.3) IFACT = 3
V = V+(TSF6(I)/T)**2*DEXP(TSF6(I)/T)/(DEXP(TSF6(I)/T)-1.0)**2*IFAC
IT
H = H+TSF6(I)/(DEXP(TSF6(I)/T)-1.0)*IFACT
51 CONTINUE
H = (H+3.0*ALPHA*BETA*T)*RR/MASS
G1 = (4.0*V)/(3.0*V)
GO TO 100

C
60 GO TO 200

C
70 V = (TOX/T)**2*DEXP(TOX/T)/(DEXP(TOX/T)-1.0)**2*0.21
H = (3.5*T+TOX)/(DEXP(TOX/T)-1.0)*0.21*2.5*ALPHA*BETA*T)*RR/MASS
G1 = (3.5*V)/(2.5*V)
GO TO 100

C
100 G = (G1/(G1-1.0)+1.0/(GO-1.0)*ALPHA*BETA)/(1.0/(G1-1.0)+1.0/(GO-1.0)*ALPHA*BETA)
GO TO 100

C
200 BBO = P/T*MASS/RR
A = DSQRT(C*P/BBO)
RETURN
END

```

8.4

```

C
C *** SUBROUTINE SUB-PROCESS INTL ***
C
SUBROUTINE INTERPSO, TMPO, THETA, MAHRS, DP, TSTEP, TPHID, TPHIL, TPFID
REAL MAHRS
DOUBLE TPFID, TPFID, DP, TSTEP, TPHID, TPHIL, TPFID
COMMON /STATO, STAT1, STAT2, STAT3, STAT4, STAT5, STAT6,
Q2 = 0.017453293
DP = DBLE(TSTEP)
DT = DBLE(TMPO)
CALL CASDEF, DP, TSTEP, TPFID, DP, TSTEP, TPFID, DP, TSTEP, TPFID
GAMMA = SIN(PI/6)
IF(GAMMA.LT.1.1) GO TO 10
TCHI = 30.70*Q2-0.75*THETA
IF(THETA.GT.2.2) TCHI = 30.70*Q2-0.75*THETA
TFACT = 1.0-0.21*(MACHS-1.0)
IF(MACHS.GT.1.0) TFACT = 0.91-0.110*(MACHS-1.0)
IF(MACHS.GT.3.0) TFACT = 0.80-0.60*(MACHS-3.0)
IF(MACHS.GT.5.0) TFACT = 0.72-0.60*(MACHS-5.0)
TCHI = TCHI*TFACT
IF(MACHS.GE.1.6) TFACT = 1.0-0.11*(MACHS-1.6)
IF(MACHS.LT.1.6) TFACT = 1.0-0.11*(MACHS-1.6)
TCHI = TCHI*TFACT
TCHI = TCHI-6.5*Q2*(1.4-GAMMA)
GO TO 20
10 TCHI = 29.85*Q2-1.165*THETA+0.013/Q2*THETA**2
TFACT = 1.0-0.47*(MACHS-1.6)
IF(MACHS.GT.2.0) TFACT = 0.812-0.25*(MACHS-2.0)
IF(MACHS.GT.3.0) TFACT = 0.563-0.106*(MACHS-3.0)
IF(MACHS.GT.5.0) TFACT = 0.352-0.036*(MACHS-5.0)
TCHI = TCHI*TFACT
TFACT = 1.0-0.11*(MACHS-1.6)*(GAMMA-1.02)/0.08
TCHI = TCHI*TFACT
20 IF(TCHI.LT.1.0*Q2) TCHI = 1.0*Q2
CSTEP = TCHI*0.2
C
TPHID = (76.48+25.446/(MACHS-0.68))*Q2
TPHID = TPHID-(1.72-0.45/(MACHS-0.80))*(THETA-5.0*Q2)
TPHID = (64.1-101.0/SQRT(MACHS+1.0))*Q2+0.6*(THETA-5.0*Q2)-0.0167
1*(THETA/Q2-5.0)**2*SQRT((ABS(MACHS-1.6))*Q2)
TFACT = 0.0
IF(GAMMA.LT.1.4) TFACT = ((1.4-GAMMA)*10.0)**1.5/8.0
IF(GAMMA.GT.1.4) TFACT = -((GAMMA-1.4)*10.0)**1.5/8.0
TPHIL = TPHID-TPHID*TFACT
IF(TPHIL.LT.5.0*Q2) TPHIL = 5.0*Q2
PSTEP = 4.0*Q2
C
RETURN
END

```

```

C      *** SUBROUTINE SUB-PROGRAM MAXTHE ***
C      -----
C
SUBROUTINE MAXTHE(MACH1,PRS1,TMP1,PH11,THETAM,MACH2,PRS2,TMP2,ILL)
  DIMENSION THETA(3),G(2)
  REAL MACH1,MACH2
  FACT21 = 0.005
  FACT22 = 1.0E-5
  Q2 = 0.017453293
  C
  C --- SET THE INITIAL VALUE FOR PH11 ---
  C
  TRR = 0.0
  DO 5 I = 1,4
    PP = (45.0+I*10.0)*Q2
    CALL SVFS(MACH1,PRS1,TMP1,PP,MACH2,PRS2,TMP2,PH112,1,ILL,2)
    IF(ILL.NE.0) GO TO 102
    IF(PP-PH112.LT.TRR) GO TO 5
    TRR = PP-PH112
    TPHI = PP
  5 CONTINUE
  TPHIF = TPHI
  STEP = 3.0*Q2
  K = 0
  C
  C --- START ITERATION ---
  C
  10 IF(MACH1*SIN(TPHI-STEP).GT.1.0) GO TO 11
  STEP = 0.4*TPHIF
  TPHI = TPHIF*0.44
  TPHIF = TPHI
  11 DO 20 I = 1,3
    PP = TPHI*(1-2)*STEP
    CALL SVFS(MACH1,PRS1,TMP1,PP,MACH2,PRS2,TMP2,PH112,1,ILL,2)
    IF(ILL.NE.0) GO TO 101
    THETA(1) = PP-PH112
  20 CONTINUE
  C
  G(1) = THETA(2)-THETA(1)
  G(2) = THETA(3)-THETA(2)
  C
  IF(G(1)*G(2).GT.0.0) GO TO 21
  IF(STEP.LT.FACT22) GO TO 30
  IF(ABS(G(1)).LT.STEP*FACT21.AND.ABS(G(2)).LT.STEP*FACT21) GO TO 30
  GO TO 22
  C
  21 IF(ABS(G(1)-G(2)).LE.ABS(G(2)*STEP/1.67)) GO TO 22
  C
  TPHIF = TPHI
  TPHI = TPHI+(G(1)+G(2))/2.0/(G(1)-G(2))*STEP
  STEP = ABS((G(1)+G(2))/2.0/(G(1)-G(2))*STEP)
  22 STEP = STEP*0.30
  K = K+1

```

```

IF(K.GT.20) GO TO 40
GO TO 10
C
  30 ILL = 0
  PH11 = TPHI
  THETAM = THETA(2)
  RETURN
C
  40 ILL = 999
  RETURN
C
  101 WRITE(6,601)
  601 FORMAT(1H,'(STOPPED AT MAXTHE 101)')
  GO TO 1000
  102 WRITE(6,602)
  602 FORMAT(1H,'(STOPPED AT MAXTHE 102)')
  1000 ILL = 999
  RETURN
  END
C
  C --- SUBROUTINE SUB-PROGRAM NR ---
  C
SUBROUTINE NR(MACHS,PRS0,TMP0,THEMIN,IC,IOUT,ILL)
  REAL MACH0,MACHS,MACH1
  DIMENSION AM(3)
  C
  Q2 = 0.017453293
  FACT = 1.0E-4
  GO TO (10,50),IC
  C
  10 TTHE = 30.0*Q2
  STEP = 0.2*TTHE
  K = 0
  C
  C --- START ITERATION ---
  C
  20 DO 30 I = 1,3
    IT = TTHE*(1-2)*STEP
    PH10 = 90.0*Q2-IT
    MACH0 = MACHS/SIN(PH10)
    CALL SVFS(MACH0,PRS0,TMP0,PH10,MACH1,PRS1,TMP1,PH101,2,ILL,1)
    IF(ILL.NE.0) GO TO 101
    AM(1) = MACH1
  30 CONTINUE
  C
  IF(ABS(AM(2)-1.0).LT.FACT) GO TO 40
  TTHE = TTHE*(AM(2)-1.0)*STEP*2.0/(AM(1)-AM(3))
  STEP = 0.3*ABS((AM(2)-1.0)*STEP*2.0/(AM(1)-AM(3)))
  IF(STEP.GT.20.0*Q2) GO TO 102
  K = K+1
  IF(K.GT.25) GO TO 103

```



```

PHI1 = APHI1(2)
CALL SVFS(MACH0, PRS0, TMP0, PHI0, MACH1, PRS1, TMP1, PHI01, 1, ILL, 1)
CALL SVFS(MACH1, PRS1, TMP1, PHI1, MACH2, PRS2, TMP2, PHI12, 1, ILL, 2)
THETW0 = 90.0*Q2-PHI0
RETURN

C
40 PHI0 = 90.0*Q2-THETW0
MACHX = THEM1N
C
C --- SET INITIAL VALUE FOR MACHS ---
C
TM = 1.2/SIN(PHI0)
TMF = TM
STEP = 0.03/SIN(PHI0)
K = 0
C
C --- START THE ITERATION ---
C
50 IF((TM-STEP)*SIN(PHI0).GT.1.0) GO TO 51
STEP = (TMF-1.0/SIN(PHI0))*0.4
TM = 1.0/SIN(PHI0)+1.1*STEP
51 IF(TM+STEP.LT.MACHX/SIN(PHI0)) GO TO 52
STEP = (MACHX/SIN(PHI0)-TMF)*0.4
TM = MACHX/SIN(PHI0)-1.1*STEP
52 TMF = TM
DO 60 I = 1,3
TM = TM+(1-2)*STEP
CALL SVFS(TM, PRS0, TMP0, PHI0, MACH1, PRS1, TMP1, PHI01, 1, ILL, 1)
IF(ILL.NE.0) GO TO 101
CALL MAXTHE(MACH1, PRS1, TMP1, PHI1, THETAM, MACH2, PRS2, TMP2, ILL)
IF(ILL.NE.0) GO TO 102
T(1) = THETAM-(PHI0-PHI01)
APHI1(1) = PHI1
60 CONTINUE
C
IF(ABS(T(2)).LT.FACT02) GO TO 70
IF((T(3)-T(1)).EQ.0.0) GO TO 65
TM = TM+STEP*2.0*T(2)/(T(1)-T(3))
STEP = ABS(STEP*2.0*T(2)/(T(1)-T(3)))
65 STEP = 0.30*STEP
IF(STEP.GT.0.2) GO TO 104
K = K+1
IF(K.GT.25) GO TO 103
GO TO 50
C
70 ILL = 0
MACH0 = TM
MACHS = TM*SIN(PHI0)
PHI1 = APHI1(2)
CALL SVFS(MACH0, PRS0, TMP0, PHI0, MACH1, PRS1, TMP1, PHI01, 1, ILL, 1)
CALL SVFS(MACH1, PRS1, TMP1, PHI1, MACH2, PRS2, TMP2, PHI12, 1, ILL, 2)
RETURN
C
101 WRITE(6,602)
602 FORMAT(1E, '(STOPPED AT REPR 101)')
GO TO 1000

```

```

102 WRITE(6,603)
603 FORMAT(1E, '(STOPPED AT REPR 102)')
GO TO 1000
103 WRITE(6,604)
604 FORMAT(1E, '(STOPPED AT REPR 103)')
GO TO 1000
104 WRITE(6,605)
605 FORMAT(1E, '(STOPPED AT REPR 104)')
1000 ILL = 999
RETURN
END

```

```

C
C
C --- SUBROUTINE SUB-PROGRAM SIMMR ---
C
SUBROUTINE SIMMR(NUM, MACHS, PRS0, TMP0, PTHWP,
REAL MACH0, MACHS, MACH1, MACH2, MACH3, MACHX, MA(3)
DOUBLE PRECISION ALPHA, BETA, GO, DPI, DP2, DP3, DT1, DT2, DT3, PRO, DR1,
IDR2, DR3, DA1, DA2, DA3, DPR, DTM, AS
DIMENSION PR(3), TM(3), PH(3), TH(3), IST(3), VRL(3)
COMMON IREAL, ICAS, GO, ALPHA, BETA, IP, IQ
COMMON /CI/SLIP
COMMON /ST/ISTAT0, ISTAT1, ISTAT2, ISTAT3, ISTAT4, ISTAT5
C
Q1 = 13.6*9.806
Q2 = 0.017453293
SLIP = 0.0
ALPHA = 0.0
BETA = 0.0
L=0
C
IF(IQ.EQ.1) GO TO 5
IQ = 0, THETA WALL AS THE PARAMETER
PTHW=PTHWP
THETAW=PTHW*Q2
CALL NR(MACHS, PRS0, TMP0, THEM1N, 1, 0, ILL)
CALL TRPLI(THETAW, MACHS, PRS0, TMP0, CHI, PHI, MACH2, MACHX, PHIK,
ITHEM1N, DELTA, PHI3, CHIP, 2, ILL)
GO TO 55
C
IQ = 1, THETA WALL PRIME AS THE PARAMETER
THWP=PTHWP*Q2
CALL NR(MACHS, PRS0, TMP0, THEM1N, 1, 0, ILL)
CALL RMR(MACHS, MACH0, PRS0, PHI0, MACH1, PRS1, TMP1, PHI01,
IMACH2, PRS2, TMP2, PHI1, PHI12, THETW0, THEM1N, 0.0, K, 1, ILL)
THETW1=2.*Q2
THETW3=THETW0
CALL TRPLI(THETW1, MACHS, PRS0, TMP0, CHI1, PHI, MACH2, MACHX, PHIK,
ITHEM1N, DELTA, PHI3, CHIP, 2, ILL)
CALL TRPLI(THETW3, MACHS, PRS0, TMP0, CHI3, PHI, MACH2, MACHX, PHIK,
ITHEM1N, DELTA, PHI3, CHIP, 2, ILL)

```

```

1 PCHI,PTHW,PCHIP,PDELTA,PWP,MACHK
  WRITE(6,608) ISTAT1,ISTAT2,ISTAT3
  WRITE(6,604) MACH1,MACH2,MACH3
  WRITE(6,602) P1,P2,P3
  WRITE(6,605) TMP1,TMP2,TMP3
  WRITE(6,607) DR1,DR2,DR3
  WRITE(6,610) DA1,DA2,DA3
  WRITE(6,603) T1,T2,T3
  WRITE(6,606) PH0,PH1,PH3
  THEWP=THETA+CHIP
  MA(1)=MACH1
  MA(2)=MACH2
  MA(3)=MACH3
  PR(1)=PRS1
  PR(2)=PRS2
  PR(3)=PRS3
  TM(1)=TMP1
  TM(2)=TMP2
  TM(3)=TMP3
  PH(1)=PH0
  PH(2)=PH1
  PH(3)=PH3
  TH(1)=T1
  TH(2)=T2
  TH(3)=T3
  ISTAT1=ISTAT1
  ISTAT2=ISTAT2
  ISTAT3=ISTAT3
  DO 60 I=1,3
    CALL VIB(ICAS,PR(1),TM(1),TAU)
    DPR=PR(1)
    DTM=TM(1)
    CALL GAS(DPR,DTM,DUM,DUM,AS,DUM,IST(1))
    V2=MA(1)*SIN((PH(1)-TH(1))*3.14159/180.)
    VRL(1)=TAU*V2*1.E-06*1000.
60 CONTINUE
    WRITE(6,609)(VRL(1),I=1,3)
    CALL TRPL2(MACH1,PRS1,TMP1,PHI1,PHI01,THEWPP)
503 FORMAT(5X,'ILL IN TRPL1 IS NOT ZERO')
505 FORMAT(5X,'ITERATION MORE THAN 25 TIMES')
C 506 FORMAT(5X,THEWP,THEW2 : ',2F10.5)
601 FORMAT(/,1H 'EXP=',I4,3X,'***** MR-SOLUTION AT MACHS=',F7.3,3X,
  1'THEWAP=',F6.2,3X,'ILL=',I3,/,9X,'IREAL=',I2,3X,'IGAS=',I2,
  23X,'PO=',F8.2, (TORR)',3X,'TO= ',
  1'F8.2, (DEG)',3X,'RHO0=',F10.7, (KG/M**3)',/9X
  1'CHI=',F7.3,3X,'THETA=',F6.2,3X,'CHIP=',F7.3,3X,'DELTA=',F8.3,
  13X,'OMEGA PRIME=',F8.3,3X,'MACHK=',F7.3,
  1//,9X,'** REGION **',9X,'1',I1X,'2',
  11X,'3')
602 FORMAT(1H ,10X,'PRESSURE',6X,3(F9.2,3X))
605 FORMAT(1H ,10X,'TEMPERATURE',3X,3(F9.2,3X))
604 FORMAT(1H ,10X,'MACH',11X,3(F7.3,5X))
603 FORMAT(1H ,10X,'THETA',10X,3(F7.3,5X))
606 FORMAT(1H ,10X,'PHI',12X,3(F7.3,5X))
607 FORMAT(1H ,8X,'DENSITY (KG/M**3)',3(F10.7,2X))
608 FORMAT(1H ,8X,'** STATE **',9X,11,11X,11,11X,11,/)

```



```

C 50 ILL = 999
C RETURN
C
C 40 ILL = 0
C PRS2 = TPRS
C TMP2 = TTMP
C CALL GAS(PRS2,TMP2,CMH2,RHO2,H2,A2,MASS,IHND)
C PH12 = DATAN(CI/RHO2)
C IF(CI.LT.0.0) PH12 = PH12+3.14159265359
C U2 = C2/RHO2/DSIN(PH12)
C MACH2 = U2/A2
C IP = 1, THERMODYN. STATES ARE AS GIVEN
C IP = 2, THERMODYN. STATES ARE TO BE DETERMINED BY THE PROGRAM
C IF(ICOUNT.EQ.IP) GOTO 1050
C
C DEFINE THE STATE OF THE FLOW REGION
C CALL VIB(IGAS,PRS2,TMP2,TAU)
C V2=U2*DSIN(PH12)
C VRL=TAU*V2*1.D-06
C IF(IP.EQ.2.AND.VRL.GT.0.001) GOTO 1025
C
C FOR VIB. EQUILIBRIUM
C IF(IREGIN.EQ.1) ISTAT1=1
C IF(IREGIN.EQ.2) ISTAT2=1
C IF(IREGIN.EQ.3) ISTAT3=1
C IF(IREGIN.EQ.4) ISTAT4=1
C IF(IREGIN.EQ.5) ISTAT5=1
C GOTO 15
C
C RESET ISTATE IF NOT IN VIB. EQUILIBRIUM
C 1025 IF(IREGIN.EQ.1) ISTAT1=0
C IF(IREGIN.EQ.2) ISTAT2=0
C IF(IREGIN.EQ.3) ISTAT3=0
C IF(IREGIN.EQ.4) ISTAT4=0
C IF(IREGIN.EQ.5) ISTAT5=0
C
C 1050 SMACH2 = SNGL(MACH2)
C SPRS2 = SNGL(PRS2)
C STMP2 = SNGL(TMP2)
C SPH12 = SNGL(PH12)
C RETURN
C END
C
C *** SUBROUTINE SUB-PROGRAM TRPL1 ***
C
C SUBROUTINE TRPL1(THETA,MACHS,PRS0,TMP0,CHI,PHI1,MACH2,MACHK,PHIK,
C ITHMIN,DELTA,PHI3,CHIP,IC,ILL)
C
C REAL MACHS,MACH0,MACH1,MACH2,MACH3,MACHK
C DIMENSION AP(3,2),AT(3,2),AM(3),APHI(3,3)
C DOUBLE PRECISION DPRS(3,2),DTMP(3,2),DRHO0,DRHO1,DUM,DPRS0,DTMP0,D
C LA0,DA2

```

```

COMMON /CI/SLIP,EPSLN
COMMON /ST/ISTAT0,ISTAT1,ISTAT2,ISTAT3,ISTAT4,ISTAT5
C
C FACT1 = 1.0E-4
C FACT2 = 1.0E-4
C Q2 = 0.017453293
C
C --- SET INITIAL VALUE FOR CHI AND PHI1 ---
C
C CALL INTL(PRS0,TMP0,THETA,MACHS,TCHI,CSTEP,TPH1,PSTEP)
C TCHI = TCHI*EPSLN
C TPH1 = TPH1*EPSLN
C IF(TCHI-CSTEP.IT.THEMIN-THETA) TCHI = THEMIN-THETA+CSTEP*1.1
C TCHIF = TCHI
C MACH0 = MACHS/SIN(90.0*Q2-THETA-TCHI+CSTEP)
C CALL SVFS(MACH0,PRS0,TMP0,90.0*Q2-THETA-TCHI+CSTEP,MACH1,PRS1,TMP
C 11,PHI01,2,ILL,1)
C IF(ILL.NE.0) GO TO 105
C IF(.MACH1*SIN(TPH1-PSTEP).IT.1.0) TPH11 = ASIN(1.0/MACH1)*1.1*PST
C IEP
C TPH11F = TPH11
C K = 0
C
C --- START ITERATION ---
C
C 10 IF(TCHI-CSTEP.GT.THEMIN-THETA+0.02*Q2.AND.TCHI-CSTEP.GT.0.0) GO T
C 10 11
C CSTEP = 0.3*(TCHIF-AMAX1((THEMIN-THETA+0.02*Q2,0.0)))
C TCHI = 1.2*CSTEP+AMAX1((THEMIN-THETA+0.02*Q2,0.0))
C TCHIF = TCHI
C 11 MACH0 = MACHS/SIN(90.0*Q2-THETA-TCHI+CSTEP)
C CALL SVFS(MACH0,PRS0,TMP0,90.0*Q2-THETA-TCHI+CSTEP,MACH1,PRS1,TMP
C 11,PHI01,2,ILL,1)
C IF(ILL.NE.0) GO TO 104
C IF(TPH11.GT.90.0*Q2) GO TO 12
C IF(MACH1*SIN(TPH1-PSTEP).GT.1.0) GO TO 14
C PSTEP = 0.4*ABS(TPH1F-ASIN(1.0/MACH1))
C TPH11 = ASIN(1.0/MACH1)*PSTEP*1.1
C TPH11F = TPH11
C GO TO 14
C 12 IF(TPH1-PSTEP.GT.180.0*Q2-PHI01) TPH11 = 180.0*Q2-PHI01-PSTEP*1.1
C IF(MACH1*SIN(TPH1-PSTEP).GT.1.0) GO TO 14
C PSTEP = 0.4*ABS(180.0*Q2-ASIN(1.0/MACH1)-TPH11F)
C TPH11 = 180.0*Q2-ASIN(1.0/MACH1)-PSTEP*1.1
C 14 IF(TPH11.GT.124.0*Q2) TPH11 = 100.0*Q2
C TPH11F = TPH11
C DO 20 I = 1,3
C DO 30 J = 1,2
C IF(I*J.EQ.4) GO TO 30
C TC = TCHI*(1-2)*(2-J)*CSTEP
C TP = TPH1*(1-2)*(J-1)*PSTEP
C PHI0 = 90.0*Q2-(THETA+TC)
C MACH0 = MACHS/SIN(PHI0)
C PHI3 = 90.0*Q2-TC+EPSLN
C CALL SVFS(MACH0,PRS0,TMP0,PHI0,MACH1,PRS1,TMP1,PHI01,2,ILL,1)
C IF(ILL.NE.0) GO TO 101

```

```

CALL SVFS(MACH1,PRS1,TMP1,TP,MACH2,PRS2,TMP2,PHI12,2,ILL,3)
IF(ILL.NE.0) GO TO 102
CALL SVFS(MACH0,PRS0,TMP0,PHI3,MACH3,PRS3,TMP3,PHI33,2,ILL,3)
IF(ILL.NE.0) GO TO 103
AP(1,J) = (PRS3-PRS2)/PRS2
AT(1,J) = (PHI33-PHI33)-(PHI0-PHI01)*TP-TPH12*-SLIP
AM(1) = MACH2
DPRS0 = PRS0
DPRS(1,1) = PRS1
DPRS(1,2) = PRS2
DTMP0 = TMP0
DTMP(1,1) = TMP1
DTMP(1,2) = TMP2
APHI(1,1) = PHI0
APHI(1,2) = PHI01
APHI(1,3) = PHI12
30 CONTINUE
20 CONTINUE
C
IF(ABS(AP(2,1)),1.T,FACT1.AND.ABS(AT(2,1)),1.T,FACT2) GO TO 40
IF(K.GT.25) GO TO 50
C
IF((AP(3,2)-AP(1,2))*(AT(3,2)-AT(1,2)).EQ.0.0) GO TO 42
B1 = (AP(3,1)-AP(1,1))/CSTEP/2.0
B2 = (AT(3,1)-AT(1,1))/CSTEP/2.0
A1 = (AP(3,2)-AP(1,2))/PSTEP/2.0
A2 = (AT(3,2)-AT(1,2))/PSTEP/2.0
BB = A1*B2-A2*B1
PP = (B1*AT(2,1)-B2*AP(2,1))/BB
IF(ABS(PP).GT.20.0*Q2) PP = 20.0*Q2*PP/ABS(PP)
TPH1LF = TPH11
TPH1L = TPH11+PP
PSTEP = 0.3*ABS(PP)
CC = (A1*AT(2,1)-A2*AP(2,1))/BB
IF(ABS(CC).GT.10.0*Q2) CC = 5.0*Q2*CC/ABS(CC)
TCHIF = TCHI
TCHI = TCHI-CC
CSTEP = ABS(CC)
GO TO 41
42 TCHIF = TCHI
TCHI = TCHI+2.0*CSTEP*AT(2,1)/(AT(1,1)-AT(3,1))
CSTEP = 0.3*ABS(2.0*CSTEP*AT(2,1)/(AT(1,1)-AT(3,1)))
41 K = K+1
GO TO 10
C
50 ILL = 999
RETURN
C
40 ILL = 0
CHI = TCHI
PH1L = TPH11
DELTA = 180.0*Q2-(APHI(2,2)+TPH11)
MACH2 = AM(2)
IF(IC.EQ.1) RETURN
CALL GAS(DPRS0,DTMP0,DUM,DRH00,DUM,DAO,DUM,1,STAT0)
CALL GAS(DPRS(2,1),DTMP(2,1),DUM,DRH01,DUM,DUM,1,STAT1)

```

```

CALL CASIDPRS(, , , TMP1,TMP2,TMP3,TMP4,TMP5,TMP6,TMP7,TMP8,TMP9,TMP10)
KHO0 = DRH00
KH01 = UKR01
AO = DA0
A1 = DA1
VW1 = KHO0/KHO1/SIN(TRP1)*EXP(-I*PI*PHI0)*COS(PHI0)
VTZ = MACH2*MA2
MACHW = MACH1*5*(RT(1.0+(VKTA/T1)**2-1.0)/T1)*VW1/VW2*(SIN(ATRIE)+SIN(
PRIK = ATAN((1.0-KRH0)/KH01)/((1.0+KRI0)/KRI1)-ATRIE/2.0*(1.0+KRI0)/KH01
IJAN(TPH11+APH1(.5))/?/?
CRIP = 90.*C2-THTAN-FTHK
WRITE(6,*)THETA,W,CHI,PHUK,(HIP
RETURN
C
C
101 WRITE(6,601)
601 FORMAT(1H,'(STOPPED AT TRPL1 101)')
GO TO 1000
102 WRITE(6,602)
602 FORMAT(1H,'(STOPPED AT TRPL1 102)')
GO TO 1000
103 WRITE(6,603)
603 FORMAT(1H,'(STOPPED AT TRPL1 103)')
GO TO 1000
104 WRITE(6,604)
604 FORMAT(1H,'(STOPPED AT TRPL1 104)')
GO TO 1000
105 WRITE(6,605)
605 FORMAT(1H,'(STOPPED AT TRPL1 105)')
1000 ILL = 999
RETURN
END
C
C
C
*** SUBROUTINE SUB-PROGRAM TRPL2 ***
SUBROUTINE TRPL2(MACH1,PRSI,TMP1,PHI1,PHI01,THEWPP)
DOUBLE PRECISION DP2P,DP4,DP5,DT2P,DT4,DT5,GMM1,GMM2P,GMM4,
.GMM5,DRE2P,DR4,DR5,DA1,DA2P,DA4,DA5,DPR,DTM,AS
REAL MACHI,MACHIP,MACH2P,MACH4,MACH5,MA(3)
DIMENSION AP(3,2),AT(3,2),AM(3),PR(3),TM(3),PH(3),TH(3),
.IST(3),VRL(3)
COMMON IREAL,IGAS,CO,ALPHA,BETA
COMMON /ST/ISTAT0,ISTAT1,ISTAT2,ISTAT3,ISTAT4,ISTAT5
COMMON /GUESS/GT2,GT4
FACT1=1.0E-4
FACT2=1.0E-4
Q1=13.6*9.806
Q2=0.017453293
PHIP=PHI1+PHI01
MACHIP=MACHI*(1.+SIN(PHI01)*SIN(PHI01))/((SIN(PHIP))*SIN(PHIP)))

```

```

-2.*SIN(PHI01)*COS(PHI1)/SIN(PHI1P))*0.5
CALL SVFS(MACH1P,PRS1,TMP1,PH1P,MACH2P,PRS2P,TMP2P,PH12P,2,
.ILL,2)
WRITE(6,511)MACH1P
511 FORMAT(/' MACH1P = ',F10.4)
IF(ILL.NE.0) GO TO 101
C NOT DMR CASE
IF(MACH2P.IT.1.0) GOTO 1000
C SET INITIAL VALUES FOR PHI4 AND PHI2
TPHI4=CT4*Q2
P4STEP=2.*Q2
TPHI2=GT2*Q2
P2STEP=2.*Q2
IF(MACH2P*SIN(TPHI2-P2STEP).LT.1.0) TPHI2=ASIN(1.0/MACH2P)
+1.1*P2STEP
TPHI2F=TPHI2
TPHI4F=TPHI4
K=0
C START ITERATION
10 IF(TPHI4+P4STEP.GT.(PH1P-5.*Q2).AND.TPHI4+P4STEP.GT.0.0)GOTO 11
P4STEP=1.1*TPHI4F
TPHI4=1.2*TPHI4+P4STEP
TPHI4F=TPHI4
11 CALL SVFS(MACH1P,PRS1,TMP1,TPHI4,MACH4,PRS4,TMP4,PHI14,2,ILL,4)
IF(ILL.NE.0) GO TO 102
IF(TPHI2.GT.90.*Q2) GO TO 12
IF(MACH2P*SIN(TPHI2-P2STEP).GT.1.0) GO TO 14
P2STEP=0.4*ABS(TPHI2F-ASIN(1.0/MACH1P))
TPHI2=ASIN(1.0/MACH1P)+P2STEP*1.1
TPHI2F=TPHI2
GO TO 14
12 IF(TPHI2+P2STEP.GT.180.*Q2-PHI12P) TPHI2=180.*Q2-PHI12P-P2STEP*1.1
IF(MACH1P*SIN(TPHI2+P2STEP).GT.1.0) GO TO 14
P2STEP=0.4*ABS(180.*Q2-ASIN(1.0/MACH1P)-TPHI2F)
TPHI2=180.*Q2-ASIN(1.0/MACH1P)-P2STEP*1.1
14 IF(TPHI2.GT.179.*Q2) TPHI2=179.*Q2
TPHI2F=TPHI2
DO 20 I=1,3
DO 30 J=1,2
IF(I*J.EQ.4) GO TO 30
TP4=TPHI4+(I-2)*(2-J)*P4STEP
TP2=TPHI2+(I-2)*(J-1)*P2STEP
PHI4=TP4
PHI2=TP2
CALL SVFS(MACH2P,PRS2P,TMP2P,PHI2,MACH5,PRS5,TMP5,PHI25,2,ILL,5)
IF(ILL.NE.0) GO TO 103
CALL SVFS(MACH1P,PRS1,TMP1,PHI4,MACH4,PRS4,TMP4,PHI14,2,ILL,4)
IF(ILL.NE.0) GO TO 104
AP(I,J)=(PRS4-PRS5)/PRS5
AT(I,J)=(PHI4-PHI14)-(PHI1P-PHI12P)*(TP2-PHI25)
AM(1)=MACH5
IF(1.NE.2) GOTO 30
IF(J.NE.1)GOTO 30

```


UTIAS Report No. 283

Institute for Aerospace Studies, University of Toronto (UTIAS)
4925 Baffertin Street, Downsview, Ontario, Canada, M3H 5T6

TABULAR AND GRAPHICAL SOLUTIONS OF REGULAR AND MACH REFLECTIONS
IN PSEUDO-STATIONARY FROZEN AND VIBRATIONAL-EQUILIBRIUM FLOWS

Hu, T. C. J. and Shirouzu, M.

1. Oblique-shock-wave reflections
2. Regular reflection
3. Mach reflection
4. Numerical and graphical solutions
5. Frozen and equilibrium flows

I. Hu, T. C. J., Shirouzu, M. II. UTIAS Report No. 283

Flow properties of pseudo-stationary oblique-shock-wave reflections are given as solutions of two-shock and three-shock theories. The calculations were performed for Ar, air, CO_2 and SF_6 using both frozen and vibrational equilibrium gas assumptions. The flow properties are tabulated for initial shock Mach numbers $1.2 < M_0 < 10.0$ and wedge angles $1^\circ < \theta_0 < 85^\circ$. The flow properties are plotted as a function of the incident shock Mach number for a series of wedge angles for both regular and Mach reflections. Another set of graphs is presented for Mach reflection with the flow properties plotted against the effective wedge angle θ_0 for a series of shock Mach numbers. The latter set is used when the effective wedge angle is chosen as the parameter for comparison. The second triple-point system, which exists only in double-Mach reflection, is solved numerically for the first time, and the solutions are presented both in tabular and graphical forms. The tables and graphs are designed to serve the analyst and experimenter working on oblique-shock-wave reflections.

Available copies of this report are limited. Return this card to UTIAS, if you require a copy.

UTIAS Report No. 283

Institute for Aerospace Studies, University of Toronto (UTIAS)
4925 Baffertin Street, Downsview, Ontario, Canada, M3H 5T6

TABULAR AND GRAPHICAL SOLUTIONS OF REGULAR AND MACH REFLECTIONS
IN PSEUDO-STATIONARY FROZEN AND VIBRATIONAL-EQUILIBRIUM FLOWS

Hu, T. C. J. and Shirouzu, M.

1. Oblique-shock-wave reflections
2. Regular reflection
3. Mach reflection
4. Numerical and graphical solutions
5. Frozen and equilibrium flows

I. Hu, T. C. J., Shirouzu, M. II. UTIAS Report No. 283

Flow properties of pseudo-stationary oblique-shock-wave reflections are given as solutions of two-shock and three-shock theories. The calculations were performed for Ar, air, CO_2 and SF_6 using both frozen and vibrational equilibrium gas assumptions. The flow properties are tabulated for initial shock Mach numbers $1.2 < M_0 < 10.0$ and wedge angles $1^\circ < \theta_0 < 85^\circ$. The flow properties are plotted as a function of the incident shock Mach number for a series of wedge angles for both regular and Mach reflections. Another set of graphs is presented for Mach reflection with the flow properties plotted against the effective wedge angle θ_0 for a series of shock Mach numbers. The latter set is used when the effective wedge angle is chosen as the parameter for comparison. The second triple-point system, which exists only in double-Mach reflection, is solved numerically for the first time, and the solutions are presented both in tabular and graphical forms. The tables and graphs are designed to serve the analyst and experimenter working on oblique-shock-wave reflections.

Available copies of this report are limited. Return this card to UTIAS, if you require a copy.

UTIAS Report No. 283

Institute for Aerospace Studies, University of Toronto (UTIAS)
4925 Baffertin Street, Downsview, Ontario, Canada, M3H 5T6

TABULAR AND GRAPHICAL SOLUTIONS OF REGULAR AND MACH REFLECTIONS
IN PSEUDO-STATIONARY FROZEN AND VIBRATIONAL-EQUILIBRIUM FLOWS

Hu, T. C. J. and Shirouzu, M.

1. Oblique-shock-wave reflections
2. Regular reflection
3. Mach reflection
4. Numerical and graphical solutions
5. Frozen and equilibrium flows

I. Hu, T. C. J., Shirouzu, M. II. UTIAS Report No. 283

Flow properties of pseudo-stationary oblique-shock-wave reflections are given as solutions of two-shock and three-shock theories. The calculations were performed for Ar, air, CO_2 and SF_6 using both frozen and vibrational equilibrium gas assumptions. The flow properties are tabulated for initial shock Mach numbers $1.2 < M_0 < 10.0$ and wedge angles $1^\circ < \theta_0 < 85^\circ$. The flow properties are plotted as a function of the incident shock Mach number for a series of wedge angles for both regular and Mach reflections. Another set of graphs is presented for Mach reflection with the flow properties plotted against the effective wedge angle θ_0 for a series of shock Mach numbers. The latter set is used when the effective wedge angle is chosen as the parameter for comparison. The second triple-point system, which exists only in double-Mach reflection, is solved numerically for the first time, and the solutions are presented both in tabular and graphical forms. The tables and graphs are designed to serve the analyst and experimenter working on oblique-shock-wave reflections.

Available copies of this report are limited. Return this card to UTIAS, if you require a copy.

UTIAS Report No. 283

Institute for Aerospace Studies, University of Toronto (UTIAS)
4925 Baffertin Street, Downsview, Ontario, Canada, M3H 5T6

TABULAR AND GRAPHICAL SOLUTIONS OF REGULAR AND MACH REFLECTIONS
IN PSEUDO-STATIONARY FROZEN AND VIBRATIONAL-EQUILIBRIUM FLOWS

Hu, T. C. J. and Shirouzu, M.

1. Oblique-shock-wave reflections
2. Regular reflection
3. Mach reflection
4. Numerical and graphical solutions
5. Frozen and equilibrium flows

I. Hu, T. C. J., Shirouzu, M. II. UTIAS Report No. 283

Flow properties of pseudo-stationary oblique-shock-wave reflections are given as solutions of two-shock and three-shock theories. The calculations were performed for Ar, air, CO_2 and SF_6 using both frozen and vibrational equilibrium gas assumptions. The flow properties are tabulated for initial shock Mach numbers $1.2 < M_0 < 10.0$ and wedge angles $1^\circ < \theta_0 < 85^\circ$. The flow properties are plotted as a function of the incident shock Mach number for a series of wedge angles for both regular and Mach reflections. Another set of graphs is presented for Mach reflection with the flow properties plotted against the effective wedge angle θ_0 for a series of shock Mach numbers. The latter set is used when the effective wedge angle is chosen as the parameter for comparison. The second triple-point system, which exists only in double-Mach reflection, is solved numerically for the first time, and the solutions are presented both in tabular and graphical forms. The tables and graphs are designed to serve the analyst and experimenter working on oblique-shock-wave reflections.

Available copies of this report are limited. Return this card to UTIAS, if you require a copy.

END

FILMED

4-86

DTIC